

Application of the Biginelli-Three-Component Reaction for the Synthesis of Novel Renewable Polymers

Anwendung der Biginelli-Drei-Komponenten-Reaktion für die Synthese neuartiger, erneuerbarer Polymere

Juni 2021

Julian Tobias Windbiel, M.Sc. Chem.

Dissertation

Application of the Biginelli-Three-Component Reaction for the Synthesis of Novel Renewable Polymers

Zur Erlangung des akademischen Grades eines
DOKTORS DER NATURWISSENSCHAFTEN

(Dr. rer. nat.)

von der KIT-Fakultät für Chemie und Biowissenschaften
des Karlsruher Instituts für Technologie (KIT)

genehmigte

DISSERTATION

von

M. Sc. Julian Tobias Windbiel

1. Referent: Prof. Dr. Michael A. R. Meier

2. Referent: Prof. Dr. Joachim Podlech

Tag der mündlichen Prüfung: 21. Juli 2021

“First thoughts are the everyday thoughts. Everyone has those. Second thoughts are the thoughts you think about the way you think. People who enjoy thinking have those. Third thoughts are thoughts that watch the world and think all by themselves. They’re rare, and often troublesome. Listening to them is part of witchcraft.”

–Terry Pratchett

Die vorliegende Arbeit wurde von Januar 2018 bis Juni 2021 unter Anleitung von Prof. Dr. Michael A. R. Meier am Karlsruher Institut für Technologie (KIT) angefertigt.

Hiermit erkläre ich wahrheitsgemäß, dass ich die vorliegende Arbeit selbständig angefertigt und keine anderen als die angegebenen Quellen und Hilfsmittel benutzt, sowie die wörtlich oder inhaltlich übernommenen Stellen als solche kenntlich gemacht und die Satzung des Karlsruher Instituts für Technologie (KIT) zur Sicherung guter wissenschaftlicher Praxis in der jeweils gültigen Fassung beachtet habe. Des Weiteren erkläre ich, dass ich mich derzeit in keinem laufenden Promotionsverfahren befinde und auch keine vorausgegangenen Promotionsversuche unternommen habe.

Ort, Datum

Unterschrift

Acknowledgements

An dieser Stelle möchte ich allen danken, die zum Gelingen dieser Arbeit beigetragen haben. Als erstes möchte ich mich bei Mike für das entgegengebrachte Vertrauen und die Möglichkeit meine Doktorarbeit in seinem Arbeitskreis durchführen zu können bedanken.

Further, I would like to thank all former and present colleagues as you created the warm productive and relaxed atmosphere that I enjoyed so much; at work and during the after hours.

Special thanks to Lab 409: Luca, Eren, Pia, Anja, and Kenny, you maintained the perfect combination of nice scientific discussions and nonsense.

I would like to thank Dafni, Roman, Bohni, Josina for their critical proofreading.

Many thanks also to Prof. Athina Anastasaki for the opportunity to spend two months in her group at the Materials Department at the ETH in Zürich. Thanks also to the group for their warm welcome and support, especially to Richard, Hyun Suk, Philipp, Takanori, and Kostas.

Weiterhin möchte ich allen Studierenden und Auszubildenden, die an dieser Arbeit mitgewirkt haben, danken.

Danken möchte ich außerdem der analytischen Abteilung des Instituts für Organische Chemie für die Instandhaltung der Messgeräte sowie die Durchführung diverser Analysen.

Ein besonderer Dank gilt meiner Mutter Uta, die mich über all die Jahre in allen Bereichen meines Lebens bedingungslos unterstützt hat und immer für mich da war.

Abstract

The sustainable and reasonable use of fossil resources and the utilisation of renewable resources is a major goal of science. This work contributes to this goal. Consequently, sustainability in the broader sense, as well as the renewability of the materials that were applied within this work were discussed. The goal of this thesis was the synthesis and characterisation of novel polymers that were prepared using the Biginelli-three-component reaction as the characteristics of multicomponent reactions correlate well with the principles of Sustainable Chemistry. Consequently, the synthesis and characterisation of novel renewable polymers using the Biginelli-three-component reaction was investigated following three different approaches.

In the first approach, the Biginelli-three-component reaction was applied for the efficient synthesis of a set of novel renewable polycondensates significantly expanding the known set of components for the Biginelli polycondensation. The structure-property relations of the resulting Biginelli polycondensates was evaluated verifying that the Biginelli polycondensates offer, overall, high glass transition temperatures. The glass transition temperature was tunable in 15°C steps by a simple variation of the applied components.

In the second approach, the end group functionalisation of Biginelli polycondensates was investigated for the first time to allow for the synthesis of block copolymers by polymer-polymer coupling. Hence, a terminal double bond was introduced as end group of the Biginelli polycondensate. Coupling was realised *via* thiol-ene reaction of the Biginelli polycondensate with a polymer equipped with thiol end group. The thermal properties of the resulting block copolymers were investigated and indicated microphase separation of the investigated block copolymers.

The third approach covered the post-polymerisation modification of renewable polymers that were equipped with acetoacetate groups in their pendant groups *via* the Biginelli-three-component reaction. The synthesis of renewable vinyl ester monomers and one methacrylate monomer that were equipped with an acetoacetate group was investigated. Subsequently, the RAFT radical polymerisation of these monomers was investigated. While the vinyl ester monomers showed strong polymerisation inhibition, RAFT polymers of the methacrylate monomer were obtained. Consequently, the possibility for chain extension and the synthesis

of block copolymers was shown. Furthermore, the resulting polymers were efficiently modified *via* the Biginelli-three-component reaction and their thermal properties were determined.

Zusammenfassung

Der nachhaltige und verantwortungsbewusste Einsatz fossiler Rohstoffe und die Verwendung nachwachsender Rohstoffe ist eines der Hauptziele der Chemie und verwandter Fachgebiete. Die in dieser Arbeit dargelegten Forschungsergebnisse tragen zu diesem Ziel bei. Daher wurde Nachhaltigkeit im Allgemeinen besprochen und die erneuerbare Synthese der in dieser Arbeit verwendeten Verbindungen diskutiert. Ziel der Arbeit war es, neuartige und nachwachsende Polymere mit Hilfe der Biginelli-Drei-Komponenten-Reaktion herzustellen, da die typischen Eigenschaften von Multikomponenten-Reaktionen gut mit den Prinzipien der Nachhaltigkeit korrelieren. Dabei wurden drei verschiedene Ansätze verfolgt.

Der erste Ansatz beschäftigte sich mit der effizienten Synthese einer Bibliothek von neuartigen Biginelli-Polykondensaten. Dabei wurde die Gesamtheit der für die Biginelli-Polykondensation bekannten Komponenten deutlich erweitert. Die Struktur-Eigenschaftsbeziehungen der erhaltenen Polykondensate wurden untersucht. Die erwarteterweise hohen Glasübergangstemperaturen konnten in 15°C-Schritten durch eine einfache Variation der verwendeten Edukte eingestellt werden.

Der zweite Ansatz beschäftigte sich mit der Endgruppenfunktionalisierung von Biginelli-Polykondensaten, um die Synthese von Blockkopolymeren durch Polymer-Polymer-Kopplung zu ermöglichen. Zum ersten Mal wurden Biginelli-Polykondensate mit einer definierten Endgruppe dargestellt. Die eingeführte terminale Doppelbindung wurde verwendet, um den Biginelli-Block mit einem Polymer, das eine Thiol-Endgruppe trug, mittels Thiol-En-Reaktion zu koppeln. Die Untersuchung der thermischen Eigenschaften der erhaltenen Blockkopolymere deuteten auf eine Mikrophasenseparation im Material hin.

Der dritte Ansatz war die Modifikation erneuerbarer Polymere mittels Biginelli-Drei-Komponenten Reaktion. Dazu wurden erneuerbare Vinylester-Monomere und ein Methacrylat-Monomer, die über eine Acetoacetat-Gruppe verfügten, dargestellt. Daraufaufgehend wurde die radikalische Polymerisation dieser Monomere untersucht. Während die Polymerisation der Vinylester-Monomer stark inhibiert war, so konnte das Methacrylat problemlos in einer RAFT-Polymerisation umgesetzt werden. Nachfolgend, wurde die Möglichkeit der Kettenverlängerung, sowie der Synthese von Blockkopolymeren

aufgezeigt. Zu guter Letzt wurden die erhaltenen Homopolymere über ihre Acetoacetat-Gruppen effizient mittels Biginelli-Drei-Komponenten Reaktion modifiziert und die thermischen Eigenschaften der Produkte wurden untersucht.

Table of Contents

1	Introduction.....	1
2	Theoretical Background.....	3
2.1	GREEN AND SUSTAINABLE CHEMISTRY – A BRIEF HISTORICAL SUMMARY	3
2.2	GREEN AND SUSTAINABLE CHEMISTRY.....	5
2.3	TOOLS TO ASSESS SUSTAINABILITY	7
2.3.1	Metrics to Optimise the Mass Balance of a Reaction.....	7
2.3.2	Metrics to Assess the Environmental Impact of a Process	10
2.3.3	Metrics to Assess the Energy Demand of a Process.....	12
2.4	HOW TO ADDRESS THE WASTE PROBLEM?.....	15
2.4.1	Efficient Reaction Design.....	15
2.4.2	Sustainable Solvents	17
2.5	BIOREFINERY – AN INTRODUCTION.....	24
2.5.1	Biobased Platforms	26
2.5.2	Available Biobased Product Classes	28
2.6	NON-FOSSIL SYNTHESIS PATHWAYS FOR IMPORTANT STARTING MATERIALS.....	30
2.6.1	Aliphatic diols.....	30
2.6.2	Aliphatic Diamines	38
2.6.3	Urea and <i>N</i> -Methylurea	40
2.6.4	Benzaldehyde and Terephthalic Aldehyde	42

2.6.5	<i>tert</i> -Butyl acetoacetate and Diketene Acetone Adduct.....	43
2.6.6	Acrylic Acid, Methacrylic Acid, and Vinyl Acetate	45
2.7	MULTICOMPONENT REACTIONS	46
2.7.1	The Biginelli-3-Component Reaction.....	51
2.7.1.1	<i>Mechanistic Discussion and the Currently Accepted Iminium Route....</i>	51
2.7.1.2	<i>Structural Variations and Applied Catalysts/Catalytic Systems.....</i>	59
2.7.1.3	<i>Applications of 3,4-dihydropyrimidin-2(1H)-ones</i>	62
2.7.2	The Biginelli-3-Component reaction in the Field of Polymer Chemistry	62
2.7.2.1	<i>Radical Polymerisation of Monomers Containing a Dihydropyrimidinone Functionality.....</i>	63
2.7.2.2	<i>Post-Polymerisation Modification using the Biginelli-Three-Component Reaction</i>	65
2.7.2.3	<i>Synthesis of Polycondensates Using the Biginelli-Three-Component Reaction</i>	66
3	Aim.....	69
4	Results and Discussion	71
4.1	SYNTHESIS OF NEW BIGINELLI HOMOPOLYCONDENSATES: RENEWABLE MATERIALS WITH TUNEABLE HIGH GLASS TRANSITION TEMPERATURES.....	71
4.1.1	Abstract.....	71
4.1.2	Synthesis of Aliphatic Diacetoacetate and Diacetoacetamide Monomers	72
4.1.3	Synthesis of Poly[3,4-dihydropyrimidin-2(1H)-one]s.....	78

4.1.3.1	<i>Poly[3,4-dihydropyrimidin-2(1H)-one]s Using Diacetoacetates</i>	78
4.1.3.2	<i>Poly[3,4 dihydropyrimidin 2(1H)-one]s Using Diacetoacetamides</i>	92
4.1.4	Conclusion and Outlook	96
4.2	END GROUP-FUNCTIONALISATION OF BIGINELLI POLYCONDENSATES AND SUBSEQUENT BLOCK COPOLYMER SYNTHESIS.....	97
4.2.1	Abstract.....	97
4.2.2	Synthesis of Starting Materials.....	98
4.2.3	Poly[3,4-dihydropyrimidin-2(1H)-one]s with Defined End Groups	103
4.2.4	Synthesis of Block Copolymers by Polymer-Polymer Coupling	113
4.2.5	Conclusion and Outlook	121
4.3	CONTROLLED RADICAL POLYMERISATION OF RICINOLEIC ACID-DERIVED VINYL MONOMERS AND SUBSEQUENT MODIFICATION <i>VIA</i> THE BIGINELLI-3-COMPONENT REACTION	122
4.3.1	Abstract.....	122
4.3.2	Synthesis of Renewable Vinyl Esters	123
4.3.3	Radical Polymerisation of Renewable Vinyl Esters.....	134
4.3.4	Synthesis and Radical Polymerisation of 2-(Methacryloyloxy)ethyl (<i>R,Z</i>)-12-((3-Oxobutanoyl)oxy)octadec-9-enoate.....	138
4.3.5	Post Polymerisation Modification <i>via</i> the Biginelli-Three-Component Reaction	151
4.3.6	Conclusion and Outlook	154

5	Conclusion and Outlook	157
6	Experimental Section	161
6.1	MATERIALS	161
6.2	GENERAL METHODS AND INSTRUMENTATION.....	161
6.2.1	Thin Layer Chromatography (TLC)	161
6.2.2	Flash Column Chromatography.....	161
6.2.3	Vacuum Oven	162
6.2.4	Nuclear Magnetic Resonance (NMR) Spectroscopy.....	162
6.2.5	Size Exclusion Chromatography (SEC)	162
6.2.6	Infrared (IR) Spectroscopy	164
6.2.7	High Resolution Mass Spectrometry (HRMS).....	164
6.2.8	Differential Scanning Calorimetry (DSC).....	164
6.2.9	Thermogravimetric Analysis (TGA)	164
6.3	SYNTHESIS PROCEDURES AND ANALYTICAL DATA RELATED TO CHAPTER 4.1	165
6.3.1	Diacetoacetates and Diacetoacetamides	165
6.3.1.1	<i>Ethane-1,2-diacetoacetate (124a)</i>	166
6.3.1.2	<i>Propane-1,3-diacetoacetate (124b)</i>	168
6.3.1.3	<i>Butane-1,4-diacetoacetate (124c)</i>	170
6.3.1.4	<i>Hexane-1,6-diacetoacetate (124d)</i>	172
6.3.1.5	<i>Decane-1,10-diacetoacetate (124e)</i>	174

6.3.1.6	<i>Isosorbide-diacetoacetate (124f)</i>	176
6.3.1.7	<i>Ethane-1,2-diacetoacetamide (126a)</i>	178
6.3.1.8	<i>Hexane-1,6-diacetoacetamide (126d)</i>	180
6.3.1.9	<i>Decane-1,10-diacetoacetamide (126e)</i>	182
6.3.2	Poly[3,4 dihydropyrimidin 2(1 <i>H</i>)-one]s.....	184
6.3.2.1	<i>Polymerisation Kinetics</i>	184
6.3.2.2	<i>Poly[3,4 dihydropyrimidin 2(1H)-one]s using Acetoacetates</i>	192
6.3.2.3	<i>Poly[3,4 dihydropyrimidin 2(1H)-one]s using Acetoacetamides</i>	207
6.3.2.4	<i>Thermogravimetric Analysis of Poly[3,4 dihydropyrimidin 2(1H)-one]s</i>	217
6.4	SYNTHESIS PROCEDURES AND ANALYTICAL DATA RELATED TO CHAPTER 4.2	218
6.4.1	Monomers and 10-Undecenyl-1-acetoacetate	218
6.4.1.1	<i>Allyl Methyl Carbonate (137)</i>	218
6.4.1.2	<i>4-(Allyloxy)-3-methoxybenzaldehyde (138)</i>	220
6.4.1.3	<i>2-Mercaptoethyl Acetoacetate (140)</i>	222
6.4.1.4	<i>2-[3-(4-Formyl-2-methoxyphenoxy)propyl]thio}ethyl acetoacetate (141)</i>	225
6.4.1.5	<i>10-Undecenyl-1-acetoacetate (143)</i>	228
6.4.2	Poly[3,4 dihydropyrimidin 2(1 <i>H</i>)-one]s.....	231
6.4.2.1	<i>End Group-Functionalised Poly[3,4 dihydropyrimidin 2(1H)-one] Homopolymers (AA/BB system)</i>	231

6.4.2.2	<i>Poly[3,4 dihydropyrimidin 2(1H)-one] Homopolymers (AB system)..</i>	239
6.4.2.3	<i>Poly[3,4-dihydropyrimidin-2(1H)-one]-b-poly(ethylene glycol)s</i>	245
6.4.2.4	<i>End Group-Functionalised Poly[3,4 dihydropyrimidin 2(1H)-one] Homopolymers (AA/BB system) using N-Methyl Urea</i>	254
6.4.2.5	<i>Poly[3,4-dihydropyrimidin-2(1H)-one]-b-poly(ethylene glycol)s using N-Methyl Urea</i>	260
6.5	SYNTHESIS PROCEDURES AND ANALYTICAL DATA RELATED TO CHAPTER 4.3	266
6.5.1	Synthesis of Monomer Precursors and Monomers	266
6.5.1.1	<i>(S)-2-[(3-Oxobutanoyl)oxy]propanoic Acid (157).....</i>	266
6.5.1.2	<i>(12R,9Z)-12-[(3-Oxobutanoyl)oxy]octadec-9-enoic Acid (159).....</i>	269
6.5.1.3	<i>(R)-12-[(3-Oxobutanoyl)oxy]octadecanoic Acid (160)</i>	272
6.5.1.4	<i>Vinyl (12R,9Z)-12-[(3-Oxobutanoyl)oxy]octadec-9-enoate (163)</i>	275
6.5.1.5	<i>Vinyl (R)-12-[(3-Oxobutanoyl)oxy]octadecanoate (164)</i>	278
6.5.1.6	<i>2-(Methacryloyloxy)ethyl (12R,9Z)-12-[(3-Oxobutanoyl)oxy]octadec-9-enoate (168)</i>	281
6.5.2	RAFT Polymerisation (169)	284
6.5.3	Chain Extension of Poly{2-(methacryloyloxy)ethyl (12R,9Z)-12-[(3-oxobutanoyl)oxy]octadec-9-enoate}	293
6.5.4	Block Copolymer Synthesis (170).....	296
6.5.5	Post-Polymerisation Modification via Biginelli-Three-Component Reaction (171).....	298

6.5.5.1	<i>171a</i>	300
6.5.5.2	<i>171b</i>	302
7	References	303
8	Appendix	335
8.1	LIST OF ABBREVIATIONS	335
8.2	LIST OF SYMBOLS	338
8.3	LIST OF FIGURES.....	341
8.4	LIST OF SCHEMES	349
8.5	LIST OF TABLES.....	356
8.6	PUBLICATIONS.....	360

1 Introduction

Worldwide, one of the most important resources is petroleum. Since mankind has begun to use fossil resources in great quantities in the 19th century, the scientific and technological understanding has grown rapidly.^[1] At the same time, the demand for petroleum never stopped rising due to the growth of the worldwide population and the advancing living conditions. The global energy supply depends, besides coal and gas, primarily on mineral oil.^[2] Apart from being the world's main energy resource, petroleum is also the prime raw material for the chemical and polymer industry. It is converted into essential platform molecules using petrochemical processes. These are cheap and high-volume starting materials that lead to all kinds of organic molecules, from bulk chemicals to highly specialised pharmaceuticals and a manifold of different polymers.^[3] Especially polymer materials are ubiquitous in large quantities in our everyday life from clothing to electronics and packaging to construction materials as it becomes apparent from the annual worldwide production of polymers of 322 million tons (as of 2015).^[4]

However, the stock of fossil resources is finite and will possibly face a shortage according to an estimation of the *Bundesanstalt für Geowissenschaften und Rohstoffe* (BGR). Although there are sufficient oil reserves left, it is technically demanding and economically not profitable to produce petroleum from the remaining sources, at least at the current technological level.^[2] Furthermore, the increasing depletion of fossil resources has been accompanied by a drastic increase of environmental pollution due the production processes itself but also due to the disposal of the respective products after their use. A prominent example is the accumulation of microplastics in every area of our environment. Thus, the sustainable and reasonable use of fossil resources and the utilisation of renewable resources for the production of chemical products as well as proper recycling is inevitable and should be a major goal of our (scientific) society.

This thesis is dedicated to adding to this goal by extending the current knowledge on polymer synthesis from renewable starting materials and by investigating the synthesis and the characteristics of novel renewable polymer structures.

2 Theoretical Background

2.1 Green and Sustainable Chemistry – A Brief Historical Summary

The field of Green and Sustainable Chemistry had its starting point in the early 1980s with the appointment of the World Commission for Environment and Development whose goal was to evaluate environmental issues and to propose solutions.^[5] Until then, the main focus of interest had been the economical development of the industry while environmental problems were usually addressed without consideration of their source.^[6] In the resulting Brundtland Report in 1987, a first definition for a sustainable development was given.^[7] A development was considered sustainable if it guaranteed “that it meets the needs of the present without compromising the ability of future generations to meet their own needs”^[7] and if “population size and growth are in harmony with the changing productive potential of the ecosystem”.^[7] Thus, sustainability comprehensively covers and discusses optimisation of any perspective of human behaviour from economics, business, and education to agriculture, chemistry, and engineering.^[8] Due to the growing environmental awareness, costs for energy, waste disposal, and the diminishing supplies of non-renewable resources increased.^[9] Together with more severe pollution fines, these expense factors motivated the industry to evolve.^[9]

In 1990, the Pollution Prevention Act in the USA was a first step towards pollution prevention as a more effective strategy against environmental issues.^[10] The following efforts were focussed on networking and exchange of information. The first symposium on the topic of Green Chemistry took place in 1993,^[11] shortly followed by a second symposium in 1994.^[12] While the contributors of the first symposium represented only institutions from the USA,^[11] the second symposium consisted of international contributions.^[12] In 1997, the Green Chemistry Institute was founded to promote a sustainable development and to enable the implementation of this topic into education, industry, and society.^[13] Later, the Green Chemistry Institute joined the American Chemical Society to facilitate addressing international environmental issues.^[13] In the meantime, Green Chemistry, the first journal that mainly addresses the topic of sustainability, was

launched with its inaugural issue in 1999.^[14] The above mentioned milestones largely contributed to the development of a strong international network with an efficient infrastructure for communication and exchange of knowledge as well as the promotion of the necessity for a sustainable future.

Indeed, the interest of scientists, the industry, and the society in general, in a more sustainable chemistry has increased during the following years until today. A clear indicator has been the strong relative increase of publications with the topic of sustainable chemistry from 1990 to 2019 compared to the total number of chemistry related publications (**Figure 2.1**). The difference between the number of search results in SciFinder[®] *versus* Scopus[®] might arise from the different coverage of chemistry related topics. SciFinder[®] is indeed reported to have a broader coverage of natural sciences, especially chemistry, compared to Scopus[®].^[15]

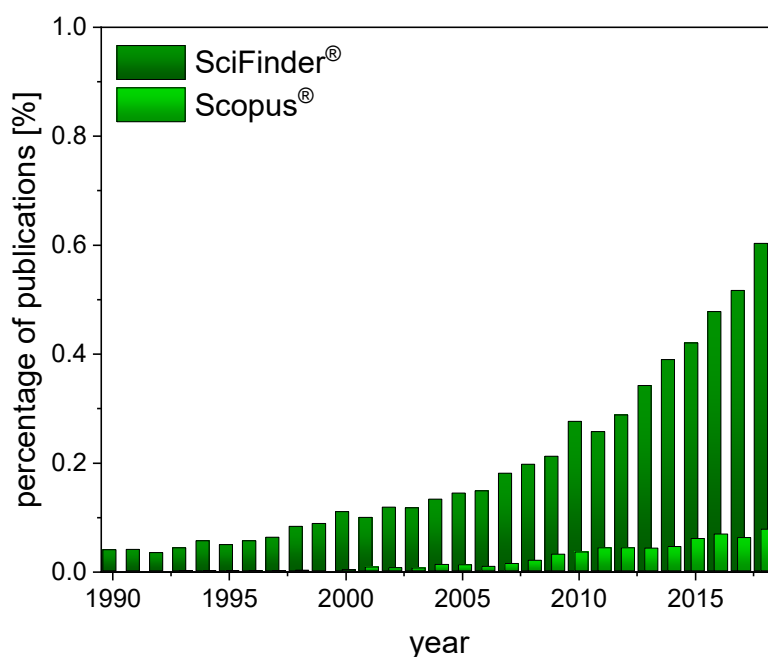


Figure 2.1 Visualization of the increase of publications related to the topic of “Sustainable Chemistry” from 1990 to 2019 relative to publications regarding the topic “chemistry” as a benchmark for the growing interest in sustainability (according to a search *via* SciFinder[®] and Scopus[®] on the research topic “Sustainable Chemistry”).

While there was no doubt regarding the importance of sustainability, the terminology of phrases like “Green Chemistry” or “Sustainable Chemistry” were not clear to begin with. In addition, no tools to assess sustainability had been developed yet. In the following sections, the current definition of important phrases are discussed and several tools and guidelines to assess the sustainability of chemical syntheses will be reviewed. Furthermore, the necessary change to renewable feedstocks to gain access to valuable platform chemicals from biomass will be addressed.

2.2 Green and Sustainable Chemistry

Since the potential risk arising from a product depends on its hazardousness and the exposure,^[16] Anastas and Warner emphasised the design of products that are as benign as possible, coining the term “Green Chemistry”.^[17] Thereby, exposure does not have to be controlled if the product and its production are not hazardous to begin with.^[16] To efficiently lower the risk, the whole lifecycle of a product has to be assessed, addressing the intrinsic safety of a product on a molecular level.^[18,19] Thus, the respective feedstock, the production process including the applied reagents and procedures, occurring intermediates, waste, energy demand, and energy source have to be considered.^[18] In addition, the product itself as well as its fate after use have to be taken into account.^[18] This concept of “Green Chemistry” was condensed into the 12 Principles of Green Chemistry (Table 2.1) as an appealing guideline that summarises all aspects that need to be coherently considered for an environmentally benign and innocuous chemical product.^[17,19] Later, the 12 Principles of Green Engineering were published to complete the above mentioned aspects from an engineers point of view, *e.g.* by adding considerations about the design of the chemical plant.^[20] Both sets of principles were condensed even further into the two mnemonics “PRODUCTIVELY”^[21] and “IMPROVEMENTS”^[22] to facilitate their communication.

To conclude, Green Chemistry is focussed on synthesis and application while chemical policy, socioeconomic aspects, and more comprehensive pollution control and remediation are left aside.^[8] Sustainable Chemistry, on the contrary, includes these aspects rendering it a guideline that strives to accommodate the demand for more environmentally friendly

products and production processes in the broader sense while taking legislation and education^[8] into account to facilitate the implementation of scientific improvements and new technologies.^[23] A descriptive and clear figure that contains all elements of Sustainable Chemistry was published by Anastas and Zimmerman^[24] by arranging them in groups and periods in the way chemical elements are ordered in the periodic table of elements.

Table 2.1 The 12 Principles of Green Chemistry published by Anastas and Warner in 1998^[17] as a guideline for the design of chemical processes and products.

The 12 Principles of Green Chemistry	
1	Prevention: It is better to prevent waste than to treat or clean up waste after it is formed
2	Atom Economy: Synthetic methods should be designed to maximise the incorporation of all materials used in the process into the final product.
3	Less Hazardous Chemical Syntheses: Wherever practical, synthetic methodologies should be designed to use and generate substances that possess little or no toxicity to human health and environment.
4	Designing Safer Chemicals: Chemical products should be designed to preserve efficacy of function while reducing toxicity.
5	Safer Solvents and Auxiliaries: The use of auxiliary substances (<i>e.g.</i> solvents, separation agents, <i>etc.</i>) should be made unnecessary wherever possible and, innocuous when used.
6	Design for Energy Efficiency: Energy requirements should be recognised for their environmental and economic impacts and should be minimised. Synthetic methods should be conducted at ambient temperature and pressure.
7	Use of Renewable Feedstocks: A raw material or feedstock should be renewable rather than depleting wherever technically and economically practicable.
8	Reduce Derivatives: Unnecessary derivatisation (blocking group, protection/deprotection, temporary physical/chemical modification processes) should be avoided whenever possible.
9	Catalysis: Catalytic reagents (as selective as possible) are superior to stoichiometric reagents.
10	Design for Degradation: Chemical products should be designed so that at the end of function they do not persist in the environment and break down into innocuous degradation products.
11	Real-Time Analysis: Analytical methodologies need to be further developed to allow for real-time in process monitoring and control prior to the formation of hazardous substances.
12	Inherently Safer Chemistry: Substances and the form of a substance used in a chemical process should be chosen as to minimise the potential for chemical accidents, including releases, explosions, and fires.

2.3 Tools to Assess Sustainability

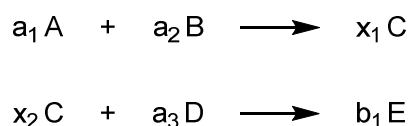
Several guidelines and tools were published to evaluate the sustainability, to increase the efficiency, and to lower the waste production of a synthesis protocol. Each covers a specific aspect of the synthetic procedure comprising advantages and disadvantages. The book *Paradigms in Green Chemistry and Technology*^[25] provides a good overview over the different available metrics. In the following sections, the most important and practical guidelines and metrics will be addressed.

2.3.1 Metrics to Optimise the Mass Balance of a Reaction

To evaluate the efficiency of a chemical reaction, it is possible to consider the mass of the product molecule/s relative to the sum of the masses of all starting materials.^[26] The method is based on the reaction equation and the stoichiometry.^[27] The resulting quotient is called atom economy (*EA*) and depends on molecular weight (*M*) and the stoichiometry coefficients *a* and *b*. It was first suggested by Trost in 1991 (Equation (1)).^[26]

$$AE = \frac{\sum_i b_i M_i(\text{product})}{\sum_i a_i M_i(\text{starting material})} \quad (1)$$

Thus, perfect economy means $AE = 1$ whereas $AE = 0$ means that none of the starting materials is reacting towards the formation of the product. Any starting material which is (partially) incorporated into the product/s is considered.^[27] As a consequence, catalysts and any excess of a starting material are not considered in the calculation.^[27] Moreover, inorganic reagents are ignored.^[27]



Scheme 2.1 Generic reaction scheme of a linear stepwise reaction: x_i refer to stoichiometric coefficients of the intermediate C which is not part of the calculation of *AE*.

The calculation of AE for stepwise linear (**Scheme 2.1**) or convergent syntheses was reported as well.^[27] For reaction sequences of any complexity, a general expression for the calculation of AE was introduced in 2004.^[28] Intermediates are ignored, while additional substances that are used to convert the intermediates are added as reagents in the calculation.^[27] This is exemplarily shown for a generic linear reaction (**Scheme 2.1**) from a starting material A to product E over the intermediate C (Equation (2)).

$$AE = \frac{b_1 M(E)}{a_1 M(A) + a_2 M(B) + a_3 M(D)} \quad (2)$$

While being a simple and quick evaluation tool, AE is defined by the exact chemical reaction. Thus, the actual yield, substoichiometric as well as hyperstoichiometric reagents, solvents, additives, or auxiliaries are not included.^[25] The removal of these limitations is possible if experimental equivalents instead of stoichiometric factors are applied and the inorganic components are added to the reaction equation. A composite metric that contains the reaction yield, hyperstoichiometric substances together with the recovered fraction of the excess was defined partly covering the limitations of AE .^[29] This metric is called global reaction mass efficiency (RME_{global}) (Equation (3)) and depends on the yield (ε), a stoichiometric factor (α), and an elaborate recovered material factor (β), with a value between 0 and 1 (Equation (4)).^[25,29]

$$RMF_{\text{global}} = \varepsilon(AE) \frac{\beta}{\alpha} \quad (3)$$

$$\alpha = 1 + \frac{\sum_i m_i(\text{excess mass of reagents})}{\sum_j m_j(\text{stoichiometric mass of reagents})} \quad (4)$$

Just like AE , RMF_{global} ranges between 0 and 1. If a reagent is used in excess, α is larger than 1 and RMF_{global} is directly attenuated.^[29] Moreover, RMF_{global} equals $\varepsilon(AE)$ if excess mass, solvent, additive, or auxiliary is recovered after the reaction.^[29]

The focus for the above metrics lies on the formation of the reaction product, whereas waste production is implicitly included. In contrast, the environmental impact factor (E),

introduced by Sheldon in 1992,^[30] explicitly describes the ratio of the masses of waste to product (Equation (5)).^[5,30]

$$E = \frac{m(\text{waste})}{m(\text{product})} \quad (5)$$

As a consequence, $E = 0$ for an ideal reaction, in which no waste is produced. E accounts for reaction yield, catalysts, hyperstoichiometric reagents, solvents, and auxiliaries used during the synthesis and purification steps.^[5] However, water is not included in the calculation as Sheldon states that extraordinarily high E -factors, that would arise from the inclusion of waste water for many processes, would hamper the comparability of processes.^[5] This is one of the biggest downsides of this metric since waste water remediation is complex and highly energy consuming^[31,32] and thus strongly affects the environmental impact. Current definitions of E include waste water as well.^[5,33] Moreover, E is defined more precisely with distinct summands for each part of the total waste mass (side products $m_{a,i}$, excess mass of reagents $m_{b,j}$, mass of auxiliaries $m_{c,k}$, and the recycled mass $m_{d,l}$) (Equation (6)).^[34] Sometimes, the energy demand is added as the mass of the CO₂ that is formed during the energy production as well.^[35]

$$E = \frac{\sum_{i,j,k,l} [m_{a,i} + m_{b,j} + m_{c,k} - m_{d,l}]}{\sum_n m_n (\text{product})} \quad (6)$$

The E -factor is often applied for industrial processes and strongly depends on the respective industrial sector (**Table 2.2**).^[25,36] For well established processes for which most products are valuable, the E -factor is expectedly low (e.g. oil refinery: $E = 0.1$).^[36] In contrast, processes for fine chemicals or pharmaceuticals produce significant amounts of waste and thus have higher E -factors.^[36] However, the total amount of waste produced by a certain sector depends on the total production. As a consequence, the oil refinery is still producing at least ten times more waste than other industrial sectors (**Table 2.2**).^[25]

Table 2.2 Annual production, accumulated waste and *E*-factors of four industrial sectors.^[25,36]

Industrial Sector	Production [t·a ⁻¹]	Waste [t·a ⁻¹]	<i>E</i> -factor
Oil Refinery	10 ⁶ – 10 ⁸	10 ⁶	0.1
Bulk Chemicals	10 ⁴ – 10 ⁶	10 ⁵	1 – 5
Fine Chemicals	10 ² – 10 ⁴	10 ⁴	5 – 50
Pharmaceuticals	10 – 10 ³	10 ³	25 – 100

A similar mass metric is the process mass intensity (*PMI*).^[37] It is defined as the ratio of the mass of materials needed to produce a specific mass of a product and the mass of the product (Equation (7)).^[37] The mass of materials needed consists of the waste and the product mass.^[37] Thus, the *PMI* is rewritten using the expression for the *E*-factor plus one which is basically the revenue that the process generates (Equation (8)).^[37]

$$PMI = \frac{\sum_i m_i(\text{material})}{\sum_j m_j(\text{product})} \quad (7)$$

$$PMI = \frac{\sum_{i,j} m_i(\text{waste}) + m_j(\text{product})}{\sum_j m_j(\text{product})} = E + 1 \quad (8)$$

2.3.2 Metrics to Assess the Environmental Impact of a Process

While the above discussed metrics cover the in- and output of materials of a chemical process, the hazardousness of the respective materials is not considered. Therefore, the effective mass yield (*EMY*) was proposed in 1999 by Hudlicky and coworkers as a first definition of a mass metric that accounts for the hazard potential of a process.^[38] It is defined as the ratio of the mass of the product to the mass of hazardous waste.^[38] However, this leaves any impact of non-hazardous waste apart.

The Environmental Assessment Tool for Organic Synthesis incorporates a more comprehensive approach.^[39] To separately account for starting materials, waste and

products, two environmental impact factors, EI_{in} and EI_{out} , are calculated using the above described metrics PMI and E , respectively (Equations (9) and (10)).^[39] The environmental impact is included *via* the specific potential environmental impact factors, Q_{in} and Q_{out} ,¹ in units of potential environmental impact (PEI) per kilogram.^[39] Q_{in} is a sum of two $Q_{i,in}$, containing the resource requirements and hazard potential of the starting materials.^[39] Q_{out} is a sum of eleven $Q_{j,out}$, containing toxicity, the influence on the ozone layer and the global climate, the tendency to degrade or accumulate in the environment and the ability to acidify soil and water.^[39] The necessary data for the evaluation is taken from readily accessible sources like safety data sheets.^[40] A small EI_{in} and EI_{out} are desirable and indicate more sustainable processes.

$$EI_{in} = PMI \cdot Q_{in} = \frac{\sum_i Q_{i,in} \cdot m_i(\text{material})}{\sum_j m_j(\text{product})} \quad (9)$$

$$EI_{out} = E \cdot Q_{out} = \frac{\sum_j Q_{j,out} \cdot m_j(\text{waste})}{\sum_k m_k(\text{product})} \quad (10)$$

Another tool to quickly assess the environmental impact of a process is the semiquantitative EcoScale.^[41] The software calculates a score between 0 (worst) and 100 (best) based on six parameters: yield, price of components, safety, technical setup, temperature and reaction time, and workup and purification.^[41] For each parameter, a certain number of penalty points P_i is given depending on the process.^[41] The score is subsequently calculated (Equation (11)) by subtracting penalty points from the highest score of 100, whereas a score below 50 indicates insufficient reaction conditions or an insufficient reaction path.^[41]

$$EcoScale = 100 - \sum_i P_i \quad (11)$$

The parameters of the EcoScale are comprehensive and provide a broad overview of the sustainability of a chemical process. However, the relative importance of the parameters

¹For detailed information on the calculation of Q_{in} and Q_{out} , please refer to Eissen.^[40]

change depending on the scale of the reaction.^[41] While, *e.g.*, few restrictions on the use of chemicals exist on the laboratory scale and the cost of reagents is of minor importance, such chemicals are likely to be banned from an industrial process due to low profit or legal restrictions.^[41] Moreover, the amount of penalty points given is based on intuition and experience rendering the EcoScale a flexible^[41] but inaccurate tool.

2.3.3 Metrics to Assess the Energy Demand of a Process

Except for the EcoScale, in which the energy demand is implicitly included *via* reaction conditions and the applied apparatuses,^[41] most of the above discussed metrics do not include the energy demand of a process. The *E*-factor, however, is completed by inclusion of the CO₂ that was generated during the production of the needed amount of energy, as waste.^[35] Indeed, the *E*-factors including the energy demand were approximately a factor of 35 higher compared to the traditional *E*-factors for the investigated microbial enzyme syntheses.^[35] Hence, it is of great importance to evaluate the energy demand and the energy source in order to correctly compare different processes.

Two similar metrics that assess the energy demand of a process are the energy efficiency (E_E) (Equation (12))^[25] and the specific productivity (sP) (Equation (13)).^[42] Both are fractions giving the amount of product relative to the energy consumption, however the used units differ.

$$E_E = \frac{\sum_i m_i(\text{product})}{\sum_j E_j} \left[\frac{kg}{kJ} \right] \quad (12)$$

$$sP = \frac{\sum_i n_i(\text{product})}{\sum_j E_j} \left[\frac{mol}{kWh} \right] \quad (13)$$

Each of the discussed metrics comprise advantages and limitations that determine their individual applicability (**Table 2.3**). The combination of different metrics that compensate for each other's downsides allow for comprehensive assessments.

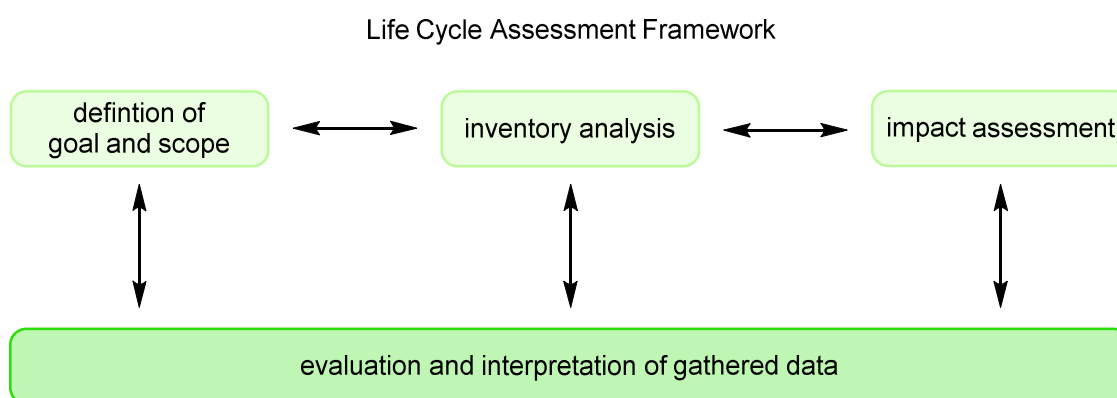
Table 2.3 Comparison of prominent Green Chemistry metrics.

metric	information	limitation/s
<i>AE</i>	weight fraction of starting material/s incorporated in product/s	exclusion of reagents, excess, yield, hazard potential, and energy demand
<i>RMF_{global}</i>		exclusion of reagents, hazard potential, and energy demand
<i>E</i>	mass of waste relative to product	exclusion of waste water, hazard potential, and energy demand
<i>PMI</i>	mass of used materials relative to product	exclusion of hazard potential and energy demand
<i>EI</i>	<i>E</i> and <i>PMI</i> adapted by an environmental factor	semi-quantitative, availability of data often difficult
<i>EcoScale</i>	comprehensive evaluation of a process	qualitative estimation
<i>E_E, sP</i>	amount of energy needed relative to product mass	any energy needed besides the production process is neglected

A comprehensive approach to determine the sustainability of a product is the Life Cycle Assessment (LCA).^[43,25] The concept of a comprehensive method to evaluate the environmental effects of products and services was simultaneously developed in Europe and the USA.^[44] During the early stages in the late 1960s,^[44] the focus of LCA was on the conservation of resources and energy.^[43] However, the approach was quickly adapted by the Society of Environmental Chemistry and Toxicology (SETAC)^[45] and the International Organization for Standardization (ISO)^[46-48] to provide a profound insight of a process. A profound review and application guide of the LCA is provided in the “Handbook on Live Cycle Assessment”.^[49]

A complete LCA consists of four mains steps: definition of goal and scope, inventory analysis, impact assessment, and interpretation of the former results (**Scheme 2.2**).^[43] In the first step, which system is to be assessed and why the analysis is conducted is defined.^[43] This includes, besides other elements, the definition of the system to elaborate limitations,

the definition of the audience the study will be addressed to as well as a peer review.^[43] In addition, the elements of the LCA that are needed to reach the defined goal are chosen since data acquisition is costly and time consuming while parts of the LCA are often sufficient.^[43] The inventory analysis lists the calculated mass and energy flows of the product during its whole life cycle from the production of raw materials through the use of the product to the waste removal or possibly recycling and reuse.^[43] The impact assessment, evaluates the results of the inventory analysis in terms of environmental aspects,^[43] which are summarised in two categories: input- and output- related aspects.^[50] The quantified data is subsequently analysed to pinpoint the main issues^[43,25] and is connected to results of assessment tools with another focus (*e.g.* finance, or safety) to complete the evaluation.^[51]



Scheme 2.2 The four parts of a complete Life Cycle Assessment; data is continuously updated and interpreted allowing for an efficient adaptation of the sections.^[49]

As stated above, such thorough analyses are not always feasible or necessary. For such cases, protocols for a simplified LCA (SLCA) are available.^[51] Furthermore, if the development of a process is in an early stage, SLCA is a valuable tool to avoid false decisions^[49] and to readily screen for the most crucial economical aspects.^[52] The LCA is simplified in various ways depending on the assessed process.^[53] For example, the actual compounds are substituted with similar substances for which the necessary data is directly available^[25] or complex parameters are substituted with similar parameters with better accessibility.^[52]

While the topic of sustainable chemistry contains many different aspects, some are of greater importance than others. In accordance to the 24 Principles of Green Chemistry and Green Engineering,^[22] two main issues are the amount and hazard of the generated waste as well as the origin of the used resources. These two aspects will be further discussed in the following chapters.

2.4 How to Address the Waste Problem?

The chemical industry is producing more than 10⁶ t of toxic waste every year,^[36] consisting of side products, auxiliaries, and solvents, besides others. The *E*-factors of the production of bulk chemicals are sufficiently lower compared to the *E*-factors of fine chemical production or pharmaceutical synthesis.^[36] Thus, the latter sectors show greater potential to lower their relative waste production and the respective environmental impact. As an example, the total mass of materials that is applied for pharmaceutical syntheses, consists of 56% of the mass of solvents,^[37] rendering solvents an important factor to increase sustainability. Additionally, the applied solvents contribute to 60% of the total energy consumption and to 50% of the greenhouse gas emissions that are formed during the post-treatment of the chemical waste.^[54,55] As a consequence, the design of new efficient reaction pathways as well as the search for less hazardous and sustainable solvents is crucial and has become a major scientific research topic in the field of sustainable chemistry. The improvement of reaction pathways is aided by above mentioned metrics whereas solvent selection guides highlight potential downsides of a specific solvent and provide more sustainable alternatives.^[54]

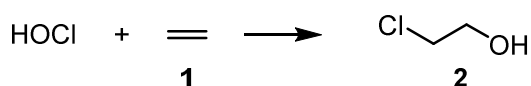
2.4.1 Efficient Reaction Design

The careful design of chemical syntheses and the respective products is necessary to prevent adverse consequences, environmentally and economically.^[19] Many processes have been reassessed and improved after sustainability has become a crucial part of production design.^[19] The industrial synthesis of oxirane **3** impressively shows how an innovative

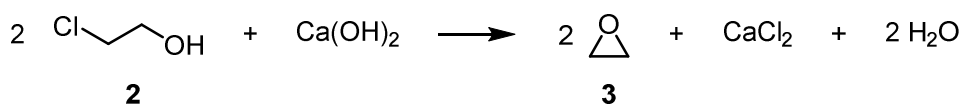
2.4 How to Address the Waste Problem?

reaction design, in which a new catalytic system is applied instead of stoichiometric reagents, increases the sustainability and efficiency of a process (**Scheme 2.3**).

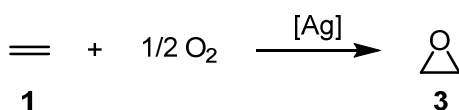
Traditional Route



E-factor = 5



Improved Route



E-factor = 0.3

Scheme 2.3 Industrial oxirane production methods: traditional route over 2-chloroethanol and subsequent elimination of hydrogen chloride, improved route *via* direct oxidation of ethene.^[56,57]

The traditional route is a two-step process:^[56] synthesis of 2-chloroethanol **2** from ethylene **1** and hypochlorous acid (*in situ* formed from water and chlorine) is followed by the elimination of hydrogen chloride using Ca(OH)_2 . The *E*-factor of this synthesis route is 5 and does not include the amount of waste water.^[19] The corresponding *AE* of 0.29 shows that less than a third of the used mass is incorporated in oxirane. In the current process, **1** is directly oxidized to **3** with molecular oxygen or air using a supported silver catalyst^[57] resulting in an *E*-factor of 0.3.^[19] The improvement of the production process consequently led to an annual waste reduction from $70.5 \cdot 10^6$ t to $4.5 \cdot 10^6$ t at an annual oxirane production of $15 \cdot 10^6$ t (in 2011).^[57] In addition, the theoretical *AE* is 1 according to the reaction equation (**Scheme 2.3**). However, only molecular oxygen is oxidizing **1** to **3**. The remaining atomic oxygen leads to total oxidation of another ethylene molecule to water and CO_2 .^[58] In

addition, small fractions of formaldehyde and acetaldehyde are formed.^[59] Thus, the actual atom economy is lower than 1 if any side reactions are considered. Nonetheless, the oxirane process was substantially improved.

The improvement of the oxiran process impressively shows the impact of an efficiently designed synthesis and purification routine on the resulting waste production on the industrial scale. However, many synthesis procedures that are currently considered as optimised rely on solvents during at least one synthetic step. As a consequence, the substitution of currently used solvents with more sustainable alternatives further reduces the environmental impact.

2.4.2 Sustainable Solvents

As stated above, solvents largely contribute to the amount of waste that is produced by the chemical industry. Therefore, it is necessary to find replacements for conventional solvents. To subsume the challenges that must be met on the search for sustainable solvents, JESSOP^[60] published The Four Challenges of Green Solvents (**Figure 2.2**). First, the available sustainable solvents need to cover the whole spectrum of possible solvent properties, otherwise the prerequisite for a substitution is not met.^[60] Second, simple methods to evaluate whether a solvent is sustainable are necessary.^[60] Typically, the energy demand for the manufacturing, the energy recovery *via* recycling or incineration, and the impact on health and environment are assessed.^[61] Polar aprotic solvents are especially useful in chemical synthesis due to their ability to dissolve organic substances and salts.^[62,60] However, their distillation is energy demanding and extraction with water causes waste which is difficult to separate and not suited for incineration.^[61,62] Thus, the third challenge is to find new polar aprotic solvents that are easier to separate and recycle.^[60] The fourth challenge is the general avoidance of distillation whenever possible.^[60]

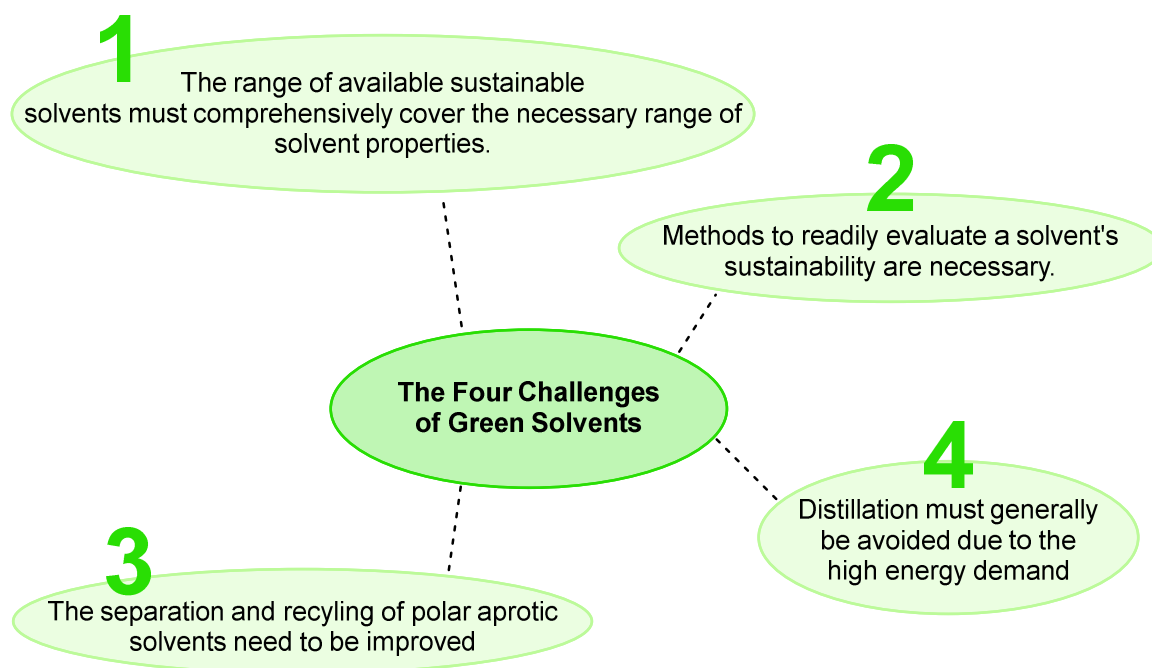


Figure 2.2 The Four Challenges of Green Solvents.^[60]

If the application of solvents is necessary, the substitution with a more sustainable solvent is usually a compromise since economical criteria and criteria for sustainability have to be considered.^[63] Various pharmaceutical companies published solvent selection guides^[61,64–66] that follow similar principles. Moreover, the Innovative Medicines Initiative provides a review^[67] that summarizes and compares those guides and provides a simple comparative overview of available solvents. The assessed solvents are categorized as recommended (green), problematic (yellow), hazardous (red), or highly hazardous (red) taking safety, health, and environmental impact into account.^[67] The assessment uses the Globally Harmonised System of Classification and Labelling of Chemicals (GHS) and physical data of the solvents.^[67] Thus, only rudimentary information was used for the evaluation, allowing only for a rough estimation of solvent sustainability that has to be applied with care and relative to one another.

Moreover, the environmental hazard does not include information like energy demand for production, recycling and disposal of a solvent, renewability, and more precise reports on toxicity towards different ecosystems. As an example, water cannot be considered a green solvent if the energy demand for the waste water treatment is taken into account.^[68] An excerpt containing the categorisation of 18 common solvents is depicted in **Table 2.4**.

Besides renewable and fossil based classical solvents, new solvent classes have been developed as sustainable substitutes.^[69] Popular examples include ionic liquids and deep eutectic solvents, as well as switchable solvents systems.^[69]

Ionic liquids are organic salts with melting temperatures (T_m) below 100°C.^[70] The typically bulky, unsymmetric organic cations and organic or inorganic anions hinder crystallization which results in a low T_m of the salt.^[71] Common ionic liquids are composed of quaternary ammonium cations or tetraalkylphosphonium cations and anions like halides, nitrate, tetrafluoroborate, hexafluorophosphate or chloroaluminates(III) (**Figure 2.3**).^[72]

2.4 How to Address the Waste Problem?

Table 2.4 Categorisation of 18 common solvents according to their safety and impact on health and environment as recommended (green), problematic (yellow), and hazardous/highly hazardous (red).^[67]

entry	solvent family	solvent	category
1	water	water	recommended
2	alcohols	methanol	
3		ethanol	
4		ethylene glycol	
5	ketones	acetone	
6		methyl ethyl ketone	
7	esters	ethyl acetate	
8	ethers	diethyl ether	highly hazardous
9		methyl <i>tert</i> -butyl ether	hazardous
10		tetrahydrofuran	problematic
11		methyl tetrahydrofuran	
12	hydrocarbons	<i>cyclo</i> -hexane	
13		toluene	
14	halogenated	dichloromethane	hazardous
15		chloroform	highly hazardous
16	polar aprotic	acetonitrile	problematic
17		dimethylformamide	hazardous
18		dimethyl sulfoxide	problematic

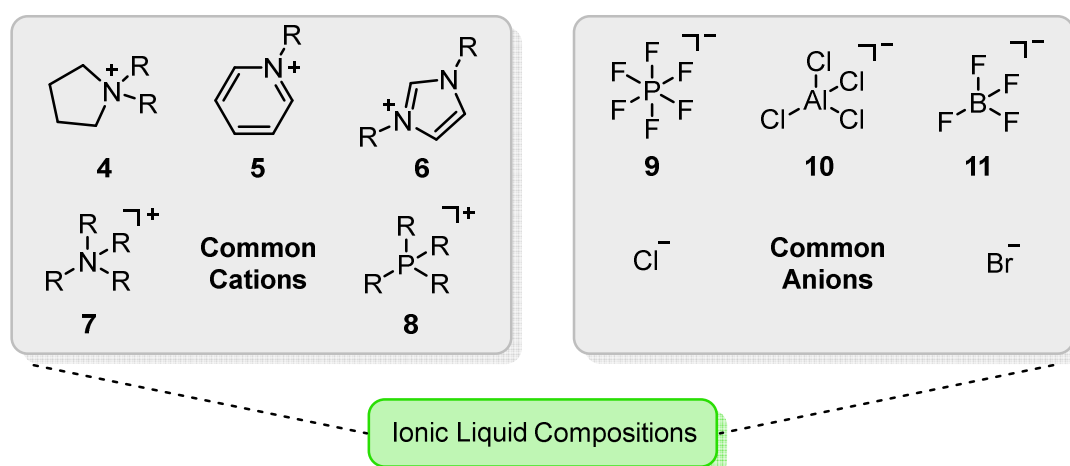


Figure 2.3 Popular cations (left) and anions (right) used in ionic liquid compositions: pyrrolidinium **4**, pyridinium **5**, imidazolium **6**, ammonium **7**, and tetraalkylphosphonium **8**, as well as hexafluorophosphate **9**, tetrachloroaluminate **10**, tetrafluoroborate **11**, chloride, and bromide.^[72,71]

Ionic liquids feature beneficial properties, such as negligible vapour pressure and flammability, high thermal stability,^[73] they dissolve a large range of compounds, and their synthesis from renewable resources is possible.^[74] In addition, the option to customise the ion structures^[75] allows for tailormade properties including biodegradability and lowered toxicity.^[76] However, ionic liquids and the resulting metabolites are typically harmful to the environment.^[77] The extent of the toxicity depends strongly on the chemical structure of the ionic liquid and the observed trophic level.^{2[77]} Another downside of ionic liquids is the limited recyclability. Due to the high boiling points, distillation is challenging as temperatures above 150°C and pressures below 5 mbar are needed.^[79] Other purification methodologies, such as liquid-liquid extraction with supercritical CO₂,^[80] nanofiltration,^[81] and melt crystallisation,^[82,83] have been reported but lack comprehensive applicability.

Deep eutectic solvents share many of the above noted characteristics of ionic liquids.^[84,85] However, they comprise an eutectic mixture of a hydrogen bond acceptor and

²A food cycle describes the feeding hierarchy in an ecological system. Trophic levels thereby define subgroups within the food cycle such as plants and algae as producers, herbivores as primary consumers and several following levels of carnivores.^[78]

a hydrogen bond donor (**Figure 2.4**).^[84] As a consequence, the intermolecular interactions in deep eutectic solvents contain a large contribution of hydrogen bonding while in ionic liquids ionic interactions dominate. Typical hydrogen bond acceptors are quaternary ammonium salts (*e.g.* choline chloride (**12**)). Prominent donors are saccharides (*e.g.* glucose), or organic acids (*e.g.* citric acid (**15**)) urea derivatives, or alcohols.^[84,85]

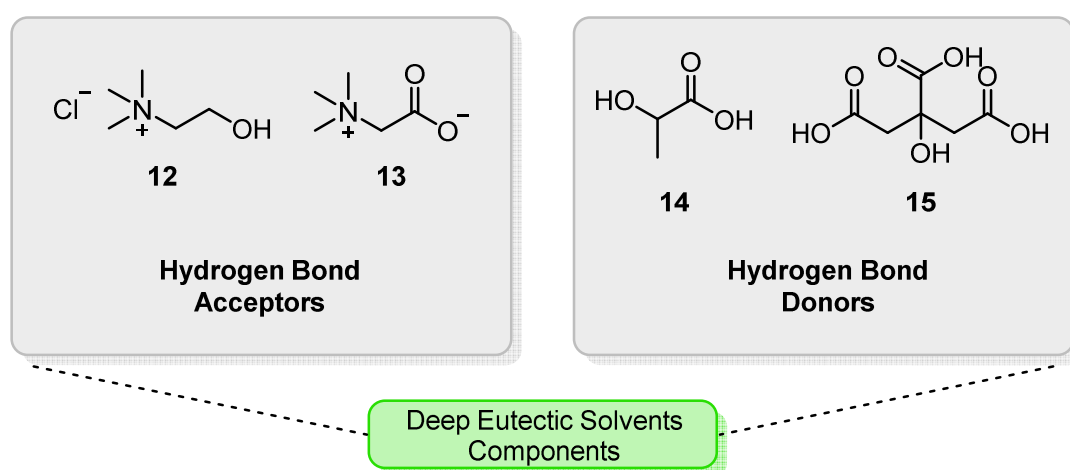
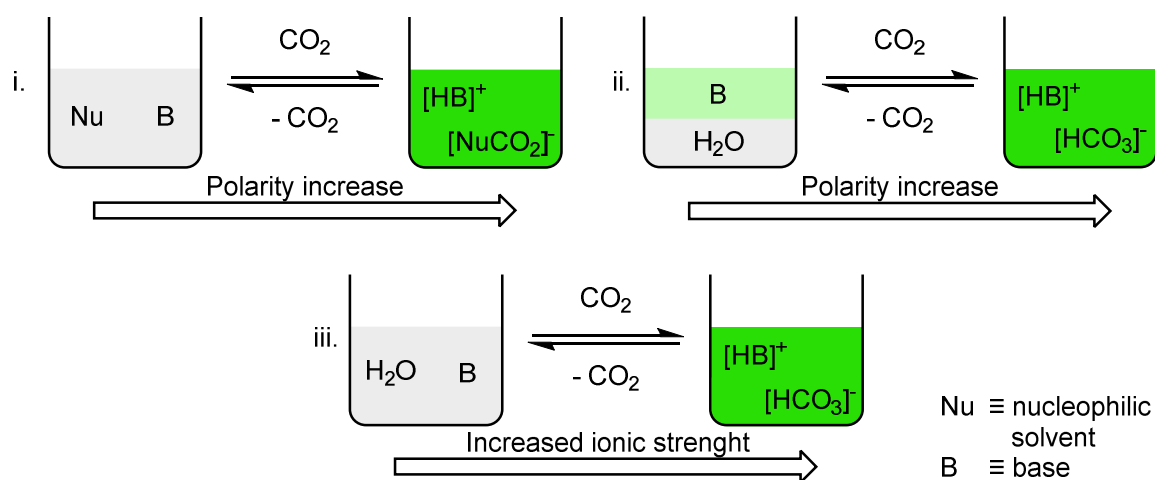


Figure 2.4 Popular hydrogen bond acceptors used for deep eutectic solvents are choline chloride (**12**) or trimethyl glycine (**13**), popular donors are lactic acid (**14**) or citric acid (**15**)

Since some of these starting materials are readily available from biomass, deep eutectic solvents are usually cheaper than ionic liquids while being of particular interest in terms of sustainability.^[71,85,86] Furthermore, the solvent production comprises simple mixing of the respective compounds instead of chemical synthesis.^[84] On the contrary, deep eutectic solvents are not as inert as ionic liquids.^[84]

Switchable solvents are defined as solvent systems with triggered property changes. The most common triggers are temperature changes^[87] and the chemical reaction with gases such as CO₂.^[88] CO₂-switchable solvents are of major interest to the scientific community as CO₂ is not only non-toxic, cheap, and produces no additional waste but the switching is simple as well: the solvents are switched by passing through CO₂ and are readily reverted by heating, sonication, or purging with another gas.^[69]

Switchable solvents are categorised according to the respective property change and the composition (**Scheme 2.4**). Switchable polarity solvents (i.) are monophasic equimolar mixtures of a nucleophilic solvent (*e.g.* alcohol, amine) and typically a nitrogenous base that form an ionic liquid if CO₂ is added to the system.^[89,90] Switchable hydrophilicity solvents (ii.) comprise biphasic systems with an aqueous layer and a hydrophobic phase (hydrophobic nitrogen compounds).^[91,92] Introduction of CO₂ leads to the formation of carbonic acid which protonates the nitrogen compound under the formation of a single ionic phase,^[91] while the polarity change is larger compared to switchable polarity solvents.^[93] Switchable water (iii.) is a monophasic mixture of water and a water miscible nitrogen species.^[94] The addition of CO₂ leads to the same ion formation as for switchable hydrophobicity solvents but the solvent mixture increases the ionic strength rather than the polarity.^[94]



Scheme 2.4 Three types of switchable solvent systems using CO₂ as trigger: i. switchable polarity solvent, ii. switchable hydrophilicity solvent, iii. switchable water.

Thus, switchable solvents combine solvation power and enhanced recyclability. As a consequence, switchable solvents are of manifold interest *e.g.* for extraction procedures to recover or purify different materials or as potent solvents for organic syntheses and catalysis with enhanced recyclability of catalysts and reagents.^[91,92,95–97]

Within chapter 2.4, reaction design and solvent sustainability and their impact on waste generation were described. The thorough design of a reaction/production process allows to find the most efficient and sustainable route towards a product. However, hazardous waste is in many cases not completely avoidable, especially the application of solvents. Hence, more sustainable solvents have the potential to largely contribute to the environmental impact of the chemical industry and chemistry overall.

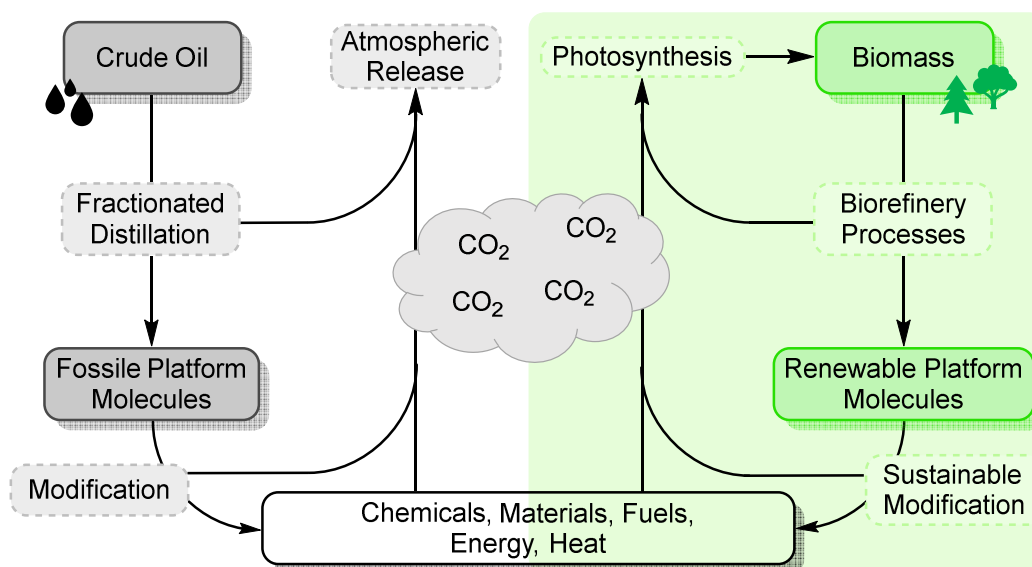
Besides, the resource of which a chemical is derived from is largely contributing to its environmental impact. Biorefineries strive to produce important platform chemicals from renewable sources as alternative to the time-tested oil refinery. Both, the production of oil-analogue platform chemicals and new platform chemicals is investigated.

2.5 Biorefinery – An Introduction

Another crucial factor for the sustainable development of the chemical industry is the exploitation of renewable resources to subsequently substitute the existing oil refineries for which biorefineries are a promising concept. Biorefinery is defined as “sustainable processing of biomass into a spectrum of marketable products [...] and energy”^[98] meaning that diverse feedstocks are converted into food, feed, a manifold of different organic molecules and materials including fuels, as well as power and heat. The development has mainly aimed to reduce the dependence on petroleum-based products and the reduction of greenhouse gases.^[98,99] The main driver for biorefinery development, however, has been the transportation sector as large parts of the consumed crude oil is used for transportation purposes.^[99] As an example, 68% of the total petroleum consumption of the USA was attributed to transportation fuels in 2019.^[100]

A problem of the biorefinery development is the current inability to economically compete with oil refineries.^[99] With fuel being the largest contribution to oil consumption, the reduction of production prices for biofuels are critical.^[99] A promising possibility for a self-dependent and economically feasible facility is the integrated biorefinery as a direct analogue to the oil refinery (**Scheme 2.5**).^[101] Thus, the whole input of biomass is used and

converted in one plant into materials, fuels, and energy.^[101] In addition, political measures like tax reduction or the enforcement to produce and use proportions of biomaterials and biofuels will help but are not able to change the need for economic feasibility on the long run.^[98]



Scheme 2.5 General concepts and comparison of traditional crude oil refinery and biorefinery: both share the same conceptual structure while biorefinery is designed as sustainable material cycle.^[101]

The development of self-sustaining biorefinery plants is a complex endeavour and is not covered within this chapter. However, additional information is available elsewhere regarding several subtopics as follows: classification methodologies have to be established for biorefinery systems to allow a comprehensive comparison of existing systems.^[99,102] The resulting product stream has to satisfy the demand and thus has to be adjusted to it.^[101,103] As a result, combinations of different feedstocks and processing technologies, as well as possible product streams have to be evaluated.^[101,103] The amount of biomass needed to be independent of fossil resources has to be evaluated in terms of available cultivation area, available resources (water, nutrients, labour), and competition to the demand of food and feed.^[104,105]

Instead, this chapter gives further insight into the available platform chemicals and describes the sustainable synthesis of frequent starting materials, some also used in this work.

2.5.1 Biobased Platforms

Platform molecules are key intermediates and serve as crosslinks between different biorefinery concepts. A certain platform is available from various feedstocks and *via* different methods.^[99] A platform is usually a mixture of substances that depends on the processing and the feedstock.^[98] Different platforms are usually combined in the end in order to allow the intended product stream.^[98] Depending on the follow-up chemistry, routes for the synthesis of a manifold of product molecules with different added values are available.^[99]

A summary of biorefinery platforms is given in **Table 2.5** together with usual processing methodologies of typical feedstocks. The different platforms are not only interconnected by the feedstocks applied but also by the side products that are formed during the production of a certain platform. Thus, it is obvious that the integrated biorefinery, as mentioned above, is the most promising approach towards a self-sustaining, economically feasible concept for a sustainable chemical industry.

Table 2.5 Summary of biorefinery platforms, possible feedstocks, processing methodologies, and main products.

entry	platform	feedstock	processing	platform components
1 ^[106]	pyrolysis oil	lignocellulosic, variable	heating above 400°C in the absence of oxygen; various methods exist	bio-oil: complex mixture of organic molecules, strongly depending on feedstock and processing, syngas and biochar (charcoal)
2 ^[107]	lignin	lignocellulosic	thermal treatment yielding carbon fibers ^[108] ; depolymerisation <i>via</i> pyrolysis, hydrogenolysis, hydrodeoxygenation, or oxidative routes	complex mixture of aromatic compounds
3 ^[109]	C-5/6 sugars	carbohydrates (C6), hemicellulose (C5/6)	combination of hydrolysis and fermentation processes	ethanol, furan-derivates, succinic acid, 3-hydroxypropionic acid/aldehyde, levulinic acid, lactic acid, sorbitol, and xylitol
4 ^[110]	organic solutions/press juice	grass, clover, alfalfa	pressing of wet, fresh biomass to obtain a liquid fraction containing water-soluble bio-molecules; the lignocellulosic press-cake is valorized differently	carbohydrates, proteins, organic acids
5 ^[111]	bio-oil	oil plants, microalgae	mechanical treatment of the plant/seeds, followed by subsequent hydrolysis or transesterification	glycerol, fatty acids, fatty acid methyl ester, waxes
6 ^[112]	syngas	lignocellulosic, variable	thermally pretreated biomass is gasified at up to 1600°C together with a gasification agent (water, oxygen, air, CO ₂) depending on the desired main component of the crude syngas	CO, H ₂ , CO ₂ , CH ₄ , (H ₂ O)
7 ^[113]	bio-gas	manure, oils, agricultural waste, macroalgae	subsequent anaerobic degradation of biomass by microbes to H ₂ , CO ₂ , and acetate; the latter is finally converted to CH ₄	CH ₄ , CO ₂
8 ^[114-116]	hydrogen	various	fermentation in the absence of light to H ₂ and organic by-products; low H ₂ yields; concomitant valorization of the by-products is necessary; application of the water-gas shift reaction on the gas stream after gasification of biomass to increase the H ₂ content	H ₂ , complex mixture of different liquid organics

While a lot of research is still needed in the field of biorefineries, especially in terms of purification and integration,^[117] 803 biorefineries are already in operation throughout the European Union of which 177 have been integrated biorefineries (as of 2018).^[118] Most biorefinery facilities are located in Germany and France and mainly use agricultural feedstocks.^[118] Other major feedstock categories are forestry, short rotation crops, waste and marine biomass.^[118]

In recent years, extensive progress has been made in order to enable the production of product classes from biomass, to sustainably transform the platform molecules into value added products. The following chapter will highlight a few of the most important biorefinery platforms and the resulting product classes and products and discuss the sustainable synthesis.

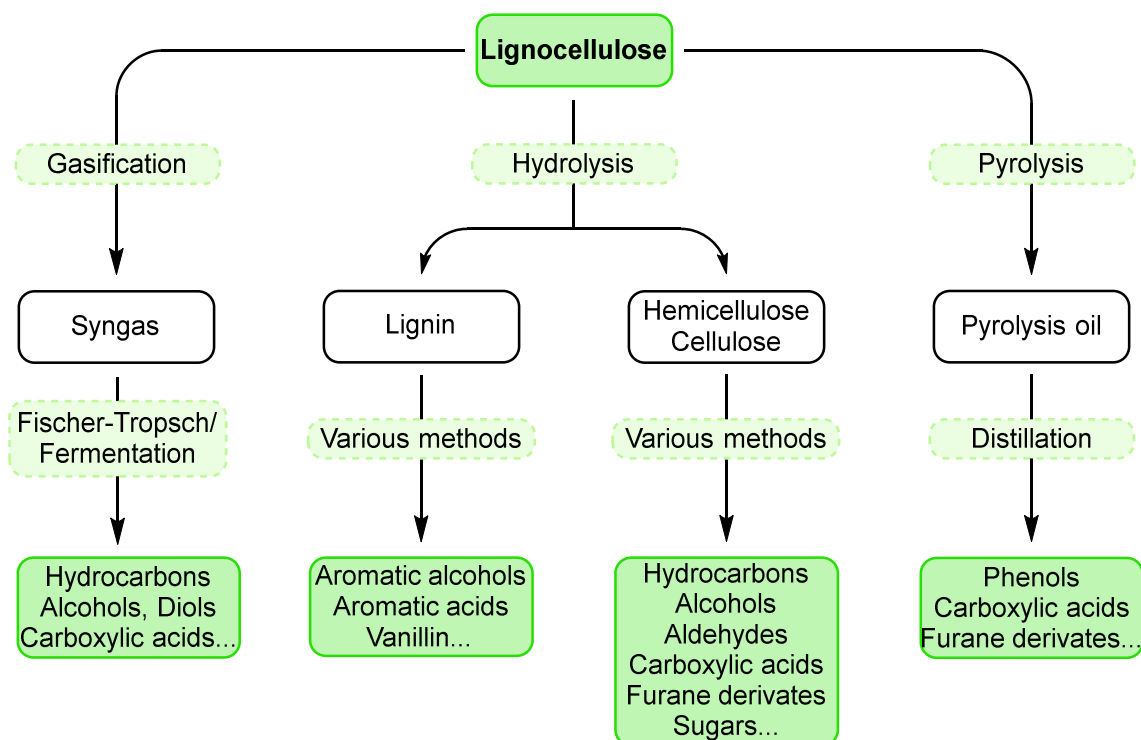
2.5.2 Available Biobased Product Classes

Nowadays, a variety of biobased materials is already industrially produced on a large scale. For other biobased materials, a large scale production is possible but has not been realised yet for economic reasons.^[98] Extensive lists of industrially produced biobased chemicals are available in a report of the International Energy Agency (IEA) of 2020^[98] and a report of the Joint Research Centre (JRC) of the European Commission of 2019.^[119]

The possible product classes, among which are alkanes, aromatics, alcohols, aldehydes, ketones, acids, and amines, as well as combinations thereof, are frequently discussed together with different feedstocks and reaction pathways underlining the current importance.^[98,119–123] Other publications focus on the synthesis of specific products from biomass.^[124]

Regarding the available biomass, lignocellulose is the most comprehensive in terms of available product classes based on the versatile chemical composition of the respective bio-source and the applied extraction/modification methods. In addition, half of the biogenic carbon is lignocellulose.^[123] In **Scheme 2.6**, examples of synthesis pathways to prominent biobased products from lignocellulosic biomass are depicted. It is apparent that a very large

spectrum of molecular weights, functional groups, and carbon-hydrogen-oxygen ratios are available allowing for a vast number of following modifications.



Scheme 2.6 Considerable valorisation pathways for lignocellulose (gasification^[125,126], hydrolysis^[120] and pyrolysis^[127]): the possible product spectrum covers a variety of valuable product classes.

In the previous chapters 2.2, 2.3, and 2.4, many aspects of sustainability and methods to improve the sustainability of chemical reactions have been discussed. However, the implementation of improvements, especially for industrial scale processes, is challenging. The economic aspects are essentially deciding if changes towards sustainability are done. It does not matter how benign a process is if the resulting product/s are sold at prices that cannot compete with prices of competitors, the process will not be implemented. As a consequence, sustainable reactions/products need to be thoroughly investigated first on laboratory scale before an industrial implementation is considered. Furthermore, the starting materials need to be available at reasonable prices. Hence, the production of chemicals from renewable sources is strongly investigated (*cf.* **Table 2.5**, page 27) covering various product

classes. In the following chapter, synthesis pathways of specific compounds are discussed in detail.

2.6 Non-fossil synthesis pathways for important starting materials

To implement the use of renewable resources in the chemical industry, it is reasonable to directly use renewable or potentially renewable starting materials during the research for potential chemical products and materials. As a consequence, renewable compounds were used within this thesis. The following sections cover the applied compound classes and discuss existing and reasonable non-fossil synthesis routes for frequently used molecules.

2.6.1 Aliphatic diols

Aliphatic diols are widely used chemical products. As an example, the global demand for 1,2-ethanediol (**18**) was 25 million tons as of 2014.^[128] They are mainly applied for the synthesis of polymer materials and, in case of the short C₂- to C₄-homologues, used as solvents or anti-freeze agents.^[129–132] The traditional crude oil-based synthesis typically involves the oxidation of unsaturated or saturated cracking products.^[130,132] In this work, six different diols, namely 1,2-ethanediol (**18**), 1,3-propanediol (**21**), 1,4-butanediol (**24**), 1,6-hexanediol (**24**), 1,10-decanediol (**34**), and isosorbide (**35**) were used as monomer precursors. Hence, possible synthesis routes from renewable resources are presented.

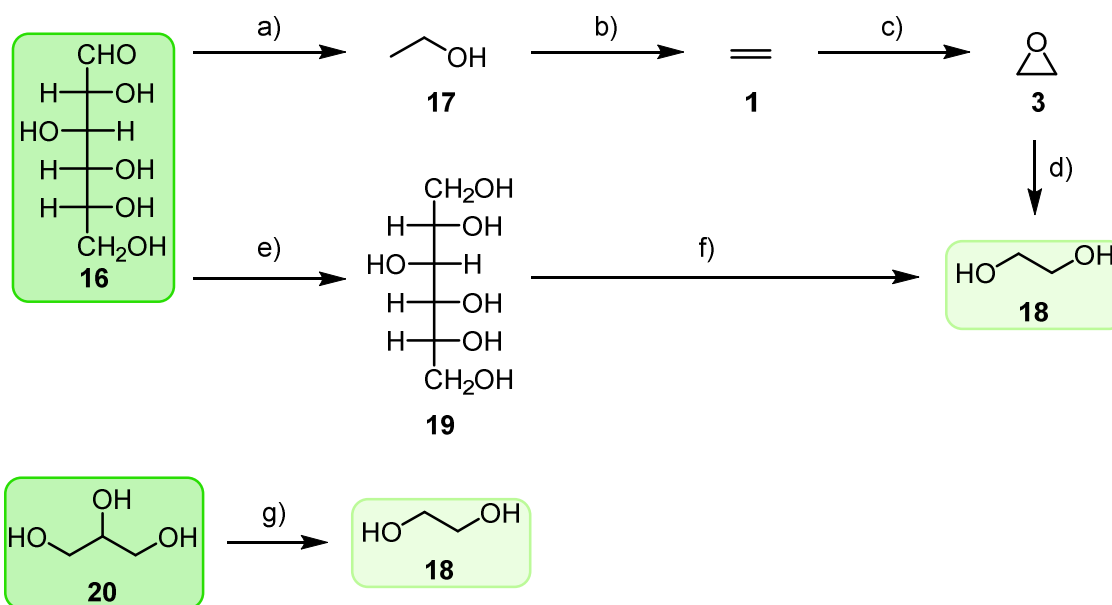
1,2-ethanediol (**18**) is often derived from ethanol (**17**), sorbitol (**19**), or glycerol, (**20**) as summarized in the literature (**Scheme 2.7**).^[128] **17**, which is typically derived from lignocellulose *via* hydrolysis and fermentation in large quantities (**Scheme 2.7, path a**),^[133] is in the first step dehydrated to ethylene (**1**) (**Scheme 2.7, path b**)^[134] followed by oxidation yielding ethylene oxide (**3**) (**Scheme 2.7, path c**).^[57] Subsequent hydration yields **18** (**Scheme 2.7, path d**).^[128,135] This method is industrially applied for example in Taiwan with a production capacity of 100 kt·a⁻¹.^[128,136] **19** is obtained from cellulose *via* hydrolysis to glucose (**16**) and subsequent hydrogenation (**Scheme 2.7, path e**).^[137] The following

hydrogenolysis step leads to **18** with conversions between 36% and 99% and selectivities between 7% and 38% depending on the applied catalyst and the reaction conditions (**Scheme 2.7**, path **f**).^[128] Approaches for direct conversion of lignocellulosic biomass to **19**^[138] or **18**^[139] exist as well. Noteworthy is the prevalent application of nickel catalysts, which are highly toxic and need to be avoided for the transition from renewability to sustainability.

As an alternative to sugar-based starting materials, **20** has been used (**Scheme 2.7**). It is obtained as a side product of the biodiesel production. The transesterification of oils with MeOH yields different fatty acid methyl esters and **20**.^[140] Subsequent hydrogenolysis of **20** leads to **18** (**Scheme 2.7**, path **g**).^[128] Conversions range between 15% and 90% with selectivities between 8% and 56% for **18** depending on the applied catalyst and the reaction conditions.^[128]

1,3-propanediol (**21**) is industrially produced from **16** by DuPont.^[141] **16** is fermented *via* the glycolytic pathway of the used microorganism *via* **20** as intermediate (**Scheme 2.8**, page 33, **a**).^[142,143] Furthermore, the direct use of **20** as feedstock for the fermentation process was reported (**Scheme 2.8**, **b**).^[144] Considering the increasing production volumes of biodiesel over the last decade, the latter is considered to be especially profitable.^[145] The catalytic hydrogenolysis of **20** to **21** is also possible but typically shows lower conversions and lower selectivity compared to the above described enzymatic reactions.^[146,147] Moreover, temperatures above 120°C and hydrogen pressures above 40 bar are necessary.^[147] Nonetheless, a boehmite-supported platinum nanoparticle/tungsten oxide catalyst was shown to reach 100% glycerol conversion at a selectivity for **21** of 66% (**Scheme 2.8**, **c**).^[148]

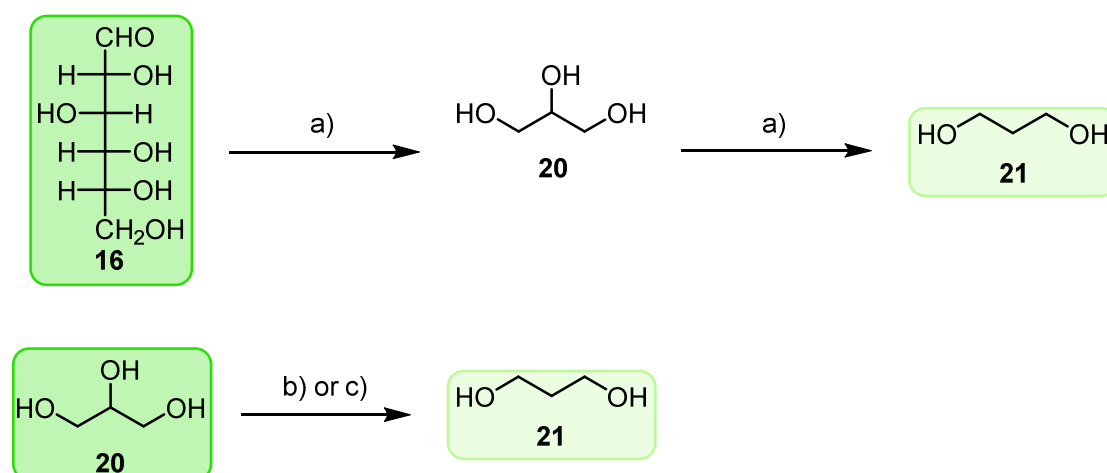
2.6 Non-fossil synthesis pathways for important starting materials



Scheme 2.7 Syntheses pathways for the production of **18** from the renewable platform molecules **16** or **20** using biochemical and catalytic steps.^[57,128,134,135,137,149,150] Example reactions/conditions: **a)** microbial fermentation, *Saccharomyces cerevisiae*, water, 35 – 45°C, 3 – 5 d, no yield reported. **b)** dehydration, 95 wt% EtOH/H₂O, alumina based cat., 300 – 500°C, 1 – 2 bar, *SV*³ 0.1 – 1 h⁻¹, 94 – 99% yield. **c)** oxidation, 2 – 10 vol% **1**, alumina supported Ag, 220 – 277°C, 10 – 30 bar air, *SV* 2000 – 4000 h⁻¹, 16 – 52% yield. **d)** hydration, carboxylate salts as cat., 10 mol% H₂O/**3**, 100 – 120°C, 15 bar, 1 h, 98% yield. **e)** hydrogenation, Cu/Cr cat. on solid support, 50 wt% **16**/H₂O, 120 – 150°C, 70 bar H₂, 2 – 4 h, no yield reported. **f)** hydrogenolysis, Ru- or Ni-based catalyst, 200 – 275°C, 40 – 270 bar H₂, 20 min – 7 h, 8 – 25% yield. **g)** hydrogenolysis, Ru- or Ni-based catalyst, 120 – 230°C, 1 – 80 bar H₂ or N₂, 1 – 72 h, 6 – 30%.

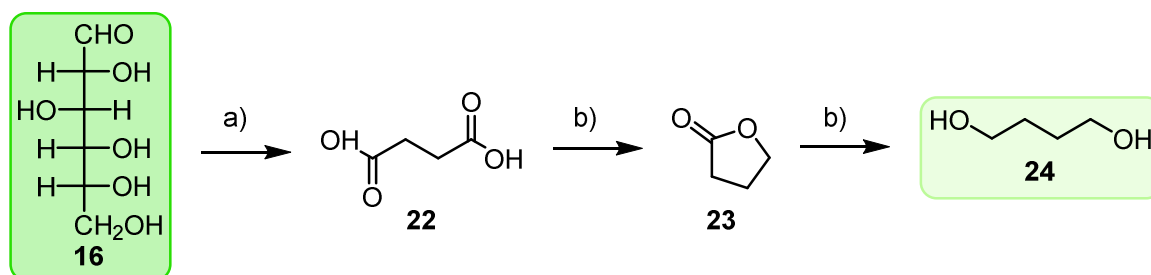
³The space velocity *SV* describes the throughput of a reactor in reactor volumes (*V_r*) per time unit. It is calculated by division of the flow rate \dot{V} by *V_r*. The mean turnover time τ equals the reciprocal of *SV*.^[151]

$$SV = \frac{\dot{V}}{V_r} = \frac{1}{\tau}$$



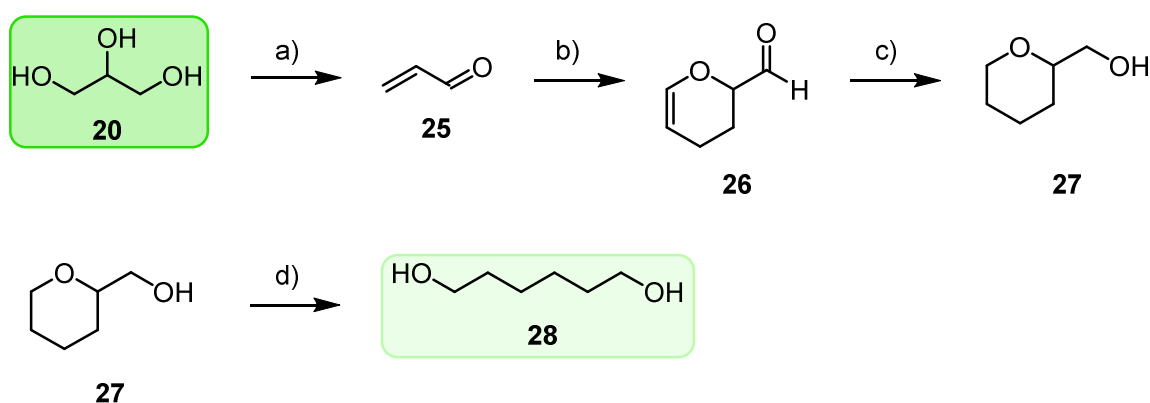
Scheme 2.8 Possible synthesis pathways for the production of **21** from the renewable platform molecules **16** and **20** via different biochemical processes or catalytic hydrogenolysis.^[142,144,146,147,152] Typical reactions/conditions: **a)** fermentation, e.g. genetically modified *Escherichia coli*, 0.2 wt% **16** in growth medium, 37°C, 1 d, 21% yield at 99% conversion. **b)** fermentation, genetically modified *Clostridium acetobutylicum*, 0.11 mol% **20** in growth medium, 35°C, volumetric productivity 3 g·L⁻¹·h⁻¹, 64% yield. **c)** hydrogenolysis, 0.33 M **20** in H₂O, bohemite-supported Pt/W-oxide cat., 180°C, 50 bar H₂, 12 h, 69% yield at 99% conversion.

The synthesis of renewable 1,4-butanediol (**24**) from succinic acid (**22**) was shown, which is mainly produced by microbial fermentation of **16** (Scheme 2.9, step a)).^[153] The following hydrogenation of **22** to **24** is a well-established process as **24** is synthesised from fossil maleic anhydride-derived **22** on an industrial scale (Scheme 2.9, path b)).^[154] Typical catalysts contain combinations of ruthenium or rhenium and a group X metal on solid support.^[155] The mechanism towards **24**, notably, has been reported to proceed via γ -butyrolactone (**23**), which forms prior to the consecutive, albeit somewhat concomitant, conversion to **24**.^[156]



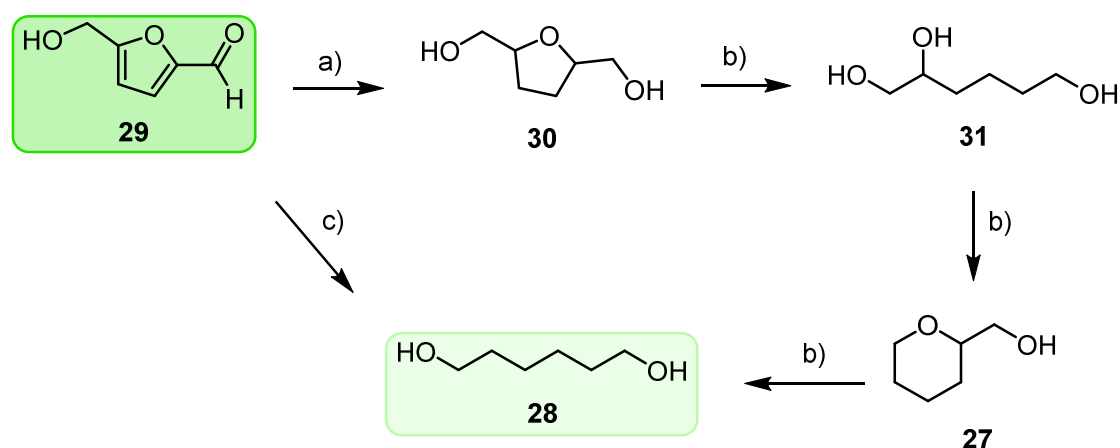
Scheme 2.9 Industrial production pathway of **24** from renewable **22** via drop-in strategy.^[153,156,157] Typical reactions/conditions: **a)** fermentation, e.g. genetically modified *Escherichia coli*, 40 – 100 g·L⁻¹ in growth medium, 30 – 40°C, volumetric productivity 1.1 – 3.8 g·L⁻¹·h⁻¹, 3 – 4 d, yield not given. **b)** hydrogenation, Ru/Sn catalyst on ZrO₂ support, 225°C, 140 bar H₂, 94% yield.

The production of 1,6-hexanediol (**28**) was reported from either **20** or 5-hydroxymethylfurfural (**29**). The route starting from **20** involves dehydration to acrolein (**25**) (**Scheme 2.10, a**).^[158] The dehydration is typically performed in the gaseous phase over an acidic heterogeneous catalyst in the presence of water at temperatures above 270°C.^[158] The latter readily undergoes thermal [4+2]-cycloaddition to the acrolein dimer (**26**) (**Scheme 2.10, b**).^[159] The subsequent hydrogenation of **26** results in mixtures of 2-hydroxymethyltetrahydropyran (**27**) and **28** (**Scheme 2.10, c**).^[160] After separation, **27** is converted to **28** via heterogeneously catalysed hydrogenolysis with selectivity up to 97% (**Scheme 2.10, d**).^[160,161]



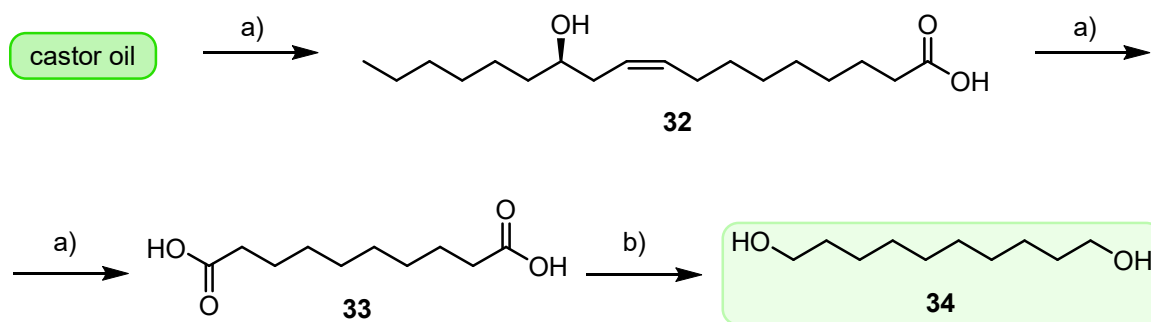
Scheme 2.10 Possible synthesis of **28** from the renewable **20** via subsequent catalytic reduction.^[158–162] Typical reactions/conditions: **a)** dehydration, 10 wt% **20** in H₂O, H₃PW₁₂O₄₀/Nb₂O₅ cat., *SV* 420 h⁻¹, 325°C, 92% yield. **b)** [4+2]-cycloaddition, 185 – 195°C, 45 – 75 min, up to 99% yield at 56% conversion. **c)** hydrogenation, 5 wt% **26** in MeOH, PtW/TiO₂ cat., 80°C, 6.6 bar H₂, 4 h, 60% yield (+27% **28**). **d)** hydrogenolysis, 2 wt% **27** in water, Rh/Re-oxide on carbon support, 100°C, 80 bar H₂, 24 h, 48% yield, at 50% conversion.

29 is an important platform molecule mainly obtained by hexose dehydration.^[163] Two routes are established for the synthesis of **28** from **29**:^[164] first, the hydrogenation of **29** to 2,5-dihydroxymethyltetrahydrofuran (**30**) (**Scheme 2.11**, path **a**)^[165] and subsequent dehydrative ring-opening towards **28** (**Scheme 2.11**, path **b**) and second, the direct hydrogenolysis of **29** to **28** (**Scheme 2.11**, path **c**).^[166] It was shown that the route over **30** preferably proceeds over 1,2,6-hexanetriol (**31**) and **27**.^[167,168]



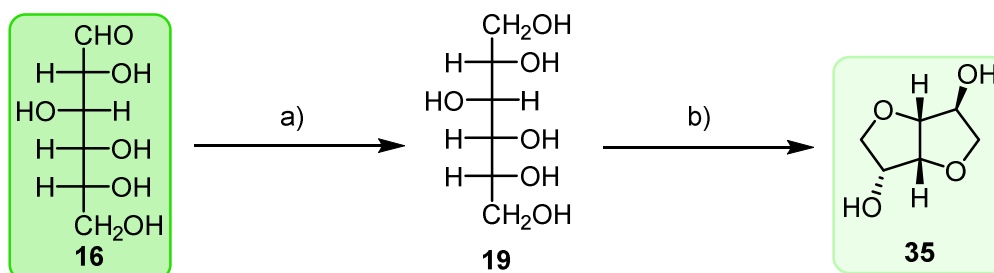
Scheme 2.11 Possible synthesis of **28** from the renewable **29** via subsequent catalytic reduction.^[164–168] Typical reactions/conditions: **a)** hydrogenation, 0.5 M **29** in H₂O, Ni–Pd/SiO₂ cat., 40°C, 80 bar H₂, 2 h, 96% yield. **b)** hydrogenolysis, 0.45 M **30** in water, Rh/Re-catalysts and NAFION™ SAC13, 120°C, 10 bar H₂, after 1 h 80 bar, 20 h, 86% yield. **c)** hydrogenolysis, 0.33 M in EtOH, Pd/ZrP, formic acid, 140°C, 21 h, 43% yield at 97% conversion.

For the production of 1,10-decanediol (**34**), castor oil-derived sebacic acid (**33**) was used. The castor oil is usually pyrolysed at 280°C in an alkaline environment yielding 70% of **33**, as well as 2-octanol as main side-product (Scheme 2.12, reaction a)).^[169] The alkaline conditions promote the *in situ* hydrolysis of the castor oil to **20** and ricinoleic acid (**32**).^[170] The latter is subsequently cleaved.^[170,171] Hydrogenation of **33** or the respective methyl ester leads to **34**.^[172]



Scheme 2.12 Possible synthesis of **34** from renewable castor oil *via* pyrolysis under alkaline conditions.^[169,170,172] Typical reactions/conditions: **a)** alkaline pyrolysis, mineral oil as solvent, NaOH, 280°C, 5 h, up to 70% yield. **b)** hydrogenation, Ru/Pd/Pt cat., 200°C, 150 bar H₂, ultrasonication, 98% yield.

Isosorbide (**35**) is readily obtained by dehydration of **19** on industrial scale (**Scheme 2.13**, reactions **a)** and **b)**).^[173,174]



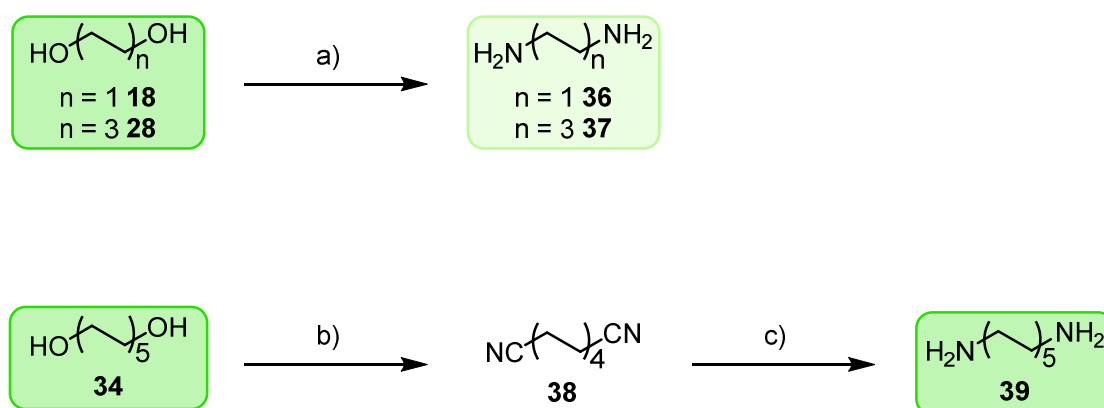
Scheme 2.13 Synthesis of **35** *via* dehydration of **19**.^[173] Typical reactions/conditions: **a)** see **Scheme 2.7 e)**. **b)** dehydration, AMBERLYST 36™, 150°C, 4 h, 99.8% yield.

This section provided an overview over the synthesis of six aliphatic diols from different renewable sources. Most of these syntheses are at least partially applied on an industrial scale.

2.6.2 Aliphatic Diamines

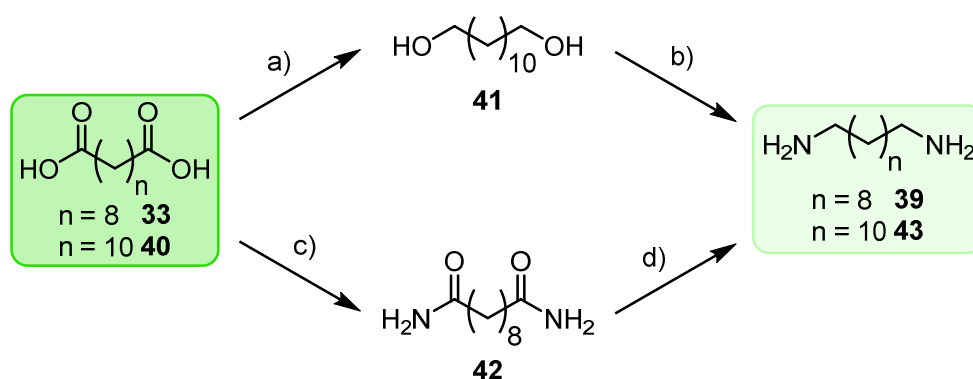
Aliphatic diamines are, just as diols, widely applied. While the longer homologues are mainly used as starting materials for the synthesis of polyamides or polyurethanes,^[175] 1,2-ethanediamine (**36**) is additionally used as precursor for pharmaceuticals or agrochemicals.^[176] **36** is traditionally produced from 1,2-dichloro ethane and ammonia.^[176] Longer chain homologues are often synthesised by hydrogenation of the respective nitriles.^[176,177] The latter are reportedly derived from haloalkanes or olefins.^[178] However, several options for the renewable synthesis of the aliphatic diamines **36**, 1,6-hexanediamine (**37**), and 1,10-decanediamine (**39**) exist from either renewable diols or diacids. These were used as monomer precursors in this work.

The production of **36** and 1,6-hexanediamine (**37**) was reported *via* direct amination of the respective diol in a flow reactor (**Scheme 2.14**, reaction **a**)).^[179] For 1,10-decanediamine (**39**), a synthesis starting from **34** is described as two-step process *via* 1,8-octanedinitrile (**38**).^[180] **34** was catalytically reacted to form **38** with ammonia under oxygen atmosphere (**Scheme 2.14**, reaction **b**)).^[180] The corresponding amine was obtained *via* hydrogenation using Raney-Ni (**Scheme 2.14**, reaction **c**)).^[180] Nonetheless, a direct conversion to the amine according to the above described procedure for **36** and **37** is conceivable. Moreover, additional catalyst systems for the conversion of a variety of aliphatic monoalcohols have been reported.^[181–183]



Scheme 2.14 Synthesis of renewable diamines **36**, **37**, and **38** by direct amination or two step synthesis over an intermediate dinitrile using diols as starting materials.^[179,180] Typical reactions/conditions: **a)** amination (e.g. of **18**), SiO₂/Al₂O₃-supported Ni/Re-cat., 130 – 225°C, 35 – 200 bar H₂/NH₃, 24% yield at 30% conversion. **b)** nitrile synthesis, 0.6 M **34** in MeCN, CuI/bipyridine/2,2,6,6-tetramethylpiperidinyl-1-oxyl (TEMPO), NH₃, oxygen atmosphere, 30°C, 24 h, 93% yield. **c)** hydrogenation, 0.2 M in EtOH, Raney Ni, 70°C, 10 bar H₂. 16 h, 51% yield.

Since the synthesis route from renewable resources to carboxylic acids is typically shorter than the route towards the respective alcohols, the conversion of carboxylic acids to primary amines is reasonable (**Scheme 2.15**). The required renewable dicarboxylic acids are accessible by electrolytic addition of carbon dioxide (**44**) and water in the case of oxalic acid^[184] or microbial reactions (adipic acid, oxalic acid).^[185,186] Long chain aliphatic diacids like **33** have reportedly been synthesised *via* biochemical routes.^[187] While the conversion of oxalic acid to **36** has not been reported yet, the syntheses of **37** and longer aliphatic diamines (1,10-decanediamine (**39**), 1,12-dodecanediamine (**43**), and 1,19-nonadecanediamine) from the respective diacids are reported with yields of approximately 80% in one-pot procedures.^[188,189]



Scheme 2.15 Reported one-pot syntheses of aliphatic diamines from dicarboxylic acids over either an intermediate diol (shown for **43**) or diamide (shown for **39**).^[188,189] Typical reactions/conditions: **a**) hydrogenation, 0.1 M **40** in dioxane/water, Ru(acetylacetonate)₃/1,1,1-tris(diphenylphosphinomethyl)ethane/methanesulfonic acid, 220°C, 10 bar H₂, 20 h. **b**) amination, same as **a**) but 0.1 M in dioxane, aqueous NH₃, 83% yield. **c**) amidation, 0.1 M **33** in *c*-pentyl methyl ether, Ru/W-oxide cat. on solid support, 200°C, 6 bar NH₃, reaction time not given. **d**) hydrogenation, same as **c**) but 6 bar NH₃/50 bar H₂, 6.5 h, 30% yield.

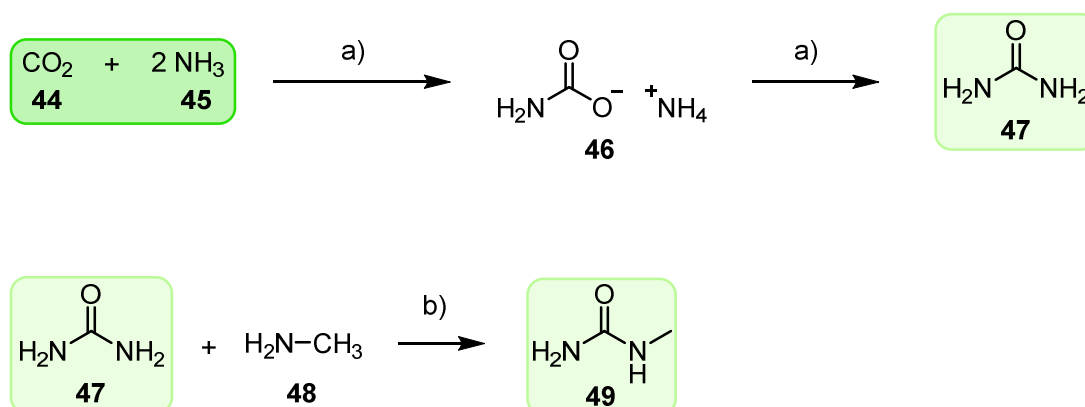
While being one-pot reactions, the conversion is still a two-step process in both cases. The first reaction route *via* the diol starts with the reduction of the carboxylic acid to the alcohol (**Scheme 2.15**, reaction **a**)).^[189] The latter is subsequently converted to the amine by addition of aqueous ammonia to the reaction mixture (**Scheme 2.15**, reaction **b**)).^[189] The second route begins with the formation of the intermediate amide (**Scheme 2.15**, reaction **c**)).^[188] Afterwards, the amide is hydrogenated to the amine (**Scheme 2.15**, reaction **d**)).^[188]

This section provided an overview over the synthesis of diamines from different renewable sources showing high yielding approaches and even one-pot procedures.

2.6.3 Urea and *N*-Methylurea

Urea (**47**) is one of the most important nitrogen fertilizers due to its high nitrogen content.^[190] Approximately 90% of the global production is applied for agricultural purposes.^[190] *N*-Methyl urea (**49**) is mainly applied for the production of plant protectives or the in the pharmaceutical industry.^[191] However in this work, both are used as one of the main reactants for the polymer synthesis.

Starting materials for the industrial **47** production are CO₂ (**44**) and NH₃ (**45**) (**Scheme 2.16**).^[192] Both react at elevated temperatures and pressures in an exothermic reaction to form ammonium carbamate (**46**) (**Scheme 2.16**, path **a**).^[192] Afterwards, **46** is dehydrated to **47** (**Scheme 2.16**, path **a**).^[192] The renewability of this process depends on the hydrogen and carbon sources. Today, hydrogen is mostly produced from natural gas by steam reforming and the subsequent water-gas-shift reaction, with **44** as by-product.^[193] However, it is possible to renewably generate hydrogen and **44**. The conversion of biomass by either gasification^[112] or fermentation^[114–116] produces renewable hydrogen. In addition, the electrolysis of water produces renewable hydrogen and oxygen if renewable energies like wind or solar power are used.^[194,195] The gasification of biomass yields syngas which also serves as source for renewable carbon besides hydrogen.^[112]



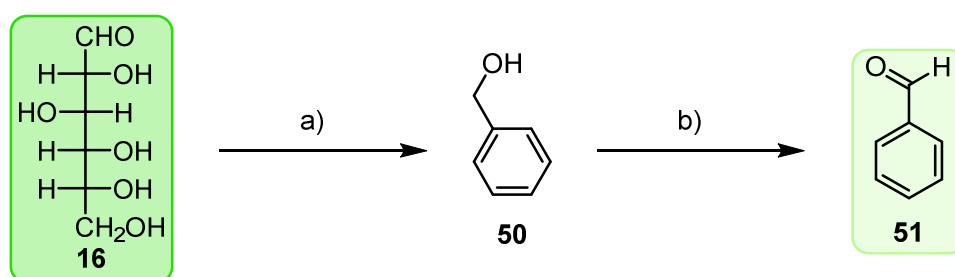
Scheme 2.16 Synthesis of **47** and **49**.^[192,196–198] Typical reactions/conditions: **a**) addition/dehydration, 150 – 250°C, 120 – 400 bar. **b**) methylation, 380°C, 1 h, 60% yield.

A consecutive production of **49** from **47** was reported using methylamine (**48**) as methylating agent (**Scheme 2.16**, reaction **b**).^[196,197] Renewable **48** is industrially produced from methanol and ammonia.^[199]

Hence, the renewability of the synthesis of **47** and **49** rather depends on the respective energy sources than the starting materials.

2.6.4 Benzaldehyde and Terephthalic Aldehyde

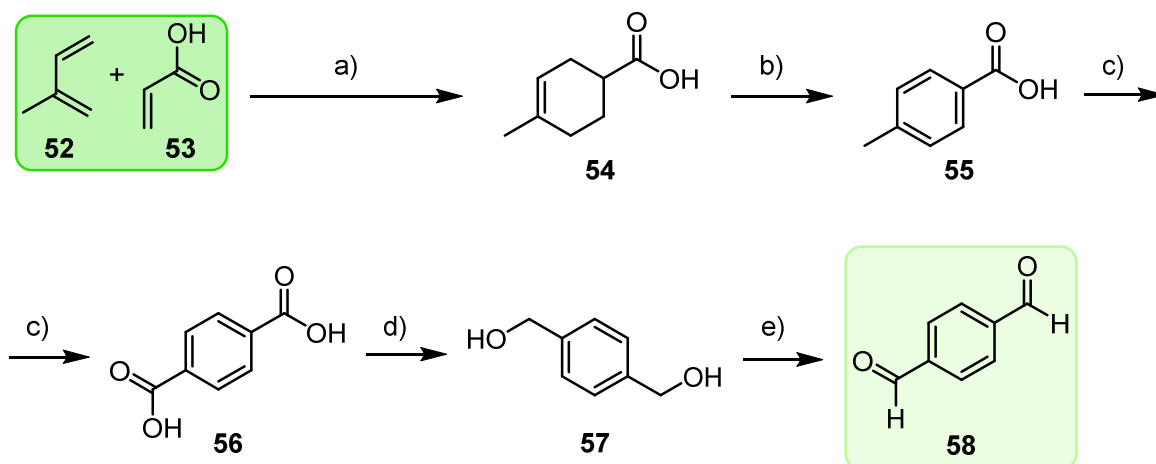
Benzaldehyde (**51**) is used in large quantities as starting material for flavours or odorants and typically synthesised from fossil toluene by either partial oxidation or radical chlorination and subsequent hydrolysis.^[200] A possible precursor for renewable **51** is benzyl alcohol (**50**). It is available by microbial conversion of **16** (Scheme 2.17, reaction a)).^[201,202] The oxidation of **50** leads to **51** (Scheme 2.17, reaction b)). Several promising catalytic systems have been reported.^[203–205]



Scheme 2.17 Synthesis of renewable **51** using carbohydrate feedstocks.^[203–205] Typical reactions/conditions: a) biosynthesis, 15 g·L⁻¹ **16** in growth medium, genetically modified *Escherichia coli*, 37°C, 96 h, 32% yield. b) oxidation, *hν* (>420 nm), 0.02 M **50** in toluene/H₃PO₄, Ru/SrTiO₃:Rh, 25°C, N₂, 18 h, >95% yield.

The traditional synthesis of terephthalic aldehyde (**58**) is performed, similarly to the synthesis of **51**, from *p*-xylene.^[206] The synthesis of biobased **58** has not been covered as such in the literature, however, the synthesis of renewable terephthalic acid (**56**) has been. Hence, a possible route to **58** includes **56** as intermediate (Scheme 2.18). **56** was obtained by [4+2]-cycloaddition of isoprene (**52**) and acrylic acid (**53**) (Scheme 2.18, reaction a)) followed by subsequent aromatisation (Scheme 2.18, reaction b)) and oxidation to **56** (Scheme 2.18, reaction c)) with a combined maximum yield of 68%.^[207,208] Syntheses of **56** starting from muconic acid ((*2E,4E*)-hexa-2,4-dienedioic acid)^[209] or **1**^[128] have also been reported. The obtained **56** or the respective esters were readily reduced to 1,4-di(hydroxymethyl)benzene (**57**) with up to quantitative yields using several different catalysts (Ru/Sn-catalyst^[210], homogeneous Ru-^[211,212], or Fe-pincer^[213] complexes) (Scheme 2.18, reaction d)). **57** was shown to undergo partial oxidation to **58** (Scheme 2.18,

reaction e)). Besides an iodine-based catalyst,^[204] a nitrogen-doped cobalt catalyst was reported to yield quantitative yields of **58** under similar conditions.^[214]



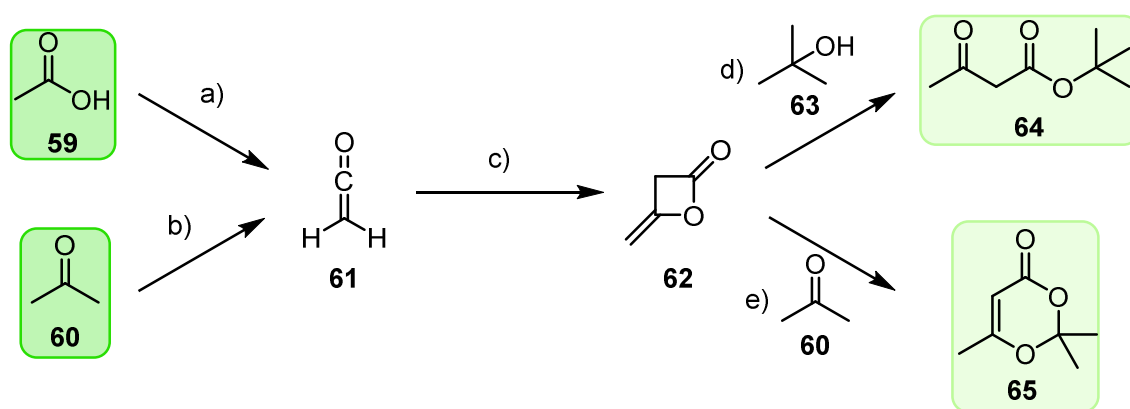
Scheme 2.18 Synthesis route for **58** via **56** as intermediate using **52** and **53** as possible renewable precursors.^[204,207,210,214] Typical reactions/conditions: **a**) [4+2]-cycloaddition, TiCl_4 -cat., 21°C , 24%, 94% yield. **b**) dehydroaromatization, Pd/C, 240°C , 0.11 bar, 77% yield. **c**) oxidation, AcOH, $\text{Co}(\text{OAc})_2/\text{Mn}(\text{OAc})_2$ cat., O_2 , 100°C , 94%. **d**) reduction, $[\text{RuCl}_2(\text{p-cumene})]_2$, NaOEt, 80°C , 50 bar H_2 , 16 h, 99% yield. **e**) oxidation, 0.2 M **57** in toluene, Co/N/C-cat., 100°C , O_2 , 36 h, 99% yield.

In this section, possible renewable routes to form **51** and **58** were proposed. While the synthesis of **51** already has been established, the production of **58** needs further investigation especially in order to decrease the number of reaction steps.

2.6.5 *tert*-Butyl acetoacetate and Diketene Acetone Adduct

Both *tert*-butyl acetoacetate (**64**) and the diketene acetone adduct (2,2,6-trimethyl-4*H*-1,3-dioxin-4-on, **65**) are important reactants for organic synthesis. Within this work, both are used as convenient alternatives to the toxic and unstable diketene.^[215,216] The starting material for both *tert*-butyl acetoacetate (**64**) and diketene acetone adduct (2,2,6-trimethyl-4*H*-1,3-dioxin-4-on, **65**) is ketene (**61**) (Scheme 2.19).^[215] The highly reactive gas is industrially produced by pyrolysis of acetic acid (**59**) **a**),^[217] acetone (**60**) **b**)^[218] or other

methods^[219] and quickly dimerises to diketene (**62**) *via* thermochemical [2+2]-cycloaddition **c**).^[220] A subsequent nucleophilic ring-opening with *tert*-butanol (**63**) yields **64 d**).^[221] The required **63** is available by acid catalysed hydration of biobased isobutene.^[222] The latter is industrially produced *via* fermentation of sugars.^[223,224] If **62** is reacted with **60** in the presence of an acid, diketene acetone adduct (**65**) is obtained with a yield of 91% **e**).^[225] The starting materials **59** and **60** are typically directly prepared from biomass by fermentation processes^[226–228].



Scheme 2.19 Synthetic pathways for renewable **64** and **65**.^[215,217,218,220,221,225] Typical reactions/conditions: **a**) pyrolysis, 740 – 760°C, PO(OEt)₃ cat., no yield given. **b**) pyrolysis, 700 – 750°C, 10 h, 95% yield. **c**) [2+2]-cycloaddition, spontaneous below 200°C, up to 85% yield. **d**) ring-opening, 21-150°C, no further information given. **e**) addition, *p*-TsOH as cat., reflux, 3 h, 91 % yield.

Hence, the renewable synthesis of **64** and **65** is possible using established processes.

2.6.6 Acrylic Acid, Methacrylic Acid, and Vinyl Acetate

Compounds with vinylic double bonds are important starting materials for polymer materials synthesised by radical polymerisation techniques. Millions of tons of vinyl type monomers are produced every year. The worldwide production of methacrylic acid alone is 1.4 million tons per year.^[229] Also in this work, acrylic acid, methacrylic acid, and vinyl acetate will be applied for the synthesis of polymers. They are typically produced from fossil resources. However, improvements towards renewable vinyl type monomers have been reported and recently summarized.^[230] In the following, established or reasonable renewable synthesis routes for acrylic acid (**53**), methacrylic acid, and vinyl acetate are given.

The synthesis of biobased **53** from lactic acid or 3-hydroxypropionic acid, both of which are available, *e.g.*, as sugar fermentation products, has been reported.^[231,232] Both are reported to undergo dehydration to **53**. 3-Hydroxypropionic acid was reacted at temperatures between 120°C and 250°C at elevated pressures of up to 10 bar over an acidic homogeneous or heterogeneous catalyst.^[233] Furthermore, 3-hydroxypropionic acid was dehydrated at temperatures between 150°C and 180°C using homogeneous acid catalysts under approximately atmospheric pressure.^[234] Lactic acid dehydration was reported by heterogeneous catalysts like zeolites, phosphate-based catalysts, and hydroxyapatites.^[235,236] Other procedures, like biochemical conversion of lactic acid or **20** to **53** with up to quantitative yields, are also known.^[237,238]

The synthesis of biobased methacrylic acid was reported from glucose (**16**) *via* different metabolites like isobutyric acid, itaconic acid, among others.^[239] In addition, the use of well-established petrochemical routes are possible as well if biobased starting materials are used. Possible starting materials are ethylene and isobutene, among others.^[240] One example is the conversion of **1** in the presence of CO and H₂ to propionaldehyde followed by the reaction with formaldehyde to methacrolein and subsequent oxidation to methacrylic acid.^[241]

Biobased vinyl acetate is already produced by Wacker in a pilot plant using renewable **1** and **59**.^[242] The reaction was patented as oxidative addition of **1** and **59** in the presence of

a rare metal catalyst on solid support at pressures between 3 bar and 30 bar at temperatures between 150°C and 250°C.^[243] In another patent, the hydrogenolytic conversion of **59** to **1** is reported followed by the oxidative addition of **1** and **59** to vinyl acetate.^[244]

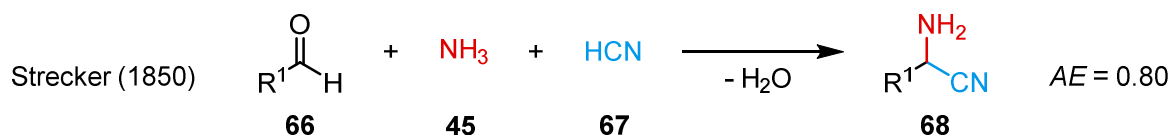
Within this chapter 2.6, renewable synthesis routes of several important compound classes have been described. Many of the shown routes are at least partly industrially applied creating a strong foundation for the investigation of new sustainable polymer materials. It furthermore shows the ubiquitous shift from fossil resources towards renewables. Besides the aspect of sustainability, the application of the Biginelli-3-component reaction, a multicomponent reaction, plays an important role in this thesis. Hence, the field of multicomponent reactions with an emphasis on the Biginelli-3-component reaction will be covered in the following chapter.

2.7 Multicomponent Reactions

Multicomponent reactions (MCRs) offer many beneficial characteristics, synthetically and in terms of sustainability. MCRs are high-yielding one-pot reactions in which three or more reactants condense or add to complex product structures that contain structural elements of each of the reactants.^[245,246] Up to all atoms of the starting materials are incorporated in the final product leading to high atom efficiencies.^[247,248] The nature of one-pot reactions allows for shorter reaction times and easier work-ups, compared to conventional step-wise syntheses, as well as facile automation.^[247,248] Thus, MCRs are promising tools for sustainable chemical syntheses. Another outstanding feature of MCRs is their modular character rendering MCRs a powerful tool in the field of combinatorial chemistry. A simple variation of the starting materials allows for the synthesis of a manifold of different products that enable the straightforward synthesis of large compound libraries.^[249,250]

The investigation of MCRs started in the 18th century with the report of the Strecker synthesis (**Scheme 2.20**), followed by many other examples.^[251] This first multicomponent reaction was the one-pot reaction of an aldehyde (**66**), ammonia (**45**) and hydrocyanic acid

(**67**) to an α -amino nitrile (**68**), which was further converted to α -amino acids *via* hydrolysis.^[251]

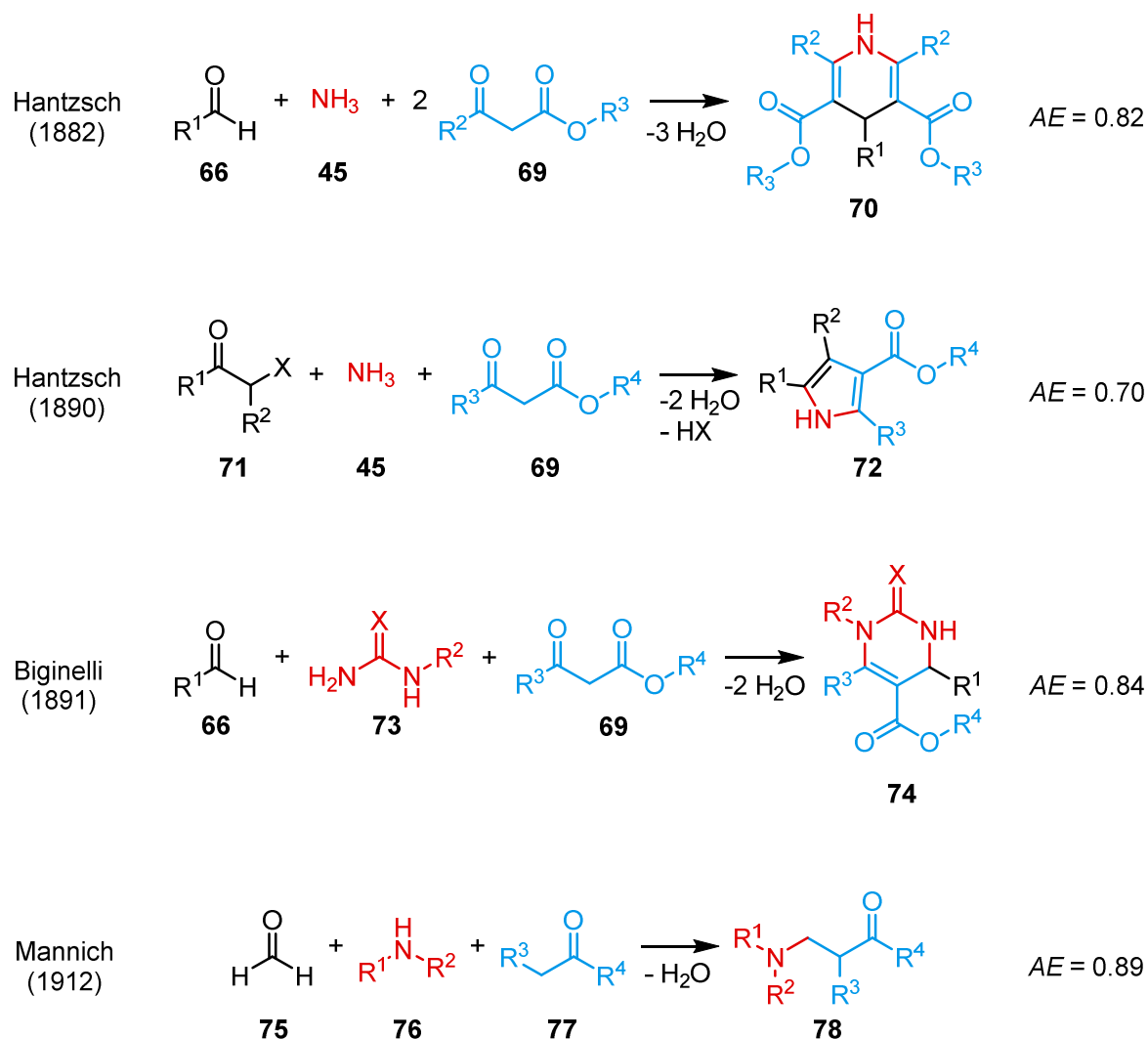


Scheme 2.20 The Strecker synthesis is the first MCR, reported in 1850; the *AE* was calculated using $\text{R}^1 = \text{CH}_3$.^[251]

A second milestone in the development of MCRs was marked by Hantzsch with his synthesis of pyrimidines in 1882 (**Scheme 2.21**).^[252] He described the condensation of **66** with two equivalents of a β -keto ester (**69**) and **45** to 1,4-dihydropyrimidines (**70**), which was oxidised to pyridines.^[252] **70** represents an important class of calcium channel blockers that are pharmaceutical compounds.^[253] A few years after, Hantzsch published the similar condensation of **69**, α -halogenated ketones (**71**), and **45** to pyrroles (**72**) (**Scheme 2.21**).^[254] The pyrrole structure is present in a variety of natural products, *e.g.*, hemes (porphyrin)^[255] or chlorophylls (chlorins).^[256]

In 1891, Biginelli observed that the acid-catalysed reaction of **66**, **69**, and urea (**47**) leads to dihydropyrimidinones (DHPMs, **74**; for further details refer to chapter 2.7.1 and 2.7.2) (**Scheme 2.21**).^[257] In the beginning of the 19th century, the aminomethylation of **66** and ketones (**77**) using paraformaldehyde and amines (**76**) in the presence of an acid was observed by Mannich.^[258] This reaction is, *inter alia*, applied for the synthesis of natural products such as the alkaloid tropinone^[259] or pharmaceutical compounds.^[260]

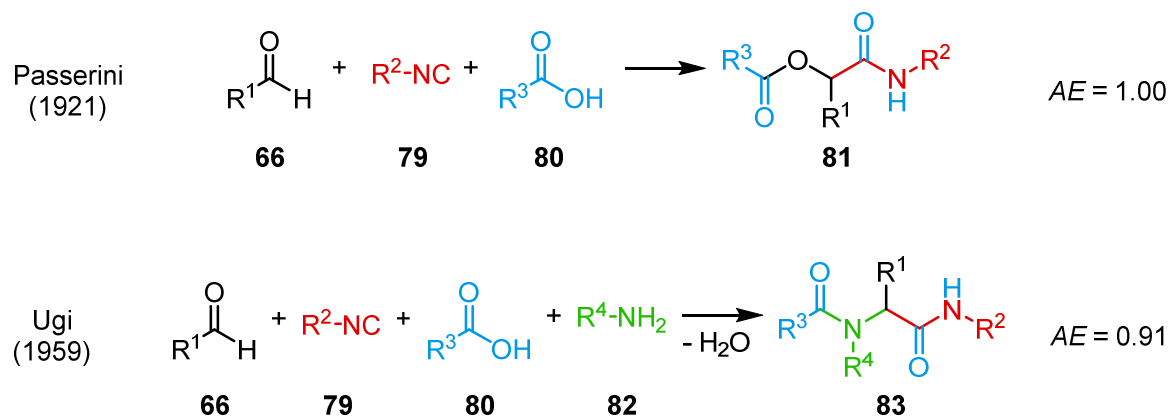
2.7 Multicomponent Reactions



Scheme 2.21 Representative milestones of the development of MCRs with the names of the lead authors in the respective publication, year of publication, and an example *AE*; the *AE* was calculated using $\text{R}^x = \text{CH}_3$ and $\text{X} = \text{Cl}$.^[252,254,257,258]

Later, the class of isocyanide-based MCRs was introduced with the Passerini-3-component reaction and the Ugi-4-component reaction as most prominent examples (**Scheme 2.22**). In 1921, Passerini discovered that the reaction of **66** with an isocyanide (**79**), and a carboxylic acid (**80**) yields α -acyloxy amides (**81**).^[261] In 1959, Ugi reported the formation of *bis*-amides (**83**) *via* reaction of **66**, **79**, **80**, and an amine (**82**).^[262] Interestingly, the Ugi-reaction is considered the aza-analogue of the Passerini-reaction. Besides the above

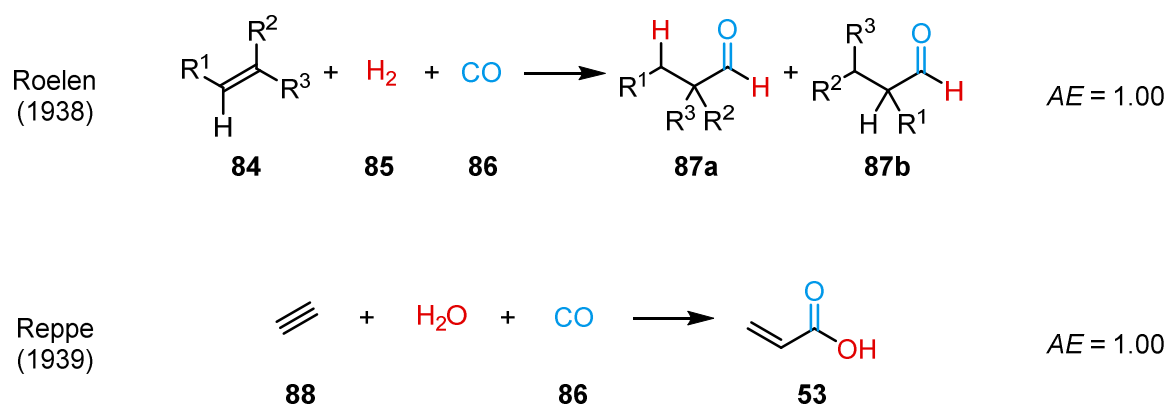
mentioned examples, further examples of MCRs such as the Orriu-2-imidazoline synthesis or the Passerini-Dömling-thiazole synthesis have been reported until today.^[248,263–266]



Scheme 2.22 Two examples for isocyanide-based MCRs are given with the names of the lead authors in the respective publication, year of publication, and an example *AE*; the *AE* was calculated using $\text{R}^x = \text{CH}_3$ and $\text{X} = \text{Cl}$.^[261,262]

MCRs have also been applied industrially (**Scheme 2.23**). Important examples are carbonylation reactions using metal catalysts. The hydroformylation of alkenes (**84**) was discovered in 1938 by Roelen^[267] and is one of the largest homogeneous catalytic processes applied industrially *e.g.* by the BASF.^[268] In 1939, Reppe reported on the hydrocarboxylation of alkynes with CO (**86**) and water, representing an important pathway for the synthesis of acrylic acid (**53**) among other vinyl compounds.^[246,269]

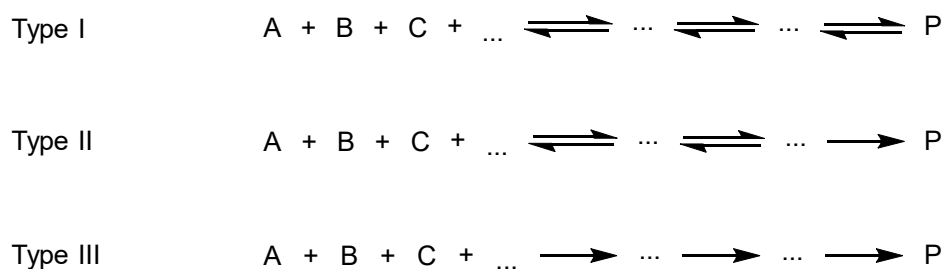
2.7 Multicomponent Reactions



Scheme 2.23 Two examples industrially applied MCRs are given with the names of the lead authors in the respective publication, year of publication, and an example AE ; the AE was calculated using $R^x = \text{CH}_3$.^[267,269]

MCRs are typically categorised regarding the reversibility of the steps of the underlying reaction mechanism. Three types of MCRs are distinguished (**Scheme 2.24**).^[270] Type I MCRs proceed *via* equilibrium reactions between starting materials, intermediates, and products. An example is the above mentioned Strecker synthesis.^[270] For Type II MCRs, the last reaction step is irreversible which usually leads to higher yields in accordance to the principle of Le Chatelier.⁴^[270] Examples are the Passerini-3-component reaction, the Ugi-4-component reaction or MCRs in which heterocyclic compounds are formed.^[271] Type III MCRs proceed *via* a sequence of practically irreversible reactions.^[270] While only a few procedures involving Type III MCRs are known,^[249] they often occur in biological systems due to the efficiency and selectivity of enzyme catalysis.^[249,272] In addition, the assignment to a particular type might be revised over time if further insight into the reaction mechanism of the respective MCR is gained.

⁴ The principle of Le Chatelier describes a general behaviour of equilibrium reactions if exposed to a particular stimulus. Accordingly, the reaction equilibrium will shift in a way to counteract the stimulus. This holds true for concentration, pressure, temperature *etc.* For example, if one of the products is removed from the equilibrium reaction, more starting materials will react to counteract the reduced concentration of the product.



Scheme 2.24 Categorisation of multicomponent reactions into three types according to the reversibility of the mechanistic steps.^[270]

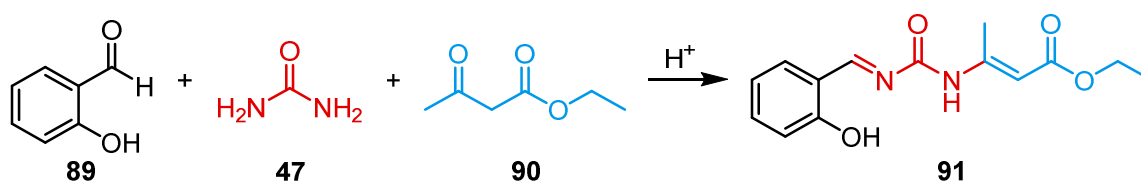
2.7.1 The Biginelli-3-Component Reaction

Within this chapter, the Biginelli-three-component reaction (B-3CR) will be discussed in detail due to its importance within this work. First, the ongoing debate regarding the actual reaction mechanism is discussed. Second, the possible structural variations of the components are displayed. Third, reports that investigate the B-3CR as a tool for polymer science are reviewed.

2.7.1.1 Mechanistic Discussion and the Currently Accepted Iminium Route

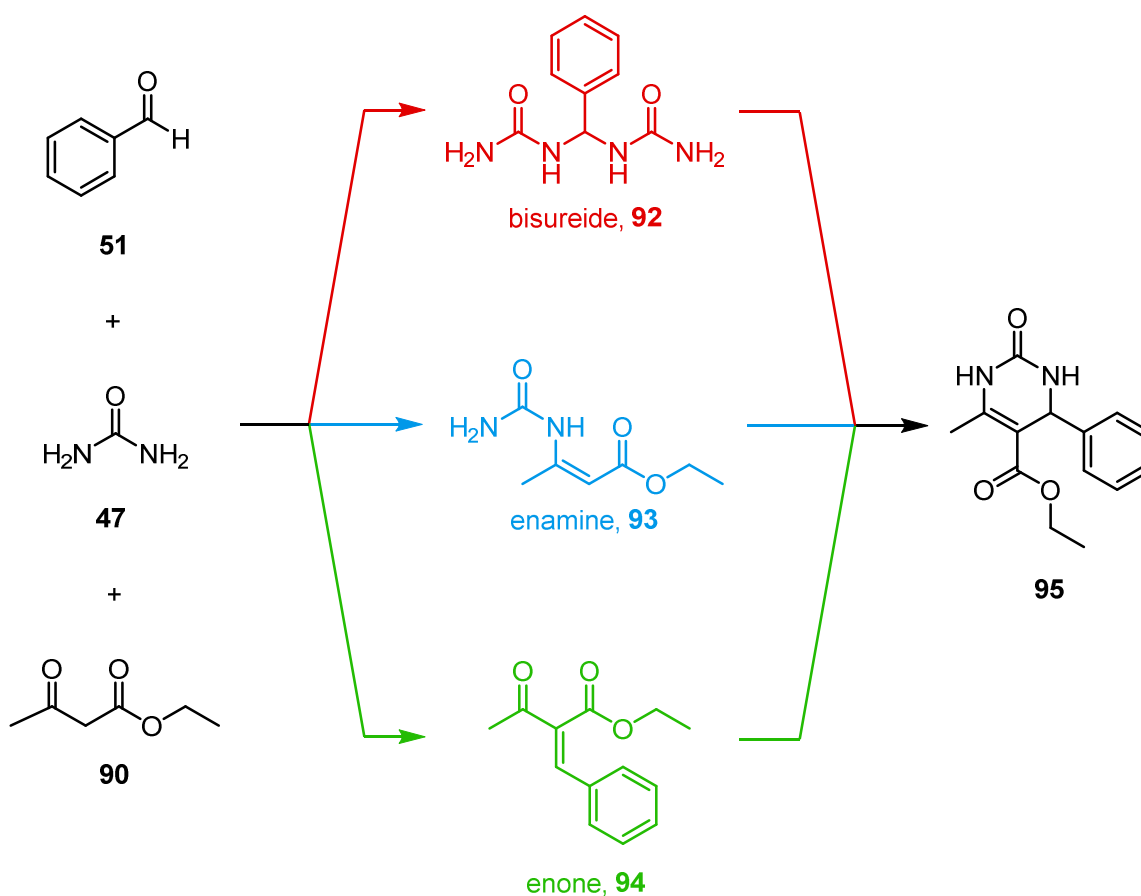
In 1891, the Italian chemist Pietro Biginelli observed the formation of a precipitate during the reaction of salicylaldehyde (**89**), urea (**47**), and ethyl acetoacetate (**90**) in the presence of hydrochloric acid in an ethanolic solution under reflux.^[257] The initially proposed molecular structure of the precipitate was an open chain β -ureidocrotonate (**91**) (**Scheme 2.25**).^[257] However, the structure elucidation was revised by Biginelli shortly after, identifying the reaction product as 3,4-dihydropyrimidin-2(1*H*)-one (DHPM, **74** (*cf.* **Scheme 2.21**, page 48)).^[273]

2.7 Multicomponent Reactions



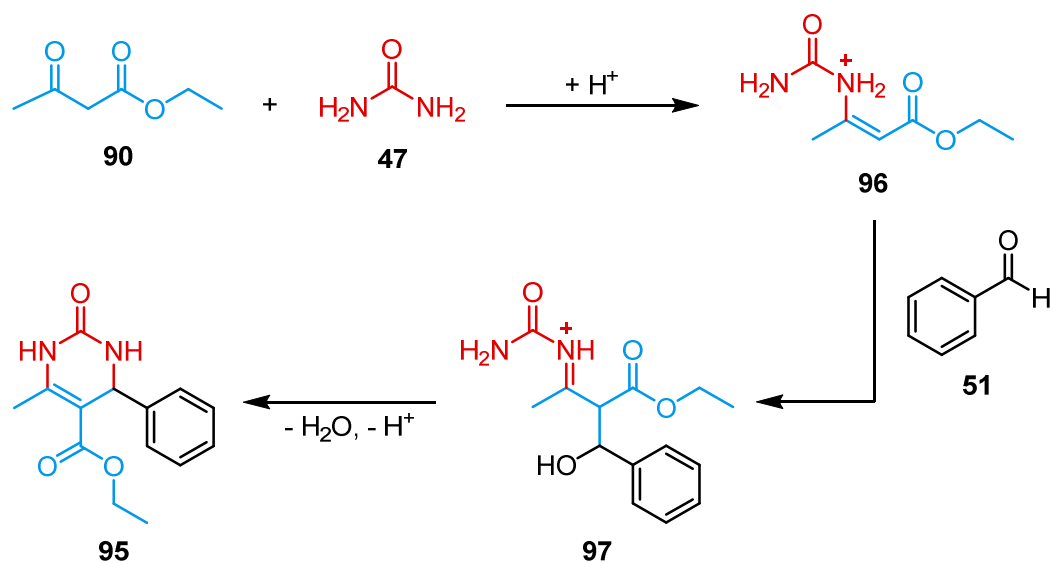
Scheme 2.25 The first Biginelli-three-component reaction yielding the proposed open chain β -ureidocrotonate as originally reported by Biginelli in 1891.^[257]

The reaction mechanism of the B-3CR has been debated for a long time. There are currently three different proposed reaction pathways, namely the enamine-, the imine-, and the Knoevenagel-mechanism which have been investigated in the presence of a Brønsted acid.^[274] First investigations on the mechanism of the B-3CR were published by in 1933 by Folkers and Johnson.^[275] They investigated the reaction of benzaldehyde (**51**), **47**, and **90** which are considered the standard components for the B-3CR.^[275] The authors suggested the intermediate formation of three possible adducts *via* different combinations of the starting materials (**Scheme 2.26**): addition of two urea molecules and benzaldehyde to a bisureide, reaction of urea with ethyl acetoacetate to an enamine, or the Knoevenagel reaction of benzaldehyde and ethyl acetoacetate to an enone.^[275]



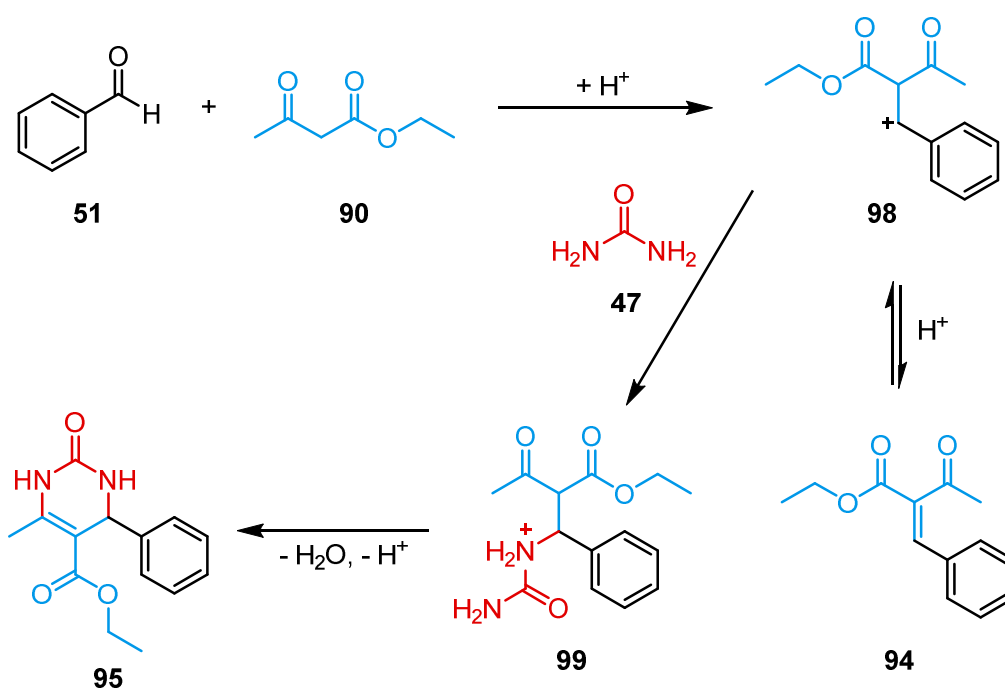
Scheme 2.26 The three possible primary reaction intermediates of a Biginelli-three-component reaction as proposed by Folkers and Johnson: a bisureide (red), an enamine (blue), or an enone (green).^[275]

Finally, the authors favoured the enamine route according to their finding that a DHPM is readily formed from a separately synthesised enamine but not from any other proposed intermediate (**Scheme 2.27**).^[275] Catalysed by a Brønsted acid, this route was proposed to proceed *via* formation of an enammonium species (**96**) that further reacts with **51** to an iminium species (**97**) subsequently undergoing cyclocondensation to **95**.^[275]



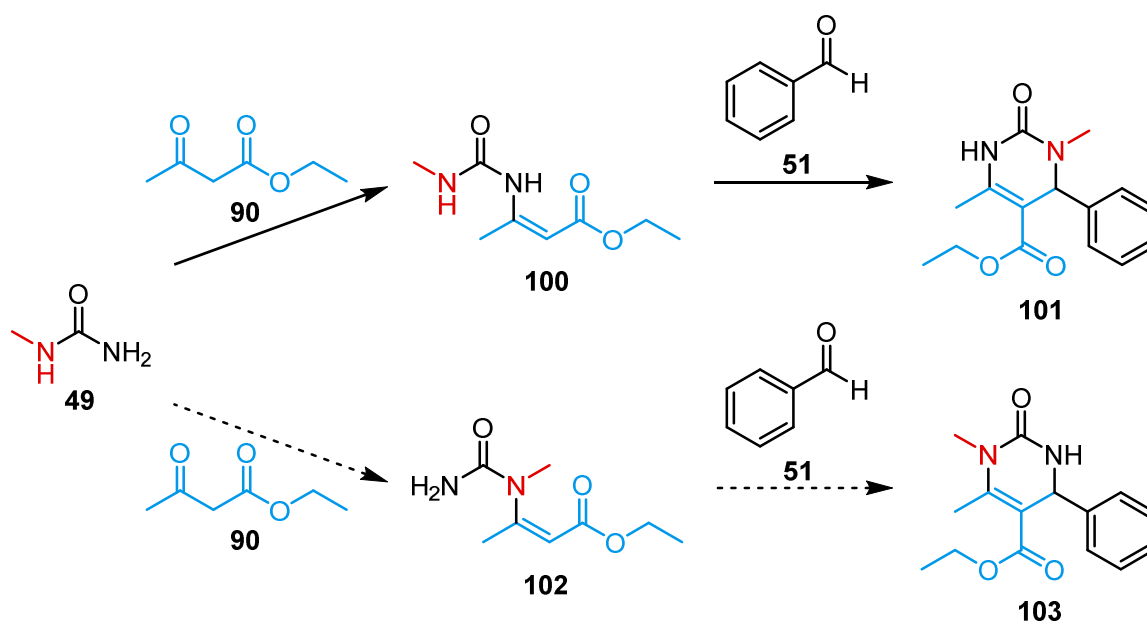
Scheme 2.27 Suggested enamine mechanism for the Biginelli-three-component reaction.^[275]

The Knoevenagel mechanism was further investigated in 1973 by Sweet and Fissekis (**Scheme 2.28**).^[276] They suggested the formation of a carbenium ion (**98**) *via* the acid catalysed reaction of **51** and **90** as a first and rate-determining step.^[276] **98** is converted in an acid catalysed equilibrium reaction to enone **94** (the Knoevenagel product) while **98** reacts to form the final DHPM **95** in the presence of **47**.^[276] The main evidence for this reaction mechanism was the formation of **95** *via* reaction of separately synthesised **94** and **47** in the presence of an acid.^[276] However, instead of evidence for the Knoevenagel-mechanism, rather contradictory findings were reported.



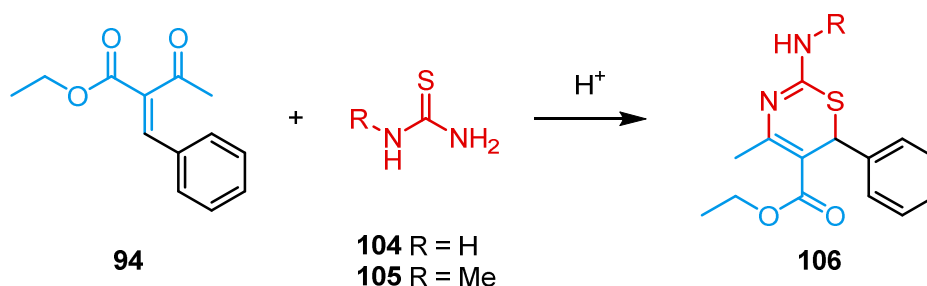
Scheme 2.28 Suggested Knoevenagel-mechanism for the Biginelli-three-component reaction.^[276]

In 1997, Kappe re-examined the previously proposed mechanisms *via* nuclear magnetic resonance (NMR) spectroscopy using the HCl catalysed reaction of benzaldehyde, urea, and ethyl acetoacetate as test system.^[277] To verify the enamine-mechanism, the proposed enamine intermediate **93** was separately synthesised under anhydrous conditions,^[277] since the sensitivity of **93** to hydrolysis had already been reported.^[275] Afterwards, the quick hydrolysis of **93** under the conditions for a B-3CR was reported leading to the conclusion that the equilibrium reaction to **93** is far on the side of the starting materials **47** and **90**. In addition, the reaction of *N*-methylurea (**49**) under anhydrous conditions yields the regioisomer **100** which led to the *N*3-substituted DHPM **101** and not the *N*1-substituted DHPM **103** that is obtained *via* the B-3CR (**Scheme 2.29**).^[277] As a consequence, Kappe dismissed this mechanism.^[277]



Scheme 2.29 Results of the separate enamine formation and subsequent reaction towards a DHPM: only the enamine **100** was accessible which led to DHPM **101**. **101** differs in the position of the Me-N group from **103**, which is solely formed by direct B-3CR of **49**, **90**, and **51**;^[277] the position of the methyl group of interest is drawn in red.

To verify the Knoevenagel mechanism, benzaldehyde and ethyl acetoacetate were reacted under standard reaction conditions for a B-3CR. However, no evidence for the formation of the aldol or any other reaction between benzaldehyde and ethyl acetoacetate was found.^[277] In addition, it is known that the B-3CR proceeds as expected if **47** is substituted with thiourea (**104**) or *N*-methylthiourea (**105**).^[278] However, if separately prepared **94** is reacted with **104** or **105**, solely the isomeric products, the 2-amino-1,3-thiazines (**106**), are obtained (Scheme 2.30).^[277] Consequently, the Knoevenagel mechanism was also dismissed.^[277]



Scheme 2.30 Reaction of separately prepared **94** with **104** or **105** led to the formation of **106**, a regioisomer of the targeted DHPM.^[277]

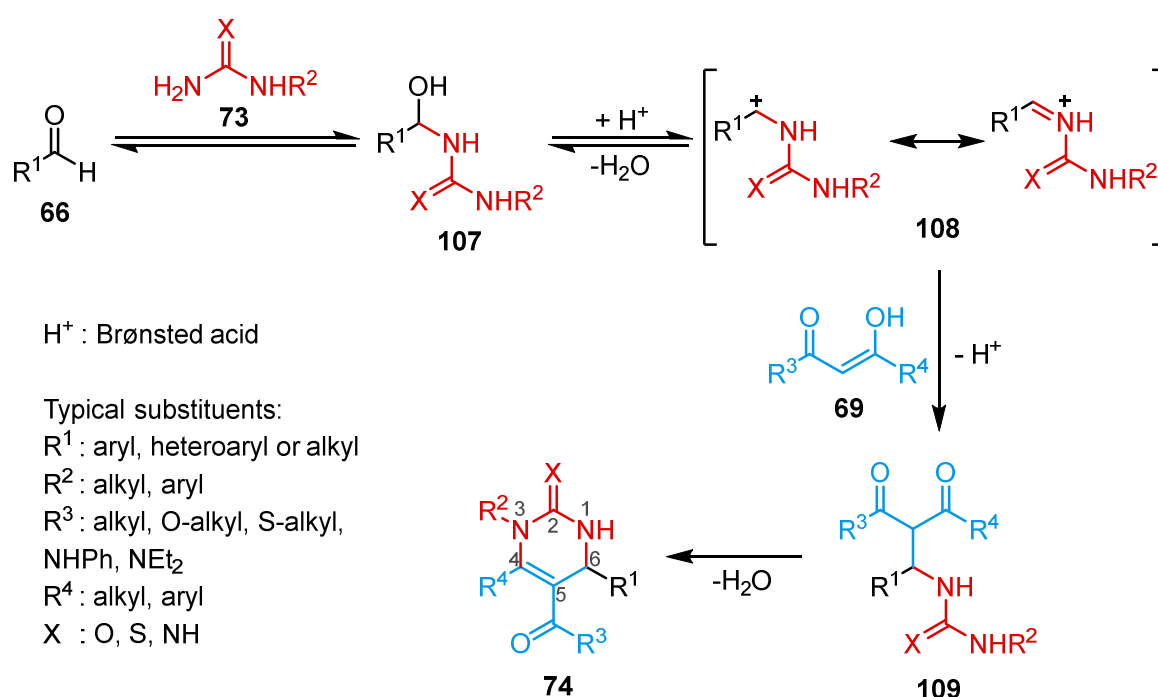
The bisureide mechanism was also re-examined. First, Kappe investigated the reaction of equimolar ratios of **51** with **47** or **49** in the presence of an acid.^[277] The formation of the proposed bisureide (**92**)^[275] in high yields was confirmed after 10 min.^[277] Second, if **90** was added to the reaction mixture, **92** was not detected while the corresponding DHPM was formed. As a consequence, Kappe suggested, just as Folkers and Johnson had, that the reaction of **51** and **47** or **49** to be the first step of the mechanism.

However, the formed hemiaminal was proposed to subsequently dehydrate to a highly reactive iminium species which is intercepted by **90** leading to the DHPM, while in the absence of **90**, a second addition of urea to the bisureide takes place.^[277] The above described findings were supported by density functional theory (DFT) calculations and online electron spray ionization mass spectrometry (ESI-MS).^[279] Interestingly, the iminium mechanism was reported to be thermodynamically and kinetically favoured under Brønsted acid catalysis.^[279] Further combined experimental and theoretical studies regarding the mechanism *via* Brønsted acid and Lewis acid catalysis provided further evidence for the iminium mechanism.^[280,281]

This is, however, contradictory to experimental investigations which indicated that the reaction proceeds *via* the enamine pathway if Lewis acid catalysts are applied.^[282,283] In the end, the underlying mechanism of the B-3CR is not yet fully understood. Mechanistic details are still under investigation, particularly regarding the catalyst-free B-3CR,^[284,285] the more unique Brønsted base catalysed variant,^[286,287] and solvent effects.^[284]

2.7 Multicomponent Reactions

The Brønsted acid-catalysed B-3CRs performed within this work are currently assumed to proceed according to the iminium mechanism (**Scheme 2.31**). The first step of the mechanism is the nucleophilic addition of a urea compound (**73**) to an aromatic or aliphatic aldehyde (**66**). The resulting hemiaminal (**107**) undergoes acid promoted dehydration to an iminium species (**108**). The following step is the nucleophilic addition of the 1,3-dicarbonyl compound (**69**) to the iminium carbon of **108**. The resulting adduct (**109**) undergoes cyclocondensation to the final DHPM (**75**).



Scheme 2.31 Commonly accepted mechanism for the Brønsted acid-catalysed Biginelli-three-component reaction *via* the iminium intermediate **107** alongside common substituents of the components.^[277,288–290]

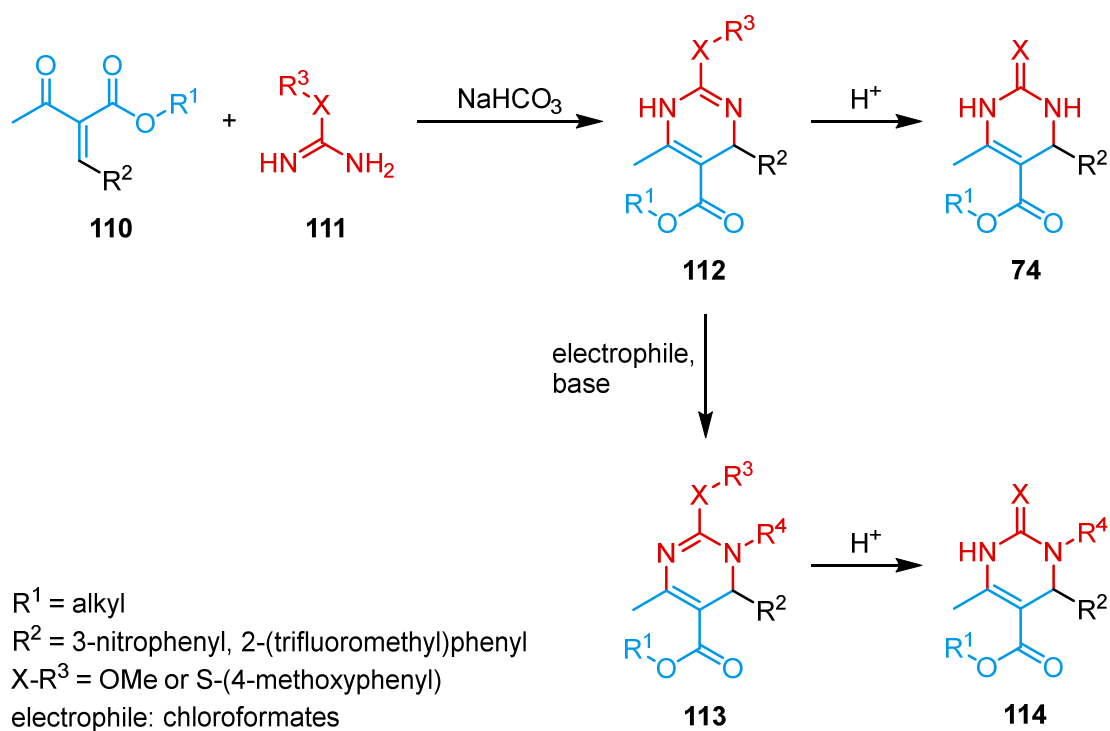
Kappe has presented strong evidence for the currently accepted mechanism of the Brønsted acid-catalysed B-3CRs. Nonetheless, the dependence of the mechanism especially on the type of catalyst or the applied reaction conditions/solvents is still under debate and not fully understood yet.

2.7.1.2 Structural Variations and Applied Catalysts/Catalytic Systems

MCRs such as the B-3CR are well known for the variability of the applied components. While MCRs are, indeed, flexible in terms of non-participating functional groups, there are limits. Within this chapter, these limits will be pointed out and the structural diversity will be illustrated.

The structural variations of the components that are applicable for a B-3CR are manifold. The aldehyde component is reported as the most flexible regarding the substituents. However, aromatic aldehydes are generally advantageous since the iminium intermediate (*cf.* **Scheme 2.31**, page 58) is stabilised *via* resonance with the aromatic system.^[277] The aromatic system may comprise different ring sizes, heteroaromatic cycles, and condensed systems and carry *ortho*- *meta*- and/or *para*-substituents of either electron withdrawing or electron donating nature.^[288–290]

Nonetheless, aliphatic aldehydes are also suitable but are reported to react slower and provide smaller yields compared to aromatic aldehydes.^[288–290] In addition, bulky substituents on the *o*-position of aromatic aldehydes were reported to lower the yields as well.^[288–290] However, a procedure called Atwal-modification was reported to yield **74** from aliphatic and sterically demanding aldehydes in larger quantities, compared to the classical B-3CR (**Scheme 2.32**).^[291] In addition, the synthesis of *N*3-substituted DHPMs (**114**) was shown.^[292] This procedure starts with the condensation of a separately prepared enone (**110**) and a protected urea compound (**111**) yielding a 1,4-dihydropyrimidine (**112**).^[292,291] The latter is converted to the respective DHPM *via* deprotection under acidic conditions.^[292,291] **114** was obtained by addition of an electrophile to the *N*3-position of **112** and subsequent deprotection.^[292]



Scheme 2.32 Atwal procedure for the synthesis of *N*3-substituted DHPMs through the efficient incorporation of aliphatic/sterically demanding aldehydes.^[292,291]

The C-H-acidic component is typically an 1,3-dicarbonyl like a β -keto ester, β -keto amide, β -keto thioester, or a 1,3-diketone.^[288–290] However, cyclic 1,3-dicarbonyls and ketones that carry an electron withdrawing substituent in α -position are reported as well, among others.^[288–290]

Most restricted are variations of the urea compound, thus, most commonly, urea itself is used.^[289] Nonetheless, simple *N*-mono-substituted ureas, thioureas, or guanidines are reported as well.^[289,290] Moreover, heterocyclic systems like diazoles, triazoles and tetrazoles have also been reported B-3CRs.^[290]

Within the last decades, a broad spectrum of catalysts and catalytic systems for the efficient synthesis of DHPMs was published. Well established examples are strong mineral acids like HCl or H₂SO₄. Nonetheless, many other Brønsted acids like acetic acid,^[275]

amidosulfonic acid,^[293] ammonium chloride,^[294] phytic acid,^[295] or *p*-toluenesulfonic^[296] acid, to mention a few, were published.

While the mechanism of Lewis acid catalysts is still debated, their performance in B-3CRs has been verified. Hundreds of different Lewis acids, mainly halides and triflates of lithium,^[297] alkaline earth metals,^[298–301] transition metals (mainly of the 4th period),^[302–306] lanthanides,^[307–309] and metals of group 13^[310] and 14^[311] were reported to increase the yield of B-3CRs at reduced reaction times. In addition, ionic liquids were reported to provide a new class of efficient catalysts for the synthesis of DHPMs, be it Brønsted acidic ionic liquids like [1-*n*-butyl-3-methylimidazolium][HSO₄],^[312] Lewis acidic ionic liquids like [1-*n*-butyl-3-methylimidazolium][FeCl₄],^[313] or immobilized ionic liquids.^[314]

Finally, B-3CRs were shown to be catalysed by different polymer-supported catalysts,^[315] ion exchange resins,^[315] acidic clays,^[316–318] and heteropolyacids,^[319] nanoparticles,^[320] and enzymes.^[321,322] More comprehensive collections of reported catalysts for the B-3CR are available elsewhere.^[288–290,315,316,323–325]

Last but not least, enantioselective B-3CRs are possible with chiral groups attached to the catalyst giving stereocontrol over the substituent at the inherently asymmetric C4. Since DHPMs are frequently applied as pharmaceutical compounds and the absolute configuration determines the pharmaceutical activity, enantioselective B-3CRs are of great interest.^[326] Despite the progress that has been made, the enantioselective B-3CR still suffers from drawbacks like low yields or long reaction times.^[325] Examples for suiting catalytic systems are chiral phosphoric acids (carrying a binaphthyl group or related substituents),^[327] asymmetric ytterbium-based Lewis acids or chiral acidic ionic liquids.^[328,329] In addition, most catalytic systems use achiral Brønsted acids together with chiral promoters as co-catalyst.^[325]

Finally, the B-3CR is a highly flexible MCR allowing for the synthesis of a manifold of different compounds. Moreover, suiting catalysts/catalytic systems enable the enantioselective synthesis of DHPMs *via* enantioinduction.

2.7.1.3 Applications of 3,4-dihydropyrimidin-2(1H)-ones

As mentioned above, DHPMs are mainly investigated for their biological activity and are, thus, frequently applied in the pharmaceutical industry. Several reviews were published covering the scope of structural diversity and the resulting biological activity.^[330–332] The most important drug classes include anti-cancer and anti-human-immunodeficiency-virus medication (anti-HIV medication), calcium channel blockers (to treat for example inflammation or hypertension), and antimicrobials (**Figure 2.5**).^[330–332]

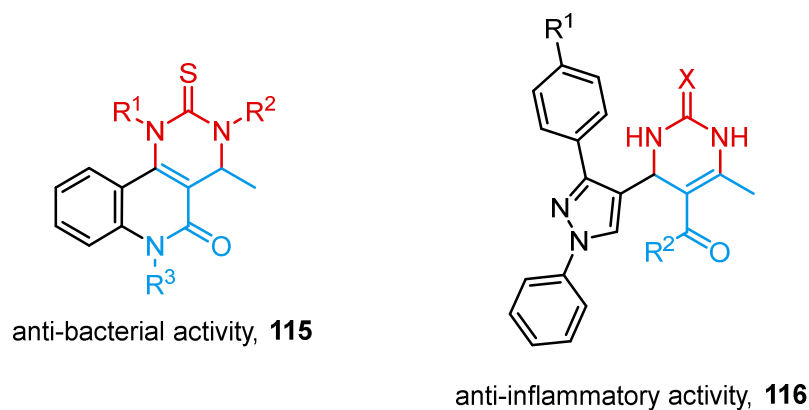


Figure 2.5 Generic DHPM structures with anti-bacterial (**115**) and anti-inflammatory (**116**) effects.^[330]

Furthermore, the interest in the B-3CR as a tool for polymer science has been of growing since the last decade. The application of the B-3CR in the field of polymer chemistry will be covered in detail in the following chapter.

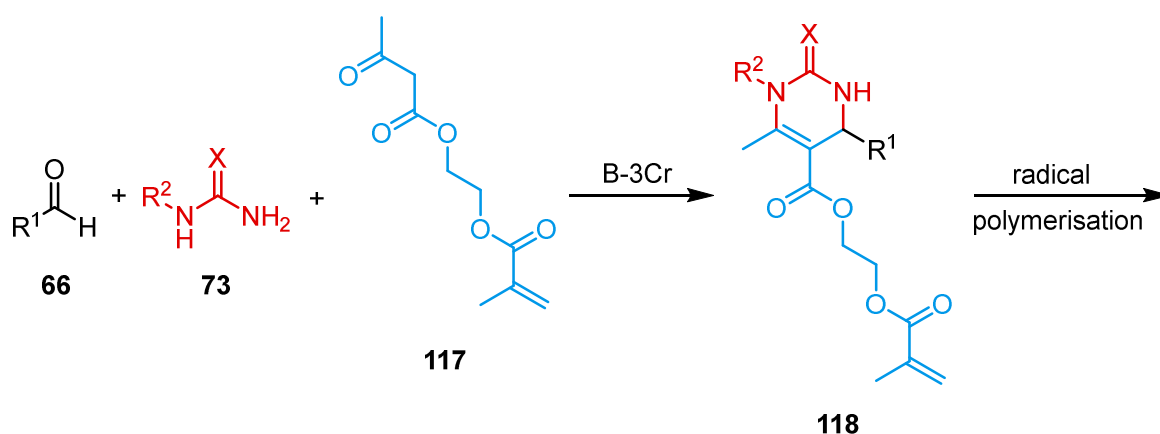
2.7.2 The Biginelli-3-Component reaction in the Field of Polymer Chemistry

The unique features of the DHPM structure as well as the efficiency and tolerance against many functional groups of the B-3CR render it an interesting tool for the synthesis of novel and useful polymeric materials. However, the B-3CR has only been applied in the field of polymer chemistry in the last decade, with the groups of Tao and Meier providing

the largest part of the available reports. The contributing publications were summarised in four reviews.^[333–336] There are, in general, four approaches for the application of the B-3CR for the preparation of new functional macromolecules: synthesis of polymerisable monomers that carry the DHPM motif, post-polymerisation modification (PPM), synthesis of copolymers using the efficiency of the B-3CR to link several homopolymers, and synthesis of Biginelli-polycondensates from suitable bifunctional monomers. These four approaches will now be discussed separately.

2.7.2.1 Radical Polymerisation of Monomers Containing a Dihydropyrimidinone Functionality

To date, all reports that use DHPM-carrying monomers used 2-acetoacetoxyethyl methacrylate (**117**) as precursor molecule. The acetoacetoxy-function was converted into different DHPM structures prior to subsequent polymerisation of the methacrylate function of **118** to polymethacrylates carrying the respective DHPM (**Scheme 2.33**). Typically, free radical polymerisation (FRP) or reversible addition-fragmentation chain transfer (RAFT) polymerisation was used.



Scheme 2.33 Synthesis of a DHPM-carrying methacrylate that is subsequently polymerised using FRP or RAFT polymerisation.

In 2018, a library of 25 potentially UV-protective polymethacrylates was synthesised using various biobased hydroxy/methoxy substituted benzaldehydes using **73**.^[337] The most promising monomers were copolymerised with poly(ethylene glycol) methyl ether methacrylate resulting in water-soluble and biocompatible UV-protective copolymers.^[337] The UV-protection was shown to arise from the ability of the dihydropyrimidine-thione moiety to act as a radical scavenger.^[337] Later, an improved version of the UV-protective polymers, was published.^[338] Here, the authors reacted the dihydropyrimidine-thione moieties of the polymer with α -chloro alkynes to form conjugated, fluorescent structures that showed strong absorption bands in the UV-range.^[338] In addition, a biocompatible hydrogel with additional antioxidant properties was reported.^[339] The antioxidant properties arose from the above mentioned ability to scavenge radical species.^[339] The DHPM containing monomer was synthesised from **117**, 4-formylphenyl boronic acid and thiourea (**104**) and was copolymerised with poly(ethylene glycol) methyl ether methacrylate to yield a water-soluble copolymer.^[339] When mixed with poly(vinyl alcohol), the mixture quickly formed a dynamic gel *via* the reversible formation of boronate esters from the boronic acid and the alcohol moieties.^[339,340]

Using RAFT to polymerise the methacrylate function, it was demonstrated that the conversion of **117** to **118** was possible in a one-pot procedure in parallel to the polymerisation.^[341] This method was applied in the one-pot synthesis of a fluorescent copolymer from **117**, urea, 4-(1,2,2-triphenylvinyl) benzaldehyde, and poly(ethylene glycol) methyl ether methacrylate.^[342] The resulting copolymer was applied for cell imaging purposes due to the fluorescence of the triphenylvinyl moiety.^[342]

The reports of polymerisations of monomers that carry the DHPM group were, as of today, limited to the use of methacrylates. In addition, the investigated field of application was mainly focussed on biomedical applications exploiting the radical scavenging properties of the prepared materials.

2.7.2.2 Post-Polymerisation Modification using the Biginelli-Three-Component Reaction

Post-polymerisation modification (PPM) describes the conversion of functional groups of a polymer after polymerisation and is a widely applied method that has been known since 1840.^[343] Such modifications are especially useful if the desired functionality is not synthesisable in the monomer due to incompatible reactivities or if it interferes with the polymerisation process.

Most reports about the PPM approach start, similar to the monomer approach, with **117** or 2-acetoacetoxyethyl acrylamide. However, the acetoacetoxy function is converted to the DHPM after the polymerisation. Hence, the synthesis of a polymer library *via* RAFT-mediated block copolymerisation of 2-acetoacetoxyethyl acrylamide, *N,N*-dimethyl acrylamide, and 4-acryloylmorpholine was reported.^[344] The resulting six block copolymers were converted *via* the B-3CR into 60 different polymers and subsequently screened for various properties presenting the combination of RAFT and subsequent B-3CR as useful high throughput method to quickly screen polymer libraries.^[344]

Furthermore, **117** was copolymerised with acrylic acid *via* RAFT polymerisation.^[345] In the following B-3CR, a fluorescent dye was added as the aldehyde component.^[345] The final copolymer was applied for cell imaging purposes.^[345] In addition, a water-soluble metal adhesive was synthesised by block copolymerisation of **117** and poly(ethylene glycol) methyl ether methacrylate and subsequent B-3CR using urea and benzaldehyde, 4-hydroxy benzaldehyde, or 4-formylphenyl boronic acid.^[346] The adhesive properties are reported to arise from interactions between the DHPM moiety and the metal surface without further explanation.^[346]

The PPM approach was moreover used to increase the solubility of carbon nanotubes.^[347] Poly(*N*-isopropylacrylamide) was synthesised *via* RAFT polymerisation using a chain transfer agent that carried an acetoacetoxy group.^[347] The latter was reacted in a B-3CR with urea and 1-formylpyrene.^[347] As a consequence, the end groups of the poly(*N*-isopropylacrylamide) carried the DHPM. The poly(*N*-isopropylacrylamide) was

bound to carbon nanotubes *via* π - π -interactions of the pyrene-moiety and the graphene structure.^[347]

Last but not least, the natural polymers cellulose^[348] and starch^[349] have been modified using the B-3CR. In both reports, acetoacetate groups were first introduced to the carbohydrate scaffold.^[348,349] Second, the acetoacetate groups were reacted in a B-3CR with urea and several aromatic aldehydes.^[348,349] The resulting polymers showed increased solubility and processability.^[348,349]

The use of the B-3CR to couple two homopolymers was also reported for two poly(ethylene glycol) monomethyl ether chains, one carrying an aromatic aldehyde and one an acetoacetamide.^[341] The polymers were efficiently coupled with urea in the presence of a LEWIS acid with almost quantitative yields to demonstrate the similarities of the B-3CR to click reactions.^[341,350]

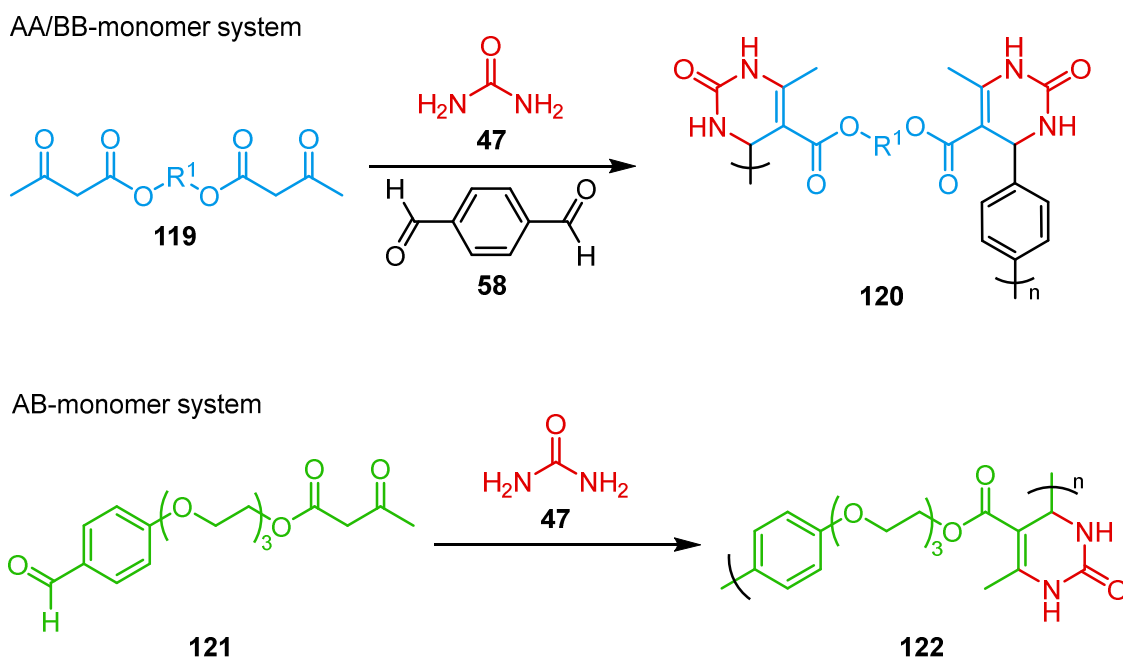
Hence, PPM using the B-3CR was shown to be a versatile tool for the synthesis of a variety of functional monomers being compatible with different polymer structures. This approach was mainly applied to improve the solubility of typically insoluble materials and to alter material properties.

2.7.2.3 Synthesis of Polycondensates Using the Biginelli-Three-Component Reaction

The last approach covers the synthesis of Biginelli-polycondensates using suitable bifunctional monomers. Hence, the DHPMs are connected forming the polymer backbone. Here, AA- and BB-monomers (dialdehydes and monomers with two C-H acidic functional groups) or AB-monomers (monomers that carry an aldehyde function and a C-H acidic group) are used as bifunctional components due to their better availability, compared to bifunctional urea compounds (**Scheme 2.34**).

Tao *et al.* prepared three different AB-monomers that were directly polymerised with urea in the presence of MgCl₂ between two metal plates, strongly gluing them together.^[351] As mentioned in above section, this effect arises from strong interactions between the

DHPM moiety and the metal surface. In addition, an AA/BB-monomer system was applied together with urea and thiourea to synthesise a library of 64 Biginelli-polycondensates to predict the glass transition temperature (T_g) of Biginelli-polycondensates within the mapped spectrum of compounds was good accuracy.^[352]



Scheme 2.34 Two possible monomer systems for the synthesis of Biginelli-polycondensates: example of an AA/BB-monomer system as applied by Meier *et al.* and an AB-monomer system as applied by Tao *et al.*^[353,351]

Moreover, Tao *et al.* reported on the synthesis of a statistical copolycondensate using the Hantzsch dihydropyridine synthesis and the B-3CR in one pot.^[354] Furthermore, the PPM of Biginelli-polycondensates which contain a thiourea moiety was reported.^[355] The authors reacted the thiourea moiety either with haloalkanes or α -chloro alkynes.^[355] Finally, Meier *et al.* reported on a series of renewable Biginelli-polycondensates with tuneable and high T_g s up to 203°C.^[353] They applied different diacetoacetates, terephthalic aldehyde (**58**) or divanillin together with urea in a Brønsted acid-catalysed polycondensation.^[356]

Not fitting to one of the above mentioned approaches, small DHPMs were blended with poly(butyl acrylate-*co*-methyl methacrylate).^[357] Polymer-coated glass plates showed an increased water resistance if coated with the blend compared to pure poly(butyl acrylate-*co*-methyl methacrylate).^[357]

In the end, the reports that cover the application of the B-3CR in the field of polymer chemistry are still rather limited. As an example, block copolymers containing the DHPM group have not been investigated as of today. In addition, the applied urea compounds have been limited to urea and thiourea. As a consequence, the versatile B-3CR offers interesting opportunities for further investigations.

3 Aim

Within this thesis, the synthesis of novel and renewable polymer structures was investigated. More precisely, the Biginelli-three-component (B-3CR) reaction was applied in three different ways within the field of polymer chemistry. The components for a B-3CR are available from renewable resources and the reaction itself is considered rather sustainable as per the characteristics of a sustainable process defined in chapter 2.2. Being a multicomponent reaction, the variability of the components was exploited to determine structure-property relationships.

First, a set of bifunctional components was applied for the B-3CR to yield a library of Biginelli polycondensates expanding the reported set of components and resulting polymer structures (chapter 4.1). For this purpose, the synthesis of various diacetoacetates and their subsequent reaction with terephthalic aldehyde and urea or *N*-methyl urea was investigated and optimised. The resulting polycondensates are compared with regard to their molecular weights and thermal properties.

Second, the synthesis of novel block copolymers containing a Biginelli polycondensate was investigated (chapter 4.2). There, a terminal double bond is introduced as endgroup to the Biginelli polycondensate using a monoacetoacetate that carries the terminal double bond. The influence of the amount of monoacetoacetate on the molecular weight as well as the efficiency of the incorporation of monoacetoacetate was examined. Subsequently, the synthesis of block copolymers was conducted by polymer-polymer coupling of the Biginelli polycondensates with poly(ethylene glycol) methyl ether thiol through the thiol-ene reaction. The thermal properties of the resulting block copolymers was explored.

Third, the synthesis of novel renewable vinyl ester monomers and a methacrylate monomer was attempted (chapter 4.3). These monomers were equipped with an acetoacetate functionality to allow for post-polymerisation modification (PPM) using the B-3CR. Consequently, the radical polymerisation behaviour of these monomers *via* FRP and RAFT polymerisation was investigated. Crucially, the control of the RAFT process was assessed

by testing the end-group retention in the polymers by chain extension and copolymerisation experiments. Finally, the resulting RAFT polymers are modified by the B-3CR.

To summarise, the versatility of the B-3CR as an efficient tool for polymer chemistry was examined and expanded throughout this work whilst ensuring that all processes are carried out with as much respect to the Green Chemistry principles as reasonably feasible.

4 Results and Discussion

As discussed in chapter 2.7.2, the B-3CR has been applied in manifold ways in the field of polymer chemistry. Within this thesis, the scope of reported Biginelli-homopolycondensates was expanded by new components. In addition, new block copolymers were synthesised *via* end group functionalisation of homopolycondensates with subsequent thiol-ene reactions. Last but not least, novel fatty acid-based vinyl monomers carrying an acetoacetate group for a possible post-polymerisation modification (PPM) *via* the B-3CR were produced and polymerised *via* radical polymerisation techniques.

4.1 Synthesis of New Biginelli Homopolycondensates: Renewable Materials with Tuneable High Glass Transition Temperatures

Parts of this chapter and the associated chapters of the experimental section (6.1, 6.2, 6.3) were already published in:

J. T. Windbiel, M. A. R. Meier, *Polym Int*, **2020 // 2021**, *70*, 506. © 2020 Polymer International published by John Wiley & Sons Ltd on behalf of Society of Industrial Chemistry. DOI: 10.1002/pi.6106

Some of the experiments were carried out by Josina Bohlen and are featured in her bachelor's thesis.^[358] These will be clearly indicated.

4.1.1 Abstract

Biginelli polycondensates have been prepared from various diacetoacetates, aromatic dialdehydes, and urea (**47**) or thiourea (**104**). AB-monomers carrying, both, an acetoacetate and an aldehyde group have also been used (*cf.* chapter 2.7.2.3). However, the variations of the starting materials are strongly limited, compared to the components used for small DHPMs. Within this chapter, we introduce new components to the Biginelli polycondensation and investigate the properties of the resulting polycondensates. Hence,

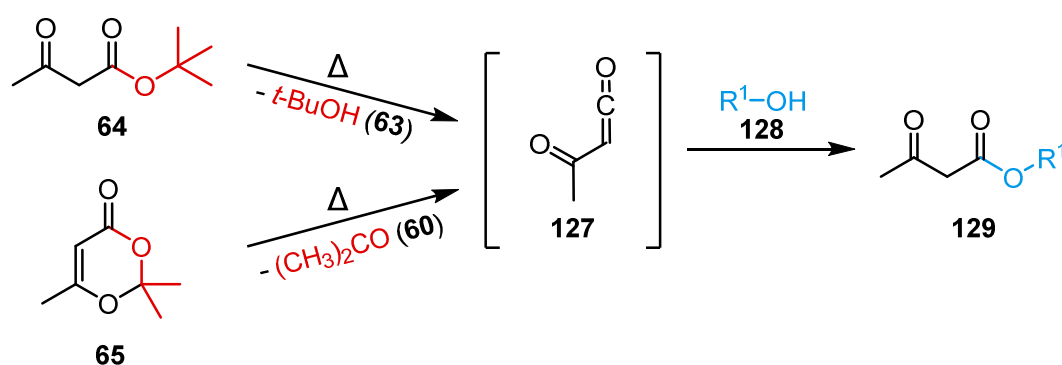
the synthesis of a set of 15 new and fully renewable poly[3,4-dihydropyrimidin-2(1*H*)-one]s (polyDHPMs) is described. One of six diacetoacetates or three diacetoacetamides (AA-monomers), terephthalic aldehyde (**58**) (BB-monomer) and **47** or *N*-methylurea (**49**) were used as renewable starting materials in various combinations, hence significantly expanding the known set of monomers, as well as polymer structures. The existing set includes **47**, thio-urea (**104**), **58**, divanillin, and diacetoacetates^[353,352] besides several AB-monomers.^[351,354] More precisely, we introduce *N*-methylurea, three diacetoacetates as well as three diacetoacetamides to this set of starting materials. The diacetoacetates and diacetoacetamides with different spacer lengths were synthesised in yields up to 99% in a one-step process. The used starting materials are all available from renewable resources as discussed in chapter 2.6.1 – 2.6.5. All obtained polyDHPMs were fully characterised. Thermal analysis of the obtained set of polymers revealed high T_g s ranging from 160°C to 308°C. The T_g was tuneable in small steps of 10°C by simple variation of diacetoacetate or diacetoacetamide monomers as well as the choice between **47** and **49**. The polyDHPMs were thermally stable well above the respective high T_g values. The results demonstrate the straight forward variation of the components for the Biginelli polycondensation and enable the synthesis of renewable high T_g polymers.

4.1.2 Synthesis of Aliphatic Diacetoacetate and Diacetoacetamide Monomers

One of the components of the B-3CR is an CH-acidic reactant, in many cases a β -keto compound. In this work, 9 different β -keto compounds have been used. Their synthesis is described within this chapter. The other components were bought and used as received.

The reaction of diketene (**62**) with nucleophiles like alcohols or amines to form the respective β -keto compounds has been known for decades.^[221] The reaction is reported to proceed quickly and selectively under mild conditions.^[221] **62** is readily formed from ketene gas (**61**) in a thermal [2+2]-cycloaddition.^[359] However, **62** is lachrymatory, toxic and prone to self oligomerisation/polymerisation if stored longer than a week.^[215,216] As an alternative to **62**, acetylketene (**127**) was reported as potent reactant for the formation of β -keto

compounds. As **127** itself is highly reactive and unstable, several stable and less harmful precursors, compared to **62**, are known. Those decompose *in situ* to **127** at temperatures above 90°C (**Scheme 4.1**). Such precursors are 4*H*-1,3-dioxin-4-ones,^[360,361] *tert*-butyl acetoacetate (**64**),^[362] or Meldrum's acid.^[363] Simpler acetoacetates, like methyl or ethyl acetoacetate, were used for transacetoacetylations as well but showed 20-fold lower reactivity compared to **64**.^[362]



Scheme 4.1 Synthesis of acetoacetates (**129**) via the thermal *in situ* formation of acetylketene (**127**) using the precursors *tert*-butyl acetoacetate (**64**) or diketene acetone adduct (**65**) as an example.

To synthesise the diacetoacetate monomers **124a-f**, a literature procedure^[353] was optimised and simplified leading to yields between 98% and 99% (**Table 4.1**). The renewable diols (**123a-f**) and a 1.25-fold excess of **64** were stirred at 150°C for 7 h in bulk and not as described in toluene. To further improve the sustainability of the monomer synthesis, up to 90% of *t*-BuOH (**63**) and 95% of excess **64** were recovered *via* distillation during the reaction and column chromatography during product purification, respectively. In addition, the solvent mixture used for the purification of **124d** was distilled and 90% of the originally applied volume was recovered. Compared to the originally applied mixture with a ratio of *c*-C₆H₁₂ to EtOAc of 90:10, the recovered mixture had a ratio of approximately 92:8 with an impurity of *t*-BuOH of 1 – 2 mol%. The recovered mixture was considered sufficient for reuse without further purification.

4.1 Synthesis of New Biginelli Homopolycondensates: Renewable Materials with Tuneable High Glass Transition Temperatures

Table 4.1 Reaction Scheme for the synthesis of six different diacetoacetates (**124a-f**) with the respective yields and relative amounts of recovered excess of **64** and by-product **63**.

123a-f + **64** $\xrightarrow[150^\circ\text{C}, 7\text{ h}]{-\text{tBuOH (63)}}$ **124a-f**

R¹: -C₂H₄- (a), -C₃H₆- (b),
 -C₄H₈- (c), -C₆H₁₂- (d),
 -C₁₀H₂₀- (e)

(f)

monomer	yield [%] ^a	recovered excess 64 [%] ^b	recovered 63 [%] ^b
124a	99	94	87
124b	99	95	90
124c	99	91	89
124d	98	92	85
124e	98	85	89
124f	99	91	82

^a isolated yield after column chromatography, ^b isolated amount of recovered substance.

In order to confirm the formation of the products, **124a-f** were characterised by ¹H and ¹³C NMR spectroscopy (**Figure 4.1**, top example shows the ¹H NMR spectrum of **124d**), infrared (IR) spectroscopy, and high-resolution mass spectrometry (HRMS). The respective ¹H NMR spectra showed the characteristic signals of the α-CH₂ protons at 3.2 ppm and the signals of the terminal γ-CH₃ protons of the β-keto ester moiety at 2.2 ppm. The signals corresponding to the respective enol-tautomer were observed as well at different ratios below 10 mol% depending on the diacetoacetate (in DMSO-*d*₆). The HO-C(CH₃)=CH signal showed a chemical shift of 12.0 ppm (not shown in **Figure 4.1**, for clarity), the HO-C(CH₃)=CH signal was visible at 5.1 ppm, and the methyl signal at 1.9 ppm. According to the NMR spectroscopy results, less than 3 mol% EtOAc remained in the purified monomers. Besides the long chain aliphatic diols, isosorbide (**35**) was also used as diol. Due to its rigid

bicyclic structure and its availability from sugars, it was employed as a suitable and available example of a renewable diol that offers high T_g s in a variety of different polymers.^[364] Hence, all diacetoacetates were obtained with up to quantitative yields and negligible impurities (*cf.* chapter 6.3.1 for detailed analytics) and were used as monomers for the synthesis of Biginelli polycondensates.

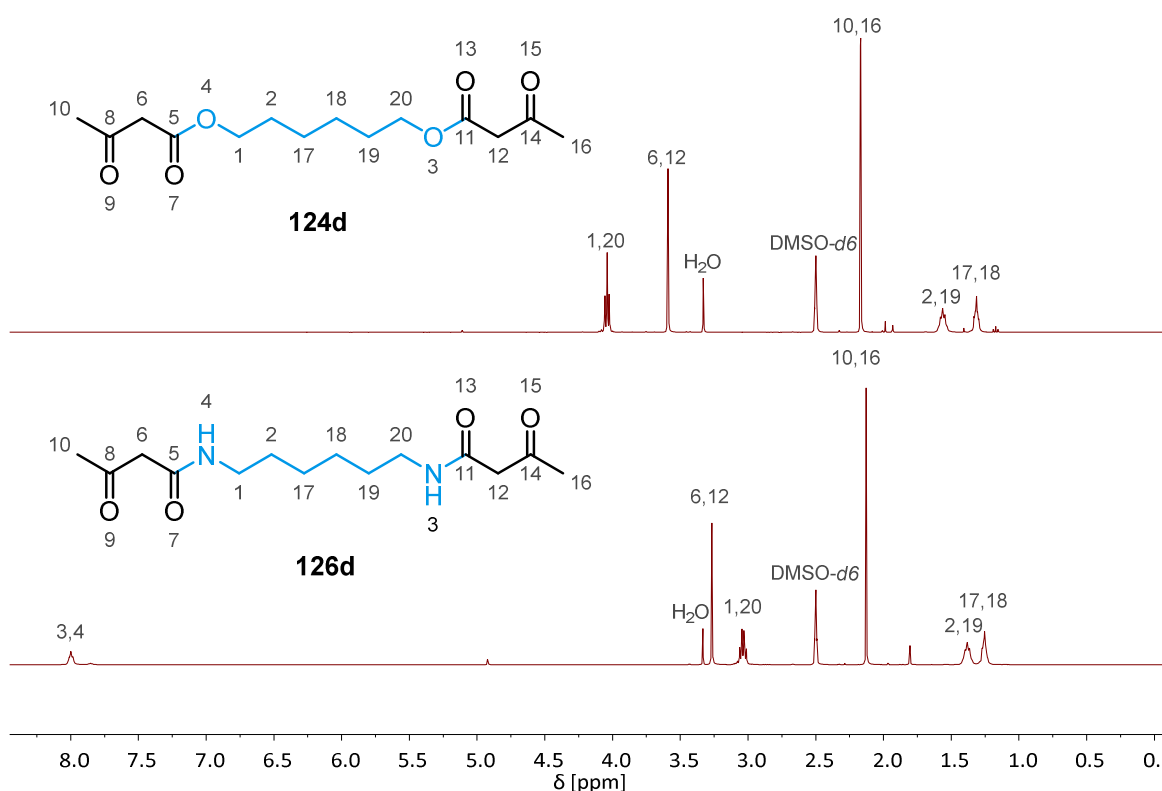


Figure 4.1 ^1H NMR spectra of **124d** (top) and **126d** (bottom) showing, as examples, the characteristic signals of diacetoacetates and diacetoacetamides.

As a second and new class of monomers for the Biginelli polycondensation, the synthesis of diacetoacetamides was attempted. For the first attempts to synthesise β -keto amides, primary amines and **64** or ethyl acetoacetate (**90**) were used as model reactants since procedures similar to the diacetoacetate synthesis indicated the feasibility of this method.^[362,365] These experiments were conducted by Josina Bohlen as part of her bachelor's thesis.^[358] Butyl amine was used as starting material. However, all attempts to

4.1 Synthesis of New Biginelli Homopolycondensates: Renewable Materials with Tuneable High Glass Transition Temperatures

reproduce the reported results solely led to the formation of the respective enamines in up to quantitative yields. For example, the simple mixture of ethyl acetoacetate and butyl amine at room temperature led to the formation of the respective enamine (**130**) in an *E/Z*-ratio of approximately 11:89 (**Figure 4.2**).^[358] In addition, the reaction of primary amines and diamines with ethyl acetoacetate (**90**) in the presence of *Candida antarctica* lipase B was reported to selectively produce β -keto amides in yields between 87% and 99%.^[366,367] While the reported^[367] batch size of 2.5 mmol led to product formation, scaling up to 250 mmol, in order to obtain enough monomer for the following polymerisations, solely yielded the enamine. As a consequence, the approach *via* transesterification of acetoacetates was abandoned and diketene acetone adduct (**65**) was used as acetylketene precursor.

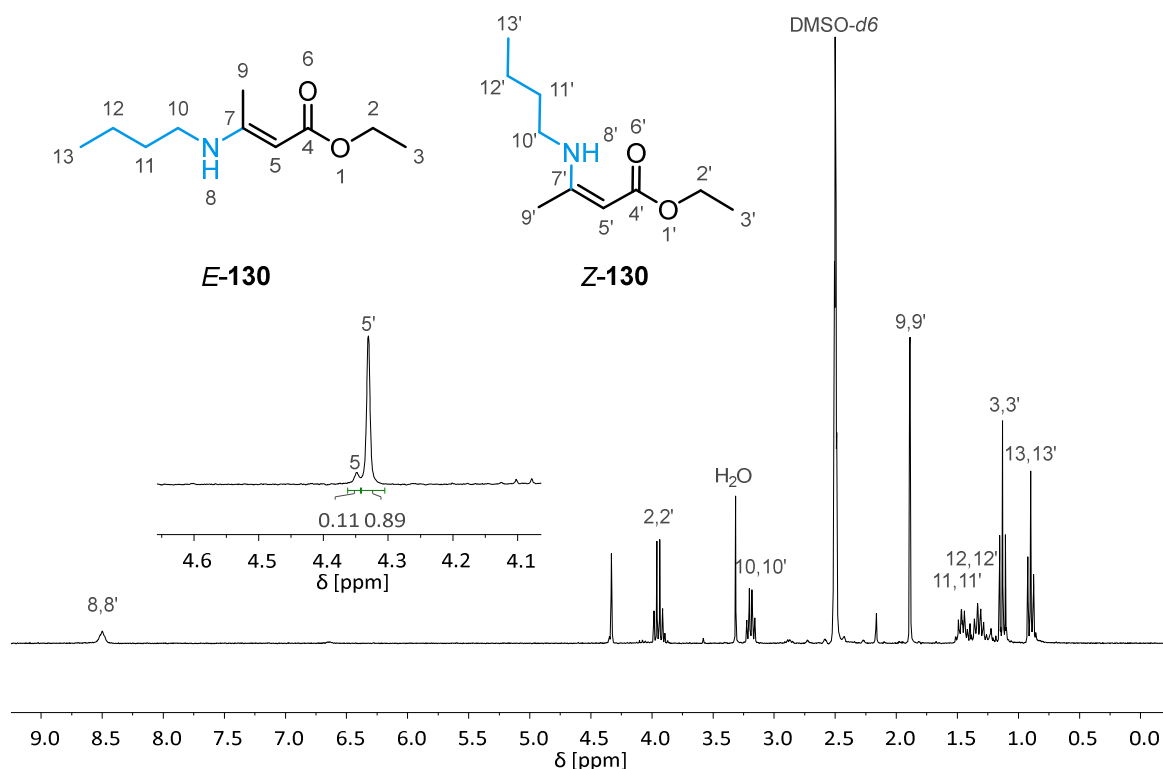


Figure 4.2 ¹H NMR spectrum of the crude product mixture of the reaction of ethyl acetoacetate (**90**) and butyl amine indicating the sole formation of an *E/Z*-mixture of the enamine (**130**) of 11:89 (signals 5 and 5' were assigned in accordance to the literature^[368,369]).

The application of **65** as reagent was successful, leading to the diacetoacetamide monomers (**126a, d, e**) with yields up to 62%. The reactions were performed similarly to a procedure by Clemens and Hyatt,^[360] by reacting a series of aliphatic primary diamines (**125a, d, e**) with **65** in bulk (**Table 4.2**). The significantly lower yields compared to the diacetoacetates arose mainly from the challenging purification. Column chromatography was not possible due to the low solubility in most eluents/eluent mixtures. Moreover, thin layer chromatography of the crude substance indicated the existence of at least 3 impurities with retention times close to that of the product ($\Delta R_f \leq 0.1$). Crystallisation was challenging due to the similar solubility of product and impurities. In addition, the ¹H NMR spectroscopy of the crude mixtures indicated, besides full conversion of the amine moieties, small amounts of enamine formation. The best results were obtained by purification *via* crystallisation from ethanol.

Table 4.2 Reaction Scheme for the synthesis of three different diacetoacetamides (**126a, d, e**) with the respective yields.

R¹: -C₂H₄- (a),
-C₆H₁₂- (d),
-C₁₀H₂₀- (e)

monomer	yield [%] ^a
126a	43
126d	62
126e	47

^a isolated yield after recrystallisation from ethanol.

The synthesis of the diacetoacetamides **126a, d, e** was confirmed by ¹H and ¹³C NMR spectroscopy, IR spectroscopy and HRMS. The ¹H NMR spectra showed the characteristic

signals of the amide NH at 8.0 ppm, the α -CH₂ protons at 3.3 ppm, and the signals of the terminal γ -CH₃ protons of the β -keto amide moiety at 2.1 ppm (**Figure 4.1** page 75, bottom example shows the ¹H NMR spectrum of **126d**). According to the NMR spectroscopy results, the pure monomers were obtained in all cases after crystallisation (see chapter 6.3.1 for detailed analytics) and used for the synthesis of Biginelli polycondensates. Nonetheless, a further improvement of the purification technique or the application of another reagent apart from **62** might increase the obtained yields.

Finally, the six different diacetoacetates **124a-f** and the three diacetoacetamides **126a, d, e** were synthesised. Their use for the synthesis of polymer materials is described in the following chapter.

4.1.3 Synthesis of Poly[3,4-dihydropyrimidin-2(1H)-one]s

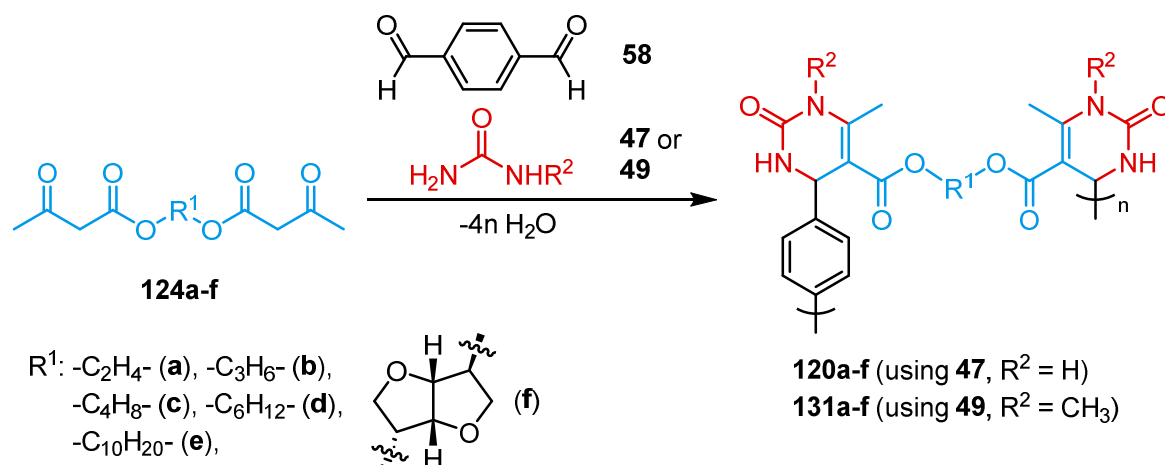
The newly introduced components for the Biginelli-polycondensation were applied with known components in various combinations in order to broaden the spectrum of available polyDHPMs and to investigate their properties. The investigations are divided in the synthesis of polyDHPMs from diacetoacetates (chapter 4.1.3.1) and the synthesis of polyDHPMs from diacetoacetamides (chapter 4.1.3.2).

4.1.3.1 Poly[3,4-dihydropyrimidin-2(1H)-one]s Using Diacetoacetates

The acid catalysed polycondensation of various combinations of the synthesised **124a-f** (chapter 4.1.2) with **58** and either **47** or **49** is discussed together with the resulting polyDHPMs. The Biginelli polycondensation was optimised in terms of resulting molecular weight and dispersity (*D*).⁵ Moreover, the reaction time was optimised following the

⁵ Polymer samples usually consist of a distribution of individual macromolecules of different molecular weights. Therefore, the polymer samples are described by a set of averaged molecular weights, the number average molecular weight M_n , the mass average molecular weight M_w , the viscosity average molecular weight M_η , and the centrifuge average molecular weight M_z .^[370] It is:^[370]

polymerisation kinetics of four polyDHPMs. Last but not least, the above mentioned library of polyDHPMs was synthesised (**Scheme 4.2**). The obtained materials were thoroughly characterised by ^1H NMR spectroscopy, size exclusion chromatography (SEC), differential scanning calorimetry (DSC), IR spectroscopy, and thermogravimetric analysis (TGA).



Scheme 4.2 Brønsted acid catalysed synthesis of polyDHPMs using six different diacetoacetates **124a-f** in combination with terephthalic aldehyde (**58**) and either urea (**47**) or *N*-methyl urea (**49**).

The optimisation of reaction conditions was performed studying the polycondensation of **124d** with **58** and **47** as test reaction (**Table 4.3**). Based on previous work of our group, dimethyl sulfoxide (DMSO) was applied as solvent and the reaction temperature was set to 125°C .^[353] Temperatures above 100°C were chosen in order to remove evolving water from the reaction mixture. First, the monomer concentration was optimised in favour of a large molecular weight. Typically, the polymerisation rate increases with increasing monomer concentration. However, if the concentration is too high, the mixture possibly becomes

$$M_n \leq M_\eta \leq M_w \leq M_z$$

The most illustrative average molecular weights M_n and M_w are typically used. How narrow a molecular weight distribution is, is indicated by the dispersity D .^[370] D is defined as ratio between M_w and M_n and equals 1 for uniform samples.^[370] For non-uniform polymer samples D is greater than 1.^[370]

$$D = M_w \cdot M_n^{-1} \geq 1$$

4.1 Synthesis of New Biginelli Homopolycondensates: Renewable Materials with Tuneable High Glass Transition Temperatures

viscous which hinders mixing and induces a broadening of D . Hence, the concentration was varied between 0.34 M and 1.40 M.

An increase of the concentration led to an increase of $M_{n,SEC}$ of the polymer from $7.6 \text{ kg}\cdot\text{mol}^{-1}$ to $13.8 \text{ kg}\cdot\text{mol}^{-1}$ together with an increase of the yield from 47% to 72%. The increase in yield was probably caused by the lower solubility of the larger macromolecules in the precipitation solvent, MeOH, facilitating the purification. However, higher concentrations led to a significant increase of the D as well, especially for 1.20 M and 1.40 M mixtures. This increase was presumably a consequence of the inhomogeneous polymerisation due to the increased viscosity of the reaction mixture for higher concentrations. Second, the Lewis acid MgCl_2 was used as catalyst (**Table 4.3**).

Table 4.3 Results of the optimisation of the Biginelli polycondensation by varying the type of the catalyst and concentration of the reaction mixture.

catalyst	c [M] ^a	$M_{n,SEC}$ [$\text{g}\cdot\text{mol}^{-1}$]	$M_{w,SEC}$ [$\text{g}\cdot\text{mol}^{-1}$]	D	yield [%] ^b
<i>p</i> -TsOH	0.34	7 600	17 300	2.27	47
	0.70	8 900	28 400	3.19	59
	1.0	9 600	36 600	3.81	67
	1.2	10 300	116 000	10.0	72
	1.4	13 800	174 600	12.7	71
MgCl_2	1.0	8 400	27 200	3.34	57

Reaction conditions: **124d** (1.0 eq), **58** (1.0 eq), **47** (3.5 eq), catalyst (0.10 eq), DMSO, 125°C, 24 h.

^aconcentration in DMSO relative to 1.00 eq; ^bisolated yield after precipitation in MeOH.

Compared to the reactions catalysed by *p*-toluenesulfonic acid, a lower yield of polymer with a lower $M_{n,SEC}$ was obtained. Nonetheless, the results were very similar. As a consequence, subsequent Biginelli polycondensations were performed at 125°C in a 1.0 M

solution regarding 1.0 eq of diacetoacetate in DMSO and 0.10 eq of *p*-toluenesulfonic acid as a satisfactory compromise between molecular weight, \bar{D} , and yield.

The polymerisation kinetics were monitored for **120e**, **131e**, **120f**, and **131f** to establish a polymerisation time that allows for high molecular weights while maintaining a moderate \bar{D} . Thus, samples for SEC were taken after certain time intervals monitoring the development of molecular weights and \bar{D} for up to 22.5 h. The polymerisation was quenched by precipitation of aliquots of the reaction mixture into water to remove **47** or **49**, thus drastically lowering the concentration of a crucial component for the B-3CR together with the reaction temperature.

The SEC data for **120e** and **120f** is shown in **Table 4.4**. The SEC data for the synthesis of **131e** and **131f**, as well as the SEC chromatograms for each sample is available in chapter 6.3.2.1. The molecular weights and \bar{D} s of **120e** and **131e** increased over time and reached an $M_{n,SEC}$ of $4.9 \text{ kg}\cdot\text{mol}^{-1}$ ($\bar{D} = 3.24$) and $8.7 \text{ kg}\cdot\text{mol}^{-1}$ ($\bar{D} = 2.88$) after 22.5 h, respectively. When **124f** was used as diacetoacetate, the $M_{n,SEC}$ of **120f** and **131f** developed similarly. The mass distributions were similar after 7 – 8 h yet significantly broader after 22.5 h ($\bar{D} = 10.1$ and 13.1 , respectively). A possible reason for this behaviour is the qualitatively more significant increase in viscosity of mixtures of polycondensates containing the rigid **124f** compared to the more flexible linear diacetoacetates. However, the broad distributions were accepted in favour of higher molecular weights. Finally, 22.5 h was chosen as standard reaction time since sufficiently high molecular weights were obtained.

4.1 Synthesis of New Biginelli Homopolycondensates: Renewable Materials with Tuneable High Glass Transition Temperatures

Table 4.4 SEC data of the kinetic investigation of **120e** and **120f**.

time [h]	120e			120f		
	$M_{n,SEC}$ [g·mol ⁻¹]	$M_{w,SEC}$ [g·mol ⁻¹]	\bar{D}	$M_{n,SEC}$ [g·mol ⁻¹]	$M_{w,SEC}$ [g·mol ⁻¹]	\bar{D}
0.25	1 300	3 700	2.8	1 300	2 500	1.91
0.5	2 500	5 000	1.98	1 600	3 700	2.23
1	2 900	6 200	2.16	1 800	4 600	2.55
1.75	3 400	8 200	2.42	2 300	6 200	2.67
3	3 800	10 000	2.61	2 700	8 700	3.19
7	4 200	12 800	3.09	3 300	14 200	4.3
22.5	4 900	15 900	3.24	4 800	48 400	10.1

Reaction conditions: **124e** or **124f** (1.0 eq), **58** (1.0 eq), **47** (3.5 eq), *p*-TsOH (0.10 eq), DMSO (1.0 M regarding 1.0 eq), 125°C.

The Biginelli-polymerisation is an acid-catalysed polycondensation of bifunctional monomers. Hence, it is reasonable to assume a step-wise growth of the polymer chains. Moreover, the development of $M_{n,SEC}$ and the degree of polymerisation (DP) were similar to the kinetics of an acid catalysed polycondensation of three components.⁶ The time

⁶The kinetics of acid catalysed polycondensations of the bifunctional monomer types AA/BB or AB were described by Flory in a simple manner making three assumptions.^[371] First, the reactivity of the reacting functional groups does not depend on the size of the molecule. Second, the tendency to undergo the reverted reaction is, as well, identical regarding the position in the molecule. Third, side-reactions are negligible. As a consequence, the following equation^[372] is derived from the respective differential equation with the extent of the reaction p , the initial concentration c_0 , the rate constant k , and time t :

$$DP = \frac{1}{1-p} = c_0kt + 1 \text{ and } \bar{D} = 1 + p$$

Consequently, for a polycondensation that obeys Flory's assumptions, the DP increases linearly with time and \bar{D} ranges between 1 and 2. The equation, expressing the proportionality between DP and p is known as Carothers equation. However, the calculation for \bar{D} is mostly erroneous due to the drastic idealisation of Flory's assumptions.^[373]

dependence of DP (calculated based on SEC data), as plotted in **Figure 4.3**, indicated a proportionality of DP to the square root of the reaction time (t) for, approximately, the first 4 h. Afterwards, the DP seemed to reach a plateau for **120e,f** and **131f**. Nonetheless, the assumption of a third order kinetic for a Biginelli polycondensation is an educated guess and needs further investigation to be verified. For a more comprehensive investigation of the polymerisation kinetics, the inclusion of ^1H NMR-derived M_n values was necessary to rule out solubility related effects during SEC measurements.

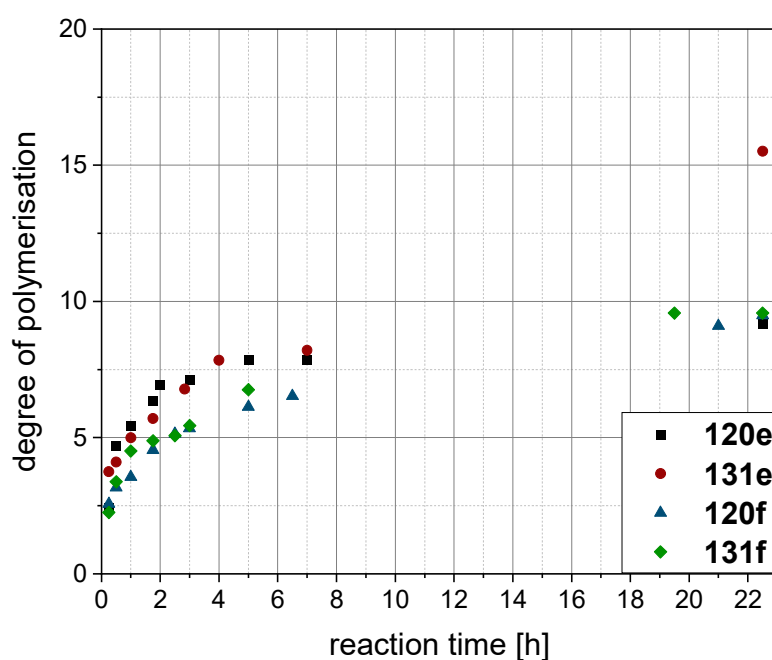


Figure 4.3 SEC-determined evolution of the DP with t during the synthesis of **120e**, **131e**, **120f**, and **131f** showing a non-linear relation of DP with respect to the reaction time with a similar final chain length of approximately 10 repeat units for **120e**, **120f**, and **131f**.

A proportionality of DP to $t^{-0.5}$ is obtained for a self-catalysed polycondensation.^[374] The same proportionality is obtained for a catalysed system with three components like the Biginelli polycondensation:

$$DP = \frac{1}{1-p} = \sqrt{k'c_0t + 1}$$

When the evolution of DP with t was determined by ^1H NMR analysis, a similar proportionality was obtained (**Figure 4.4**). $M_{n,\text{NMR}}$ was obtained by integration of the signals of the aldehyde end group at approximately 9.96 ppm relative to the CH -protons of the DHPM-ring at approximately 5.1 ppm. The acetoacetate end group was not used for molecular weight determination as the signals overlap with the polymer signals. The DP did not seem to stagnate after 4 h of reaction time, indicating that the observed stagnation in **Figure 4.3** was related to the molecular weight determination by SEC. It is conceivable that, starting from a certain chain length on, the polymer chains started to coil tightly due to reduced solubility in the eluent hexafluoroisopropanol/0.1 wt% $\text{KCO}_2(\text{CF}_3)_2$. This would lead to minor changes in the retention time relative to an increase in chain length.

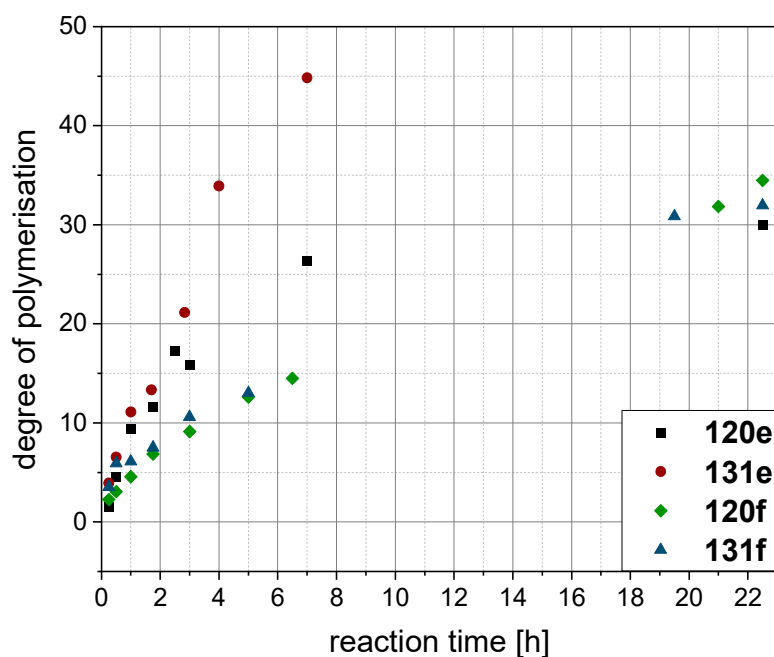


Figure 4.4 Evolution of the degree of polymerisation with the reaction time during the synthesis of **120e**, **131e**, **120f**, and **131f** determined *via* ^1H NMR analysis.

Furthermore, the obtained DP -values were with 30 – 45 a factor of 3 higher compared to the DP s observed by SEC. As a consequence, solvent effects during the SEC analysis led, in particular for larger polymers, to an underestimation of M_n . However, the DP s

obtained *via* ^1H NMR spectroscopy were probably an overestimation due to the challenging integration of the respective peaks. The baseline was properly corrected in the region of the aldehyde end group at approximately 10 ppm. However, the baseline around the integrated signal of the *CH*-proton of the DHPM-structure of the repeat unit at approximately 5.1 ppm showed a positive offset. This led to an overestimation of the ratio of the end group signal to the polymer signal and thus to an overestimation of *DP*. As a consequence, the actual M_n of the polyDHPMs was probably in between $M_{n,\text{SEC}}$ and $M_{n,\text{NMR}}$.

Noteworthy, the M_n -values of the samples of the kinetics after 22.5 h are smaller compared to the M_n -values given in **Table 4.5** for the same polymer structure. The reason is the different workup. The samples for the kinetic were precipitated in water to prevent loss of low molecular weight oligomers. The final polymers in **Table 4.5**, however, were precipitated in MeOH or MeOH/water mixtures also removing low molecular weight impurities.

Finally, the polymerisation rate was not significantly limited within the investigated time frame. Hence, higher molecular weights seemed possible at reaction times larger than 22.5 h. However, the use of a mechanical stirrer is recommended in order to avoid inhomogeneous mixtures. Moreover, the Biginelli polycondensation seemed to proceed similarly to the proposed kinetic for a polycondensation of three components. For further insight, the application of a third complementary method to determine the molecular weight of polymers, such as viscometry or light scattering, is conceivable.

Afterwards, the optimised reaction conditions were applied to synthesise a set of different polyDHPMs. Consequently, the polyDHPMs **120a-f** and **131a-f** were synthesised using stoichiometric amounts of **124a-f** and **58**, as well as a 1.75-fold excess of **47** or **49** and 10 mol% of *p*-toluenesulfonic acid as a catalyst in DMSO. After the reaction, the polymers were precipitated and subsequently dried in a vacuum oven yielding the final polymer in yields up to 86%. The polymers were fully characterised using ^1H NMR spectroscopy, SEC, DSC, IR spectroscopy, and TGA.

The synthesis of the polyDHPMs was verified by investigation of the polymer samples by ^1H NMR spectroscopy. The ^1H NMR spectra of the polyDHPMs **120a-f** showed the characteristic signals (Figure 4.5, top example shows the ^1H NMR spectrum of **120d**) of the $\text{NHC}=\text{C}$ protons at 9.2 ppm, the $\text{NHC}-\text{C}$ at 7.7 ppm, the aromatic protons around 7.2 ppm, the $\text{NH}-\text{CH}-\text{CAr}$ protons at 5.1 ppm and the $\text{O}=\text{CO}-\text{CH}_2$ protons at 3.9 ppm. The signal of the $\text{C}=\text{C}-\text{CH}_3$ protons was visible at 2.3 ppm. Signals for aliphatic protons were furthermore visible between 1.5 and 1.1 ppm for polyDHPMs with aliphatic spacers longer than C_2H_4 (chapter 6.3.2.2).

For **131a-f** (Figure 4.5, bottom example shows the ^1H NMR spectrum of **123d**), the signal at 9.2 ppm was absent while a new signal for the $\text{H}_3\text{C}-\text{NC}=\text{C}$ protons at 3.0 ppm was observed. The $\text{NHC}-\text{C}$ proton was shifted by +0.2 ppm to 7.9 ppm and the $\text{C}=\text{C}-\text{CH}_3$ protons were shifted by +0.2 ppm to 2.5 ppm. The signals of the aldehyde end-groups were observed around 9.96 ppm and were used to calculate the $M_{n,\text{NMRs}}$ of the polyDHPMs (Table 4.5). The obtained results indicate a higher degree of polymerisation for longer spacer units and **49**, possibly due to better solubility of the respective polymers in the reaction solvent DMSO. **120b, d, e** have already been reported prior to this work.^[353] The ^1H NMR spectra and IR spectra correlate well, while molecular weights were higher by a factor of approximately two compared to this work. T_g s for **120b** and **120d** were not found in these previous reports.^[353]

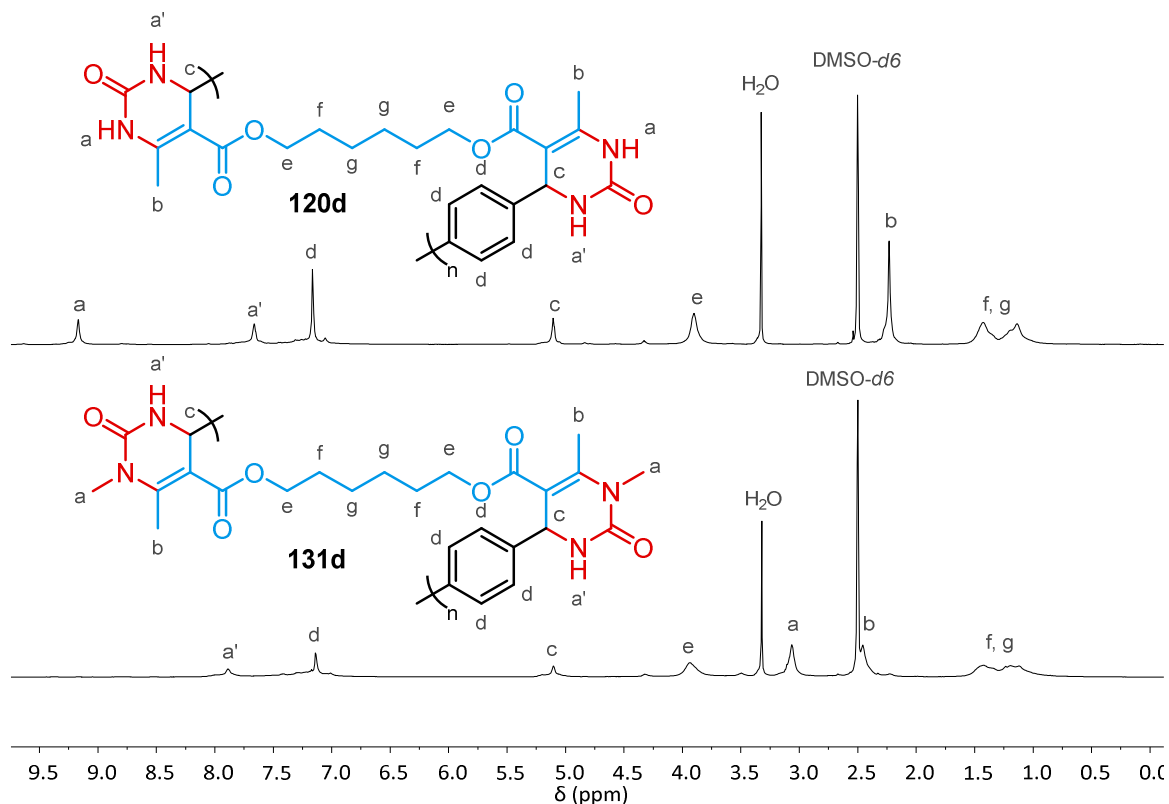


Figure 4.5 ^1H NMR spectra of **120d** (top) and **131d** (bottom) showing, as examples, the characteristic signals of polyDHPMs from diacetoacetates.

The molecular weight distributions of the polyDHPMs were investigated *via* SEC using hexafluoroisopropanol with 0.1 wt% $\text{KCO}_2(\text{CF}_3)_2$ as eluent (Table 4.5; for SEC chromatograms see Figure 6.16 on page 193). The results clearly showed that macromolecular polycondensates were obtained. **120a-d** showed increasing $M_{n,\text{SEC}}$ values from 3.80 to 8.30 $\text{kg}\cdot\text{mol}^{-1}$ ($M_{n,\text{NMR}}$ up to 12.2 $\text{kg}\cdot\text{mol}^{-1}$) with varying D from 2.8 to 4.2. Other eluents were not suitable due to the insolubility of the polyDHPMs in water, acetonitrile, methanol, ethanol, dimethylacetamide, or tetrahydrofuran. Low solubility and problems using SEC analysis, especially for higher degrees of polymerisation, have already been reported for polyDHPMs and are generally known for polymers with strong hydrogen bonding, such as polyamides or polyureas.^[353]

4.1 Synthesis of New Biginelli Homopolycondensates: Renewable Materials with Tuneable High Glass Transition Temperatures

Table 4.5 Molecular weight and DSC data for the polyDHPMs from diacetoacetates (**120a-f** and **131a-f**).

polymer	R ^{1a}	$M_{n,NMR}^b$ [g·mol ⁻¹]	$M_{n,SEC}$ [g·mol ⁻¹]	$M_{w,SEC}$ [g·mol ⁻¹]	D	T_g^c [°C]
120a	C ₂ H ₄	5 500	3 800	14 800	3.88	280
120b	C ₃ H ₆	5 700	4 900	18 000	3.65	255
120c	C ₄ H ₈	6 100	5 600	16 600	2.85	239
120d	C ₆ H ₁₂	10 100	8 300	34 700	4.20	220
120e	C ₁₀ H ₂₀	12 200	6 600	18 200	2.76	198
120f	isosorbide	30 700	6 200	50 000	8.07	308
131a	C ₂ H ₄	11 300	10 800	43 000	3.99	248
131b	C ₃ H ₆	24 000	10 500	33 800	3.21	222
131c	C ₄ H ₈	21 400	7 600	19 700	2.58	211
131d	C ₆ H ₁₂	31 800	9 500	42 800	4.94	175
131e	C ₁₀ H ₂₀	36 700	8 700	24 900	2.88	159
131f	isosorbide	23 000	8 400	73 100	8.71	266

Reaction conditions: **124a-f** (1.0 eq), **58** (1.0 eq), **47** or **49** (3.5 eq), *p*-TsOH (0.10 eq), DMSO (1.0 M regarding 1.0 eq), 125°C, 22.5 h. ^aspacer of the diacetoacetate, *cf.* Scheme 4.2; ^bcalculated by integration of the aldehyde end-group signals; ^cthe inflection point of the DSC curve was chosen as T_g .

Two possible reasons for the increasing $M_{n,SEC}$ for longer spacers were considered in accordance with the NMR results. First, the larger size of the spacer unit naturally resulted in a larger hydrodynamic volume and consequently a higher $M_{n,SEC}$. Second, in a material with longer aliphatic spacer units, the frequency of hydrogen bonds throughout the material is lower which possibly results in less intramolecular hydrogen bonding and thus a larger hydrodynamic volume. The $M_{n,SEC}$ of **120e** did not follow this trend, perhaps due to the lower solubility of **120e** in hexafluoroisopropanol with 0.1 wt% KCO₂(CF₃)₂. This possibly led to lower hydrodynamic volumes by an overcompensation of above explanations for higher $M_{n,SEC}$ values.

The $M_{n,NMR}$ values of **131a-e** obtained by 1H NMR end-group analysis show a similar trend with increasing $M_{n,NMR}$ for longer spacer units up to $36.7 \text{ kg}\cdot\text{mol}^{-1}$, while being considerably higher compared to **120a-e** (Table 4.5). The $M_{n,SEC}$ values, however, are decreasing with longer spacer units. Interestingly, this trend was observed (for $M_{n,NMR} > 11 \text{ kg}\cdot\text{mol}^{-1}$) for both polyDHPMs from **47** as well as **49**. These findings indicate that polyDHPMs start to form tight random coils if a certain $M_{n,NMR}$ is reached. Moreover, neither the usage of **47** or **49** seemed to influence the $M_{n,NMR}$ at which this phenomenon started to occur.

The synthesis of **120f** and **131f** led to polymers with a high $M_{n,NMR}$ of $30.7 \text{ kg}\cdot\text{mol}^{-1}$ and $23.0 \text{ kg}\cdot\text{mol}^{-1}$, respectively (Table 4.5). The $M_{n,SEC}$ values were $6.2 \text{ kg}\cdot\text{mol}^{-1}$ and $8.4 \text{ kg}\cdot\text{mol}^{-1}$ with broad dispersities ($D = 8.07, 8.71$). Since the reaction mixtures of **120f** and **131f** were very viscous, the stirring was possibly not sufficient thus leading to inhomogeneous polymerisation mixtures throughout the reaction and hence to a bimodal molecular weight distribution (Figure 4.6).

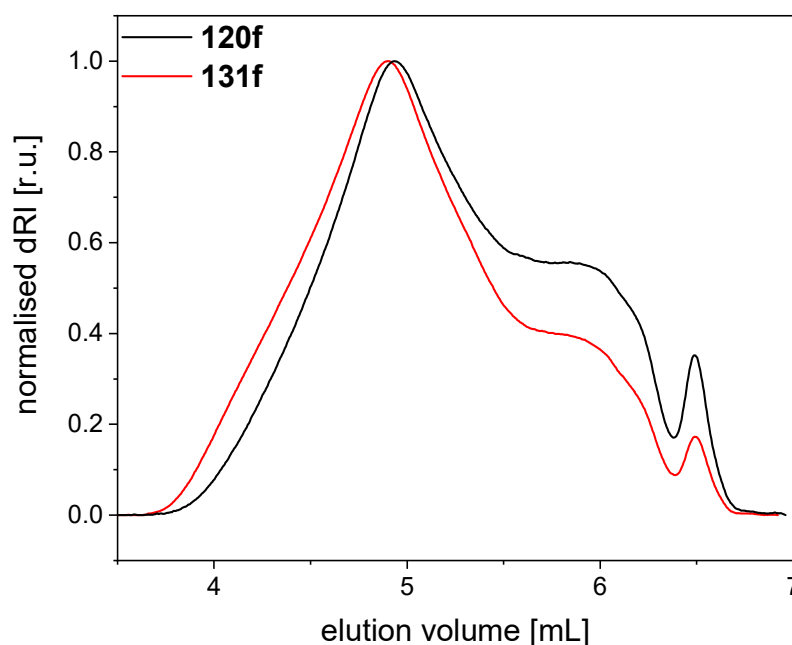


Figure 4.6 SEC graphs of **120f** and **131f** showing a bimodal, broad shape.

The results discussed are a significant indication that the intramolecular hydrogen bonding in polyDHPMs, which is more pronounced for **120a-e**, influences the reaction progress and leads to a compact structure in solution. Thus, small hydrodynamic volumes were observed by SEC. Furthermore, the use of **49** seemed to accelerate the polymerisation compared to **47**, while retention time was dependent on the molecular weight rather than the molecular structure. In any case, reasonable control of the macromolecular characteristics of the polyDHPMs were obtained.

The influence of the choice of either **47** or **49** and the respective diacetoacetate on the thermal properties of the polyDHPMs was investigated *via* DSC (**Figure 4.7**) showing a clear trend regarding the type of urea compound and the length of the applied spacer. Generally, **120a-f** and **131a-f** showed T_g values between 160°C and 308°C (**Table 4.5** on page 88), as expected from the highly rigid and strongly hydrogen bonding repeating units. Comparing the T_g s, a clear trend was observed: The T_g s were lower for polymers with longer spacers. This seems reasonable considering the above assumptions that an increasing spacer length resulted in decreasing hydrogen bond frequency and thus increased flexibility of the polymer backbone. In addition, when the same diacetoacetate was used, the respective T_g was lower for polymers **131a-e** compared to **120a-e**. In line with above considerations, **120f** and **131f** showed the highest T_g s of 308°C and 266°C, respectively, which was attributed to the rigid bicyclic structure of isosorbide (**35**).

Considering the whole data-set (**Table 4.5** on page 88), it was possible to adjust the T_g of the polyDHPMs (**120a-f** and **131a-f**) in small steps (<10°C) within a 150°C range from 160 – 308°C by simple variation of the combination of starting materials. It is notable that the T_g s of other renewable polymers from various resources are usually below 150°C.^[364] Nevertheless, several other renewable polymers with a comparable T_g are known. For example, polyamides with a T_g of 273°C were obtained using monomers synthesised *via* [2 + 2]-cycloaddition of 4-aminocinnamic acid.^[375] Applying isosorbide and its diastereomers isomannide and isoidide as monomers, different polyesters with a T_g between 180°C and 196°C^[376–379] and polycarbonates with a T_g up to 175°C were obtained.^[380,381]

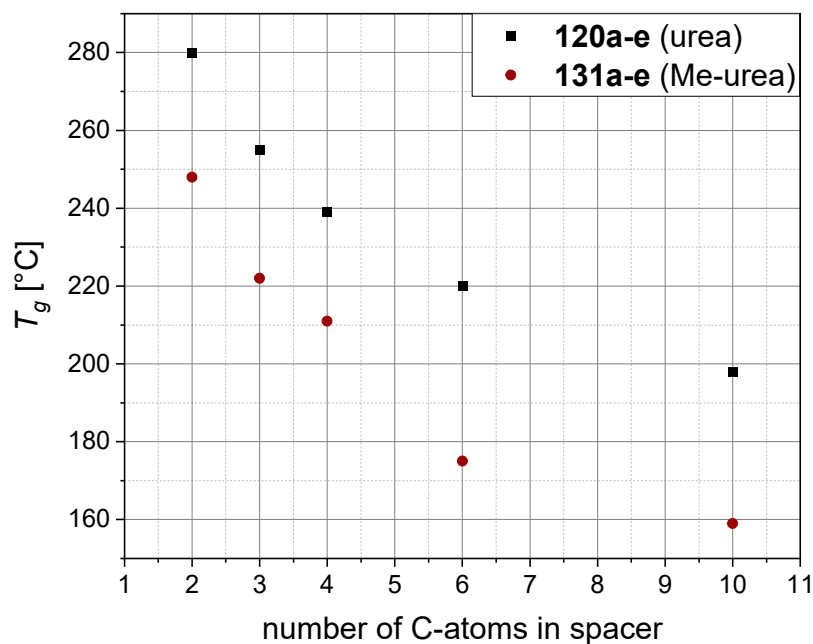
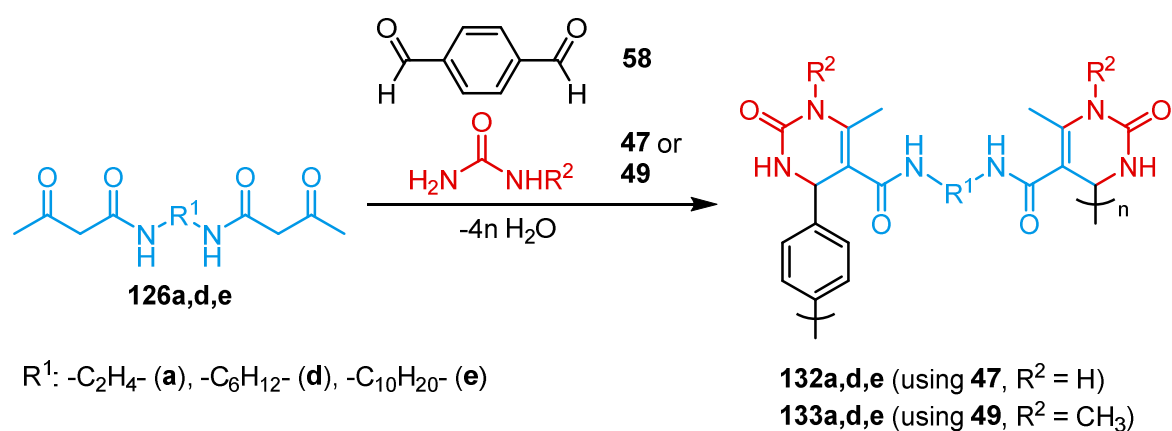


Figure 4.7 Dependence of the T_g of polyDHPMs on the spacer-length and the choice of either urea (**47**) or Me-urea (**49**).

TGA revealed that the polyDHPMs from diacetoacetates have high thermal stability under synthetic air flow. The observed $T_{d5\%}$ values of **120a-e** and **131a-f** were between 264°C and 314°C surpassing the respective T_g s indicating a possible thermal processing of these polymers (**Table 6.9** on page 217). Solely the $T_{d5\%}$ of **120f** was lower (289°C) than its T_g at 308°C. An investigation of the mechanical properties by stress-strain measurements of **120e** and **131e** was attempted since a long spacer was considered to likely result in a deformable material. Hot pressing as well as the formation of a polymer film *via* evaporation from solution in *N*-methyl-2-pyrrolidone or *N,N*-dimethylacetamide were attempted. However, the brittleness of the material did not allow the manufacture of a specimen suitable for mechanical analysis.

4.1.3.2 Poly[3,4 dihydropyrimidin 2(1H)-one]s Using Diacetoacetamides

Within this chapter the set of polyDHPMs from diacetoacetamides (**Scheme 4.3**) was synthesised and characterised. At first however, the reaction kinetics were investigated for **132e** and **133e** using the optimised reaction conditions for **120a-f** and **131a-f** (*cf.* chapter 4.1.3.1). These investigations revealed that an insoluble gel is formed if the reaction time is longer than approximately 2.5 h for **132e** and 0.5 h for **133e**. The gelation is indicated by a broadening of the molecular weight distribution (shoulder at high molecular weights) prior to gelation (see **Figure 6.30** on page 208). Consequently, the synthesis of **132e** was stopped after 1.5 h. The reaction time of **132a** and **132d** was kept at 22.5 h, since no gelation was observed. The polymerisations yielding **133a, d, e** were stopped after 0.5 h to avoid gelation. Using these optimised polymerisation conditions the set of **132a, d, e** and **133a, d, e** was obtained with isolated yields of up to 67%.



Scheme 4.3 Synthesis scheme of polyDHPMs using three different diacetoacetamides **126a, d, e** in combination with terephthalic aldehyde (**58**) and either urea (**47**) or *N*-methyl urea (**49**).

The evolution of DP with t was observed by 1H NMR analysis for **132e**. The resulting plot indicated a similar increase of DP with t (**Figure 4.8**) compared to the polyDHPMs from diacetoacetates (*cf.* **Figure 4.4**, page 84). However, the reaction process was only monitored up to 3 h due to the insolubility of the resulting polymer.

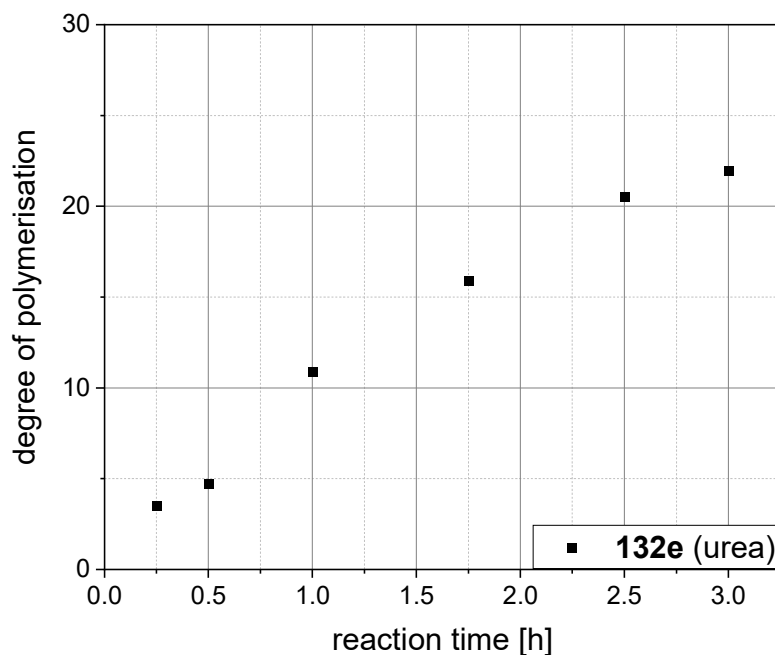


Figure 4.8 Evolution of the degree of polymerisation with reaction time during the synthesis of **132e** determined *via* ^1H NMR analysis.

Afterwards, **132a,d,e** and **133a,d,e** were synthesised and fully characterised using ^1H NMR spectroscopy, SEC, DSC, IR spectroscopy and TGA. The ^1H NMR spectra confirmed the successful synthesis. The spectra of **132a, d, e** showed the characteristic signals (**Figure 4.9**, top example shows the ^1H NMR spectrum of **132d**) of the $\text{NHC}=\text{C}$ protons at 8.5 ppm, the $\text{NHC}-\text{C}$ at 7.6 ppm, the $\text{O}=\text{C}(\text{NH})-\text{CH}_2$ at 7.5 ppm, the aromatic protons around 7.2 ppm, the $\text{NH}-\text{CH}-\text{C}_{\text{Ar}}$ proton at 5.2 ppm and the $\text{O}=\text{C}(\text{NH})-\text{CH}_2$ protons at 3.1 ppm. The signal of the $\text{C}=\text{C}-\text{CH}_3$ protons was observed at 2.0 ppm. Signals for aliphatic protons were furthermore visible between 1.5 ppm and 0.9 ppm for polyDHPMs with aliphatic spacers longer than C_2H_4 (*cf.* chapter 6.3.1). For **133a, d, e** (**Figure 4.9**, bottom example shows the ^1H NMR spectrum of **133d**), the signal at 8.5 ppm was absent while a new signal for the $\text{H}_3\text{C}-\text{NC}=\text{C}$ protons at 3.0 ppm was observed, overlapping with the broad $\text{O}=\text{C}(\text{NH})-\text{CH}_2$ signal. The latter was confirmed *via* phase-edited heteronuclear single quantum coherence (HSQC) spectroscopy (**Figure 6.37** on page 215). The $\text{NHC}-\text{C}$ proton remained at 7.6 ppm, the $\text{O}=\text{C}(\text{NH})-\text{CH}_2$ was shifted by +0.3 ppm to 7.8 ppm, the

NH-CH-CAr proton was shifted -0.1 ppm to 5.1 ppm, and the C=C-CH₃ protons were shifted by $+0.2$ ppm to 2.2 ppm.

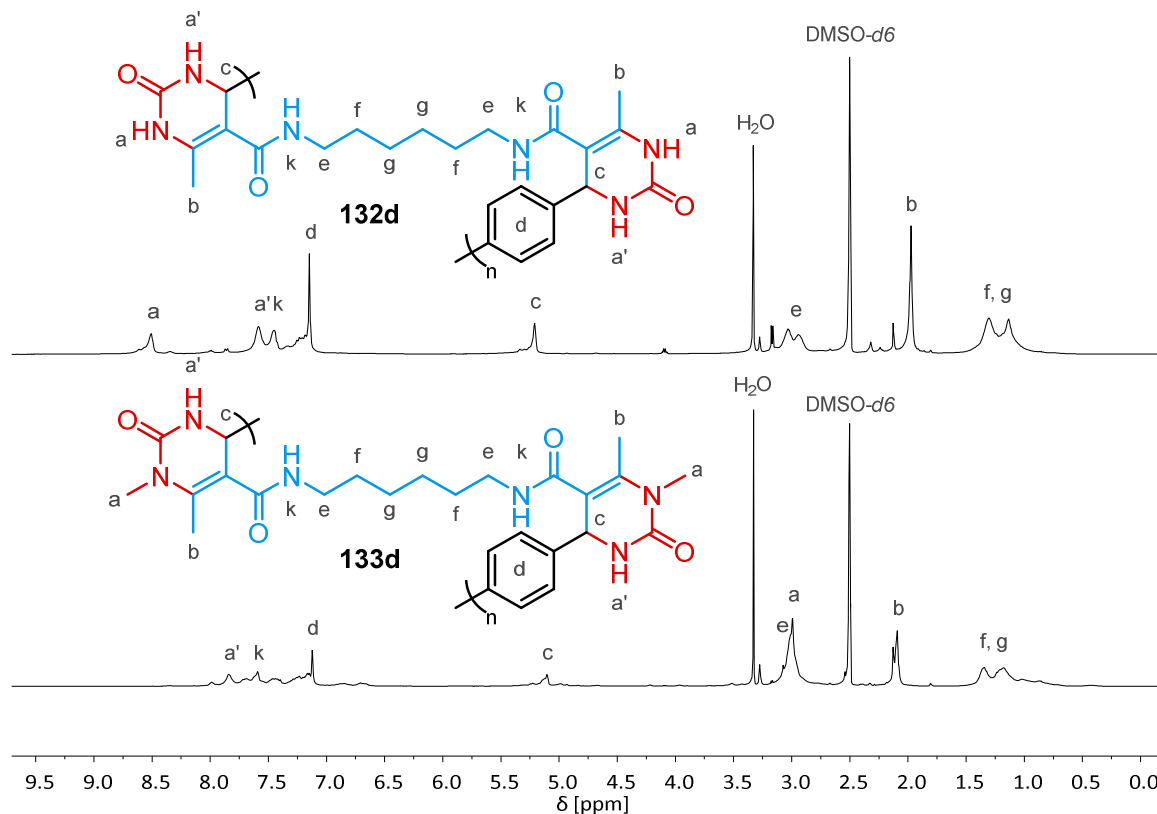


Figure 4.9 ¹H NMR spectra of **132d** (top) and **133d** (bottom) showing, as examples, the characteristic signals of polyDHPMs from diacetoacetamides.

The molecular weight distributions of the polyDHPMs were investigated *via* SEC using hexafluoroisopropanol with 0.1 wt% KCO₂(CF₃)₂ as eluent (**Table 4.6**; for SEC chromatograms see **Figure 6.30** on page 208). The results clearly showed that macromolecular polycondensates were obtained. The obtained molecular weights ($M_{n,SEC}$) of the resulting polymers were $5.00 \text{ kg}\cdot\text{mol}^{-1}$ (**132a**), $12.4 \text{ kg}\cdot\text{mol}^{-1}$ (**132d**) and $11.8 \text{ kg}\cdot\text{mol}^{-1}$ (**132e**), $6.00 \text{ kg}\cdot\text{mol}^{-1}$ (**133a**), $5.30 \text{ kg}\cdot\text{mol}^{-1}$ (**133e**), and $15.2 \text{ kg}\cdot\text{mol}^{-1}$ (**133d**). D ranged from 2.06 to 7.71 (**Table 4.6**).

Table 4.6 Molecular weight data and DSC data for the polyDHPMs from diacetoacetamides (**132a**, **d**, **e** and **133a**, **d**, **e**).

polymer	R ^{1a}	M _{n,NMR} ^b [g·mol ⁻¹]	M _{n,SEC} [g·mol ⁻¹]	M _{w,SEC} [g·mol ⁻¹]	<i>D</i>	T _g ^c [°C]
132a	C ₂ H ₄	9 600	5 000	23 400	4.17	– ^d
132d	C ₆ H ₁₂	5 300	12 400	63 000	5.07	265
132e ^e	C ₁₀ H ₂₀	5 500	11 800	40 300	3.40	235
133a ^f	C ₂ H ₄	2 400	6 000	12 400	2.06	– ^d
133d ^f	C ₆ H ₁₂	3 900	5 300	13 000	2.47	– ^d
133e ^f	C ₁₀ H ₂₀	3 800	15 200	71 100	7.71	194

Reaction conditions: **126a,d,e** (1.0 eq), **58** (1.0 eq), **47** or **49** (3.5 eq), *p*-TsOH (0.10 eq), DMSO (1.0 M regarding 1.0 eq), 125°C, 22.5 h. ^aspacer of the diacetoacetamide, *cf.* Scheme 4.3; ^bby integration of the aldehyde end-group signals; ^cthe inflection point of the DSC curve was chosen as T_g; ^dnot observed within the observed temperature range (–50 – 350°C); ^e0.5 h reaction time; ^f1.5 h reaction time.

The influence of the choice of either **47** or **49** and the respective diacetoacetamide on the thermal properties of the polyDHPMs was investigated *via* DSC (**Table 4.6**) showing a clear trend regarding the type of urea compound and the length of the applied spacer. A T_g was observed for **132d** (265°C), **132e** (235°C) and **133e** (194°C). Compared to **120d** (220°C), **120e** (198°C), and **131e** (159°C), respectively, the T_{gs} were expectedly higher (35 – 45°C higher compared to polyDHPMs from diacetoacetates) for the polymers that contained an amide moiety, which was attributed to additional hydrogen bonding through the amide. No thermal transition was observed for **132a**, **133a**, **d**, although different heating/cooling rates for DSC investigations (range of 5 – 35 K·min⁻¹ and 5 – 20 K·min⁻¹, respectively) were attempted. For **132a** it is possible that the T_g is above the T_{d5%} and is therefore not observable.

Consequently, the T_{gs} for diacetoacetamide-derived polyDHPMs seem to be tuneable in a manner similar to diacetoacetate-derived polyDHPMs. TGA showed that the polyDHPMs from diacetoacetamides have high thermal stability under synthetic air flow. The observed

$T_{d5\%}$ values ranged from 278°C to 314°C (**Table 6.9** on page 217) and are thus in a similar range to the T_g s of **120a-f** and **131a-f**.

4.1.4 Conclusion and Outlook

Herein, we synthesised a set of 15 new polyDHPMs *via* the Biginelli polycondensation introducing **49** and several diacetoacetate and diacetoacetamide monomers as new building blocks. In addition, three literature-known polyDHPMs, which fit in this series of investigated polymers, were prepared. The T_g of two of them was analysed for the first time. The monomers are available from renewable resources in yields from up to 62% for the diacetoacetamides and up to 99% for the diacetoacetates. The T_g s of the resulting polymers were tunable in small steps of approximately 10°C from 160 – 308°C by exploitation of the established structure–property relations, rendering polyDHPMs sustainable alternatives for high T_g polymers. In addition, the high thermal stability of the polyDHPMs potentially allows for thermal processing techniques.

The Biginelli polycondensation is overall a promising tool for future applications. However, more insight into the characteristics of the Biginelli polymerisation, and thus control over the resulting polymers regarding molecular weight and dispersity, are needed. To further regulate the molecular weight the application of end-capping agents are conceivable allowing high conversions alongside specific molecular weights depending on the ration of end-capping agent. Additional investigations of the polymerisation kinetics and the development of the dispersity, especially at reaction times longer than 22.5 h, are needed for more sophisticated insight into the polymerisation process. The application of mechanical stirring might, albeit, avoid inhomogeneous polymerisation and allow for higher molecular weights and lower dispersities. In addition, the synthesis of copolymers or the application of monomers with substituents that disrupt the hydrogen bonding might reduce the brittleness and allow for processing, determination of mechanical properties, and application. Finally, the application of an external plasticiser is anticipated to enhance the mechanical properties.

4.2 End Group-Functionalisation of Biginelli Polycondensates and Subsequent Block Copolymer Synthesis

Chapters 6.1, 6.2, and 6.4 of the experimental section correspond to the following investigations within this chapter.

4.2.1 Abstract

The synthesis of Biginelli polycondensates was previously reported from various diacetoacetates, aromatic dialdehydes, and urea (**47**) or thiourea (**104**). AB-monomers carrying both an acetoacetate and an aldehyde group have also been used (cf. chapter 2.7.2.3). However, each of the reports featured homopolymers with one exception: a statistical copolycondensate containing DHPM motifs *via* the B-3CR and dihydropyridine motifs *via* the Hantzsch synthesis. Within this chapter, the synthesis of block copolymers that contain a polyDHPM block was investigated. The copolymer was prepared by introduction of a reactive end group to the polyDHPM and subsequent coupling with another polymer. Hence, we prepared six polyDHPMs with terminal double bonds as end groups and investigated their conversion in a thiol-ene reaction. The reactivity was first investigated with butane thiol (**145**) and second with poly(ethylene glycol) methylether thiol (**147**) to obtain block copolymers.

Five diacetoacetates (**124a-e**, AA-monomer), terephthalic aldehyde (**58**, BB-monomer), urea (**47**), and *N*-methyl urea (**49**) were used as renewable starting materials. Additionally, 2- $\{[3-(4\text{-formyl-2-methoxyphenoxy})\text{propyl}]\text{thio}\}$ ethyl acetoacetate (**141**) was used as a renewable AB-monomer. In both approaches, end groups were introduced by addition of 10-undecenyl-1-acetoacetate (**143**) to the monomer mixture. This led to six different polyDHPMs (**144a-f**) with terminal double bonds as end groups in yields of up to 76%. Moreover, the molecular weight of the end group-functionalised polyDHPMs was tuned between $4\,200\text{ g}\cdot\text{mol}^{-1}$ and $6\,800\text{ g}\cdot\text{mol}^{-1}$ by the variation of the amount of **143** added. Subsequently, the **144a-f** were reacted *via* thiol-ene reaction with **147** to form the polyDHPM-*b*-poly(ethylene glycol)s (**148a-f**) with yields of up to 76%. All obtained **144a-f**

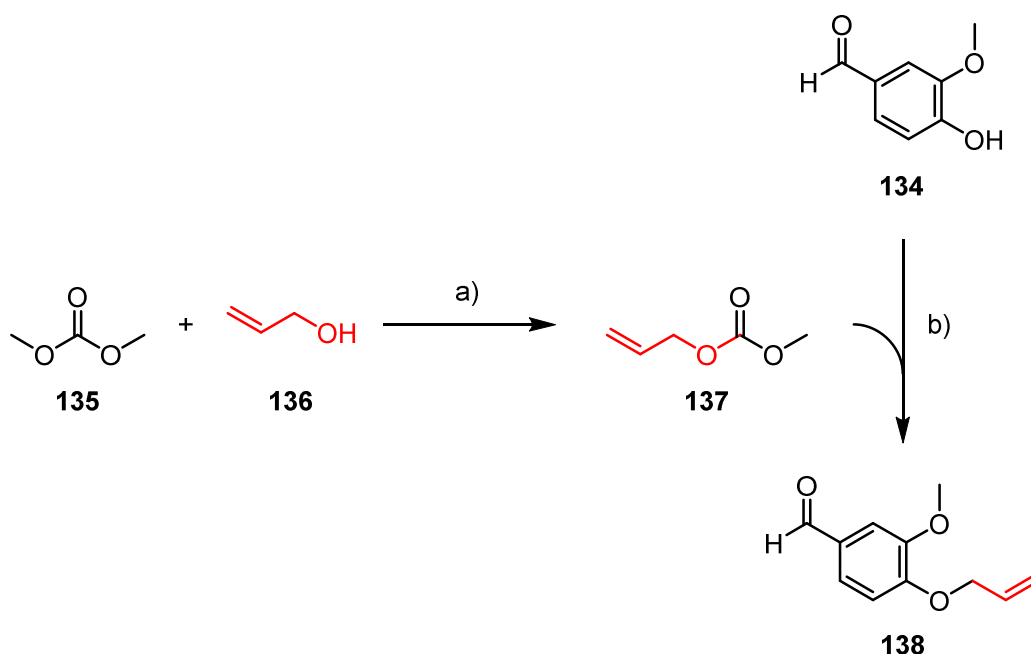
and **148a-f** were fully characterised. DSC analysis of **148a-e** revealed two distinct thermal transitions for the block copolymers. While the T_{gs} of the polyDHPM blocks ranged, depending on the monomer structure, between 265°C and 159°C, the melting point (T_m) of the poly(ethylene glycol) block (PEG block) remained between 49°C and 52°C matching the T_m of pure **147**. This behaviour indicated microphase separation of the applied polymer blocks possibly allowing for self-assembling polymers or the synthesis of thermoplastic elastomers.

4.2.2 Synthesis of Starting Materials

The diacetoacetates used within this chapter are the same as the ones used in chapter 4.1. Therefore, the applied diacetoacetates (**124a-e**) were synthesised according to the procedure described in chapter 6.3.1 from the respective diols (**123a-e**) and *tert*-butyl acetoacetate (**64**). Besides these AA-monomers, a novel AB-monomer was synthesised from renewable starting materials and used to complement the monomer spectrum with a new type.

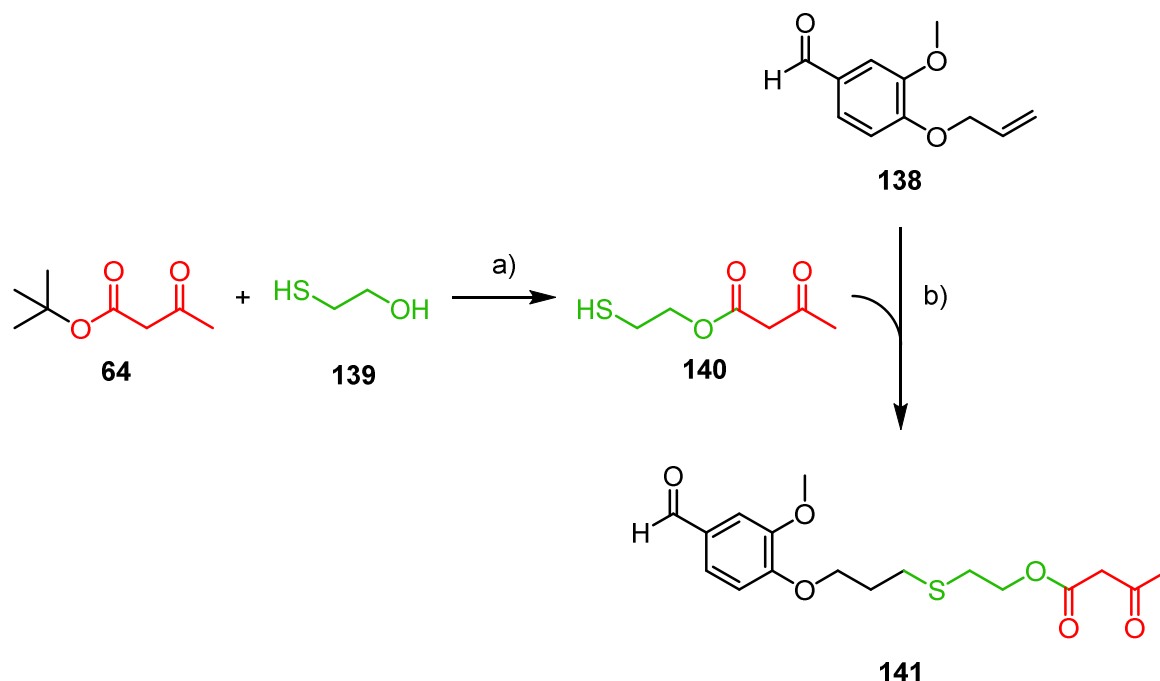
The renewable AB-monomer, 2-{{[3-(4-formyl-2-methoxy-phenoxy)propyl]thio}ethyl acetoacetate (**141**), was synthesised *via* a four-step route (**Scheme 4.5**) while the overall sustainability was carefully considered. Each step was mainly verified using ^1H NMR spectroscopy supported by ^{13}C NMR spectroscopy, IR spectroscopy, and HRMS.

The first two reaction steps towards 4-(allyloxy)-3-methoxybenzaldehyde (**138**) were performed as described in the literature.^[382,383] First, allyl methyl carbonate (**137**) was synthesised by 1,5,7-triazabicyclo[4.4.0]dec-5-ene (TBD)-catalysed transesterification of dimethyl carbonate (**135**) with allyl alcohol (**136**) (**Scheme 4.4, a**). Second, **137** and vanillin (**134**) were reacted in a Tsuji-Trost reaction to form the allyl ether **138** (**Scheme 4.4, b**). As catalyst, Pd⁰ nanoparticles in water, stabilised with poly(vinylpyrrolidone), were applied. The obtained results were in accordance with the literature.^[382,383]



Scheme 4.4 Literature-known two-step synthesis of **138** from **134**, **135**, and **136**; reaction conditions: **a)** 7.50 eq **135**, 1.00 eq **136**, 0.01 eq TBD, 80°C, 1 h, 31% yield. **b)** 1.00 eq **134**, 2.50 eq **137**, 0.05 eq triphenyl phosphine, 0.001 eq Pd⁰/poly(vinylpyrrolidone), 0.370M in water, 90°C, 22 h, 80% yield.^[382,383]

Third, 2-mercapto ethanol (**139**) and *tert*-butyl acetoacetate (**64**) were reacted to form 2-mercaptoethyl acetoacetate (**140**) (Scheme 4.5, **a**)) using a procedure similar to the procedure for the synthesis of diacetoacetates (*cf.* chapter 4.1.2). However, **139** and **64** were applied in a ratio of 1:1 to decrease double functionalisation of **139**. The pure product was obtained with a yield of 63%. The favoured formation of the ester compared to the thioester was attributed to the higher stability of the ester compared to the thioester. Thus, the reaction temperature of 150°C probably led to the favoured formation of the thermodynamically favoured product. ¹H NMR analysis confirmed the product formation showing the characteristic product signals, in particular the γ -CH₃- and α -CH₂-protons of the β -keto moiety and the thiol-protons at 2.19 ppm, 3.63 ppm, and 2.56 – 2.51 ppm, respectively.



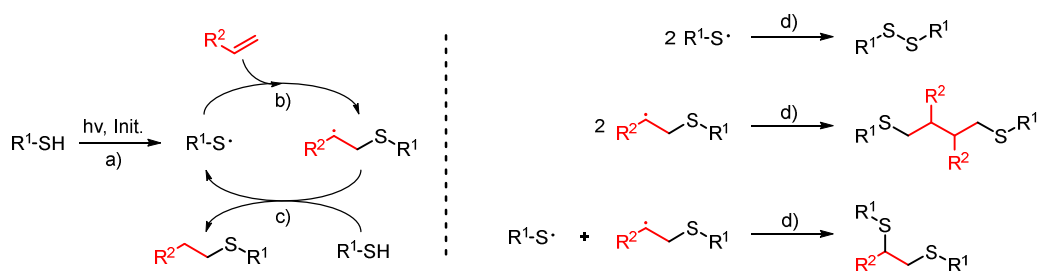
Scheme 4.5 Four step synthesis route to the renewable AB-monomer **141**; optimised reaction conditions: **a)** 1.00 eq **139**, 1.00 eq **64**, 150°C, 4.5 h, 63% yield. **b)** 1.00 eq **138**, 1.00 eq **140**, 0.01 eq DMPA, irradiation at 365 nm, over night, 85% yield.

The fourth step was a photoinitiated thiol-ene reaction⁷ between **138** and **140** yielding the AB-monomer (**141**) (Scheme 4.5, b)). The first experiment was conducted in EtOAc (2M). **138** and **140** were applied in a 1:1 ratio with 2,2-dimethoxy-1,2-diphenylethan-1-one (DMPA) as photoinitiator. The respective conversions were observed by ¹H NMR spectroscopy of samples of the crude reaction mixture.

⁷ The thiol-ene reaction is the anti-Markovnikov addition of a thiol to a double bond.^[384] The reaction proceeds over a radical pathway. The typical reaction cycle for a photoinduced thiol-ene reaction starts with the formation of a thiyl-radical (a), also possible without initiator). The following addition of the thiyl-radical to the olefin (b) and subsequent proton abstraction from another thiol molecule (c) results in the formation of the product and another thiyl-radical.^[384] Termination (d) occurs by radical-radical coupling under formation of disulfides or dithioethers.^[384]

The use of EtOAc as solvent led to no conversion of the double bond of **138**. However, a conversion of approximately 30% of the aldehyde function to an unknown compound was observed. Furthermore, a slight shift of -0.02 ppm and -0.01 ppm of the γ - CH_3 - and α - CH_2 -protons of the β -keto moiety and $+0.03$ ppm of the $(CO)O-CH_2$ -signals of **140** was observed. Integration of the respective signals indicate a conversion of 80% of **140**. The reaction of **140** in EtOAc and DMPA as initiator without the addition of an olefin showed no conversion of **140**. Hence, the conceivable formation of a disulfide as side product in the above thiol-ene reaction was excluded. Nonetheless, the resulting structure/s remained unknown.

As a consequence, the thiol-ene reaction was investigated with respect to the applied solvent. The reaction was performed in bulk, in CH_2Cl_2 (2 M), and in DMSO (2 M) leading, according to the integration of the respective proton signals at 6.06 ppm, 5.42 ppm, and 5.29 ppm, to ene-conversions of 92%, 96%, and 88%, respectively (**Figure 4.10**, example 1H NMR spectrum of the crude product of the thiol-ene in bulk). Moreover, characteristic product signals besides negligible side products indicated high theoretical yields. Due to the similar conversions and selectivities between these three conditions, **141** was, for sustainability reasons, synthesised in bulk with a yield of 85% after purification by column chromatography.



4.2 End Group-Functionalisation of Biginelli Polycondensates and Subsequent Block Copolymer Synthesis

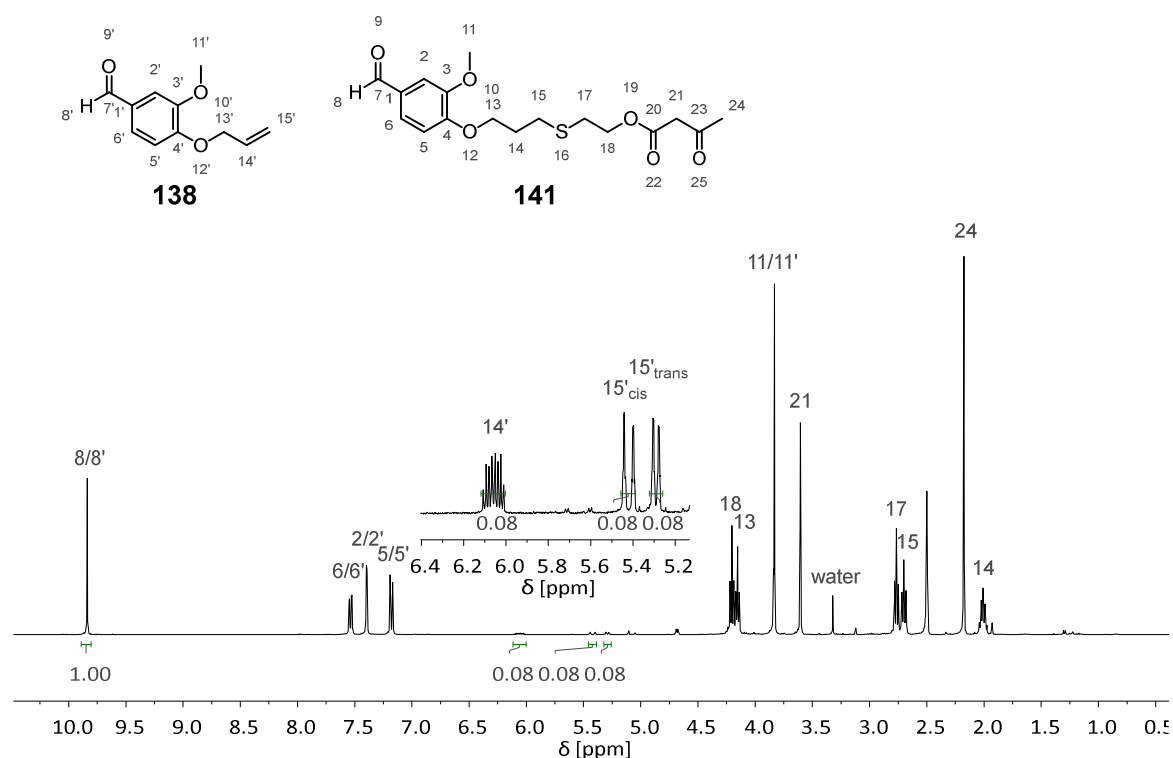
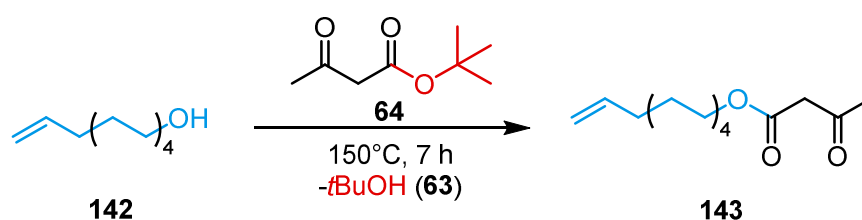


Figure 4.10 Optimisation of the synthesis of **141**, here shown by the results of the thiol-ene reaction in bulk: The crude ^1H NMR spectrum shows 92% conversion of the allyl double bond of **138** relative to the aldehyde signal; the product signals are visible besides minor impurities; the respective spectra of the reactions in CH_2Cl_2 or DMSO as solvent are comparable.

The end-capping agent to introduce terminal double bonds to the polyDHPMs, 10-undecenyl-1-acetoacetate (**143**), was synthesised similar to the diacetoacetates described in chapter 4.1.2. Accordingly, 10-undecenyl-1-ol (**142**) was stirred with 2.50 eq of **64** at 150°C yielding 99% of **143** after purification. ^1H NMR analysis confirmed the product formation showing the characteristic product signals, in particular the $\gamma\text{-CH}_3$ - and $\alpha\text{-CH}_2$ -protons of the β -keto moiety at 2.17 ppm and 3.58 ppm, respectively, as well as the $\text{H}_2\text{C}=\text{CH}$ - and the $\text{H}_2\text{C}=\text{CH}$ -signals at 4.89 – 5.05 ppm and 5.79 ppm. The successful synthesis was further supported by ^{13}C NMR spectroscopy, IR spectroscopy, and HRMS.



Scheme 4.6 Reaction scheme for the synthesis of **143** by esterification of the respective alcohol **142** in bulk, 99% yield.

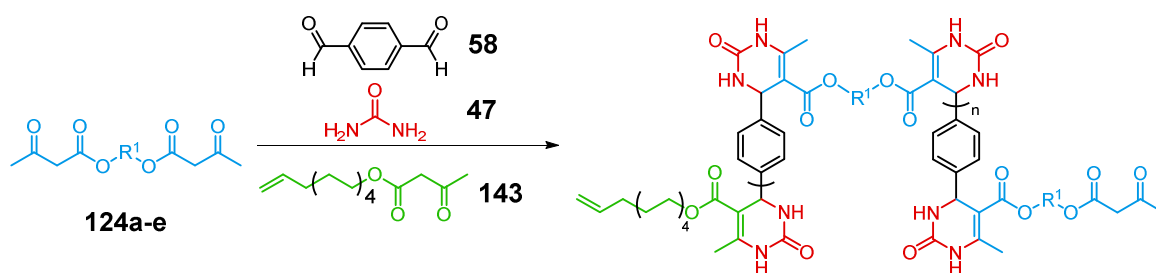
To conclude, the pure starting materials **124a-e** and **141**, as well as the pure end-capping agent **143** were synthesised. Their application for the synthesis of polyDHPMs with terminal double bonds is described within the following chapter.

4.2.3 Poly[3,4-dihydropyrimidin-2(1H)-one]s with Defined End Groups

Within this chapter, the Brønsted acid catalysed (*p*-toluenesulfonic acid) polycondensations of the above described diacetoacetates (**124a-e**) with terephthalic aldehyde (**58**) and urea (**47**) as well as the polycondensation of the AB-monomer **141** with **47** is discussed (**Scheme 4.7**). The procedure resembles that for the synthesis of the polyDHPMs **120a-f** (chapter 4.1.3.1). However, different amounts of **143** were added to the reaction mixture prior to heating to efficiently introduce a terminal double bond as end group of the polymer chain. The resulting end group-functionalised polyDHPMs (**144a-f**) were characterised by NMR spectroscopy, SEC, DSC, and IR.

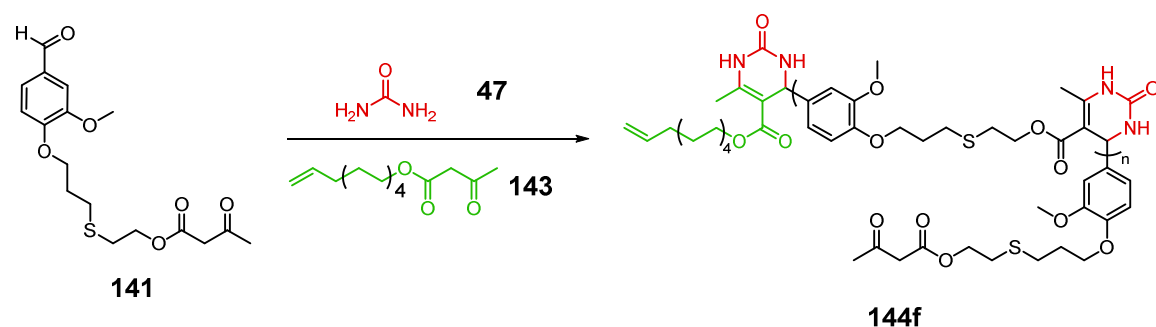
4.2 End Group-Functionalisation of Biginelli Polycondensates and Subsequent Block Copolymer Synthesis

AA/BB-monomer system:



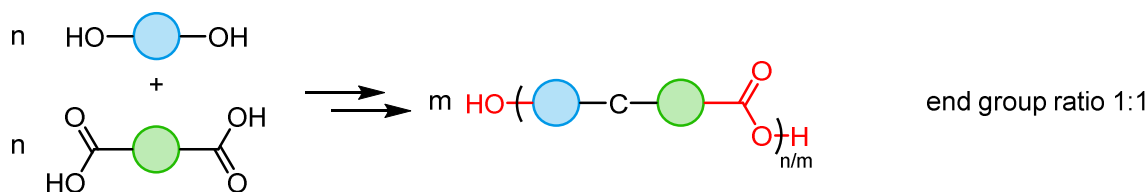
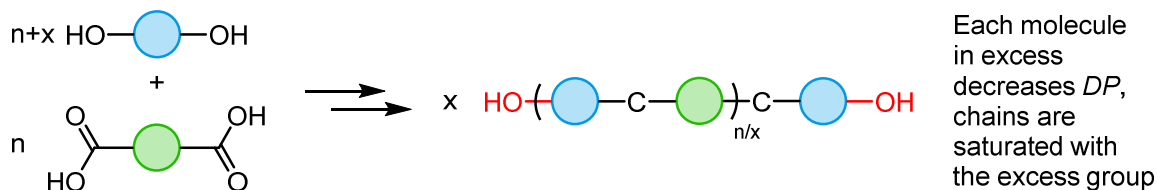
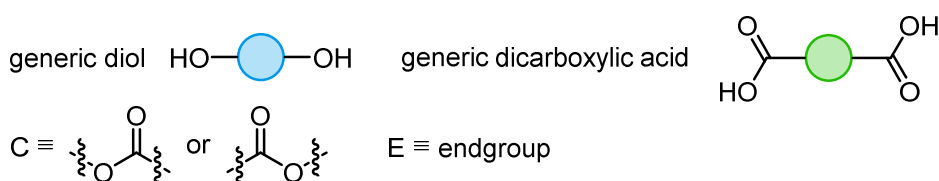
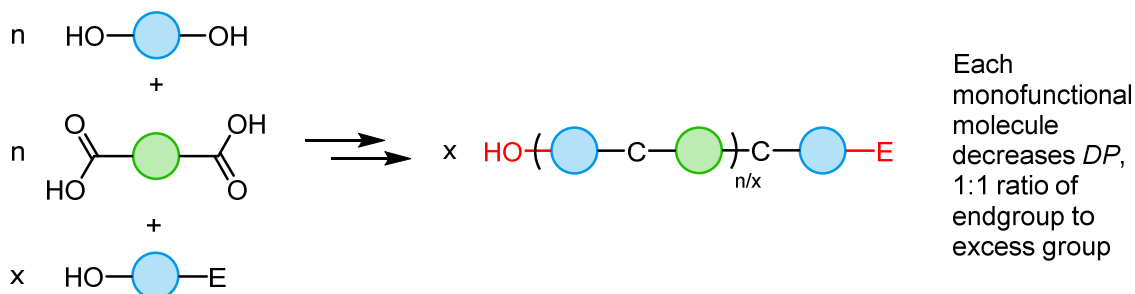
R¹: -C₂H₄- (a), -C₃H₆- (b), -C₄H₈- (c),
-C₆H₁₂- (d), -C₁₀H₂₀- (e)

AB-monomer system:



Scheme 4.7 Brønsted acid catalysed synthesis of end group functionalised polyDHPMs: top: using AA/BB-monomers, particularly the diacetoacetates **124a-e** in combination with terephthalic aldehyde (**58**) and urea (**47**), bottom: using the AB-monomer **141** together with **47**.

The Biginelli-polycondensation is supposed to proceed step-wise (see chapter 4.1.3.1). Such step-growth polymerisations are sensitive towards the stoichiometry of the reactants, therefore also towards the addition of monofunctional reactants. This is shortly illustrated in **Scheme 4.8** in a generic polycondensation of a diol and a dicarboxylic acid.

Polycondensation with stoichiometric balance between diol and dicarboxylic acid:**Stoichiometric imbalance, excess diol, situation at full conversion:****Stoichiometric imbalance, additional monofunctional alcohol, situation at full conversion:**

Scheme 4.8 Idealised scheme of a generic polycondensation of a diol and a dicarboxylic acid: if both monomers are present in equal amounts, polymer chains with a statistical ratio of alcohol:dicarboxylic acid of 1:1 are formed; an excess of, e.g., diol lowers the maximum DP and produces polymer diols at full conversion; addition of monofunctional alcohols equally lowers the DP and yields polymers with alcohol and “E” endgroups.

If the diol and dicarboxylic acid are present in equimolar amounts, the resulting polycondensates statistically carry one alcohol function and one carboxylic acid function each. In addition, the DP is only limited by p according to the Carothers equation.⁸ However, this only holds true if the monomers are added in stoichiometrically equal amounts and no monofunctional monomer is present (**Scheme 4.8**). If the stoichiometry is imbalanced, the excess of one functionality over the other causes an excess of polymer chains where α - and ω -chain ends both correspond to the excess functionality which also hinders the step-growth. Therefore, the DP decreases with increasing excess of one functional group.⁸ The addition of a monofunctional reactant similarly lowers the maximum DP and leads to polymer chains that statistically carry the structure (E) of the monofunctional monomer and the excess polymerisable function, respectively. Moreover, if the conversion is below 100%, the deficient functional group is also present. Their amount, together with the amount of E-groups, equals the amount of present excess functionality.

As a consequence, it was reasonable to assume that the α - and ω -chain ends of a polyDHPM chain are an aldehyde and a β -keto ester, respectively, and that they statistically occur in a ratio of 1:1. Furthermore, by addition of the monoacetoacetate **143** to the reaction

⁸ The Carothers equation expresses the proportionality of degree of polymerisation DP and extent of the reaction p for step-growth polymerisations.^[385] It is for stoichiometrically balanced polymerisations:^[385]

$$DP = \frac{1}{1-p}$$

To calculate DP in the case of an imbalanced stoichiometry, the ratio of polymerisable functional groups r is introduced with the number of A-groups N_A and the number of B-groups N_B .^[385]

$$DP = \frac{1+r}{1+r-2rp} \text{ and } r = \frac{N_A}{N_B}$$

Conventionally N_B is the excess functionality, hence $r \leq 1$.^[385] Above equation is also applicable for the presence of a number of monofunctional reagent $N_{B,mono}$ if r is adapted. Since the presence of one monofunctional molecule has the same effect on DP as one difunctional, a factor of two arises and r is defined as:^[385]

$$r = \frac{N_A}{N_B + 2N_{B,mono}}$$

mixture, the resulting polyDHPMs would carry an acetoacetate and a terminal double bond introduced by **143**, each.

To investigate this assumption, a set of polyDHPMs with double bond end groups was synthesised using **141** or **124d** together with **47** and **58** in the case of **124d** (*cf.* Scheme 4.7). Different amounts of **143** were added to the reaction mixture at the beginning of the polymerisation to maximise the incorporation of the end-capping agent. This resulted in the polyDHPMs **144d** and **144f** (Table 4.7). The products were analysed by SEC and ¹H NMR spectroscopy.

Table 4.7 ¹H NMR and SEC data of polyDHPMs using **124d** or **141** with different amounts of **143**.

entry	polymer	mol% of 143 added	mol% of 143 incorporated ^a	$M_{n,NMR}^b$ [g·mol ⁻¹]	$M_{n,SEC}^c$ [g·mol ⁻¹]	$M_{w,SEC}^c$ [g·mol ⁻¹]	\bar{D}
1		0	-	10 100	7 100	20 900	2.95
2		1	- ^d	11 500	6 800	24 600	3.59
3		5	97	7 400	5 800	16 300	2.82
4	144f	10	78	4 600	5 500	15 200	2.78
5 ^e		10	75	4 800	5 600	16 100	2.86
6		15	44	5 500	5 300	15 100	2.83
7 ^f		15	47	5 400	5 500	17 600	3.23
9		30	56	2 200	4 200	9 500	2.29
10		5	92	4 700	6 800	28 800	4.21
11	144d	10	66	3 400	6 400	20 900	3.25
12		15	61	2 500	5 900	17 100	2.92

^a¹H NMR determination of mol% of **143** incorporated in purified polyDHPM relative to the amount of **143** added to the reaction mixture; ^bdetermined by integration of the aldehyde and the double bond end group signals, end groups were not implemented into the calculation; ^cSEC measurements were conducted in hexafluoroisopropanol with 0.1 wt% KO₂CCF₃ as eluent; ^dsignal of the double bond not visible in ¹H NMR spectrum; ^eaddition of a second portion of **143** after 16 h of reaction time; ^f45 h reaction time.

Nine different samples of **144f** were prepared using 1.0 mol% to 30 mol% of **143** (Table 4.7, entry 1 – 9). As expected, the $M_{n,SEC}$ decreased with increasing amount of **143**. The highest $M_{n,SEC}$ of 7 100 g·mol⁻¹ was reached without addition of end-capping agent, the lowest $M_{n,SEC}$ of 4 200 g·mol⁻¹ with 30 mol% of **143**. The D ranged between 2.29 and 3.59 and did not follow an obvious trend.

The $M_{n,NMRS}$ were calculated using the integrals of the CH-protons of the DHPM unit at 5.1 ppm relative to the sum of the integrals of aldehyde and double bond end groups at 9.9 ppm and 5.8 ppm, respectively. As an example, the ¹H NMR spectrum of **144f**, prepared with 5 mol% of **143**, is shown in Figure 4.11. Besides the signals of the double bond end group, the characteristic signals of the NHC=C protons at 9.2 ppm, the NHC-C at 7.7 ppm, the aromatic protons around 6.7 ppm and 6.9 ppm, the NH-CH-C_{Ar} protons at 5.1 ppm, and the O-CH₃ protons at 3.7 ppm were observed. The signal of the C=C-CH₃ protons was visible at 2.3 ppm. The signals of the remaining CH₂ protons are visible between 4.3 – 3.8 ppm and 2.9 – 2.5 ppm, and at 1.9 ppm.

Like the $M_{n,SEC}$, the $M_{n,NMR}$ also decreased with increasing amount of **143** (Table 4.7, entry 1 – 9). However, the $M_{n,NMRS}$ of entries 4 and 5 were smaller than the $M_{n,NMRS}$ of entries 6 and 7. This was attributed to the inaccuracy during the integration of the respective signals of the ¹H NMR spectra. The baseline was properly corrected in the region of the aldehyde end group at approximately 10 ppm. However, the baseline around the integrated signal of the double bond end group at 5.8 ppm and the CH-proton of the DHPM-structure of the repeat unit at 5.1 ppm showed a positive offset. Furthermore, due to the low concentration of end groups, minor impurity signals distort the integration.

Nonetheless, the ¹H NMR spectra were also used to estimate the ratio of end-capping agent that was incorporated into the polymer compared to the added amount. Interestingly, the incorporated amount decreased from 97% to approximately 50% with increasing addition of **143**. Nonetheless, the amount of double bond end groups incorporated in the polymer increased from 4.9% to 17%. The signals of the acetoacetate end group at 3.6 ppm and 2.2 ppm were not distinguishable due to the overlap with signals of the polyDHPM and

were thus not integrated. To be able to determine the amount of acetoacetate end groups, a quantitative reaction that introduces, upon conversion of the acetoacetate, a moiety whose NMR signals do not overlap with the polyDHPM signals, is conceivable – for example the reaction with an excess of a trimethylsilyl-functionalised primary or secondary amine. However, this approach was, due to time restraints, not sought in this context.

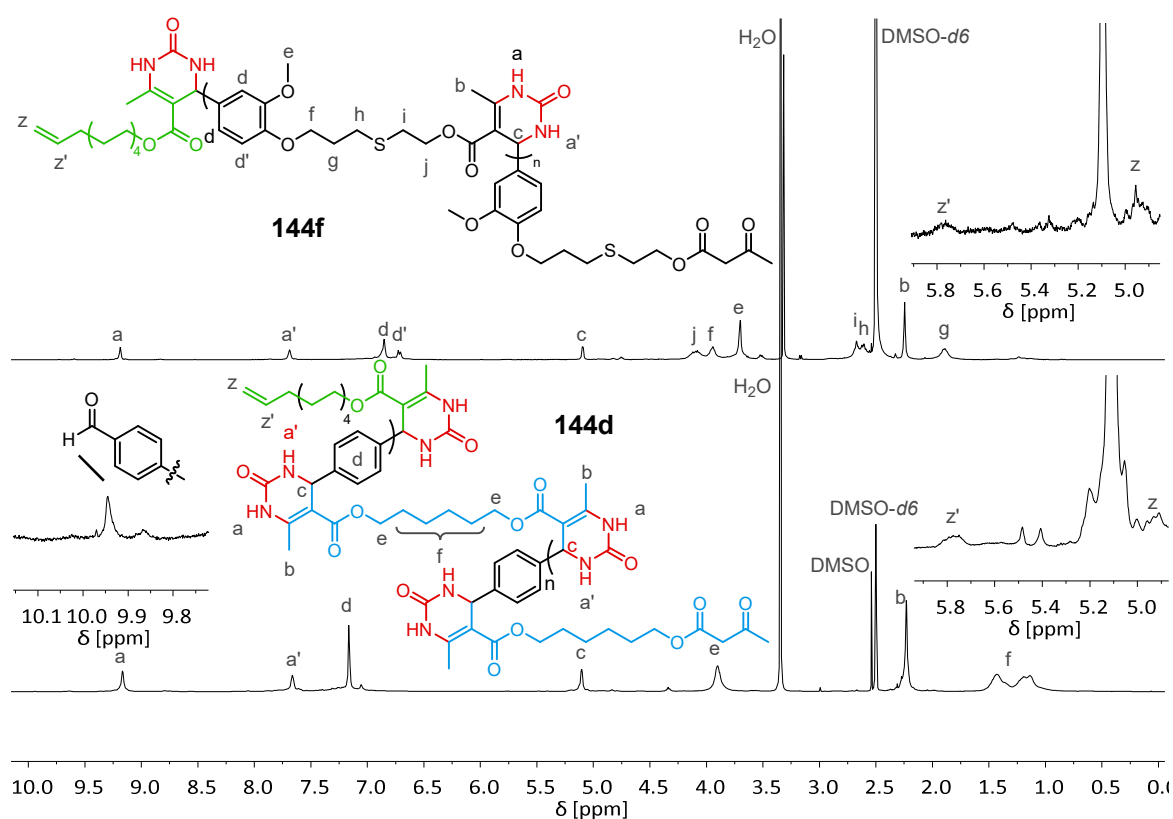


Figure 4.11 Typical ¹H NMR spectrum of **144f** (top) and **144d** (bottom) with 5 mol% of **143**, the aldehyde end group signal is shown for **144d**.

Furthermore, to investigate the possibility to increase the amount of incorporated double bond end group, a second portion of **143** was added after 16 h of reaction time (**Table 4.7**, entry 5). However, no significant change was observed compared to a single addition at the start of the reaction (entry 4). More precisely, the second addition seemed not to be incorporated. Last but not least, the influence of reaction times longer than 22.5 h was

investigated, comparing entry 6 (22.5 h) and entry 7 (48 h). No significant change of the $M_{n,SEC}$ or the $M_{n,NMR}$ were observed while an increase of the D was found. Hence, the polymerisation seemed to not proceed any further within a reasonable time frame after 22.5 h while side reactions seemed to occur.

Similarly to **144f**, three reactions to form **144d** were conducted with 5 mol%, 10 mol%, and 15 mol% of **143** (Table 4.7, entry 10 – 12). $M_{n,SEC}$ and $M_{n,NMR}$ followed the same trend as for **144f** ranging from 6 800 g·mol⁻¹ to 5 900 g·mol⁻¹ and from 4 700 g·mol⁻¹ to 2 500 g·mol⁻¹, respectively. The D decreased with increasing amount of end-capping agent from 4.21 to 2.92 possibly due to the following reason. The SEC graphs of polyDHPMs without double bond end groups show large shoulders to or even bimodal distributions towards lower molecular weights possibly due to the formation of rings or the oxidation of some of the aldehyde endgroups (Figure 6.16, page 193). As the end-capped polyDHPMs only reached lower molecular weights, the peak of the respective molecular weight distribution overlaps with what would form the shoulder. Consequently, the size distribution appears to be narrower. An example ¹H NMR spectrum of **144d** with 5 mol% of **143** is shown in Figure 4.11.

Finally, various molecular weights of end group-functionalised polyDHPMs were achieved by addition of different amounts of the end-capping agent for the polymerisation of an AA/BB-monomer and an AB-monomer. The incorporation of the end-capping agent was quantified by ¹H NMR spectroscopy. It was found that more than 92% of **143** were incorporated by addition of 5 mol%. This percentage, however, decreased when larger amounts of **143** were added. As a consequence, 5 mol% of **143** were chosen for the synthesis of a series of six end group functionalised polyDHPMs using **124a-e** as AA-monomer and **141** as AB-monomer (cf. Scheme 4.7, page 104).

Since, the addition of 5 mol% of end-capping agent led to the highest efficiency for end group incorporation, the same amount was used for the preparation of four additional polyDHPMs, **144a-c,e**. Consequently, five different aliphatic, linear diacetoacetates **124a-e** with chain lengths between C₂ and C₁₀ and the AB-monomer **141** were applied. The results

of the SEC analysis and the ^1H NMR spectroscopy are shown in **Table 4.8** and resemble the results obtained for **144f** and **144d**. The end-capping agent was incorporated at percentages above 92% and similar DP s were reached. Furthermore, yields between 69% and 76% were reached after purification by precipitation.

Table 4.8 ^1H NMR and SEC data of polyDHPMs using **124a-e** or **141** with 5 mol% of **143**.

entry	polymer	mol% of 143 incorporated ^a	$M_{n,\text{NMR}}^b$ [g·mol ⁻¹]	$M_{n,\text{SEC}}$ [g·mol ⁻¹]	$M_{w,\text{SEC}}$ [g·mol ⁻¹]	\bar{D}
1	144a	99	4 100	4 500	16 400	3.68
2	144b	101	3 800	4 500	14 000	3.01
3	144c	99	4 300	5 700	14 700	2.52
4	144d	92	4 700	6 800	28 800	4.21
5	144e	92	5 300	6 900	29 600	4.32
6	144f	97	7 400	5 800	16 300	2.82

^a ^1H NMR determination of mol% of **143** incorporated in purified polyDHPM relative to the amount of **143** added to the reaction mixture; ^bdetermined by integration of the aldehyde and the double bond end group signals.

Finally, **144a-f** were investigated by DSC to compare the thermal transitions to those of the non-end-capped polyDHPMs **120a-e** described in chapter 4.1.3.1 (*cf.* **Table 4.5**). For the polyDHPMs from AA/BB monomers, the observed T_g s expectedly ranged from 268°C for the C₂ diacetoacetate to 176°C for the C₁₀ diacetoacetate with a gradually lower T_g for longer spacers (*cf.* chapter 6.4.2.1 and 6.4.2.2). Compared to the non-end-capped polyDHPMs, the T_g s of **144a-e** were up to 20°C lower (*cf.* **Table 6.7** and **Table 6.10**). This was attributed to the lower molecular weights of **144a-e**.⁹ The end-capped **144f** showed a

⁹ The dependence of the glass transition temperature, T_g , of the number average molecular weight, M_n , was shown by Flory and Fox by investigation of poly(styrenes) of different M_n s.^[386] The resulting Flory-Fox equation gives, for linear polymers, a linear dependence of T_g to M_n^{-1} with the glass transition temperature at infinite M_n , $T_{g,\infty}$, and an empirical factor K :^[386] $T_g = T_{g,\infty} - K \cdot M_n^{-1}$

considerably lower T_g of 59°C which was consistent with the finding that the non-capped **144f** showed a comparably low T_g of 94°C. The lower T_g was considered to be caused by the lower symmetry of the AB-monomer compared to the AA/BB system hindering the formation of hydrogen bonds.

To investigate whether the terminal double bond end group is suited for further functionalisation, **144d**, prepared with 10 mol% of **143**, was reacted with 5.00 eq of butanethiol (**145**) relative to the double bond end group in a photoinitiated thiol-ene reaction. Samples were taken after 15 h, 24 h and 48 h to estimate the conversion by integration of the terminal double bond signal at 5.8 ppm *via* ^1H NMR spectroscopy (**Figure 4.12**).

The reaction reached a conversion of 79% after 48 h of reaction time. While the thiol-ene reaction proceeded slowly, high conversions were still possible. As a consequence, the application of the thiol-ene reaction for polymer-polymer coupling reactions of the end group functionalised polyDHPMs **144a-f** with another polymer that contains a thiol end group was considered principally feasible.

To conclude, the efficiency of the end group functionalisation by introduction of a double bond and the dependence of the molecular weights of the polyDHPMs **144d** and **144f** were investigated using various amounts of the end-capping agent **143** between 1 mol% and 30 mol%. The highest percentage was incorporated for the addition of 5 mol% of **143**. The molecular weight of the resulting polyDHPMs decreased with increasing addition of end-capping agent. Moreover, a set of six end group functionalised polyDHPMs, **144a-f** was synthesised using the established protocol with 5 mol% of **143** showing $M_{n,SECS}$ between 4 500 g·mol⁻¹ and 6 900 g·mol⁻¹ and T_g s between 268°C and 59°C. Finally, the reactivity of the terminal double bond in a photoinitiated thiol-ene reaction was tested using **145** as test reagent resulting in a double bond conversion of 79% after 48 h.

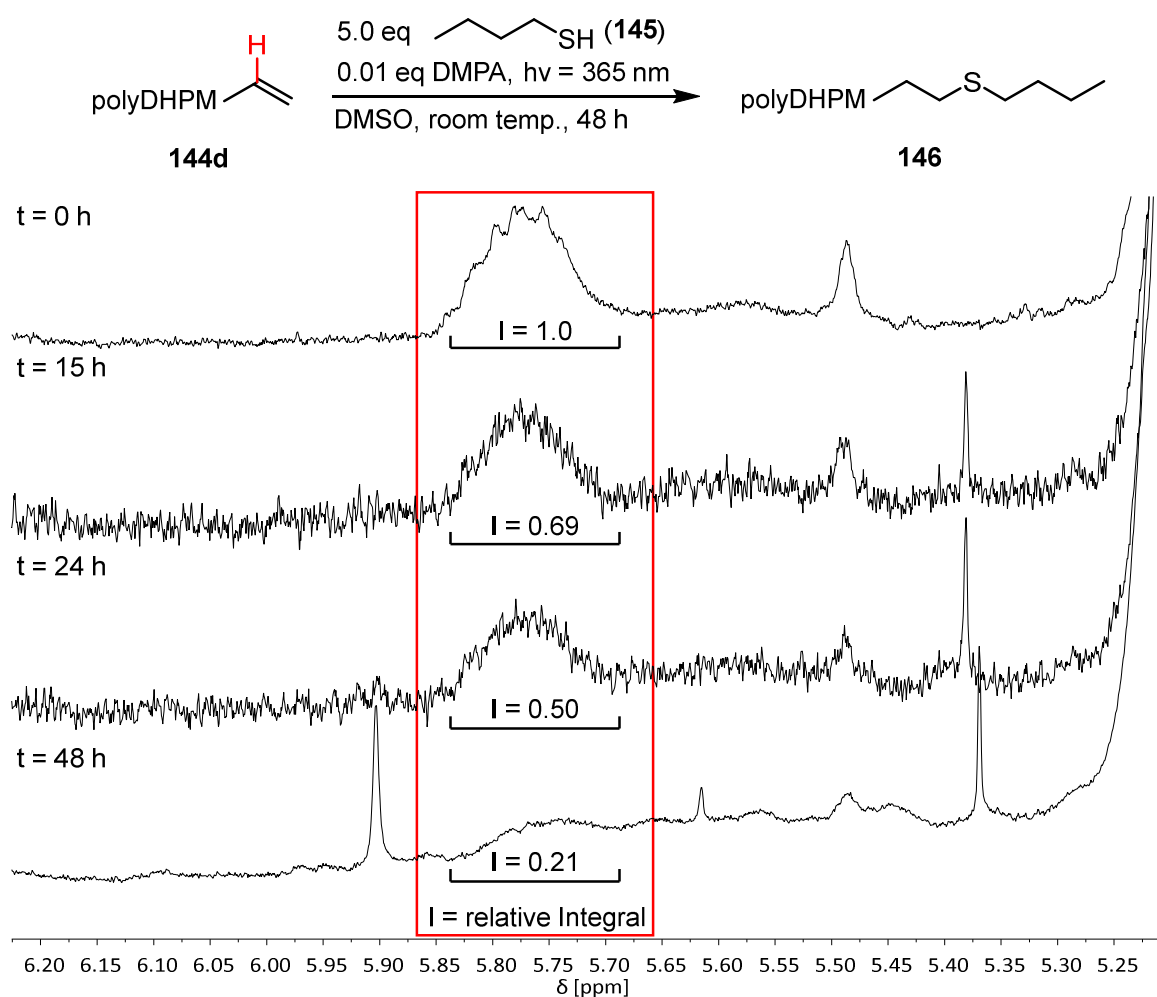


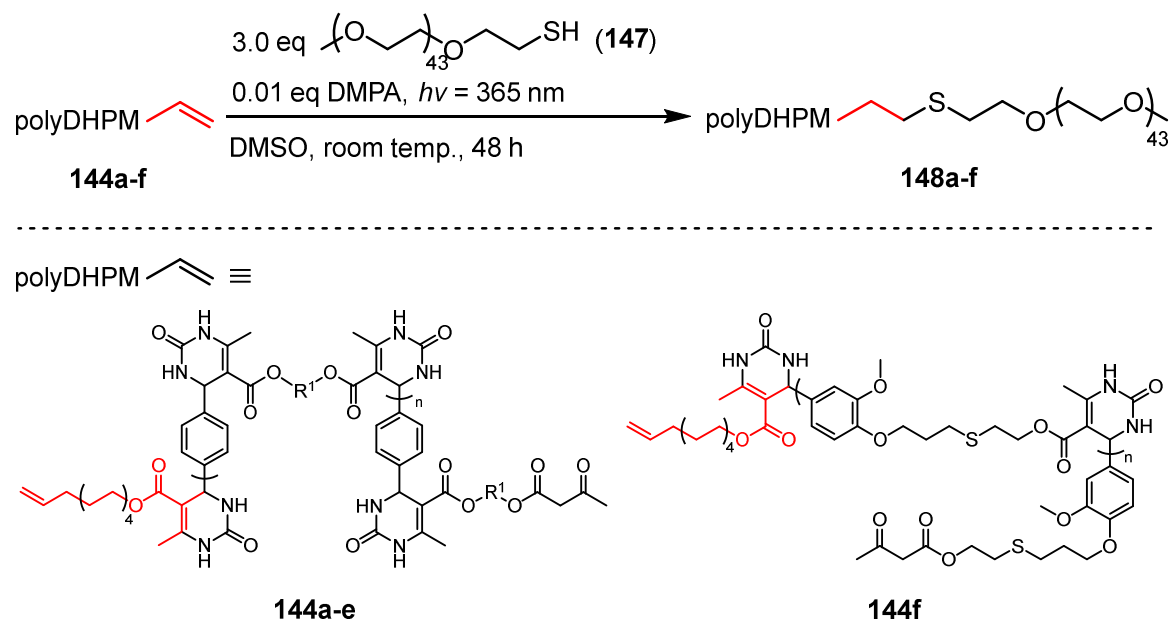
Figure 4.12 Estimation of end group conversion of **144d** in photoinitiated thiol-ene reaction with **145**: Integrals of the end group CH signal are given for reaction times of 15 h, 24 h, and 48 h relative to the starting material ($t = 0$ h), the signal of the CH proton of the polyDHPM backbone is used as reference.

4.2.4 Synthesis of Block Copolymers by Polymer-Polymer Coupling

The occurrence of Biginelli-polycondensates as part of copolymers has been rarely reported. The only example is a statistical copolycondensate containing dihydropyrimidine and DHPM moieties in the polymer backbone for which the authors simply combined the Hantzsch- and Biginelli-reactions in one pot.^[354] This chapter aims to investigate the synthesis of block copolymers containing a polyDHPM block. The in the last chapter introduced terminal double bond was used to couple the polyDHPMs **144a-f** with

4.2 End Group-Functionalisation of Biginelli Polycondensates and Subsequent Block Copolymer Synthesis

poly(ethylene glycol) methylether thiol (**147**, $M_n = 2\,000\text{ g}\cdot\text{mol}^{-1}$) via thiol-ene reaction (**Scheme 4.9**).



Scheme 4.9 Reaction scheme of the photoinitiated thiol-ene reaction of **144a-f** with **147**.

The resulting polyDHPM-*b*-poly(ethylene glycol)s, **148a-f**, were synthesised with yields between 69% and 76%. Investigation by SEC, ^1H NMR spectroscopy, and DSC verified the formation of block copolymers and gave insight into the respective thermal properties (**Table 4.9**). The SEC data showed larger $M_{n,\text{SECS}}$ and similar D_s compared to the starting materials, **144a-f** (**Table 4.8**, page 111), indicating the coupling of **144a-f** with **147** by thiol-ene reaction. The resulting $M_{n,\text{SECS}}$ ranged from $5\,700\text{ g}\cdot\text{mol}^{-1}$ to $11\,800\text{ g}\cdot\text{mol}^{-1}$. It is noteworthy that the polymer samples were precipitated twice in acetone from DMSO prior to washing with water as **148f** was highly soluble in water if it was directly precipitated from the reaction mixture in water. Washing was continued until no unreacted PEG signal was observable anymore. Hence, the existence of a blend instead of a block copolymer was excluded. Afterwards, the filtrate was evaporated to dryness and analysed by ^1H NMR spectroscopy.

Table 4.9 ¹H NMR, SEC, and DSC data and yields of polyDHPM-*b*-poly(ethylene glycol), **148a-f**.

polymer	R ¹	$M_{n, \text{NMR}}^{\text{a}}$ [g·mol ⁻¹]	$M_{n, \text{SEC}}$ [g·mol ⁻¹]	$M_{w, \text{SEC}}$ [g·mol ⁻¹]	\bar{D}	T_g/T_m^{b} [°C]	Yield ^c [%]
148a	C ₂ H ₄	5 700	5 700	18 600	3.27	265/49	76
148b	C ₃ H ₆	5 400	6 200	21 200	3.44	238/49	73
148c	C ₄ H ₈	5 800	5 900	14 700	2.51	232/49	75
148d	C ₆ H ₁₂	6 200	7 100	28 800	4.03	205/49	70
148e	C ₁₀ H ₂₀	6 700	8 900	53 700	6.00	159/52	69
148f^d	- ^e	4 400	11 800	30 300	2.56	55/-	76

^acalculated by integration of the aldehyde end group signals and the PEG CH₂ signals; ^bthe inflection point of the DSC curve was chosen as T_g , the minimum as T_m ; ^cisolated yields calculated by comparison with theoretical amount of mass at 100% conversion; ^dprecipitated two times in acetone from DMSO, washed with water; ^eAB-monomer.

The spectrum of the purified polymers showed the signal of the CH₂ protons of the ethylene glycol unit of **147** at 3.5 ppm besides the signals of the polyDHPM (**Figure 4.13**). The typical polyDHPM proton signals are described in chapter 4.1.3.1 in detail. Furthermore, the integral of the terminal double bond at 5.8 ppm decreased compared to the respective starting material. However, full conversion of the double bond end group was not possible. Using the integrals of the aldehyde end group, the double bond end group, the CH₂ signal of the PEG-block, and the CH signal of the polyDHPM, $M_{n, \text{NMR}}$ was estimated (**Table 4.9**). Expectedly, the estimated $M_{n, \text{NMR}}$ s were lower compared to the respective $M_{n, \text{SEC}}$ s.

Furthermore, the conversion to form the copolymer was estimated comparing the integral of the double bond end groups per polyDHPM unit of the respective starting material with the integral of the PEG signal of **148a-f**. Hence, conversions between 24% and 37% were determined. A separation of block copolymer and end group-functionalised polyDHPM was not investigated due to the similar solubility between the respective end group-functionalised polyDHPM and the block copolymer. A purification *via* preparative SEC or was considered challenging as well due to the broad molecular weight dispersion and its

similarity between the starting material and the resulting copolymer (*cf.* **Figure 6.44** and **Figure 6.55**, pages 232 and 246).

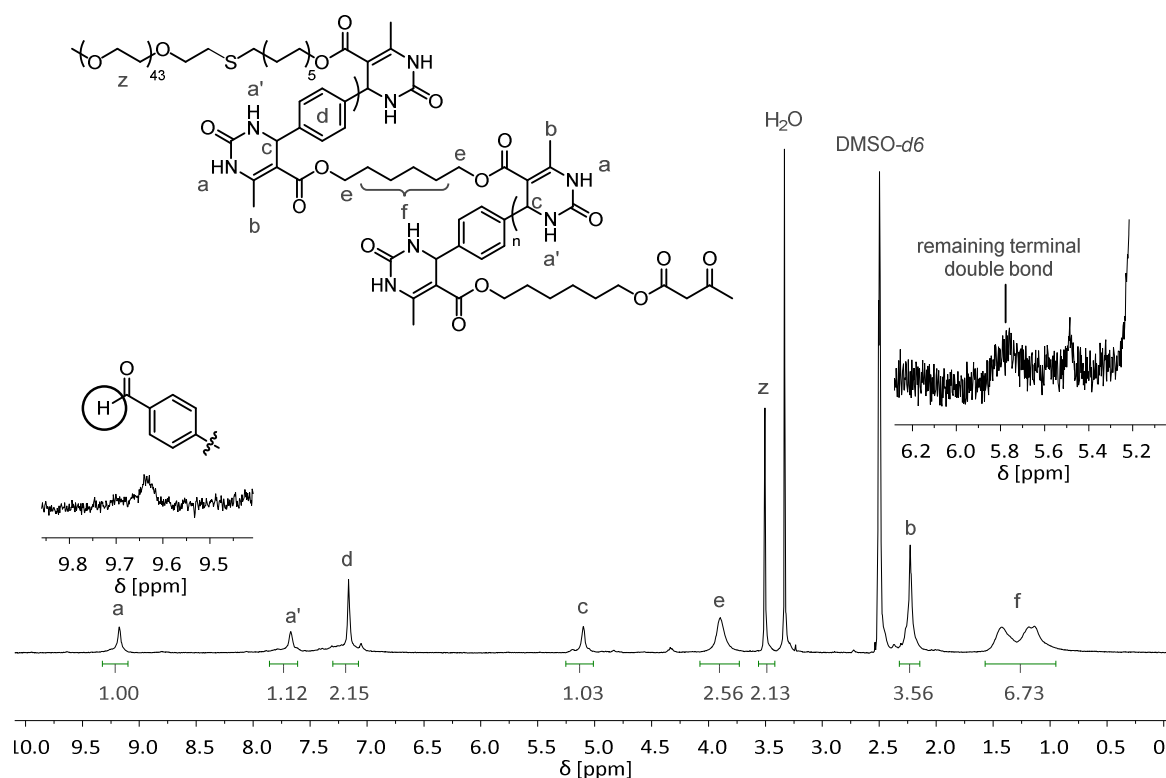


Figure 4.13 ¹H NMR spectrum of **144d** showing the typical signals of a polyDHPM-*b*-poly(ethylene glycol): besides the signal of the CH₂ groups of poly(ethylene glycol) at 3.5 ppm, the remaining signal of unreacted double bond end group at 5.8 ppm is visible.

To increase the conversion of the thiol-ene reaction, several experiments were conducted. First, one of the copolymer samples **148a** was reacted again in a thiol-ene reaction using the same conditions as for the first thiol-ene reaction. However, the conversion remained the same. The conversion of **144a** to **148a** with 6.0 eq of **147** gave the same conversion as for 3.0 eq. However, the addition of a second portion of 0.01 eq of DMPA after 24 h of reaction time allowed the increase of the conversion by approximately 10% to 44%. The improved yield after a second addition of photoinitiator indicated that an additional radical source was

needed. Since the reaction proceeds slowly and was conducted under air atmosphere, the radicals formed by the first portion of initiator were possibly scavenged by oxygen before the thiol-ene reaction was able to proceed to more than 37%. While the thiol-ene reaction does not necessarily need a radical initiator since the UV-irradiation is typically creating enough radicals, the radical concentration was probably too low in the case of the polymer-polymer coupling as the formed radicals were scavenged before the thiol-ene reaction proceeded and prolonged reaction times under constant irradiation were also not able to increase the conversion. Consequently, oxygen-free reaction conditions were considered to improve the conversion for future investigations.

Moreover, the thermal properties of **148a-f** were investigated by DSC (**Figure 4.14**, **Table 4.9**). Interestingly, two distinct thermal transitions, a T_g and a T_m , were observed for **148a-e**. The observed T_g s resembled those of the end-capped polyDHPMs indicating microphase separation between the polymer blocks since an interaction between blocks leads to an influence of the observed thermal transitions.^[387,388] The T_m s, which resembled the T_m of pure **147** at 51°C gave further evidence for this assumption. The T_g of PEG was not investigated since measurements of the expected T_g at about -50°C exceeded the lower temperature limit of the applied device.^[389] The thermal behaviour of **148f** differed from those of the other block copolymers. The T_m of the PEG block was not visible and a single T_g at 55°C was observed while the T_g of the respective end-capped polyDHPM **144f** was observed at slightly higher temperatures at 59°C (*cf.* **Table 6.11**, page 239). This indicated an interaction between the two polymer blocks.^[388]

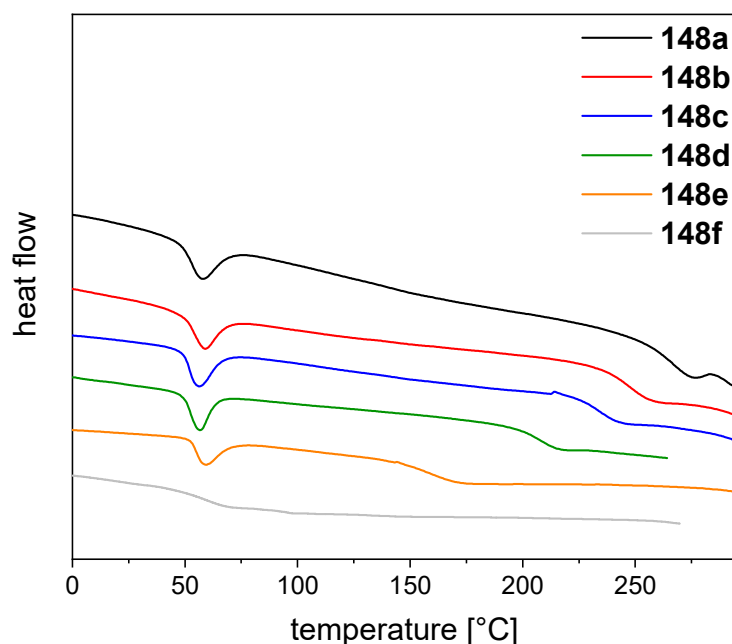
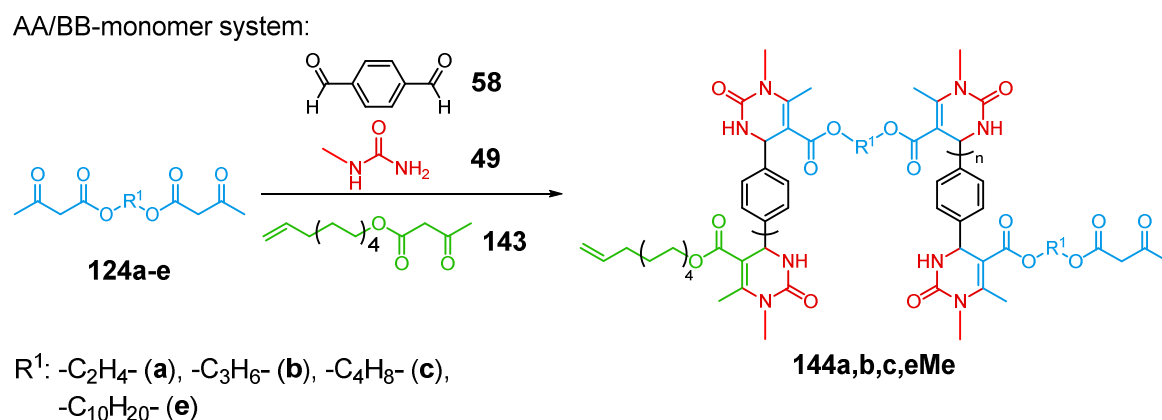


Figure 4.14 DSC graphs of **148a-e** showing two distinct thermal transitions, the T_m of the PEG block and the T_g of the respective polyDHPM block; the DSC graph of **148f** showed only one T_g .

In addition, a similar set of block copolymers was prepared using *N*-methyl urea (**49**) instead of **46** for the synthesis of the end group-functionalised polyDHPMs (**144a-eMe**) to demonstrate the feasibility of the established procedure for a broader scope of components using the same procedure as for **144a-e** yielding up to 80% of product (**Scheme 4.10**, **Table 4.10**). The synthesis of the resulting polymers was verified by ^1H NMR spectroscopy and SEC while the thermal properties were investigated by DSC. The respective spectra and graphs are available in chapter 6.4.2.4. Indeed, the obtained results were similar to those of the end group functionalised polyDHPMs and the copolymers for which **47** was used. In particular, the $M_{n,SEC}$ of **144a,b,c,eMe** ranged from 8 900 $\text{g}\cdot\text{mol}^{-1}$ to 12 700 $\text{g}\cdot\text{mol}^{-1}$ with D_s from 2.51 to 3.69. The T_g s decreased with increasing length of the spacer from 234 C to 144°C and were lower compared to those measured for the polyDHPMs from **47** as it was already discussed in detail in chapter 4.1.3.



Scheme 4.10 Brønsted acid catalysed synthesis of end group functionalised polyDHPMs (**144a,b,c,eMe**) using AA/BB-monomers, particularly the diacetoacetates **124a,b,c,e** in combination with terephthalic aldehyde (**58**) and *N*-methyl urea (**49**)

Table 4.10 SEC and DSC data and yields of the end group functionalised polyDHPMs (**144a,b,c,eMe**) and the polyDHPM-*b*-poly(ethylene glycol)s (**148a,b,c,eMe**).

polymer	R ¹	$M_{n,SEC}$ [g·mol ⁻¹]	$M_{w,SEC}$ [g·mol ⁻¹]	\bar{D}	T_g/T_m^a [°C]	Yield ^b [%]
144aMe	C ₂ H ₄	8 900	26 200	2.94	234/-	72
144bMe	C ₃ H ₆	12 700	46 900	3.69	212/-	75
144cMe	C ₄ H ₈	9 200	24 900	2.7	190/-	80
144eMe	C ₁₀ H ₂₀	6 400	16 000	2.51	144/-	68
148a	C ₂ H ₄	9 800	29 400	2.99	234/51	77
148b	C ₃ H ₆	11 900	47 800	4.03	204/51	72
148c	C ₄ H ₈	9 100	24 700	2.72	185/51	74
148e	C ₁₀ H ₂₀	6 600	16 800	2.53	140/52	72

^athe inflection point of the DSC curve was chosen as T_g , the minimum as T_m ; ^bisolated yields calculated by comparison with theoretical amount of mass at 100% conversion.

Subsequently, the polyDHPM-*b*-poly(ethylene glycol)s **148a,b,c,eMe** were prepared using the same procedure as for **148a-f**. The $M_{n,SECS}$ and the respective T_g s resembled those of **144a,b,c,eMe** while the D s increased slightly (Table 4.10). Also, the T_m of the PEG-block was observed in the DSC graphs at approximately 51°C confirming the successful synthesis of the block copolymers as discussed above for **148a-f**. In the end, the substrate scope and range of available T_g s was broadened by the application of **49** as component for the Biginelli-polycondensation and the subsequent block copolymer synthesis.

Consequently, the high and tunable T_g s of the polyDHPM block and the possibility for the synthesis of block copolymers that show microphase separation possibly allows for the synthesis of thermoplastic elastomers.^[390] In combination with PEG, however, the preparation of samples to investigate the mechanical properties of the copolymers was not possible. Hot pressing, as well as the formation of a polymer film *via* evaporation from solution in *N*-methyl-2-pyrrolidone or *N,N*-dimethylacetamide were attempted. The brittleness of the material hindered the preparation of a specimen suitable for stress-strain analysis and dynamic mechanical analysis. To obtain processable block copolymers, the usage of amorphous low T_g blocks, like poly(styrene) or polymethacrylates instead of the crystalline PEG is conceivable. Furthermore, the usage of shorter polyDHPM blocks might reduce the brittleness.

To conclude, the end group functionalisation of polyDHPMs with a terminal double bond was shown using the unsaturated monoacetoacetate **143** as end-capping agent. The $M_{n,SEC}$ of the resulting end-capped polyDHPMs was tuned between 6 800 g·mol⁻¹ and 4 200 g·mol⁻¹ by addition of different amounts of end-capping agent between 1 mol% and 30 mol% for the polyDHPMs **144f** using the AB-monomer **141**. Using the AA-monomers **124a-e**, the polyDHPMs **144a-e** were obtained with $M_{n,SECS}$ between 6 800 g·mol⁻¹ and 5 900 g·mol⁻¹ using 5-15 mol% of **143**. Afterwards, a set of six block copolymers was synthesised reacting the end-capped polyDHPMs **144a-f** in a thiol-ene reaction with poly(ethylene glycol) methylether thiol (**147**). Conversions of up to 44% were reached. Further investigations are necessary to obtain higher degrees of functionalisation and thus

pure block copolymers. The thermal analysis *via* DSC revealed the original thermal transitions of the polymer blocks indicating microphase separation.

4.2.5 Conclusion and Outlook

Within this chapter, the end group functionalisation of polyDHPMs and the subsequent synthesis of block copolymers exploiting the reactivity this end group were investigated. The synthesis of the end group-functionalised polyDHPMs **144a-f** using the monoacetoacetate **143** as end-capping agent was shown. Furthermore, the molecular weights of the resulting end-capped polyDHPMs were tuned by addition of different amounts of **143**. The resulting $M_{n,SEC}$ was expectedly lower for larger amounts of **143**. The end-capped polyDHPMs were subsequently converted to block copolymers **148a-f** by polymer-polymer coupling with poly(ethylene glycol) methylether thiol (**147**) in a thiol-ene reaction. DSC analysis of the resulting block copolymers **148a-e** indicated microphase separation enabling a possible application as thermoplastic elastomers.

For future investigations, the optimisation of the incorporation of end groups into the polyDHPMs and optimisation of the coupling reaction is highly interesting as it simplifies purification and allows for the synthesis of ABA block copolymers if the non-polyDHPM block has two reactive endgroups. For this purpose, a closer investigation on possible side reactions during the Biginelli polycondensation that hinder the incorporation of the end group or leads to its degradation is needed. Furthermore, the introduction of end groups that allow for a more efficient polymer-polymer coupling reaction are feasible. Possible examples are click reactions.^[391]

4.3 Controlled Radical Polymerisation of Ricinoleic Acid-Derived Vinyl Monomers and Subsequent Modification *via* the Biginelli-3-Component Reaction

Chapters 6.1, 6.2, and 6.5 of the experimental section correspond to the following investigations within this chapter.

4.3.1 Abstract

The search for renewable monomers for radical polymerisation techniques is of current interest due to the shift towards sustainability in the chemical industry. Renewable starting materials and the subsequent conversion to suitable monomers have recently been critically reviewed.^[230,392] Most monomer syntheses depend on the coupling of a renewable carboxylic acid or alcohol with toxic compounds such as 2-hydroxymethyl methacrylate (**167**), 4-(chloromethyl)styrene or methacrylic acid to obtain monomers capable of radical polymerisation.^[230,392]

Consequently, the synthesis of renewable monomers from carboxylic acids and the less toxic vinyl acetate (**161**) was herein attempted. In order to introduce further functionality and the possibility for post polymerisation modification (PPM) by the B-3CR, the introduction of an acetoacetate moiety was also investigated. Finally, the conversion of six renewable starting materials with a carboxylic acid group and a hydroxy group was investigated. However, only ricinoleic acid (**32**) was converted to two vinyl ester monomers with additional acetoacetate moieties, **162** and **163**. The radical polymerisation of **162** and **163** *via* FRP or RAFT polymerisation showed strong inhibition. Hence, no conversion of the monomers was observed. The source of inhibition remained unknown.

Thus, the more toxic methacrylate **167** was used to synthesise the ricinoleic acid-based methacrylate monomer (**168**). Subsequent RAFT polymerisation yielded polymers with a molecular weight of up to 15 000 g·mol⁻¹ and expectedly narrow molecular weight

distributions with D_s around 1.13. The feasibility of the resulting polymer for chain extension and block copolymer synthesis was demonstrated by qualitative determination of the end group fidelity of the RAFT polymers (**169**) and subsequent chain extension with monomer **168** and the block copolymer synthesis using methyl methacrylate as second monomer. Last but not least, the PPM of the acetoacetate moiety within **169** was investigated.

4.3.2 Synthesis of Renewable Vinyl Esters

The number of sustainable monomers suited for radical polymerisation techniques is limited.^[392] For the synthesis of renewable vinyl monomers with a functionality suitable for modification *via* B-3CR after radical polymerisation, appropriate starting materials had to be found. A vinyl ester was planned to be introduced by transvinylation of a carboxylic acid function with vinyl acetate. Hence, a carboxylic acid function was needed in the starting material. For the B-3CR, a urea moiety, an aldehyde, or an acetoacetate is needed within the final monomer. The introduction of acetoacetates by conversion of alcohols using *tert*-butyl acetoacetate (**64**) or a diketene acetone adduct (**65**) was considered more efficient and sustainable compared to the introduction of either an urea moiety or an aldehyde. Additionally, several renewable compounds that carry a carboxylic acid and a hydroxy group are commercially available.

Hence, the synthesis of renewable vinyl esters was investigated starting from five renewable hydroxy acids (**Figure 4.15**): vinyl guaiacol (**149**, 1-hydroxy-2-methoxy-4-vinylbenzene), ferulic acid (**150**, (*E*)-3-(4-hydroxy-3-methoxyphenyl)prop-2-enoic acid), hydroferulic acid (**151**, 3-(4-hydroxy-3-methoxyphenyl)propanoic acid), L-lactic acid (**152**, (*S*)-2-hydroxypropanoic acid), and ricinoleic acid (**32**, (*9Z,12R*)-12-hydroxyoctadec-9-enoic acid). Noteworthy, **149** was an exceptional monomer in the sense that it already carries a vinyl group that is polymerisable by radical polymerisation techniques. Hence, only the acetoacetylation of the phenolic hydroxy group was necessary to yield the intended monomer structure.

4.3 Controlled Radical Polymerisation of Ricinoleic Acid-Derived Vinyl Monomers and Subsequent Modification via the Biginelli-3-Component Reaction

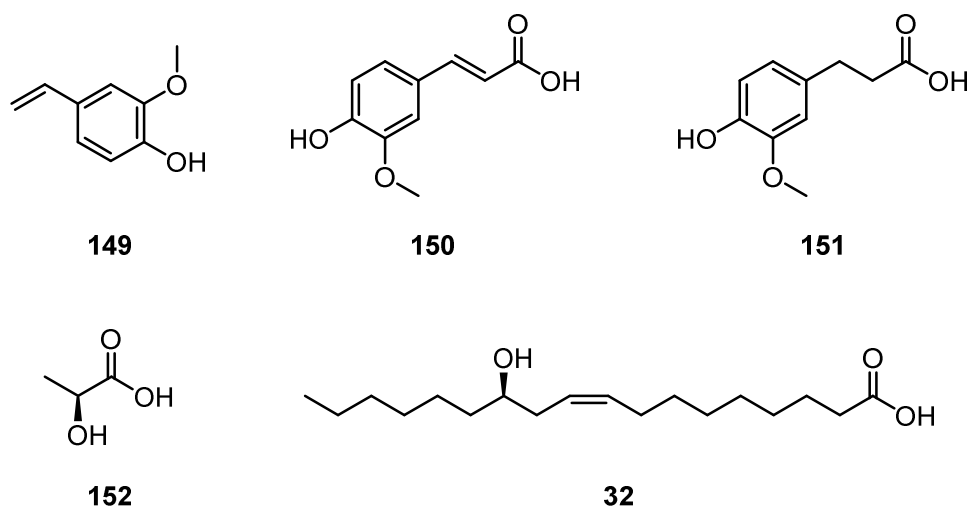
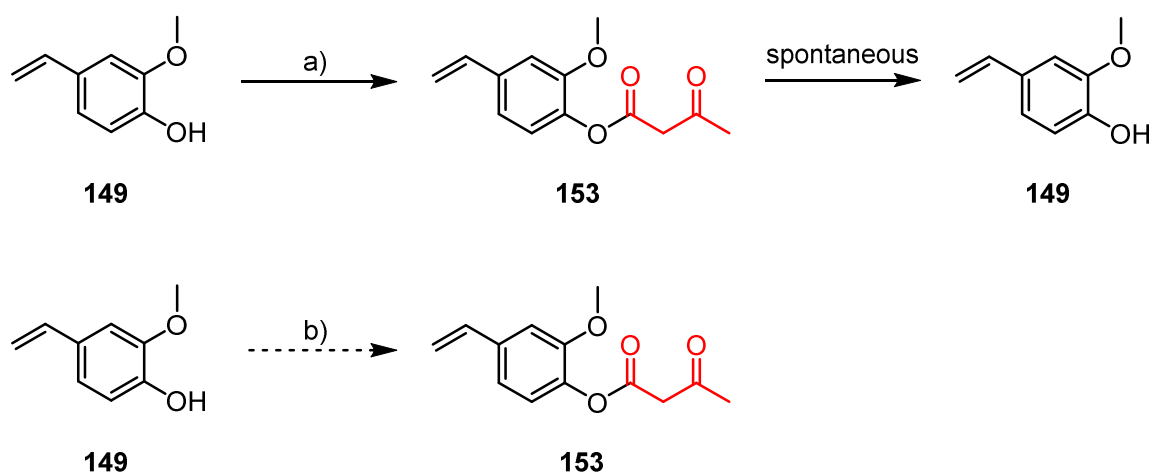


Figure 4.15 Possible renewable starting materials for the synthesis of vinyl esters that carry an acetoacetate group.

The conversion of alcohols to acetoacetates is typically performed at reaction temperatures above 100°C (*cf.* chapter 4.1.2 and 4.2.2). Thus, it was reasonable to perform the acetoacetylation prior to transvinylation as sidereactions of the vinyl group, such as oligomerisation or polymerisation, was considered possible at elevated temperatures. Nonetheless, the acetoacetylation of **149** was investigated first since only one reaction step was needed in order to obtain a monomer with the desired functionality. Hence, **149** was reacted with 3.00 eq of **64** at 140°C and with 3.00 eq of **65** at 95°C in bulk despite the possibility for thermal self-initiated polymerisation, which is well known for styrene (**Scheme 4.11**).^[393]



Scheme 4.11 Attempts for the synthesis of **153**: **a)** 3.0 eq **64**, bulk, 140°C, 4.5 h, 30% yield, degradation upon isolation; **b)** 3.0 eq **65**, bulk, 95°C, 2 h, 0% yield.

The reaction progress was monitored by ^1H NMR spectroscopy (**Figure 4.16**). Samples of the crude mixture were taken and measured after certain reaction times. The conversion was calculated by comparison of the signals of the vinyl protons of **149** at 5.63 ppm and 5.06 ppm and the signals of the vinyl protons of **153** at 5.87 ppm and 5.29 ppm. Using **64**, a crude yield of to 30% after 4 h of reaction time was determined while the reaction with **65** led to no conversion of **149** within 4 h. The integrals of the aromatic protons and the methoxy groups of **149** and **153**, respectively, and the integrals of the newly introduced acetoacetate verified the assumption of 30% conversion with **64**. At reaction times longer than 4 h, the broadening of the signals in the aromatic region together with a relative decrease of the signals of the double bond signals indicated polymerisation/oligomerisation. Consequently, the reaction was repeated and stopped after 4 h.

4.3 Controlled Radical Polymerisation of Ricinoleic Acid-Derived Vinyl Monomers and Subsequent Modification via the Biginelli-3-Component Reaction

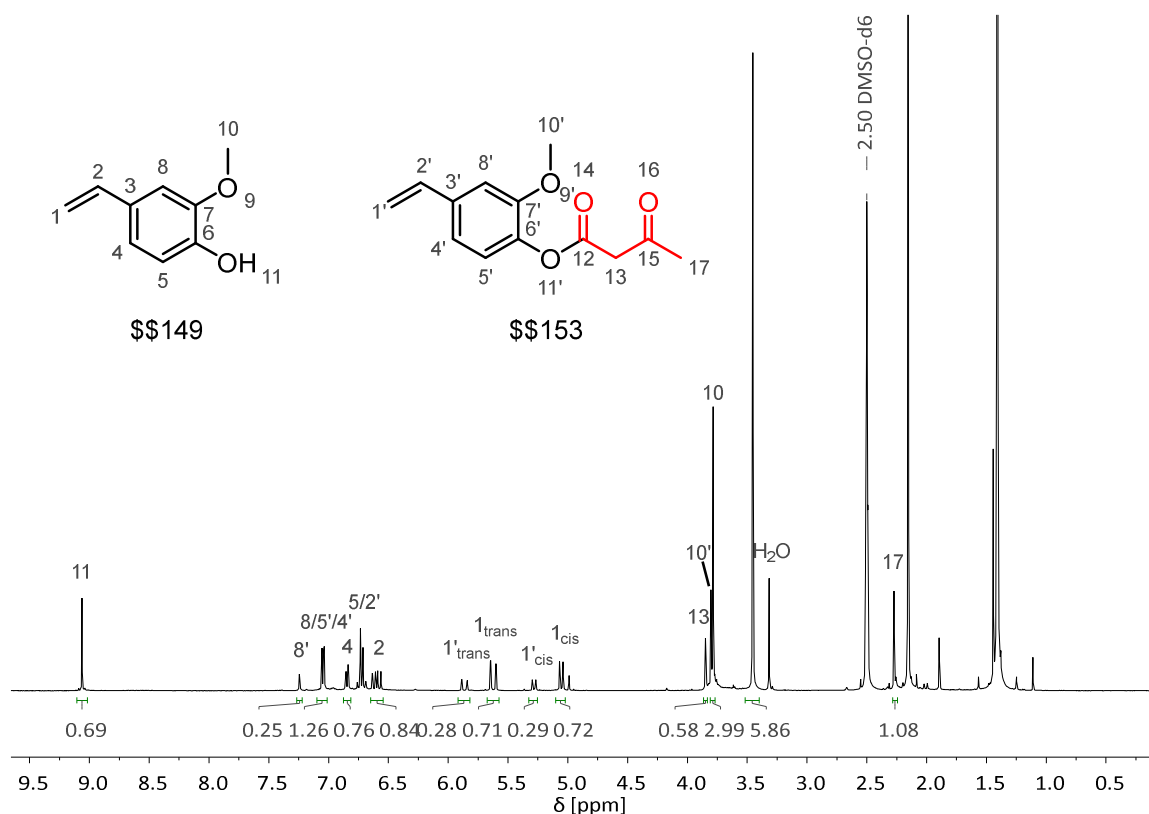


Figure 4.16 ^1H NMR spectrum of the crude reaction mixture of the synthesis of **153** from **149** using **64** after a reaction time of 4 h: the spectrum indicated approximately 30% conversion to the desired product.

Afterwards, the mixture was attempted to be purified by column chromatography over silica gel. Even though the product was obtained as a pure fraction according to thin layer chromatography, the ^1H NMR spectrum after the evaporation of the solvent at 40°C showed 10 mol% of starting material relative to **153**. The existence of starting material was attributed to the hydrolysis of **153** with small amounts of water to **149** and acetoacetic acid. The latter is known to readily decompose to the volatile acetone and CO_2 already at 30°C .^[394] Hence, no decomposition product was visible in the ^1H NMR spectrum. Furthermore, the broadening of the methoxy signal at 3.80 ppm and the appearance of a broad signal at approximately 1.42 ppm, which was attributed to the oligomer/polymer of **149** and/or **153**, indicated the presence of oligomers/polymers. The spontaneous decomposition of the acetoacetate moiety of **153** back to **149** was probably favoured by the

negative mesomeric effect of the aromatic system attached to the ester rendering the phenol a sufficient leaving group for its substitution with water.

As a consequence, the desired product was formed to a maximum of 30 mol% relative to the starting material during the reaction. The share of 30 mol% was probably not surpassed due to the mentioned polymerisation reaction and the simultaneous decomposition. The attempted purification led, however, to an impure product due to partial decomposition and oligomerisation/polymerisation of **153** upon concentration of the product fraction. Finally, the application of **149** as monomer precursor for the desired purpose was abandoned due to the supposed instability of **153** and the low yield. Although **150** and **151** are also aromatic alcohols, the acetoacetylation of **150** and **151** was nevertheless attempted due to their higher thermal stability with regards to spontaneous polymerisation. The same procedures as for the attempted synthesis of **153** were used. Reaction of **150** with **64** at 140°C led to decarboxylation ($\geq 95\%$) of **150** to **149**. The same reaction at 95°C led to no conversion of any of the starting materials. Hence, the more reactive **65** was applied at 95°C.^[362]

The ¹H NMR spectrum of the crude mixture indicated the conversion to the product at a yield of 90% in the absence of significant side reactions after 1 h of reaction time (**Figure 4.17**). However, during the concentration of the sample after purification by column chromatography, the acetoacetate degraded leading to the formation of the starting material **150**. Notably, acetic acid, besides *c*-C₆H₁₂ and EtOAc, was applied for the purification by column chromatography. Here, the water content of the acetic acid possibly led to decomposition of the acetoacetate upon concentration during the evaporation of the solvent mixture similar to the findings for the synthesis of **153**. Additionally, the acidic conditions possibly catalysed the decomposition. Hence, a different purification strategy, for example the use of reverse phase silica gel to avoid the application of an acid as part of the eluent, was deemed possible but was not attempted.

4.3 Controlled Radical Polymerisation of Ricinoleic Acid-Derived Vinyl Monomers and Subsequent Modification via the Biginelli-3-Component Reaction

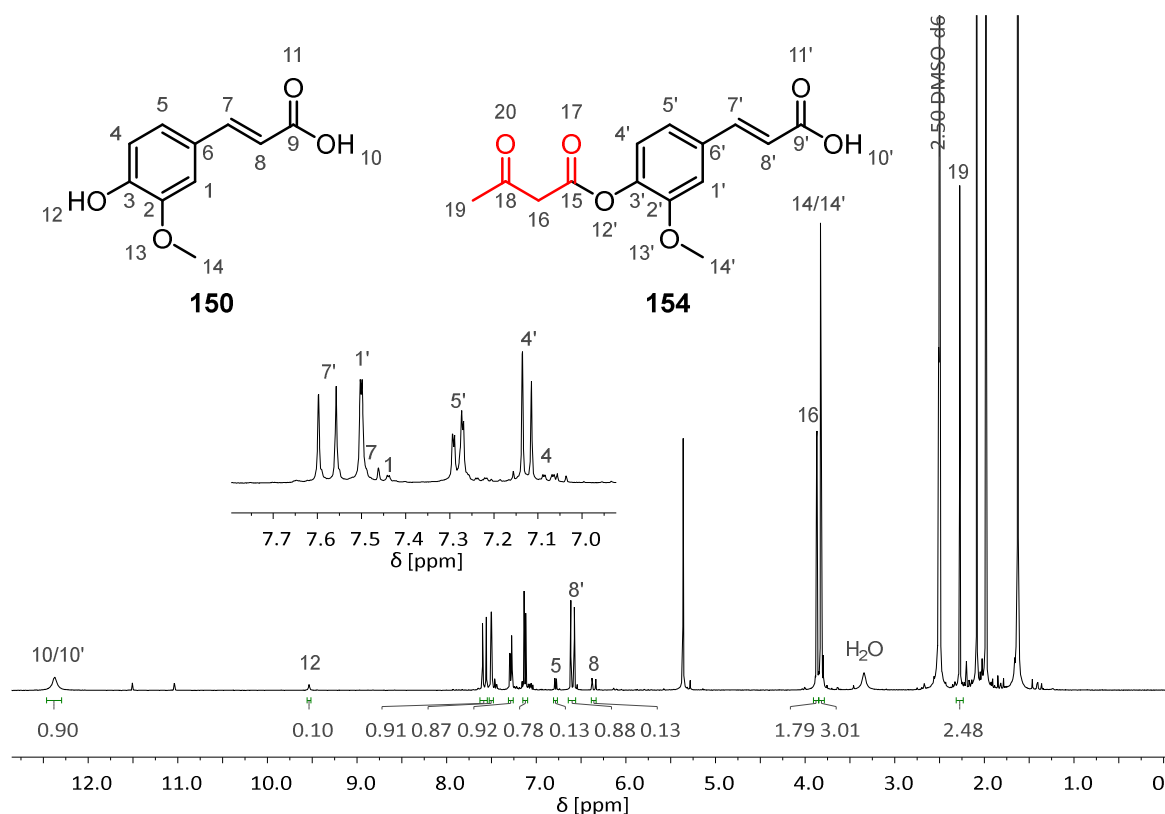


Figure 4.17 ¹H NMR spectrum of the crude reaction mixture of the synthesis of **154** from **150** using **65** after a reaction time of 1 h: the spectrum indicated approximately 90% conversion to the desired product.

While the reaction of **151** with **64** at 140°C led to an insoluble, unknown solid, the reaction with **65** at 95°C led to approximately 70% conversion to the product according to the ¹H NMR spectrum of the crude mixture. However, after column chromatography using a mixture of *c*-C₆H₁₂ and EtOAc and AcOH, only mixtures of **151** and the respective acetoacetate were obtained. Notably, the use of an acid was necessary to achieve an adequate separation.

To conclude, the reaction of **150** and **151** to aromatic acetoacetates using **65** led to yields between 70% and 90% within the crude mixture after a reaction time of 1 h. However, purification led, in both cases, to a degradation of the product to the respective starting materials. While improvement of the purification might lead to the final product in the desired product, the instability of the aromatic acetoacetates was apparent. Thus, the

aromatic acetoacetates were abandoned to avoid possible problems at a later stage of the project since the origin of their instability was not clearly determined.

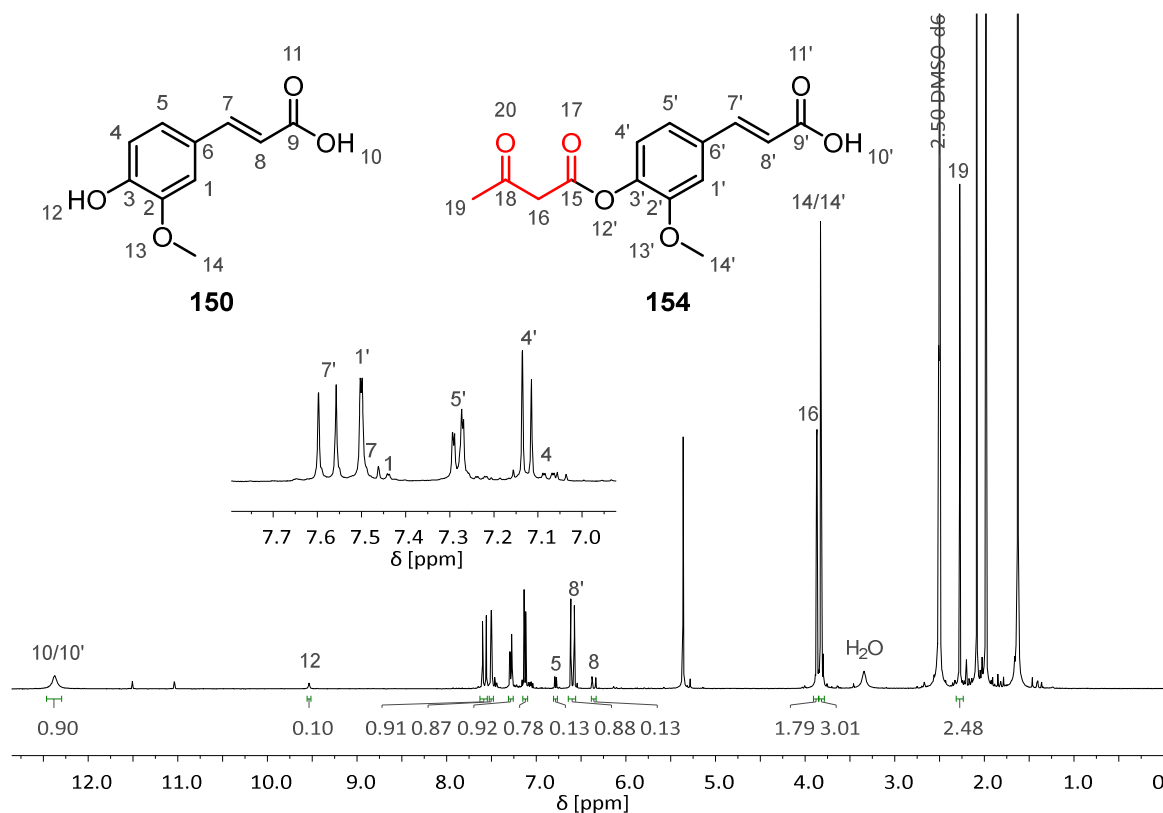
Subsequently, the acetoacetylation of **152** was investigated. Again **64** and **65** were applied as reactants for the transesterification (**Scheme 4.12**). Since **152** typically contains oligomeric species due to condensation reactions, sodium L-lactate (**155**) was used instead. The reactions were performed as above at 140°C and 95°C, respectively. However, due to the insolubility of **155** in **64**, DMSO (10 M solution) was added to the reaction mixture leading to a homogeneous solution. After 3 h of reaction time, the ¹H NMR spectra of the crude reaction mixtures of both variations indicated conversions to sodium 2-[(3-oxobutanoyl)oxy]propanoate (**156**) above 95%. After purification *via* extraction and subsequent acidification to the respective carboxylic acid, both variations yielded up to 90% of product. However, for the reaction with **64**, DMSO still remained in the product and was removed by extraction with a product loss of 40%. Hence, variation **b**), using **65** in bulk, was preferred. Finally, the synthesis of **157** was verified by NMR spectroscopy and HRMS (chapter 6.5.1.1).

Last but not least, the synthesis of (9Z,12R)-12-[(3-oxobutanoyl)oxy]octadec-9-enoic acid (**159**) from **32** was investigated. As starting material, sodium ricinoleate (**158**, sodium (9Z,12R)-12-hydroxyoctadec-9-enoate) was applied since higher purities, compared to the acid, were commercially available. Common impurities in **32** are other fatty acids, mainly oleic acid, linoleic acid, linolenic acid, palmitic acid, and stearic acid.^[395] These are challenging to separate from ricinoleic acid and likely react similar in the following transvinilation.

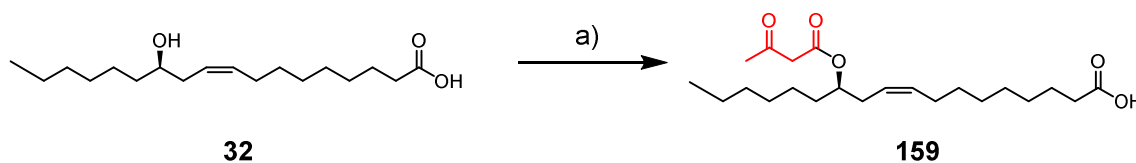
Since the milder reaction conditions at 95°C with **65** were advantageous for above acetoacetylations, these conditions were directly applied for the synthesis of **159** (**Scheme 4.13**). However, **158** was largely insoluble in either **65** or common solvents such as DMSO, toluene, acetonitrile, or ethanol. Hence, **158** was converted to **32** using 1 M HCl_{aq}. Pure **32** was obtained in quantitative yields after extraction of the aqueous phase with EtOAc. Subsequently, **32** was reacted with **65** in bulk. Full conversion of the hydroxy group was observed by ¹H NMR spectroscopy after 1 h of reaction time. Notably, full conversion was

4.3 Controlled Radical Polymerisation of Ricinoleic Acid-Derived Vinyl Monomers and Subsequent Modification via the Biginelli-3-Component Reaction

reached after up to two hours for multi-gram batches yielding 68% of pure product. The synthesis was confirmed by NMR spectroscopy and HRMS (chapter 6.5.1.2).

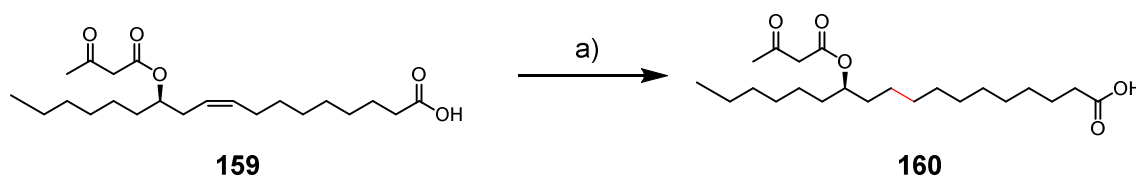


Scheme 4.12 Reaction scheme for the synthesis of **157** using **64** or **65**: **a)** 3.00 eq **64**, 10 M in DMSO, 140°C, 3 h, 95% yield (not isolated); **b)** 3.00 eq **65**, bulk, 95°C, 3 h, 90% yield (not isolated); **c)** 1.10 eq 1M HCl_{aq}, room temperature, 30 min, 90 % yield (when **156** was prepared *via a*), extraction of the DMSO with EtOAc was necessary leading to a yield of 50%).



Scheme 4.13 Reaction scheme for the synthesis of **159** using **65**: **a)** 3.0 eq **65**, bulk, 95°C, 1 h, 68%.

Additionally to **159**, (12*R*)-12-[(3-oxobutanoyl)oxy]octadecanoic acid (**160**) was synthesised by simple hydrogenation of a solution of **159** in EtOAc with hydrogen and Pd on charcoal in quantitative yields (**Scheme 4.14**). After filtration to remove the heterogeneous catalyst and removal of the solvent, no further purification was necessary. The synthesis was confirmed by NMR spectroscopy and HRMS (chapter 6.5.1.3).



Scheme 4.14 Reaction scheme for the hydrogenation of **159** to **160**: a) 0.00125 eq Pd/C (10% Pd basis), 0.15M in EtOAc, room temperature, 15 bar H₂, 24 h, quantitative yield.

Finally, the three renewable carboxylic acids with an acetoacetate function, **157**, **159**, and **160**, were synthesised. Subsequently, the transvinylation of these compounds towards the desired vinyl ester monomers was investigated. First, the transvinylation of **157** was investigated using several catalytic systems and conditions similar to the respective literature reports (**Table 4.11**). The applied catalysts were palladium(II)acetate, ruthenium(III)chloride hydrate, triruthenium dodecacarbonyl, and di- μ -chlorobis[(1,2,5,6- η^2)-1,5-cyclooctadiene]diiridium ([Ir(cod)Cl]₂), respectively.^[396-400]

The product formation was determined by ¹H NMR spectroscopy of samples of the crude reaction mixture using the *CH* proton of the vinyl group which is shifted +0.4 ppm to 7.21 ppm compared to the respective shift in **161**. As a reference, the *H*₃C-*CH* proton signal of **157** was used. For most catalyst systems and conditions, less than 5% of **162** was found in the crude mixtures. Moreover, for reaction temperatures above 60°C, degradation of **157** to unknown degradation products was observed. Only the application of Pd(OAc)₂ as catalyst led to 34% of product in the crude mixture. However, after column chromatography, approximately 5% of yield of impure **162** was obtained. Due to the inefficient

4.3 Controlled Radical Polymerisation of Ricinoleic Acid-Derived Vinyl Monomers and Subsequent Modification via the Biginelli-3-Component Reaction

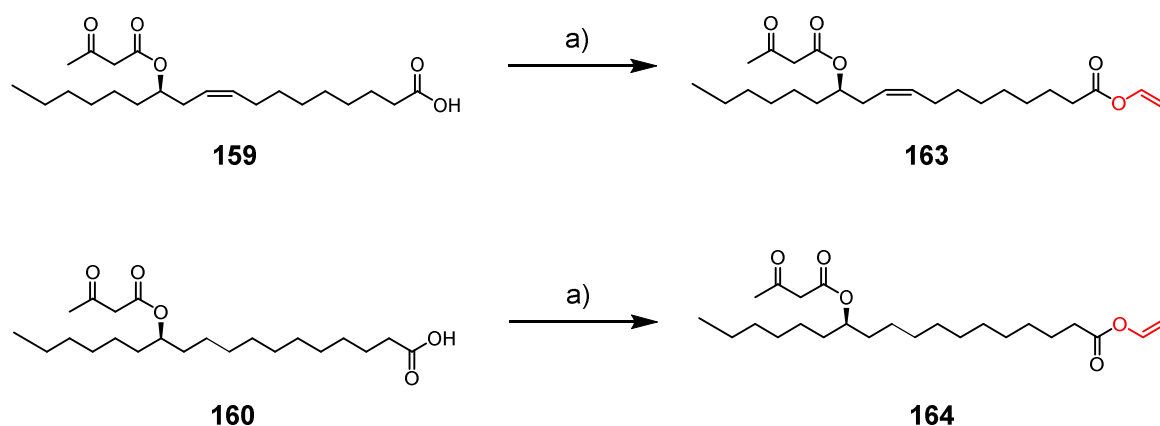
transvinylation in combination with the challenging purification the synthesis of **162** was also abandoned.

Table 4.11 Screening of conditions for the synthesis of **162** from **157** and **161**: a maximum of 34% of product was obtained within the crude mixture.

catalyst /eq	cocatalyst /eq	solvent	temperature [°C]	reaction time [h]	yield ^a [%]
Pd(OAc) ₂ /0.10	H ₂ SO ₄ ^b /0.15	tetrahydrofuran	40	16	10
				24	34
	<i>p</i> -TSA/0.1		60	72	<5
RuCl ₃ ·xH ₂ O/0.03 ^c			120	16	0
Ru ₃ (CO) ₁₂ /0.03	NaOAc/0.090	-	100	24	<5
[Ir(cod)Cl] ₂ /0.03			100	16	<5

^a yield in the crude reaction mixture, estimated by ¹H NMR spectroscopy; ^b 10 wt% of concentrated H₂SO₄ in tetrahydrofuran; ^c the added mass was calculated using the molecular weight of anhydrous RuCl₃.

Finally, the vinylation of the ricinoleic acid-derived acetoacetates, **159** and **160**, was attempted. The catalytic system using [Ir(cod)Cl]₂ and NaOAc was applied first since the respective report showed the vinylation of oleic acid, an unsaturated fatty acid (**Scheme 4.15**).^[400] Surprisingly, both vinyl esters, **163** and **164** were obtained after column chromatography with yields of 68% and 72%, respectively. The formation of the products was confirmed by NMR spectroscopy and HRMS (chapters 6.5.1.4 and 6.5.1.5).



Scheme 4.15 Synthesis routes of the ricinoleic acid based vinyl esters **163** and **164**: a) 10 eq **161**, 0.01 eq $[\text{Ir}(\text{cod})\text{Cl}]_2$, 0.03 eq NaOAc, degassed with Ar, 100°C, 16 h, 68% yield for **163**, 72% yield for **164**.

^1H NMR spectroscopy of **163** and **164** showed the characteristic product signals, particularly the two singlets of the acetoacetate moiety at 3.57 ppm and 2.16 ppm and the doublet of doublets of the vinyl group at 7.21 ppm, 4.88 ppm, and 4.64 ppm. The ^1H NMR spectra of **163** and **164** are depicted in **Figure 4.18**.

To conclude, the synthesis of renewable vinyl esters that carry an acetoacetate moiety was attempted starting from five different renewable compounds. The synthesis was attempted by acetoacetylation and subsequent transvinylation. However, for **149**, **150**, and **151** the formed aromatic acetoacetate was found to be unstable. Product formation was observed in the crude mixture but upon purification, or concentration of the product after purification, only starting material or mixtures of starting material and product were obtained.

For **152** and **32**, the acetoacetylation was successful yielding **157** and **159** at 90% and 68%, respectively. In addition, **159** was quantitatively hydrogenated yielding **160**. The subsequent transvinylation to the desired vinyl esters for **157** was attempted using three different catalyst systems and various conditions. However, only $\text{Pd}(\text{OAc})_2$ was able to yield up to 34% of **162** in the crude mixture. Unfortunately, the purification led to the formation of an unknown compound and only approximately 5% of impure **162** was obtained. The transvinylation of the ricinoleic acid derivatives with $[\text{Ir}(\text{cod})\text{Cl}]_2$ readily yielded the desired

vinyl ester monomers, **163** and **164**, at a yield of 68% and 72%, respectively. Hence, the radical polymerisation of **163** and **164** was subsequently investigated within the following chapter.

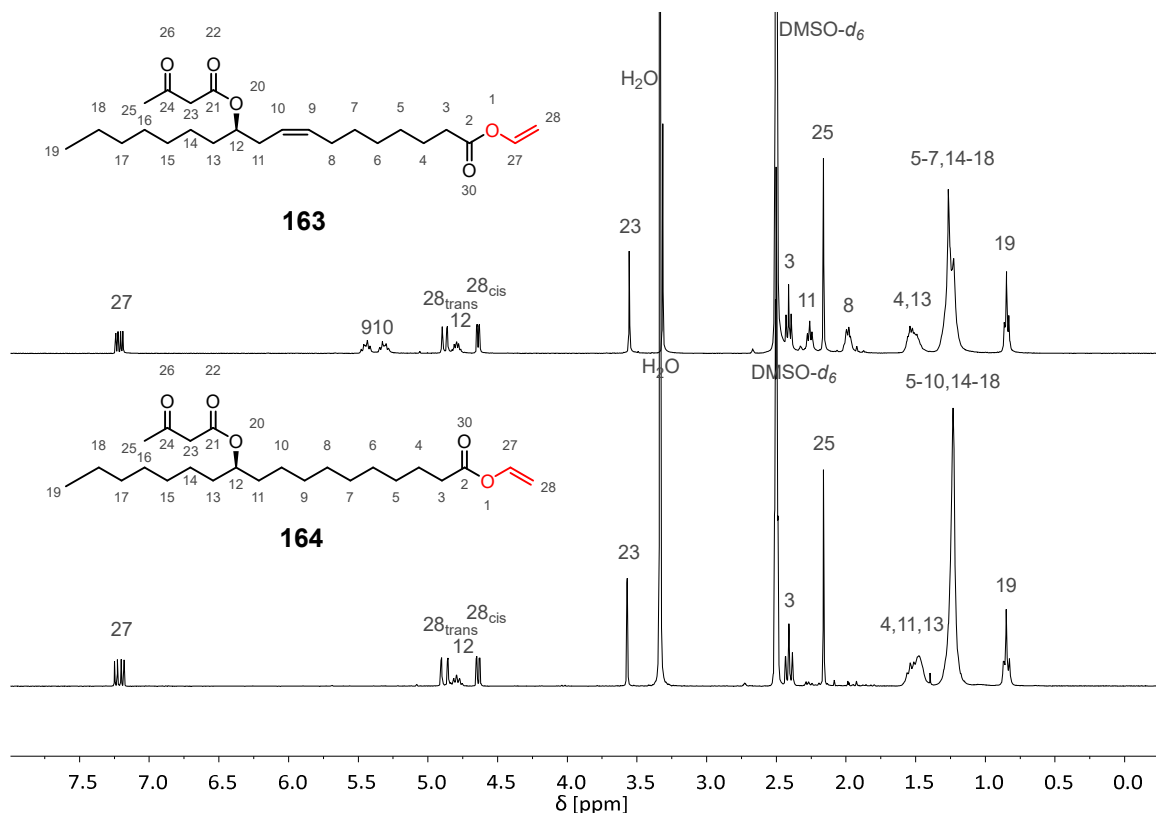


Figure 4.18 ^1H NMR spectra of **163** and **164** after purification.

4.3.3 Radical Polymerisation of Renewable Vinyl Esters

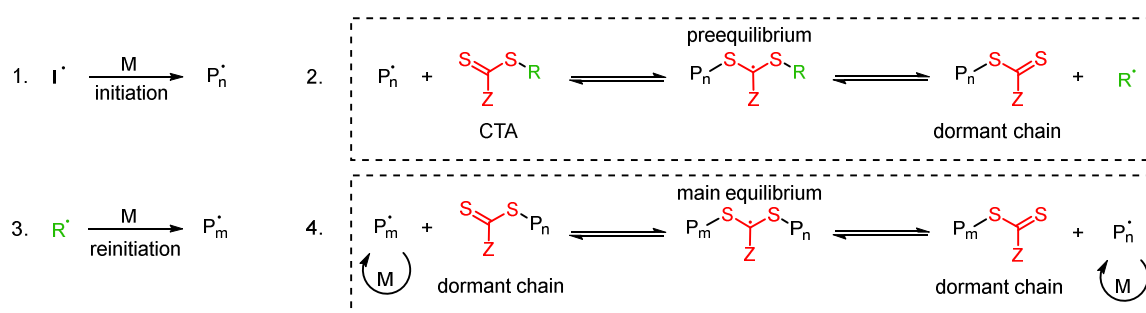
Within this chapter, the radical polymerisation of the vinyl esters **163** and **164** was investigated. The radical polymerisation of similar fatty acid monomers has been reported.^[401–405] For FRPs, it was shown that the polymerisation rate and the final conversions were drastically lowered with increasing degree of unsaturation.^[406,407] This was explained by the combination of the rather slow propagation of the vinyl ester monomer and the formation of stable allyl radicals by hydrogen abstraction of hydrogen atoms located in α -position to the double bond.^[406] Hence, propagating radicals and initiator radicals are

scavenged by the monomer itself while radical-radical combination of the allyl radicals continuously lowers the radical concentration and quenches the polymerisation.

Nonetheless, vinyl oleate, containing one double bond, was still polymerised with conversions of about 60% after 24 h.^[406] Moreover, conversions of up to 100% were shown for saturated fatty acid vinyl esters.^[406,407] A similar trend with overall higher polymerisation rates was observed for the FRP of fatty acid acrylates^[408] and acrylamides,^[409] as well. This trend regarding the degree of unsaturation was also reported for the RAFT¹⁰ polymerisation of fatty acid vinyl esters^[401–403] and other monomer classes like fatty acid methacrylates.^[414,415]

Consequently, the polymerisation of **163** and **164** was attempted *via* RAFT polymerisation and FRP. All reactions were performed at 65°C with

¹⁰ RAFT polymerisation is a type of reversible deactivation radical polymerisation.^[410,411] Such polymerisations have characteristics of a living polymerisation: a linear proportionality of M_n and conversion and narrow molecular weight distributions (D typically smaller 1.2).^[410–412] The mechanism is based on an equilibrium between dormant polymer chains (attached to the CTA) and propagating polymer chains P_n^{\cdot} or P_m^{\cdot} .^[413] The radical concentration is not changed during the RAFT equilibrium.^[413] Hence, an external radical source is needed. Consequently, the mechanism starts with the initiation of the polymerisation by reaction of an initiator radical with a monomer (M) to a propagating chain.^[413] This chain reacts in an equilibrium reaction with a CTA to form an intermediate radical to finally release the R group of the CTA as active radical.^[413] This R $^{\cdot}$ also forms a propagating chain which either reacts with a CTA or enters the main equilibrium by reaction with a dormant chain.^[413]



In an effective RAFT process, the rate of the chain transfer is faster than the rate of the propagation. Hence, all chains have a similar DP .^[413] Consequently, the choice of the Z- and R-group of the CTA with respect to the polymerised monomer is crucial. A comprehensive review on the choice and synthesis of a suitable CTA and explanations on the influence of the Z- and R- groups has been published.^[411] Application of a non-suitable CTA leads to complications such as poor control over the M_n and broader D s or retardation/inhibition of the polymerisation.^[411] Furthermore, the ratio of monomer to CTA naturally defines the maximum DP for full conversion of the monomer.^[413]

2,2'-azobis(2-methylpropionitrile) (AIBN) as initiator. For the RAFT polymerisation, methyl 2-[(ethoxycarbonothioyl)thio]acetate was used as chain transfer agent (CTA) since xanthates were reported to control the polymerisation of vinyl esters.^[403] Furthermore, the applied solvent was varied. All reaction mixtures were degassed and backfilled with N₂ prior to heating.

The investigated conditions and results are summarised in **Table 4.12**. Prior to the investigation of **163** and **164**, the RAFT polymerisation and the FRP of vinyl stearate was carried to evaluate the suitability of the chosen experimental conditions (**Table 4.12**, entries 1 and 2). The conversion was determined by ¹H NMR spectroscopy through the integration of the vinyl protons at 4.88 ppm and 4.56 ppm relatively to the signals of the (CO)OCH protons at 4.82 ppm that are formed during the polymerisation. Both cases verified the polymerisation under the chosen reaction conditions. In addition, the inhibition effect of the acetoacetate moiety was excluded by the investigation of ethyl acetoacetate as solvent (entry 3). This led to a conversion of 20% after 3 h. The lower conversion compared to the polymerisation in toluene was hypothesised to be caused by a higher chain transfer to solvent constant for ethyl acetoacetate. However, such constants for acetoacetates were not reported in the literature to the best of my knowledge.

First, the radical polymerisation of **163** was investigated in toluene as solvent and in bulk (**Table 4.12**, entries 4 – 8). Neither the RAFT polymerisation nor the FRP showed any monomer conversion after 18 – 24 h of reaction time. Subsequently, a FRP of **164** was attempted using 0.5 eq of AIBN. After 3 h of reaction time, a conversion of approximately 33% was observed indicating that the monomer itself or an impurity within the polymer are substantially inhibiting radical polymerisation. In addition, the polymerisation of the saturated monomer **164** was investigated due to its probably higher polymerisation rate (entries 9 – 11). Unfortunately, also no monomer conversion was observed for the RAFT polymerisation or the FRP in bulk or in DMSO for reaction times longer than 19 h.

Table 4.12 Tested polymerisation conditions for **163** and **164** via RAFT polymerisation and FRP at 65°C.

entry	monomer	[M]/[CTA]/[AIBN] ^a	solvent ^b	reaction time [h]	conversion ^c [%]
1		40/1/0.15		28	75
2	Vinyl stearate	40/-/0.15	toluene	3	53
3		40/-/0.15	ethyl acetoacetate	3	20
4		50/1/0.15		18	0
5		50/-/0.15	-	24	0
6	164	50/1/0.15		23	0
7		50/-/0.15	toluene	24	0
8		50/-/25 ^d		3	33 ^e
9		50/1/0.15	-	19	0
10	163	50/1/0.15	DMSO	32	0
11		50/-/0.15	toluene	19	0

^aratio of monomer to CTA to AIBN; ^b13 M; ^ccalculated using the ¹H NMR spectra of the crude reaction mixture; ^dthe used amounts of AIBN were only partially soluble at 65°C; ^epartly insoluble in CDCl₃.

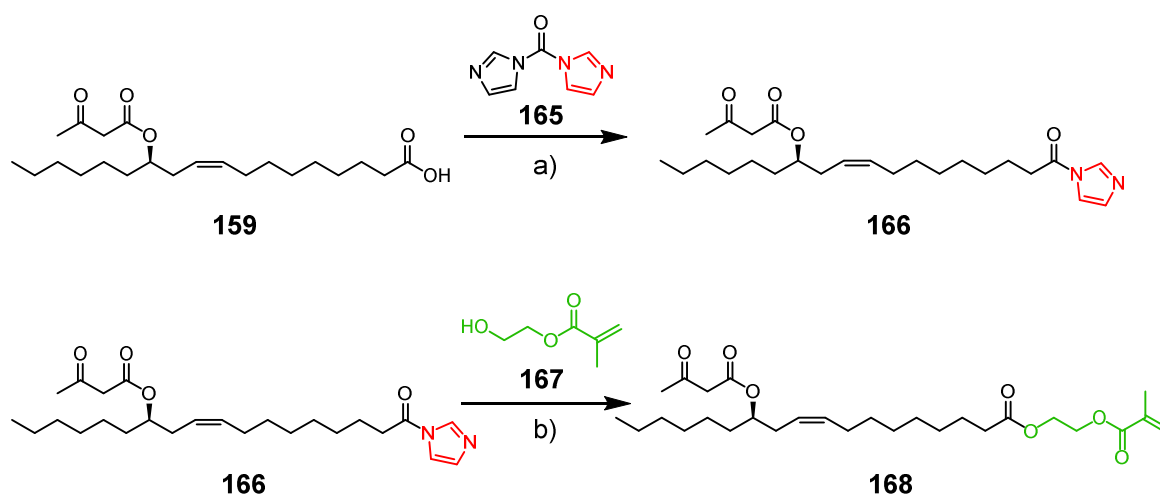
However, inhibition by the monomer itself is unlikely since apart from the acetoacetate moiety, **164** does not differ from vinyl stearate. One probable source of impurities was the starting material **158**. The main impurities are other fatty acid salts, like sodium linoleate and sodium linolenate, with higher degrees of unsaturation.^[395] These might have caused the inhibition since they were not removed during the synthesis steps towards **164** as the aliphatic chain dominates the solubility and the retention factor during column chromatography. To confirm this hypothesis, gas chromatography-mass spectrometry of **164** was performed in order to identify other trace impurities. The signal of **164** was very weak and broad. While it was possible that the signal of another fatty acid derivate was

contained in signal of **164**, no other impurity was detected. Hence, the absence of impurities other than fatty acid derivatives is likely but not proven.

To conclude, the cause of the inhibition was not resolved and the synthesis and polymerisation of vinyl esters was not pursued further. While vinyl esters were chosen over other vinyl monomer classes due to their lower toxicity, the synthesis and polymerisation of a methacrylate monomer similar to **164** is described within the following chapters 4.3.4. Interestingly, the FRP or RAFT polymerisation of the methacrylate monomer **168** did not seem to be inhibited. And since the purification steps towards **168** were the same as towards **163** or **164**, the inhibitor probably got into the monomer during the transvinilation reaction but remained unknown.

4.3.4 Synthesis and Radical Polymerisation of 2-(Methacryloyloxy)ethyl (*R,Z*)-12-((3-Oxobutanoyl)oxy)octadec-9-enoate

After the polymerisation of the fatty acid vinyl esters was deemed to be challenging, the synthesis of a similar fatty acid methacrylate was investigated. Consequently, **163** was esterified with carbonyldiimidazole (**165**, CDI) and 2-hydroxyethyl methacrylate (**167**) (**Scheme 4.16**). The activation of the carboxylic acid for the subsequent esterification was preferred over a simple acid catalysed esterification to reduce side reactions between the acetoacetate moiety and **167**. The reaction consisted of two steps: first, the reaction of **163** with **165** to the acylimidazole (**166**), second, without previous workup of **166**, heating of the mixture to 65°C with subsequent addition of **167**. After 8 h of reaction time at 65°C, the pure **168** was obtained with a yield of 92% after column chromatography. Notably, the direct addition of all reactants was also attempted. However, **165** reacted preferentially with **167** to form the respective carbamate.



Scheme 4.16 Reaction scheme for the preparation of **166** from **159** using CDI and 2-hydroxyethyl methacrylate (**165**) and the subsequent esterification with **167** to **168**: **a**) 1.05 eq **165**, 0.43 M in anhydrous toluene, room temperature, 16 h, quantitative (^1H NMR, no workup); **b**) 1.00 eq **167**, 0.43 M in toluene, 65°C, 8 h, 92%.

The synthesis of the pure product was verified by ^1H NMR spectroscopy and HRMS. The ^1H NMR spectrum showed the characteristic signals of **168**, *i.e.*, the proton signals of the double bond of the methacrylate moiety at 6.13 ppm and 5.59 ppm, the proton signals of the double bond of the ricinoleic acid at 5.48 ppm and 5.31 ppm, and the signals of the CH_2 and CH_3 protons of the acetoacetate group at 3.42 ppm and 2.26 ppm, respectively (**Figure 4.19**). Afterwards, the radical polymerisation of **168** was investigated.

4.3 Controlled Radical Polymerisation of Ricinoleic Acid-Derived Vinyl Monomers and Subsequent Modification via the Biginelli-3-Component Reaction

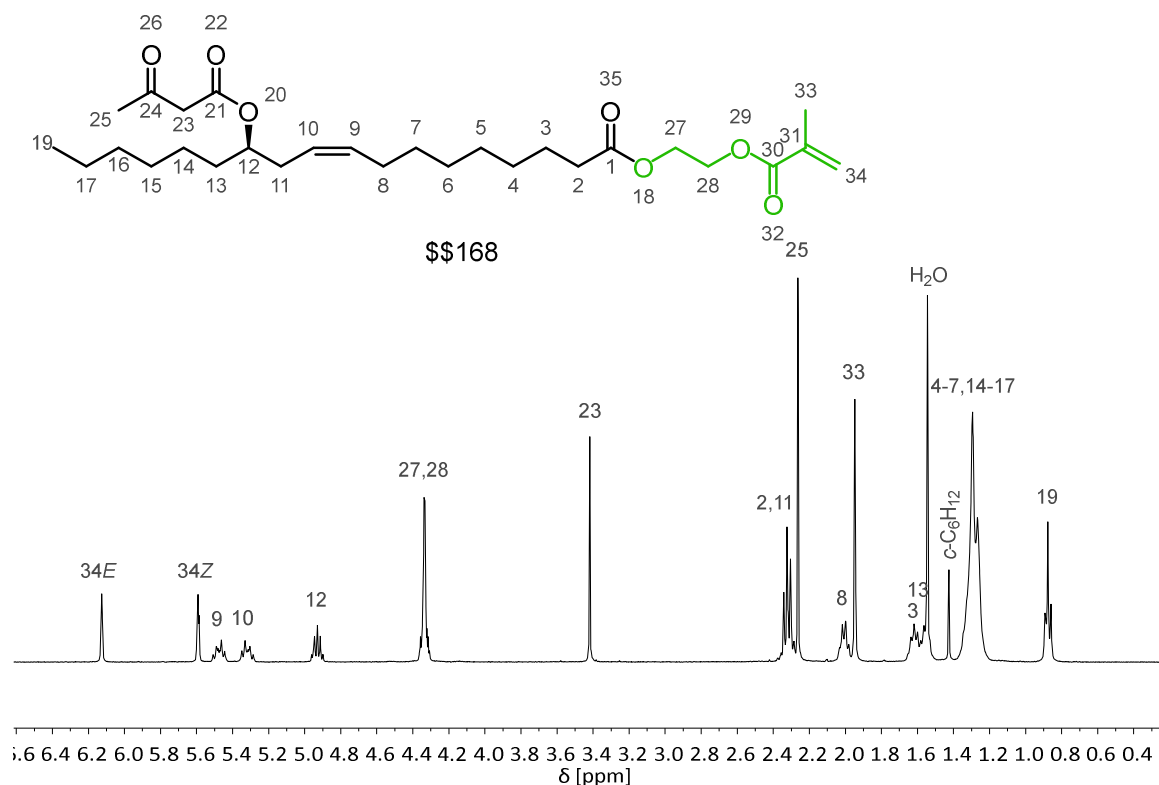


Figure 4.19 ^1H NMR spectrum of **168**.

To test if **168** was similarly inhibited like **163** and **164**, a simple free radical polymerisation in bulk using AIBN as initiator was performed. After 10 h, a gel-like material, insoluble in CHCl_3 , toluene, tetrahydrofuran, and hexafluoroisopropanol, was obtained indicating the successful polymerisation. The insolubility was probably caused by crosslinking between the polymer chains due to chain transfer to polymer reactions. As a consequence, the RAFT polymerisation of **168** was investigated as the RAFT equilibrium prevents such side reactions. Similar to the RAFT polymerisations in chapter 4.3.3, the experiments were performed at different concentrations in toluene at a temperature of 65°C with AIBN as the radical initiator. Furthermore, two CTAs previously reported to allow control of the polymerisation of methacrylates, namely 2-cyanoprop-2-yl benzodithioate (CTA1) and *S*-(2-cyanoprop-2-yl)-*S*-dodecyltrithiocarbonate (CTA2), were applied and the respective results compared.^[411] The ratio of monomer to CTA to AIBN was kept at 50 to 1

to 0.1. All reaction mixtures were thoroughly degassed and backfilled with argon prior to heating to avoid inhibition by formation of peroxy radicals with triplet oxygen.

Samples were taken after certain time intervals to screen the reaction progress *via* ^1H NMR spectroscopy and SEC. Thus, samples of the crude reaction mixture were directly dissolved in CDCl_3 or tetrahydrofuran with 2 vol% triethylamine, respectively. To calculate the conversion by NMR spectroscopy, the decrease of the integrals of the proton signals of the methacrylate double bond was observed in relation to the integrals of the double bond protons of the ricinoleic acid and the *CH* next to the acetoacetate.

The first experiments were conducted with a 7.5 M concentration of **168** in toluene (**Table 4.13**). For both CTAs, the $M_{n,\text{NMR}}$ and $M_{n,\text{SEC}}$ increased over time, verifying the polymerisation under RAFT conditions while the polymerisation rate for CTA2 was lower compared to CTA1. The lower polymerisation rate was unexpected as trithiocarbonates, compared dithiobenzoates, typically feature lower chain transfer constants and larger fragmentation rates of the intermediate radicals due to the lower stability of the intermediate radical.^[416] Hence, the lower polymerisation rate was rather attributed to an erroneous degassing prior to the polymerisation and subsequent inhibition by oxygen. This assumption was confirmed by the comparison of the polymerisation rates of the RAFT polymerisations at a 1.88 M concentration with CTA1 and CTA2, respectively (**Table 6.16**, page 289). Here, the polymerisation rate was a factor of two higher for CTA2.

4.3 Controlled Radical Polymerisation of Ricinoleic Acid-Derived Vinyl Monomers and Subsequent Modification via the Biginelli-3-Component Reaction

Table 4.13 ^1H NMR and SEC results of the screening of the RAFT polymerisation of **168** at a 7.5 M concentration.

entry	CTA ^a	reaction time [h]	$M_{n,\text{NMR}}^{\text{b}}$ [g·mol ⁻¹] (conversion [%])	$M_{n,\text{SEC}}$ [g·mol ⁻¹]	\mathcal{D}
1	CTA1	1	2 450 (9)	14 900	1.34
2		2	7 150 (28)	31 000	1.19
3		3	11 350 (45)	45 800	1.25
4		5	17 530 (70)	115 000	2.51
5	CTA2	1	1 580 (5)	- ^c	-
6		2	1 830 (6)	8 100	1.25
7		3	3 810 (14)	9 800	1.34
8		4	6 030 (23)	12 000	1.36
9		5	10 730 (42)	15 700	1.34
10		6	15 430 (61)	18 700	1.39
11		7	17 660 (70)	22 100	1.35

^aratio of monomer to CTA to AIBN is 50:1:0.1; ^b $M_{n,\text{NMR}}$ is calculated using the monomer conversion; ^csignal not visible in chromatogram.

Moreover, regarding the polymerisations at 7.5 M concentration, the \mathcal{D} s were higher than expected for a RAFT polymerisation and a large deviation between $M_{n,\text{NMR}}$ and $M_{n,\text{SEC}}$ was observed for each sample. These observations were attributed to the formation of a highly viscous solution 30 min after the start of the reaction. As the viscosity increases, the chain end diffusion was considered to drastically decrease, consequently decreasing chain transfer of the active polymer chain to CTA-end groups. Thus, chain transfer reactions to polymer (not end-groups) became more pronounced compared to chain transfer to CTA-end groups which finally led to branching (higher \mathcal{D}) and finally crosslinking at high conversions. These assumptions were supported by the observation of bimodal mass distributions starting after

2 – 3 h of reaction time and the formation of a partly insoluble gel after approximately 4 h of reaction time (**Figure 4.20**, the respective dRI vs retention time plots are shown in chapter 6.5.2). Finally, a deviation between $M_{n,NMR}$ and $M_{n,SEC}$ is naturally caused by the calculation of $M_{n,SEC}$ using linear poly(methyl methacrylate) standards due to their different hydrodynamic volume (at the same molecular weight) compared to the sample polymer. Additionally, this deviation becomes more pronounced if the polymer architecture of sample differs from the architecture of the standard.

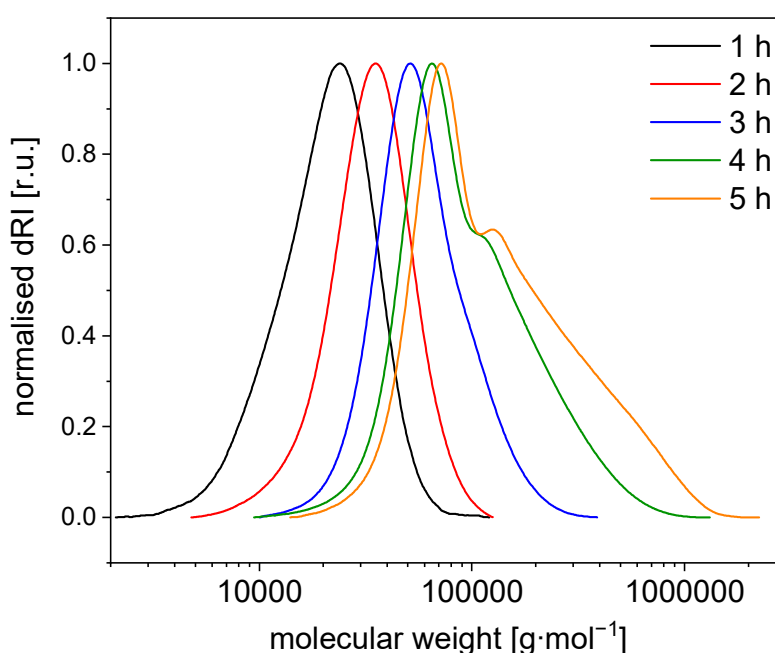


Figure 4.20 SEC chromatograms of the RAFT polymerisation of **168** with CTA1 in a 7.5 M reaction mixture showing the development of a bimodal molecular weight distribution at reaction times longer than 2 – 3 h.

Consequently, the concentration was lowered for polymerisations with CTA1 to maintain sufficient mixing throughout the polymerisation process, thus preventing temperature and concentration gradients. Polymerisations with CTA1 were screened with 3.75 M and 1.88 M solutions of **168** (**Table 4.14**). While 3.75 M concentration still showed the same problems as described above, 1.88 M mixtures led to polymers with narrow molecular weight distributions with \bar{D} s between 1.15 and 1.17. Moreover, the molecular

4.3 Controlled Radical Polymerisation of Ricinoleic Acid-Derived Vinyl Monomers and Subsequent Modification via the Biginelli-3-Component Reaction

weight linearly increased with time and $M_{n,NMR}$ and $M_{n,SEC}$ were expectedly similar indicating a controlled polymerisation. Nonetheless, a qualitative increase in viscosity of the polymerisation mixture was observed for conversions above 55%. Hence, if higher conversions are intended, lower concentrations are considered beneficial. Afterwards, CTA2 was also applied in a 1.88 M reaction mixture to investigate if it offers better control over the RAFT polymerisation of **168** (Table 6.16, page 289). However, the higher D s between 1.18 and 1.35 and the larger deviation between $M_{n,NMR}$ and $M_{n,SEC}$ indicated only partial control during the polymerisation. Hence, CTA1 was used for the following investigations and syntheses.

Table 4.14 1H NMR and SEC results from the screening of two different concentrations of the RAFT polymerisation of **168** with CTA1.^a

entry	concentration [M]	reaction time [h]	$M_{n,NMR}^b$ [g·mol ⁻¹] (conversion [%])	$M_{n,SEC}$ [g·mol ⁻¹]	D
1	3.75	1	3 400 (13)	18 100	1.27
2		2	9 200 (36)	29 400	1.23
3		3	12 600 (50)	50 900	1.24
4		4	16 600 (66)	74 600	1.55
5	1.88	1	2 200 (8)	5 355	1.15
6		2	3 930 (15)	6 560	1.17
7		3	5 420 (21)	7 880	1.17
8		4	8 630 (34)	9 690	1.17
9		5	11 100 (44)	11 750	1.15
10		6	13 580 (54)	13 480	1.17
11		6.5	14 810 (59)	14 400	1.18

^aratio of monomer to CTA to AIBN is 50:1:0.1; ^b $M_{n,NMR}$ is calculated using the monomer conversion.

The pseudo first-order rate plot for the RAFT polymerisation of **168** with CTA1 in a 1.88 M solution is given in **Figure 4.21**. The polymerisation shows significant rate retardation of a factor of approximately 2.4 within the first 3 h compared to the rate for reaction times longer than 3 h. This is a well known behaviour of RAFT polymerisations of methacrylates with dithiobenzoate CTAs but also for other monomer and CTA classes while the polymerisation is still in the preequilibrium phase.^[417] Retardation after the induction period is also known, while it has been shown that higher CTA concentrations lead to lower polymerisation rates.^[412]

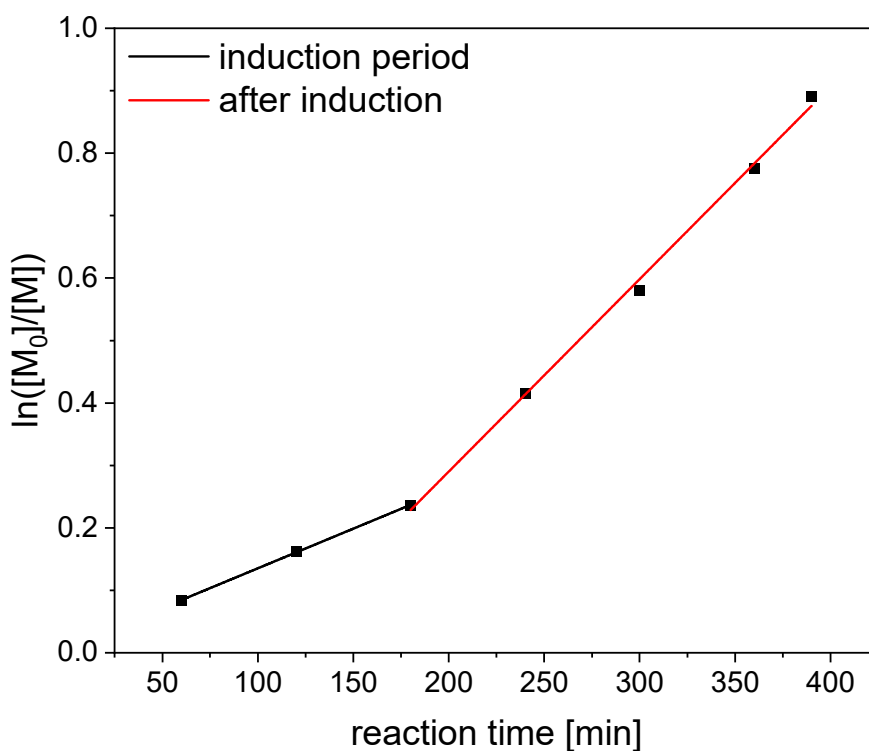


Figure 4.21 Pseudo-first order kinetic plot showing the relation between $\ln([M_0]/[M])$ and the reaction time; a rate retarded induction period of 3 h was observed, the conversion was determined by ¹H NMR spectroscopy.

Afterwards, the found relation between $\ln([M_0]/[M])$ and t was used to determine the reaction times needed to reach monomer conversions of 40%, 50%, and 60% , respectively (**Table 4.15**). Hence, the respective polymerisation experiments were stopped after

4.3 Controlled Radical Polymerisation of Ricinoleic Acid-Derived Vinyl Monomers and Subsequent Modification via the Biginelli-3-Component Reaction

222 min, 276 min, and 333 min. The reached conversions resembled the desired molecular weights with a deviation between 1% and 3%. Furthermore, $M_{n,NMR}$ and $M_{n,SEC}$ were comparable and the D s of 1.12 to 1.13 verified the controlled polymerisation.

Table 4.15 SEC and 1H NMR data for the synthesis of RAFT polymers of specific molecular weights.^a

entry	reaction ^b time [min]	intended $M_{n,NMR}$ ^b [g·mol ⁻¹] (conversion [%])	$M_{n,NMR}$ ^c [g·mol ⁻¹] (conversion [%])	$M_{n,SEC}$ [g·mol ⁻¹]	D
1	222	10 200 (40)	10 620 (42)	11 410	1.14
2	276	12 700 (50)	11 950 (51)	11 680	1.12
3	333	15 200 (60)	14 450 (57)	13 920	1.13

^aratio of monomer to CTA to AIBN is 50:1:0.1; ^bcalculated using the found relation between $\ln([M_0]/[M])$ and t (**Figure 4.21**) ^c $M_{n,NMR}$ is calculated using the signals of the dithiobenzoate end group.

Since the resulting polymers **169** were purified, the conversions and $M_{n,NMR}$ were calculated using one of the proton signals of the dithiobenzoate end group at 7.87 ppm in relation to the signals of the internal double bonds at 5.48 ppm and 5.31 ppm (**Figure 4.22**). Notably, the thermal properties of the polymers **169** were also investigated using DSC finding a consistent T_g of $-50^\circ C$ (**Figure 6.84**, page 292).

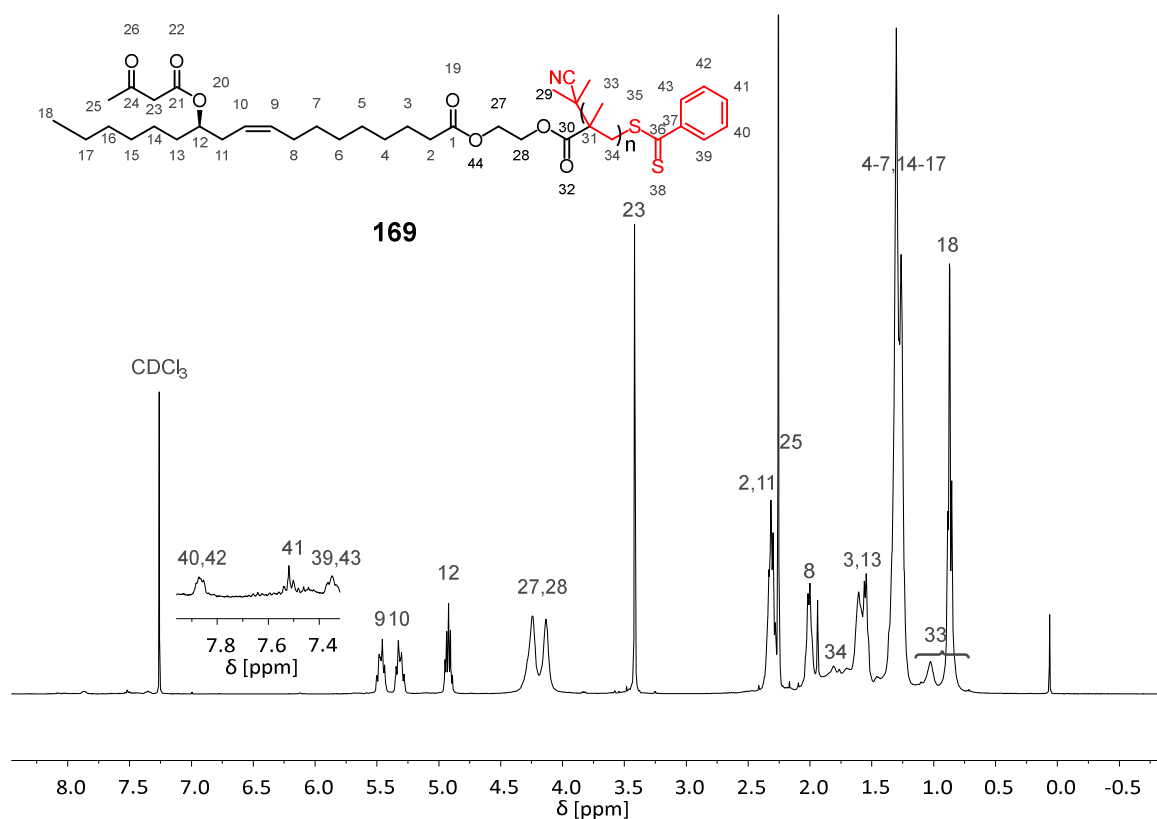


Figure 4.22 ^1H NMR spectrum of RAFT polymer **169** with a DP of 21.

The resulting polymer chains of a RAFT process still carry the, in this case, dithiobenzoate function, thus, function as macro CTA. Consequently, chain extension and the synthesis of block copolymers is possible if the macro CTA is applied for the RAFT polymerisation of another suitable monomer. A prerequisite is, however, the end group fidelity over the whole molecular weight distribution so that the polymers of each chain length are extended. To investigate the end group fidelity, the **169** samples were measured by SEC using both an RI detector and a UV detector set at a wavelength of 305 nm, which is well suited to detect the absorption of the dithiobenzoate group.^[418] For maximum end group fidelity, the peak shapes were expected to be identical.

After correction of the data of the UV detector regarding the concentration, both distributions qualitatively showed identical peak shapes indicating high end group fidelity (**Figure 4.23**).^[419] For the quantitative determination of the end group fidelity, the

determination of the dn/dc and dA/dc values regarding the two detectors is necessary. Otherwise, the two distributions differ by an unknown factor. Hence, the measurement of a standard with the same CTA end group as the polymer sample with known end group fidelity is necessary.^[418]

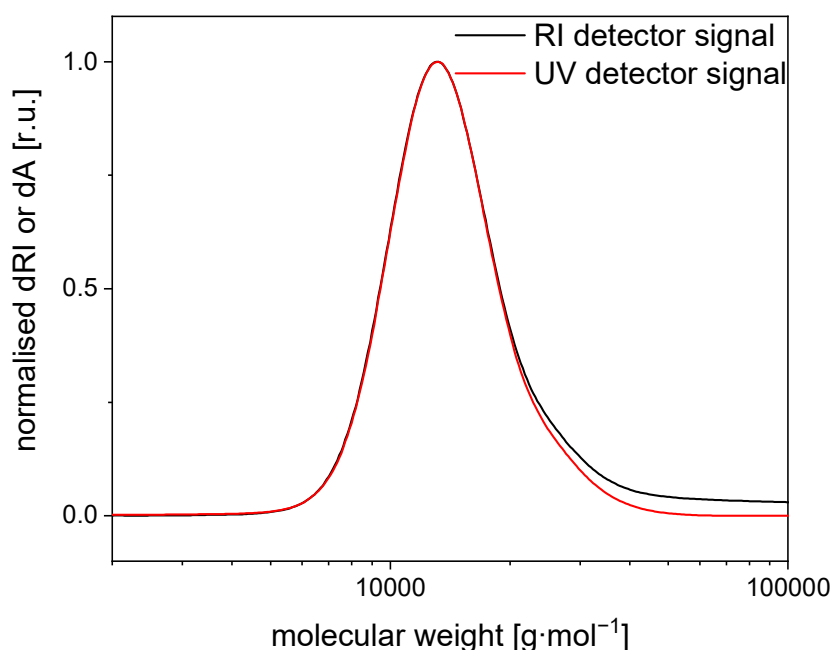


Figure 4.23 Example overlay of the normalised molecular weight distributions of the RI- and UV detector of **169** showing strong resemblance.

Instead, the end group fidelity was indirectly shown by a chain extension experiment as the presence of dead chain ends (resembling a deficiency in end group fidelity) leads to the formation of a low molecular weight shoulder or the formation of a bimodal distribution. Thus, **169** with a DP of 21 was used as macro CTA for the polymerisation of **168** using the same conditions as above (**Table 4.15**) to confirm the feasibility of the chain extension. A ratio of monomer to macro CTA to AIBN of 50:1:0.1 was used.

Since the inhibition phenomena at the beginning of a polymerisation are only reported for small CTAs but not for macro CTAs, the polymerisation rate after the induction period

(*cf.* **Figure 4.21**, page 145) was used to calculate the reaction time for a monomer conversion of 35%.^[412] A conversion of 35% was chosen to avoid an increase in viscosity and a subsequent loss of control as discussed above. Consequently, the reaction time of 144 min was determined in order to reach a final $M_{n,NMR}$ of approximately $19\,300\text{ g}\cdot\text{mol}^{-1}$.

The $M_{n,NMR}$ was found to be $18\,730\text{ g}\cdot\text{mol}^{-1}$ corresponding to a conversion of 33%. The $M_{n,SEC}$ of $18\,700\text{ g}\cdot\text{mol}^{-1}$ and the \mathcal{D} of 1.15 verified the controlled polymerisation (**Figure 4.24**). The formation of the high molecular weight shoulder was attributed to the above discussed increase in viscosity for higher molecular weights. The results of the chain extension experiments, therefore, confirm the high end group fidelity of the macro CTA that was obtained by RAFT polymerisation of **168**, as well as the feasibility of the synthesis of block copolymers.

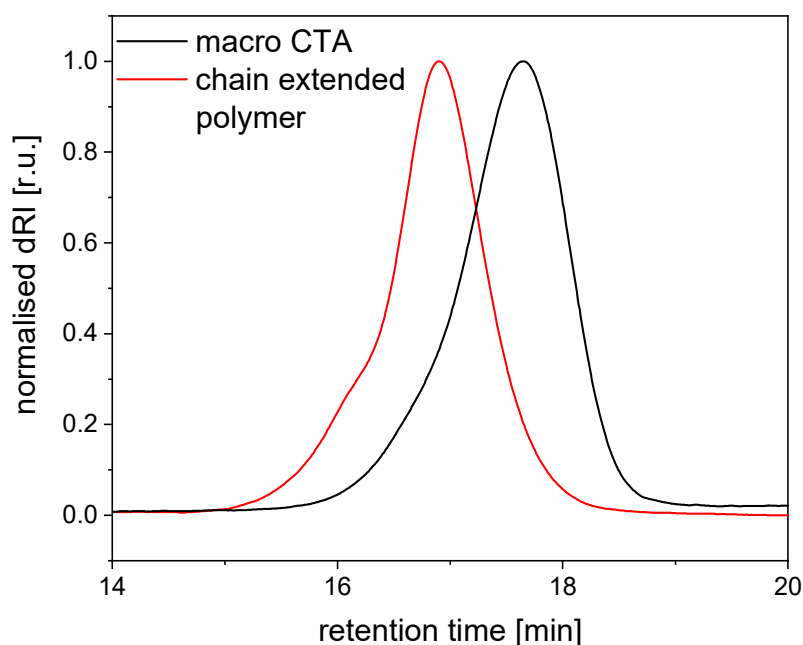


Figure 4.24 SEC chromatograms of the macro CTA and the chain extended polymer.

As such, a block copolymer (**170**) was synthesised using methyl methacrylate as monomer and **169** with a DP of 21 as macro CTA (*cf.* chapter 6.5.4 for detailed data). The

same conditions as for the chain extension were used with a ratio of monomer to macro CTA to AIBN of 50:1:0.1. The synthesis of a block copolymer was confirmed by ^1H NMR spectroscopy showing the characteristic signals of the methyl ester of the poly(methyl methacrylate) block at approximately 3.6 ppm (**Figure 4.25**). While the D of 1.13 indicated the controlled polymerisation of methyl methacrylate, the $M_{n,\text{SEC}}$ of $10\,325\text{ g}\cdot\text{mol}^{-1}$ was smaller compared to the $M_{n,\text{SEC}}$ of the macro CTA. This was attributed to the different chemical structure of the poly(methyl methacrylate) block which led to an overall smaller hydrodynamic volume compared to the macro CTA. The $M_{n,\text{NMR}}$ of $18\,130\text{ g}\cdot\text{mol}^{-1}$ showed an increase of approximately $1\,000\text{ g}\cdot\text{mol}^{-1}$ indicating a DP of the poly(methyl methacrylate) block of 10.

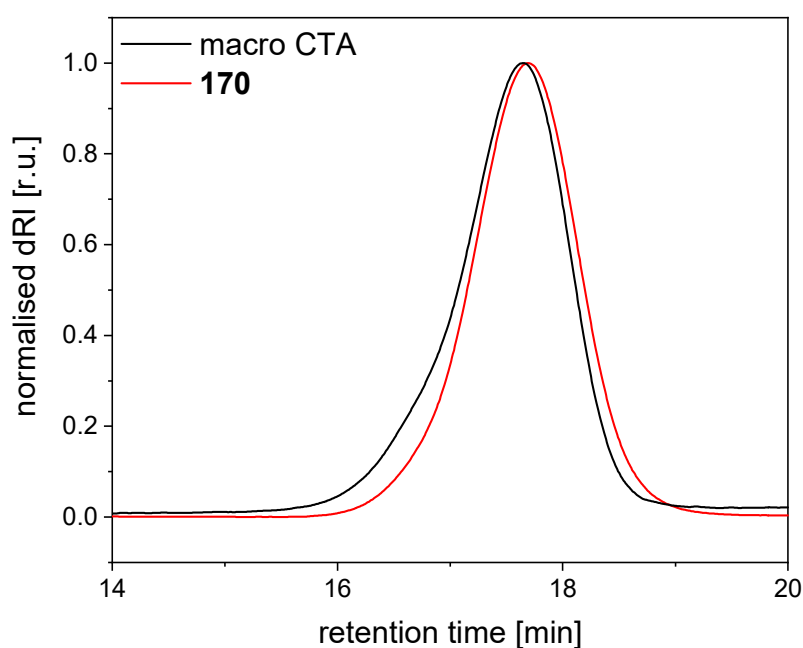


Figure 4.25 ^1H NMR spectrum of the block copolymer **170** in CDCl_3 .

To conclude, the ricinoleic acid-derived methacrylate monomer **168** was synthesised and its RAFT polymerisation was investigated. It was shown that rather diluted reaction mixtures were needed to obtain narrow molecular weight distributions. Concentrations

lower than 1.88 M were found suitable to obtain D_s lower than 1.15. While the application of the dithiobenzoate CTA, 2-cyanoprop-2-yl benzodithioate, led to D_s lower than 1.15, the trithiocarbonate CTA, *S*-(2-cyanoprop-2-yl)-*S*-dodecyltrithiocarbonate, only led to partial control over the molecular weight. In order to apply RAFT polymers from **168** for the synthesis of block copolymers, high end group fidelity and the possibility of a controlled chain extension are prerequisites. Both excellent end group fidelity and control over the molecular weight during chain extension were successfully shown. As such, **168** was shown to be a renewable monomer suitable for the synthesis of homo- and block copolymers *via* RAFT polymerisation.

The application of the incorporated acetoacetate functionality for post-polymerisation modification by the B-3CR will be addressed in the following chapter.

4.3.5 Post Polymerisation Modification *via* the Biginelli-Three-Component Reaction

Post-polymerisation modifications (PPM) are a valuable tool to include functionalities in polymers or to alter the macroscopic properties of a polymer material in a way that was not possible prior to polymerisation at the stage of the monomer. Within this chapter the PPM of the RAFT polymers **169** was investigated using the **169** with a DP of 21 as example. The acetoacetate moiety that was present within the monomer structure was retained during the polymerisation (*cf.* **Figure 4.22**, page 147) and its exploitation in a subsequent B-3CR was investigated.

Hence, **169** with DP 21 was dissolved in AcOH, and stirred together with 1.33 eq of benzaldehyde (**51**), 1.33 eq urea (**47**), and 0.07 eq MgCl₂ as catalyst according to an adapted procedure of Tao *et al.*^[346] This procedure was preferred over the, in this work typically used, Brønsted acid-catalysed B-3CR due to the milder temperature of 100°C to prevent side reactions of the polymer. The reaction progress was monitored by ¹H NMR spectroscopy referencing the *CH* proton of the polyDHPM to the signal of the *CH* adjacent to the acetoacetate of the ricinoleic acid structure (**Figure 4.26**) showing a conversion of approximately 95% of the acetoacetate moiety after 25h of reaction time. The formation of

4.3 Controlled Radical Polymerisation of Ricinoleic Acid-Derived Vinyl Monomers and Subsequent Modification via the Biginelli-3-Component Reaction

the typical signals of a DHPM, namely the signals of the *NH*-protons at 9.15 ppm and 7.68 ppm and the signal of the *CH* proton of the DHPM ring at 5.11 ppm, was also observed. After precipitation in MeOH and washing therein, the pure polymer obtained with a yield of 92%.

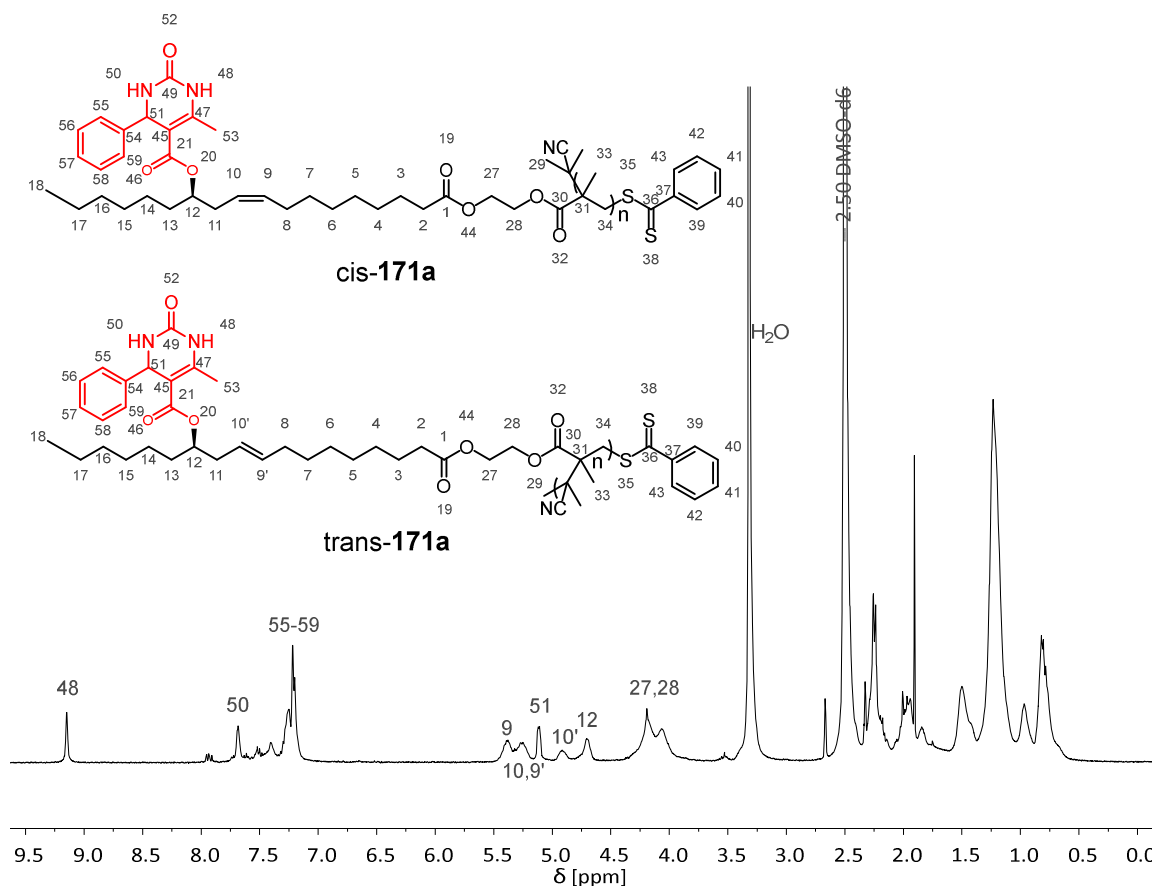


Figure 4.26 ^1H NMR spectrum of the purified polymer **171a** after PPM of **169** by B-3CR: both of the *cis*/*trans*-isomers of **171a** are visible.

Interestingly, the two multiplet signals of the double bond protons of **169** split to four different signals (**Figure 4.26**). It was assumed that the *cis*-double bond was partly isomerised to the *trans*-isomer. This was confirmed by the phase edited HSQC NMR spectrum of **171a** with reference to reported chemical shifts for *cis*/*trans* isomers of aliphatic olefins (**Figure 6.91**, page 301).^[420] The chemical shifts of the ^{13}C carbon signals of 9 and

9' as well as 10 and 10', respectively, resembled each other while the ^1H signals of the protons at 9' and 10' were shifted to higher ppm values compared to the chemical shifts of the protons at 9 and 10. Finally, a ratio of cis/trans of 60/40 was determined.

The SEC analysis of **171a** revealed the formation of a small shoulder towards higher molecular weights, while the main signal was shifted to lower molecular weights compared to the starting material (**169**) resulting in a $M_{n,\text{SEC}}$ of $8\,600\text{ g}\cdot\text{mol}^{-1}$ ($D = 1.24$) compared to a $M_{n,\text{SEC}}$ of $10\,200\text{ g}\cdot\text{mol}^{-1}$ ($D = 1.13$) of the starting material (**Figure 4.27**).

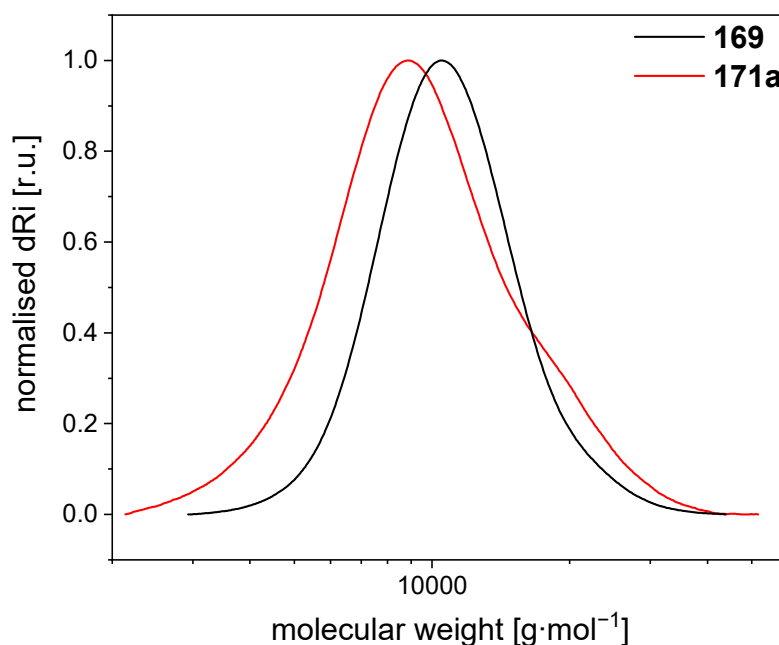


Figure 4.27 SEC graphs of **169** and **171a**.

The shift of the signal towards lower molecular weights was attributed to the tendency of polymers that contain the DHPM motif to form, due to hydrogen bonding, compact coils in solution as it was already discussed in above chapters 4.1.3 and 4.2.3. Finally, a DSC analysis revealed a shift of the original T_g at -50°C to -13°C (**Figure 6.89**, page 299).

Afterwards, the reaction was repeated with anisaldehyde (*p*-methoxy benzaldehyde) to verify the feasibility of the PPM approach (*cf.* chapter 6.5.5 for the respective

spectra/graphs). The ^1H NMR spectrum of the resulting **171b** verified the formation of the expected DHPM moiety while a conversion of the acetoacetate to the DHPM of 81% was determined. Similar to the ^1H NMR spectrum of **171a**, a cis/trans ratio of 61/39 was determined. The SEC data showed a $M_{n,SEC}$ of $9\,700\text{ g}\cdot\text{mol}^{-1}$ ($D = 1.23$) and the DSC result a T_g of 29°C .

To conclude, it was shown that the B-3CR is an efficient tool for the PPM of **169** reaching high conversions of up to 95% accompanied by a significant change of the T_g . The PPM approach was considered promising in order to synthesise block copolymers that contain the DHPM motif by synthesis of a block copolymer *via* RAFT polymerisation and subsequent PPM by the B-3CR of the block that carries the acetoacetate moiety. This way, some of the challenges regarding the block copolymer synthesis described in chapter 4.2.3 and 4.2.4 might be circumvented. This is, however, part of future investigations.

4.3.6 Conclusion and Outlook

Within this chapter the synthesis of new renewable monomers for radical polymerisation, especially RAFT polymerisation, was attempted. Due to vinyl ester being less toxic compared to acrylates or methacrylates. The synthesis of vinyl esters *via* transvinilation of renewable carboxylic acids was carried out. Furthermore, starting materials with an additional hydroxy group were chosen to introduce an acetoacetate moiety suitable for PPM. Out of six monomers, **163** and **164** were synthesised with overall yields of 46% and 49%, respectively. The investigated aromatic starting materials **149**, **150**, and **151** appeared to form the respective acetoacetates *in situ*. The latter, however, were not stable and reacted back to the starting material. Hence, the transvinilation was not attempted even though the vinyl esters were possibly readily available. A proper investigation of the decomposition for these aromatic acetoacetates might allow their purification and the further conversion to the vinyl ester as well as the application in FRP or RAFT polymerization. While **152** was converted to acetoacetate **157** with a yield of 90%, the subsequent transvinilation to **162** was inefficient with maximum yields of 34% in the crude

reaction mixture. Furthermore, purification was challenging since it led to the decomposition of **162** to unknown compounds. Hence no pure **162** was isolated.

The FRP or RAFT polymerisation of **162** and **163** were attempted. However, the polymerisations seemed to be severely inhibited albeit the similar vinyl stearate was readily polymerizable under similar reaction conditions. Being the only significant difference between **163** and stearic acid, the acetoacetate group was deemed a potential inhibitor, a hypothesis that was tested by application of ethyl acetoacetate as solvent for the polymerisation of vinyl stearate. However, no inhibition was observed and the cause for the inhibition remained unknown as no impurity within **162** or **163** were identified. Nonetheless, it was conceivable that the inhibitor was formed or added during the transvinylation, since **168** was synthesised from **159**, just as **162** was. A different approach for the vinylation might avoid the introduction of the unknown inhibitor.

As a consequence, the vinyl esters were deemed unsuitable for the purposes of this study, and the more toxic methacrylate **168** was synthesised. The RAFT polymerisation of **168** was investigated in terms of reaction conditions, molecular weight control, end group fidelity, and the possibility for chain extension and the synthesis of block copolymers. Overall, **168** was found to be a valuable renewable monomer for RAFT polymerisation. Furthermore, the resulting polymers **169** were considered suitable for the synthesis of block copolymers due to the feasibility of the investigated chain extension.

Subsequently, the PPM of **169** *via* the B-3CR was investigated. The B-3CR was shown to convert the acetoacetate moiety in the pendant groups of the polymer to up to 95% while significantly increasing the T_g of the starting material by up to 80°C. Hence, the PPM approach was considered a promising tool for the synthesis of new polymer materials. As such, the investigation of the block copolymer synthesis *via* RAFT polymerisation and subsequent PPM using the B-3CR was deemed a promising alternative to the block copolymer synthesis *via* end group functionalisation (chapter 4.2).

Finally, while the vinyl ester synthesis remained highly challenging, the transvinylation of the investigated starting materials without prior acetoacetylation possibly leads to

valuable sustainable monomers for radical polymerisations. Regarding the RAFT polymerisation of **168**, especially the synthesis of various copolymer materials with other sustainable monomers is of interest, especially in combination with the PPM by the B-3CR. However, the introduction of a suitable functional group in a monomer for subsequent B-3CR was deemed to be the most challenging part. Moreover, the brittleness of polymers that contain the DHPM motif is probably drastically lowered in combination with the flexible fatty acid compound. As microphase separation was already shown for polyDHPM-*b*-poly(ethylene glycol)s (**148a-f**), such behaviour of a block copolymer consisting of modified **169** and another block is likely. Hence, the resulting materials possibly show characteristics of a thermoplastic elastomer or shape memory polymer.

5 Conclusion and Outlook

Within this thesis, the synthesis of novel and renewable polymer structures was investigated. More precisely, the Biginelli-three-component (B-3CR) reaction was applied in three different ways within the field of polymer chemistry.

First, new components for the the Biginelli polycondensation were introduced and the resulting properties of the respective polycondensates were investigated (chapter 4.1). Hence, the synthesis of 15 new and renewable polyDHPMs was described. Six diacetoacetates, three diacetoacetamides (AA-monomers), terephthalic aldehyde (BB-monomer), urea, and *N*-methylurea were used as components for the B-3CR in various combinations significantly expanding the known library of monomers, as well as polymer structures. The diacetoacetates and diacetoacetamides with different spacer lengths were synthesised in yields up to 99% in a one-step process. The used starting materials are all available from renewable resources as discussed in chapter 2.6.1 – 2.6.5. Thermal analysis of the obtained set of polymers revealed high T_g s ranging from 160°C to 308°C. The T_g was tuneable in small steps of 10°C. The polyDHPMs were thermally stable well above the respective high T_g values. The results demonstrate the straight-forward variation of the components for the Biginelli polycondensation and enable the synthesis of renewable high T_g polymers.

Second, the synthesis of block copolymers containing a Biginelli polycondensate block was investigated and the thermal properties of the resulting block copolymers were explored (chapter 4.2). Hence, six polyDHPMs with terminal double bonds as end groups were prepared in yields up to 76% using five diacetoacetates (AA-monomer), terephthalic aldehyde (BB-monomer), urea, and *N*-methyl urea as components for the B-3CR. Additionally, 2- $\{[3-(4\text{-formyl-2-methoxyphenoxy})\text{propyl}]\text{thio}\}$ ethyl acetoacetate was used as renewable AB-monomer. The end groups were introduced by addition of 10-undecenyl-1-acetoacetate (**143**) to the monomer mixture. The molecular weight of the end group-functionalised polyDHPMs was, moreover, tuned between 6 800 g·mol⁻¹ and 4 200 g·mol⁻¹ by variation of the amount of monoacetoacetate. Afterwards, the conversion of the end group-functionalised polyDHPMs in a thiol-ene reaction was investigated. The

reactivity was first investigated with butane thiol and second with poly(ethylene glycol) methylether thiol to obtain block copolymers. Finally, polyDHPM-*b*-poly(ethylene glycol)s were obtained yielding up to 76%. DSC analysis of the block copolymers revealed two distinct thermal transitions. While the T_g s of the polyDHPM blocks ranged, depending on the monomer structure, between 265°C and 159°C, the melting point (T_m) of the poly(ethylene glycol) block (PEG block) remained between 49°C and 52°C matching the T_m of pure **147**. This behaviour indicated microphase separation of the applied polymer blocks but needs further evidence, *e.g.* using dynamic mechanical analysis and or microscopic techniques.^[421]

Third, the synthesis of novel, renewable vinyl ester monomers and a methacrylate monomer with additional acetoacetate function was attempted (chapter 4.3) to allow for post-polymerisation modification (PPM) using the B-3CR. Hence, the acetoacetylation of six suitable starting materials was attempted but was only successful for lactic acid, ricinoleic acid, and 12-hydroxystearic acid. Subsequently, the transvinylation of the three acetoacetylated carboxylic acids was attempted. However, only the two fatty acid vinyl esters were obtained. Afterwards, the polymerisation behaviour of the two vinyl esters by FRP and RAFT polymerisation was explored and showed strong inhibition preventing the formation of polyvinyl esters. The source of inhibition remained unknown.

Consequently, a ricinoleic acid-based methacrylate monomer was synthesised (chapter 4.3.4). Subsequent RAFT polymerisation yielded polymers with a molecular weight of up to 15 000 g·mol⁻¹ and narrow molecular weight distributions (D s around 1.13). Furthermore, the suitability of the resulting material for chain extension and thus block copolymer synthesis was demonstrated by determination of the end group fidelity of the RAFT polymers, the subsequent chain extension under RAFT conditions, and the synthesis of a block copolymer with poly(methyl methacrylate) as second block. Finally, the PPM of the acetoacetate moiety within **169** was investigated using the B-3CR (chapter 4.3.5). Conversions of up to 95% of the acetoacetate moiety towards the desired DHPM motif were shown rendering the PPM by B-3CR. Furthermore, the T_g s were increased by up to 80°C.

Finally, the novel ricinoleic acid-based methacrylate monomer was deemed a promising starting material for the synthesis of various polymer materials.

To conclude, the B-3CR was proven to be a valuable tool for the preparation of novel and interesting polymer structures. However, one of the main challenges remains the processability of the obtained materials as their brittleness has, so far, prevented the investigation of the respective mechanical properties. To reduce the brittleness, the introduction of larger and/or bulkier spacer units to reduce the hydrogen bonding and thus the T_g is proposed. Alternatively, the synthesis of block copolymers with a very low T_g block possibly allows for a simplified processing.

Furthermore, deeper insight in the mechanistic details and the polymerisation kinetics of the Biginelli polycondensation are needed to gain more control over the polymerisation process and finally allow higher molecular weights. Consequently, the implementation of analyses to obtain absolute molecular weight data, for example static light scattering, avoids uncertainties in the interpretation of NMR spectra and SEC chromatograms. Finally, the investigation of possible side reactions during the Biginelli polycondensation is anticipated to help understanding synthetic challenges. Especially important is the degree of oxidation of the aldehyde component during the polymerisation as it leads to dead chain ends.

Last but not least, the RAFT polymerisation of monomers that carry an acetoacetate is a promising candidate for the synthesis of interesting polymer materials. However, further investigations on the block copolymer synthesis regarding the possible monomer spectrum and the resulting material properties are needed. While the PPM *via* the B-3CR was shown to be efficient for two examples, the investigation of the product scope, in particular also for block copolymers, is needed in order to determine the value of this method.

4.3 Controlled Radical Polymerisation of Ricinoleic Acid-Derived Vinyl Monomers and Subsequent Modification via the Biginelli-3-Component Reaction

6 Experimental Section

6.1 Materials

All commercially available materials were used as received and were ordered from the following suppliers: Acros Organics, Air Liquide, Alfa Aesar, Carl Roth, Eurisotop, Fischer Scientific, Fluka, Merck, Sigma Aldrich, VWR.

6.2 General Methods and Instrumentation

6.2.1 Thin Layer Chromatography (TLC)

Fluorescent silica coated aluminium plates were used for TLC. The plates were developed using either a UV-lamp to quench fluorescence at 254 nm or to excite fluorescence of the compounds at 365 nm, or Seebach stain (phosphomolybdic acid, cerium(IV) sulfate, sulfuric acid, water) to visualise UV-inactive compounds. The R_f values and used solvent mixtures are given at the respective synthesis procedure of each compound.

6.2.2 Flash Column Chromatography

Flash column chromatography was performed using a method similar to that introduced by Still *et al.*^[422] The glass column with built-in fritted glass filter was filled with a slurry of eluent (the eluent is given at the respective synthesis procedure of each compound) and stationary phase (silica, Aldrich, technical grade, 60 Å pore size, 230 – 400 mesh size, 40 – 63 µm particle size). The crude substance was applied in a liquid state dissolved in a small amount of eluent. Pressure was applied with a manual pump.

6.2.3 Vacuum Oven

Polymer samples were dried in a ThermoScientific™ Vacutherm VT6025 S vacuum drying oven at 85°C under vacuum prior to analysis.

6.2.4 Nuclear Magnetic Resonance (NMR) Spectroscopy

^1H and ^{13}C NMR spectra were recorded on a Bruker Avance NEO spectrometer at a frequency of 400.13 MHz and 100.62 MHz, respectively. All spectra were measured at ambient temperature. For sample preparation, 10 – 15 mg of substance were dissolved in 0.40 ml DMSO- d_6 (99.80 atom% D) or CDCl_3 (99.80 atom% D) in an NMR tube with a diameter of 5 mm. The chemical shift (δ) was given in parts per million (ppm) relative to the δ of tetramethylsilane ($\delta(\text{TMS}) = 0.00$ ppm).

The chemical shifts of the residual DMSO- d_5 (^1H NMR: 2.50 ppm; ^{13}C NMR: 39.52 ppm) or CHCl_3 (^1H NMR: 7.26 ppm; ^{13}C NMR: 77.16 ppm) were used for referencing. Splitting patterns were denoted as follows: s (singlet), d (doublet), t (triplet), q (quartet), p (pentet), m (multiplet), dd (doublet of doublets), ddd (doublet of doublets of doublets), ddt (doublet of doublets of triplets), and br (broad). The respective coupling constants xJ were given in Hertz (Hz). The signals were listed from low field (large ppm) to high field (small ppm).

In addition, 2D-spectra were recorded to support signal structure assignments. The following experiments were used: ^1H , ^1H -Correlated Spectroscopy (^1H , ^1H -COSY), phase edited ^1H , ^{13}C -Heteronuclear Single Quantum Coherence (^1H , ^{13}C -HSQCed), and ^1H , ^{13}C -Heteronuclear Multiple Bond Correlation (^1H , ^{13}C -HMBC).

6.2.5 Size Exclusion Chromatography (SEC)

For SEC, three different systems were used, depending on the solubility of the polymers and the need for a UV detector in some cases: SEC was performed on a Tosoh EcoSEC

HLC-8320 SEC system. For sample preparation, 2 mg of sample were dissolved in 2 ml hexafluoroisopropanol with 0.1 wt% potassium trifluoroacetate. The same solvent mixture was used as mobile phase. The solvent flow was $0.40 \text{ mL}\cdot\text{min}^{-1}$ at $35 \text{ }^\circ\text{C}$. The analysis was performed on a three-column system: PSS PFG Micro pre-column ($3.0\cdot 0.46 \text{ cm}^2$, 10000 \AA), PSS PFG Micro ($25.0\cdot 0.46 \text{ cm}^2$, 1000 \AA) and PSS PFG Micro ($25.0\cdot 0.46 \text{ cm}^2$, 100 \AA). The system was calibrated with linear poly(methyl methacrylate) standards (PSS, $M_p: 102 - 981 \text{ kg}\cdot\text{mol}^{-1}$).

Alternatively, samples were measured on a Shimadzu LS 20A system equipped with a SIL-20A autosampler and a RID-20A refractive index detector. For sample preparation, 2 mg of sample were dissolved in 2 ml tetrahydrofuran/2 vol% NEt_3 . The same solvent mixture was used as mobile phase. The solvent flow was $1.00 \text{ mL}\cdot\text{min}^{-1}$ at 30°C . The analysis was performed on a three-column system: PSS SDV analytical ($5 \mu\text{m}$, $300\cdot 8.0 \text{ mm}^2$, 1000 \AA), PSS SDV analytical ($5 \mu\text{m}$, $300\cdot 8.0 \text{ mm}^2$, 100000 \AA), and a PSS SDV analytical precolumn ($5 \mu\text{m}$, $50\cdot 8.0 \text{ mm}^2$). For the calibration, narrow linear poly(methyl methacrylate) standards (Polymer Standards Service, PPS, Germany) ranging from $1\ 100$ to $981\ 000 \text{ g}\cdot\text{mol}^{-1}$ were used.

Furthermore, samples were measured on an Agilent 1260 Infinity II system equipped with UV/Vis-detector and RI-detector. For sample preparation, 2 mg of sample were dissolved in 2 ml tetrahydrofuran. The same solvent mixture was used as mobile phase. The solvent flow was $1.00 \text{ mL}\cdot\text{min}^{-1}$ at 35°C . The analysis was performed on a three-column system: SDV Lux pre-column ($8\cdot 50 \text{ mm}$), SDV Lux ($8\cdot 300 \text{ mm}$, 1000 \AA) and SDV Lux ($8\cdot 300 \text{ mm}$, 100000 \AA). The system was calibrated with linear poly(methyl methacrylate) standards (PSS, $M_p: 102 - 981 \text{ kg}\cdot\text{mol}^{-1}$).

6.2.6 Infrared (IR) Spectroscopy

IR spectra were recorded on a Bruker Alpha FTIR spectrometer equipped with Platinum ATR technology. The resulting transmittance spectra are averaged from 24 measurements. The energies of the IR bands were given as wavenumbers ν in cm^{-1} . The signals were noted from large to small wavenumbers.

6.2.7 High Resolution Mass Spectrometry (HRMS)

High resolution mass spectra were recorded on a Finnigan MAT 95 spectrometer using electron ionization (EI) or fast atom bombardment (FAB). The signal of the singly charged radical cation of the analyte was referred to as $[\text{M}]^{+\bullet}$, the protonated singly charged cation of the molecule was referred to as $[\text{M}+\text{H}]^+$.

6.2.8 Differential Scanning Calorimetry (DSC)

DSC experiments were performed on a DSC821e (Mettler Toledo) calorimeter. Samples were prepared by compressing 15 – 20 mg of sample in a 100 μl aluminium crucible. The measurements were performed under nitrogen atmosphere with two heating cycles in the temperature range of $-50 - 300^\circ\text{C}$ (or $-50 - 350^\circ\text{C}$) with a cooling rate of $15 \text{ K}\cdot\text{min}^{-1}$ and a heating rate of $30 \text{ K}\cdot\text{min}^{-1}$. Alternatively, a temperature range of $-70 - 250^\circ\text{C}$ was used.

For the calculation of the thermal transitions, the second heating cycle was used. The T_{gs} were determined using the inflection points of the respective second order transitions. T_{ms} were determined using the minima of the respective first order transitions.

6.2.9 Thermogravimetric Analysis (TGA)

Thermogravimetric analysis was performed on a Netzsch STA 490C with Al_2O_3 as crucible material and reference sample. The samples of 10 – 20 mg were heated from room

temperature to 500 °C with a temperature gradient of 5 K·min⁻¹ under synthetic air flow. The temperature at which a weight loss of 5% is reached ($T_{d5\%}$) was determined *via* intersection of the TGA curve with a line at $y = 0.95 - \alpha$, where α is the weight loss at 105 °C (to exclude the weight loss due to water evaporation).

6.3 Synthesis Procedures and Analytical Data Related to Chapter 4.1

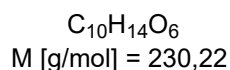
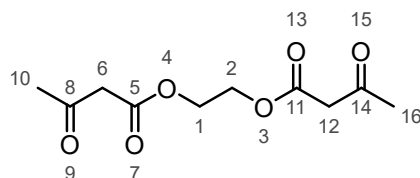
6.3.1 Diacetoacetates and Diacetoacetamides

All diacetoacetates were synthesised using the following general procedure: The respective diol (1.00 eq) was mixed with *tert*-butyl acetoacetate (5.00 eq) in a round bottom flask and stirred in a preheated oil bath at 150°C for 7 h. Evolving *t*-BuOH was continuously removed *via* distillation. Afterwards, the crude product was purified by column chromatography using a mixture of *c*-C₆H₁₂ and EtOAc. The formed *t*-BuOH, as well as the excess of *tert*-butyl acetoacetate, were recovered *via* distillation and column chromatography, respectively.

All diacetoacetamides were synthesised using the same procedure. The respective diamine (1.00 eq) was added dropwise to preheated (130°C) diketene acetone adduct (2,2,6-trimethyl-4H-1,3-dioxin-4-one, 2.10 eq) under vigorous stirring. Afterwards, the mixture was stirred at 130 °C for 5 h. Subsequently, the mixture was cooled to 80°C and EtOH was directly added to the hot mixture to crystallize the pure product from the crude mixture. The resulting white/off-white crystals were filtered, washed with cold ethanol and dried under high vacuum ($< 10^{-2}$ mbar).

Detailed information on synthesis, purification, and analytical data of all diacetoacetates and diacetoacetamides is available below.

6.3.1.1 Ethane-1,2-diacetoacetate (124a)



used diol	ethylene glycol
yield	99% (29.4 g, 128 mmol, slightly yellow oil)
eluent	<i>c</i> -C ₆ H ₁₂ :EtOAc = 7:3 → 55:45
<i>R</i> _f (product)	0.30 in <i>c</i> -C ₆ H ₁₂ :EtOAc = 1:1
Recovered <i>t</i> -butyl acetoacetate & <i>t</i> -BuOH	94% & 87%

¹H NMR (400 MHz, DMSO-*d*₆): δ (ppm) = 4.26 (s, 4H, H_{1,2}), 3.62 (s, 4H, H_{6,12}), 2.17 (s, 6H, H_{10,16}).

¹³C NMR (101 MHz DMSO-*d*₆): δ (ppm) = 201.32 (C_{8,14}), 167.09 (C_{5,11}), 62.29 (C_{1,2}), 49.37 (C_{6,12}), 29.98 (C_{10,16}).

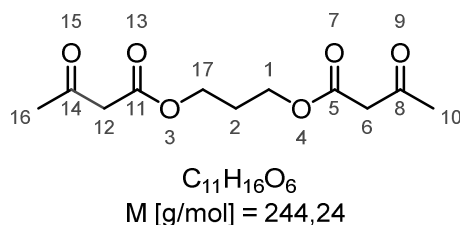
IR: ν (cm⁻¹) = 2965, 2932, 1740, 1710, 1653, 1411, 1361, 1314, 1252, 1143, 1043, 963, 856, 804, 739, 623, 542, 496, 412.

HRMS (EI): *m/z* for C₁₀H₁₄O₆⁺ [M]⁺: calculated: 230.0785; found: 230.0790.



Figure 6.1 ^1H and ^{13}C NMR spectra of **124a** in $\text{DMSO-}d_6$.

6.3.1.2 Propane-1,3-diacetoacetate (124b)



used diol	1,3-dihydroxypropane
yield	99% (31.2 g, 128 mmol, slightly yellow oil)
eluent	<i>c</i> -C ₆ H ₁₂ :EtOAc = 7:3 → 1:1
<i>R_f</i> (product)	0.35 in <i>c</i> -C ₆ H ₁₂ :EtOAc = 1:1
Recovered <i>t</i> -butyl acetoacetate & <i>t</i> -BuOH	95% & 90%

¹H-NMR (400 MHz, DMSO-*d*₆): δ (ppm) = 4.12 (t, ³*J*_{H1,17;H2} = 6.4 Hz, 4H, H_{1,17}), 3.61 (s, 4H, H_{6,12}), 2.17 (s, 6H, H_{10,16}), 1.90 (p, ³*J*_{H2;H1,17} = 6.4 Hz, 2H, H₂).

¹³C-NMR (101 MHz DMSO-*d*₆): δ (ppm) = 201.69 (C_{8,14}), 167.28 (C_{5,11}), 61.25 (C_{1,17}), 49.53 (C_{6,12}), 30.09 (C_{10,16}), 27.39 (C₂).

IR: ν (cm⁻¹) = 2970, 2934, 1737, 1710, 1650, 1411, 1360, 1313, 1262, 1146, 1043, 915, 805, 624, 541, 953.

HRMS (EI): *m/z* for C₁₁H₁₆O₆⁺ [M]⁺: calculated: 244.0941; found: 244.0949.

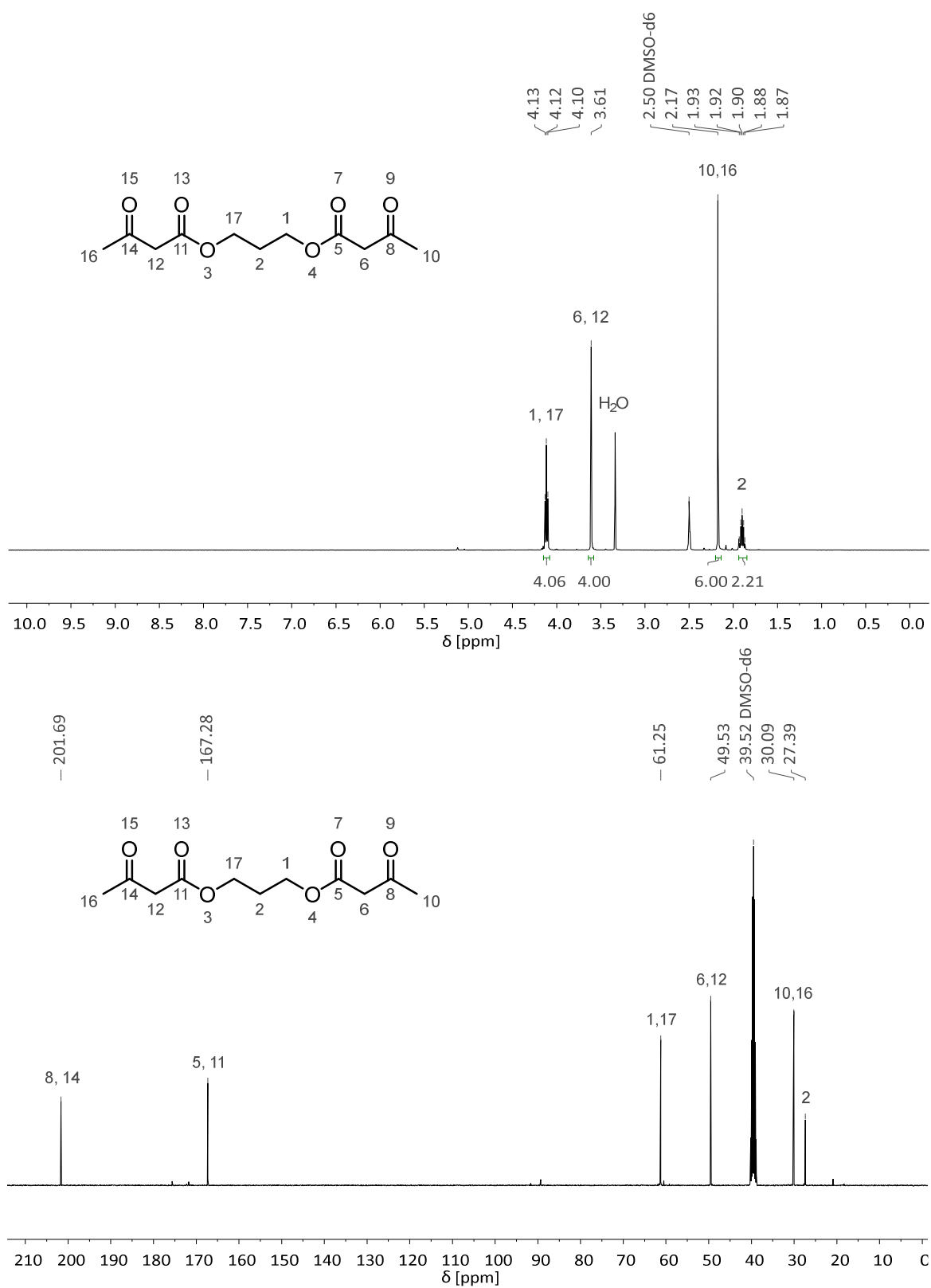
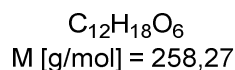
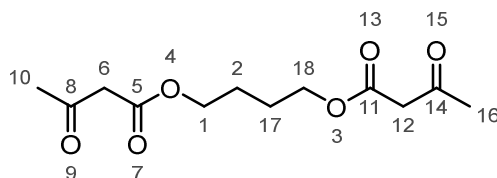


Figure 6.2 ^1H and ^{13}C NMR spectra of **124b** in $\text{DMSO-}d_6$.

6.3.1.3 Butane-1,4-diacetoacetate (124c)



used diol	1,4-dihydroxybutane
yield	99% (33.2 g, 128 mmol, slightly yellow oil)
eluent	<i>c</i> -C ₆ H ₁₂ :EtOAc = 7:3 → 1:1
<i>R_f</i> (product)	0.45 in <i>c</i> -C ₆ H ₁₂ :EtOAc = 1:1
Recovered <i>t</i> -butyl acetoacetate & <i>t</i> -BuOH	91% & 89%

¹H-NMR (400 MHz, DMSO-*d*₆): δ (ppm) = 4.12 – 4.03 (m, 4H, H_{1,18}), 3.60 (s, 4H, H_{6,12}), 2.17 (s, 6H, H_{10,16}), 1.67–1.57 (m, 4H, H_{2,17}).

¹³C-NMR (101 MHz DMSO-*d*₆): δ (ppm) = 201.58 (C_{8,14}), 167.25 (C_{5,11}), 63.95 (C_{1,18}), 49.54 (C_{6,12}), 30.05 (C_{10,16}), 24.60 (C_{2,17}).

IR: ν (cm⁻¹) = 2962, 1711, 1649, 1411, 1360, 1314, 1259, 1147, 1036, 954, 803, 740, 624, 541, 500.

HRMS (EI): m/z for C₁₂H₁₈O₆⁺ [M]⁺: calculated: 258.1098; found: 258.1102.

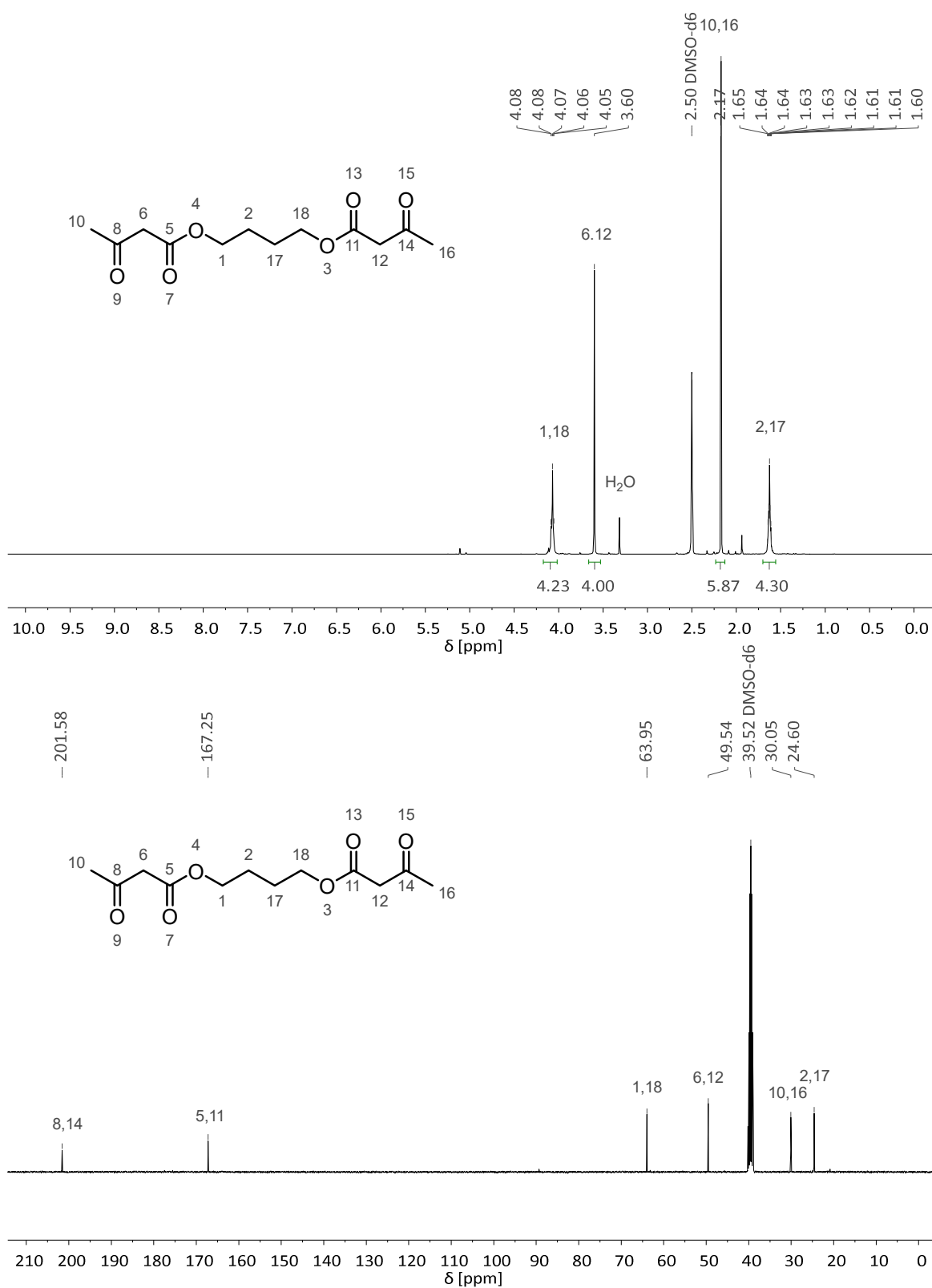
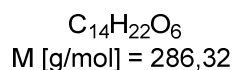
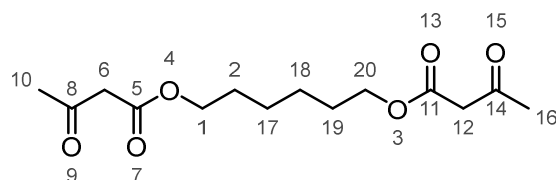


Figure 6.3 ^1H and ^{13}C NMR spectra of **124c** in $\text{DMSO-}d_6$.

6.3.1.4 Hexane-1,6-diacetoacetate (124d)



used diol	1,6-dihydroxyhexane
yield	98% (36.2 g, 126 mmol, slightly yellow oil)
eluent	<i>c</i> -C ₆ H ₁₂ :EtOAc = 90:10 → 1:1
<i>R_f</i> (product)	0.54 in <i>c</i> -C ₆ H ₁₂ :EtOAc = 1:1
Recovered <i>t</i> -butyl acetoacetate & <i>t</i> -BuOH	92% & 85%

¹H-NMR (400 MHz, DMSO-*d*₆): δ (ppm) = 4.04 (t, $^3J_{\text{H}_{1,20};\text{H}_{2,19}} = 6.6$ Hz, 4H, H_{1,20}), 3.59 (s, 4H, H_{6,12}), 2.17 (s, 6H, H_{10,16}), 1.63 – 1.50 (m, 4H, H_{2,19}), 1.37 – 1.26 (m, 4H, H_{17,18}).

¹³C-NMR (101 MHz DMSO-*d*₆): δ (ppm) = 201.61 (C_{8,14}), 167.30 (C_{5,11}), 64.33 (C_{1,20}), 49.58 (C_{6,12}), 30.07 (C_{10,16}), 27.89 (C_{2,19}), 24.87 (C_{17,18}).

IR: ν (cm⁻¹) = 2939, 2863, 1712, 1645, 1558, 1411, 1359, 1314, 1239, 1148, 1031, 978, 802, 731, 624, 542, 497.

HRMS (EI): m/z for C₁₄H₂₂O₆⁺ [M]⁺: calculated: 286.1411; found: 286.1418.

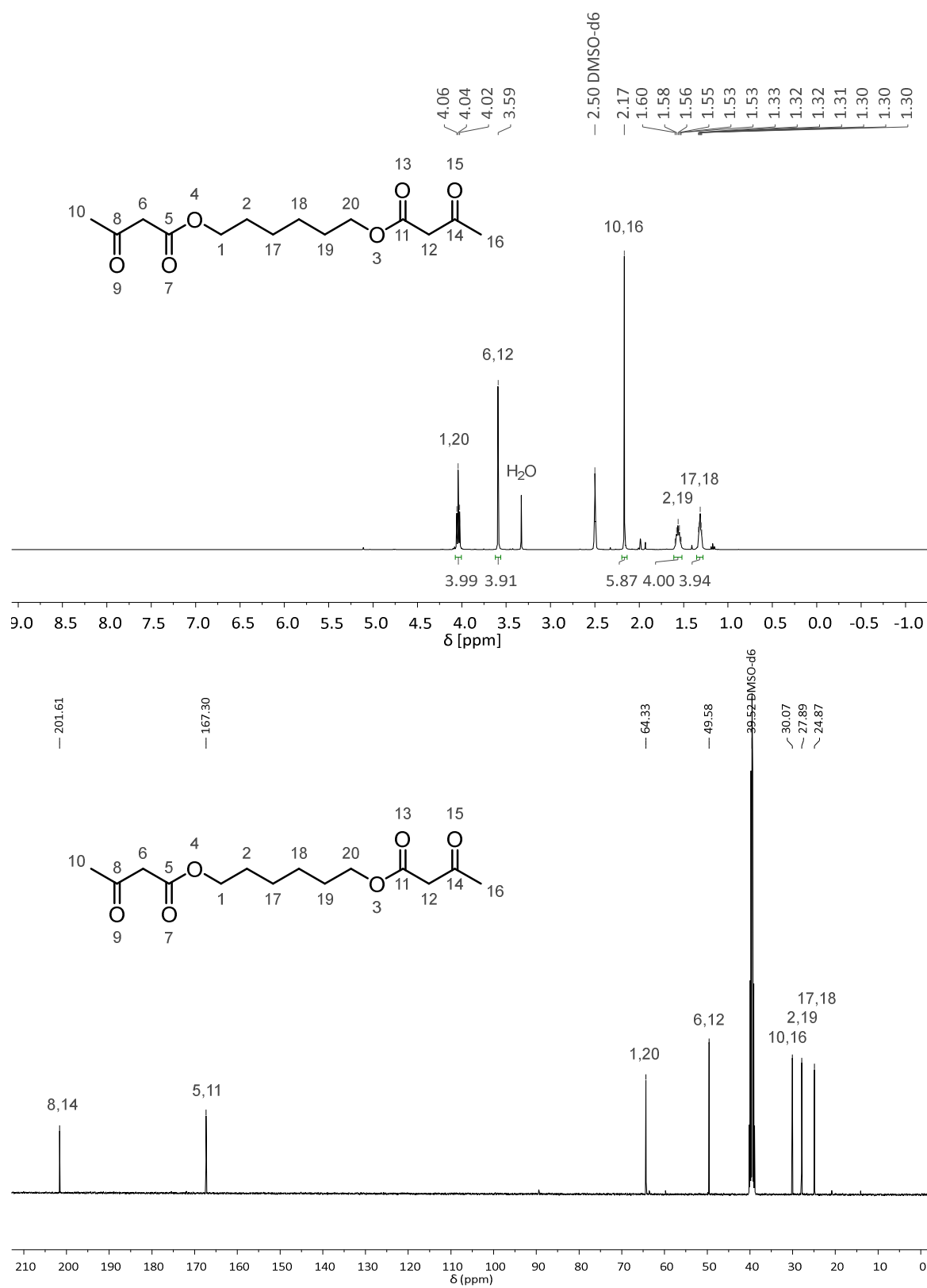
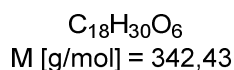
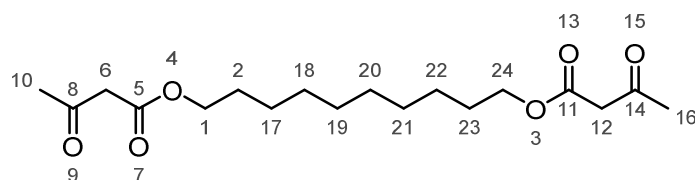


Figure 6.4 ^1H and ^{13}C NMR spectra of **124d** in $\text{DMSO-}d_6$.

6.3.1.5 Decane-1,10-diacetoacetate (124e)



used diol	1,10-dihydroxydecane
yield	98% (33.2 g, 63.2 mmol, slightly yellow solid)
eluent	<i>c</i> -C ₆ H ₁₂ :EtOAc = 98:2 → 7:3
<i>R</i> _f (product)	0.27 in <i>c</i> -C ₆ H ₁₂ :EtOAc = 7:3
Recovered <i>t</i> -butyl acetoacetate & <i>t</i> -BuOH	85% & 89%

¹H-NMR (400 MHz, DMSO-*d*₆): δ (ppm) = 4.04 (t, ³*J*_{H1,24;H2,23} = 6.6 Hz, 4H, H_{1,24}), 3.58 (s, 4H, H_{6,12}), 2.17 (s, 6H, H_{10,16}), 1.61 – 1.50 (m, 4H, H_{2,23}), 1.35 – 1.19 (m, 12H, H₁₇₋₂₂).

¹³C-NMR (101 MHz DMSO-*d*₆): δ (ppm) = 201.57 (C_{8,14}), 167.29 (C_{5,11}), 64.42 (C_{1,24}), 49.58 (C_{6,12}), 30.06 (C_{10,16}), 28.81+28.55+28.01+25.25 (C_{2,17-23}).

IR: ν (cm⁻¹) = 2936, 2865, 1733, 1705, 1479, 1466, 1411, 1362, 1322, 1267, 1175, 1151, 1069, 1046, 1027, 1005, 970, 862, 813, 734, 629, 540, 529, 416.

HRMS (ESI): *m/z* for C₁₈H₂₀O₆H⁺ [M+H]⁺: calculated: 343.2115; found: 343.2109.

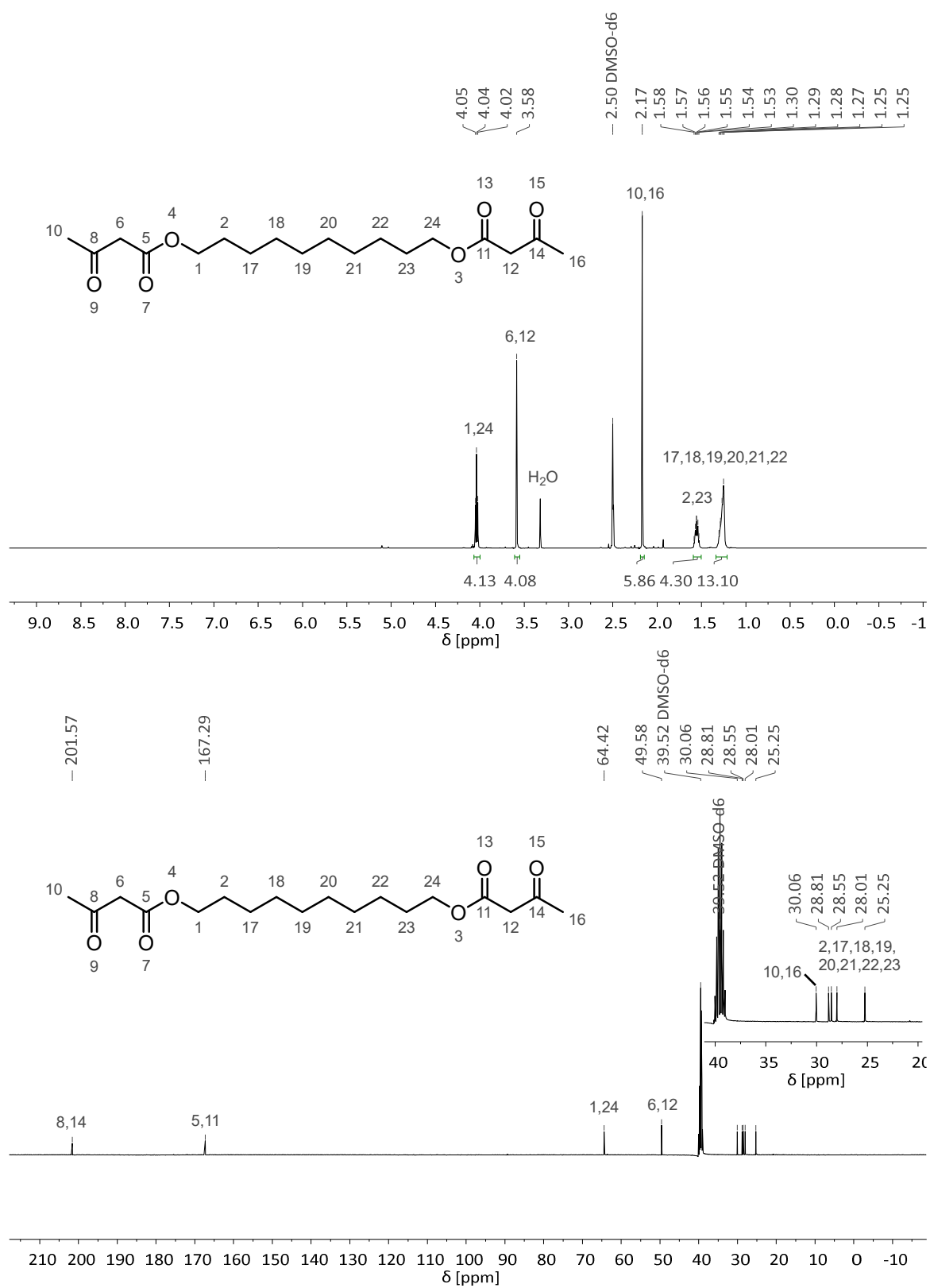
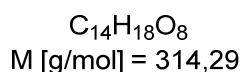
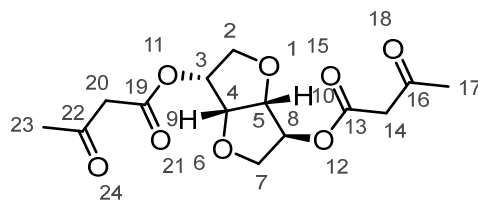


Figure 6.5 ^1H and ^{13}C NMR spectra of **124e** in $\text{DMSO-}d_6$.

6.3.1.6 Isosorbide-diacetoacetate (124f)



used diol	isosorbide
yield	99% (40.1 g, 128 mmol, slightly yellow oil)
eluent	<i>c</i> -C ₆ H ₁₂ :EtOAc = 20:80
<i>R_f</i> (product)	0.5 in <i>c</i> -C ₆ H ₁₂ :EtOAc = 20:80
Recovered <i>t</i> -BuAA & <i>t</i> -BuOH	91% & 82%

¹H-NMR (400 MHz, DMSO-*d*₆): δ (ppm) = 5.19 – 5.12 (m, 1H, H₃), 5.09 (d, ³*J*_{H8;H7} = 3.0 Hz, 1H, H₈), 4.76 (dd, ³*J*_{H9;H3;H10} = 5.3 Hz, 1H, H₉), 4.42 (d, ³*J*_{H10;H9} = 5.0 Hz, 1H, H₁₀), 3.90 – 3.78 (m, 2H, H₇), 3.89 – 3.72 (m, 2H, H₂), 3.69 – 3.58 (m, 2H, H₁₄ or 20), 3.69 – 3.58 (m, 2H, H₁₄ or 20), 2.19 (s, 3H, H₁₄ or 23), 2.18 (s, 3H, H₁₄ or 23).

¹³C-NMR (101 MHz DMSO-*d*₆): δ (ppm) = 201.49 (C₁₆ or 22), 201.08 (C₁₆ or 22), 166.66 (C₁₃ or 19), 166.52 (C₁₃ or 19), 85.32 (C₅), 80.36 (C₄), 77.90 (C₈), 74.29 (C₃), 72.32 (C₇), 70.15 (C₂), 49.42 (C₁₄ or 20), 49.33 (C₁₄ or 20), 30.03 (C₁₇ or 23), 29.90 (C₁₇ or 23).

IR: ν (cm⁻¹) = 2980, 2933, 2879, 1741, 1711, 1631, 1411, 1359, 1313, 1257, 1146, 1091, 1028, 976, 916, 889, 856, 770, 609, 539, 493.

HRMS (EI): *m/z* for C₁₄H₂₂O₆⁺ [M]⁺: calculated: 314.0996; found: 314.1002.

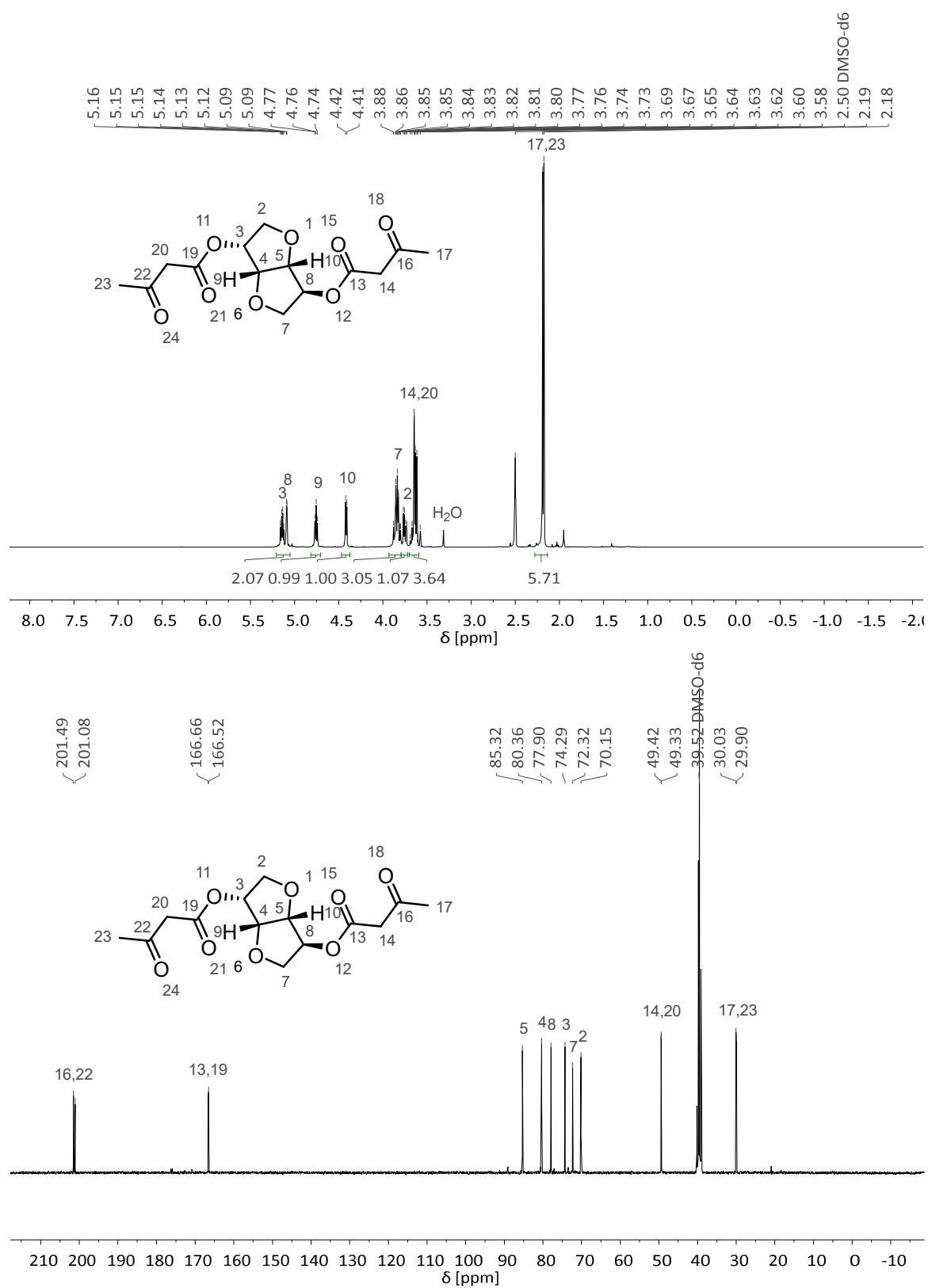
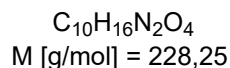
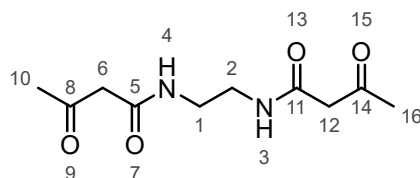


Figure 6.6 ^1H and ^{13}C NMR spectra of **124f** in $\text{DMSO-}d_6$.

6.3.1.7 Ethane-1,2-diacetoacetamide (126a)

used diamine	1,2-diaminoethane
yield	43% (4.96 g, 21.7 mmol, white crystalline solid)

$^1\text{H-NMR}$ (400 MHz, $\text{DMSO-}d_6$): δ (ppm) = 8.08 (s, 2H, $\text{H}_{3,4}$), 3.28 (s, 4H, $\text{H}_{6,12}$), 3.20 – 3.07 (m, 4H, $\text{H}_{1,2}$), 2.14 (s, 6H, $\text{H}_{10,16}$).

$^{13}\text{C-NMR}$ (101 MHz $\text{DMSO-}d_6$): δ (ppm) = 203.04 ($\text{C}_{8,14}$), 166.26 ($\text{C}_{5,11}$), 51.30 ($\text{C}_{6,12}$), 38.30 ($\text{C}_{1,2}$), 29.98 ($\text{C}_{10,16}$).

IR: ν (cm^{-1}) = 3277, 3093, 2947, 1729, 1709, 1641, 1557, 1447, 1418, 1362, 1346, 1309, 1293, 1245, 1189, 1165, 1021, 993, 943, 857, 780, 744, 711, 620, 543, 476, 418.

HRMS (EI): m/z for $\text{C}_{10}\text{H}_{16}\text{N}_2\text{O}_4^{*+} [\text{M}]^+$: calculated: 228.1105; found: 228.1111.

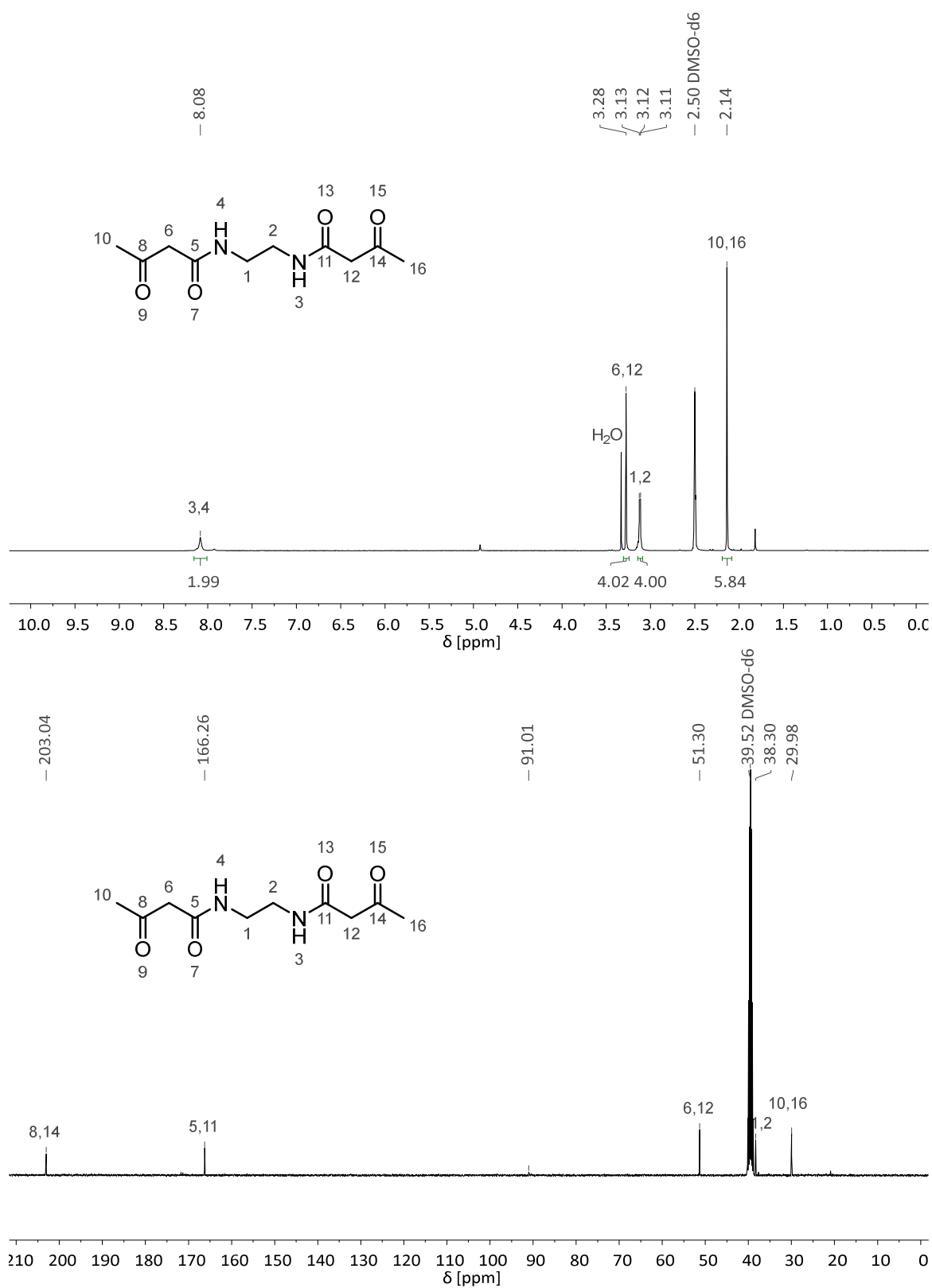
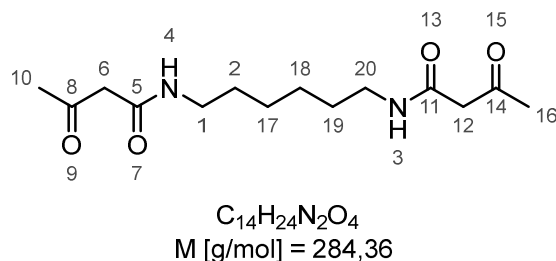


Figure 6.7 ^1H and ^{13}C NMR spectra of **126a** in $\text{DMSO-}d_6$.

6.3.1.8 Hexane-1,6-diacetoacetamide (126d)



used diamine	1,6-diaminohexane
yield	62% (8.87 g, 31.2 mmol, off-white crystalline solid)

1H -NMR (400 MHz, DMSO-*d*₆): δ (ppm) = 8.00 (t, $^3J_{H_{3,4};H_{1,20}} = 5.1$ Hz, 2H, H_{3,4}), 3.27 (s, 4H, H_{6,12}), 3.04 (td, $^3J_{H_{1,20};H_{2,19}} = 6.9$ Hz, $^3J_{H_{1,20};H_{3,4}} = 6.8$ Hz, 4H, H_{1,20}), 2.13 (s, 6H, H_{10,16}), 1.45 – 1.32 (m, 4H, H_{2,19}), 1.31 – 1.21 (m, 4H, H_{17,18}).

^{13}C -NMR (101 MHz DMSO-*d*₆): δ (ppm) = 203.14 (C_{8,14}), 165.80 (C_{5,11}), 51.36 (C_{6,12}), 38.53 (C_{1,20}), 29.96 (C_{10,16}), 28.94+26.03 (C_{2,17-19}).

IR: ν (cm⁻¹) = 3272, 3100, 2917, 2851, 1709, 1644, 1564, 1466, 1420, 1362, 1345, 1324, 1297, 1283, 1189, 1167, 1090, 1002, 920, 790, 752, 722, 621, 558, 504.

HRMS (EI): m/z for C₁₄H₂₄N₂O₄⁺ [M]⁺: calculated: 284.1731; found: 284.1734.

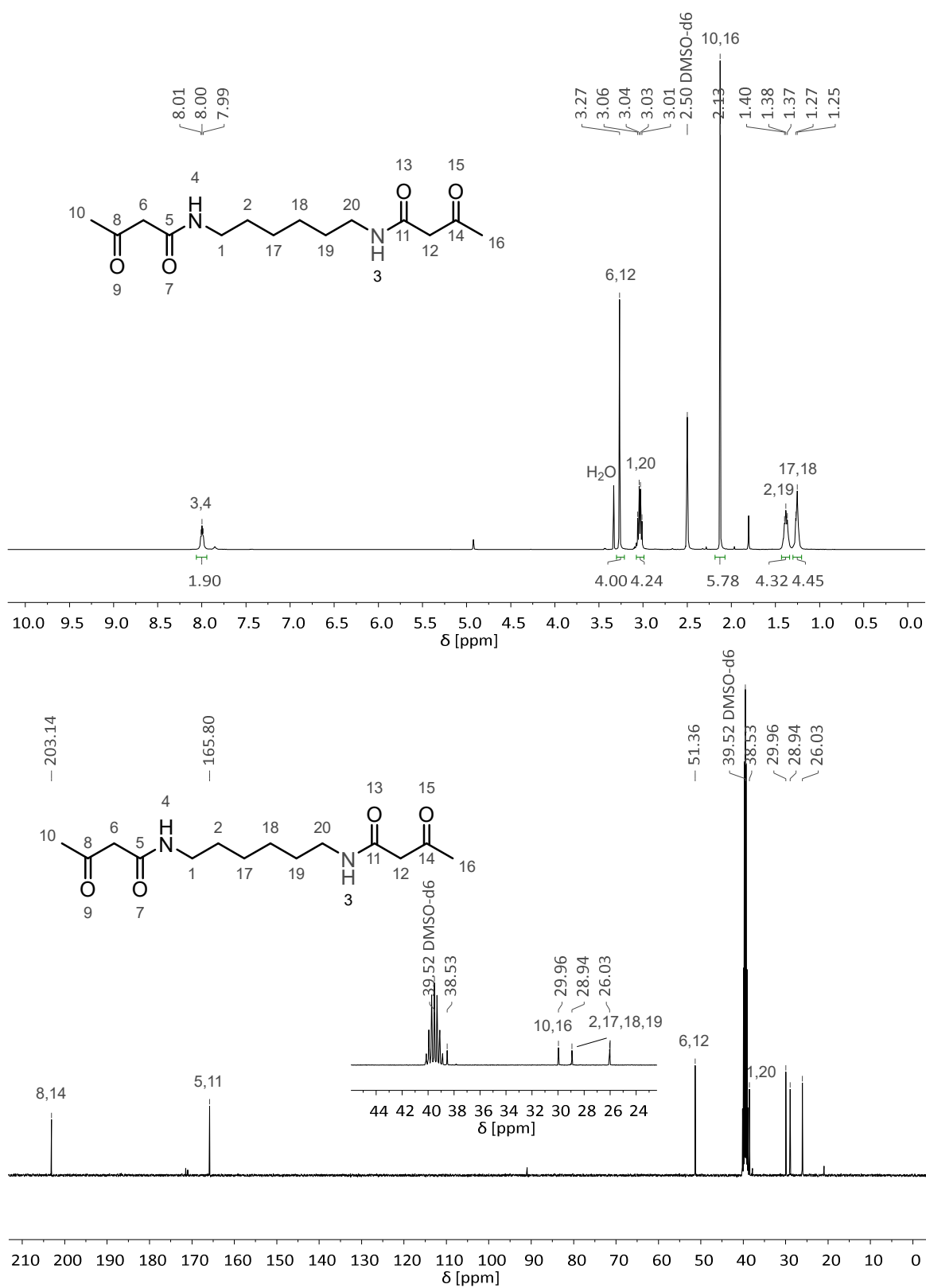
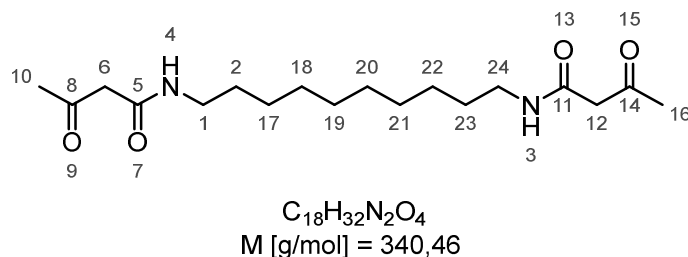


Figure 6.8 ^1H and ^{13}C NMR spectra of **126d** in $\text{DMSO-}d_6$.

6.3.1.9 Decane-1,10-diacetoacetamide (126e)



used diamine	1,10-diaminodecane
yield	47% (7,93 g, 23,3 mmol, off-white crystalline solid)

1H -NMR (400 MHz, DMSO- d_6): δ (ppm) = 8.00 (t, $^3J_{H_{3,4};H_{1,24}} = 5.7$ Hz, 2H, H_{3,4}), 3.27 (s, 4H, H_{6,12}), 3.04 (td, $^3J_{H_{1,24};H_{2,23}} = 6.7$ Hz, $^3J_{H_{1,24};H_{3,4}} = 6.7$ Hz, 4H, H_{1,24}), 2.13 (s, 6H, H_{10,16}), 1.47 – 1.32 (m, 4H, H_{2,23}), 1.25 (s, 12H, H₁₇₋₂₂).

^{13}C -NMR (101 MHz DMSO- d_6): δ (ppm) = 203.12 (C_{8,14}), 165.78 (C_{5,11}), 51.36 (C_{6,12}), 29.95 (C_{1,24}), 28.97 (C_{10,16}), 28.95+28.71+26.35 (C_{2,17-23}).

IR: ν (cm⁻¹) = 3273, 3099, 2915, 2849, 1708, 1643, 1565, 1467, 1420, 1361, 1344, 1292, 1237, 1190, 1167, 1062, 1028, 994, 949, 790, 757, 721, 618, 564, 521, 476, 438, 416.

HRMS (EI): m/z for C₁₈H₃₂N₂O₄⁺ [M]⁺: calculated: 340.2357; found: 340.2362.

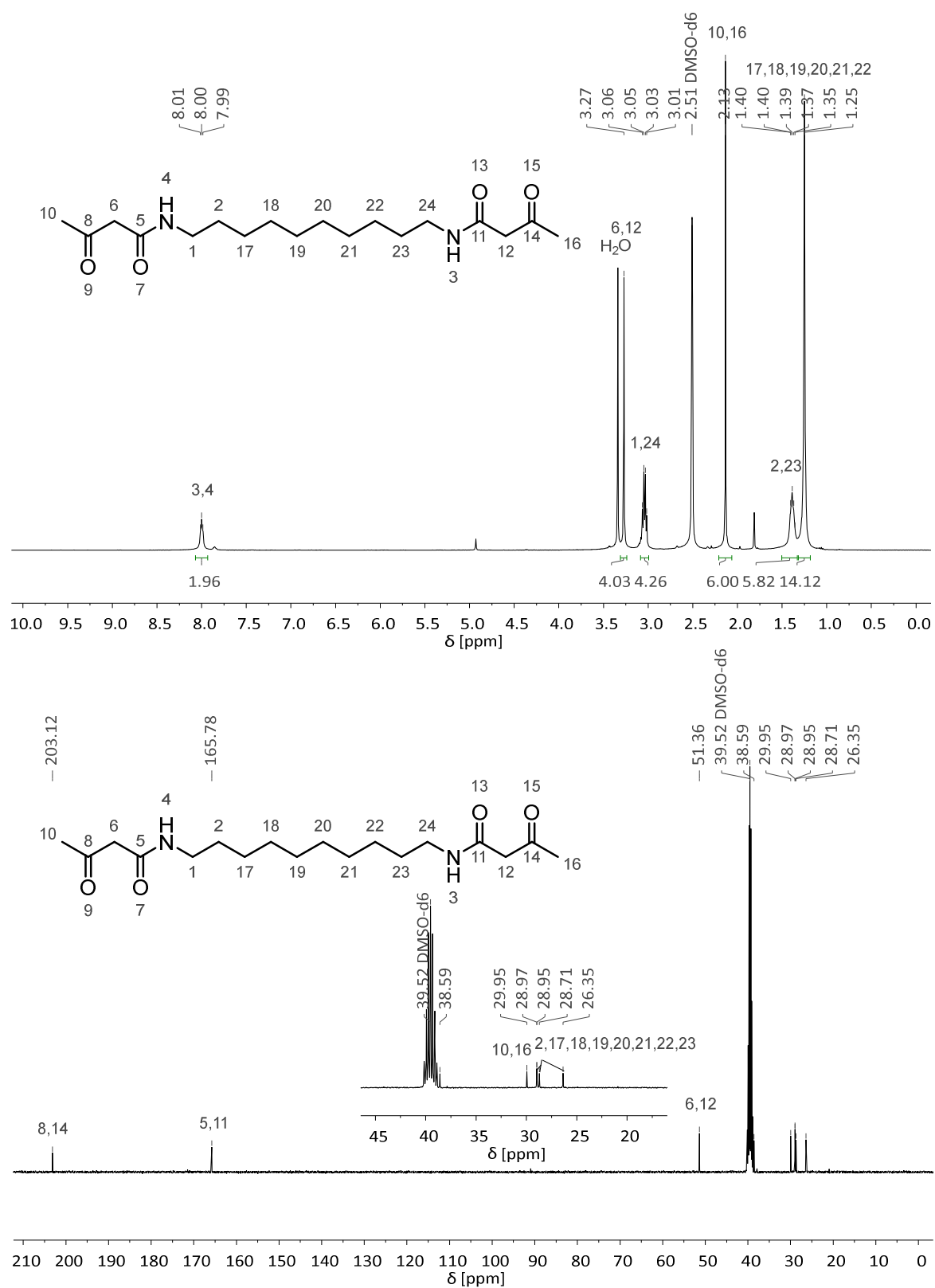


Figure 6.9 ^1H and ^{13}C NMR spectra of 126e in $\text{DMSO-}d_6$.

6.3.2 Poly[3,4 dihydropyrimidin 2(1*H*)-one]s

All polyDHPMs were synthesised according to the same general procedure. Nevertheless, the reaction times and the solvent/solvent mixture that were used for precipitation and washing (depending on the polymer structure (details are shown for the respective polymer)) differed.

The urea compound (3.50 eq) and the respective diacetoacetate (or diacetoacetamide) (6.99 mmol, 1.00 eq) were mixed with DMSO (1 M solution regarding 1.00 eq of diacetoacetate) in a round bottom flask. Afterwards, terephthalic aldehyde (1.00 eq) and *p*-toluenesulfonic acid (0.10 eq) were added.

The mixture was immediately heated to 125°C in a preheated oil bath and stirred for 22.5 h (30 min for **133a**, **133d**, and **133e**, each and 1.5 h for **132e**). The flask was left open to allow water to evaporate. Afterwards, the polymer solution was precipitated into 100 ml of the respective solvent/solvent mixture and stirred for 3 h. Subsequently, the precipitated polymer was filtered and washed with the same solvent/solvent mixture. The resulting material was dried in a vacuum drying oven over night at 85°C under reduced pressure resulting in the final polymers as yellow to orange glassy solid.

6.3.2.1 Polymerisation Kinetics

Samples for the kinetic investigation *via* SEC were prepared by precipitating 5 µL of the reaction mixture in water. After decanting and drying in a vacuum oven, the samples were dissolved in 2 ml hexafluoroisopropanol with 0.1 wt% KCO₂(CF₃).

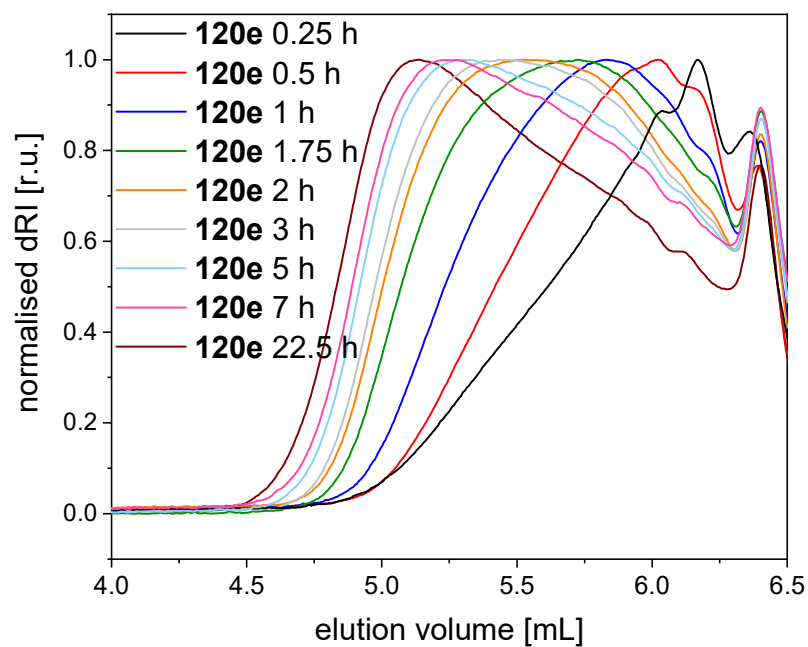
Kinetics of **120e**

Figure 6.10 Size exclusion chromatograms of the samples obtained from the polymerisation kinetics of **120e**.

Table 6.1 SEC data of the polymerisation kinetics of **120e**.

entry	t [h]	M_n [$\text{g}\cdot\text{mol}^{-1}$]	M_w [$\text{g}\cdot\text{mol}^{-1}$]	\bar{D}
1	0.25	1 300	3 700	2.8
2	0.5	2 500	5 000	1.98
3	1	2 900	6 200	2.16
4	1.75	3 400	8 200	2.42
5	2	3 700	9 500	2.56
6	3	3 800	10 000	2.61
7	5	4 200	11 700	2.82
8	7	4 200	12 800	3.09
9	22.5	4 900	15 900	3.24

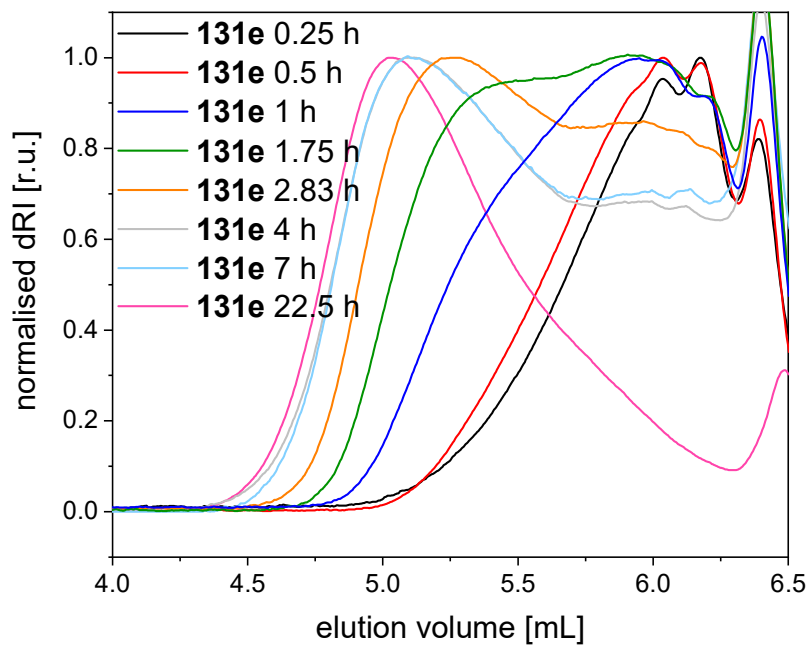
Kinetics of 131e

Figure 6.11 Size exclusion chromatograms of the samples obtained from the polymerization kinetics of **131e**.

Table 6.2 SEC data of the polymerisation kinetics of **131e**.

entry	t [h]	M_n [g·mol ⁻¹]	M_w [g·mol ⁻¹]	\bar{D}
1	0.25	2 100	3 500	1.67
2	0.5	2 300	3 900	1.70
3	1	2 800	6 200	2.17
4	1.75	3 200	8 500	2.62
5	2.83	3 800	11 700	3.06
6	4	4 400	16 800	3.80
7	7	4 600	16 200	3.54
8	22.5	8 700	24 900	2.88

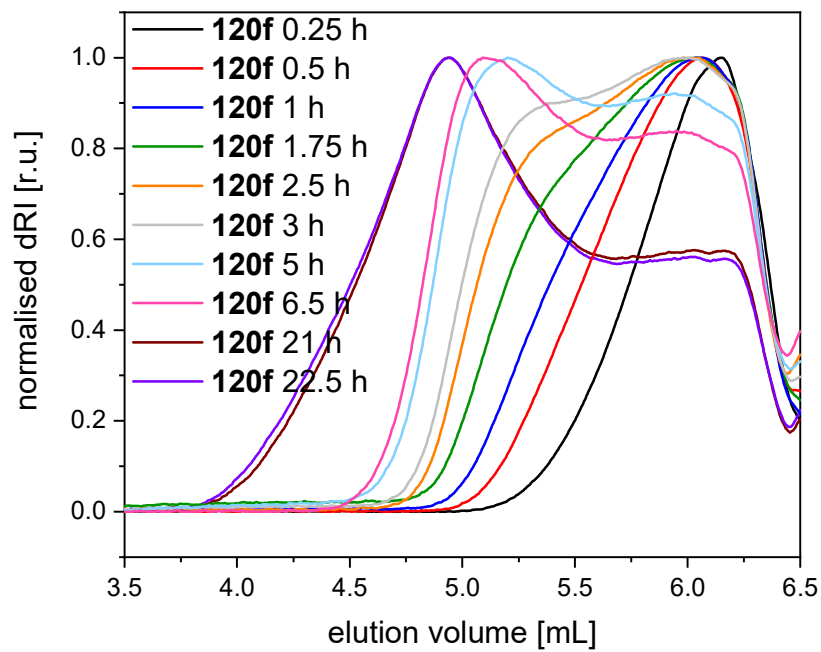
Kinetics of 120f

Figure 6.12 Size exclusion chromatograms of the samples obtained from the polymerisation kinetics of **120f**.

Table 6.3 SEC data of the polymerization kinetics of **120f**.

entry	t [h]	M_n [g·mol ⁻¹]	M_w [g·mol ⁻¹]	\bar{D}
1	0.25	1 300	2 500	1.91
2	0.5	1 600	3 700	2.23
3	1	1 800	4 600	2.55
4	1.75	2 300	6 200	2.67
5	2.5	2 600	7 600	2.96
6	3	2 700	8 700	3.19
7	5	3 100	12 200	3.97
8	6.5	3 300	14 200	4.30
9	21	4 600	43 800	9.49
10	22.5	4 800	48 400	10.1

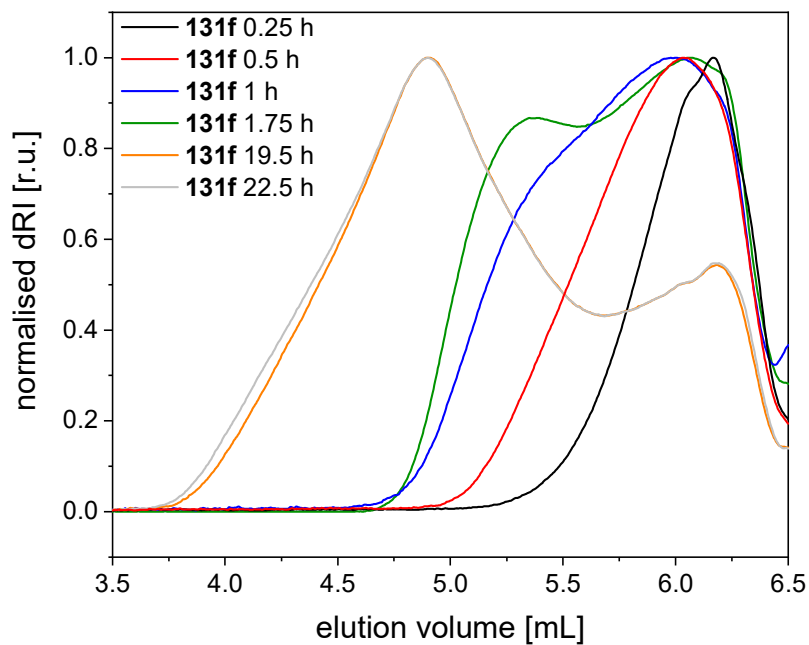
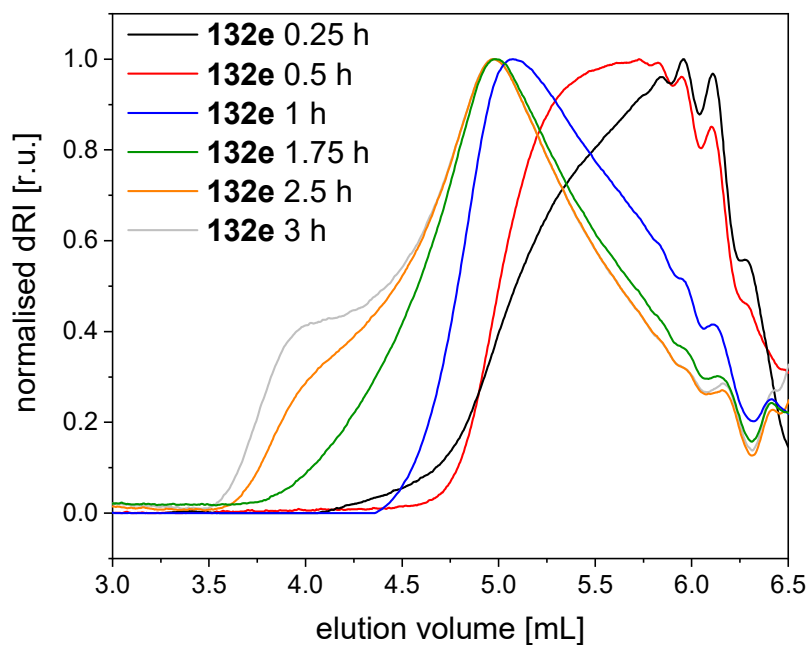
Kinetics of 131f

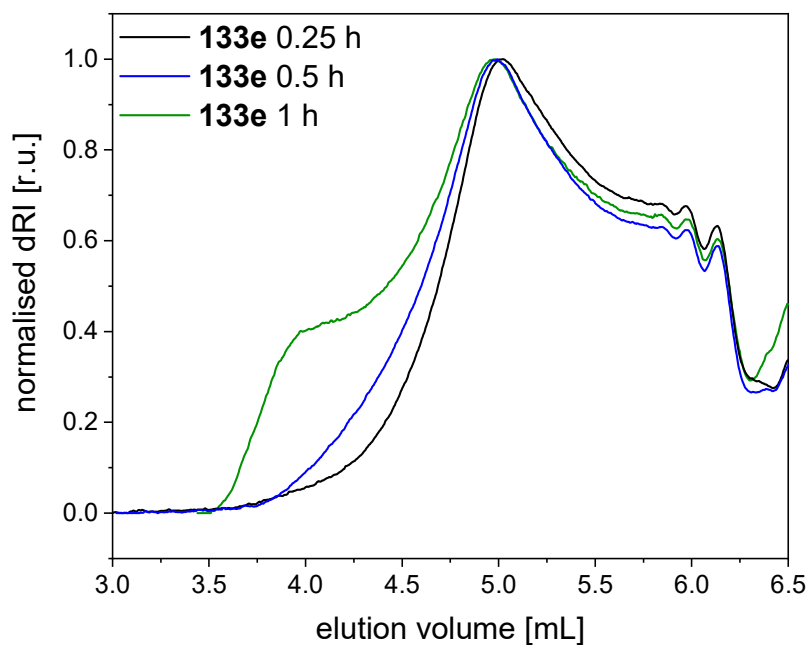
Figure 6.13 Size exclusion chromatograms of the samples obtained from the polymerisation kinetics of **131f**.

Table 6.4 SEC data of the polymerization kinetics of **131f**.

entry	t [h]	M_n [g·mol ⁻¹]	M_w [g·mol ⁻¹]	\bar{D}
1	0.25	1 200	2 200	1.80
2	0.5	1 800	3 800	2.11
3	1	2 400	6 900	2.87
4	1.75	2 600	8 200	3.20
5	2.5	2 700	10 700	4.04
6	3	2 900	12 200	4.18
7	5	3 600	19 100	5.31
8	19.5	5 100	60 100	11.8
9	22.5	5 100	66 200	13.1

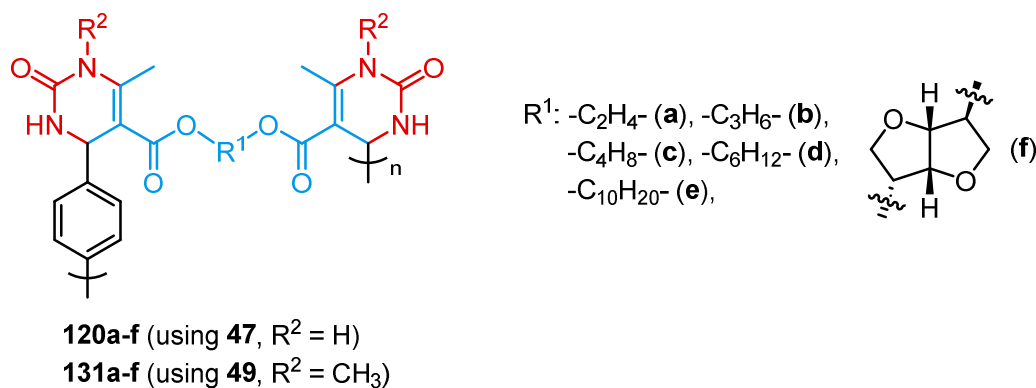
Kinetics of 132e**Figure 6.14** Size exclusion chromatograms of the samples obtained from the polymerisation kinetics of **132e**.**Table 6.5** SEC data of the polymerization kinetics of **132e**.

entry	t [h]	M_n [g·mol ⁻¹]	M_w [g·mol ⁻¹]	\mathcal{D}
1	0.25	1 900	9 400	4.95
2	0.5	2 200	8 900	4.00
3	1	3 000	18 500	6.11
4	1.75	7 600	52 800	6.92
5	2.5	9 200	94 700	10.3
6	3	9 800	12 8900	13.2

Kinetics of 133e**Figure 6.15** Size exclusion chromatograms of the samples obtained from the polymerisation kinetics of **133e**.**Table 6.6** SEC data of the polymerization kinetics of **133e**.

entry	t [h]	M_n [g·mol ⁻¹]	M_w [g·mol ⁻¹]	\bar{D}
1	0.25	5 000	29 300	5.81
2	0.5	5 700	43 400	7.69
3	1	6 900	108 600	15.7

6.3.2.2 Poly[3,4 dihydropyrimidin 2(1H)-one]s using Acetoacetates

Table 6.7 SEC and DSC data and yields of polyDHPMs **120a-f** and **131a-f** using diacetoacetates.

polymer	R ¹	$M_{n,NMR}$ [g·mol ⁻¹]	$M_{n,SEC}$ [g·mol ⁻¹]	$M_{w,SEC}$ [g·mol ⁻¹]	\bar{D}	T_g [°C]	Yield ^a [%]
120a	C ₂ H ₄	5 500	3 800	14 800	3.88	280	77
120b	C ₃ H ₆	5 700	4 900	18 000	3.65	255	65
120c	C ₄ H ₈	6 100	5 600	16 600	2.85	239	63
120d	C ₆ H ₁₂	10 100	8 300	34 700	4.20	220	69
120e	C ₁₀ H ₂₀	12 200	6 600	18 200	2.76	198	72
120f	isosorbide	30 700	6 200	50 000	8.07	308	78
131a	C ₂ H ₄	11 300	10 800	43 000	3.99	248	71
131b	C ₃ H ₆	24 000	10 500	33 800	3.21	222	63
131c	C ₄ H ₈	21 400	7 600	19 700	2.58	211	70
131d	C ₆ H ₁₂	31 800	9 500	42 800	4.94	175	69
131e	C ₁₀ H ₂₀	36 700	8 700	24 900	2.88	159	65
131f	isosorbide	23 000	8 400	73 100	8.71	266	75

^aisolated yields.

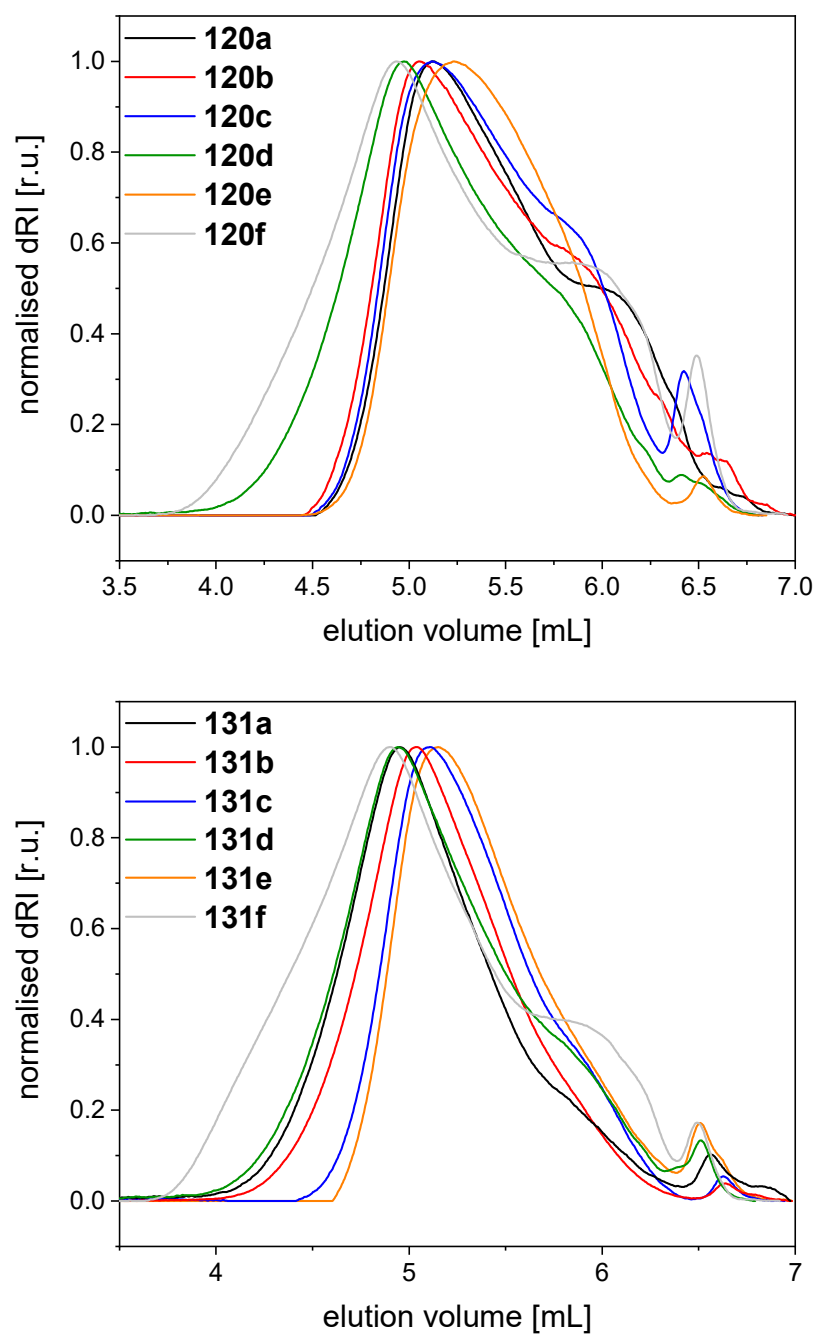


Figure 6.16 SEC chromatograms of polyDHMPs using acetoacetates and urea (**120a-f**, top) or Me-urea (**131a-f**, bottom).

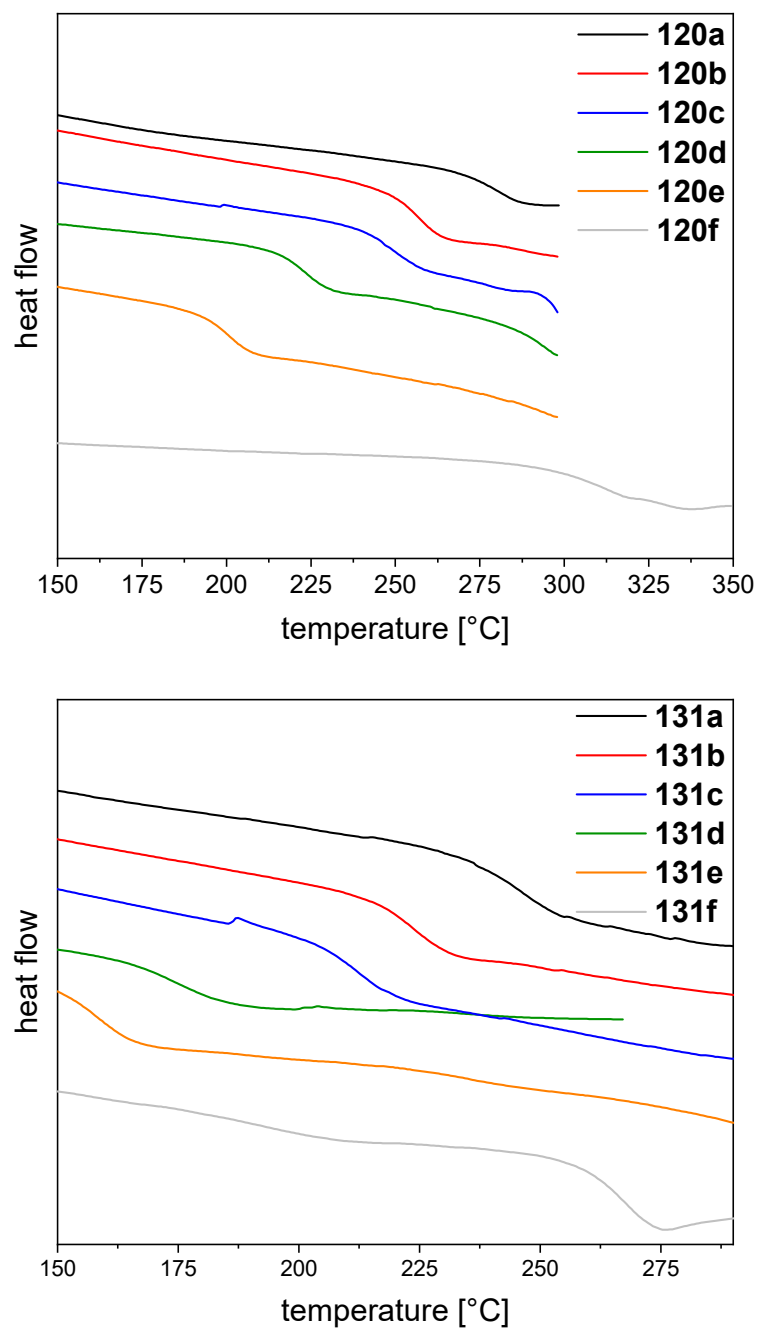


Figure 6.17 DSC curves of polyDHMPs using acetoacetates and urea (**120a-f**, top) or Me-urea (**131a-f**, bottom) showing the respective T_g s.

120a

Precipitated in and washed with MeOH/H₂O (90/10).

¹H-NMR (400 MHz, DMSO-*d*₆): δ (ppm) = 9.21 (br s, H_a), 7.71 (br s, H_{a'}), 7.33 – 6.84 (m, H_d), 5.31 – 4.96 (m, H_c), 4.28 – 3.94 (m, H_e), 2.36 – 2.06 (m, H_b).

IR: ν (cm⁻¹) = 3276, 1688, 1641, 1434, 1381, 1311, 1279, 1224, 1078, 758, 661, 503.

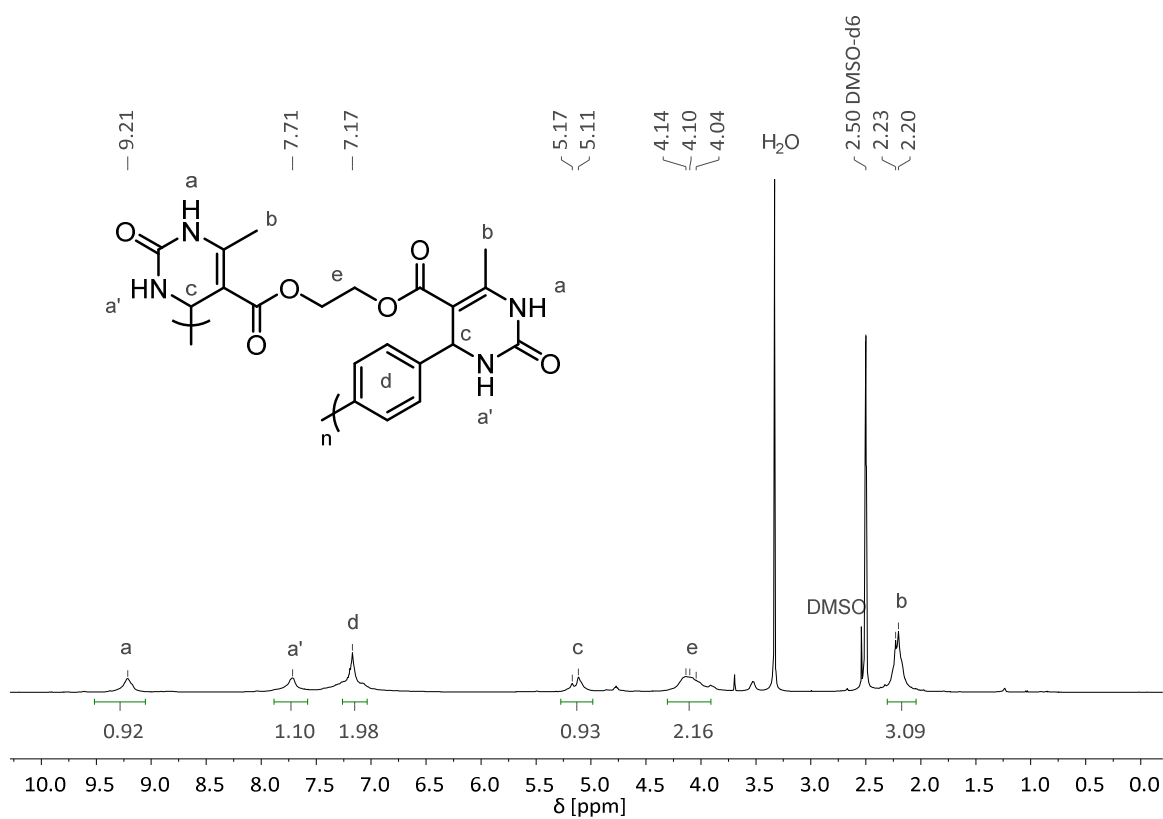


Figure 6.18 ¹H NMR spectrum of **120a** in DMSO-*d*₆.

120b

Precipitated in and washed with MeOH/H₂O (90/10).

¹H-NMR (400 MHz, DMSO-*d*₆): δ (ppm) = 9.19 (br s, H_a), 7.67 (br s, H_{a'}), 7.25 – 7.00 (m, H_d), 5.10 (br s, H_c), 4.07 – 3.75 (m, H_e), 2.22 (br s, H_b), 1.90 – 1.54 (m, H_f).

IR: ν (cm⁻¹) = 3258, 2957, 1689, 1640, 1447, 1383, 1311, 1223, 1080, 949, 758. 663, 507, 459.

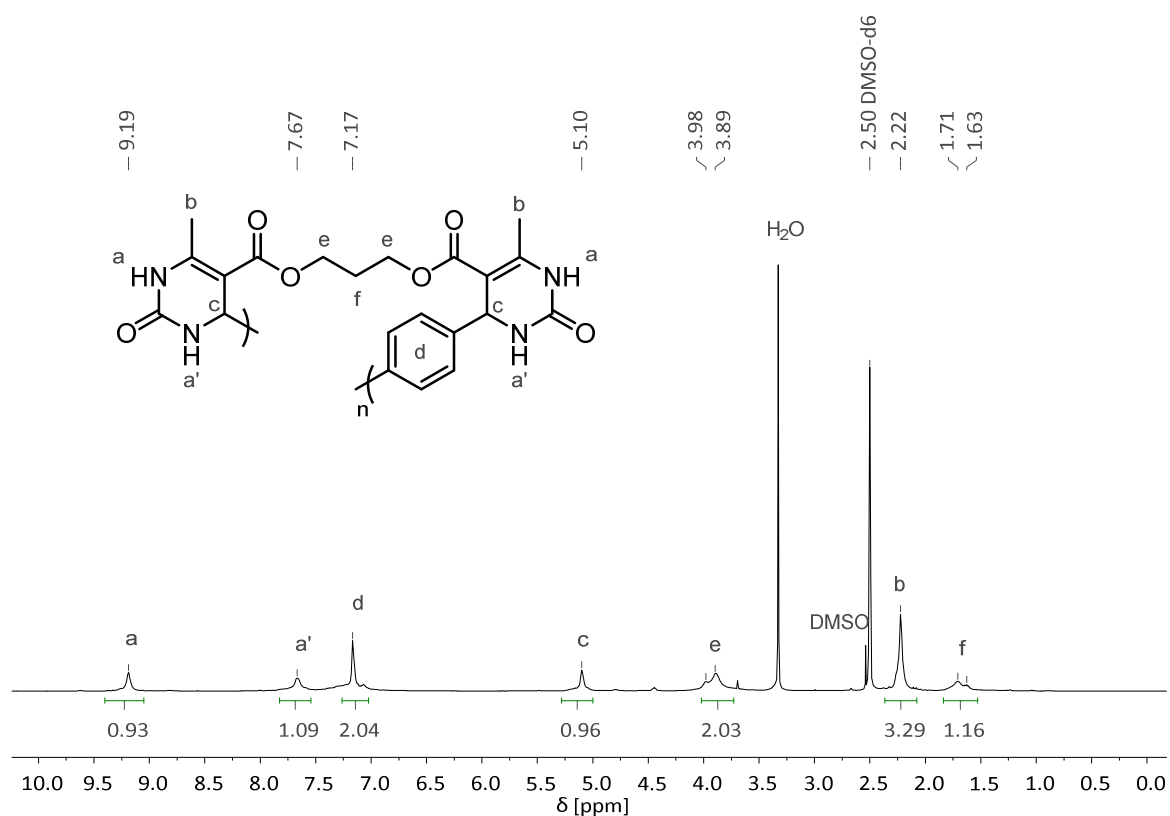


Figure 6.19 ¹H NMR spectrum of **120b** in DMSO-*d*₆.

120c

Precipitated in MeOH/H₂O (50/50) and washed with MeOH/H₂O (50/50) and MeOH/H₂O (90/10) subsequently.

¹H-NMR (400 MHz, DMSO-*d*₆): δ (ppm) = 9.17 (br s, H_a), 7.67 (br s, H_{a'}), 7.29 – 7.08 (m, H_d), 5.09 (br s, H_c), 4.09 – 3.73 (m, H_e), 2.23 (br s, H_b), 1.69 – 1.27 (m, H_f).

IR: ν (cm⁻¹) = 3258, 2953, 1688, 1639, 1445, 1383, 1312, 1223, 1082, 944, 757, 660, 509.

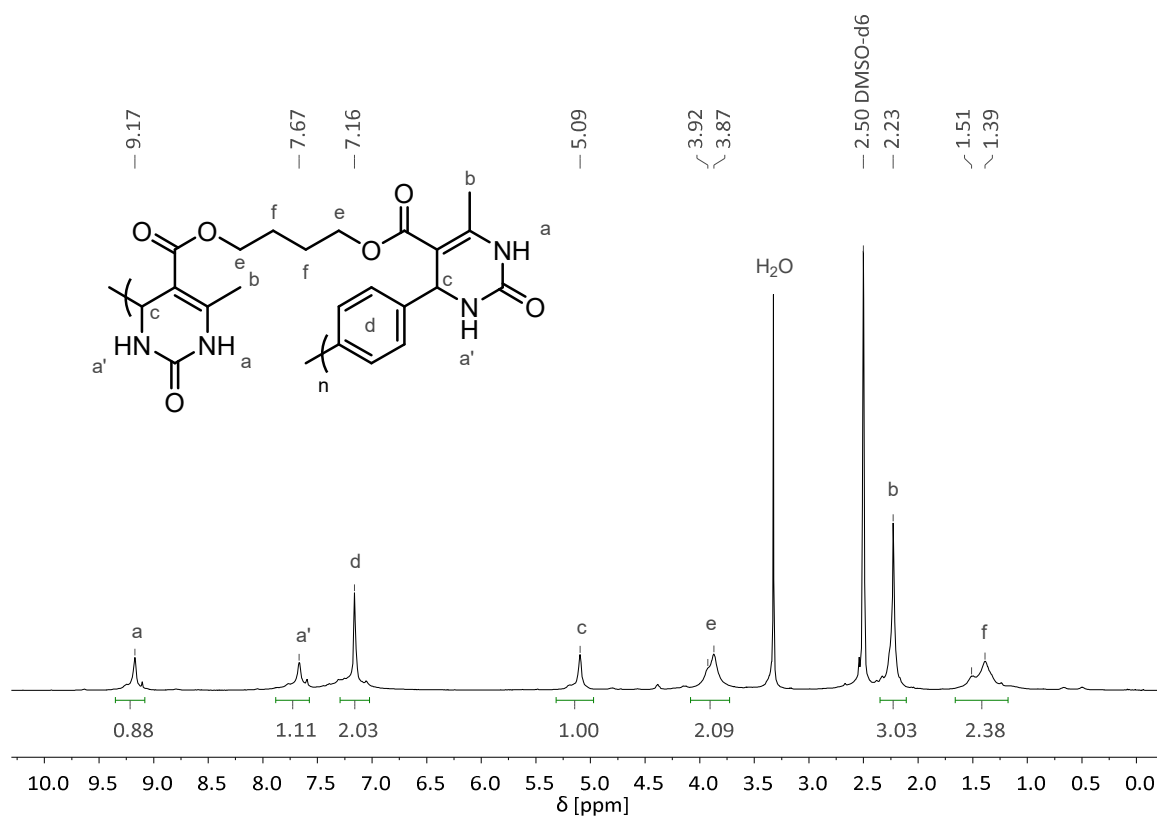


Figure 6.20 ¹H NMR spectrum of **120c** in DMSO-*d*₆.

120d

Precipitated in MeOH/H₂O (50/50) and washed with MeOH/H₂O (50/50) and MeOH/H₂O (90/10) subsequently.

¹H-NMR (400 MHz, DMSO-*d*₆): δ (ppm) = 9.17 (s, H_a), 7.66 (s, H_{a'}), 7.16 (s, H_d), 5.10 (s, H_c), 3.90 (br s, H_e), 2.23 (br s, H_b), 1.43 (br s, H_f), 1.30 – 0.99 (m, H_g).

IR: ν (cm⁻¹) = 3243, 2937, 1693, 1640, 1446, 1383, 1312, 1223, 1085, 1018, 758, 661, 508.

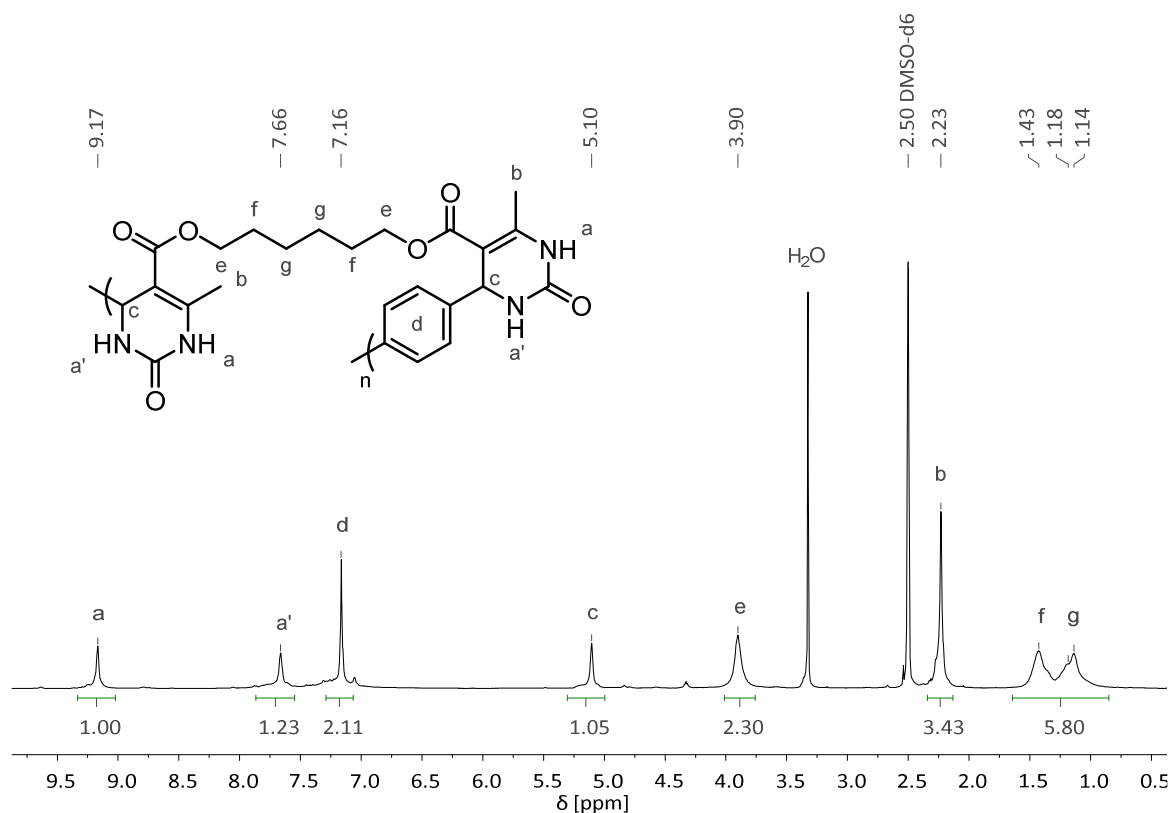


Figure 6.21 ¹H NMR spectrum of **120d** in DMSO-*d*₆.

120e

Precipitated in MeOH/H₂O (30/70) and washed with MeOH/H₂O (30/70) and MeOH/H₂O (90/10) subsequently.

¹H-NMR (400 MHz, DMSO-*d*₆): δ (ppm) = 9.17 (s, H_a), 7.66 (s, H_{a'}), 7.16 (s, H_d), 5.10 (s, H_c), 3.90 (br s, H_e), 2.23 (br s, H_b), 1.43 (br s, H_f), 1.30 – 1.02 (m, H_{g,h,i}).

IR: ν (cm⁻¹) = 3241, 2936, 1692, 1640, 1448, 1383, 1312, 1223, 1085, 1018, 758, 664, 505.

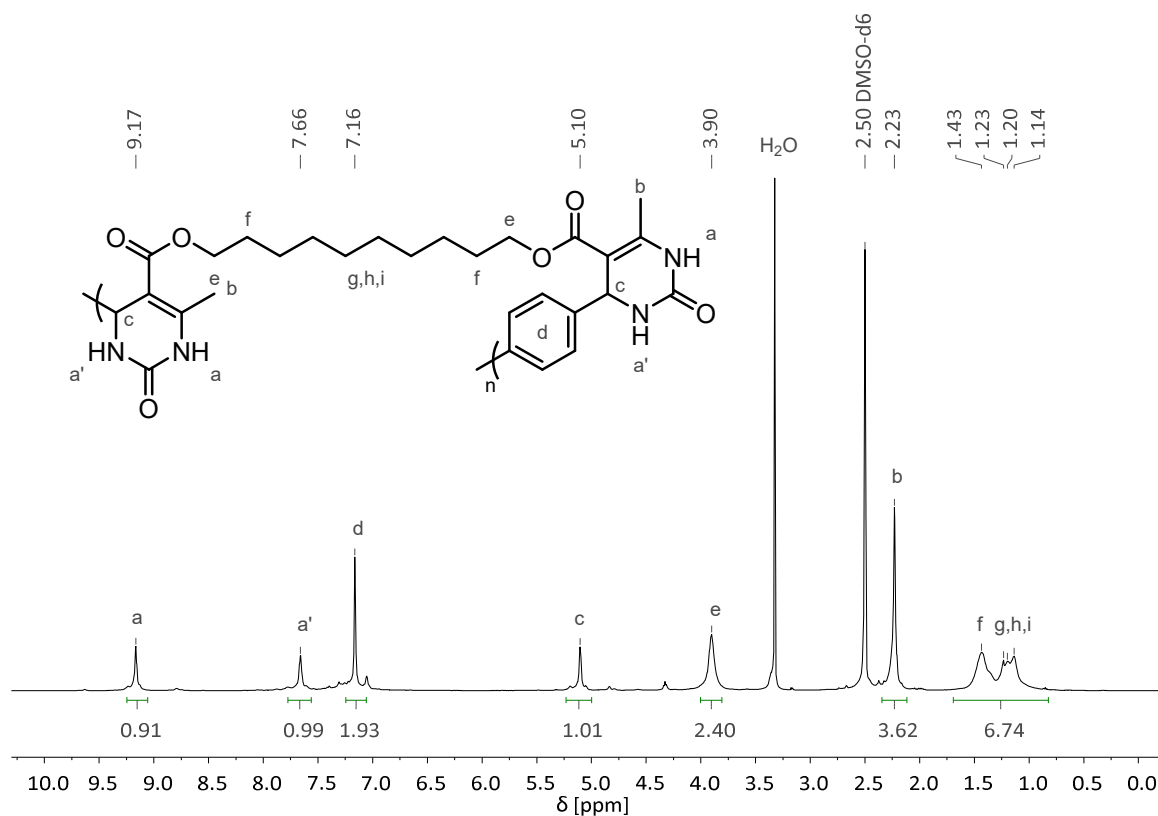


Figure 6.22 ¹H NMR spectrum of **120e**.

120f

Precipitated in MeOH and washed with MeOH.

¹H-NMR (400 MHz, DMSO-*d*₆): δ (ppm) = 9.27 (br s, H_a), 7.72 (br s, H_{a'}), 7.17 (s, H_d), 5.08 (br s, H_c), 5.06 – 3.50 (H_{isorbide}), 2.24 (br s, H_b).

IR: ν (cm⁻¹) = 3282, 3116, 2945, 2875, 1693, 1635, 1430, 1383, 1349, 1313, 1279, 1223, 1077, 1016, 805, 757, 658, 601, 506, 443, 411.

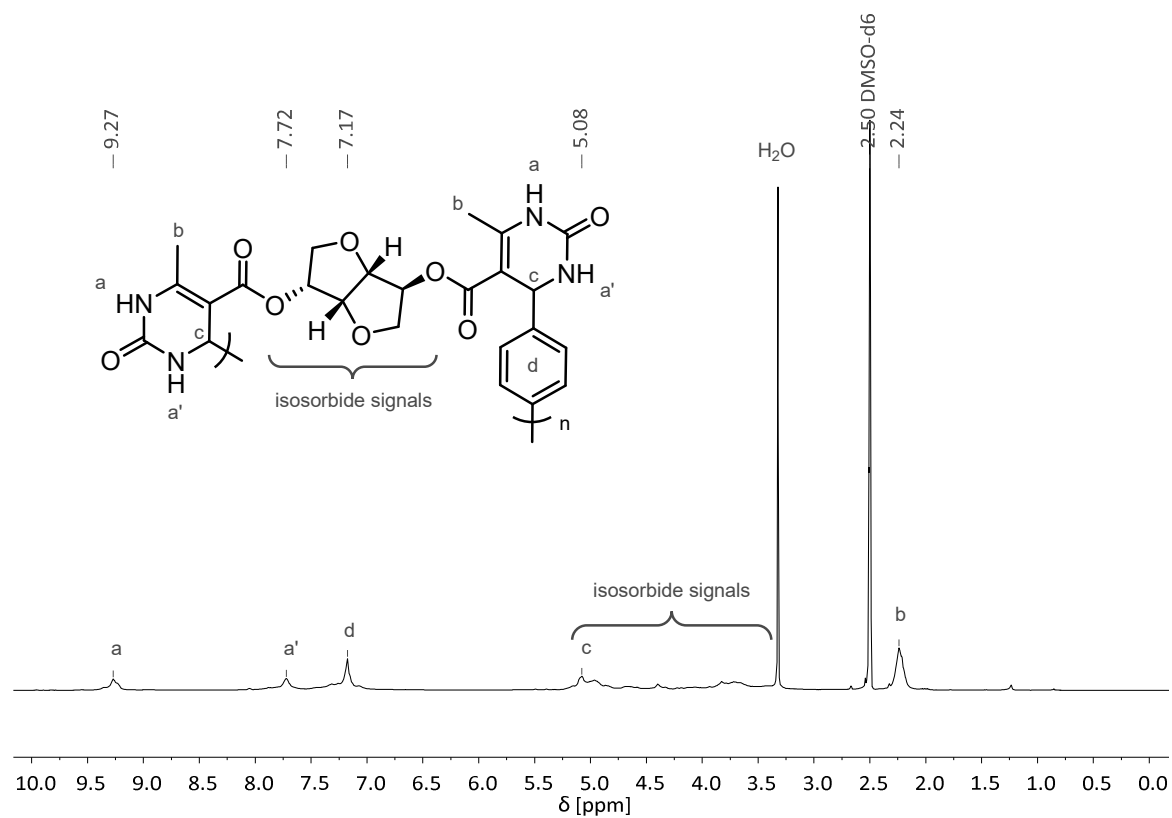


Figure 6.23 ¹H NMR spectrum of **120f** in DMSO-*d*₆.

131a

Precipitated in MeOH/H₂O (90/10) and washed with MeOH/H₂O (90/10).

¹H-NMR (400 MHz, DMSO-*d*₆): δ (ppm) = 7.92 (br s, H_{a'}), 7.14 (s, H_d), 5.29 – 4.97 (m, H_c), 4.32 – 3.99 (m, H_e), 3.08 (s, H_a), 2.44 (s, H_b).

IR: ν (cm⁻¹) = 3341, 2951, 1673, 1506, 1448, 1382, 1350, 1299, 1243, 1186, 1150, 1075, 973, 800, 758, 613, 495.

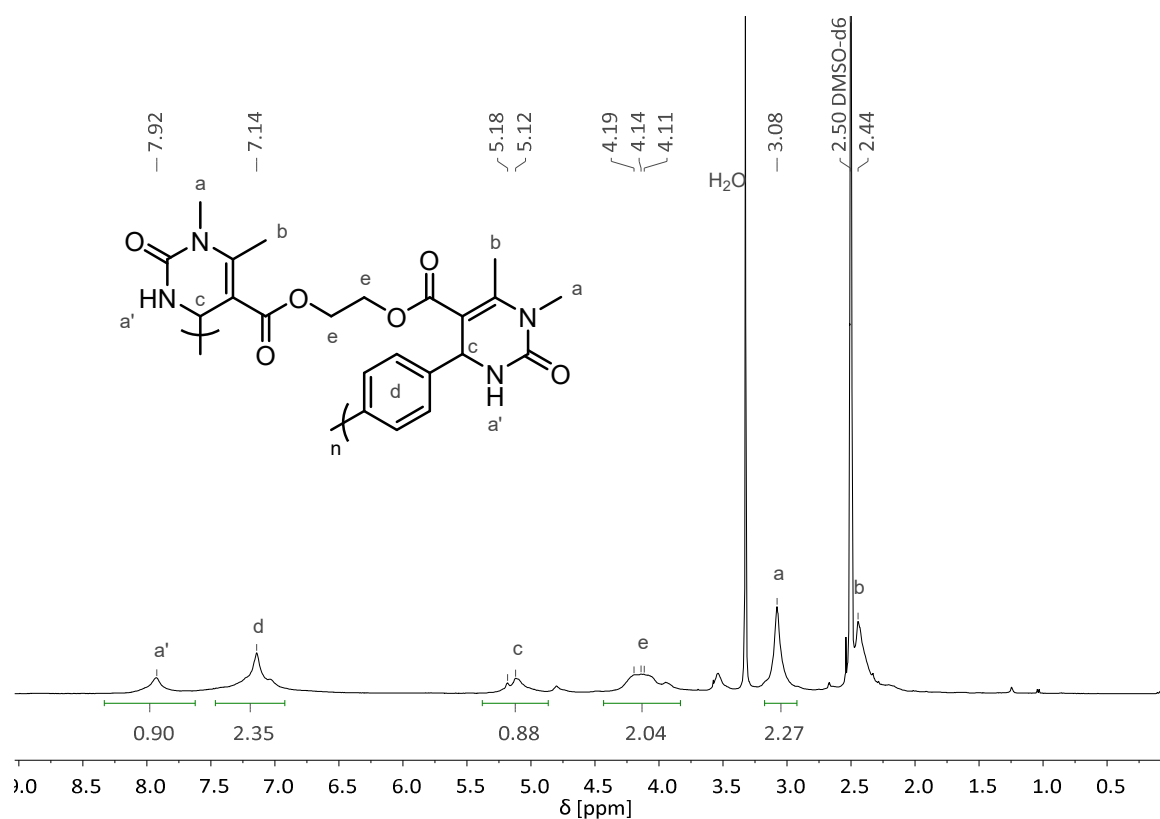


Figure 6.24 ¹H NMR spectrum of **131a** in DMSO-*d*₆.

131b

Precipitated in MeOH/H₂O (90/10) and washed with MeOH/H₂O (90/10).

¹H-NMR (400 MHz, DMSO-*d*₆): δ (ppm) = 7.88 (br s, H_{a'}), 7.14 (br s, H_d), 5.10 (br s, H_c), 4.16 – 3.80 (m, H_e), 3.06 (br s, H_a), 2.45 (br s, H_b), 1.89 – 1.55 (m, H_f).

IR: ν (cm⁻¹) = 3332, 2952, 1671, 1505, 1452, 1419, 1382, 1350, 1299, 1243, 1185, 1152, 1050, 976, 801, 757, 614, 495.

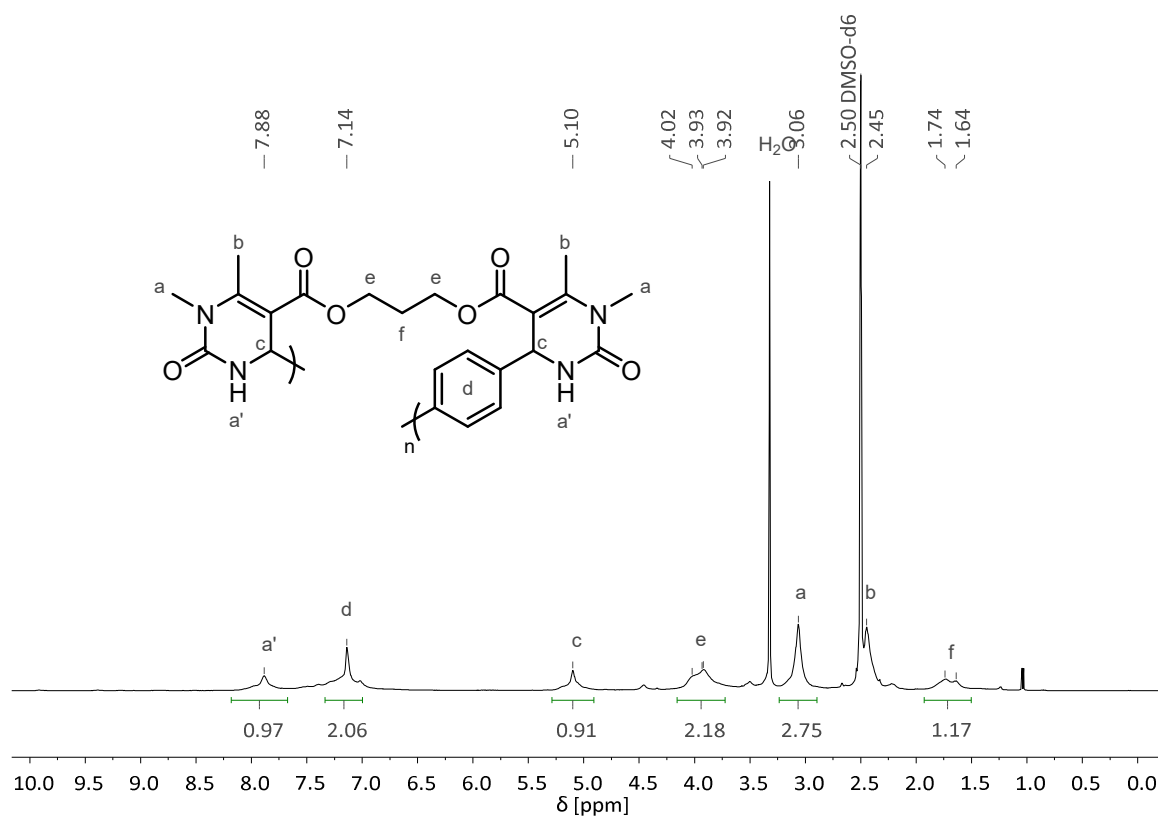


Figure 6.25 ¹H NMR spectrum of **131b** in DMSO-*d*₆.

131c

Precipitated in MeOH/H₂O (50/50) and washed with MeOH/H₂O (50/50) and MeOH/H₂O (90/10) subsequently.

¹H-NMR (400 MHz, DMSO-*d*₆): δ (ppm) = 7.89 (br s, H_{a'}), 7.14 (br s, H_d), 5.09 (br s, H_c), 3.89 (br s, H_e), 3.06 (br s, H_a), 2.45 (br s, H_b), 1.65 – 1.20 (m, H_f).

IR: ν (cm⁻¹) = 3315, 2948, 1667, 1505, 1447, 1382, 1348, 1298, 1242, 1183, 1152, 1070, 1047, 975, 798, 756, 613, 496, 415.

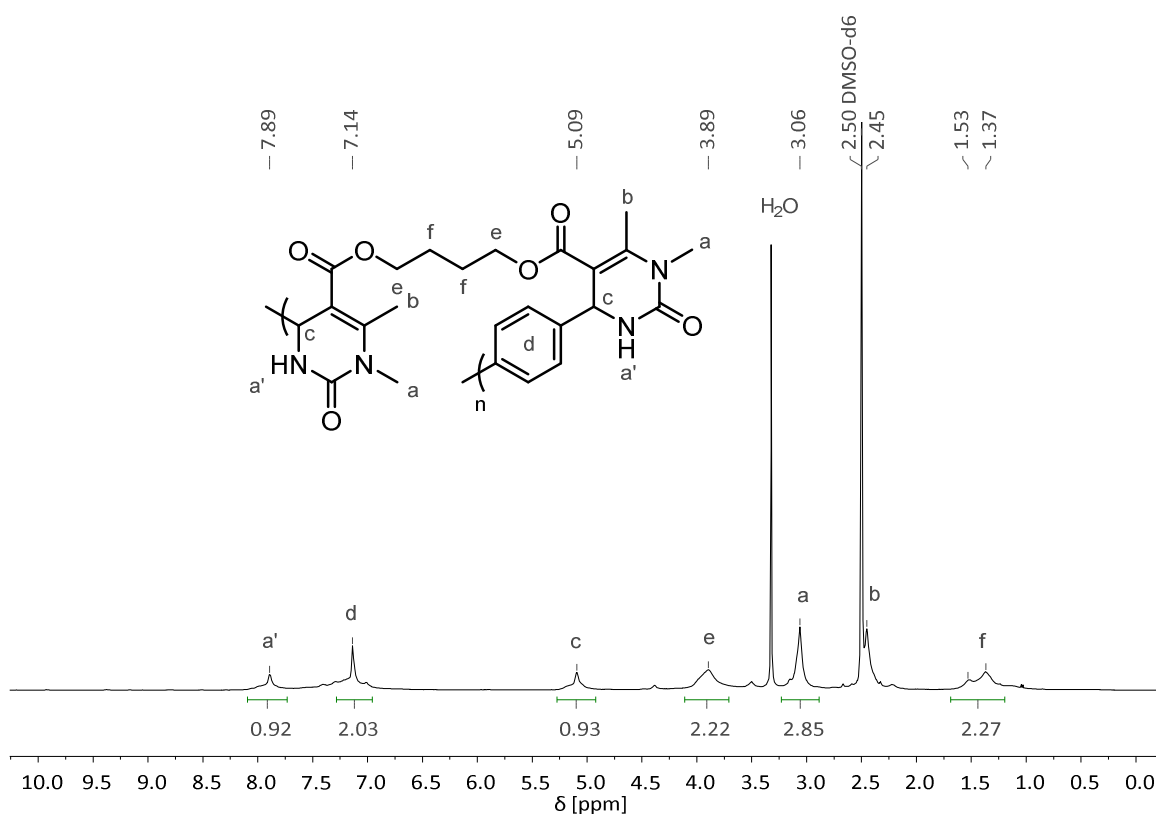


Figure 6.26 ¹H NMR spectrum of **131c** in DMSO-*d*₆.

131d

Precipitated in MeOH/H₂O (50/50) and washed with MeOH/H₂O (50/50) and MeOH/H₂O (90/10) subsequently.

¹H-NMR (400 MHz, DMSO-*d*₆): δ (ppm) = 7.89 (br s, H_{a'}), 7.14 (br s, H_d), 5.10 (br s, H_c), 3.94 (br s, H_e), 3.06 (br s, H_a), 2.46 (br s, H_b), 1.58 – 0.93 (m, H_{f,g}).

IR: ν (cm⁻¹) = 3301, 2938, 2115, 1668, 1505, 1453, 1382, 1348, 1298, 1241, 1184, 1151, 1070, 975, 797, 755, 611, 498, 431.

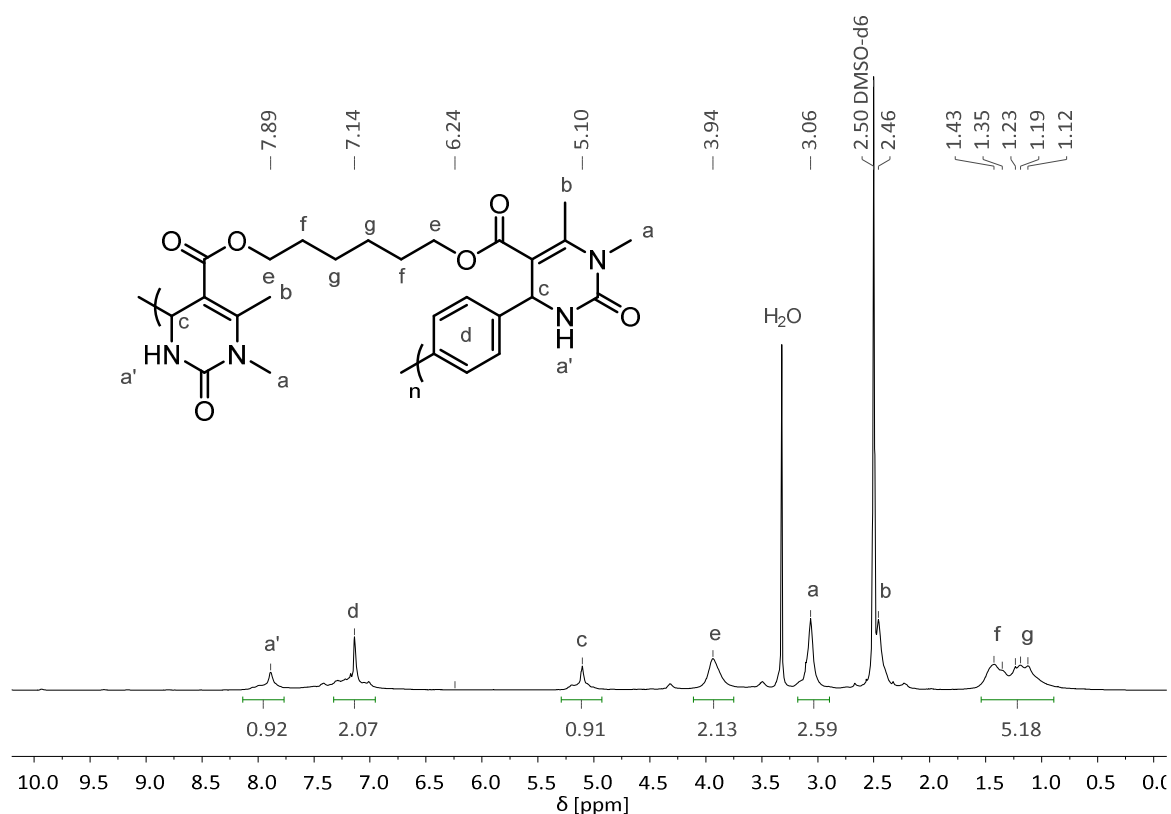


Figure 6.27 ¹H NMR spectrum of **131d** in DMSO-*d*₆.

131e

Precipitated in MeOH/H₂O (30/70) and washed with MeOH/H₂O (30/70) and MeOH/H₂O (90/10) subsequently.

¹H-NMR (400 MHz, DMSO-*d*₆): δ (ppm) = 7.89 (s, H_{a'}), 7.14 (s, H_d), 5.10 (s, H_c), 3.94 (br s, H_e), 3.06 (br s, H_a), 2.46 (br s, H_b), 1.61 – 0.92 (m, H_{f,g,h,i}).

IR: ν (cm⁻¹) = 3320, 2931, 2074, 1668, 1621, 1506, 1450, 1382, 1349, 1299, 1242, 1183, 1152, 1070, 976, 799, 756, 614, 495, 447, 425.

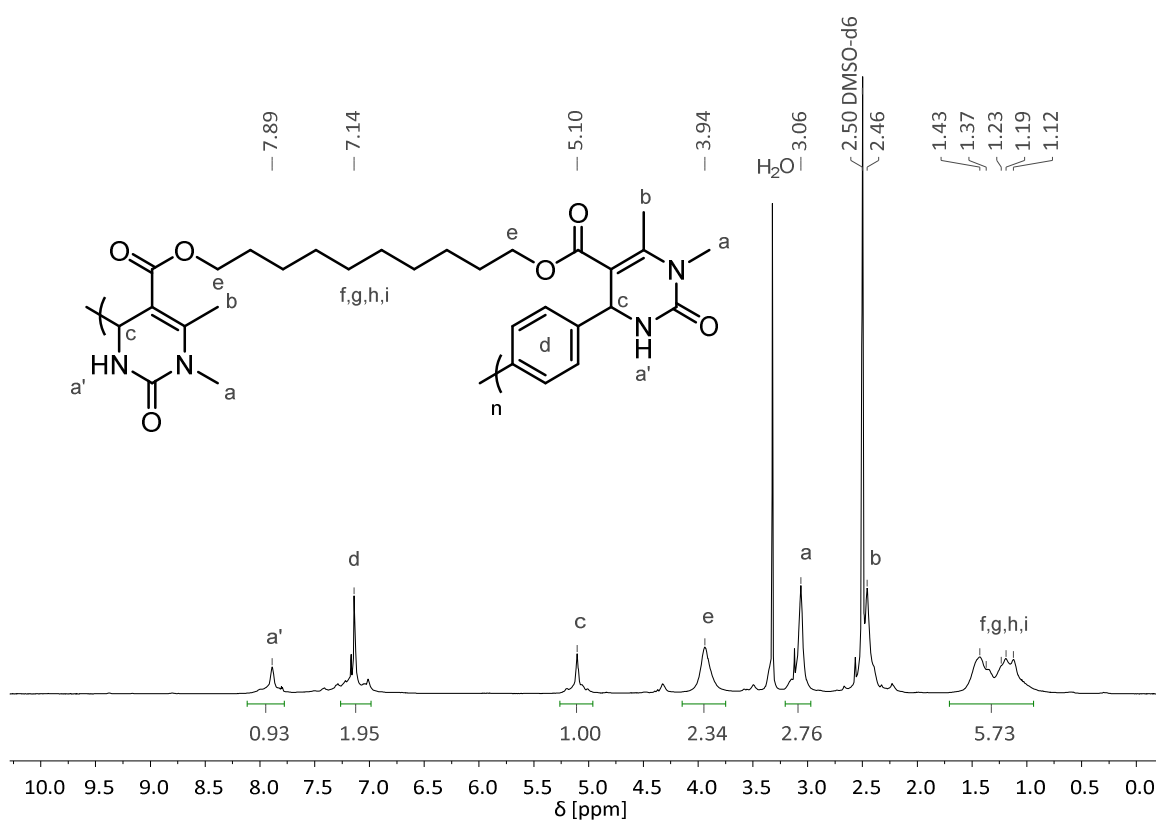


Figure 6.28 ¹H NMR spectrum of **131e** in DMSO-*d*₆.

131f

Precipitated in MeOH and washed with MeOH subsequently.

¹H-NMR (400 MHz, DMSO-*d*₆): δ (ppm) = 7.95 (br s, H_{a'}), 7.15 (br s, H_d), 5.10 – 3.51 (H_{isoborbide}), 5.07 (br s, H_c), 3.09 (br s, H_a), 2.50 (br s, H_b).

IR: ν (cm⁻¹) = 3308, 2940, 2884, 1680, 1622, 1454, 1420, 1384, 1355, 1302, 1243, 1187, 1152, 1073, 974, 871, 803, 757, 604, 492, 415.

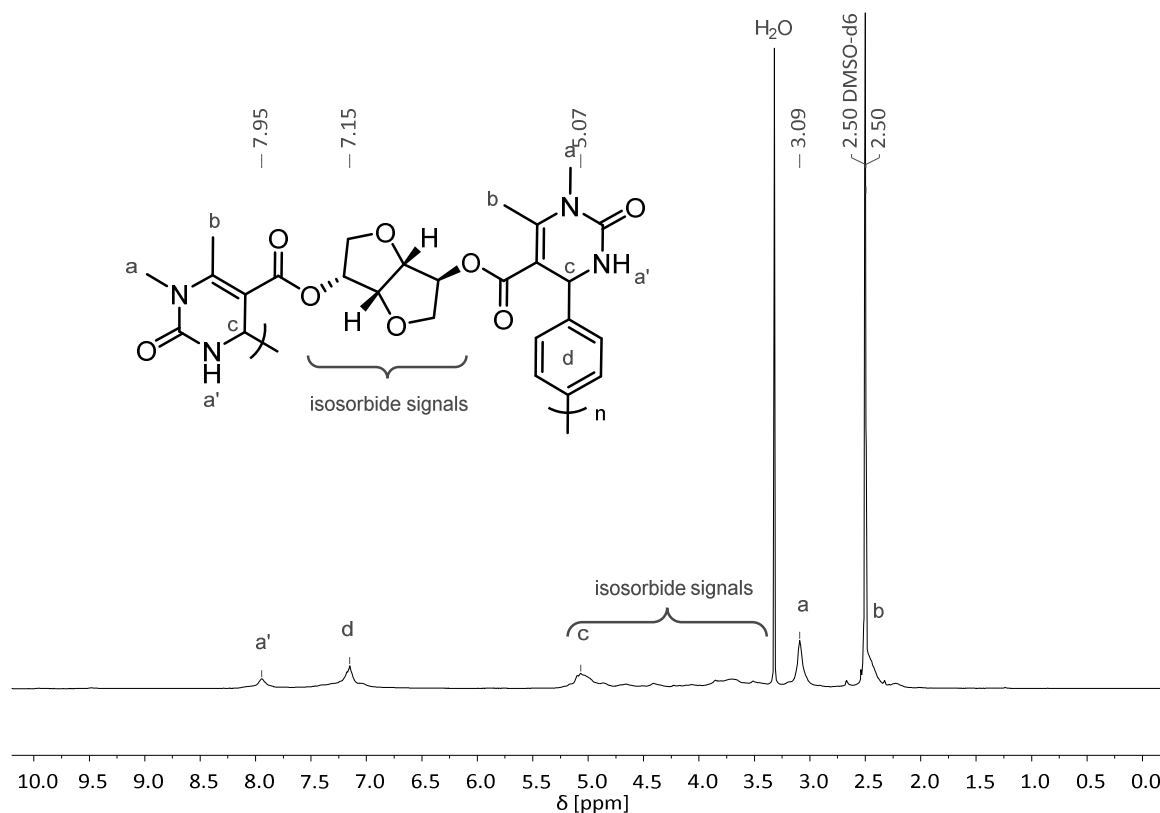
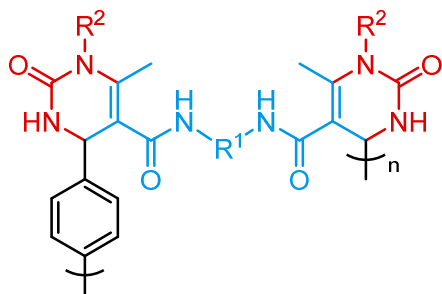


Figure 6.29 ¹H NMR spectrum of **131f** in DMSO-*d*₆.

6.3.2.3 Poly[3,4 dihydropyrimidin 2(1*H*)-one]s using Acetoacetamides

R¹: -C₂H₄- (**a**), -C₆H₁₂- (**d**), -C₁₀H₂₀- (**e**)

132a,d,e (using **47**, R² = H)

133a,d,e (using **49**, R² = CH₃)

Table 6.8 SEC and DSC data and yields of polyDHPMs **132a-e** using diacetoacetamides.

polymer	R ¹	$M_{n,NMR}$ [g·mol ⁻¹]	$M_{n,SEC}$ [g·mol ⁻¹]	$M_{w,SEC}$ [g·mol ⁻¹]	D	T_g [°C]	Yield ^a [%]
132a	C ₂ H ₄	9 600	5 000	23 400	4.71	- ^b	53
132d	C ₆ H ₁₂	5 300	12 400	63 000	5.07	265	61
132e	C ₁₀ H ₂₀	5 500	11 800	40 300	3.40	235	57
133a	C ₂ H ₄	2 400	6 000	12 400	2.06	- ^b	45
133d	C ₆ H ₁₂	3 900	5 300	13 000	2.47	- ^b	48
133e	C ₁₀ H ₂₀	3 800	15 200	71 100	4.71	194	59

^aisolated yield; ^bnot observed within the investigated temperature range.

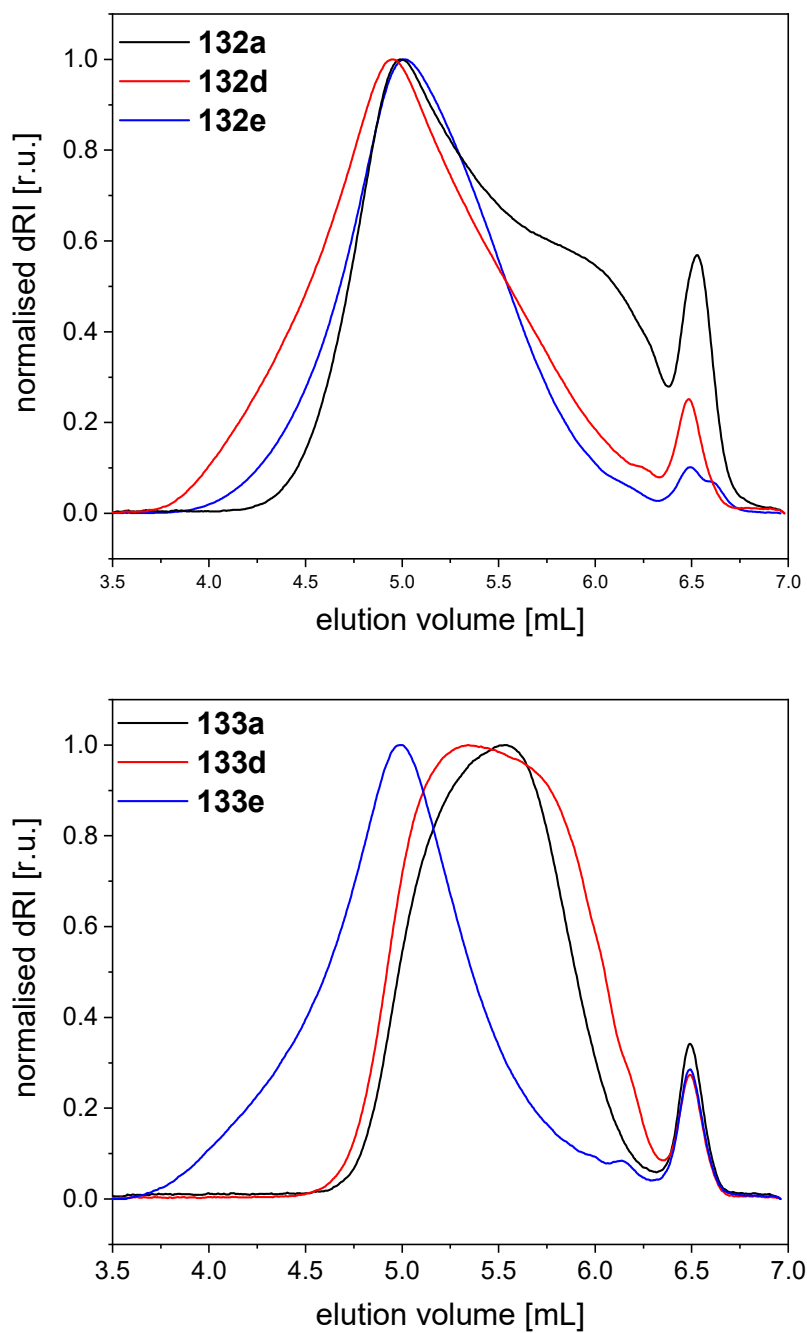


Figure 6.30 SEC chromatograms of the polyDHMPs using acetoacetamides and urea (**132a,d,e**, top) or Me-urea (**133a,d,e**, bottom).

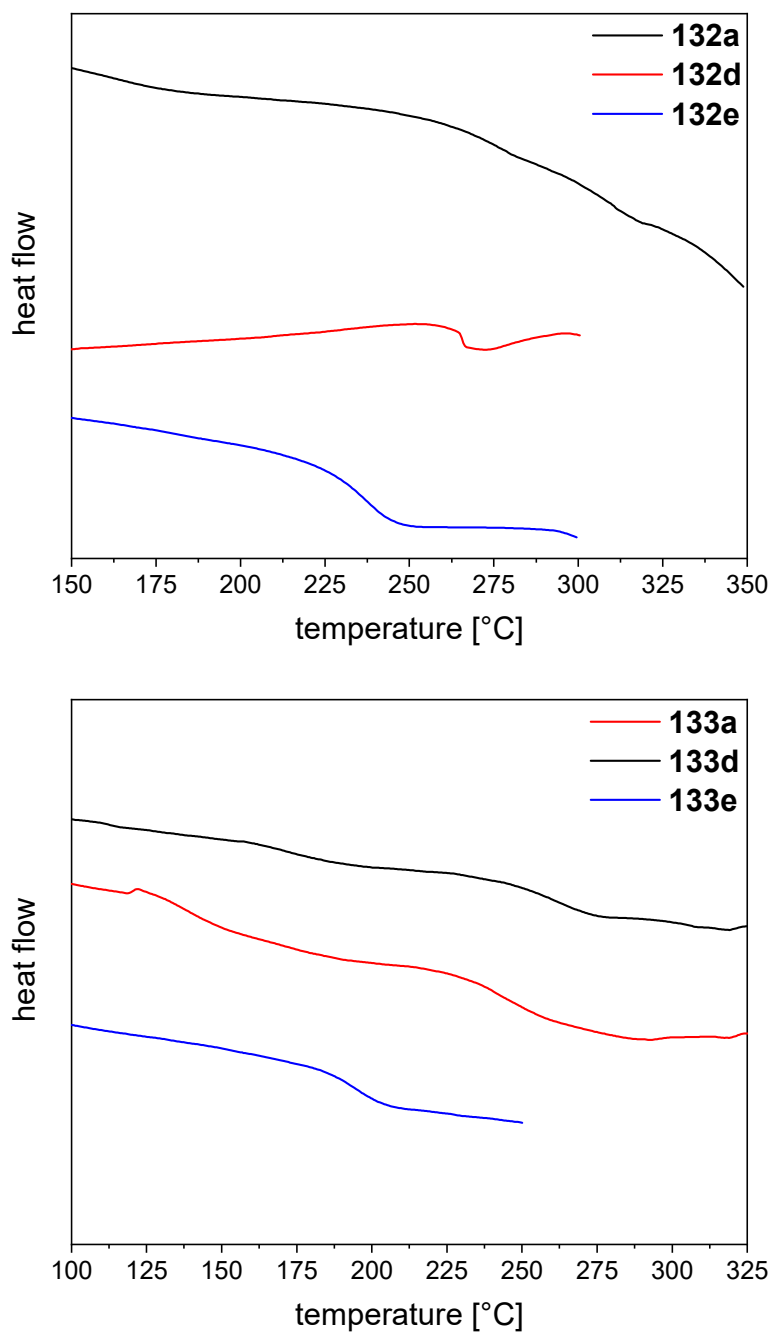


Figure 6.31 DSC curves of the polyDHMPs **132a,d,e** and **133a,d,e** using acetoacetamides and urea (top) or Me-urea (bottom) showing the respective T_g s; the baselines for the measurements of **132a**, **133a**, and **133d** were not stable.

132a

Precipitated in MeOH and washed with MeOH.

¹H-NMR (400 MHz, DMSO-*d*₆): δ (ppm) = 8.58 (br s, H_a), 7.75 – 7.46 (m, H_a’, H_k), 7.15 (s, H_d), 5.18 (s, H_c), 3.06 (br s, H_e), 1.97 (br s, H_b).

IR: ν (cm⁻¹) = 3275, 3101, 2917, 1651, 1538, 1433, 1387, 1300, 1239, 1115, 1019, 972, 798, 759, 652, 583, 498.

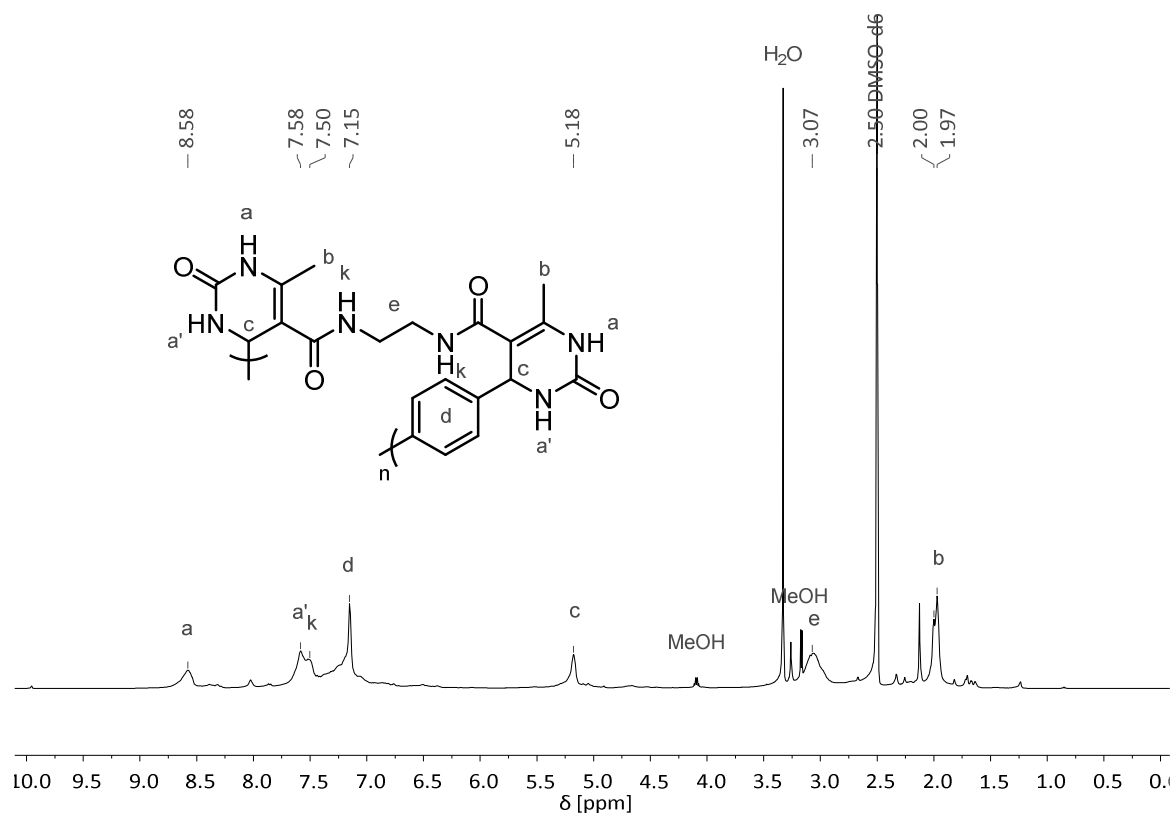


Figure 6.32 ¹H NMR spectrum of **132a** in DMSO-*d*₆.

132d

Precipitated in MeOH and washed with MeOH.

¹H-NMR (400 MHz, DMSO-*d*₆): δ (ppm) = 8.51 (br s, H_a), 7.59 (br s, H_{a'}), 7.44 (br s, H_k), 7.15 (s, H_d), 5.21 (s, H_c), 3.14 – 2.85 (m, H_e), 1.97 (s, H_b), 1.30 (br s, H_f), 1.13 (br s, H_g).

IR: ν (cm⁻¹) = 3260, 3089, 2933, 2859, 1644, 1604, 1539, 1435, 1294, 1240, 1104, 1019, 800, 758, 648, 421.

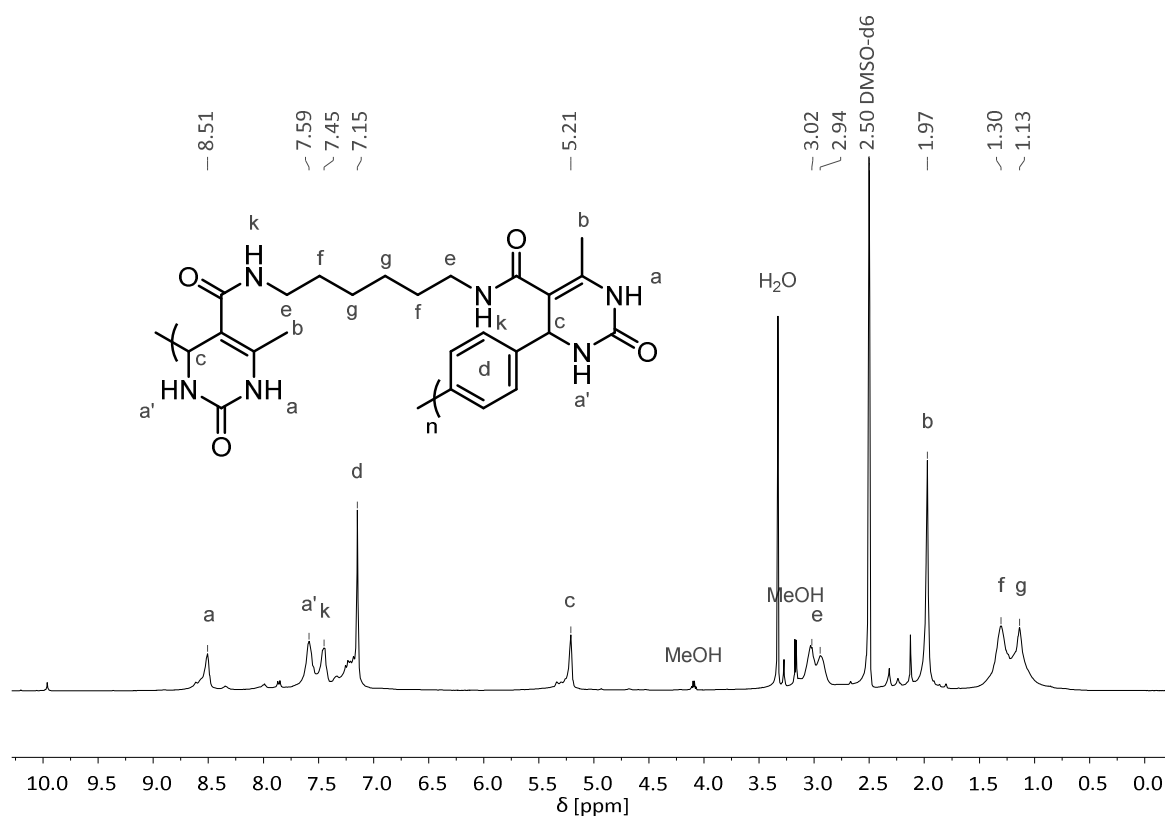


Figure 6.33 ¹H NMR spectrum of **132d** in DMSO-*d*₆.

132e

Precipitated in MeOH and washed with MeOH.

¹H-NMR (400 MHz, DMSO-*d*₆): δ (ppm) = 8.49 (br s, H_a), 7.57 (br s, H_{a'}), 7.44 (br s, H_k), 7.14 (s, H_d), 5.20 (s, H_d), 3.11 – 2.81 (m, H_e), 1.97 (s, H_b), 1.46 – 1.00 (m, H_{f,g,h,i}).

IR: ν (cm⁻¹) = 3250, 3104, 2925, 2852, 1661, 1614, 1516, 1433, 1311, 1235, 1130, 1101, 1018, 947, 755, 710, 628, 503, 419.

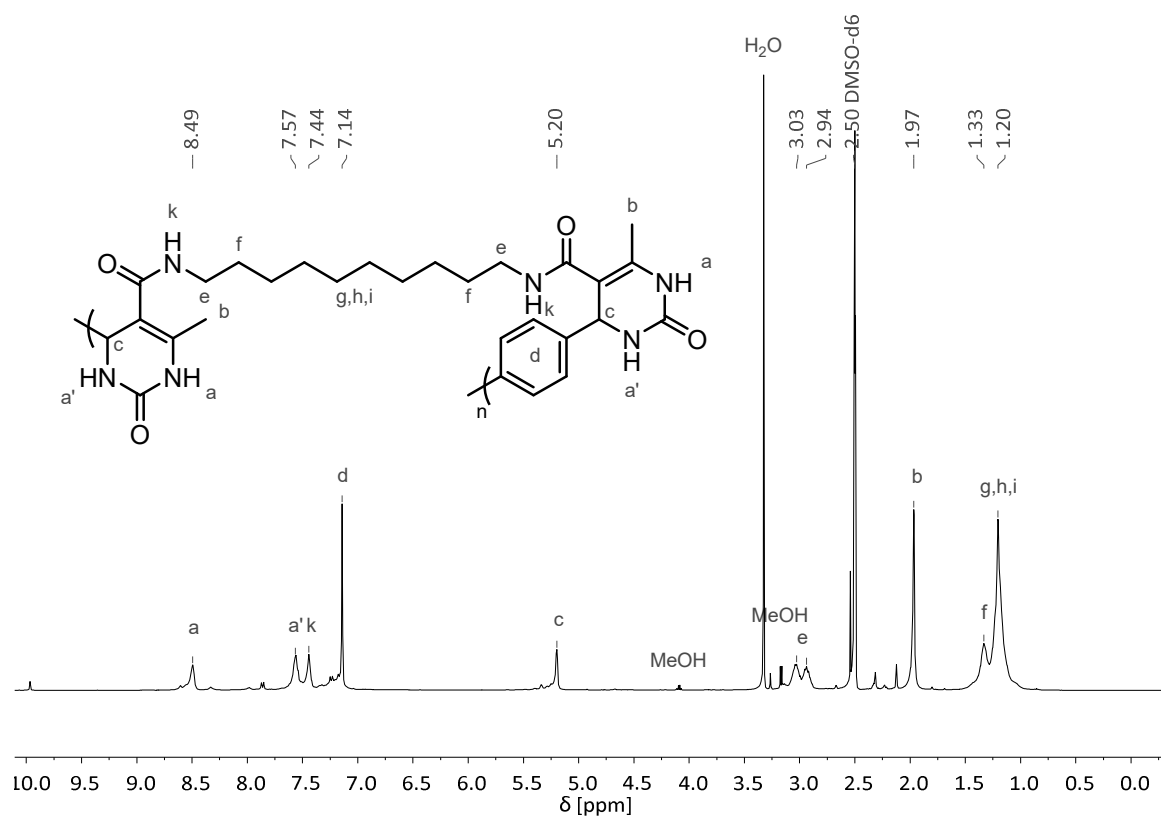


Figure 6.34 ¹H NMR spectrum of **132e** in DMSO-*d*₆.

133a

Precipitated in MeOH and washed with MeOH.

¹H-NMR (400 MHz, DMSO-*d*₆): δ (ppm) = 7.86 (br s, H_{a'}), 7.64 (br s, H_k), 7.13 (br s, H_d), 5.08 (br s, H_c), 3.26 – 2.81 (m, H_{e,a}), 2.12 (br, H_b).

IR: ν (cm⁻¹) = 3261, 3064, 2922, 2045, 1635, 1510, 1454, 1389, 1344, 1252, 1210, 1097, 975, 755, 493.

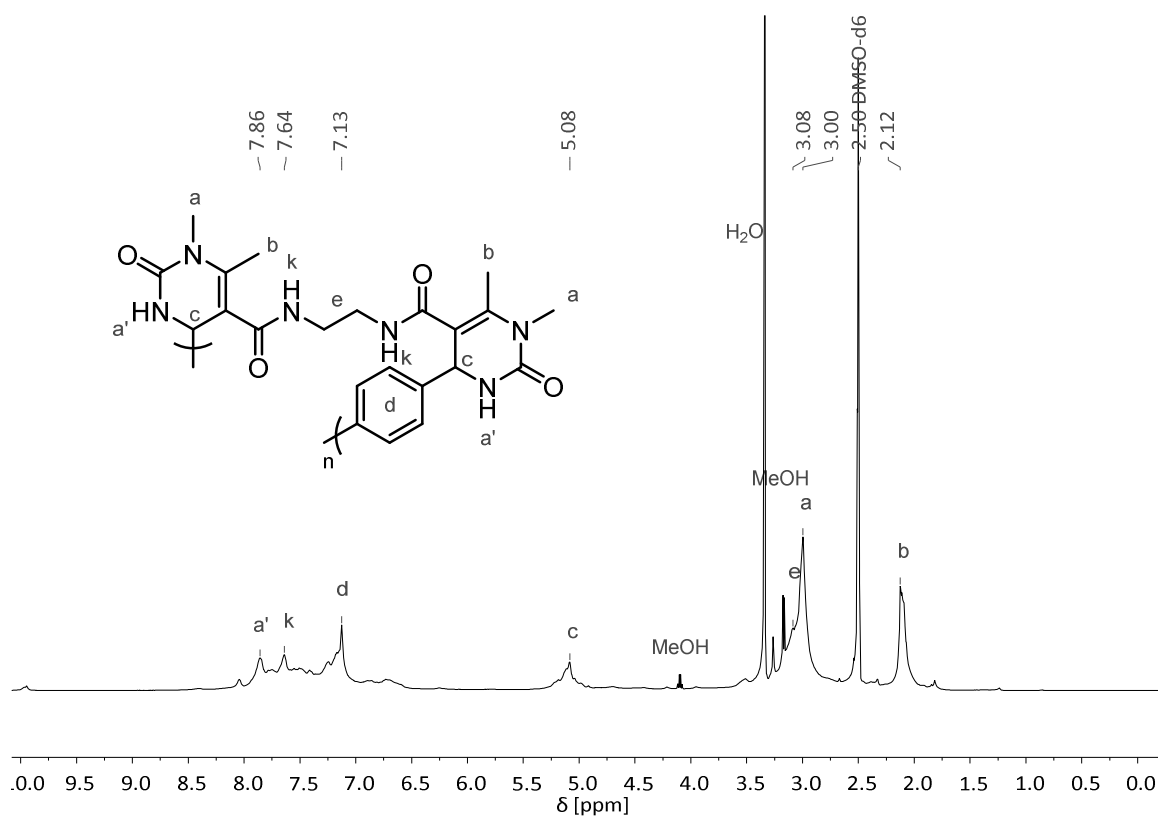


Figure 6.35 ¹H NMR spectrum of **133a** in DMSO-*d*₆.

133d

Precipitated in H₂O and washed with MeOH.

¹H-NMR (400 MHz, DMSO-*d*₆): δ (ppm) = 7.84 (br, H_{a'}), 7.59 (br, H_k), 7.12 (br, H_d), 5.10 (br, H_c), 3.07 (br, H_e), 3.21 – 2.78 (m, H_{a,e}), 2.09 (m, H_b), 1.45 – 0.79 (m, H_{f,g}).

IR: ν (cm⁻¹) = 3273, 2929, 2050, 1625, 1515, 1454, 1388, 1344, 1252, 1210, 1091, 974, 755, 488.

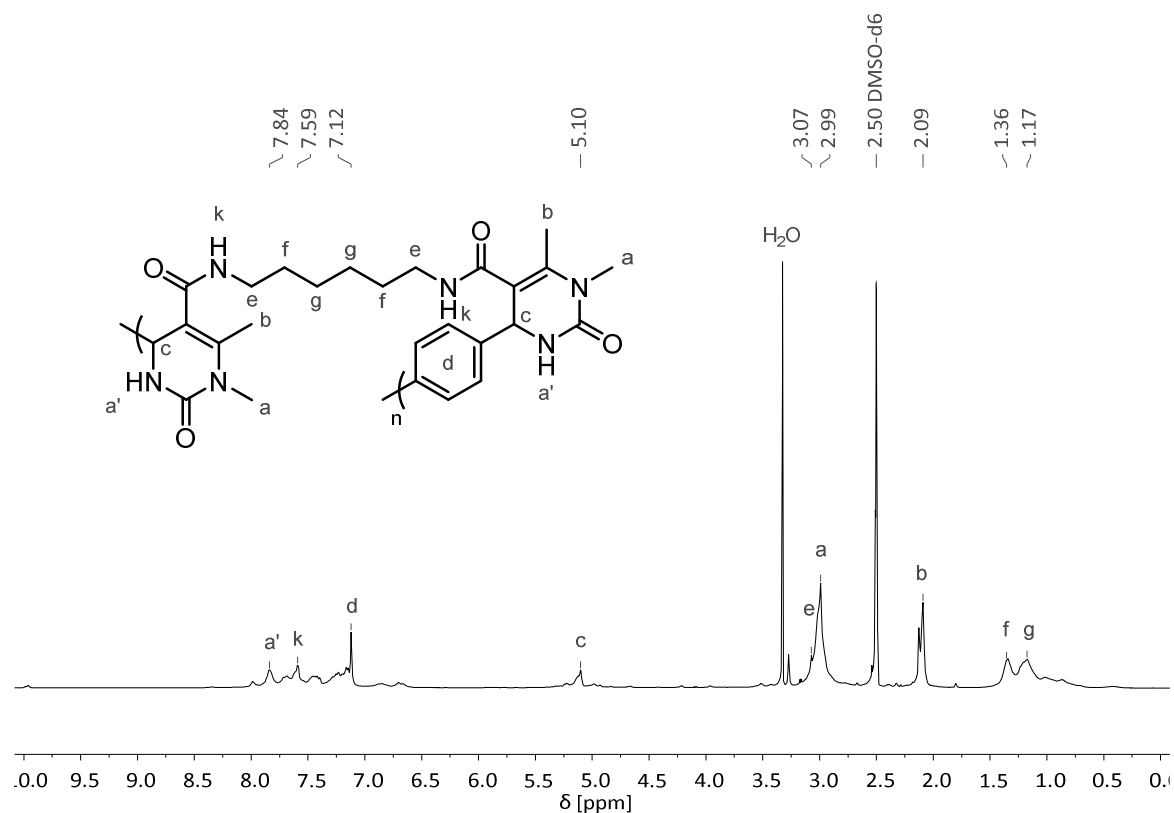


Figure 6.36 ¹H NMR spectrum of **133d** in DMSO-*d*₆.

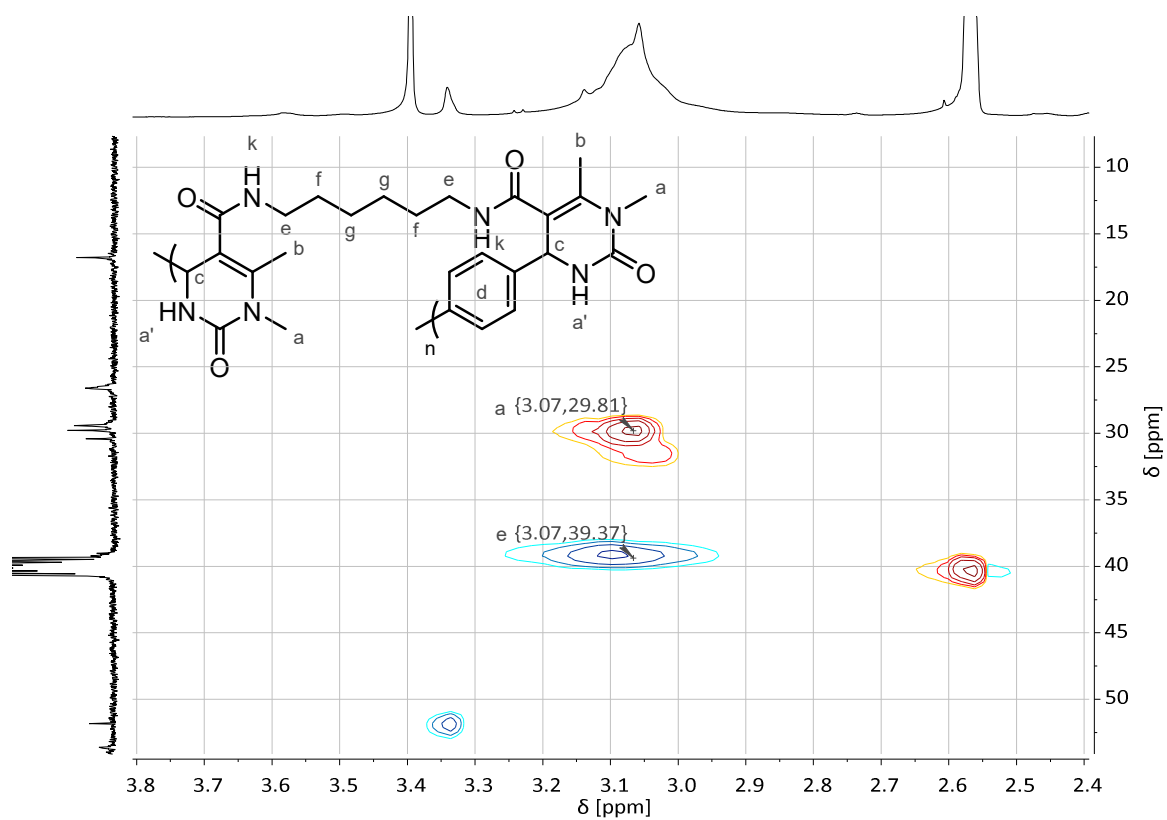


Figure 6.37 HSQC spectrum of **133d**.

The 2D-HSQC-NMR spectrum clearly shows an overlap of the CH_3 -protons of Me-urea with the $-(\text{NH})\text{CH}_2$ -protons of the spacer. A similar overlap is observed for **133a** and **133e**.

133e

Precipitated in H₂O and washed with MeOH.

¹H-NMR (400 MHz, DMSO-*d*₆): δ (ppm) = 7.82 (br s, H_{a'}), 7.59 (br s, H_k), 7.11 (br s, H_d), 5.10 (br s, H_c), 3.17 – 2.86 (m, H_{e,a}), 2.08 (br s, H_b), 1.55 – 0.95 (m, H_{f,g,h,i}).

IR: ν (cm⁻¹) = 3288, 3078, 2923, 2852, 1651, 1520, 1454, 1417, 1387, 1345, 1254, 1212, 1163, 1094, 974, 798, 755, 607, 505, 457.

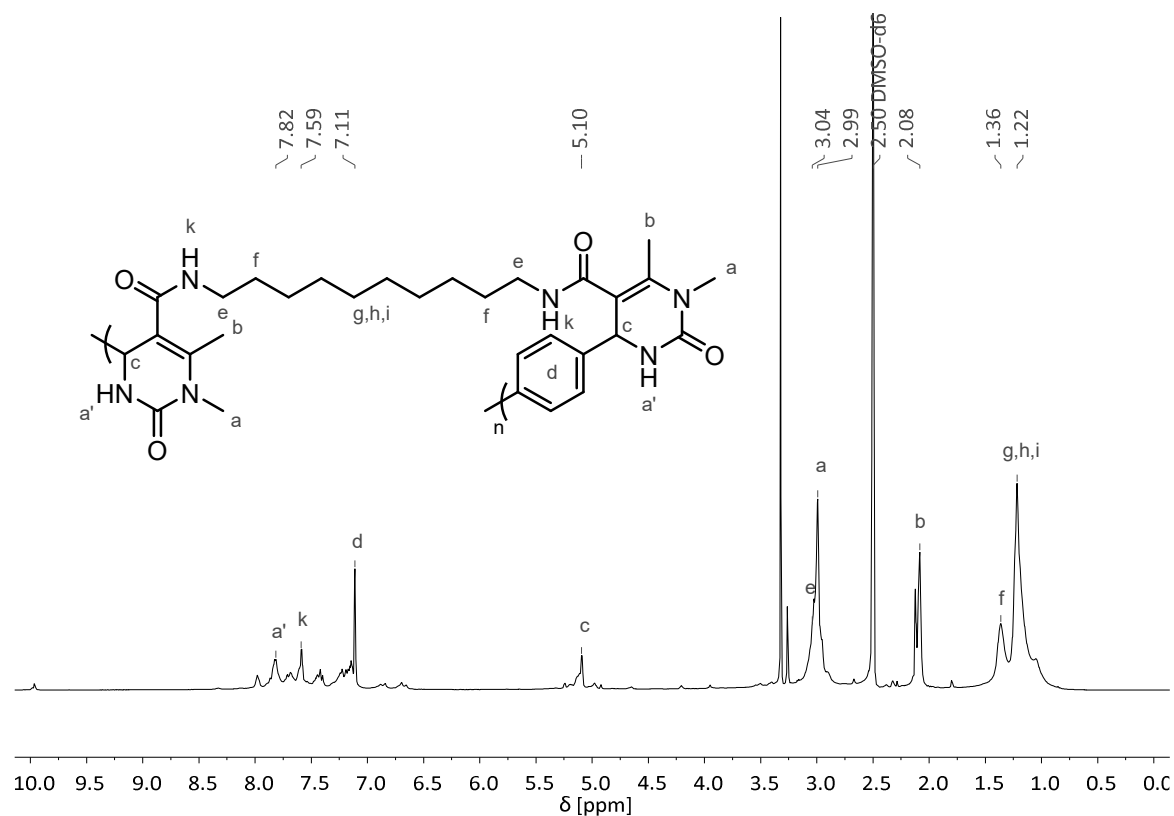


Figure 6.38 ¹H NMR spectrum of **133e** in DMSO-*d*₆.

6.3.2.4 Thermogravimetric Analysis of Poly[3,4 dihydropyrimidin 2(1*H*)-one]s

Table 6.9 Results of the TGA of the whole set of polyDHPMs.

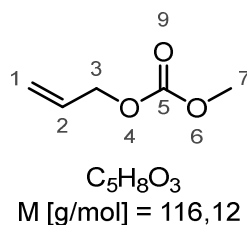
polymer	R ¹	T _{d5%} [°C]
120a	C ₂ H ₄	280
120b	C ₃ H ₆	278
120c	C ₄ H ₈	274
120d	C ₆ H ₁₂	282
120e	C ₁₀ H ₂₀	307
120f	isosorbide	289
131a	C ₂ H ₄	266
131b	C ₃ H ₆	264
131c	C ₄ H ₈	278
131d	C ₆ H ₁₂	286
131e	C ₁₀ H ₂₀	314
131f	isosorbide	282
132a	C ₂ H ₄	296
132d	C ₆ H ₁₂	282
132e	C ₁₀ H ₂₀	278
133a	C ₂ H ₄	284
133d	C ₆ H ₁₂	286
133e	C ₁₀ H ₂₀	278

6.4 Synthesis Procedures and Analytical Data Related to Chapter 4.2

6.4.1 Monomers and 10-Undecenyl-1-acetoacetate

The applied diacetoacetates were prepared according to chapter 6.3.1.

6.4.1.1 Allyl Methyl Carbonate (137)



The synthesis of allyl methyl carbonate (**137**) was carried out according to literature.^[382]

A mixture of allyl alcohol (594 mmol, 1.00 eq) and dimethyl carbonate (7.50 eq) was stirred at 80°C for 3 min. Subsequently, 1,5,7-triazabicyclo[4.4.0]dec-5-en (0.01 eq) was added. The mixture was stirred for 1 h at 80°C. The resulting mixture of dimethyl carbonate, allyl methyl carbonate, and diallyl carbonate was fractionated by vacuum distillation.

yield	31% (21.4 g, 184 mmol, colourless liquid)
distillation	dimethyl carbonate: 35°C, 100 mbar; allyl methyl carbonate: 50 – 60°C, 100 mbar, residue contained mainly diallyl carbonate

$^1\text{H-NMR}$ (400 MHz, $\text{DMSO-}d_6$): δ (ppm) = 5.93 (ddt, $^3J_{\text{H}_2;\text{H}_{1\text{cis}};\text{H}_{1\text{trans}};\text{H}_3} = 17.2, 10.5, 5.8$ Hz, 1H, H_2), 5.36 (ddt, $^2J_{\text{H}_{1\text{cis}};\text{H}_{1\text{trans}}} = 1.5$ Hz, $^3J_{\text{H}_{1\text{cis}};\text{H}_2} = 17.2$ Hz, $^4J_{\text{H}_{1\text{cis}};\text{H}_3} = 1.5$ Hz, 1H, $\text{H}_{1\text{cis}}$), 5.27 (ddt, $^2J_{\text{H}_{1\text{trans}};\text{H}_{1\text{cis}}} = 1.2$ Hz, $^3J_{\text{H}_{1\text{trans}};\text{H}_2} = 10.4$ Hz, $^4J_{\text{H}_{1\text{trans}};\text{H}_3} = 1.2$ Hz, 1H, $\text{H}_{1\text{trans}}$), 4.63 (ddd, $^3J_{\text{H}_3;\text{H}_2} = 5.8$ Hz, $^4J_{\text{H}_3;\text{H}_{1\text{cis}};\text{H}_{1\text{trans}}} = 1.4, 1.4$ Hz, 2H, H_3), 3.79 (s, 3H, H_7).

Further analyses were omitted due to the resemblance of the measured ^1H NMR spectrum with reported results.^[382]

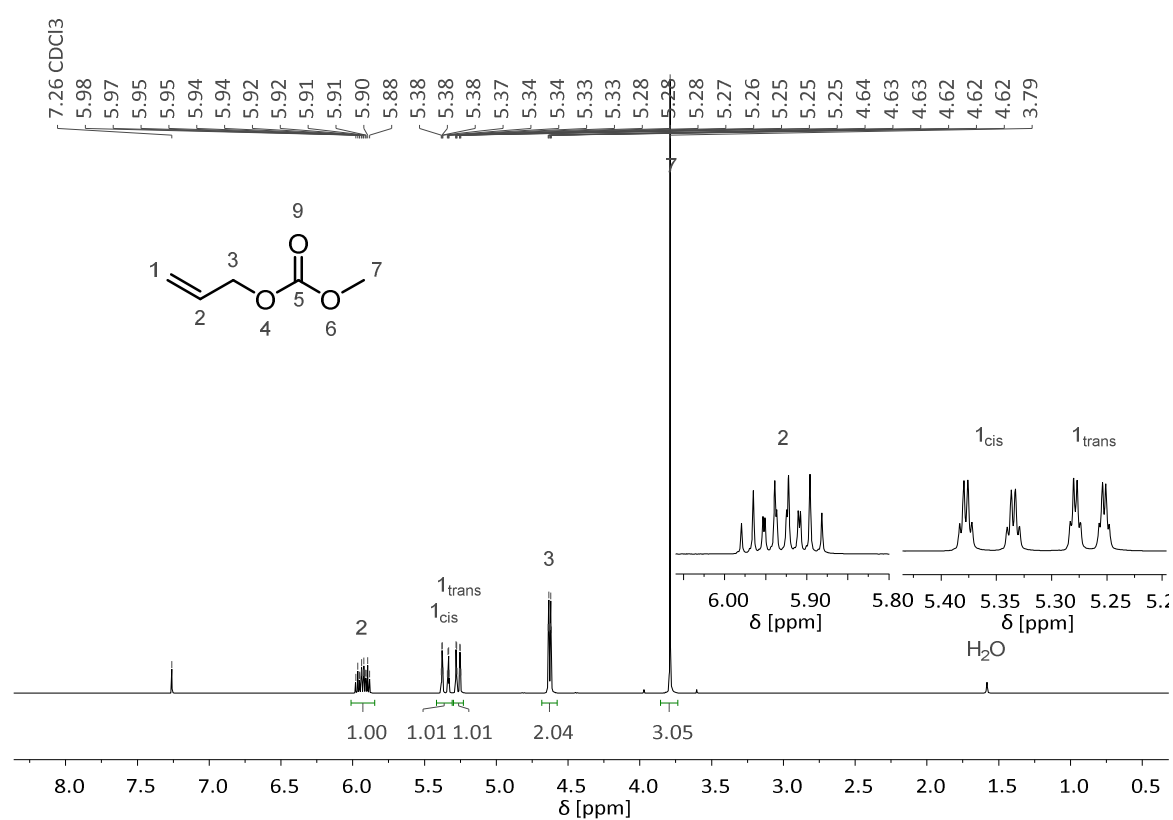
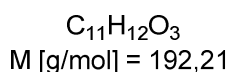
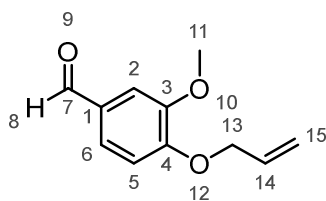


Figure 6.39 ^1H NMR spectrum of **137** in CDCl_3 .

6.4.1.2 4-(Allyloxy)-3-methoxybenzaldehyde (**138**)

The synthesis of 4-(allyloxy)-3-methoxybenzaldehyde (**138**) was carried out according to literature.^[383]

Vanillin (52.0 mmol, 1.00 eq) was mixed with allyl methyl carbonate (2.50 eq) and triphenyl phosphine (0.05 eq) in water (0.37M). Palladium nanoparticles stabilized with poly(vinylpyrrolidone) in water (0.001 eq, 2.44 mL) were added to the mixture and the mixture was stirred at 90°C for 22 h. The reaction mixture was extracted with EtOAc (five times with 50 ml). The combined organic phases were dried over Na₂SO₄ and the solvent was removed under reduced pressure. The crude product was purified by column chromatography using a mixture of *c*-C₆H₁₂ and EtOAc.

yield	80% (7.93 g, 41.2 mmol, slightly yellow oil)
eluent	<i>c</i> -C ₆ H ₁₂ :EtOAc = 98:2 → 60:40
R _f (product)	0.56 in <i>c</i> -C ₆ H ₁₂ :EtOAc = 60:40

¹H-NMR (400 MHz, DMSO-*d*₆): δ (ppm) = 9.85 (s, 1H, H₈), 7.54 (dd, ³J_{H₆;H₅} = 8.2 Hz, ⁴J_{H₆;H₂} = 1.9 Hz, 1H, H₆), 7.41 (d, ⁴J_{H₂;H₆} = 1.9 Hz, 1H, H₂), 7.18 (d, ³J_{H₅;H₆} = 8.3 Hz, 1H, H₅), 6.07 (ddt, ³J_{H₁₄;H_{15cis};H_{15trans};H₁₃} = 17.2, 10.6, 5.4 Hz, 1H, H₁₄), 5.43 (ddt, ²J_{H_{15cis};H_{15trans}} = 1.7 Hz, ³J_{H_{15cis};H₁₄} = 17.3 Hz, ⁴J_{H_{15cis};H₁₃} = 1.7 Hz, 1H, H_{15cis}), 5.30 (ddt, ²J_{H_{15trans};H_{15cis}} = 1.4 Hz, ³J_{H_{15trans};H₁₄} = 10.5 Hz, ⁴J_{H_{15trans};H₁₃} = 1.4 Hz, 1H, H_{15trans}), 4.69 (ddd, ³J_{H₁₃;H₁₄} = 5.4 Hz, ⁴J_{H₁₃;H_{15cis};H_{15trans}} = 1.5, 1.5 Hz, 2H, H₁₃), 3.85 (s, 3H, H₁₁).

Further analyses were omitted due to the resemblance of the measured ¹H NMR spectrum with reported results.^[383]

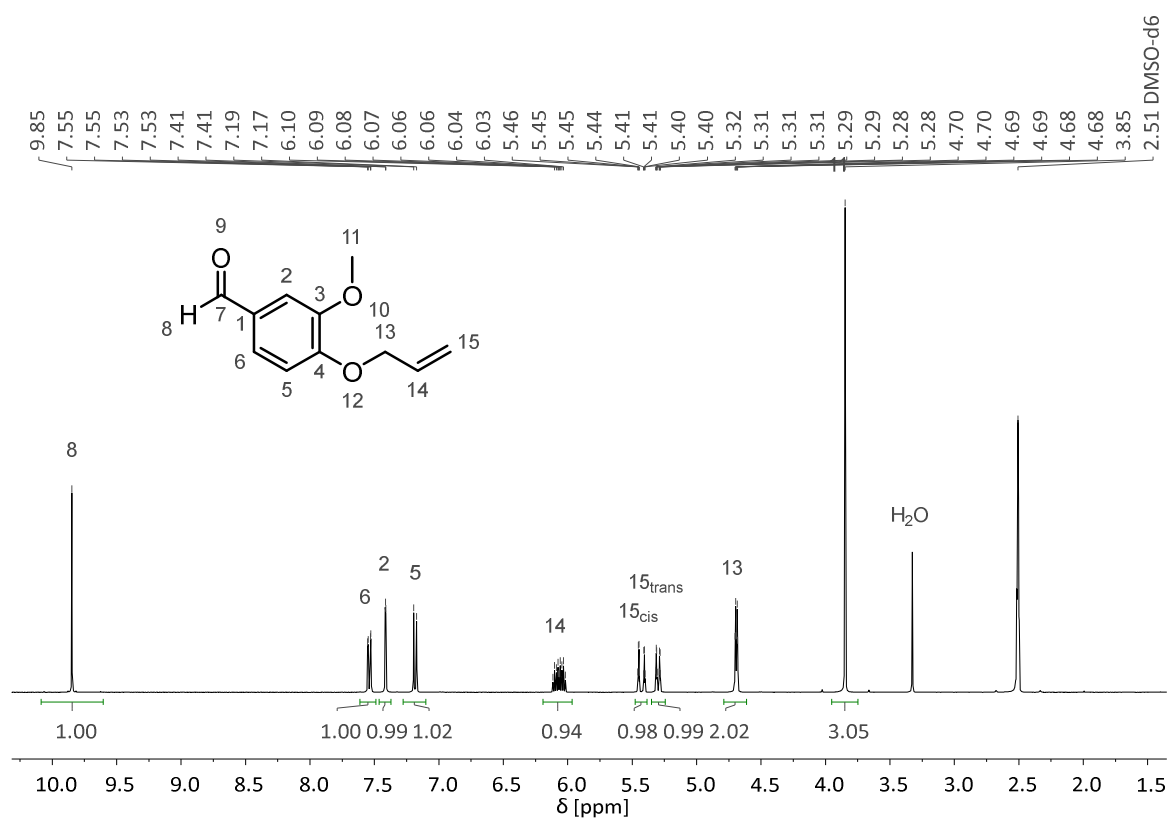
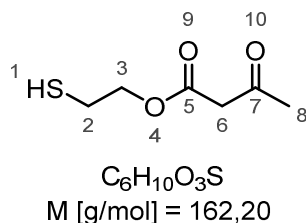


Figure 6.40 ¹H NMR spectrum of **138** in DMSO-*d*₆.

6.4.1.3 2-Mercaptoethyl Acetoacetate (140)

Mercaptoethanol (150 mmol, 1.00 eq) was mixed with *t*-butyl acetoacetate (1.00 eq) and stirred in a preheated oil bath at 150°C for 4.5 h. Evolving *t*-BuOH was continuously removed *via* distillation. Afterwards, the crude product was purified by column chromatography using a mixture of *c*-C₆H₁₂ and EtOAc.

yield	63% (15.2 g, 93.9 mmol, slightly yellow oil)
eluent	<i>c</i> -C ₆ H ₁₂ :EtOAc = 84:16
R _f (product)	0.50 in <i>c</i> -C ₆ H ₁₂ :EtOAc = 60:20

¹H-NMR (400 MHz, DMSO-*d*₆): δ (ppm) = 4.14 (t, ³J_{H₃;H₂} = 6.7 Hz, 2H, H₃), 3.63 (s, 2H, H₆), 2.70 (dt, ³J_{H₂;H₁;H₃} = 8.3, 6.6 Hz, 2H, H₂), 2.56 – 2.51 (m, 1H, H₁), 2.19 (s, 3H, H₈).

¹³C-NMR (101 MHz DMSO-*d*₆): δ (ppm) = 201.52 (C₇), 167.06 (C₅), 65.85 (C₃), 49.46 (C₆), 30.07 (C₈), 22.39 (C₂).

IR: ν (cm⁻¹) = 3434, 2947, 2896, 2571, 1738, 1652, 1631, 1451, 1409, 1360, 1314, 1263, 1244, 1172, 1146, 1033, 974, 856, 804, 742, 666, 623, 541, 497, 476, 452, 409.

HRMS (EI): m/z for C₆H₁₀O₃S⁺ [M]⁺: calculated: 162.0345; found: 162.0344.

6.4 Synthesis Procedures and Analytical Data Related to Chapter 4.2

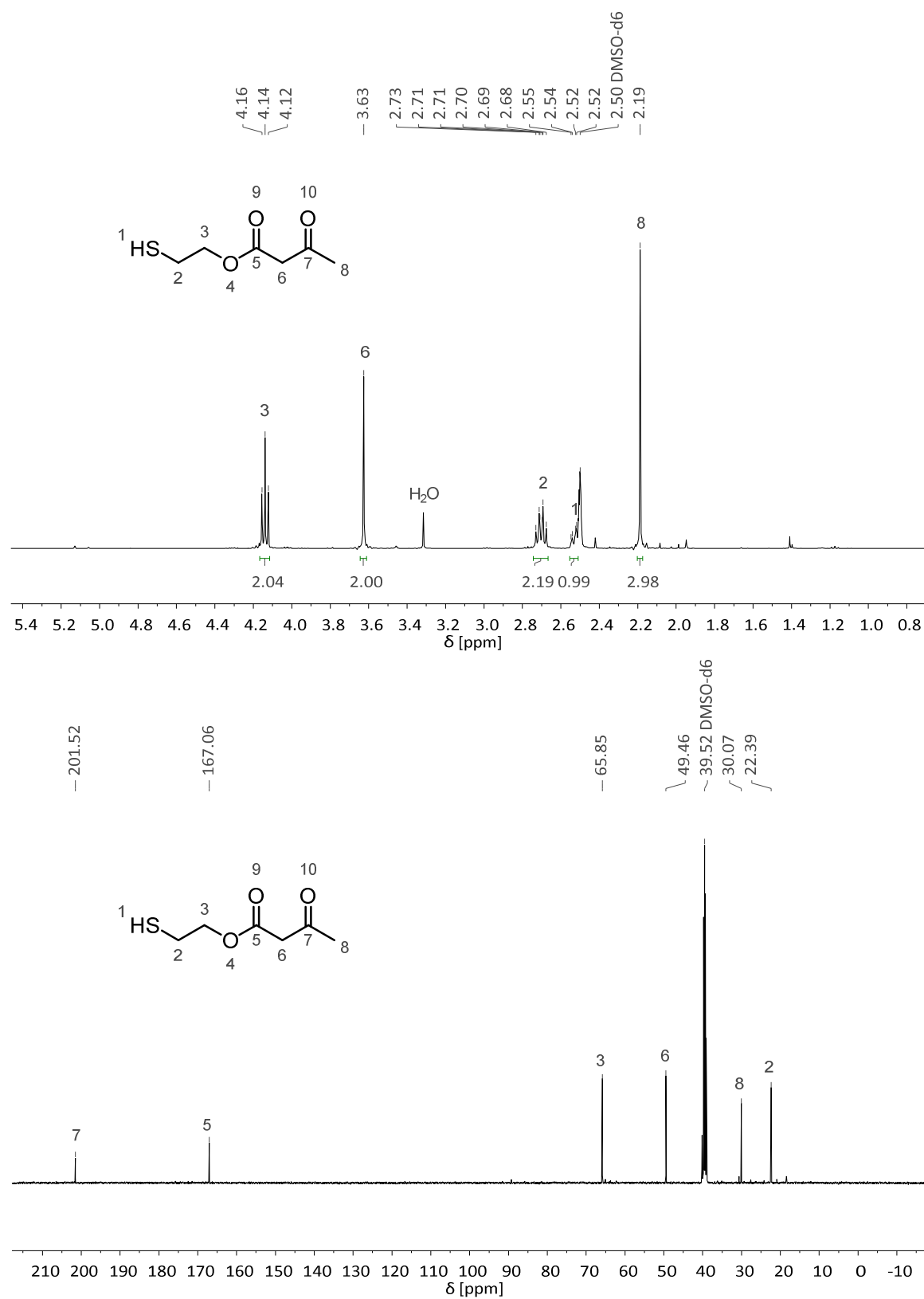
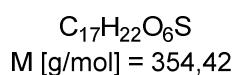
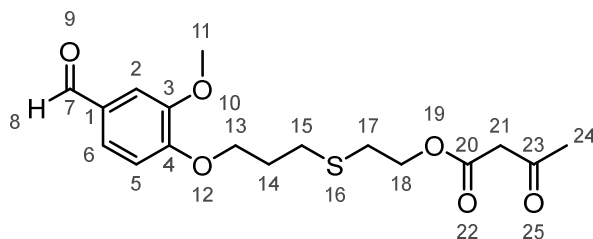


Figure 6.41 ¹H and ¹³C NMR spectra of **140** in DMSO-*d*₆.

6.4.1.4 2-{{3-(4-Formyl-2-methoxyphenoxy)propyl}thio}ethyl acetoacetate (141)

4-(Allyloxy)-3-methoxybenzaldehyde (47.4 mmol, 1.00 eq), 2-mercaptoethyl acetoacetate (1.00 eq), and 2,2-dimethoxy-1,2-diphenylethan-1-one (0.01 eq) were mixed. The mixture was stirred over night under UV irradiation (365 nm, 15 W). The resulting mixture was subjected to column chromatography using a mixture of *c*-C₆H₁₂ and EtOAc.

yield	85% (14.3 g, 40.3 mmol, slightly yellow oil)
eluent	<i>c</i> -C ₆ H ₁₂ :EtOAc = 60:40
R _f (product)	0.31 in <i>c</i> -C ₆ H ₁₂ :EtOAc = 50:50

¹H-NMR (400 MHz, DMSO-*d*₆): δ (ppm) = 9.84 (s, 1H, H₈), 7.54 (dd, ³J_{H₆,H₅} = 8.2 Hz, ⁴J_{H₆,H₂} = 1.9 Hz, 1H, H₆), 7.39 (d, ⁴J_{H₂,H₆} = 1.9 Hz, 1H, H₂), 7.18 (d, ³J_{H₅,H₆} = 8.3 Hz, 1H, H₅), 4.20 (t, ³J_{H₁₈,H₁₇} = 6.7 Hz, 2H, H₁₈), 4.15 (t, ³J_{H₁₃,H₁₄} = 6.3 Hz, 2H, H₁₃), 3.83 (s, 3H, H₁₁), 3.60 (s, 2H, H₂₁), 2.76 (t, ³J_{H₁₇,H₁₈} = 6.7 Hz, 2H, H₁₇), 2.70 (t, ³J_{H₁₅,H₁₄} = 7.3 Hz, 2H, H₁₅), 2.17 (s, 3H, H₂₄), 2.05 – 1.96 (m, 3H, H₁₄).

¹³C-NMR (101 MHz DMSO-*d*₆): δ (ppm) = 201.42 (C₂₃), 191.40 (C₇), 167.13 (C₂₀), 153.41 (C₄), 149.29 (C₃), 129.69 (C₁), 126.04 (C₆), 112.21 (C₅), 109.74 (C₂), 66.96 (C₁₃), 63.66 (C₁₈), 55.59 (C₁₁), 49.50 (C₂₁), 30.06 (C₂₄), 29.43 (C₁₇), 28.64 (C₁₄), 27.59 (C₁₅).

IR: ν (cm⁻¹) = 3010, 2927, 2856, 1719, 1639, 1453, 1410, 1359, 1317, 1296, 1239, 1152, 1029, 942, 879, 846, 814, 726, 651, 603, 542, 491.

HRMS (FAB): m/z for C₁₇H₂₂O₆S⁺ [M]⁺: calculated: 354.1132; found: 354.1132.

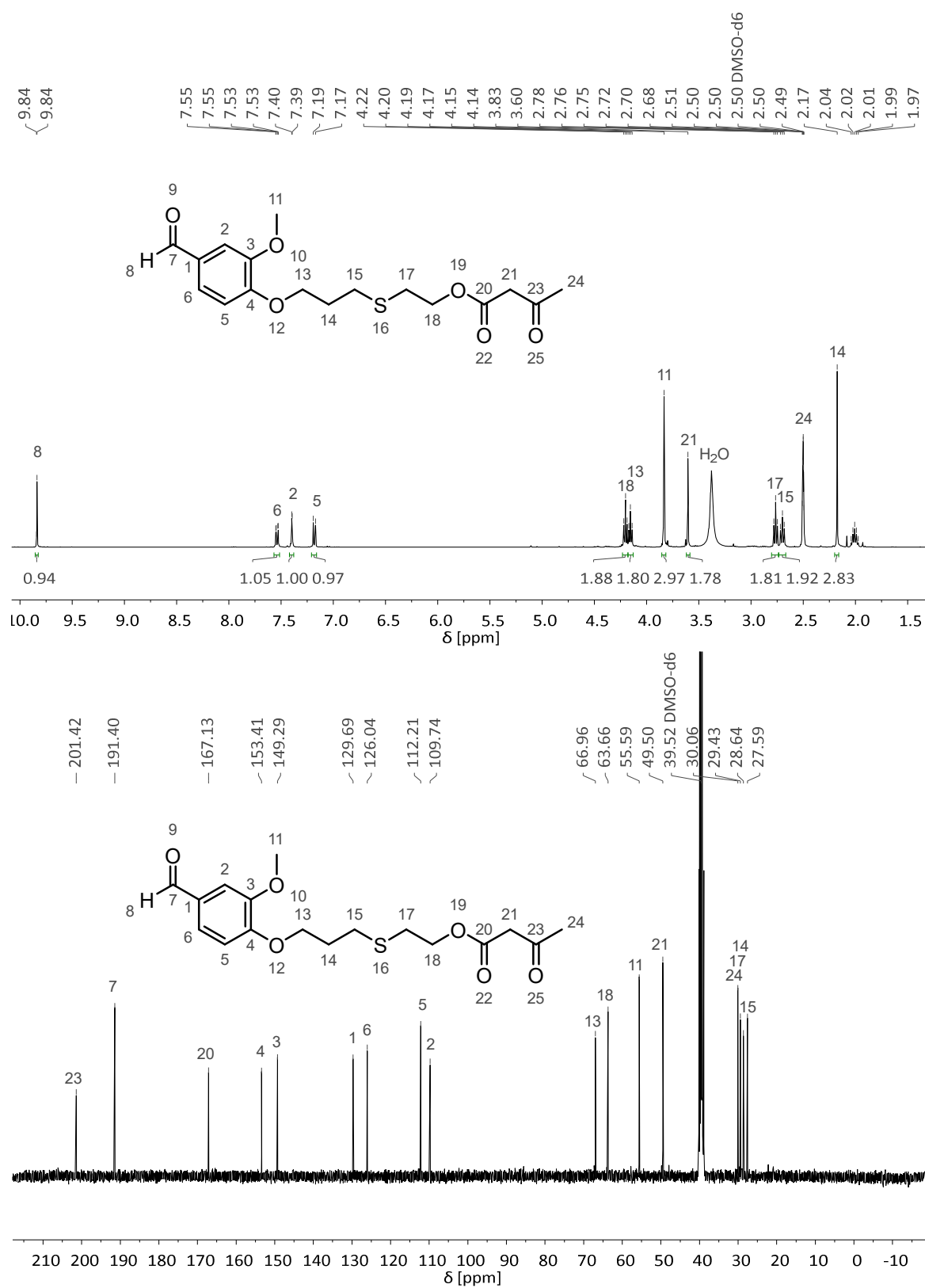
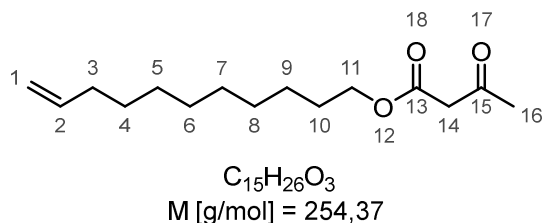


Figure 6.42 ^1H and ^{13}C NMR spectra of **141** in DMSO-d_6 .

6.4.1.5 10-Undecenyl-1-acetoacetate (143)

10-undecenyl-1-ol (130 mmol, 1.00 eq) was mixed with *t*-butyl acetoacetate (2.50 eq) and stirred in a preheated oil bath at 150°C for 7 h. Evolving *t*-BuOH was continuously removed *via* distillation. Afterwards, the crude product was purified by column chromatography using a mixture of *c*-C₆H₁₂ and EtOAc.

yield	99% (29.4 g, 128 mmol, slightly yellow oil)
eluent	<i>c</i> -C ₆ H ₁₂ :EtOAc = 95:5 → 55:45
R _f (product)	0.85 in <i>c</i> -C ₆ H ₁₂ :EtOAc = 1:1

¹H-NMR (400 MHz, DMSO-*d*₆): δ (ppm) = 5.79 (ddt, ³J_{H2;H1cis/trans;H3} = 17.0, 10.2, 6.7 Hz, 1H, H₂), 5.05 – 4.89 (m, 2H, H₁), 4.03 (t, ³J_{H11;H10} = 6.6 Hz, 2H, H₁₁), 3.58 (s, 2H, H₁₄), 2.17 (s, 3H, H₁₆), 2.06 – 1.95 (m, 2H, H₃), 1.62 – 1.50 (m, 2H, H₁₀), 1.39 – 1.21 (br m, 12H, H₄₋₉).

¹³C-NMR (101 MHz DMSO-*d*₆): δ (ppm) = 201.53 (C₁₅), 167.27 (C₁₃), 138.82 (C₂), 114.62 (C₁), 64.40 (C₁₁), 49.57 (C₁₄), 33.15 (C₃), 30.04 (C₁₆), 28.85+28.73+28.55+28.46+28.24+27.99+25.22 (C₄₋₁₀).

IR: ν (cm⁻¹) = 2925, 2854, 1741, 1718, 1640, 1414, 1359, 1314, 1236, 1150, 1033, 993, 909, 800, 723, 629, 542, 1464, 846, 492.

HRMS (FAB): m/z for C₁₅H₂₆O₃H⁺ [M+H]⁺: calculated: 245.1955; found: 255.1956.

6.4 Synthesis Procedures and Analytical Data Related to Chapter 4.2

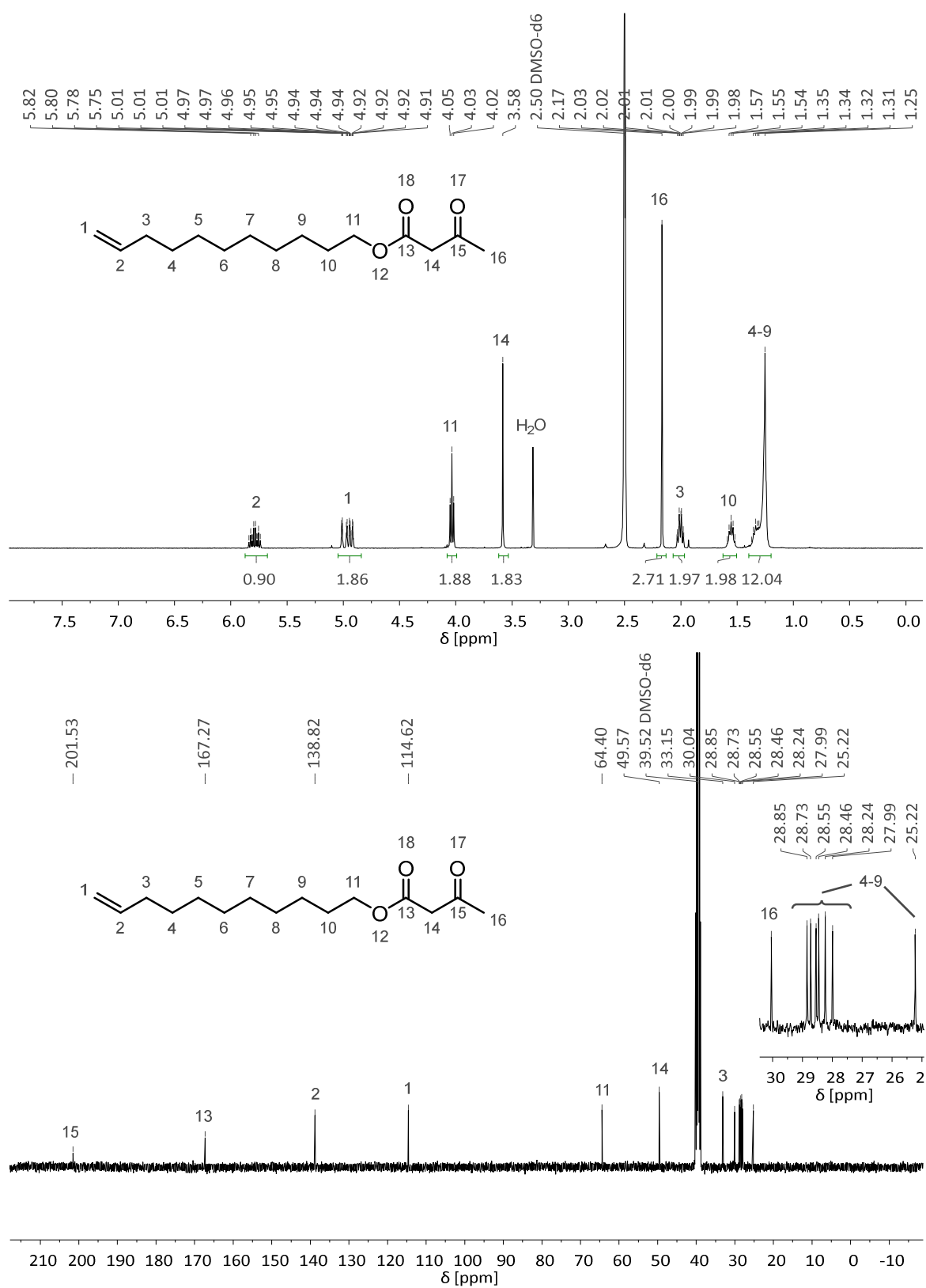
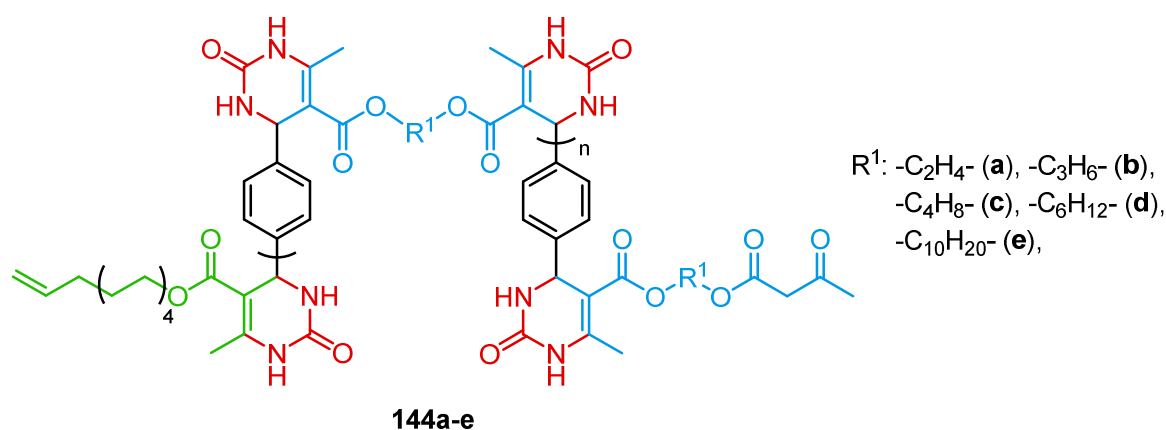


Figure 6.43 ^1H and ^{13}C NMR spectra of **143** in $\text{DMSO-}d_6$.

6.4.2 Poly[3,4 dihydropyrimidin 2(1*H*)-one]s

6.4.2.1 End Group-Functionalised Poly[3,4 dihydropyrimidin 2(1*H*)-one] Homopolymers (AA/BB system)



All end group functionalised polyDHPM homopolymers from diacetoacetates and terephthalic aldehyde were synthesised according to the same general procedure. Nevertheless, the solvent/solvent mixtures that were used for precipitation and washing differed depending on the polymer structure (details are shown for the respective polymer).

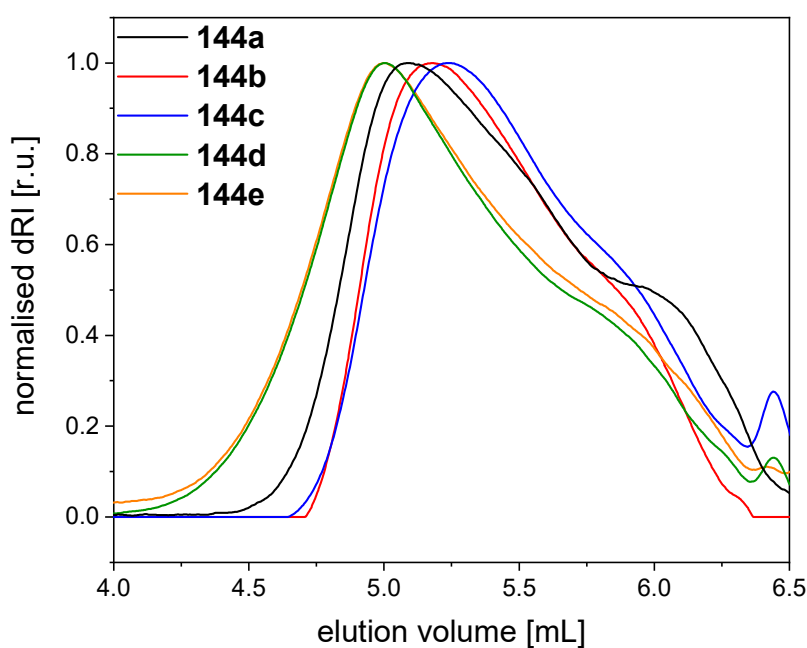
Urea (3.50 eq), the respective diacetoacetate (6.99 mmol, 1.00 eq), and 10-undecenyl-1-acetoacetate (0.05 eq) were mixed in DMSO (1 M solution regarding 1.00 eq). Afterwards, terephthalic aldehyde (1.00 eq) and *p*-toluenesulfonic acid (0.10 eq) were added. The mixture was immediately heated to 125°C on a preheated oil bath and stirred for 22.5 h. The flask was left open to allow water to evaporate. Afterwards, the polymer solution was precipitated into 100 ml of the respective solvent/solvent mixture and stirred for 3 h. Subsequently, the precipitated polymer was filtered and washed with the same solvent/solvent mixture. The resulting material was dried in a vacuum drying oven over night at 85°C under reduced pressure resulting in the final product.

Summarised analytics are given as follows.

Table 6.10 SEC and DSC data and yields of end group functionalised polyDHPMs **144a-e** from diacetoacetates **124a-e**.

polymer	R ¹	$M_{n,NMR}^a$ [g·mol ⁻¹]	$M_{n,SEC}$ [g·mol ⁻¹]	$M_{w,SEC}$ [g·mol ⁻¹]	\mathcal{D}	T_g^b [°C]	Yield ^c [%]
144a	C ₂ H ₄	4 200	4 500	16 400	3.68	268	76
144b	C ₃ H ₆	3 900	4 500	14 000	3.01	244	73
144c	C ₄ H ₈	4 300	5 700	14 700	2.52	242	75
144d	C ₆ H ₁₂	4 700	6 800	28 800	4.21	203	70
144e	C ₁₀ H ₂₀	5 300	6 900	29 600	4.32	176	69

^acalculated by integration of aldehyde and terminal double bond end group signals relative to the signal of the CH-protons of the polyDHPM ring; ^bthe inflection point of the DSC curve was chosen as T_g ; ^cisolated yields.

**Figure 6.44** SEC chromatograms of end group functionalised polyDHPMs **144a-e**.

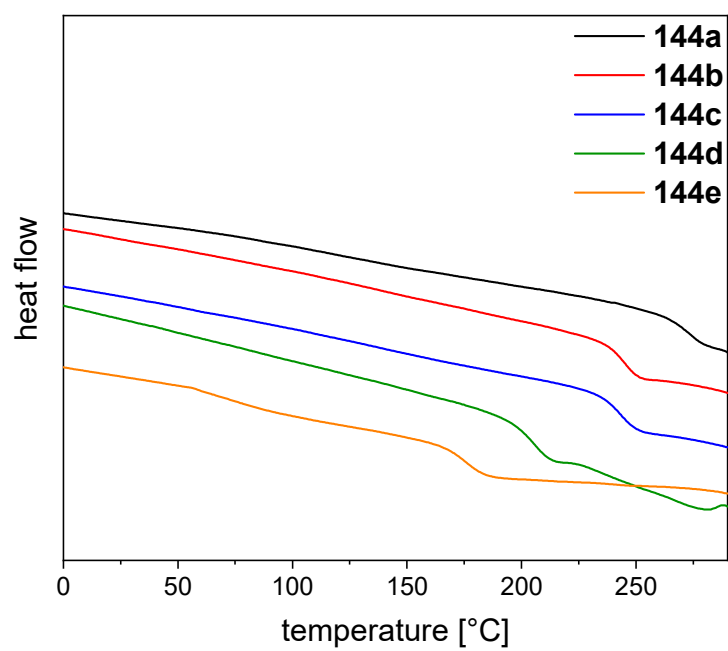


Figure 6.45 DSC curves of end group functionalised polyDHMPs **144a-e** showing the respective T_g s.

144a

Precipitated in and washed with MeOH.

$^1\text{H-NMR}$ (400 MHz, $\text{DMSO-}d_6$): δ (ppm) = 9.22 (s, H_a), 7.72 (s, $\text{H}_{a'}$), 7.17 (s, H_d), 5.84 – 5.72 (m, $\text{H}_{z'}$), 5.11 (s, H_c), 4.98 – 4.89 (m, H_z), 4.32 – 3.93 (br, H_e), 2.34 – 2.08 (br, H_b).

IR: ν (cm^{-1}) = 3252, 2949, 1685, 1640, 1435, 1381, 1311, 1223, 1078, 758, 658, 505.

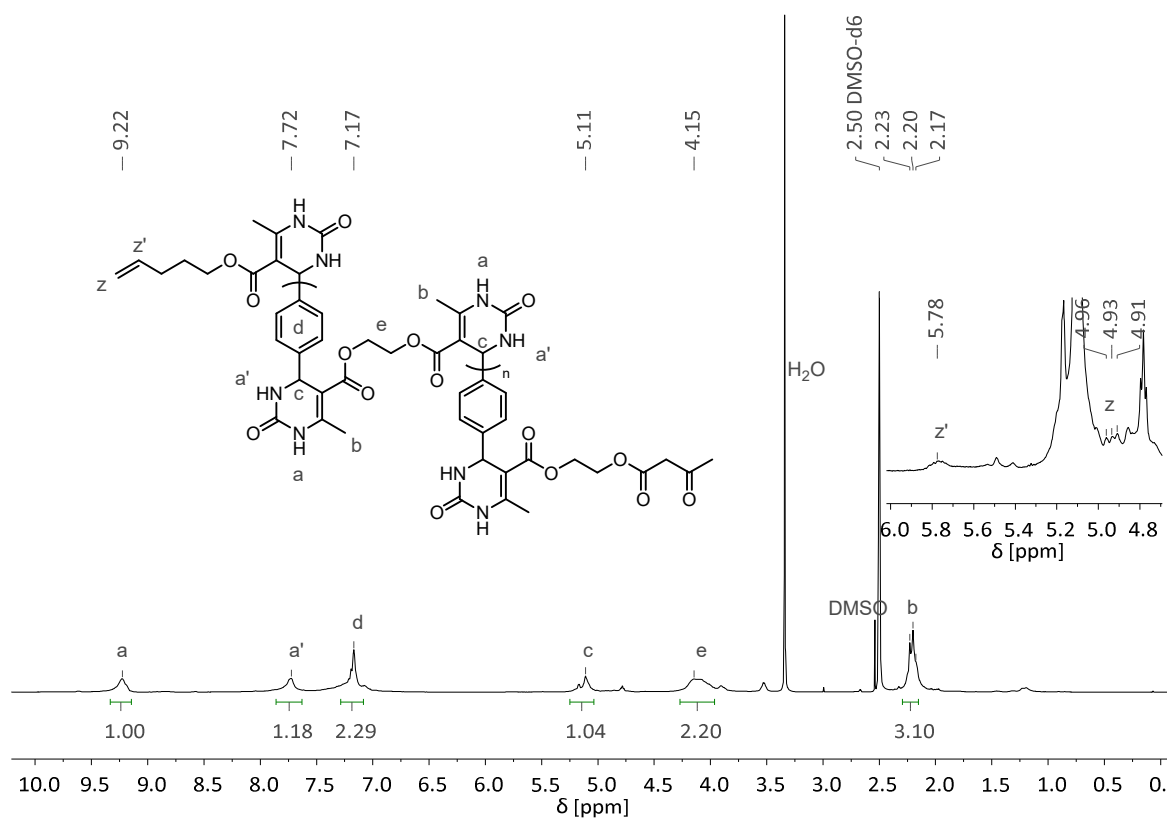


Figure 6.46 $^1\text{H-NMR}$ spectrum of **144a** in $\text{DMSO-}d_6$.

144b

Precipitated in and washed with MeOH.

$^1\text{H-NMR}$ (400 MHz, $\text{DMSO-}d_6$): δ (ppm) = 9.19 (s, H_a), 7.66 (s, $\text{H}_{a'}$), 7.16 (s, H_d), 5.85 – 5.70 (m, $\text{H}_{z'}$), 5.10 (s, H_c), 4.97 – 4.88 (m, H_z), 4.06 – 3.79 (br s, H_e), 2.22 (s, H_b), 1.81 – 1.59 (br, H_f).

IR: ν (cm^{-1}) = 3240, 2955, 1690, 1640, 1448, 1383, 1312, 1223, 1081, 949, 758, 666, 507, 458.

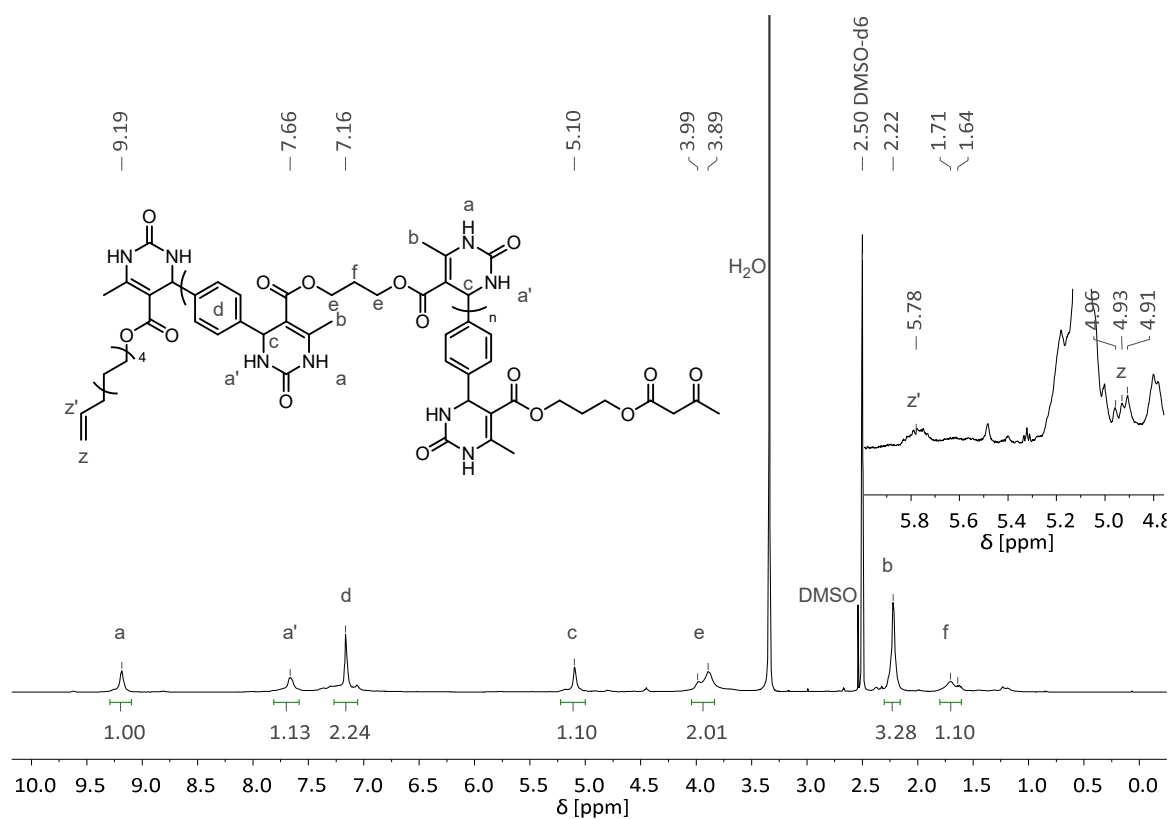


Figure 6.47 ^1H NMR spectrum of **144b** in $\text{DMSO-}d_6$.

144c

Precipitated in and washed with MeOH.

$^1\text{H-NMR}$ (400 MHz, $\text{DMSO-}d_6$): δ (ppm) = 9.18 (s, H_a), 7.68 (s, $\text{H}_{a'}$), 7.16 (s, H_d), 5.82 – 5.72 (m, $\text{H}_{z'}$), 5.09 (s, H_c), 4.97 – 4.89 (m, H_z), 4.06 – 3.73 (br, H_e), 2.23 (s, H_b), 1.59 – 1.19 (br, H_f).

IR: ν (cm^{-1}) = 3252, 2955, 1689, 1642, 1446, 1384, 1313, 1224, 1082, 942, 757, 659, 510.

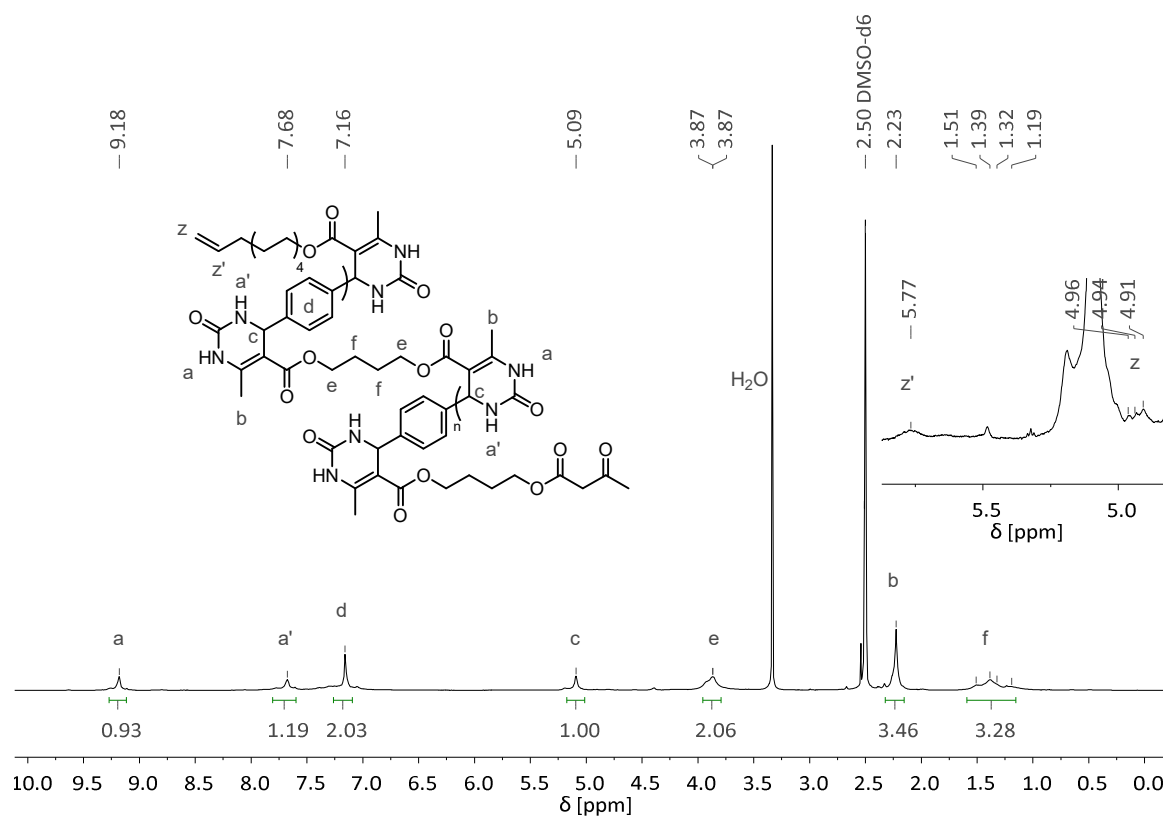


Figure 6.48 $^1\text{H-NMR}$ spectrum of **144c** in $\text{DMSO-}d_6$.

144d

Precipitated in and washed with MeOH.

¹H-NMR (400 MHz, DMSO-*d*₆): δ (ppm) = 9.17 (s, H_a), 7.66 (s, H_{a'}), 7.16 (s, H_d), 5.85 – 5.71 (m, H_{z'}), 5.10 (s, H_c), 4.98 – 4.89 (m, H_z), 3.90 (s, H_e), 2.23 (s, H_b), 1.54 – 1.04 (br, H_f).

IR: ν (cm⁻¹) = 3232, 2934, 1683, 1637, 1432, 1383, 1312, 1223, 1084, 1018, 758, 663, 505.

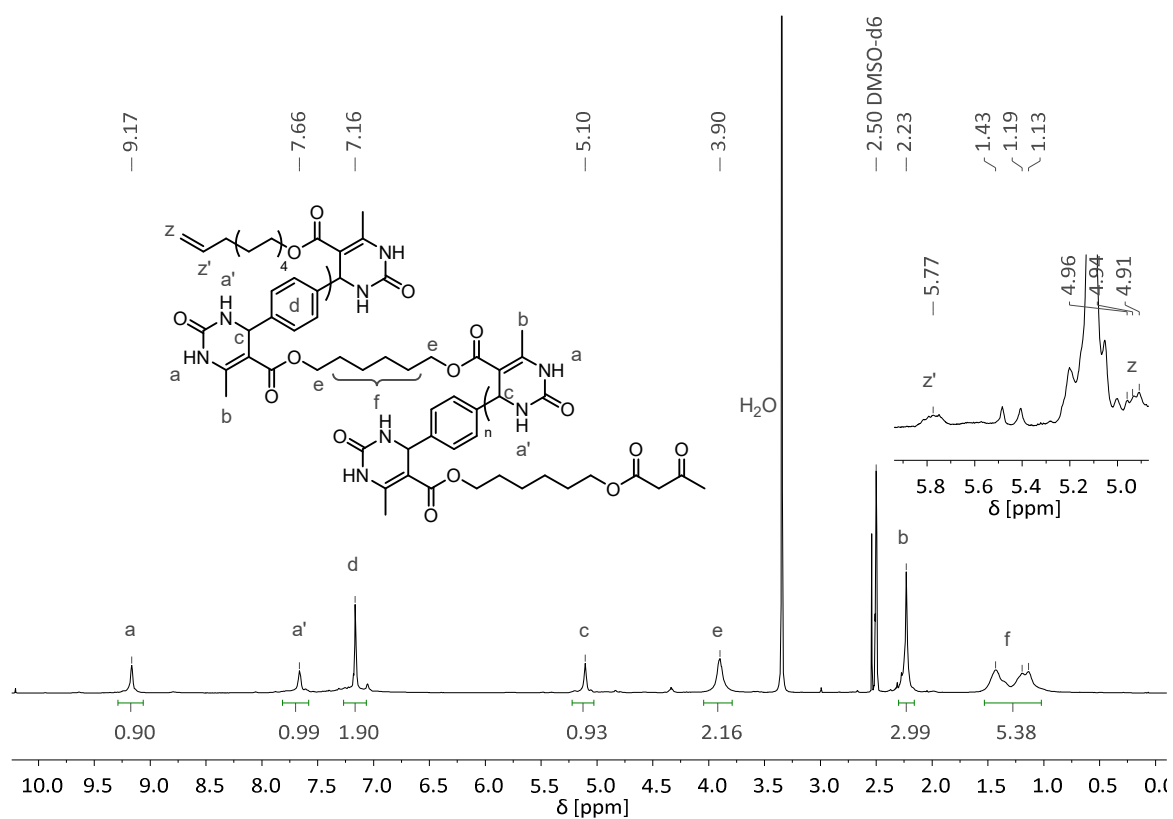


Figure 6.49 ¹H NMR spectrum of 144d in DMSO-*d*₆.

144e

Precipitated in and washed with MeOH.

¹H-NMR (400 MHz, DMSO-*d*₆): δ (ppm) = 9.18 (s, H_a), 7.68 (s, H_{a'}), 7.15 (s, H_d), 5.85 – 5.71 (m, H_{z'}), 5.09 (s, H_c), 4.97 – 4.88 (m, H_z), 4.05 – 3.77 (br, H_e), 2.23 (s, H_b), 1.66 – 0.99 (br, H_f).

IR: ν (cm⁻¹) = 3237, 2926, 2853, 2036, 1682, 1635, 1431, 1383, 1309, 1220, 1082, 1018, 756, 659, 503, 429.

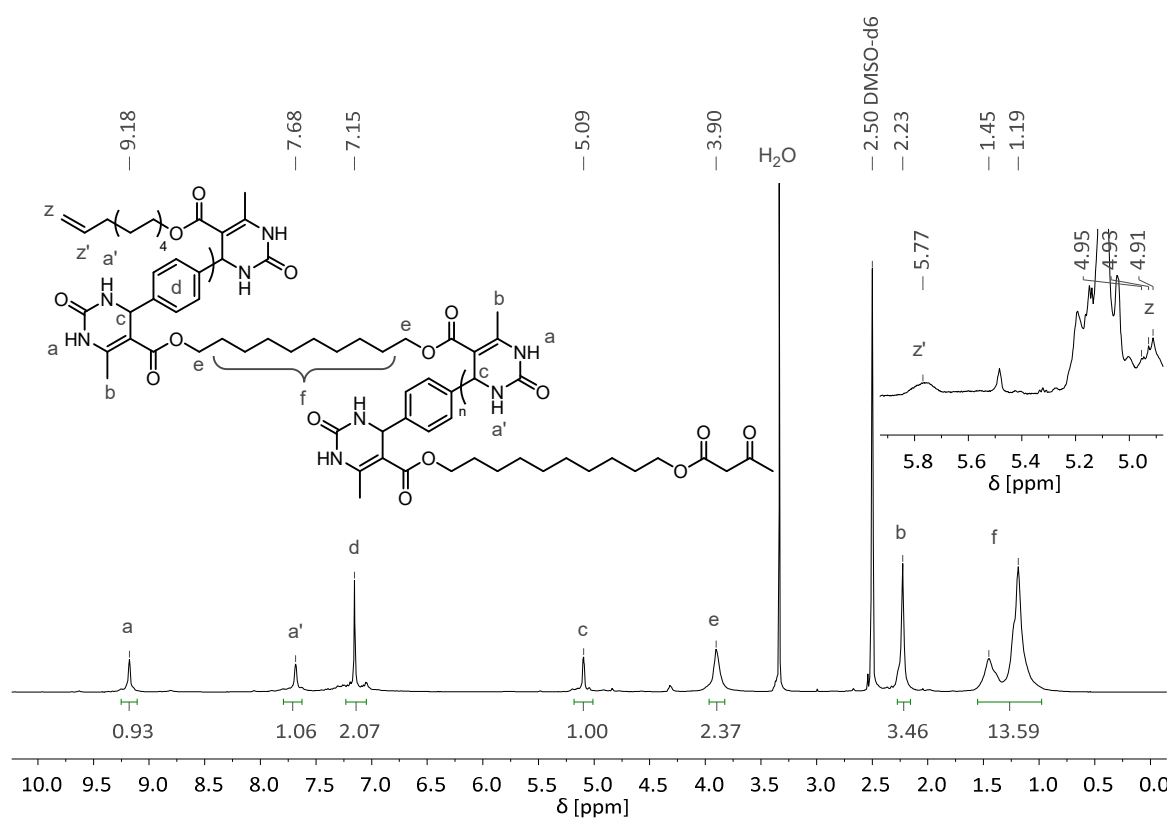


Figure 6.50 ¹H NMR spectrum of 144e in DMSO-*d*₆.

6.4.2.2 Poly[3,4 dihydropyrimidin 2(1*H*)-one] Homopolymers (AB system)

The two polyDHPMs using **141** as monomer were synthesised in a similar fashion. End group functionalisation was enabled by addition of 10-undecenyl-1-acetoacetate to the reaction mixture. The detailed synthesis procedures are given below. Summarized analytics are given as follows:

Table 6.11 Analytical data (SEC, DSC, NMR, yield) of polyDHPMs **144f**.

polymer	$M_{n,NMR}^a$ [g·mol ⁻¹]	$M_{n,SEC}$ [g·mol ⁻¹]	$M_{w,SEC}$ [g·mol ⁻¹]	\bar{D}	T_g^b [°C]	Yield ^c [%]
144f^d	10 100	7 100	20 900	2.95	94	81
144f^e	7 100	5 000	17 300	3.46	59	86

^acalculated by integration of aldehyde and terminal double bond end group signals; ^bthe inflection point of the DSC curve was chosen as T_g ; ^cisolated yields; ^dwithout end-capping agent **143**, ^e5 mol% of **143**.

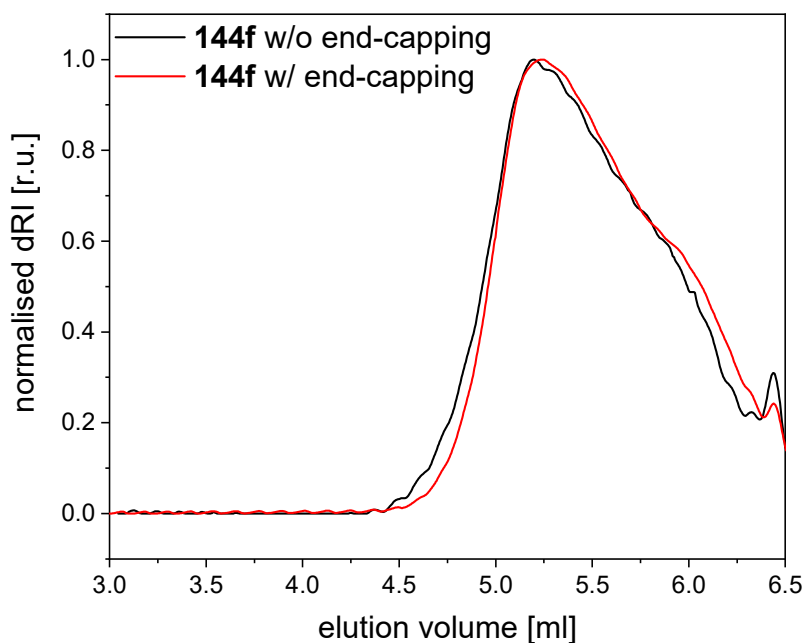


Figure 6.51 SEC chromatograms of polyDHPMs **144f** with and without end-capping.

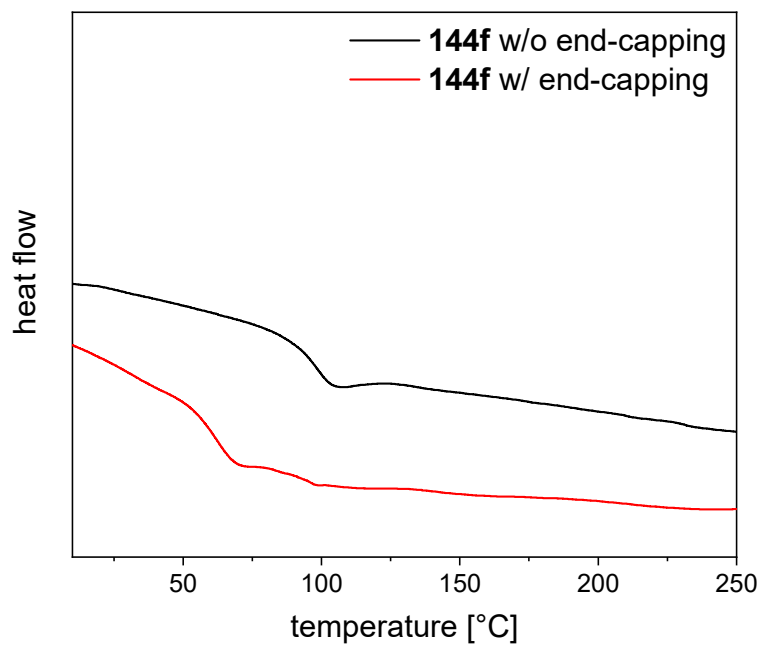
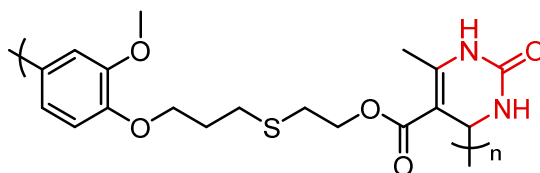


Figure 6.52 DSC curves showing the respective T_g s of the end group functionalised polyDHMPs **144f** with and without end-capping.

144f (without end group functionalisation)

Urea (1.75 eq) and 2-{[3-(4-formyl-2-methoxyphenoxy)propyl]thio}ethyl acetoacetate (0.461 mmol, 1.00 eq) were mixed in DMSO (1 M solution regarding 1.00 eq). Afterwards, *p*-toluenesulfonic acid (0.10 eq) was added. The mixture was immediately heated to 125°C on a preheated oil bath and stirred for 22.5 h. The flask was left open to allow water to evaporate. Afterwards, the polymer solution was precipitated into 30 ml of MeOH and stirred for 3 h. Subsequently, the precipitated polymer was filtered and washed with MeOH. The resulting material was dried in a vacuum drying oven over night at 85°C under reduced pressure resulting in the final product in form of a yellow powder in a yield of 79%.

¹H-NMR (400 MHz, DMSO-*d*₆): δ (ppm) = 9.19 (s, H_a), 7.69 (s, H_{a'}), 6.97 – 6.80 (m, H_d), 6.78 – 6.65 (m, H_{d'}), 5.10 (d, ³J_{H_c,H_a} = 2.9 Hz, H_c), 4.23 – 4.01 (br, H_j), 4.01 – 3.87 (br, H_f), 3.70 (s, H_e), 2.73 – 2.64 (br, H_i), 2.64 – 2.57 (br, H_h), 2.25 (s, H_b), 1.94 – 1.83 (br, H_g).

IR: ν (cm⁻¹) = 3237, 2926, 2853, 2036, 1682, 1635, 1431, 1383, 1309, 1220, 1082, 1018, 756, 659, 503, 429.

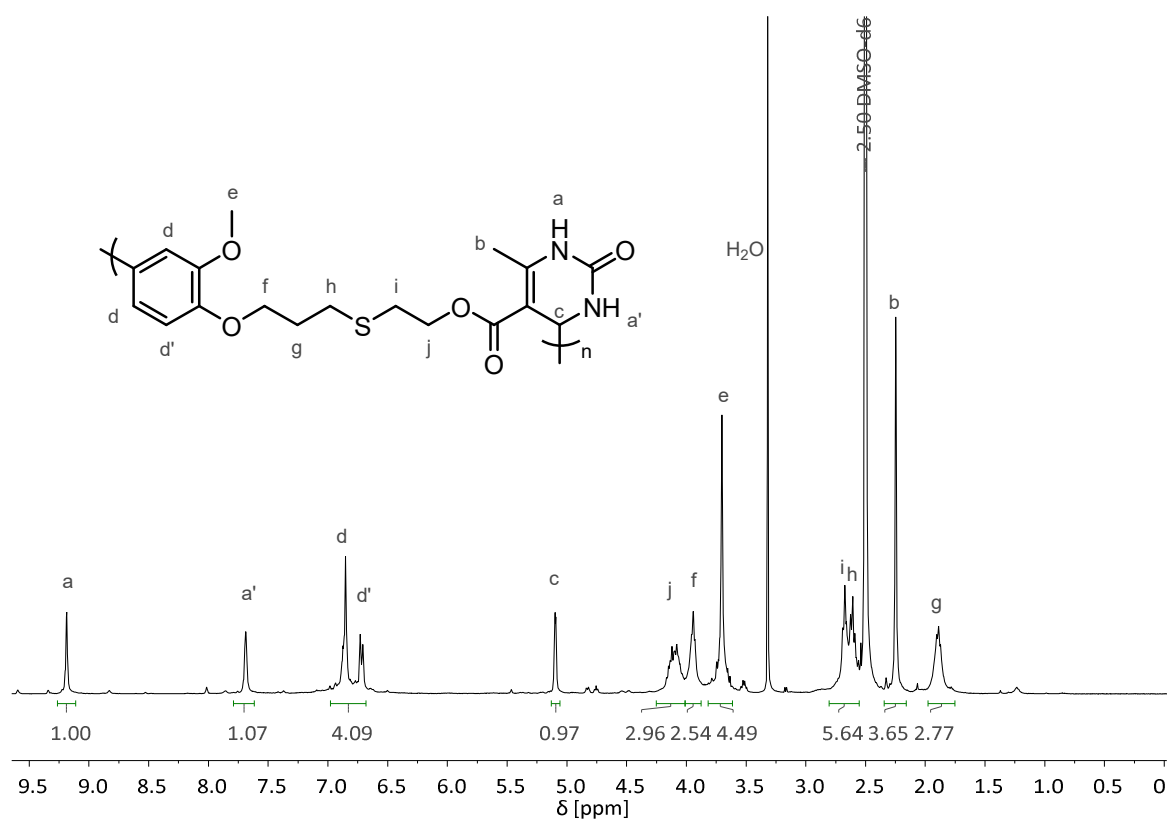
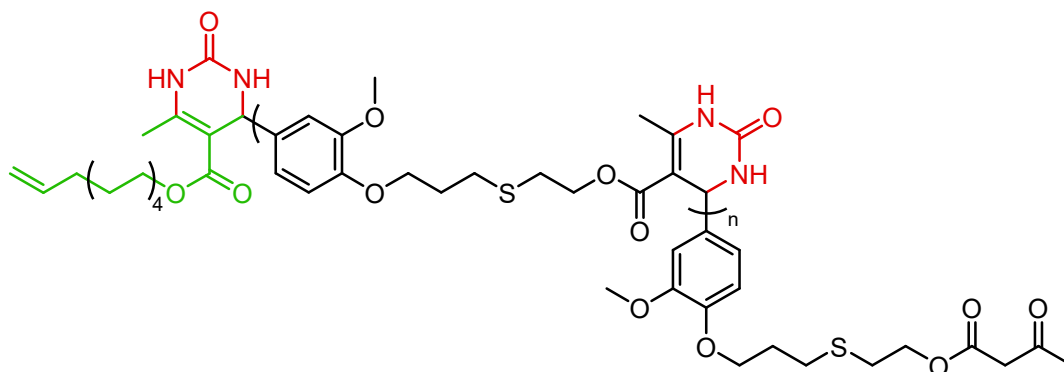


Figure 6.53 ^1H NMR spectrum of **144f** in $\text{DMSO-}d_6$.

144f (with end group functionalisation)

Urea (1.75 eq), 2-{{[3-(4-formyl-2-methoxyphenoxy)propyl]thio}ethyl acetoacetate (0.461 mmol, 1.00 eq) and 10-undecenyl-1-acetoacetate (0.05 eq) were mixed in DMSO (1 M solution regarding 1.00 eq). Afterwards, *p*-toluenesulfonic acid (0.10 eq) was added. The mixture was immediately heated to 125°C on a preheated oil bath and stirred for 22.5 h. The flask was left open to allow water to evaporate. Afterwards, the polymer solution was precipitated into 30 ml of MeOH and stirred for 3 h. Subsequently, the precipitated polymer was filtered and washed with MeOH. The resulting material was dried in a vacuum drying oven over night at 85°C under reduced pressure resulting in the final product in form of a yellow powder in a yield of 81%.

¹H-NMR (400 MHz, DMSO-*d*₆): δ (ppm) = 9.19 (s, H_a), 7.69 (s, H_{a'}), 6.95 – 6.80 (m, H_d), 6.79 – 6.66 (m, H_{d'}), 5.84 – 5.72 (m, H_{z'}), 5.09 (d, ³*J*_{H_c,H_a} = 2.8 Hz, H_c), 4.98 – 4.89 (m, H_z), 4.23 – 4.03 (br, H_j), 4.03 – 3.89 (br, H_f), 3.70 (s, H_e), 2.76 – 2.64 (br, H_i), 2.65 – 2.57 (br, H_h), 2.25 (s, H_b), 1.98 – 1.76 (br, H_g).

IR: ν (cm⁻¹) = 3429, 3339, 3211, 3116, 2934, 1675, 1633, 1510, 1448, 1419, 1381, 1315, 1255, 1159, 1134, 1082, 1022, 951, 852, 756, 680, 636, 586, 561, 513, 465.

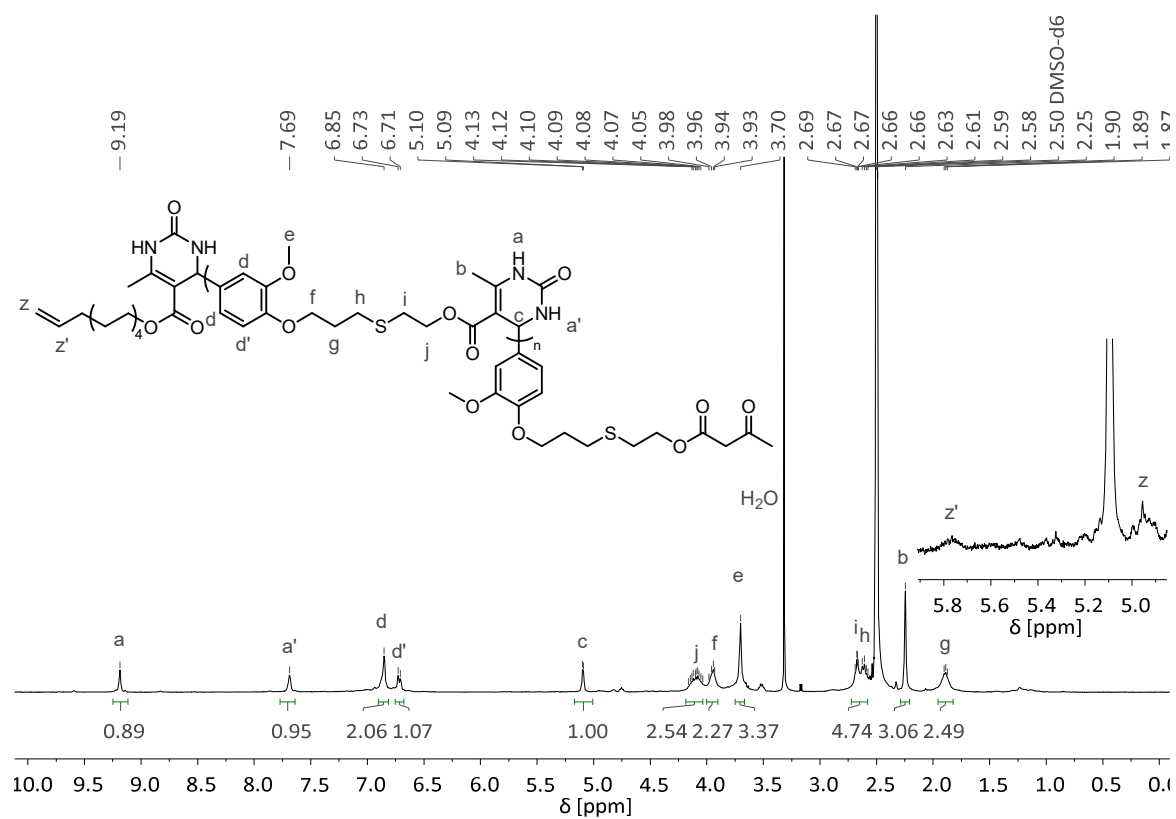
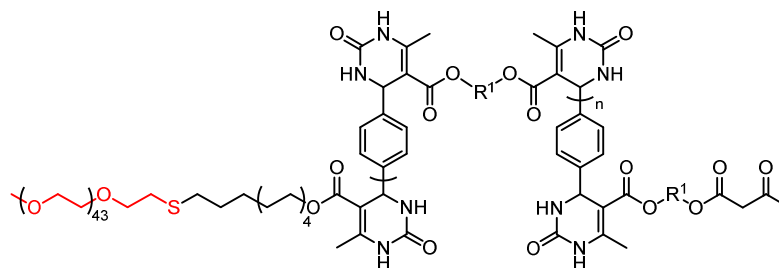
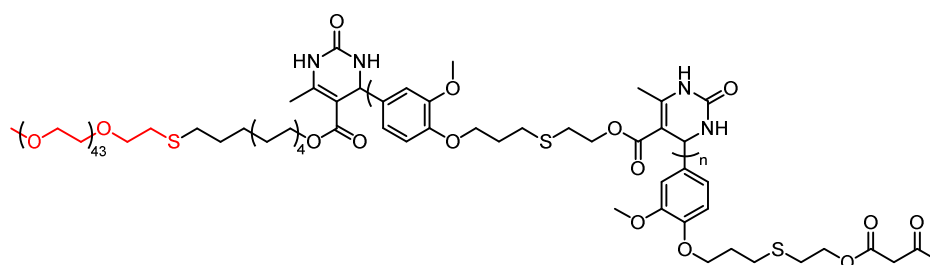


Figure 6.54 ^1H NMR spectrum of **144f** in $\text{DMSO-}d_6$.

6.4.2.3 Poly[3,4-dihydropyrimidin-2(1*H*)-one]-*b*-poly(ethylene glycol)s

144a-e

R¹: -C₂H₄- (a), -C₃H₆- (b), -C₄H₈- (c), -C₆H₁₂- (d), -C₁₀H₂₀- (e),



144f

All copolymerisations were conducted according to the same general procedure.

500 mg of the respective end group functionalized poly[3,4-dihydropyrimidin-2(1*H*)-one] were dissolved in 3.00 ml of DMSO. Afterwards, 0.01 eq 2,2-dimethoxy-2-phenylacetophenone and 1.5 eq of poly(ethylene glycol) methylether thiol ($M_n = 2\,000\text{ g}\cdot\text{mol}^{-1}$) with respect to terminal double bond end groups present were added.¹¹ The resulting mixture was stirred for 30 min at room temperature until the mixture was clear. Afterwards, the solution was stirred at room temperature for 48 h under UV-

¹¹ For the calculation of 1.00 eq, it was assumed that the 10-undecenyl-1-acetoacetate was completely incorporated in the end group functionalised polyDHPM. 1.00 eq is calculated as follows with the maximum moles of terminal double bonds $n(\text{DB}_{\text{max}})$ in the end-capped polyDHPM, the yield of end-capped polyDHPM after its synthesis $m(\text{polyDHPM}_{\text{yield}})$, and the used weight of end-capped polyDHPM for the copolymer synthesis $m(\text{polyDHPM})$:

$$1.00\text{ eq} \equiv \frac{n(\text{DB}_{\text{max}})}{m(\text{polyDHPM}_{\text{yield}})} \cdot m(\text{polyDHPM})$$

irradiation (365 nm, 15 W). Subsequent precipitation in water, and thorough washing with water led to the final polymer material as yellow to orange glassy solids.

Table 6.12 SEC and DSC data and yields of polyDHPM-*b*-poly(ethylene glycol)s **148a-f**.

polymer	R ¹	$M_{n,NMR}^a$ [g·mol ⁻¹]	$M_{n,SEC}$ [g·mol ⁻¹]	$M_{w,SEC}$ [g·mol ⁻¹]	\mathcal{D}	T_g/T_m^b [°C]	Yield ^c [%]
148a	C ₂ H ₄	5 700	5 700	18 600	3.27	265/49	76
148b	C ₃ H ₆	5 400	6 200	21 200	3.44	238/49	73
148c	C ₄ H ₈	5 800	5 900	14 700	2.51	232/49	75
148d	C ₆ H ₁₂	6 200	7 100	28 800	4.03	205/49	70
148e	C ₁₀ H ₂₀	6 700	8 900	53 700	6.00	159/52	69
148f^d	- ^e	4 400	11 800	30 300	2.56	56/-	76

^acalculated by integration of aldehyde end group signals and PEG signals; ^bthe inflection point of the DSC curve was chosen as T_g , the minimum as T_m ; ^cisolated yields; ^dprecipitated two times in acetone from DMSO and washed with water; ^eAB-monomer.

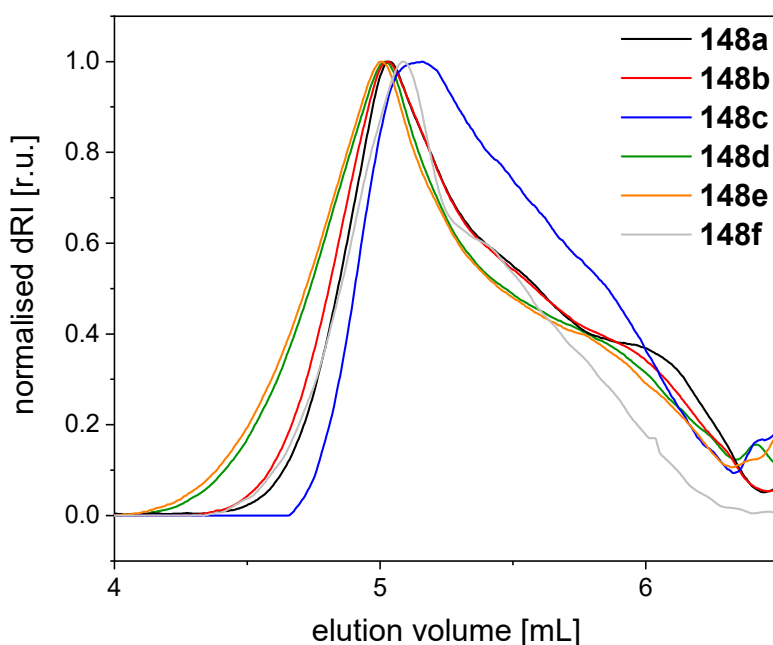


Figure 6.55 SEC chromatograms of the polyDHPM-*b*-poly(ethylene glycol)s **148a-f**.

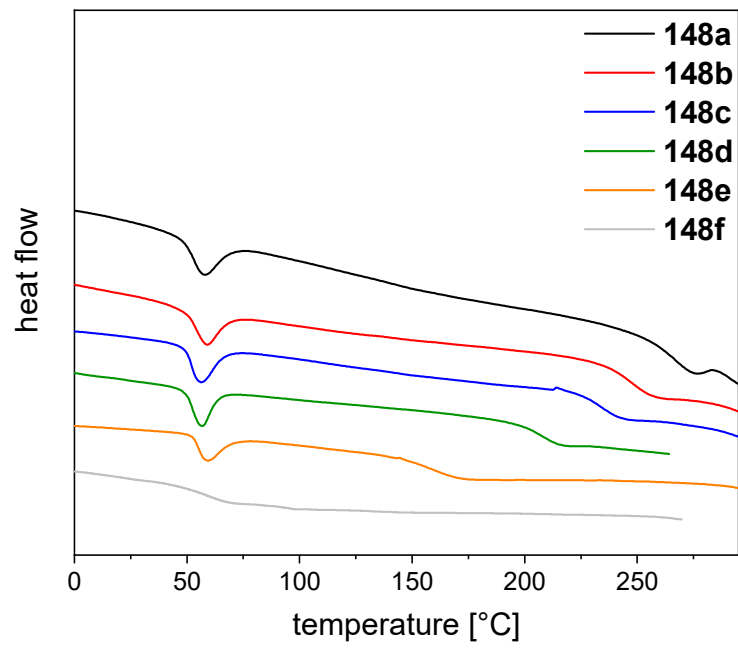


Figure 6.56 DSC curves showing the respective T_g s/ T_m s of the polyDHPM-*b*-poly(ethylene glycol)s **148a-f**.

148a

Precipitated in and washed with H₂O.

¹H-NMR (400 MHz, DMSO-*d*₆): δ (ppm) = 9.22 (s, H_a), 7.72 (s, H_{a'}), 7.17 (s, H_d), 5.28 – 5.00 (m, H_c), 4.27 – 3.96 (br, H_e), 3.51 (s, H_z), 2.23 (s, H_b).

IR: ν (cm⁻¹) = 3271, 3121, 2928, 1682, 1640, 1434, 1381, 1311, 1277, 1222, 1077, 758, 790, 659, 502.

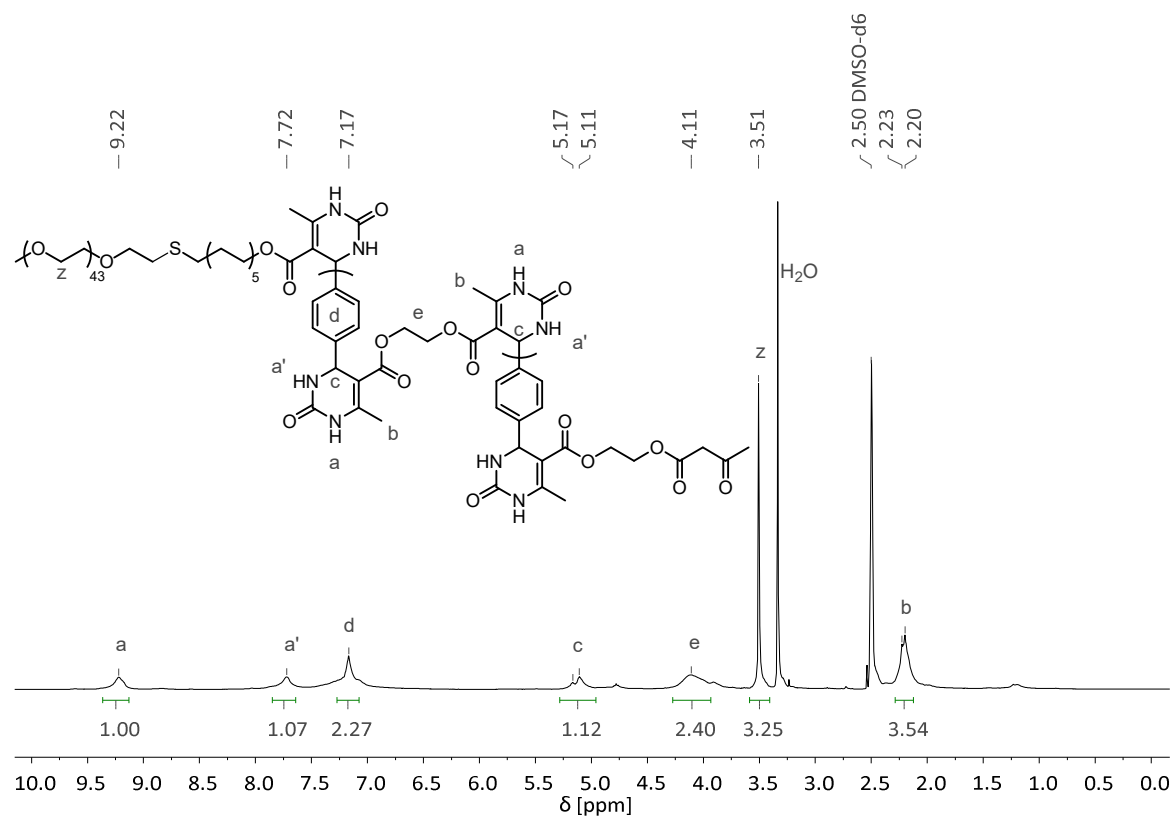


Figure 6.57 ¹H NMR spectrum of **148a** in DMSO-*d*₆.

148b

Precipitated in and washed with H₂O.

¹H-NMR (400 MHz, DMSO-*d*₆): δ (ppm) = 9.20 (s, H_a), 7.68 (s, H_{a'}), 7.17 (s, H_d), 5.09 (s, H_c), 4.10 – 3.78 (br, H_e), 3.51 (s, H_z), 2.23 (s, H_b), 1.78 – 1.56 (br, H_f).

IR: ν (cm⁻¹) = 3251, 3128, 2925, 1690, 1641, 1443, 1383, 1309, 1279, 1223, 1080, 802, 757, 659, 525, 452.

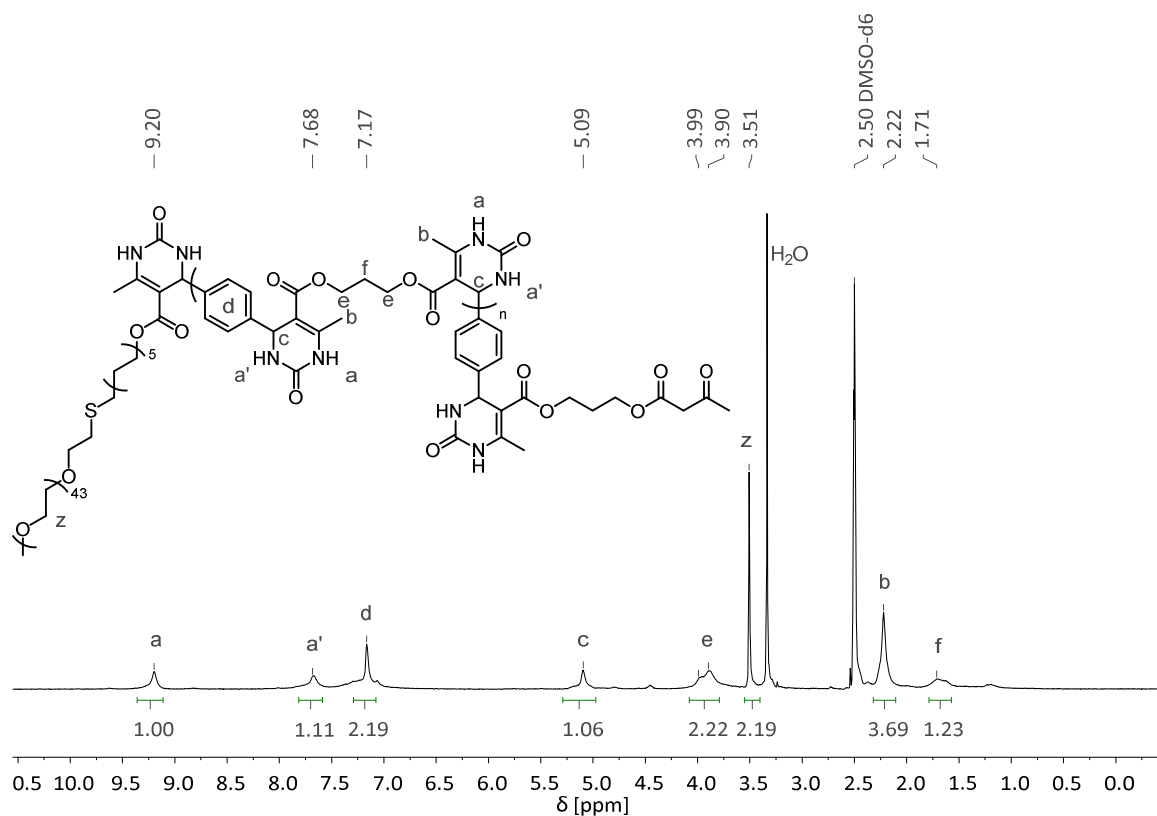


Figure 6.58 ¹H NMR spectrum of **148b** in DMSO-*d*₆.

148c

Precipitated in and washed with H₂O.

¹H-NMR (400 MHz, DMSO-*d*₆): δ (ppm) = 9.18 (s, H_a), 7.68 (s, H_{a'}), 7.16 (s, H_d), 5.09 (s, H_c), 3.99 – 3.77 (br, H_e), 3.51 (s, H_z), 2.23 (s, H_b), 1.60 – 1.08 (br, H_f).

IR: ν (cm⁻¹) = 3254, 2944, 1687, 1640, 1432, 1384, 1311, 1280, 1223, 1082, 943, 758, 662, 506.

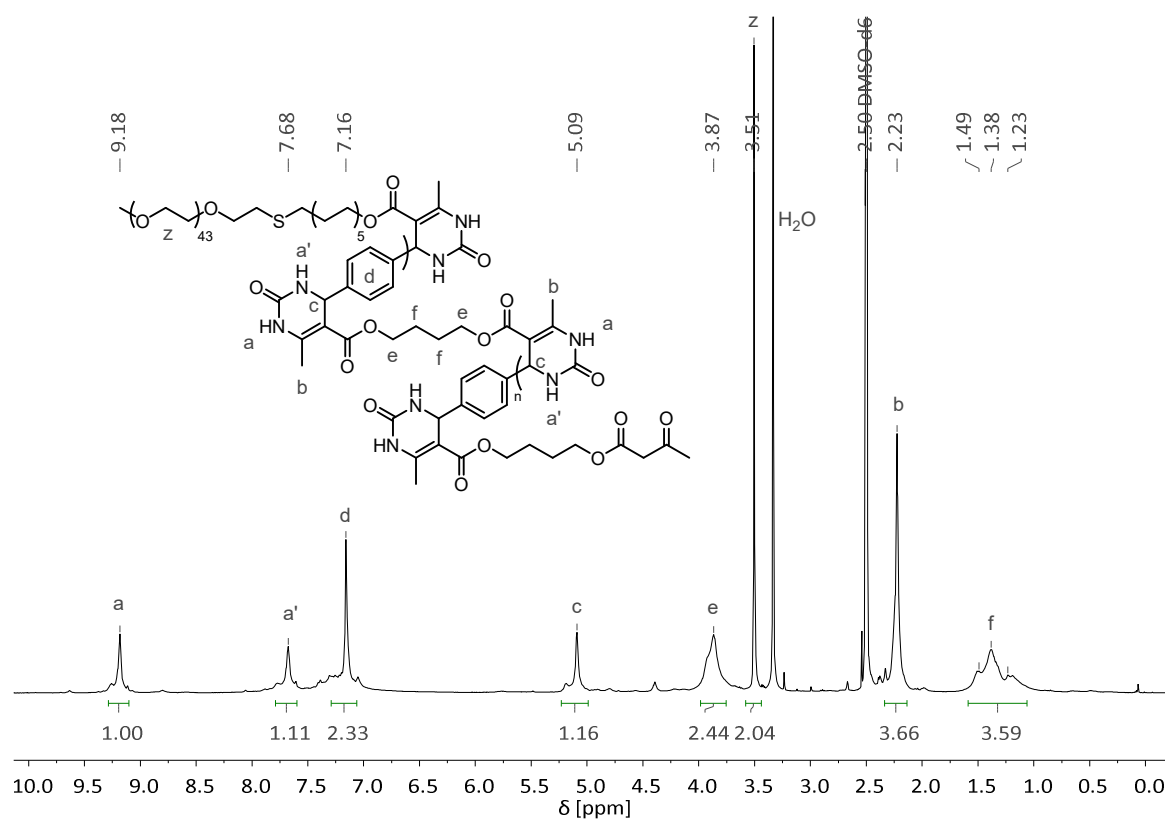


Figure 6.59 ¹H NMR spectrum of **148c** in DMSO-*d*₆.

148d

Precipitated in and washed with H₂O.

¹H-NMR (400 MHz, DMSO-*d*₆): δ (ppm) = 9.18 (s, H_a), 7.67 (s, H_{a'}), 7.16 (s, H_d), 5.10 (s, H_c), 3.90 (s, H_e), 3.51 (s, H_z), 2.23 (s, H_b), 1.58 – 0.94 (br, H_f).

IR: ν (cm⁻¹) = 3272, 3116, 2935, 2864, 1694, 1642, 1447, 1434, 1384, 1311, 1281, 1224, 1085, 970, 803, 758, 664, 510.

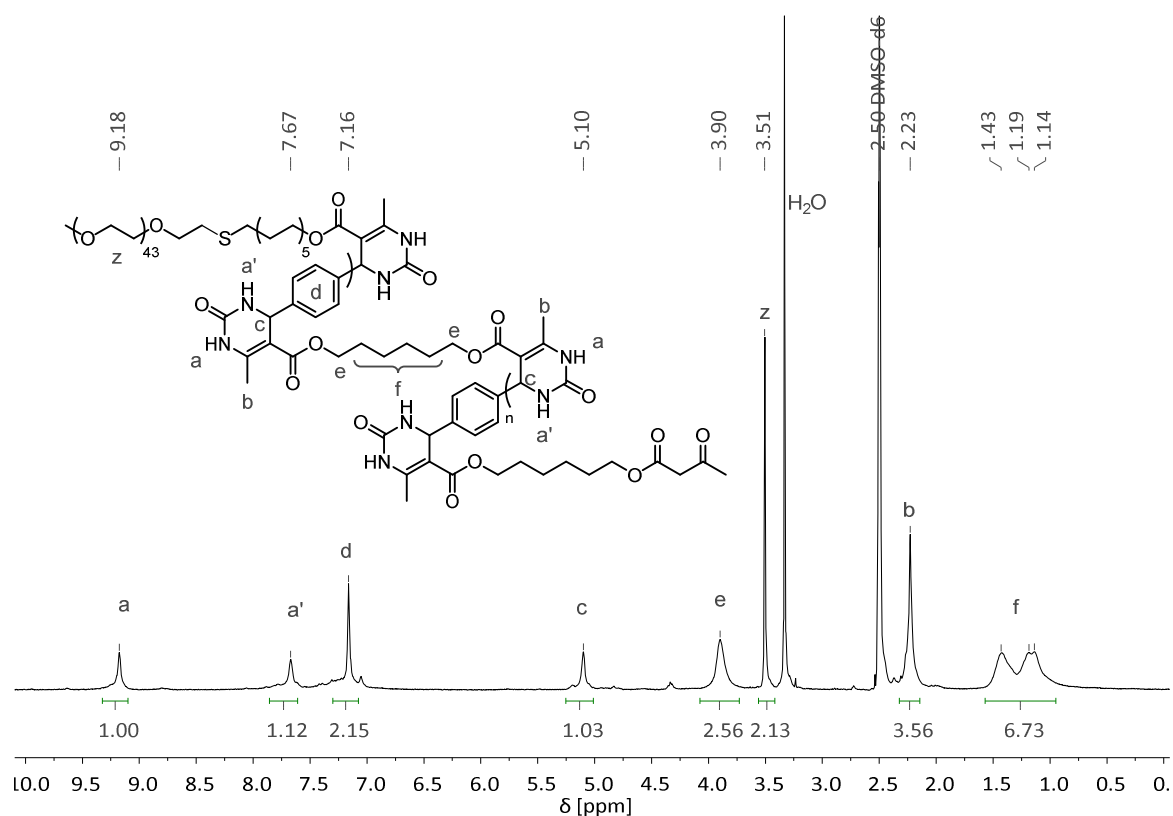


Figure 6.60 ¹H NMR spectrum of **148d** in DMSO-*d*₆.

148e

Precipitated in and washed with H₂O.

¹H-NMR (400 MHz, DMSO-*d*₆): δ (ppm) = 9.17 (s, H_a), 7.68 (s, H_{a'}), 7.15 (s, H_d), 5.10 (s, H_c), 3.90 (s, H_e), 3.51 (s, H_z), 2.23 (s, H_b), 1.60 – 1.03 (br, H_f).

IR: ν (cm⁻¹) = 3240, 2926, 2855, 1697, 1640, 1447, 1384, 1311, 1223, 1086, 1019, 952, 757, 662.

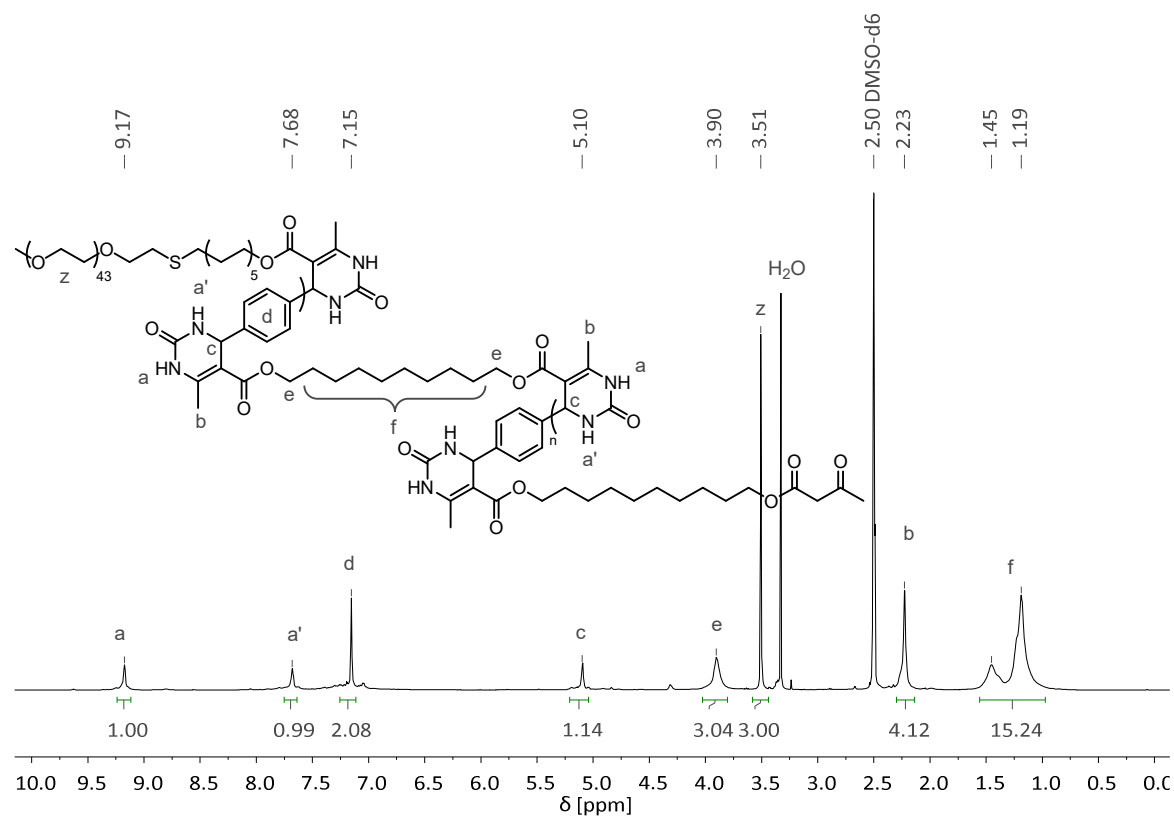


Figure 6.61 ¹H NMR spectrum of 148e in DMSO-*d*₆.

148f

Precipitated in acetone and washed with H₂O.

¹H-NMR (400 MHz, DMSO-*d*₆): δ (ppm) = 9.19 (s, H_a), 7.69 (s, H_{a'}), 6.95 – 6.80 (m, H_d), 6.79 – 6.66 (m, H_{d'}), 5.12 – 5.08 (m, H_c), 4.20 – 4.03 (br, H_j), 4.03 – 3.85 (br, H_f), 3.70 (s, H_e), 3.50 (s, H_z), 2.76 – 2.64 (br, H_i), 2.65 – 2.57 (br, H_h), 2.25 (s, H_b), 1.98 – 1.76 (br, H_g).

IR: ν (cm⁻¹) = 3259, 3112, 2923, 1681, 1638, 1509, 1449, 1420, 1381, 1255, 1221, 1134, 1081, 1023, 794, 755, 462.

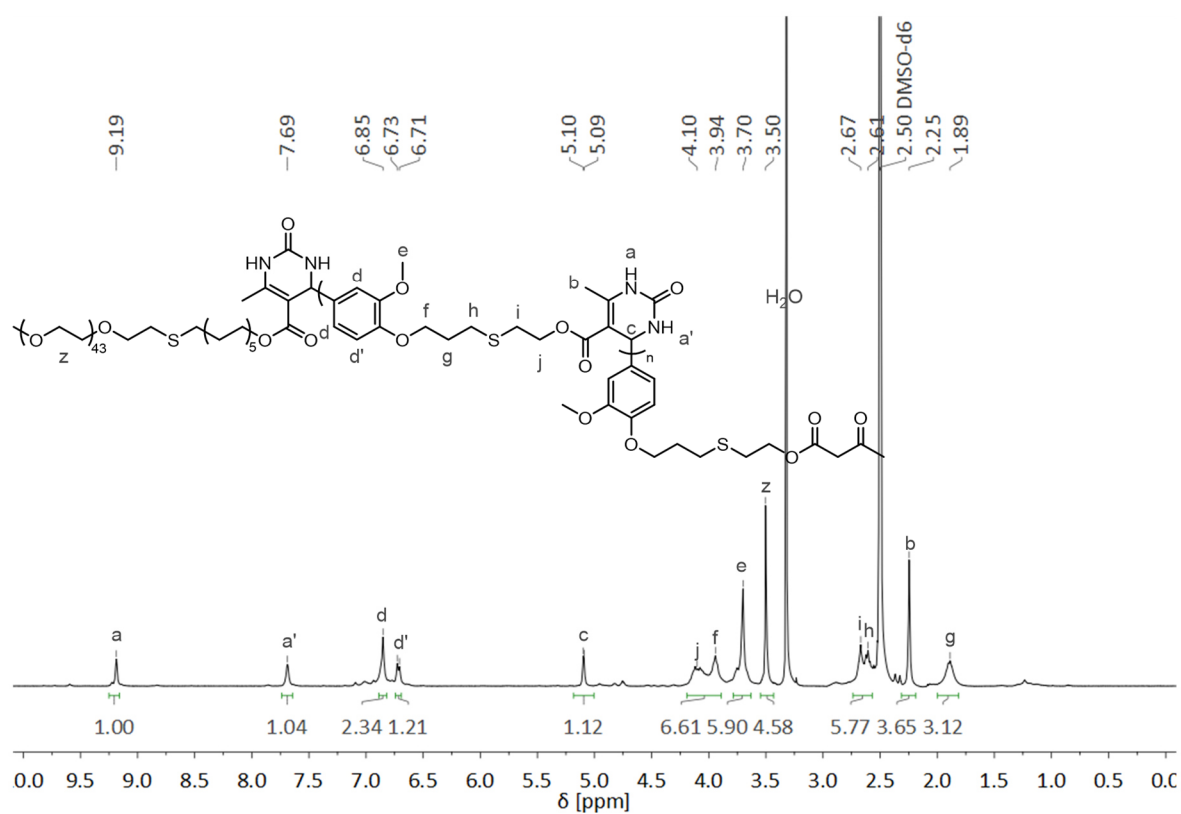


Figure 6.62 ¹H NMR spectrum of 148f in DMSO-*d*₆.

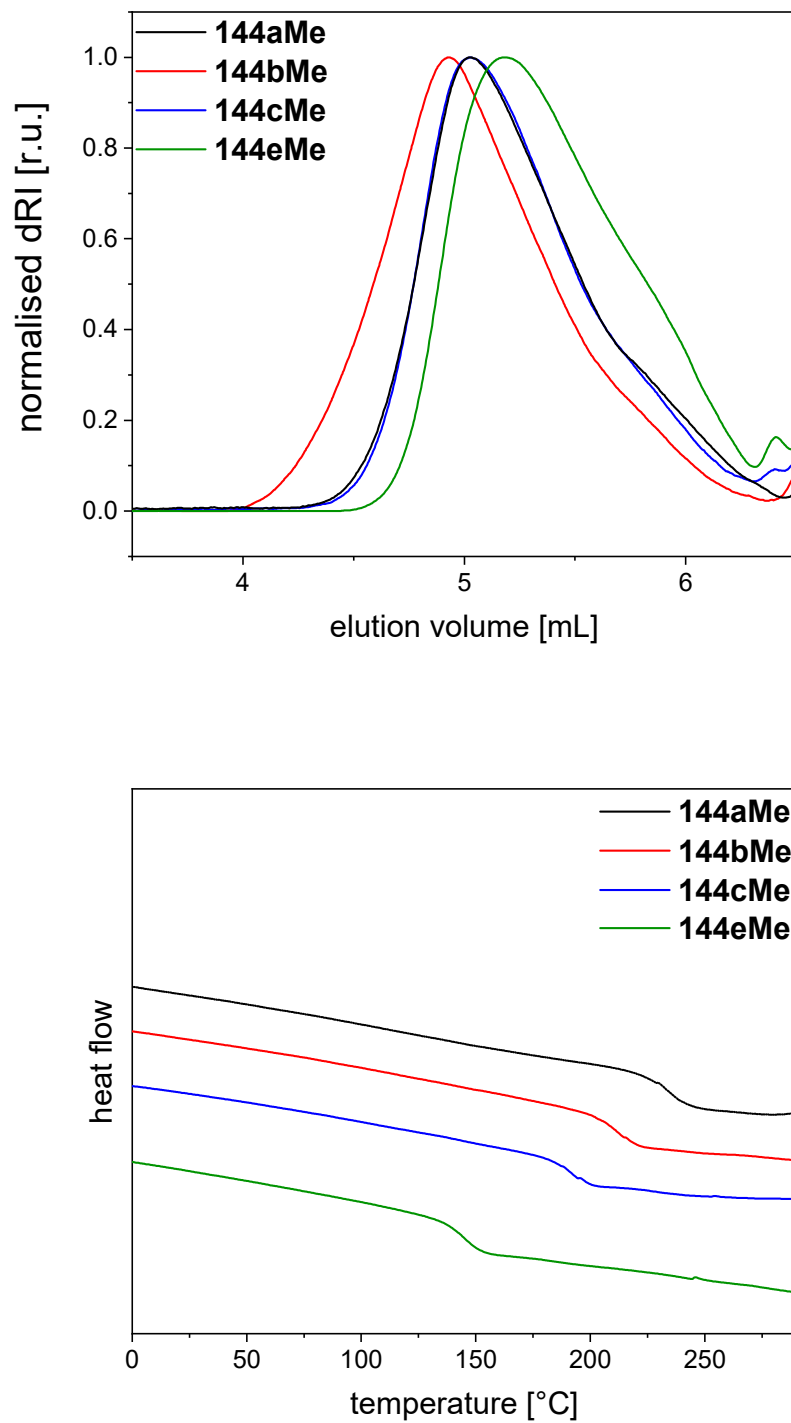


Figure 6.63 SEC chromatograms and DSC curves of end group functionalised polyDHMPs **144a,b,c,eMe**.

144aMe

Precipitated in and washed with MeOH.

$^1\text{H-NMR}$ (400 MHz, $\text{DMSO-}d_6$): δ (ppm) = 7.95 (br s, $\text{H}_{a'}$), 7.36 – 7.00 (m, H_d), 5.30 – 5.00 (m, H_c), 4.34 – 3.86 (m, H_e), 3.08 (s, H_a), 2.45 (s, H_b).

IR: ν (cm^{-1}) = 3293, 2952, 1673, 1451, 1383, 1350, 1299, 1244, 1186, 1150, 1075, 973, 799, 758, 613, 494.

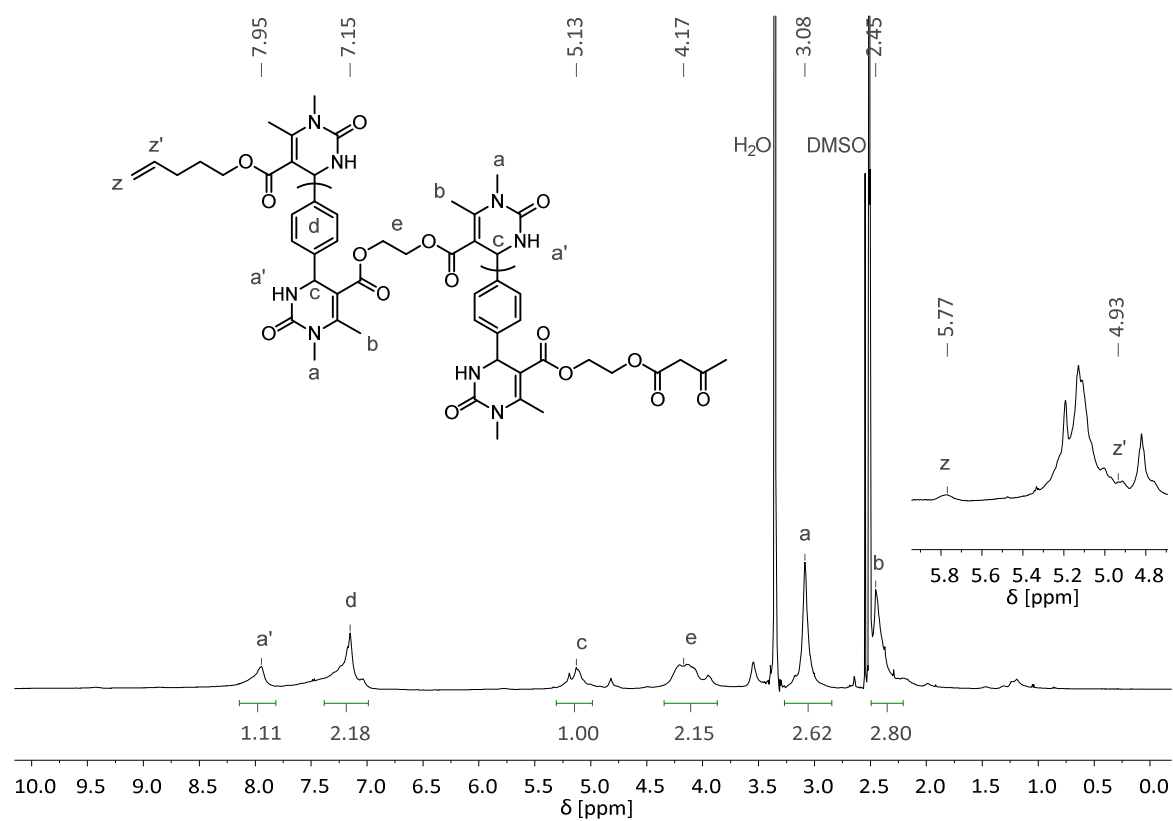


Figure 6.64 $^1\text{H-NMR}$ spectrum of **144aMe** in $\text{DMSO-}d_6$.

144bMe

Precipitated in and washed with MeOH.

¹H-NMR (400 MHz, DMSO-*d*₆): δ (ppm) = 7.90 (br s, H_{a'}), 7.32 – 6.97 (m, H_d), 5.10 (br s, H_c), 4.10 – 3.82 (m, H_e), 3.06 (s, H_a), 2.45 (s, H_b), 1.83 – 1.58 (m, H_f).

IR: ν (cm⁻¹) = 3304, 2923, 1669, 1506, 1453, 1419, 1382, 1299, 1243, 1184, 1151, 1050, 975, 756, 612, 495.

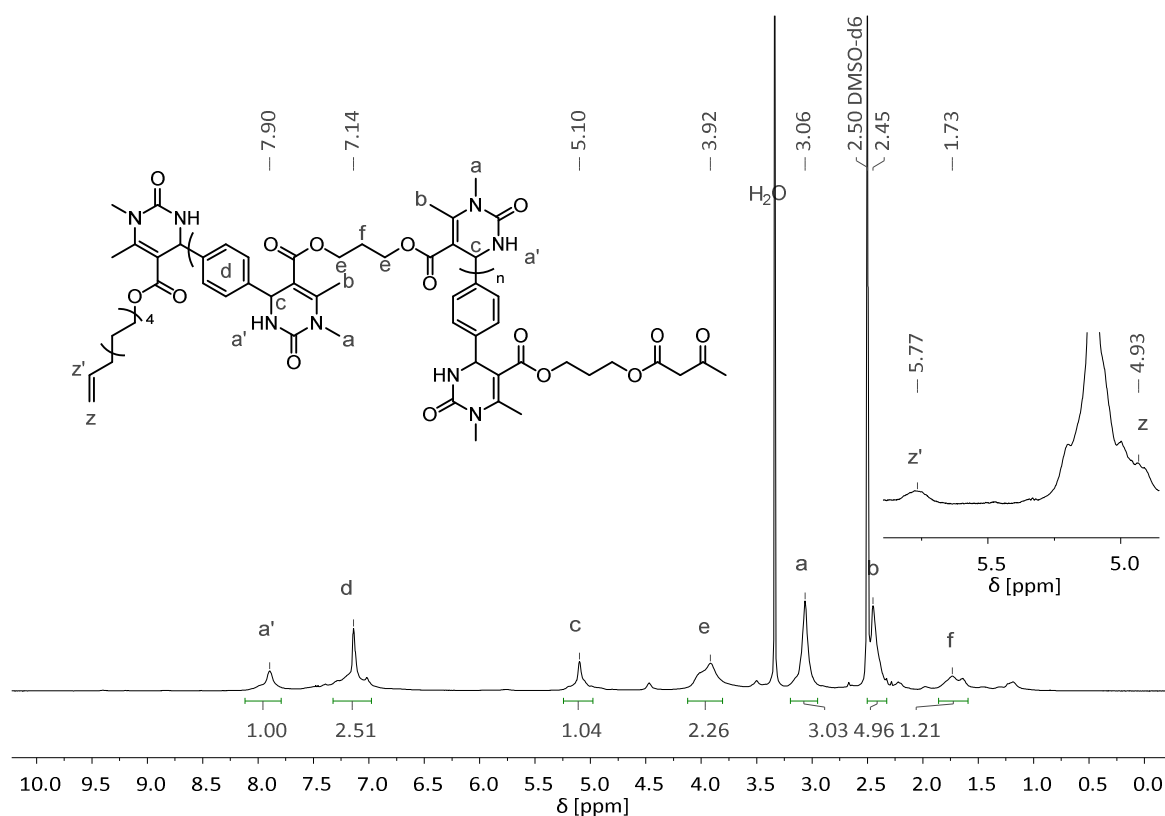


Figure 6.65 ¹H NMR spectrum of 144bMe in DMSO-*d*₆.

144cMe

Precipitated in and washed with MeOH.

¹H-NMR (400 MHz, DMSO-*d*₆): δ (ppm) = 7.90 (br s, H_{a'}), 7.32 – 7.01 (m, H_d), 5.09 (br s, H_c), 3.89 (br s, H_e), 3.06 (s, H_a), 2.45 (s, H_b), 1.65 – 1.03 (m, H_f).

IR: ν (cm⁻¹) = 3297, 2925, 1668, 1505, 1447, 1382, 1349, 1299, 1242, 1183, 1152, 1070, 1047, 975, 798, 755, 611, 495.

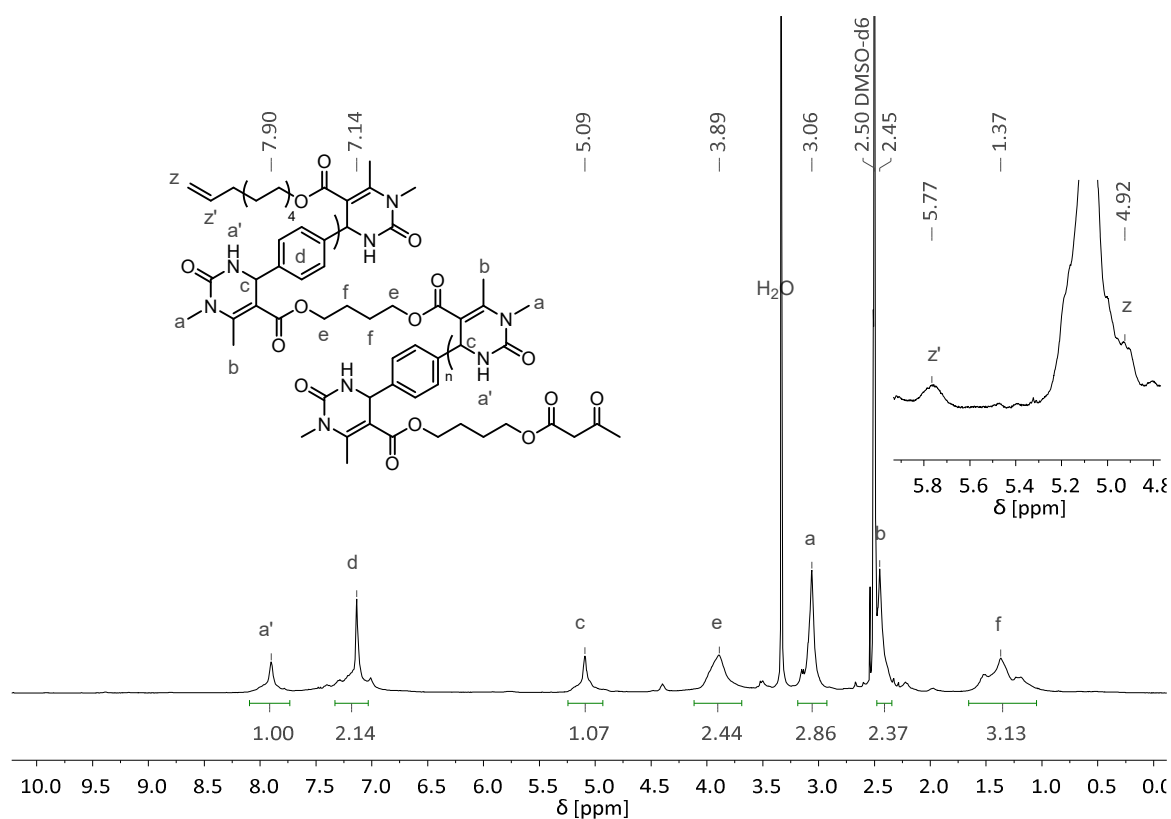


Figure 6.66 ¹H NMR spectrum of **144cMe** in DMSO-*d*₆.

144eMe

Precipitated in and washed with MeOH.

$^1\text{H-NMR}$ (400 MHz, $\text{DMSO-}d_6$): δ (ppm) = 7.90 (br s, $\text{H}_{a'}$), 7.27 – 7.04 (m, H_d), 5.10 (br s, H_c), 3.94 (br s, H_e), 3.06 (s, H_a), 2.46 (s, H_b), 1.71 – 0.84 (m, H_f).

IR: ν (cm^{-1}) = 3297, 2925, 1668, 1505, 1447, 1382, 1349, 1299, 1242, 1183, 1152, 1070, 1047, 975, 798, 755, 611, 495.

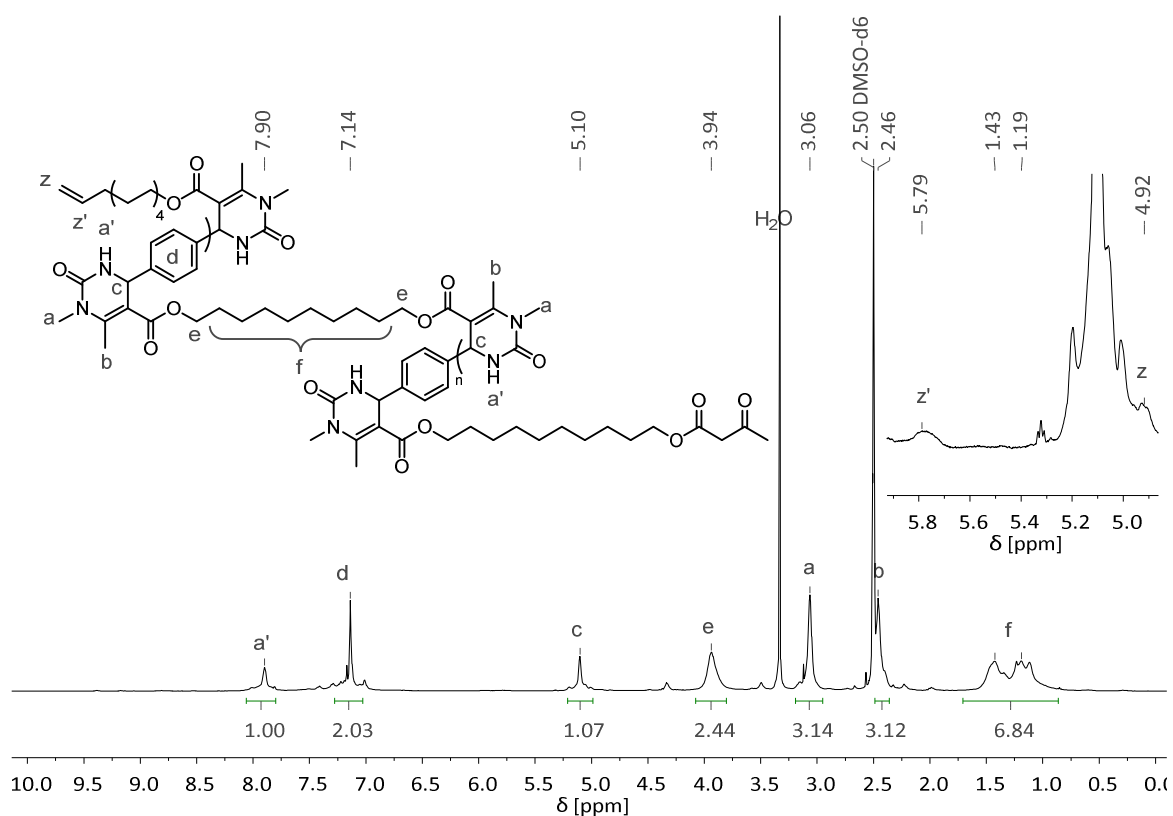
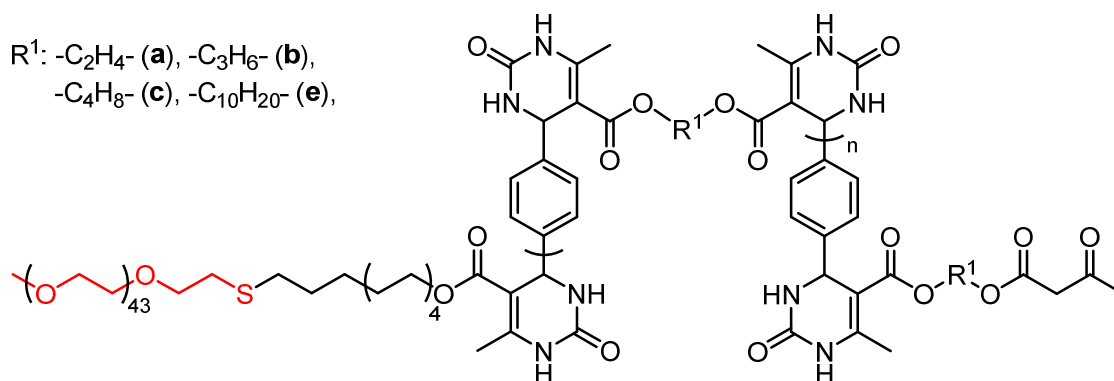


Figure 6.67 $^1\text{H-NMR}$ spectrum of **144eMe** in $\text{DMSO-}d_6$.

6.4.2.5 Poly[3,4-dihydropyrimidin-2(1H)-one]-*b*-poly(ethylene glycol)s using *N*-Methyl Urea



Each poly[3,4-dihydropyrimidin-2(1H)-one]-*b*-poly(ethylene glycol) (**148a,b,c,eMe**) from *N*-methyl urea was synthesised according to the same general procedure for the synthesis of poly[3,4-dihydropyrimidin-2(1H)-one]-*b*-poly(ethylene glycol)s from urea (chapter 6.4.2.3). However, instead of urea, *N*-methyl urea was used.

Summarised analytics are given as follows.

Table 6.14 SEC and DSC data and yields of the the polyDHPM-*b*-poly(ethylene glycol)s (**148a,b,c,eMe**).

polymer	R ¹	$M_{n,SEC}$ [g·mol ⁻¹]	$M_{w,SEC}$ [g·mol ⁻¹]	\bar{D}	T_g/T_m^a [°C]	Yield ^b [%]
148aMe	C ₂ H ₄	9 800	29 400	2.99	234/51	77
148bMe	C ₃ H ₆	11 900	47 800	4.03	204/51	72
148cMe	C ₄ H ₈	9 100	24 700	2.72	185/51	74
148eMe	C ₁₀ H ₂₀	6 600	16 800	2.53	140/52	72

^athe inflection point of the DSC curve was chosen as T_g , the minimum as T_m ; ^bisolated yields calculated by comparison with theoretical amount of mass at 100% conversion.

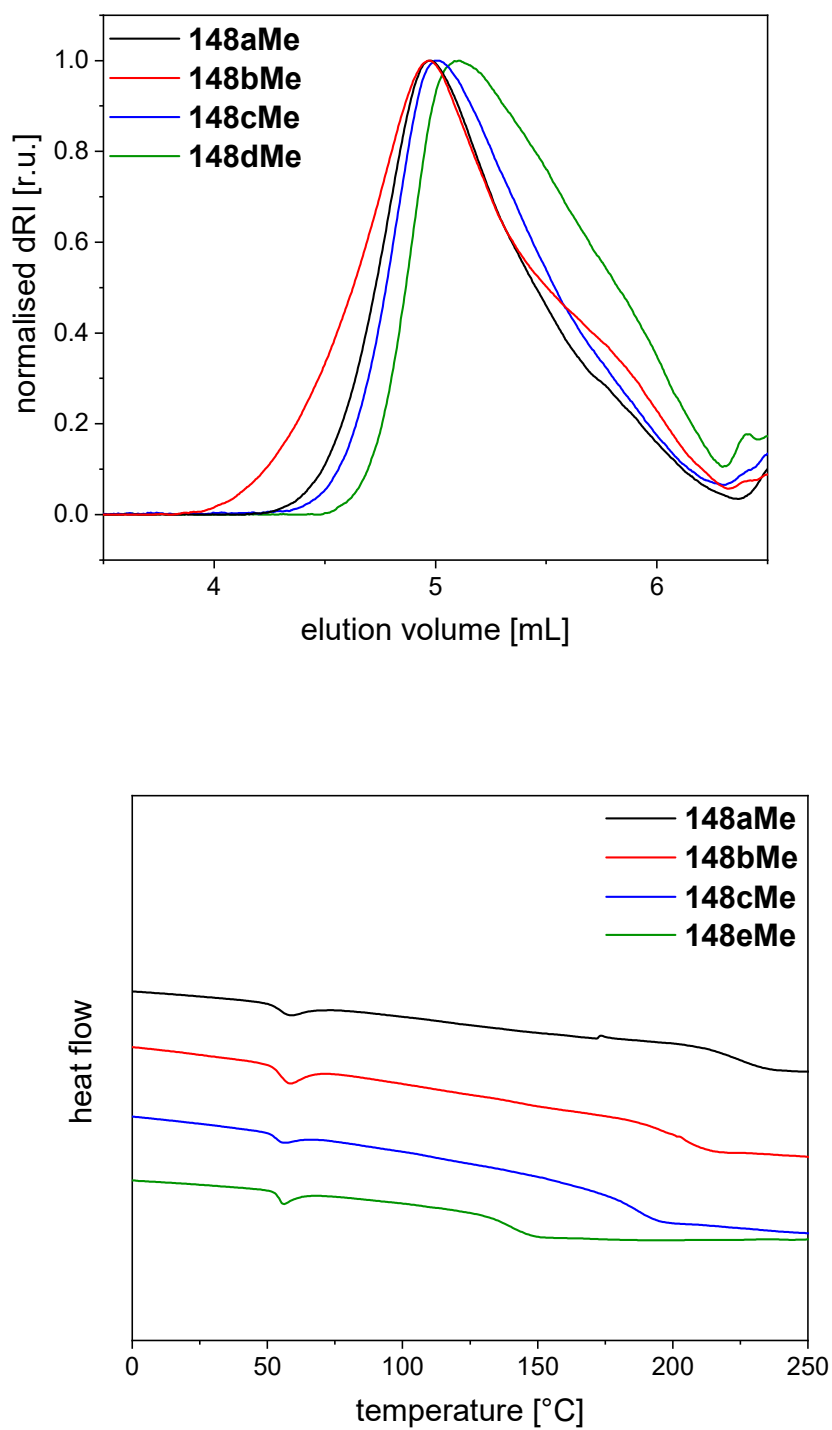


Figure 6.68 SEC chromatograms and DSC curves of polyDHPM-*b*-poly(ethylene glycol)s (**148a,b,c,eMe**).

148aMe

Precipitated in and washed with H₂O.

¹H-NMR (400 MHz, DMSO-*d*₆): δ (ppm) = 7.94 (br s, H_{a'}), 7.28 – 7.04 (m, H_d), 5.26 – 5.01 (m, H_c), 4.36 – 3.99 (m, H_e), 3.51 (s, H_z), 3.08 (s, H_a), 2.45 (s, H_b).

IR: ν (cm⁻¹) = 3314, 2948, 1672, 1507, 1448, 1382, 1350, 1299, 1242, 1186, 1145, 1073, 972, 798, 757, 612.

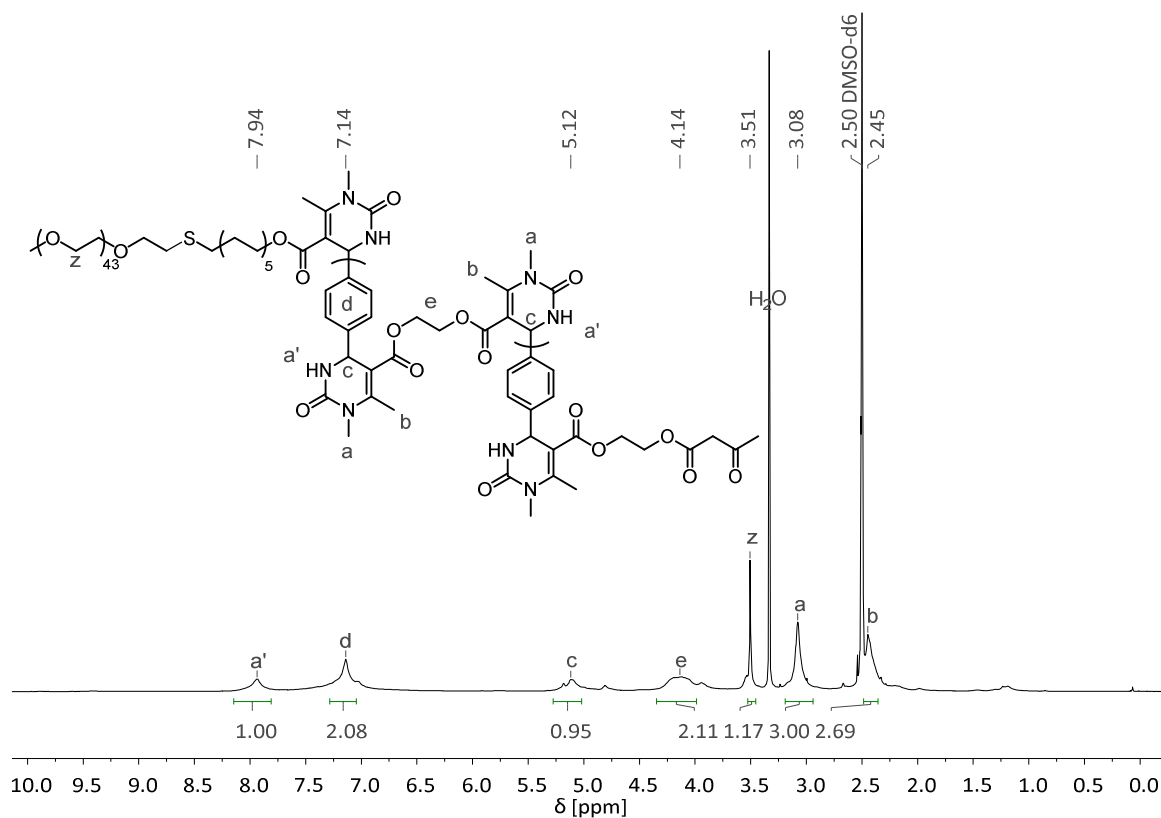


Figure 6.69 ¹H NMR spectrum of 148aMe in DMSO-*d*₆.

148bMe

Precipitated in and washed with H₂O.

¹H-NMR (400 MHz, DMSO-*d*₆): δ (ppm) = 7.90 (br s, H_{a'}), 7.27 – 6.99 (m, H_d), 5.10 (br s, H_c), 4.10 – 3.80 (m, H_e), 3.51 (s, H_z), 3.06 (s, H_a), 2.45 (s, H_b), 1.89 – 1.52 (m, H_f).

IR: ν (cm⁻¹) = 3315, 2928, 1673, 1507, 1453, 1420, 1383, 1350, 1299, 1244, 1185, 1152, 1071, 1051, 976, 801, 757, 613, 496.

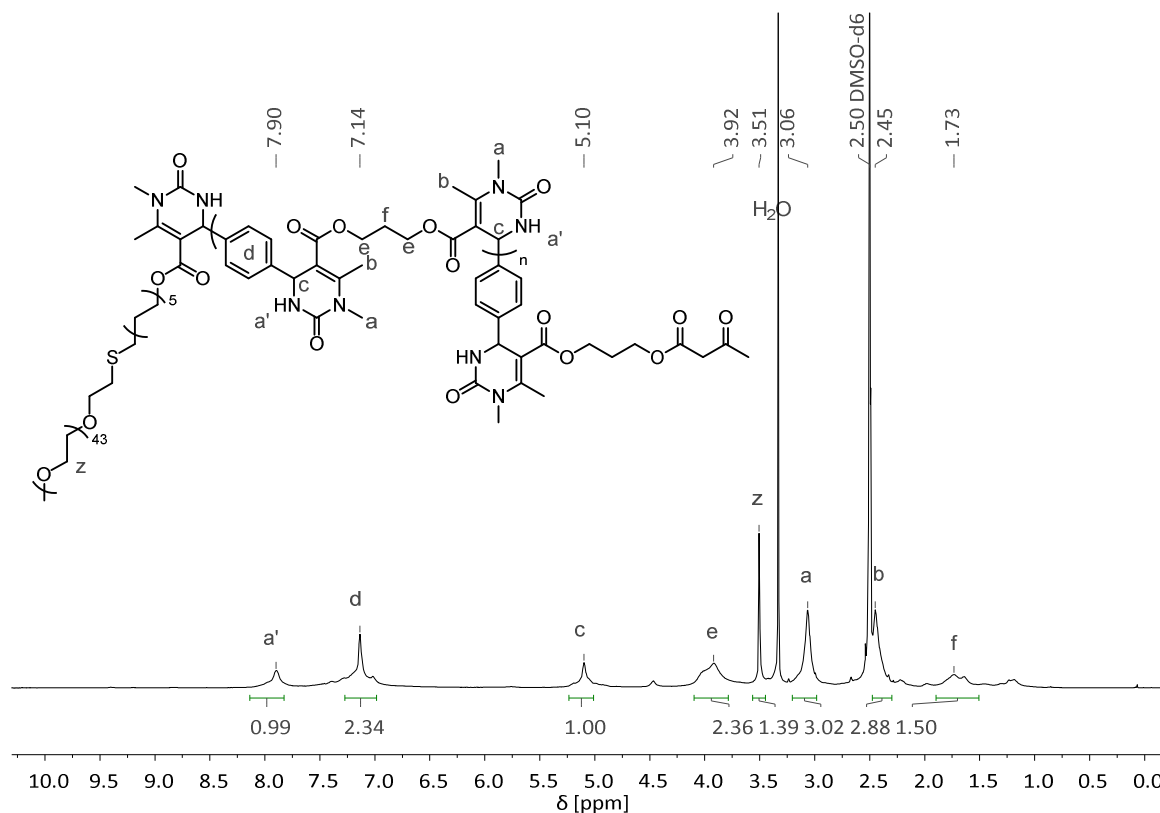


Figure 6.70 ¹H NMR spectrum of 148bMe in DMSO-*d*₆.

148cMe

Precipitated in and washed with H₂O.

¹H-NMR (400 MHz, DMSO-*d*₆): δ (ppm) = 7.90 (br s, H_{a'}), 7.24 – 7.00 (m, H_d), 5.09 (br s, H_c), 3.89 (br s, H_e), 3.51 (s, H_z), 3.06 (s, H_a), 2.45 (s, H_b), 1.65 – 1.00 (m, H_f).

IR: ν (cm⁻¹) = 3319, 2952, 1674, 1506, 1449, 1383, 1350, 1300, 1244, 1184, 1154, 1072, 1049, 977, 800, 757, 613, 495.

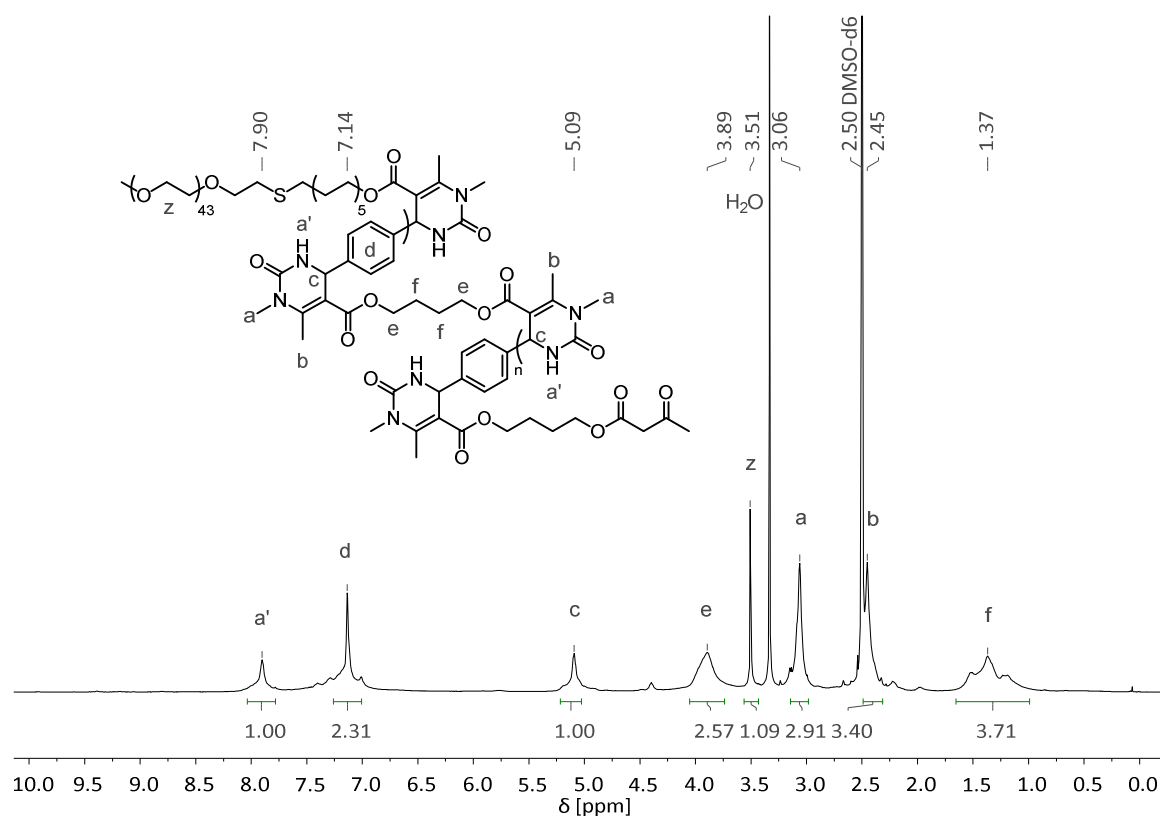


Figure 6.71 ¹H NMR spectrum of 148cMe in DMSO-*d*₆.

148eMe

Precipitated in and washed with H₂O.

¹H-NMR (400 MHz, DMSO-*d*₆): δ (ppm) = 7.90 (br s, H_{a'}), 7.24 – 7.02 (m, H_d), 5.10 (br s, H_c), 3.94 (br s, H_e), 3.51 (s, H_z), 3.06 (s, H_a), 2.46 (s, H_b), 1.79 – 0.68 (m, H_f).

IR: ν (cm⁻¹) = 3315, 2928, 1673, 1507, 1453, 1420, 1383, 1350, 1299, 1244, 1185, 1152, 1071, 1051, 976, 801, 757, 613, 496.

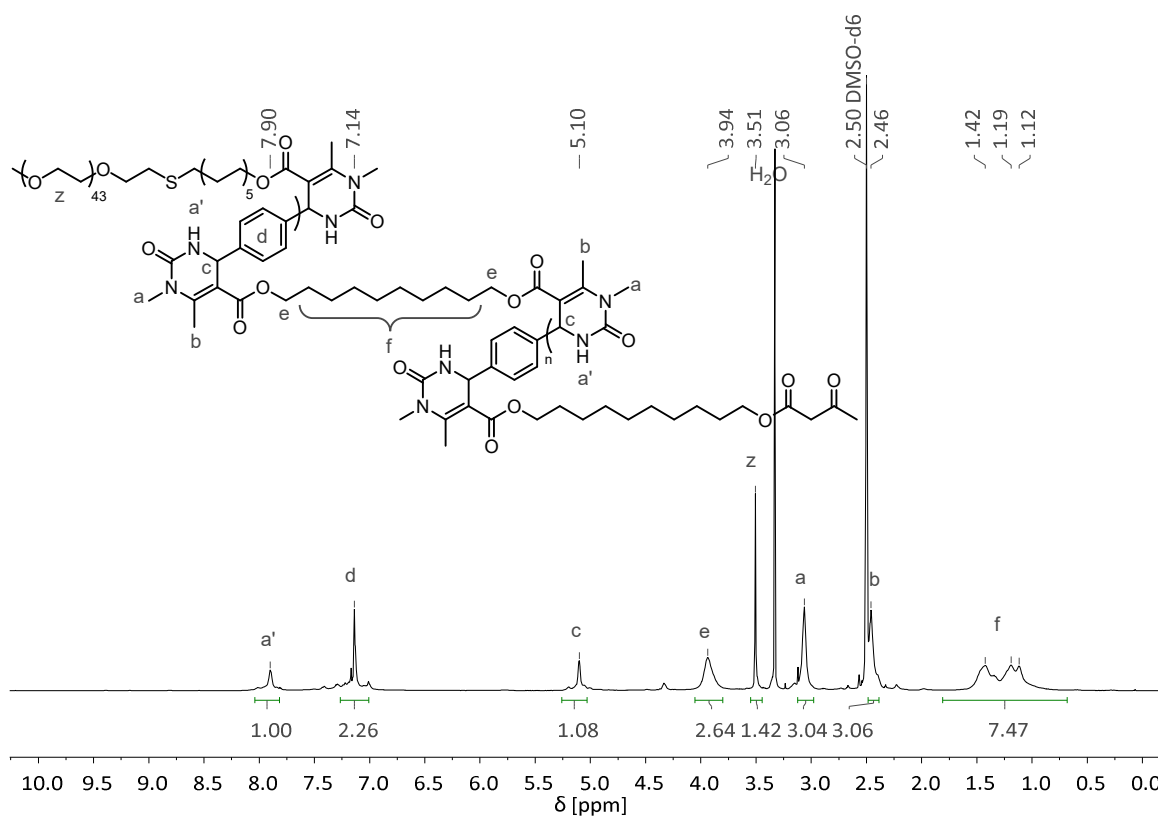
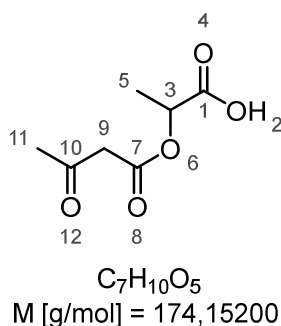


Figure 6.72 ¹H NMR spectrum of 148eMe in DMSO-*d*₆.

6.5 Synthesis Procedures and Analytical Data Related to Chapter 4.3

6.5.1 Synthesis of Monomer Precursors and Monomers

6.5.1.1 (*S*)-2-[(3-Oxobutanoyl)oxy]propanoic Acid (157)



Sodium (*S*)-2-hydroxypropanoate (60 mmol, 1.00 eq) was mixed with diketene acetone adduct (2,2,6-trimethyl-4*H*-1,3-dioxin-4-on, 3.00 eq) and stirred in a preheated oil bath at 95°C for 3 h. Afterwards, 150 mL H₂O were added to the reaction mixture and the mixture was washed with toluene (six times 100 mL). Later, the aqueous phase was acidified with 1 M HCl_{aq}. Subsequently, the solvent was removed under reduced pressure and the residue was mixed with EtOAc. After filtration and removal of the solvent the product was obtained.

yield

| 90% (9.45 g, 54.2 mmol, slightly yellow oil)

¹H-NMR (400 MHz, DMSO-*d*₆): δ (ppm) = 13.03 (s, 1H, H₂), 4.95 (q, ³*J*_{H3;H5} = 7.1 Hz, 1H, H₃), 3.63 ppm (q_{AB}, ^{AB}*J* = 15.9 Hz, δ_A = 3.64, δ_B = 3.62, 2H, H₉), 2.20 (s, 3H), 1.40 (d, ³*J*_{H5;H3} = 7.1 Hz, 3H, H₅)

¹³C-NMR (101 MHz DMSO-*d*₆): δ (ppm) = 200.95 (C₁₀), 171.52 (C₁), 166.66 (C₇), 68.91 (C₃), 49.35 (C₉), 29.93 (C₁₁), 16.62 (C₅).

HRMS (EI): *m/z* for C₇H₁₀O₅⁺ [M]⁺: calculated: 174.0523; found: 174.0524.

6.5 Synthesis Procedures and Analytical Data Related to Chapter 4.3

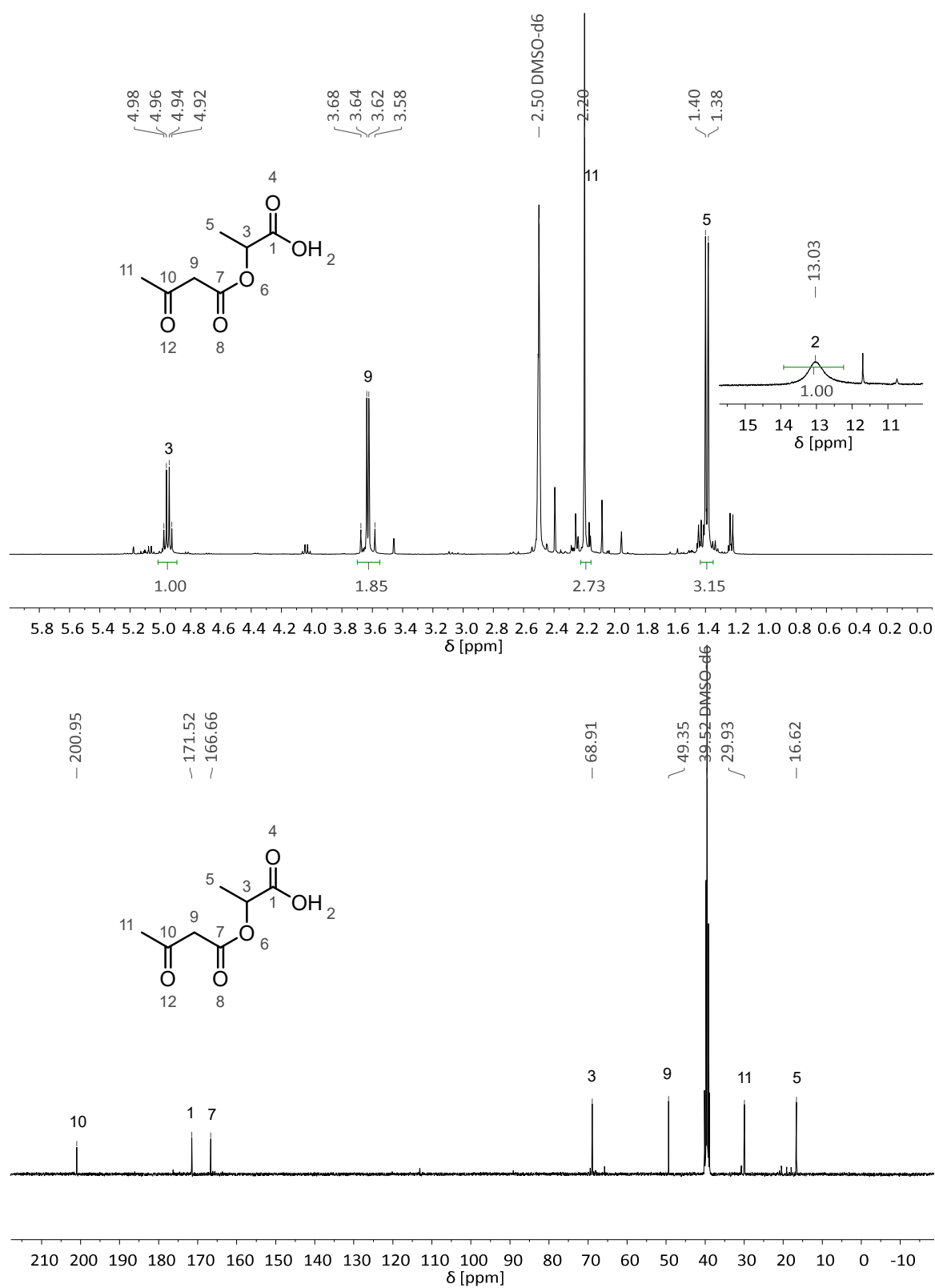
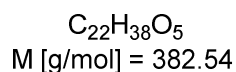
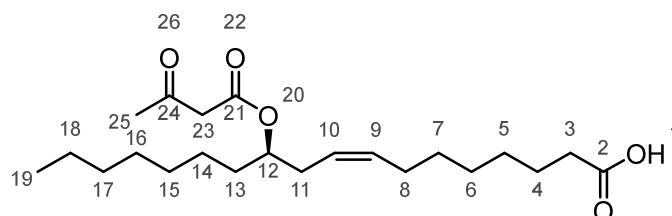


Figure 6.73 ^1H and ^{13}C NMR spectra of **157** in $\text{DMSO-}d_6$.

6.5.1.2 (12*R*,9*Z*)-12-[(3-Oxobutanoyl)oxy]octadec-9-enoic Acid (159)

(9*Z*,12*R*)-12-Hydroxyoctadec-9-enoic acid (14.0 mmol, 1.00 eq) and diketene acetone adduct (2,2,6-trimethyl-4*H*-1,3-dioxin-4-one, 3.00 eq) are mixed in an open round bottom flask and stirred for 1 h at 95°C. Afterwards, the mixture was subjected to column chromatography using silica gel.

yield	68% (3.64 g, 9.51 mmol, dark orange oil)
eluent	<i>c</i> -C ₆ H ₁₂ :EtOAc = 90:10 + 1 vol% AcOH
R _f (product)	0.70 in <i>c</i> -C ₆ H ₁₂ :EtOAc = 90:10 + 1 vol% AcOH

¹H-NMR (400 MHz, DMSO-*d*₆): δ (ppm) = 11.96 (s, 1H, H₁₉), 5.51 – 5.41 (m, 1H, H₉), 5.39 – 5.27 (m, 1H, H₁₀), 4.85 – 4.76 (m, 1H, H₁₂), 3.56 (s, 2H, H₂₃), 2.27 (dd, ³*J*_{H11;H12;H10} = 7.8, 5.9 Hz, 2H, H₁₁), 2.19 (t, ³*J*_{H3;H4} = 7.3 Hz, 2H, H₃), 2.17 (s, 3H, H₂₅), 2.04 – 1.96 (m, 2H, H₈), 1.55 – 1.42 (m, 4H, H_{4,13}), 1.36 – 1.17 (m, 16H, H_{5-7,14-18}), 0.89 – 0.83 (m, 3H, H₁₉).

¹³C-NMR (101 MHz DMSO-*d*₆): δ (ppm) = 201.40 (C₂₄), 174.45 (C₂), 166.88 (C₂₁), 132.25 (C₉), 124.26 (C₁₀), 74.00 (C₁₂), 49.77 (C₂₃), 33.64(C₃), 32.89 (C₁₃), 31.34 (C₁₁), 31.11 (C_{4-7,14-18}), 30.02 (C₂₅), 28.91 (C_{4-7,14-18}), 28.58 (C_{4-7,4-18}), 28.51 (C_{4-7,14-18}), 28.50 (C_{4-7,14-18}), 28.42 (C_{4-7,14-18}), 26.96 (C₈), 24.57 (C_{4-7,14-18}), 24.47 (C_{4-7,14-18}), 21.96 (C_{4-7,14-18}), 13.89 (C₁₉).

HRMS (FAB): *m/z* for C₂₂H₃₈O₅H⁺ [M+H]⁺: calculated: 383.2792; found: 383.2794.

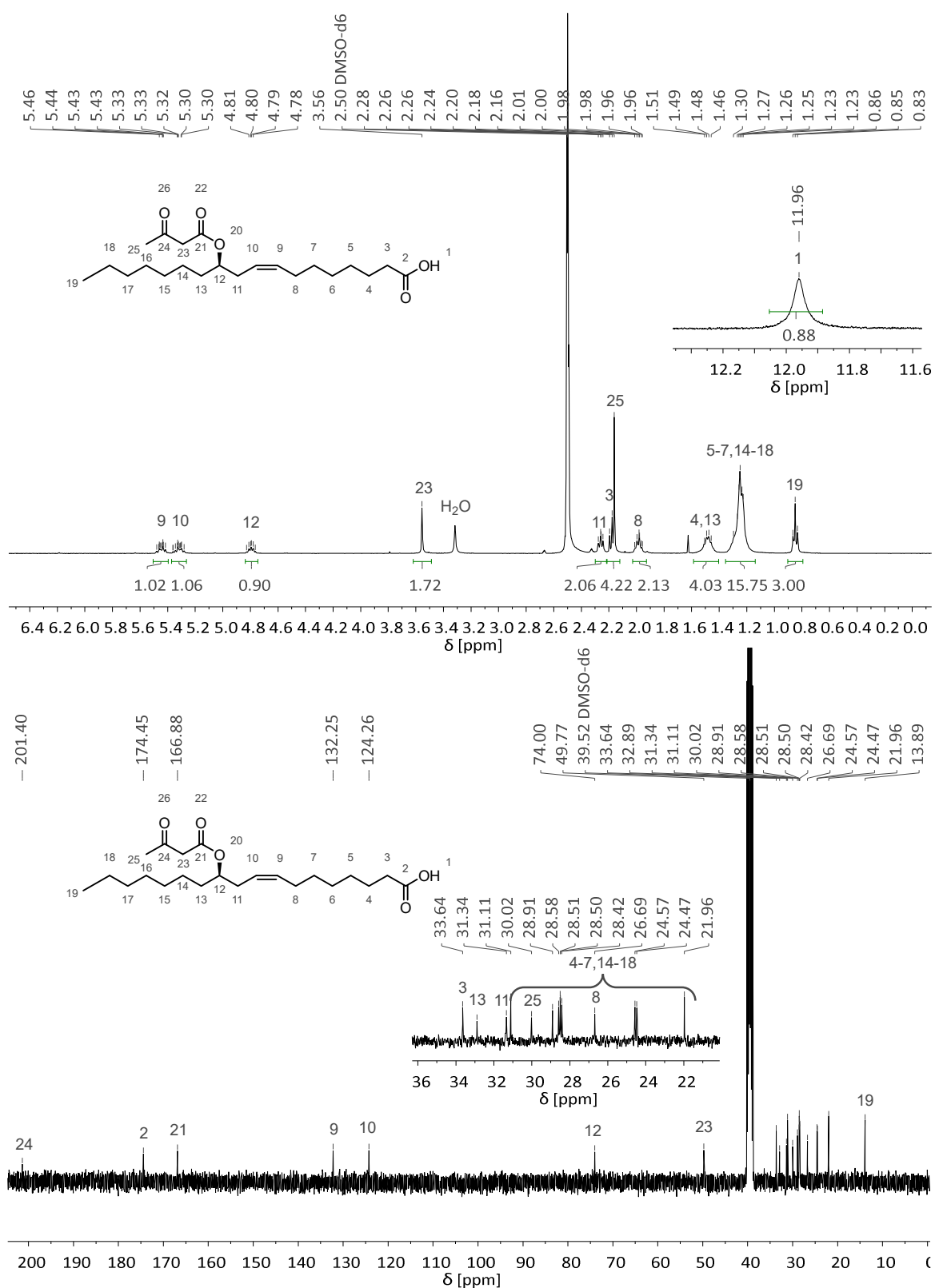
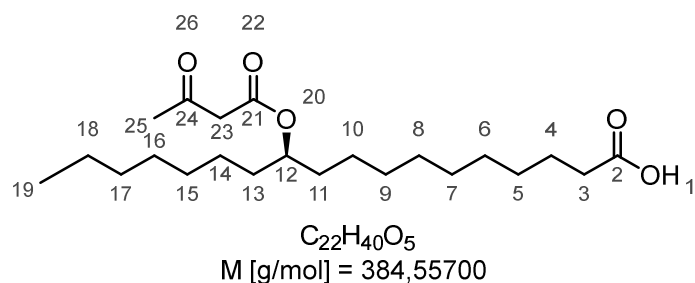


Figure 6.74 ^1H and ^{13}C NMR spectra of **159** in $\text{DMSO-}d_6$.

6.5.1.3 (R)-12-[(3-Oxobutanoyl)oxy]octadecanoic Acid (160)

(9Z,12R)-12-[(3-Oxobutanoyl)oxy]octadec-9-enoic acid (20.5 mmol, 1.00 eq) was dissolved in 140 ml of EtOAc and Pd on activated charcoal (10% Pd basis, 11.7 mg) was added. In a pressure reactor, the mixture was purged three times with hydrogen and subsequently stirred for 24 h at room temperature under 15 bar hydrogen pressure. Afterwards, the catalyst was filtered off and the filtrate was evaporated under vacuum to remove the solvent yielding the final product.

yield | $\geq 99\%$ (7.88 g, 20.5 mmol, yellow oil)

¹H-NMR (400 MHz, DMSO-*d*₆): δ (ppm) = 11.95 (s, 1H, H₁), 4.92 – 4.67 (m, 1H, H₁₂), 3.57 (s, 2H, H₂₃), 2.19 (t, ³J_{H3;H4} = 7.4 Hz, 2H, H₃), 2.16 (s, 3H, H₂₅), 1.52 – 1.43 (m, 6H, H_{4,11,13}), 1.23 (s, 22H, H_{5-10,14-18}), 0.85 (t, ³J_{H19;H18} = 6.7 Hz, 3H, H₁₉).

¹³C-NMR (101 MHz DMSO-*d*₆): δ (ppm) = 201.44 (C₂₄), 174.50 (C₂), 167.00 (C₂₁), 74.16 (C₁₂), 49.75 (C₂₃), 33.64 (C₃), 33.46 (C₂₅), 31.12 (C_{4-11,13-18}), 30.04 (C_{4-11,13-18}), 28.84 (C_{4-11,13-18}), 28.76 (C_{4-11,13-18}), 28.70 (C_{4-11,13-18}), 28.52 (C_{4-11,13-18}), 28.45 (C_{4-11,13-18}), 24.58 (C_{4-11,13-18}), 24.48 (C_{4-11,13-18}), 21.97 (C_{4-11,13-18}), 13.90 (C₁₉).

HRMS (FAB): m/z for C₂₂H₄₀O₅H⁺ [M+H]⁺: calculated: 385.2949; found: 385.2947.

6.5 Synthesis Procedures and Analytical Data Related to Chapter 4.3

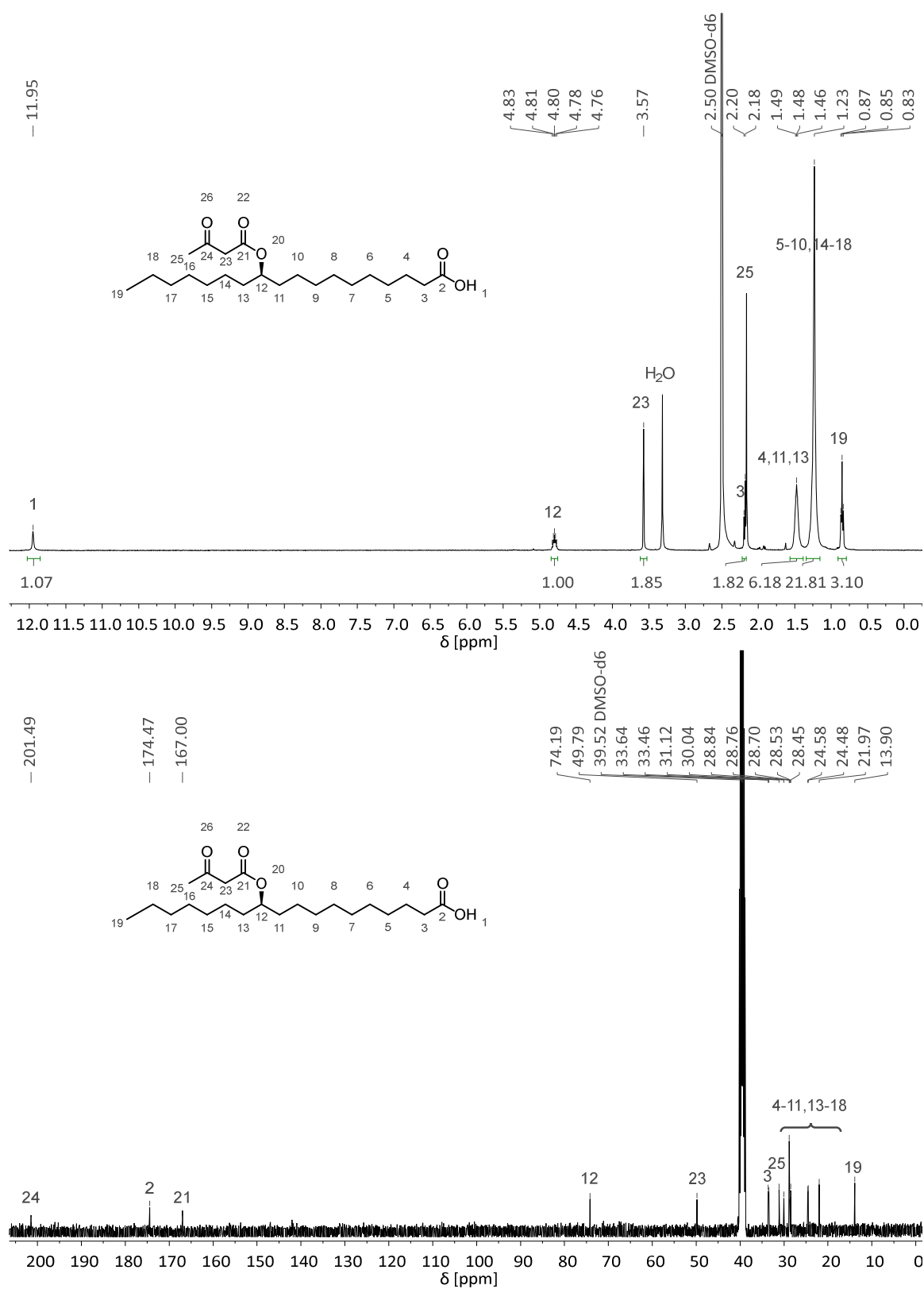
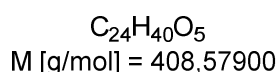
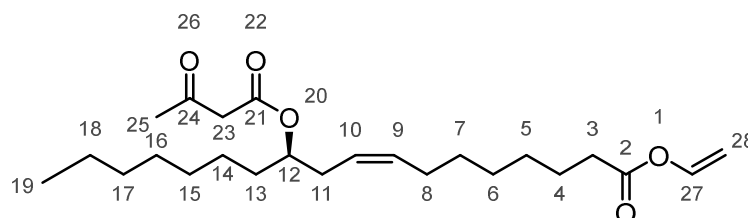


Figure 6.75 ¹H and ¹³C NMR spectra of **160** in DMSO-*d*₆.

6.5.1.4 Vinyl (12*R*,9*Z*)-12-[(3-Oxobutanoyl)oxy]octadec-9-enoate (163)

(9*Z*,12*R*)-12-[(3-Oxobutanoyl)oxy]octadec-9-enoic acid (7.84 mmol, 1.00 eq), di- μ -chlorobis[(1,2,5,6- η^2)-1,5-cyclooctadiene]diiridium (0.0100 eq), NaOAc (0.0300 eq), and vinyl acetate (10.0 eq) were combined in a pressure tube. The mixture was degassed with argon for 5 min and then sealed. In a preheated oil bath at 100°C, the mixture was stirred for 24 h. The resulting mixture was poured over 10 ml water. The solution was extracted with EtOAc (five times 30 mL). The combined organic phases were dried over anhydrous Na₂SO₄ and the solvent was evaporated under reduced pressure. The resulting crude product was purified using column chromatography over silica gel.

yield	63% (2.03 g, 4.94 mmol, yellow oil)
eluent	<i>c</i> -C ₆ H ₁₂ :EtOAc = 90:10
R _f (product)	0.75 in <i>c</i> -C ₆ H ₁₂ :EtOAc = 90:10

¹H-NMR (400 MHz, DMSO-*d*₆): δ (ppm) = 7.22 (dd, $^3J_{\text{H}27;\text{H}28\text{trans};\text{H}28\text{cis}} = 14.0, 6.3$ Hz, 1H, H₂₇), 5.50 – 5.41 (m, 1H, H₉), 5.37 – 5.28 (m, 1H, H₁₀), 4.89 (dd, $^3J_{\text{H}28\text{trans};\text{H}27} = 14.0$ Hz, $^2J_{\text{H}28\text{trans};\text{H}28\text{cis}} = 1.5$ Hz, 1H, H_{28trans}), 4.84 – 4.76 (m, 1H, H₁₂), 4.65 (dd, $^3J_{\text{H}28\text{cis};\text{H}27} = 6.3$ Hz, $^2J_{\text{H}28\text{cis};\text{H}28\text{trans}} = 1.5$ Hz, 1H, H_{28cis}), 3.55 (s, 2H, H₂₃), 2.41 (t, $^3J_{\text{H}3;\text{H}4} = 7.4$ Hz, 2H, H₃), 2.30 – 2.24 (m, 2H, H₁₁), 2.16 (s, 3H, H₂₅) 2.04 – 1.95 (m, 2H, H₈), 1.59 – 1.45 (m, 4H, H_{4,13}), 1.35 – 1.17 (m, 14H, H_{5-7,14-18}), 0.85 (t, $^3J_{\text{H}19;\text{H}18} = 6.7$ Hz, 3H, H₁₉).

¹³C-NMR (101 MHz DMSO-*d*₆): δ (ppm) = 201.39 (C₂₄), 170.39 (C₂), 166.88 (C₂₁), 141.22 (C₂₇), 132.24 (C₉), 124.27 (C₁₀), 97.95 (C₂₈), 74.00 (C₁₂), 49.77 (C₂₃), 32.99 (C₃), 32.88 (C_{4-7,13-18}), 31.33 (C₁₁), 31.11 (C_{4-7,13-18}), 30.01 (C₂₅), 28.86 (C_{4-7,13-18}), 28.45 (C_{4-7,13-18}), 28.42 (C_{4-7,13-18}), 28.27 (C_{4-7,13-18}), 26.66 (C₈), 24.57 (C_{4-7,13-18}), 24.00 (C_{4-7,13-18}), 21.96 (C_{4-7,13-18}), 13.89 (C₁₉).

HRMS (FAB): m/z for C₂₄H₄₀O₅H⁺ [M+H]⁺: calculated: 409.2949; found: 409.2948.

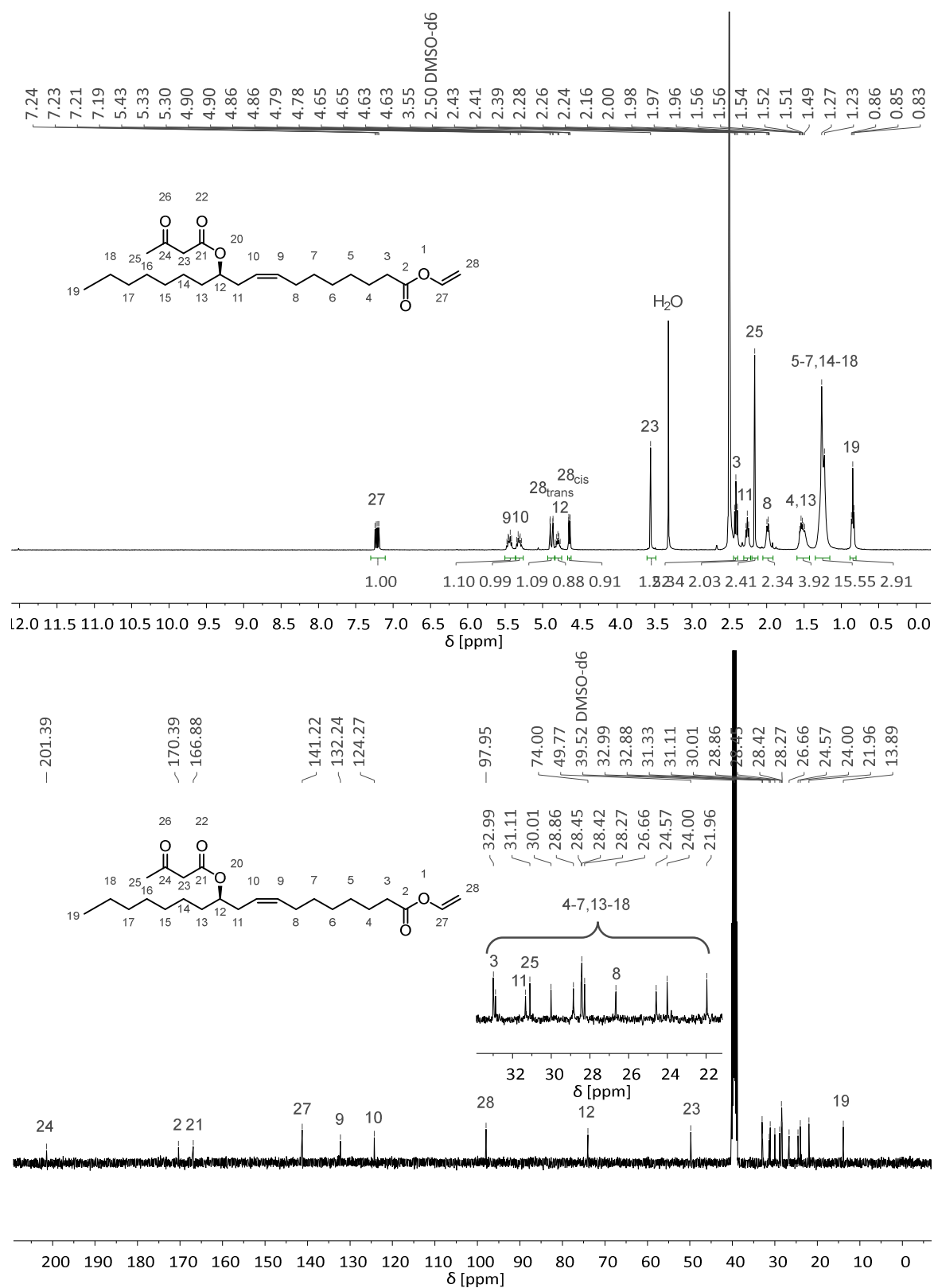
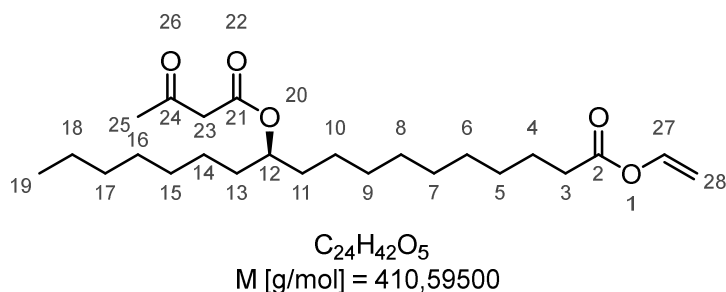


Figure 6.76 ^1H and ^{13}C NMR spectra of **163** in $\text{DMSO-}d_6$.

6.5.1.5 Vinyl (*R*)-12-[(3-Oxobutanoyl)oxy]octadecanoate (164)

(12*R*)-12-[(3-Oxobutanoyl)oxy]octadecanoic acid (14.6 mmol, 1.00 eq) di- μ -chlorobis[(1,2,5,6- η^2)-1,5-cyclooctadiene]diiridium (0.0100 eq), NaOAc (0.0300 eq), and vinyl acetate (10.0 eq) were combined in a pressure tube. The mixture was degassed with argon for 5 min and then sealed. In a preheated oil bath at 100°C, the mixture was stirred for 24 h. The resulting mixture was poured over 20 ml water. The solution was extracted with EtOAc (five times 60 mL). The combined organic phases were dried over anhydrous Na₂SO₄ and the solvent was evaporated under reduced pressure. The resulting crude product was purified using column chromatography over silica gel.

yield	63% (3.78 g, 9.20 mmol, yellow oil)
eluent	<i>c</i> -C ₆ H ₁₂ :EtOAc = 90:10
R _f (product)	0.65 in <i>c</i> -C ₆ H ₁₂ :EtOAc = 90:10

¹H-NMR (400 MHz, DMSO-*d*₆): δ (ppm) = 7.21 (dd, $^3J_{\text{H27};\text{H28trans};\text{H28cis}} = 14.0, 6.3$ Hz, 1H, H₂₇), 4.88 (dd, $^3J_{\text{H28trans};\text{H27}} = 14.0$ Hz, $^2J_{\text{H28trans};\text{H28cis}} = 1.5$ Hz, 1H, H_{28trans}), 4.84 – 4.74 (m, 1H, H₁₂), 4.64 (dd, $^3J_{\text{H28cis};\text{H27}} = 6.3$ Hz, $^2J_{\text{H28cis};\text{H28trans}} = 1.5$ Hz, 1H, H_{28cis}), 3.57 (s, 2H, H₂₃), 2.41 (t, $^3J_{\text{H3};\text{H4}} = 7.3$ Hz, 2H, H₃), 2.16 (s, 3H, H₂₅), 1.60 – 1.41 (m, 6H, H_{4,11,13}), 1.36 – 1.14 (m, 22H, H_{5-10,14-18}), 0.91 – 0.80 (m, 3H, H₁₉).

¹³C-NMR (101 MHz DMSO-*d*₆): δ (ppm) = 201.46 (C₂₄), 170.42 (C₂), 166.98 (C₂₁), 141.24 (C₂₇), 97.96 (C₂₈), 74.19 (C₁₂), 49.80 (C₂₃), 33.45 (C_{4-11,13-18}), 33.02 (C₃), 31.13 (C_{4-11,13-18}), 30.04 (C₂₅), 28.81 (C_{4-11,13-18}), 28.80 (C_{4-11,13-18}), 28.77 (C_{4-11,13-18}), 28.58 (C_{4-11,13-18}), 28.46 (C_{4-11,13-18}), 28.30 (C_{4-11,13-18}), 24.58 (C_{4-11,13-18}), 24.03 (C_{4-11,13-18}), 21.98 (C_{4-11,13-18}), 13.90 (C₁₉).

HRMS (FAB): m/z for C₂₄H₄₂O₅H⁺ [M+H]⁺: calculated: 411.3105; found: 411.3103.

6.5 Synthesis Procedures and Analytical Data Related to Chapter 4.3

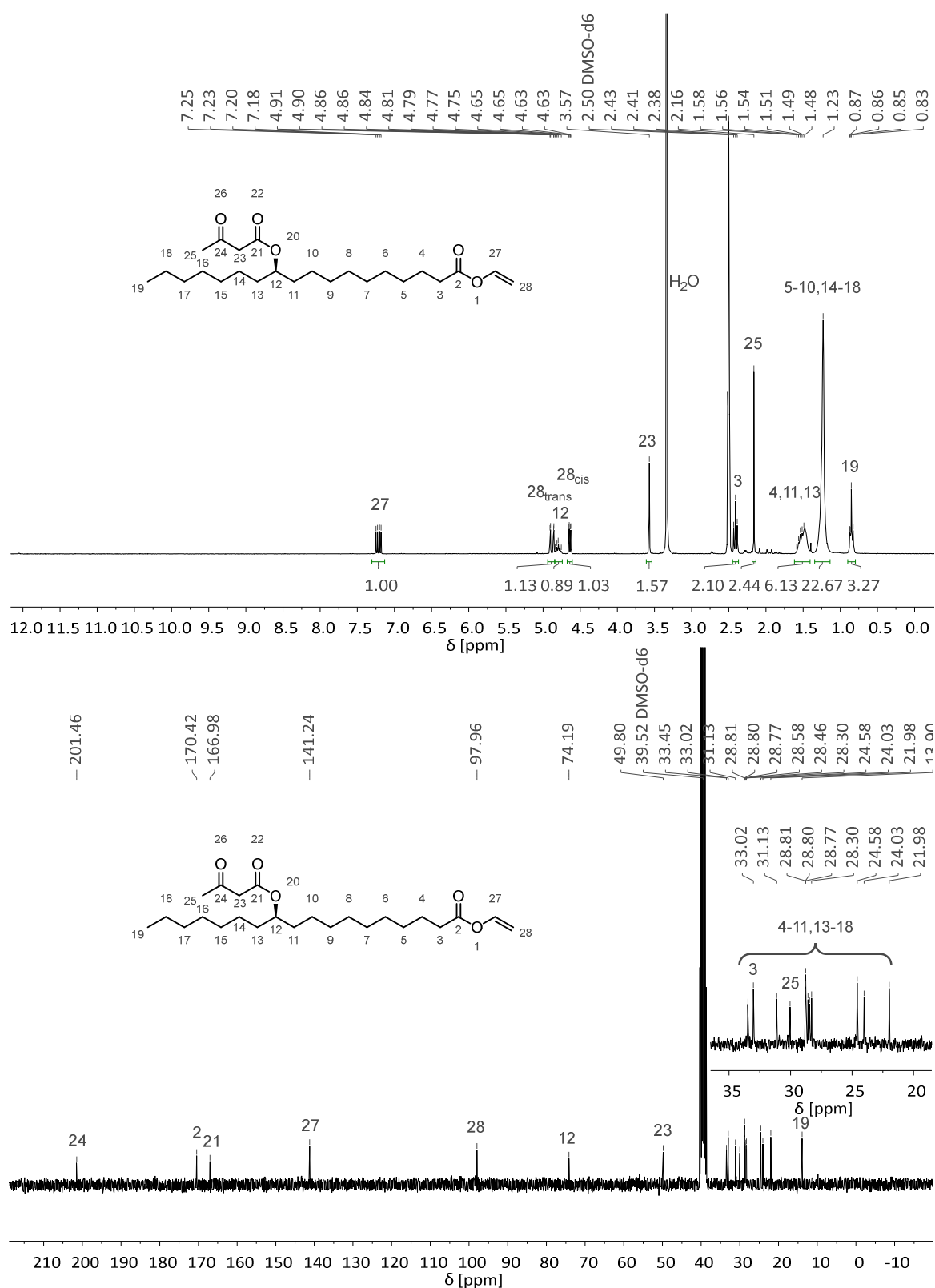
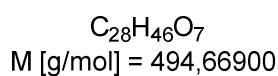
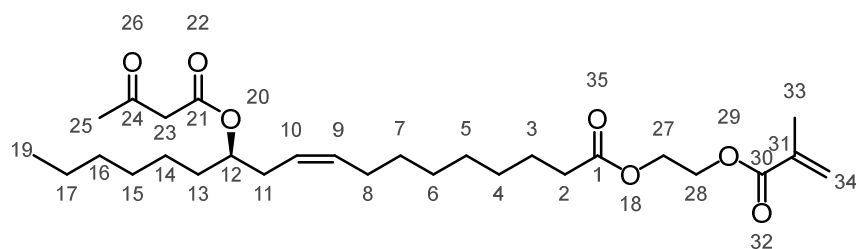


Figure 6.77 ^1H and ^{13}C NMR spectra of **164** in $\text{DMSO-}d_6$.

6.5.1.6 2-(Methacryloyloxy)ethyl (12*R*,9*Z*)-12-[(3-Oxobutanoyl)oxy]octadec-9-enoate (168)



(12*R*,9*Z*)-11-[(3-oxobutanoyl)oxy]octadec-8-enoic acid (38.98 mmol, 1.00 eq) was dissolved in 90 mL of toluene. After the addition of carbonyldiimidazole (1.05 eq), the mixture was stirred at room temperature for 16 h. Subsequently, 2-hydroxyethyl methacrylate (1.00 eq) was added to the mixture and the stirring was continued for 8 h at 65°C. The crude product was purified by column chromatography over silica gel.

yield	92% (17.7 g, 35.9 mmol, colourless oil)
eluent	<i>c</i> -C ₆ H ₁₂ :EtOAc = 90:10
R _f (product)	0.78 in <i>c</i> -C ₆ H ₁₂ :EtOAc = 50:50

¹H-NMR (400 MHz, CDCl₃): δ (ppm) = 6.15 – 6.10 (m, 1H, H_{34E}), 5.61 – 5.57 (m, 1H, H_{34Z}), 5.52 – 5.42 (m, 1H, H₉), 5.37 – 5.27 (m, 1H, H₁₀), 4.97 – 4.88 (m, 1H, H₁₂), 4.38 – 4.29 (m, 4H, H_{27,28}), 3.42 (s, 2H, H₂₃), 2.35 – 2.29 (m, 4H, H_{2,11}), 2.26 (s, 3H, H₂₅), 2.04 – 1.97 (m, 2H, H₈), 1.97 – 1.93 (m, 3H, H₃₃), 1.66 – 1.59 (m, 2H, H₃), 1.59 – 1.52 (m, 2H, H₁₃), 1.38 – 1.20 (m, 16H, H_{4-7,14-17}), 0.92 – 0.84 (m, 3H, H₁₉).

¹³C-NMR (101 MHz CDCl₃): δ (ppm) = 200.72 (C₂₄), 173.70 (C₁), 167.25 (C₃₀), 166.97 (C₂₁), 136.11 (C₃₁), 133.03 (C₉), 126.14 (C₃₄), 124.08 (C₁₀), 75.54 (C₁₂), 62.61 (C_{27/28}), 62.02 (C_{27/28}), 50.59 (C₂₃), 34.28 (C₂), 33.64 (C₁₃), 31.97 (C_{4-7,14-17}), 31.85 (C_{4-7,14-17}), 30.23 (C₂₅), 29.64 (C_{4-7,14-17}), 29.31 (C_{4-7,14-17}), 29.25 (C_{4-7,14-17}), 29.24 (C_{4-7,14-17}), 29.20 (C_{4-7,14-17}), 27.48 (C₈), 25.41, 25.03 (C₃), 22.71, 18.41 (C₃₃), 14.20 (C₁₉).

HRMS (FAB): m/z for C₂₈H₄₆O₇H⁺ [M+H]⁺: calculated: 495.3316; found: 495.3318.

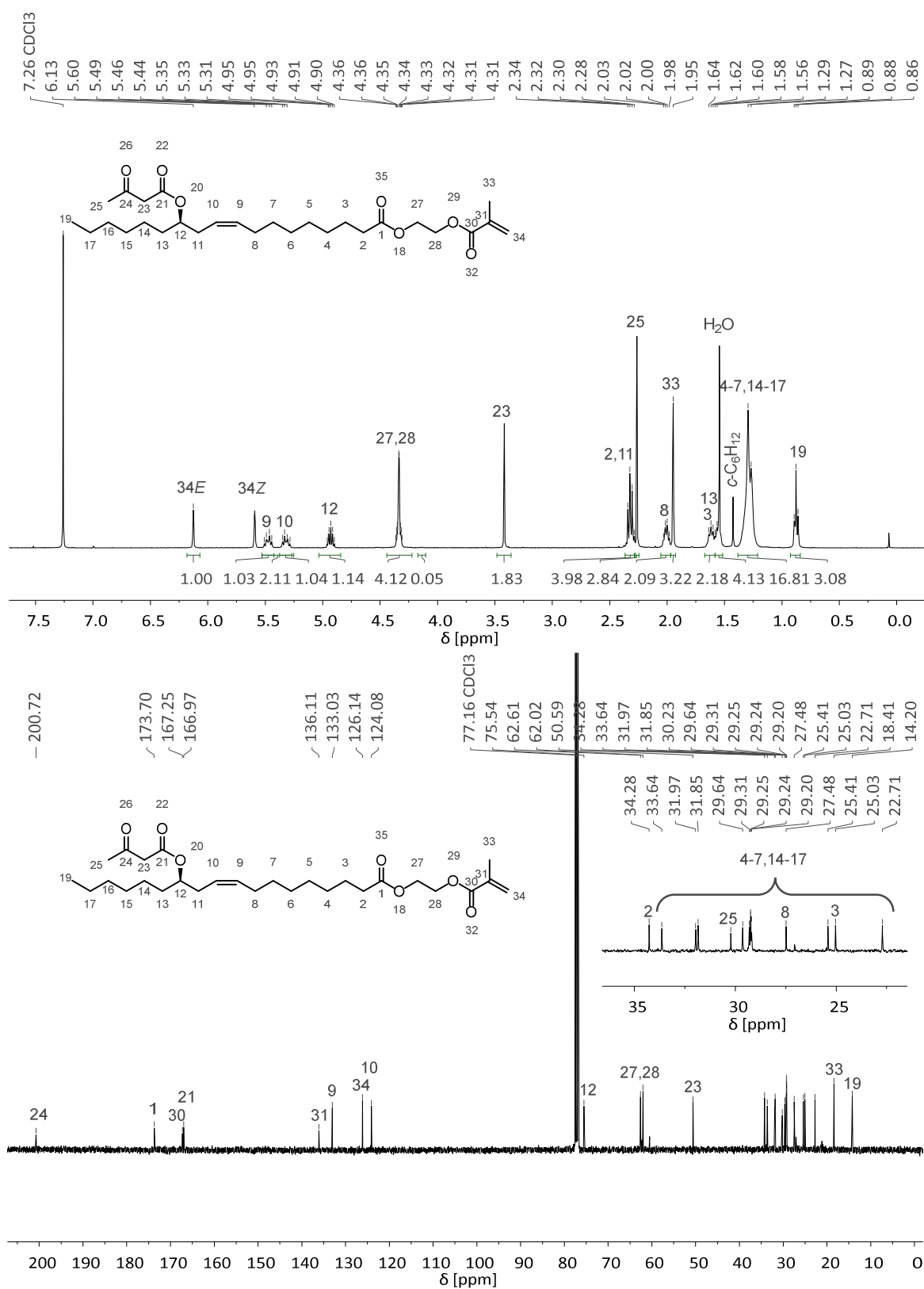
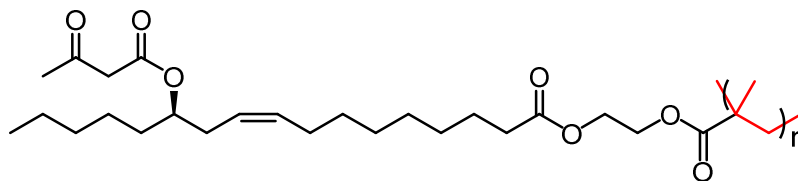


Figure 6.78 ¹H and ¹³C NMR spectra of **164** in DMSO-*d*₆.

6.5.2 RAFT Polymerisation (169)



All RAFT polymerisations were conducted according to the same general procedure if not denoted otherwise. The optimised procedure for the RAFT polymerisation of 2-(methacryloyloxy)ethyl (12*R*,9*Z*)-12-[(3-oxobutanoyl)oxy]octadec-9-enoate (**168**) with 2-cyanoprop-2-yl benzodithioate as CTA is given as follows:

2-(Methacryloyloxy)ethyl (12*R*,9*Z*)-12-[(3-oxobutanoyl)oxy]octadec-9-enoate (**168**, 1.01 mmol, 50.0 eq) and 2-cyanoprop-2-yl benzodithioate (1.00 eq) were dissolved in 495 μL toluene in 5 mL glass vial. Afterwards 44 μL of a AIBN stock solution (0.10 eq, 0.0075 $\text{mg}\cdot\mu\text{L}^{-1}$ in toluene) were added and the vial was closed with a rubber septum. The mixture was degassed with argon for 15 min. Subsequently, the mixture was stirred under argon at 65°C for several hours, depending on the desired molecular weight. Afterwards, the reaction mixture was cooled in an ice bath for 10 min, opened to the atmosphere and precipitated in 40 mL MeOH. The mixture was three times decanted and backfilled with 40 mL MeOH, each. After the last decantation, the MeOH was removed under high vacuum. Finally, the purified polymer was stored under the absence of light at 4°C.

$^1\text{H-NMR}$ (400 MHz, CDCl_3): δ (ppm) = 5.54 – 5.42 (m, H_9), 5.37 – 5.26 (m, H_{10}), 4.97 – 4.88 (m, H_{12}), 4.24 (s, H_{23}), 4.13 (br s, $\text{H}_{27/28}$), 3.42 (br s, $\text{H}_{27/28}$), 2.38 – 2.27 (m, $\text{H}_{2,11}$), 2.26 (s, H_{25}), 2.06 – 1.97 (m, H_8), 1.90 – 1.67 (br, H_{34}), 1.67 – 1.58 (m, H_3), 1.58 – 1.51 (m, H_{13}), 1.39 – 1.20 (m, $\text{H}_{4-7,14-17}$), 1.10 – 0.79 (br m, H_{33}), 0.87 (t, $^3J_{\text{H}_{18},\text{H}_{17}} = 6.7 \text{ Hz}$, H_{18}).

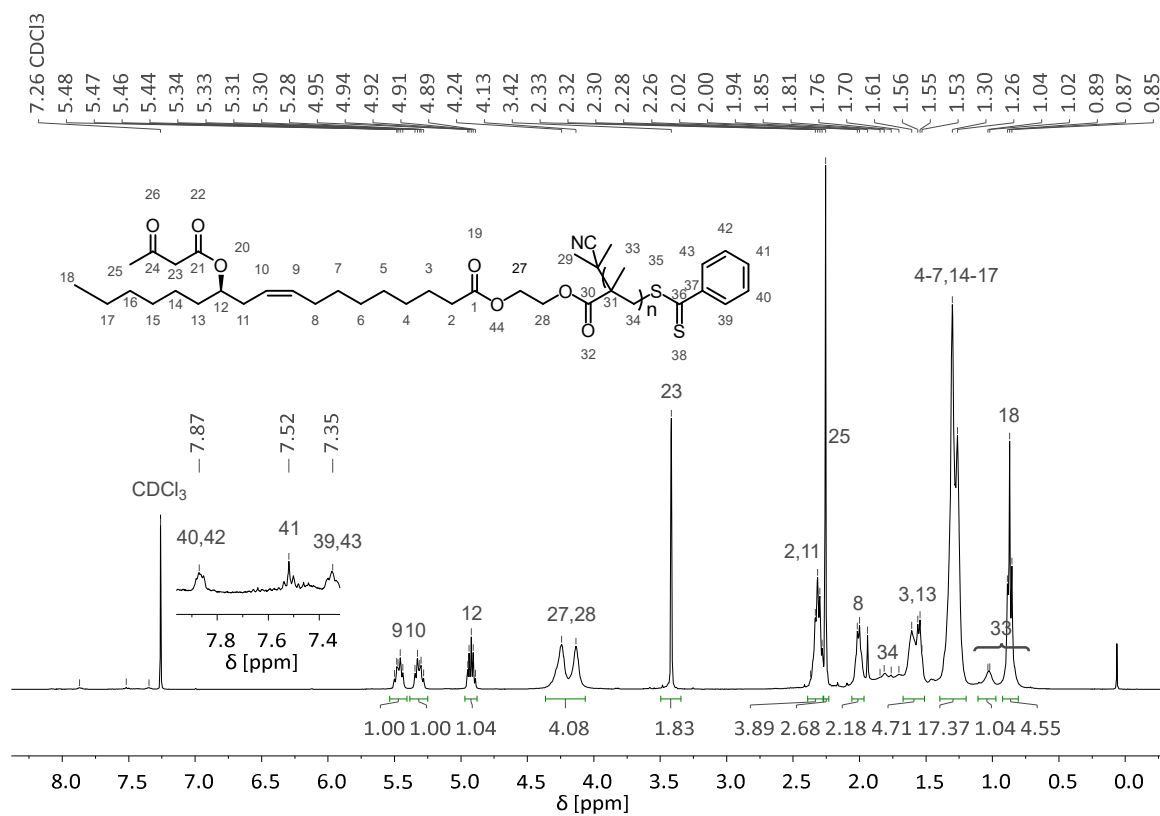


Figure 6.79 Example ¹H spectrum of **169** in CDCl₃.

The results of the screenings regarding the applied CTAs, the investigated concentrations and the thermal analyses are given as follows.

Table 6.15 ^1H NMR and SEC results of the screening of the RAFT polymerisation of **168** at a 7.5 M and 3.75 M concentration using CTA1 or CTA2.

entry	CTA ^a	concentration [M]	reaction time [h]	$M_{n,\text{NMR}}^{\text{b}}$ [g·mol ⁻¹] (conversion [%])	$M_{n,\text{SEC}}$ [g·mol ⁻¹]	\bar{D}
1			1	2 450 (9)	14 900	1.34
2	CTA1	7.5	2.2	7 150 (28)	31 000	1.19
3			3	11 350 (45)	45 800	1.25
4			5	17 530 (70)	115 000	2.51
5			1	1 580 (5)	- ^c	-
6			2	1 830 (6)	8 100	1.25
7			3	3 810 (14)	9 800	1.34
8	CTA2	7.5	4	6 030 (23)	12 000	1.36
9			5	10 730 (42)	15 700	1.34
10			6	15 430 (61)	18 700	1.39
11			7	17 660 (70)	22 100	1.35
12			1	3 400 (13)	18 100	1.27
13			2	9 200 (36)	29 400	1.23
14	CTA1	3.75	3	12 600 (50)	50 900	1.24
15			4	16 600 (66)	74 600	1.55
16			5	18 600 (74)	120 000	2.5

^aratio of monomer to CTA to AIBN is 50:1:0.1; ^b $M_{n,\text{NMR}}$ is calculated using the monomer conversion; ^csignal not visible in SEC chromatogram.

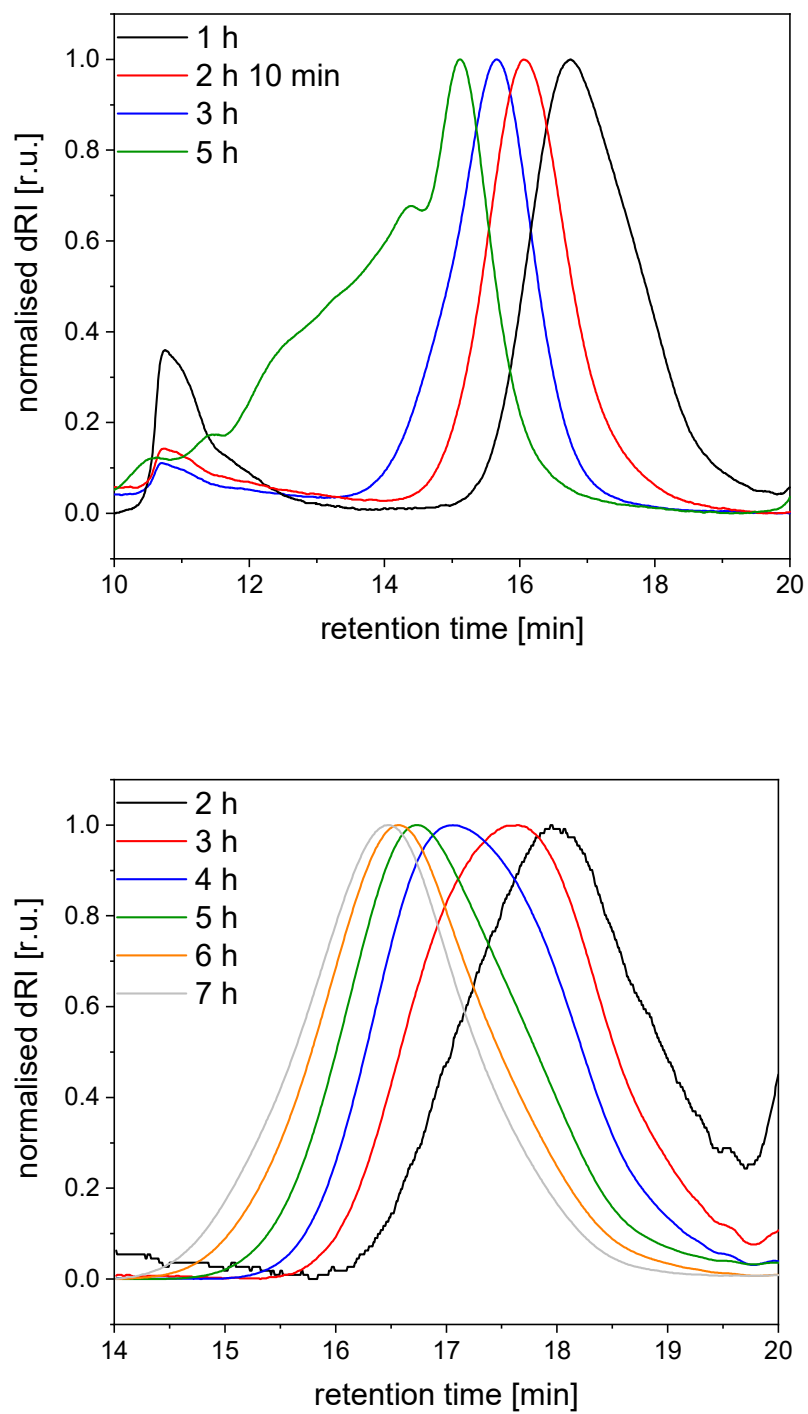


Figure 6.80 SEC graphs of the screening of the RAFT polymerisation of **168** at a 7.5 M concentration with CTA1 (top) and CTA2 (bottom).

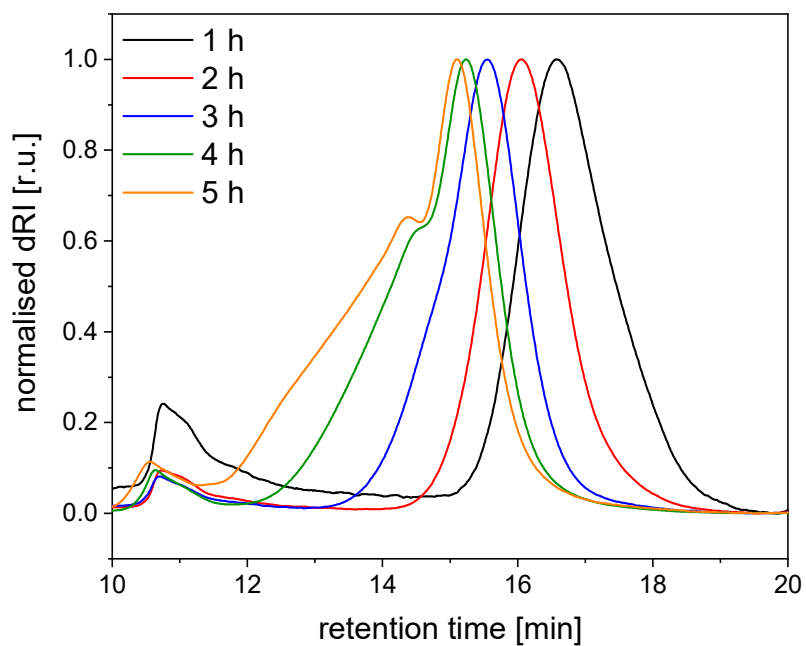


Figure 6.81 SEC graphs of the screening of the RAFT polymerisation of **168** at a 3.75 M concentration with CTA1.

Table 6.16 ^1H NMR and SEC results of the screening of the RAFT polymerisation of **168** at a 1.88 M concentration using CTA1 or CTA2.

entry	CTA ^a	concentration [M]	reaction time [h]	$M_{n,\text{NMR}}^{\text{b}}$ [$\text{g}\cdot\text{mol}^{-1}$] (conversion [%])	$M_{n,\text{SEC}}$ [$\text{g}\cdot\text{mol}^{-1}$]	D
1			1	2 200 (8)	5 355	1.15
2			2	3 930 (15)	6 560	1.17
3			3	5 420 (21)	7 880	1.17
4	CTA1	1.88	4	8 630 (34)	9 690	1.17
5			5	11 100 (44)	11 750	1.15
6			6	13 580 (54)	13 480	1.17
7			6.5	14 810 (59)	14 400	1.18
8			1	1 090 (3)	- ^c	- ^c
9			2	2 820 (10)	8 370	1.29
10			3	4 800 (18)	10 520	1.31
11	CTA2	1.88	4	7 770 (30)	12 610	1.33
12			5	11 970 (47)	15 690	1.32
13			6	16 180 (64)	18 360	1.35
14			7	19 390 (77)	22 460	1.29

^aratio of monomer to CTA to AIBN is 50:1:0.1; ^b $M_{n,\text{NMR}}$ is calculated using the monomer conversion; ^csignal not visible in SEC chromatogram.

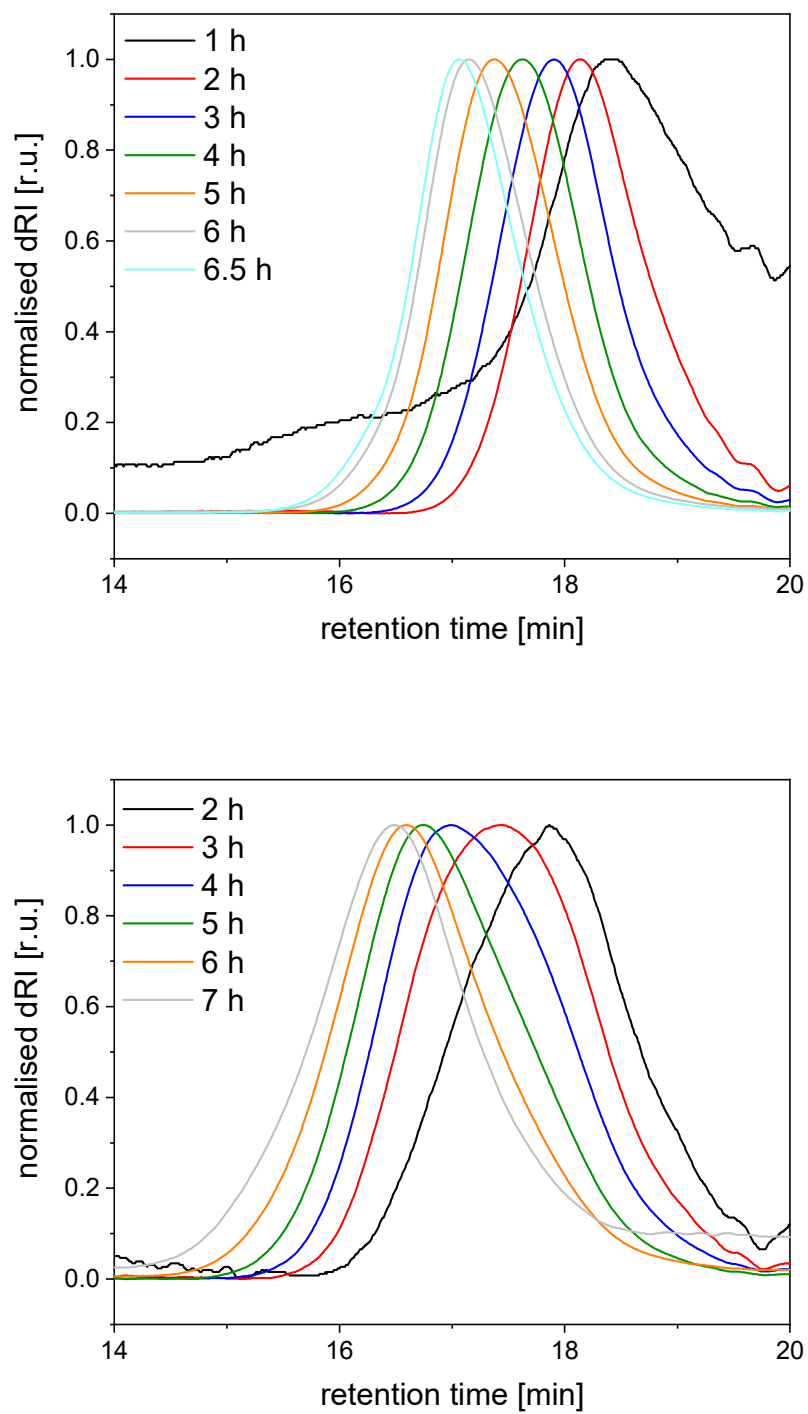


Figure 6.82 SEC graphs of the screening of the RAFT polymerisation of **168** at a 1.8 M concentration with CTA1 (top) and CTA2 (bottom).

Table 6.17 SEC and ^1H NMR data for the synthesis of RAFT polymers of specific molecular weights.^a

entry	reaction ^b time [min]	intended $M_{n,\text{NMR}}^b$ [g·mol ⁻¹] (conversion [%])	$M_{n,\text{NMR}}^c$ [g·mol ⁻¹] (conversion [%])	$M_{n,\text{SEC}}$ [g·mol ⁻¹]	D
1	222	10 200 (40)	10 620 (42)	11 410	1.14
2	276	12 700 (50)	11 950 (51)	11 680	1.12
3	333	15 200 (60)	14 450 (57)	13 920	1.13

^aratio of monomer to CTA to AIBN is 50:1:0.1; ^bcalculated using the found relation between $\ln([M_0]/[M])$ and t (**Figure 4.21**) ^c $M_{n,\text{NMR}}$ is calculated using the signals of the dithiobenzoate end group.

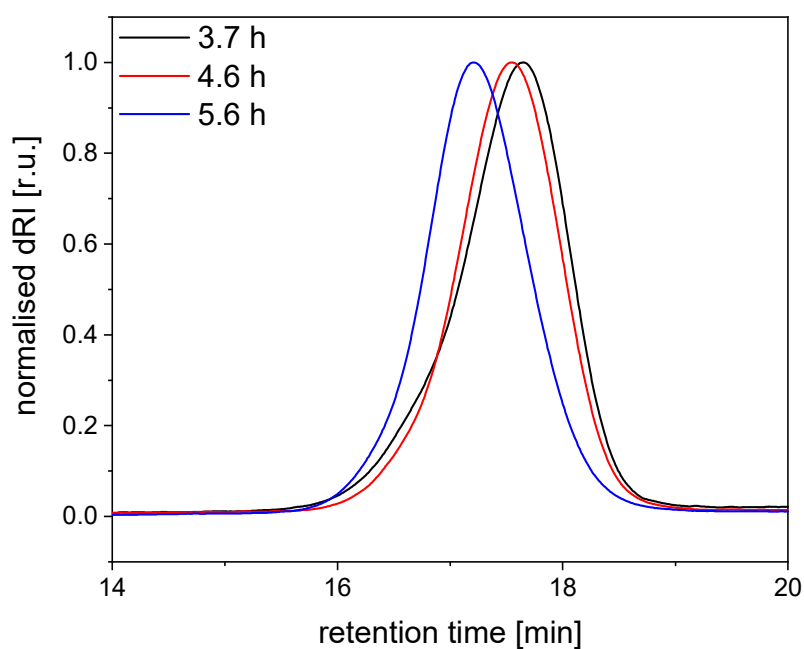


Figure 6.83 SEC graphs of the RAFT polymerisations of **168** at a 1.8 M concentration with CTA1, stopped after certain reaction times to reach specific conversions.

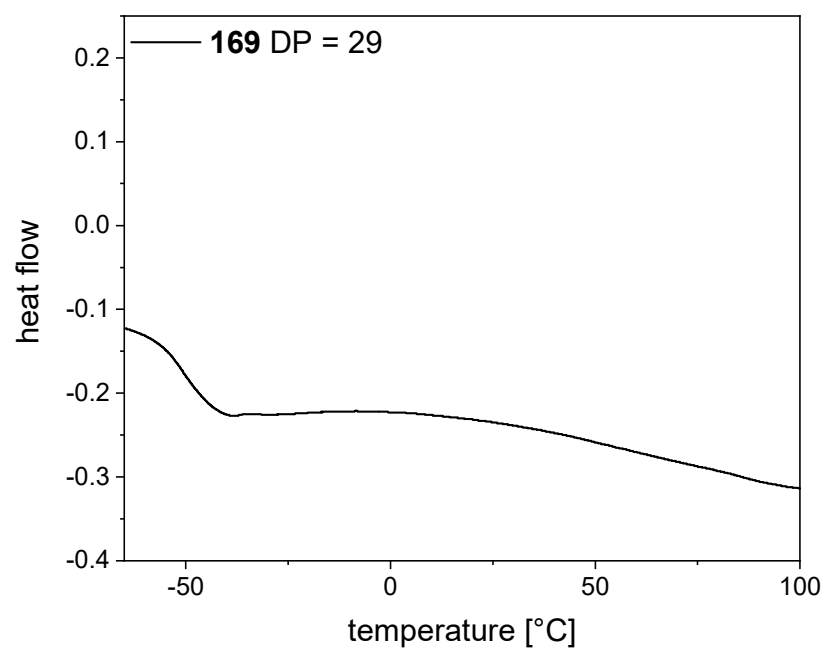
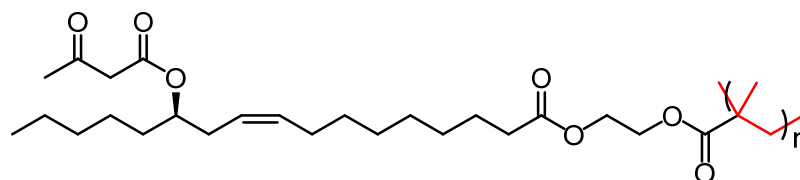


Figure 6.84 DSC graph of **169**.

6.5.3 Chain Extension of Poly{2-(methacryloyloxy)ethyl (12*R*,9*Z*)-12-[(3-oxobutanoyl)oxy]octadic-9-enoate}



For the chain extension of the RAFT polymer (**169**), **169** was applied as macro CTA ($M_{n,NMR} = 12\,011\text{ g}\cdot\text{mol}^{-1}$, 0.0202 mmol, 1.00 eq). Subsequently, 795 μL of toluene and 2-(methacryloyloxy)ethyl (12*R*,9*Z*)-12-[(3-oxobutanoyl)oxy]octadic-9-enoate (**168**, 1.01 mmol, 50.0 eq) were added. Afterwards, 44 μL of an AIBN stock solution (0.10 eq, 0.0075 $\text{mg}\cdot\mu\text{L}^{-1}$ in toluene) were added and the mixture was degassed with argon for 15 min. Subsequently, the mixture was stirred under argon at 65°C for 2.4 h (35% monomer conversion). Afterwards, the reaction mixture was cooled in an ice bath for 10 min, opened to the atmosphere and precipitated in 40 mL MeOH. The mixture was decanted three times and backfilled with 40 mL MeOH, each. After the last decantation the MeOH was removed under high vacuum. Finally, the purified polymer was stored under the absence of light at 4°C. The final polymer showed a $M_{n,NMR}$ of 18 700 $\text{g}\cdot\text{mol}^{-1}$ (35% monomer conversion) and a $M_{n,SEC}$ of 18 700 $\text{g}\cdot\text{mol}^{-1}$ with $D = 1.15$.

¹H-NMR (400 MHz, CDCl_3): δ (ppm) = 5.54 – 5.42 (m, H₉), 5.37 – 5.26 (m, H₁₀), 4.97 – 4.88 (m, H₁₂), 4.24 (s, H₂₃), 4.13 (br s, H_{27/28}), 3.42 (br s, H_{27/28}), 2.38 – 2.27 (m, H_{2,11}), 2.26 (s, H₂₅), 2.06 – 1.97 (m, H₈), 1.90 – 1.67 (br, H₃₄), 1.67 – 1.58 (m, H₃), 1.58 – 1.51 (m, H₁₃), 1.39 – 1.20 (m, H_{4-7,14-17}), 1.10 – 0.79 (br m, H₃₃), 0.87 (t, $^3J_{H_{18},H_{17}} = 6.7\text{ Hz}$, H₁₈).

6.5 Synthesis Procedures and Analytical Data Related to Chapter 4.3

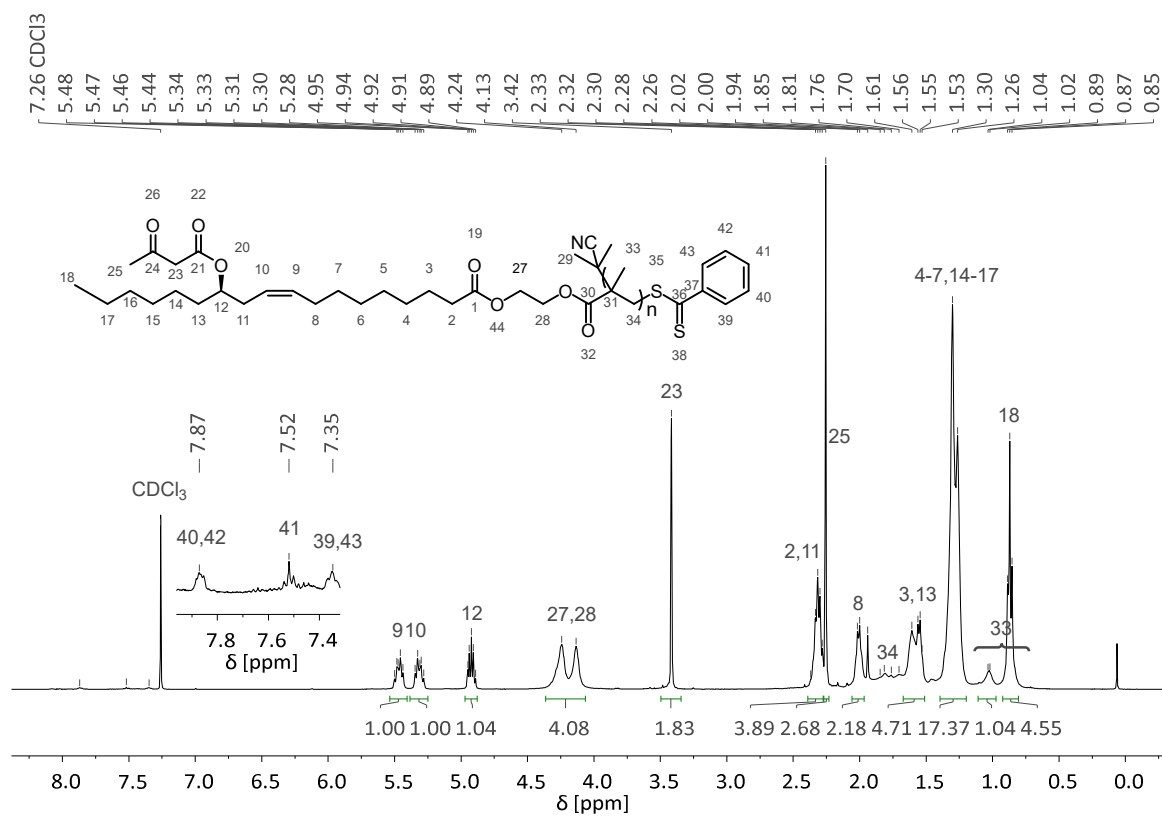


Figure 6.85 Example ¹H spectrum of **169** in CDCl₃.

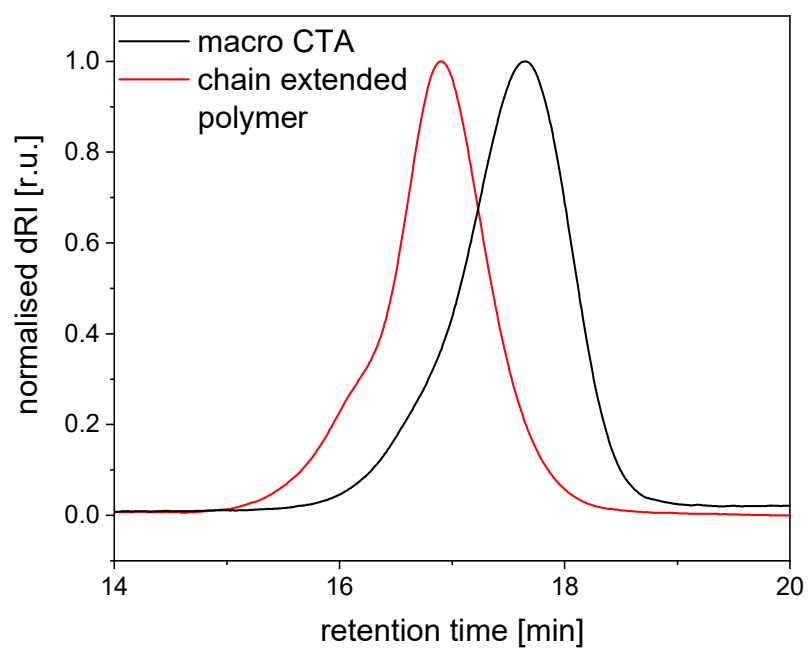
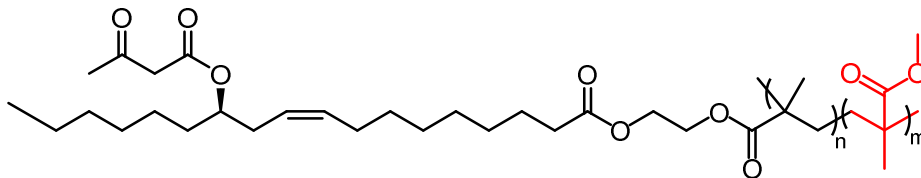


Figure 6.86 SEC graphs of the applied macro CTA and the resulting polymer after chain extension *via* RAFT polymerisation.

6.5.4 Block Copolymer Synthesis (170)



The block copolymer synthesis was performed using **169** as macro CTA and methyl methacrylate as monomer. Methyl methacrylate was filtered over basic aluminium oxide prior to usage. The macro CTA ($M_{n,NMR} = 17\,020\text{ g}\cdot\text{mol}^{-1}$, 0.0202 mmol, 1.00 eq) was dissolved in 795 μL of toluene. Afterwards, methyl methacrylate (1.01 mmol, 50.0 eq) and 44 μL of an AIBN stock solution (0.10 eq, 0.0075 $\text{mg}\cdot\mu\text{L}^{-1}$ in toluene) were added and the mixture was degassed with argon for 15 min. Subsequently, the mixture was stirred under argon at 65°C for 5.6 h. Afterwards, the reaction mixture was cooled in an ice bath for 10 min, opened to the atmosphere and precipitated in 40 mL MeOH. The mixture was decanted three times and backfilled with 40 mL MeOH, each. After the last decantation the MeOH was removed under high vacuum. Finally, the purified polymer was stored under the absence of light at 4°C. The final polymer (**170**) showed a $M_{n,NMR}$ of 18 130 $\text{g}\cdot\text{mol}^{-1}$ and a $M_{n,SEC}$ of 10 325 $\text{g}\cdot\text{mol}^{-1}$ with $D = 1.13$.

$^1\text{H-NMR}$ (400 MHz, CDCl_3): δ (ppm) = 5.46 – 5.36 (m, H_9), 5.31 – 5.20 (m, H_{10}), 4.91 – 4.81 (m, H_{12}), 4.18 (br s, $\text{H}_{27/28}$), 4.07 (br s, $\text{H}_{27/28}$), 3.64 – 3.48 (m, H_{44}), 3.35 (s, H_{23}), 2.32 – 2.21 (m, $\text{H}_{2,11}$), 2.19 (s, H_{25}), 1.99 – 1.91 (m, H_8), 1.86 – 1.60 (m, $\text{H}_{31,45}$), 1.60 – 1.52 (m, H_3), 1.52 – 1.45 (m, H_{13}), 1.32 – 1.14 (m, $\text{H}_{4-7,14-17}$), 1.05 – 0.72 (m, $\text{H}_{33,35}$), 0.86 – 0.75 (m, H_{18}).

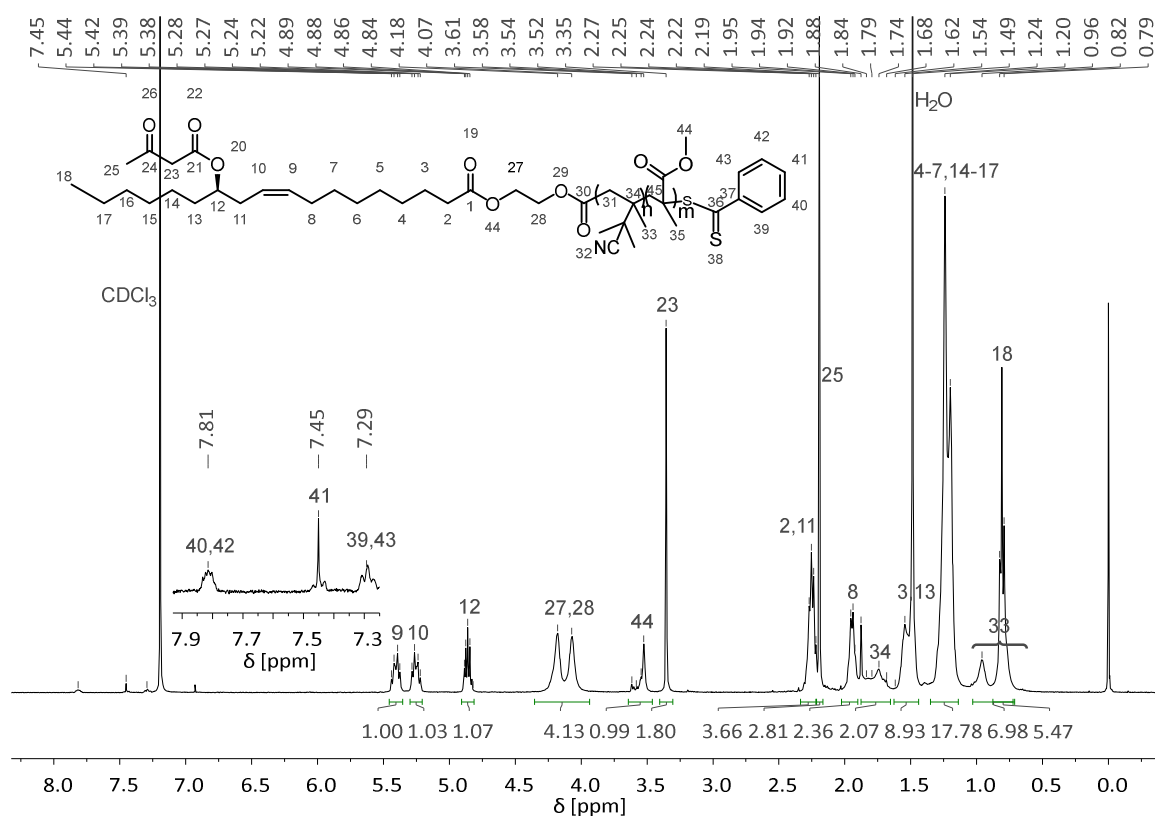


Figure 6.87 Example ¹H spectrum of **170** in CDCl₃.

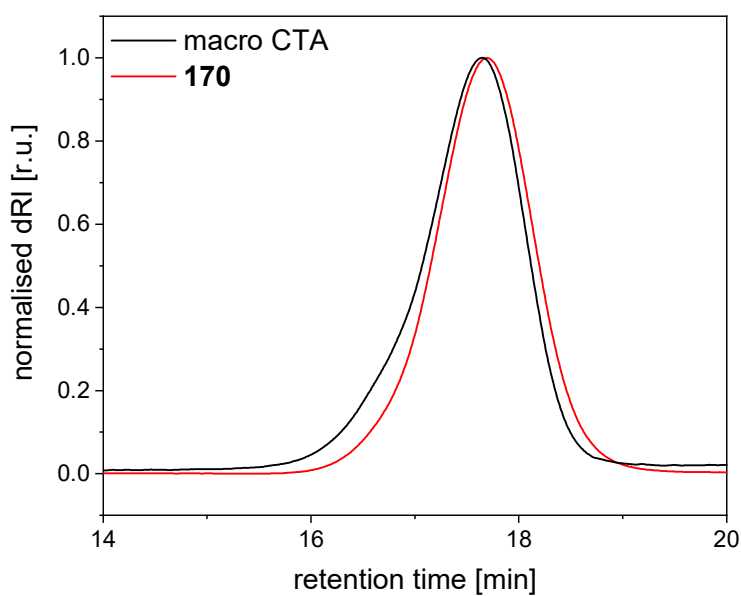
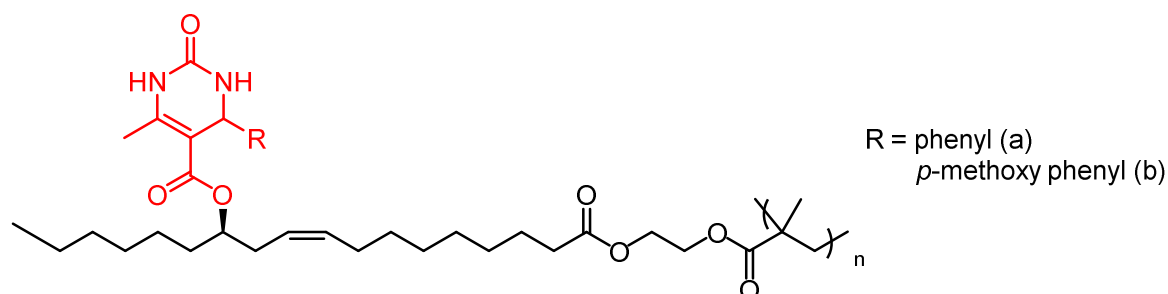


Figure 6.88 SEC graphs of the applied macro CTA and the resulting block copolymer **170**.

6.5.5 Post-Polymerisation Modification *via* Biginelli-Three-Component Reaction (171)



The post-polymerisation modifications were conducted according to the same general procedure while either benzaldehyde or anisaldehyde were used as aldehyde component leading to **171a** or **171b**, respectively.

169 ($M_{n,NMR} = 10\,150\text{ g}\cdot\text{mol}^{-1}$, $9.85\ \mu\text{mol}$, corresponds to 0.197 mmol acetoacetate, 1.00 eq) was dissolved in 0.8 mL AcOH in a 5 mL vial. Subsequently, the aldehyde component (1.33 eq), urea (1.33 eq), and $\text{MgCl}_2\cdot 6\text{ H}_2\text{O}$ (0.0667 eq) are added. After dissolution, the mixture was stirred at 100°C for 20 h . Afterwards, the polymer was precipitated in 40 mL H_2O . The suspension was three times decanted and backfilled with 40 mL MeOH, each. After the last decantation, the remaining MeOH was removed under high vacuum yielding the final polymer.

Detailed analytics by SEC, DSC, and ^1H NMR spectroscopy are given as follows.

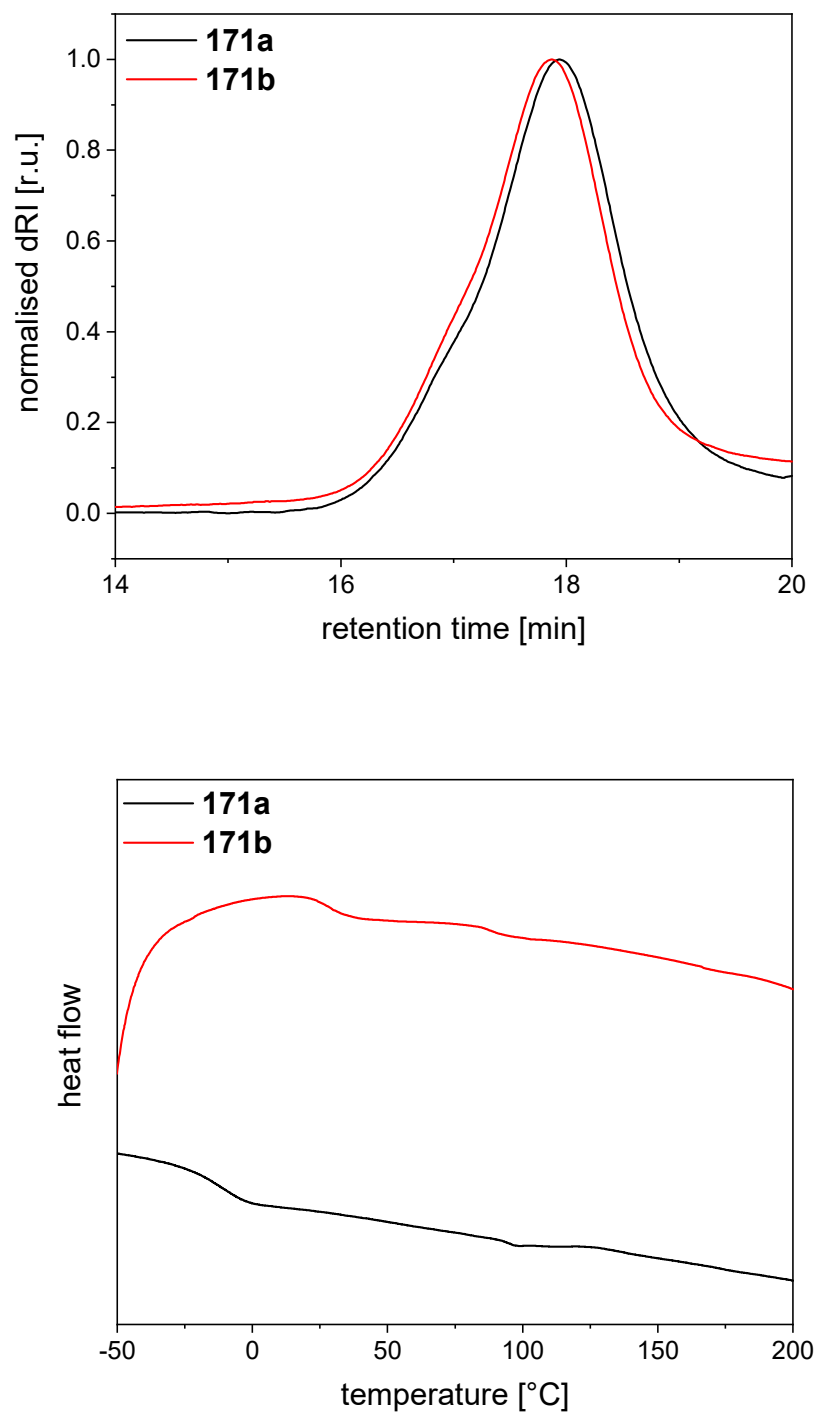


Figure 6.89 SEC and DSC graphs of **171a** and **171b**.

6.5.5.1 171a

$^1\text{H-NMR}$ (400 MHz, $\text{DMSO-}d_6$): δ (ppm) = 9.15 (s, H₄₈), 7.68 (s, H₅₀), 7.48 – 7.16 (m, H₅₅₋₅₉), 5.48 – 5.32 (m, H₉), 5.31 – 5.18 (m, H_{9',10}), 5.16 – 5.08 (m, H₅₁), 4.97 – 4.86 (m, H_{10'}), 4.77 – 4.63 (m, H₁₂), 4.31 – 3.93 (m, H_{27,28}), 2.32 – 2.12 (m, H_{2,11}), 2.08 – 1.76 (m, H₈), 2.08 – 1.61 (m, H₃₄), 1.60 – 1.38 (m, H_{3,13}), 1.39 – 1.05 (m, H_{4-7,14-17}), 1.06 – 0.60 (br, H₃₃), 0.89 – 0.63 (m, H₁₈).

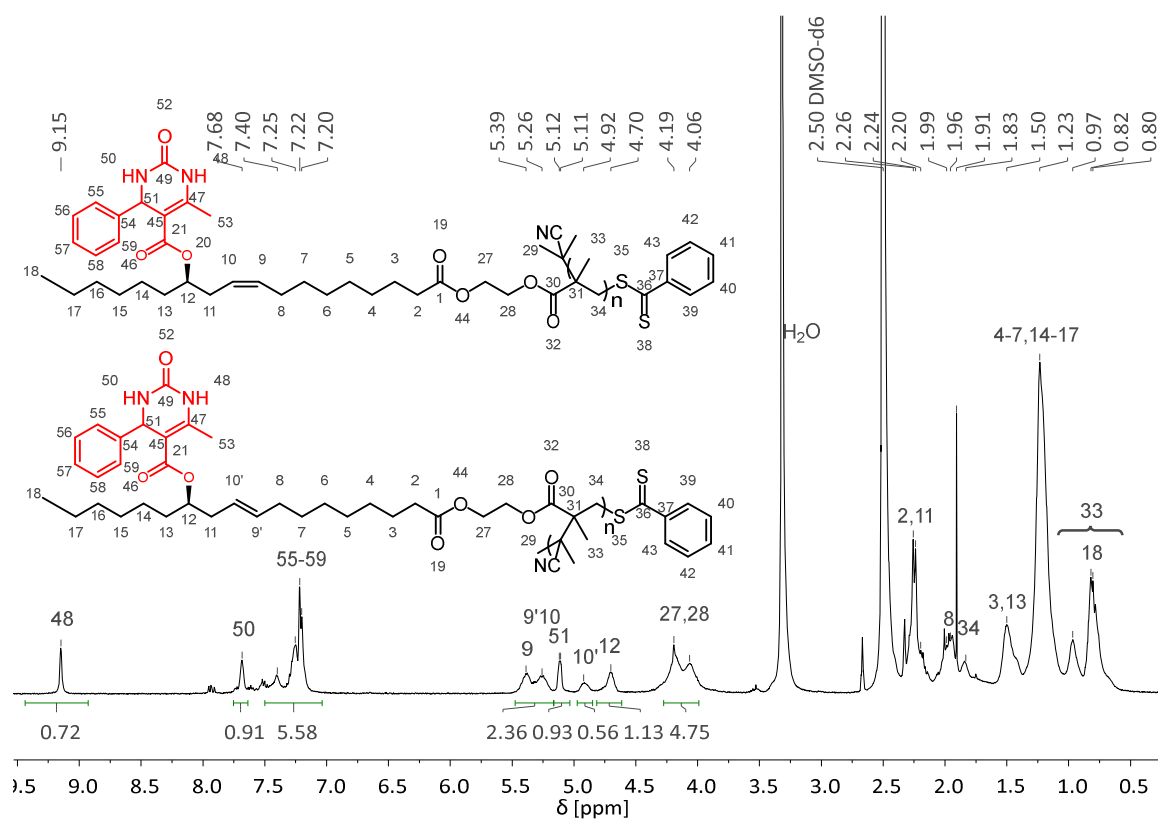


Figure 6.90 $^1\text{H-NMR}$ spectrum of **171a** in $\text{DMSO-}d_6$.

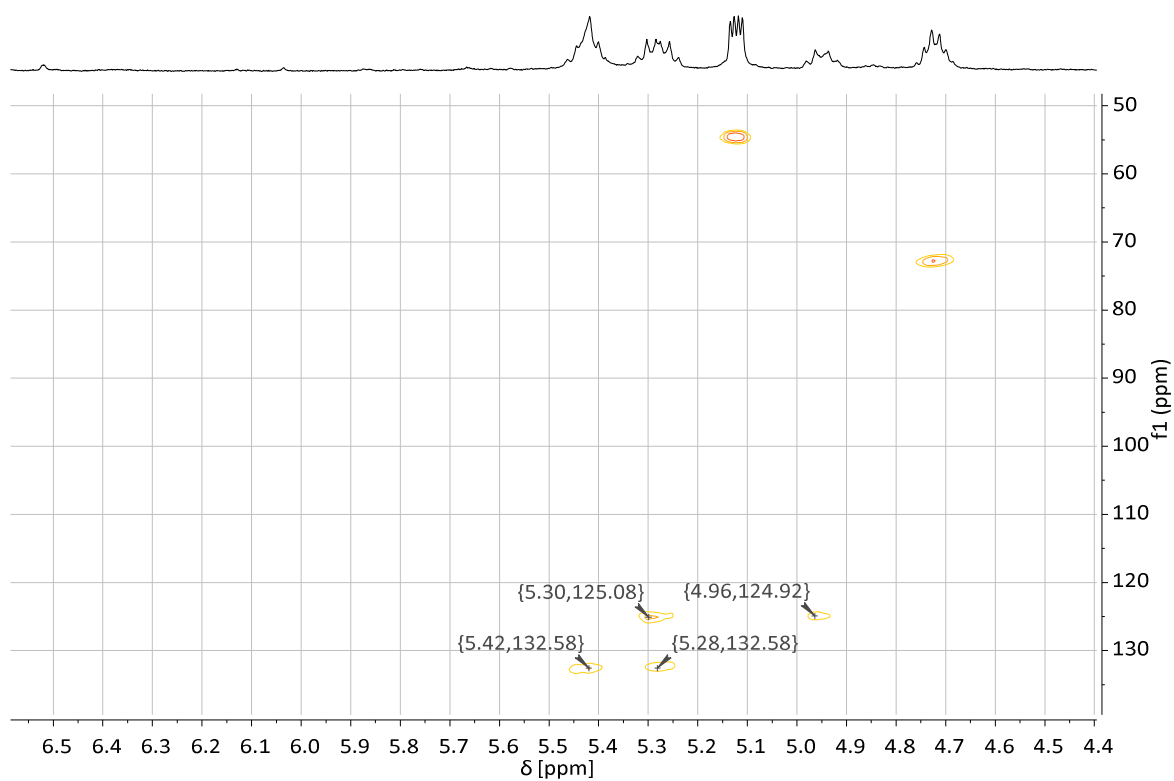


Figure 6.91 Phase edited HSQC spectrum of **171a**: the picked signals indicate existence of an internal cis double bond and an internal trans double bond as the ^{13}C shift hardly differs between cis and trans while the ^1H shift does.^[420]

6.5.5.2 171b

$^1\text{H-NMR}$ (400 MHz, $\text{DMSO-}d_6$): δ (ppm) = 9.10 (s, H₄₈), 7.60 (s, H₅₀), 7.21 – 7.05 (m, H_{55,59}), 6.93 – 6.71 (m, H_{56,58}), 5.49 – 5.32 (m, H₉), 5.33 – 5.21 (m, H_{9',10}), 5.10 – 5.03 (m, H₅₁), 5.01 – 4.87 (m, H_{10'}), 4.80 – 4.65 (m, H₁₂), 4.34 – 3.99 (m, H_{27,28}), 3.68 (s, H₆₀), 2.36 – 2.16 (m, H_{2,11}), 2.12 – 1.38 (m, H_{3,8,13,34}), 1.38 – 1.09 (m, H₄₋₇₋₁₄₋₁₇), 1.03 – 0.89 (m, H₃₃), 0.87 – 0.70 (m, H₁₈).

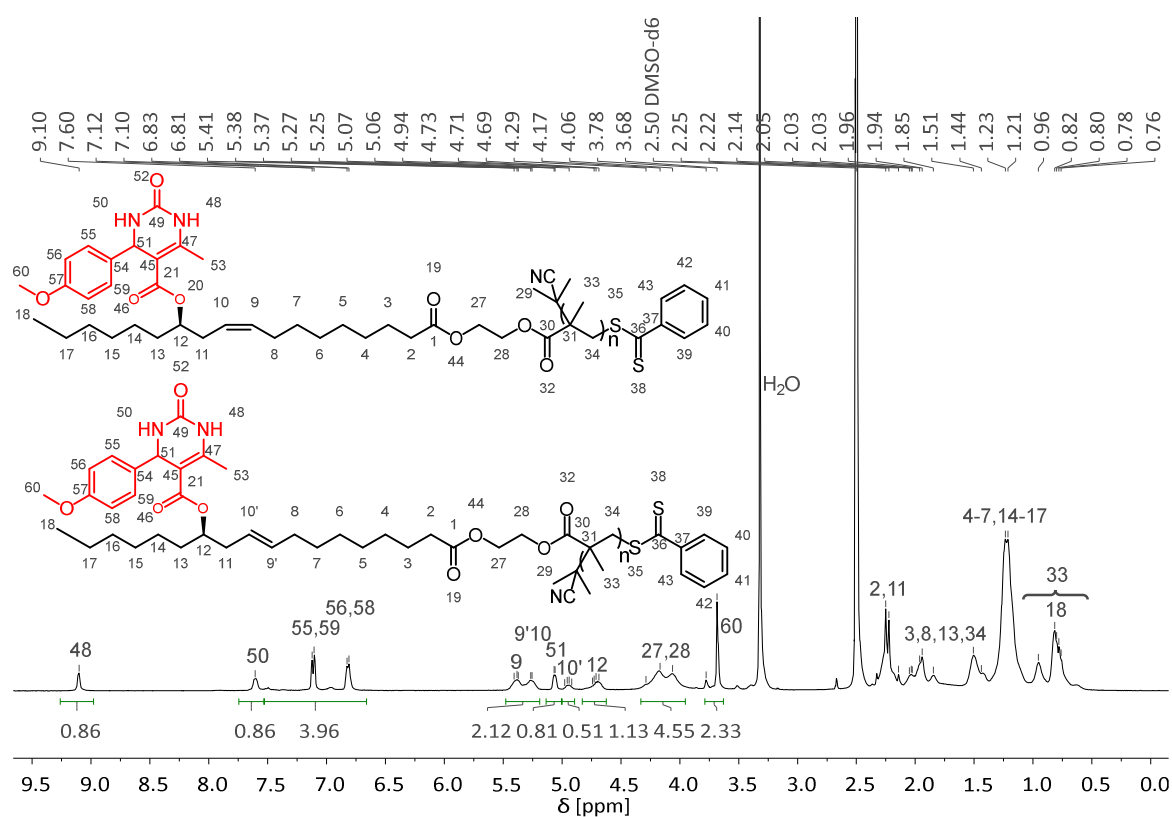


Figure 6.92 $^1\text{H-NMR}$ spectrum of 171b in $\text{DMSO-}d_6$.

7 References

- [1] L. R. Berlanstein, *The Industrial Revolution and work in nineteenth-century Europe*, Routledge, London, England, New York, **1992**.
- [2] Bundesanstalt für Geowissenschaften und Rohstoffe (BGR), “Energiestudie 2015. Reserven, Ressourcen und Verfügbarkeit von Energierohstoffen”, **2015**.
- [3] J. H. Clark, V. Budarin, F. E. I. Deswarte, J. J. E. Hardy, F. M. Kerton, A. J. Hunt, R. Luque, D. J. Macquarrie, K. Milkowski, A. Rodriguez et al., *Green Chem.*, **2006**, *8*, 853.
- [4] “Plastics-the Facts 2016”, URL:
http://www.plasticseurope.org/documents/document/20161014113313-plastics_the_facts_2016_final_version.pdf, **2016**, accessed 03.01.18.
- [5] R. A. Sheldon, *Chem. Soc. Rev.*, **2012**, *41*, 1437.
- [6] P. T. Anastas, M. M. Kirchhoff, *Acc. Chem. Res.*, **2002**, *35*, 686.
- [7] G. H. Brundtland, *Our common future*, Univ. Press, Oxford, **1991**.
- [8] A. S. Cannon, J. L. Pont, J. C. Warner in *Green Techniques for Organic Synthesis and Medicinal Chemistry* (Eds.: W. Zhang, B. Cue), Wiley, s.l., **2012**.
- [9] J. H. Clark, *Green Chem.*, **2006**, *8*, 17.
- [10] *Pollution Prevention Act of 1990*, 42 U.S.C., §§ 13101 – 13109, **1990**.
- [11] P. T. Anastas, C. A. Farris, *Benign by Design. Alternative Synthetic Design for Pollution Prevention*, Am. Chem. Soc., Washington, DC, **1994**.
- [12] P. T. Anastas, T. C. Williamson, *Green chemistry. Designing chemistry for the environment; developed from a symposium sponsored by the Division of*

Environmental Chemistry, Inc., at the 208th national meeting of the American Chemical Society, Washington, DC, August 21 - 25, 1994, American Chemical Society, Washington, DC, 1998.

- [13] “ACS Green Chemistry Institute”, URL:
<https://www.acs.org/content/acs/en/greenchemistry/about.html>, accessed 2020.08.06.
- [14] J. Clark, *Green Chem.*, **1999**, *1*, G1.
- [15] J. Li, J. F. Burnham, T. Lemley, R. M. Britton, *J. Electron. Resour. Med. Libr.*, **2010**, *7*, 196.
- [16] M. Poliakoff, J. M. Fitzpatrick, T. R. Farren, P. T. Anastas, *Science*, **2002**, *297*, 807.
- [17] P. T. Anastas, J. C. Warner, *Green chemistry. Theory and practice*, Oxford Univ. Press, New York, **1998**.
- [18] P. T. Anastas, T. C. Williamson in *Green chemistry, Vol. 626* (Ed.: P. T. Anastas), American Chemical Society, Washington, DC, **1998**.
- [19] P. Anastas, N. Eghbali, *Chem. Soc. Rev.*, **2010**, *39*, 301.
- [20] P. T. Anastas, J. B. Zimmerman, *Environ. Sci. Technol.*, **2003**, *37*, 94A-101A.
- [21] S. L. Y. Tang, R. L. Smith, M. Poliakoff, *Green Chem.*, **2005**, *7*, 761.
- [22] S. Y. Tang, R. A. Bourne, R. L. Smith, M. Poliakoff, *Green Chem.*, **2008**, *10*, 268.
- [23] T. Collins, *Science*, **2001**, *291*, 48.
- [24] P. T. Anastas, J. B. Zimmerman, *Green Chem.*, **2019**, *21*, 6545.
- [25] A. Albini, S. Protti, *Paradigms in Green Chemistry and Technology*, Springer International Publishing, Cham, **2016**.
- [26] B. M. Trost, *Science*, **1991**, *254*, 1471.

-
- [27] D. J. C. Constable, A. D. Curzons, V. L. Cunningham, *Green Chem.*, **2002**, *4*, 521.
- [28] M. Eissen, R. Mazur, H.-G. Quebbemann, K.-H. Pennemann, *Helv. Chim. Acta*, **2004**, *87*, 524.
- [29] J. Andraos, *Org. Process Res. Dev.*, **2005**, *9*, 149.
- [30] R. A. Sheldon, *Green Chem.*, **2007**, *9*, 1273.
- [31] M. Gandiglio, A. Lanzini, A. Soto, P. Leone, M. Santarelli, *Front. Environ. Sci.*, **2017**, *5*.
- [32] X.-T. Bui, C. Chiemchaisri, T. Fujioka, S. Varjani, *Water and Wastewater Treatment Technologies*, Springer Singapore, Singapore, **2019**.
- [33] R. A. Sheldon, *Green Chem.*, **2017**, *19*, 18.
- [34] A. P. Dicks, A. Hent, *Green chemistry metrics. A guide to determining and evaluating process greenness*, Springer, Cham, **2015**.
- [35] F. Tieves, F. Tonin, E. Fernández-Fueyo, J. M. Robbins, B. Bommarius, A. S. Bommarius, M. Alcalde, F. Hollmann, *Tetrahedron*, **2019**, *75*, 1311.
- [36] R. A. Sheldon in *Precision Process Technology. Perspectives for Pollution Prevention* (Eds.: M. P. C. Weijnen, A. A. H. Drinkenburg), Springer Netherlands, Dordrecht, **2013**.
- [37] C. Jimenez-Gonzalez, C. S. Ponder, Q. B. Broxterman, J. B. Manley, *Org. Process Res. Dev.*, **2011**, *15*, 912.
- [38] T. Hudlicky, D. A. Frey, L. Koroniak, C. D. Claeboe, L. E. Brammer Jr., *Green Chem.*, **1999**, *1*, 57.
- [39] M. Eissen, J. O. Metzger, *Chem. Eur. J.*, **2002**, *8*, 3580.

-
- [40] M. Eissen, *Bewertung der Umweltverträglichkeit organisch-chemischer Synthesen*. Zugl.: Oldenburg, Univ., Diss, 2001, Bis, Oldenburg, **2002**.
- [41] K. van Aken, L. Streckowski, L. Patiny, *Beilstein J. Org. Chem.*, **2006**, 2, 3.
- [42] D. Ravelli, S. Protti, M. Fagnoni, A. Albini, *Curr. Org. Chem.*, **2013**, 17, 2366.
- [43] W. Klöpffer, *Environ. Sci. Pollut. Res.*, **1997**, 4, 223.
- [44] R. G. Hunt, W. E. Franklin, R. G. Hunt, *Int. J. Life Cycle Assess.*, **1996**, 1, 4.
- [45] R. J. Perriman, *J. Cleaner Prod.*, **1993**, 1, 209.
- [46] H.-J. Klüppel, *Int. J. Life Cycle Assess.*, **2005**, 10, 165.
- [47] *DIN EN ISO 14040:2009-11, Umweltmanagement_Ökobilanz_Grundsätze und Rahmenbedingungen (ISO_14040:2006); Deutsche und Englische Fassung EN_ISO_14040:2006*, Beuth Verlag GmbH, Berlin.
- [48] *DIN EN ISO 14044:2018-05, Umweltmanagement_Ökobilanz_Anforderungen und Anleitungen (ISO_14044:2006_Amd_1:2017); Deutsche Fassung EN_ISO_14044:2006_A1:2018*, Beuth Verlag GmbH, Berlin.
- [49] H. Bruijn, R. Duin, M. A. J. Huijbregts, J. B. Guinee, M. Gorree, R. Heijungs, G. Huppes, R. Kleijn, A. Koning, L. Oers et al., *Handbook on Life Cycle Assessment. Operational Guide to the ISO Standards*, Kluwer Academic Publishers, Dordrecht, **2004**.
- [50] H. A. U. de Haes (Ed.) *Towards a Methodology for Life Cycle Impact Assessment*, SETAC, Brussels, **1996**.
- [51] D. Kralisch, C. Staffel, D. Ott, S. Bensaid, G. Saracco, P. Bellantoni, P. Loeb, *Green Chem.*, **2013**, 15, 463.
- [52] D. Kralisch, D. Reinhardt, G. Kreisel, *Green Chem.*, **2007**, 9, 1308.

-
- [53] K. Christiansen, *Simplifying LCA. Just a cut?*, Society of Environmental Toxicology and Chemistry - Europe, Brussels, Belgium, **1997**.
- [54] C. Jimnez-Gonzlez, A. D. Curzons, D. J. C. Constable, V. L. Cunningham, *Clean Technn Environn Policy*, **2004**, 7, 42.
- [55] S. Abou-Shehada, J. H. Clark, G. Paggiola, J. Sherwood, *Chem. Eng. Process.*, **2016**, 99, 88.
- [56] P. P. McClellan, *Ind. Eng. Chem.*, **1950**, 42, 2402.
- [57] S. Rebsdat, D. Mayer in *Ullmann's encyclopedia of industrial chemistry*, Wiley, Chichester, **2010**.
- [58] W. M. H. Sachtler, C. Backx, R. A. van Santen, *Catal. Rev.*, **1981**, 23, 127.
- [59] I. WACHS, *J. Catal.*, **1981**, 72, 160.
- [60] P. G. Jessop, *Green Chem.*, **2011**, 13, 1391.
- [61] C. Capello, U. Fischer, K. Hungerbühler, *Green Chem.*, **2007**, 9, 927.
- [62] D. J. C. Constable, P. J. Dunn, J. D. Hayler, G. R. Humphrey, J. J. L. Leazer, R. J. Linderman, K. Lorenz, J. Manley, B. A. Pearlman, A. Wells et al., *Green Chem.*, **2007**, 9, 411.
- [63] D. Prat, J. Hayler, A. Wells, *Green Chem.*, **2014**, 16, 4546.
- [64] K. Alfonsi, J. Colberg, P. J. Dunn, T. Fevig, S. Jennings, T. A. Johnson, H. P. Kleine, C. Knight, M. A. Nagy, D. A. Perry et al., *Green Chem.*, **2008**, 10, 31.
- [65] D. Prat, O. Pardigon, H.-W. Flemming, S. Letestu, V. Ducandas, P. Isnard, E. Guntrum, T. Senac, S. Ruisseau, P. Cruciani et al., *Org. Process Res. Dev.*, **2013**, 17, 1517.

-
- [66] R. K. Henderson, C. Jiménez-González, D. J. C. Constable, S. R. Alston, G. G. A. Inglis, G. Fisher, J. Sherwood, S. P. Binks, A. D. Curzons, *Green Chem.*, **2011**, *13*, 854.
- [67] D. Prat, A. Wells, J. Hayler, H. Sneddon, C. R. McElroy, S. Abou-Shehada, P. J. Dunn, *Green Chem.*, **2016**, *18*, 288.
- [68] D. G. Blackmond, A. Armstrong, V. Coombe, A. Wells, *Angew. Chem. Int. Ed.*, **2007**, *46*, 3798.
- [69] C. J. Clarke, W.-C. Tu, O. Levers, A. Bröhl, J. P. Hallett, *Chem. Rev.*, **2018**, *118*, 747.
- [70] J. Dupont, R. F. de Souza, P. A. Z. Suarez, *Chem. Rev.*, **2002**, *102*, 3667.
- [71] I. S. Cardoso, A. Q. Pedro, A. J. D. Silvestre, M. G. Freire in *Green analytical chemistry* (Eds.: J. Płotka-Wasyłka, J. Namieśnik), Springer, Singapore, **2019**.
- [72] P. Wasserscheid, T. Welton, *Ionic liquids in synthesis*, Wiley-VCH, Weinheim, **2008**.
- [73] M. J. Earle, J. M. S. S. Esperança, M. A. Gilea, J. N. C. Lopes, L. P. N. Rebelo, J. W. Magee, K. R. Seddon, J. A. Widegren, *Nature*, **2006**, *439*, 831.
- [74] H. Passos, M. G. Freire, J. A. P. Coutinho, *Green Chem.*, **2014**, *16*, 4786.
- [75] R. D. Rogers, K. R. Seddon, *Science*, **2003**, *302*, 792.
- [76] J. Ranke, S. Stolte, R. Störmann, J. Arning, B. Jastorff, *Chem. Rev.*, **2007**, *107*, 2183.
- [77] T. P. T. Pham, C.-W. Cho, Y.-S. Yun, *Water Res.*, **2010**, *44*, 352.
- [78] S. L. Pimm, *Theor. Popul. Biol.*, **1979**, *16*, 144.
- [79] K. Massonne, M. Siemer, W. Mormann, W. Leng, WO2009027250A2, **2009**.

-
- [80] L. A. Blanchard, Z. Gu, J. F. Brennecke, *J. Phys. Chem. B*, **2001**, *105*, 2437.
- [81] J. Kröckel, U. Kragl, *Chem. Eng. Technol.*, **2003**, *26*, 1166.
- [82] A. R. Choudhury, N. Winterton, A. Steiner, A. I. Cooper, K. A. Johnson, *J. Am. Chem. Soc.*, **2005**, *127*, 16792.
- [83] M. Fiene, Rust, Harald, K. Massonne, V. Stegmann, O. Huttenloch, J. Heilek, US20090250409A1, **2009**.
- [84] E. L. Smith, A. P. Abbott, K. S. Ryder, *Chem. Rev.*, **2014**, *114*, 11060.
- [85] A. Paiva, R. Craveiro, I. Aroso, M. Martins, R. L. Reis, A. R. C. Duarte, *ACS Sustainable Chem. Eng.*, **2014**, *2*, 1063.
- [86] H. Vanda, Y. Dai, E. G. Wilson, R. Verpoorte, Y. H. Choi, *C. R. Chim*, **2018**, *21*, 628.
- [87] S. K. Shahvandi, M. H. Banitaba, H. Ahmar, P. Karimi, *Microchem. J.*, **2020**, *152*, 104300.
- [88] P. G. Jessop, S. M. Mercer, D. J. Heldebrant, *Energy Environ. Sci.*, **2012**, *5*, 7240.
- [89] T. Yamada, P. J. Lukac, M. George, R. G. Weiss, *Chem. Mater.*, **2007**, *19*, 967.
- [90] L. Phan, D. Chiu, D. J. Heldebrant, H. Huttenhower, E. John, X. Li, P. Pollet, R. Wang, C. A. Eckert, C. L. Liotta et al., *Ind. Eng. Chem. Res.*, **2008**, *47*, 539.
- [91] P. Jessop, L. Phan, A. Carrier, R. Resendes, Wechsler Dominik, US8900444B2, **2014**.
- [92] V. Eta, J.-P. Mikkola, *Carbohydr. Polym.*, **2016**, *136*, 459.
- [93] P. G. Jessop, L. Phan, A. Carrier, S. Robinson, C. J. Dürr, J. R. Harjani, *Green Chem.*, **2010**, *12*, 809.
- [94] A. Darabi, P. G. Jessop, M. F. Cunningham, *Chem. Soc. Rev.*, **2016**, *45*, 4391.
-

-
- [95] H. Plaumann, *Phys. Sci. Rev.*, **2017**, 2.
- [96] J. Großeheilmann, J. R. Vanderveen, P. G. Jessop, U. Kragl, *ChemSusChem*, **2016**, 9, 696.
- [97] S. M. Mercer, T. Robert, D. V. Dixon, P. G. Jessop, *Catal. Sci. Technol.*, **2012**, 2, 1315.
- [98] E. de Jong, H. Stichnothe, G. Bell, H. Jorgensen, *Bio-based chemicals: a 2020 update*, IEA Bioenergy, **2020**.
- [99] F. Cherubini, G. Jungmeier, M. Wellisch, T. Willke, I. Skiadas, R. van Ree, E. de Jong, *Biofuels, Bioprod. Bioref.*, **2009**, 3, 534.
- [100] U.S. Energy Administration Information (eia), “Oil and petroleum products explained. Use of oil”, URL: <https://www.eia.gov/energyexplained/oil-and-petroleum-products/use-of-oil.php>, accessed 2020.12.12.
- [101] N. G. Chemmangattuvalappil, D. K. Ng, *A systematic methodology for optimal product design in an integrated biorefinery Computer Aided Chemical Engineering*, 32, **2013**, Elsevier, pp. 91–96.
- [102] E. Gnansounou, A. Pandey, *Life-cycle assessment of biorefineries Life-Cycle Assessment of Biorefineries*, **2017**, Elsevier, Amsterdam, Oxford, Cambridge, MA.
- [103] V. Aristizábal-Marulanda, C. A. Cardona Alzate, *Biofuels, Bioprod. Bioref.*, **2019**, 13, 789.
- [104] A. Muscat, E. M. de Olde, I. de Boer, R. Ripoll-Bosch, *Glob. Food Sec.*, **2020**, 25, 100330.
- [105] S. Serna-Loaiza, M. Miltner, A. Miltner, A. Friedl, *Sustainability*, **2019**, 11, 6765.
- [106] D. A. Laird, R. C. Brown, J. E. Amonette, J. Lehmann, *Biofuels, Bioprod. Bioref.*, **2009**, 3, 547.

-
- [107] A. J. Ragauskas, G. T. Beckham, M. J. Bidy, R. Chandra, F. Chen, M. F. Davis, B. H. Davison, R. A. Dixon, P. Gilna, M. Keller et al., *Science*, **2014**, *344*, 1246843.
- [108] I. Brodin, M. Ernstsson, G. Gellerstedt, E. Sjöholm, *Holzforschung*, **2012**, *66*.
- [109] S. Takkellapati, T. Li, M. A. Gonzalez, *Clean Techn Environ Policy*, **2018**, *20*, 1615.
- [110] M. Andersen, P. Kiel, *Ind. Crops Prod.*, **2000**, *11*, 129.
- [111] R. Kumar, I. S. Sundari, S. Sen, N. Dasgupta, R. Chidambaram in *Platform Chemical Biorefinery. Future Green Chemistry* (Eds.: S. Kaur Brar, S. Jyoti Sarma, K. Pakshirajan), Elsevier Science, s.l., **2016**.
- [112] N. Dahmen, E. Henrich, T. Henrich, *Adv. Biochem. Eng./Biotechnol.*, **2019**, *166*, 217.
- [113] P. G. Kougias, I. Angelidaki, *Front. Environ. Sci. Eng.*, **2018**, *12*.
- [114] S. J. Sarma, V. Pachapur, S. K. Brar, Y. Le Bihan, G. Buelna, *Renewable Sustainable Energy Rev.*, **2015**, *50*, 942.
- [115] S. Rittmann, C. Herwig, *Microb. Cell Fact.*, **2012**, *11*, 115.
- [116] A. Giuliano, C. Freda, E. Catizzone, *Bioengineering*, **2020**, *7*.
- [117] T. Benzing, T. Böhlend, U. R. Fritsche, M. Fröhling, A. Gröngröft, A. Günther, M. Hempel, A. Hiltermann, T. Hirth, N. Holst et al., *Biorefineries Roadmap as part of the German Federal Government action plans for the material and energetic utilisation of renewable raw materials*, Federal Ministry of Agriculture and Consumer Protection (BMELV), Berlin, **2012**.
- [118] C. Parisi, *Biorefineries distribution in the EU*, Publications Office of the European Union, Luxembourg, **2018**.

-
- [119] J. Spekrijse, T. Lammens, C. Parisi, T. Ronzon, M. Vis, *Insights into the European market for bio-based chemicals*, Publications Office of the European Union, Luxembourg, **2019**.
- [120] R. A. Sheldon, *J. Mol. Catal. A: Chem.*, **2016**, *422*, 3.
- [121] R. A. Sheldon, *Green Chem.*, **2014**, *16*, 950.
- [122] Z. Fang, R. L. Smith, X. Qi, *Production of Platform Chemicals from Sustainable Resources*, Springer Singapore, Singapore, **2017**.
- [123] K. Kohli, R. Prajapati, B. Sharma, *Energies*, **2019**, *12*, 233.
- [124] P. Gallezot, *Chem. Soc. Rev.*, **2012**, *41*, 1538.
- [125] X. Sun, H. K. Atiyeh, R. L. Huhnke, R. S. Tanner, *Bioresour. Technol.*, **2019**, *7*, 100279.
- [126] H. Jahangiri, J. Bennett, P. Mahjoubi, K. Wilson, S. Gu, *Catal. Sci. Technol.*, **2014**, *4*, 2210.
- [127] X.-S. Zhang, G.-X. Yang, H. Jiang, W.-J. Liu, H.-S. Ding, *Sci. Rep.*, **2013**, *3*, 1120.
- [128] J. Pang, M. Zheng, R. Sun, A. Wang, X. Wang, T. Zhang, *Green Chem.*, **2016**, *18*, 342.
- [129] H. Köpnick, M. Schmidt, W. Brüggling, J. Rüter, W. Kaminsky in *Ullmann's encyclopedia of industrial chemistry*, Wiley, Chichester, **2010**.
- [130] P. Werle, M. Morawietz, S. Lundmark, K. Sørensen, E. Karvinen, J. Lehtonen in *Ullmann's encyclopedia of industrial chemistry*, Wiley, Chichester, **2010**.
- [131] C. J. Sullivan, A. Kuenz, K.-D. Vorlop in *Ullmann's encyclopedia of industrial chemistry*, Wiley, Chichester, **2010**.

-
- [132] S. Rebsdatt, D. Mayer in *Ullmann's encyclopedia of industrial chemistry*, Wiley, Chichester, **2010**.
- [133] C. de Blasio in *Fundamentals of biofuels engineering and technology* (Ed.: C. de Blasio), Springer International Publishing, Cham, **2019**.
- [134] M. Zhang, Y. Yu, *Ind. Eng. Chem. Res.*, **2013**, *52*, 9505.
- [135] H. Yue, Y. Zhao, X. Ma, J. Gong, *Chem. Soc. Rev.*, **2012**, *41*, 4218.
- [136] Chemicals Technology, "Greencol Taiwan Corporation Bio-MEG Plant", URL: <https://www.chemicals-technology.com/projects/greencolbiomegplant/>, accessed 2021.04.30.
- [137] C. Marques, R. Tarek, M. Sara, S. K. Brar in *Platform Chemical Biorefinery. Future Green Chemistry* (Eds.: S. Kaur Brar, S. Jyoti Sarma, K. Pakshirajan), Elsevier Science, s.l., **2016**.
- [138] L. S. Ribeiro, J. J. Órfão, M. F. R. Pereira, *Green Process. Synth.*, **2015**, *4*.
- [139] K. Zhang, S. Wu, H. Yang, H. Yin, G. Li, *RSC Adv.*, **2016**, *6*, 77499.
- [140] S. Soltani, U. Rashid, R. Yunus, Y. H. Taufiq-Yap, *Catal. Rev.*, **2015**, *57*, 407.
- [141] J. V. Kurian, *J. Polym. Environ.*, **2005**, *13*, 159.
- [142] L. A. Laffend, V. Nagarajan, C. E. Nakamura, US5686276A, **1997**.
- [143] J. J. Bozell, G. R. Petersen, *Green Chem.*, **2010**, *12*, 539.
- [144] D. C. Cameron, N. E. Altaras, M. L. Hoffman, A. J. Shaw, *Biotechnol. Prog.*, **1998**, *14*, 116.
- [145] D. Bockey, *OCL*, **2019**, *26*, 40.
- [146] B. Tabah, A. Varvak, I. N. Pulidindi, E. Foran, E. Banin, A. Gedanken, *Green Chem.*, **2016**, *18*, 4657.

-
- [147] Y. Wang, J. Zhou, X. Guo, *RSC Adv.*, **2015**, *5*, 74611.
- [148] R. Arundhathi, T. Mizugaki, T. Mitsudome, K. Jitsukawa, K. Kaneda, *ChemSusChem*, **2013**, *6*, 1345.
- [149] M. Zakhartsev, X. Yang, M. Reuss, H. O. Pörtner, *J. Therm. Biol.*, **2015**, *52*, 117.
- [150] Z.-J. Yang, N. Ren, Y.-H. Zhang, Y. Tang, *Catal. Commun.*, **2010**, *11*, 447.
- [151] H. S. Fogler, *Elements of chemical reaction engineering*, Pearson Education International/Prentice Hall PTR, Upper Saddle River, NJ, **2006**.
- [152] M. González-Pajuelo, I. Meynial-Salles, F. Mendes, J. C. Andrade, I. Vasconcelos, P. Soucaille, *Metab. Eng.*, **2005**, *7*, 329.
- [153] J. B. McKinlay, C. Vieille, J. G. Zeikus, *Appl. Microbiol. Biotechnol.*, **2007**, *76*, 727.
- [154] D. Sun, S. Sato, W. Ueda, A. Primo, H. Garcia, A. Corma, *Green Chem.*, **2016**, *18*, 2579.
- [155] C. Delhomme, D. Weuster-Botz, F. E. Kühn, *Green Chem.*, **2009**, *11*, 13.
- [156] Y. Takeda, M. Tamura, Y. Nakagawa, K. Okumura, K. Tomishige, *Catal. Sci. Technol.*, **2016**, *6*, 5668.
- [157] P. A. Tooley, Black, Jesse Raymond, US5985789A, **1999**.
- [158] I. Pala Rosas, J. Luis Contreras Larios, B. Zeifert, J. Salmones Blásquez in *Glycerine Production and Transformation - An Innovative Platform for Sustainable Biorefinery and Energy* (Eds.: M. Bartoli, L. Rosi, M. Frediani), IntechOpen, London, **2019**.
- [159] G. F. Johnson, L. C. Teague, US3159651A, **1964**.

-
- [160] R. J. Davis, C. A. Menning, J. E. Murphy, J. C. Ritter, S. K. Sengupta, US20160159715A1, **2016**.
- [161] K. Chen, S. Koso, T. Kubota, Y. Nakagawa, K. Tomishige, *ChemCatChem*, **2010**, *2*, 547.
- [162] B. Viswanadham, V. Pavankumar, K. V. R. Chary, *Catal. Lett.*, **2014**, *144*, 744.
- [163] R.-J. van Putten, J. C. van der Waal, E. de Jong, C. B. Rasrendra, H. J. Heeres, J. G. de Vries, *Chem. Rev.*, **2013**, *113*, 1499.
- [164] X. Kong, Y. Zhu, Z. Fang, J. A. Kozinski, I. S. Butler, L. Xu, H. Song, X. Wei, *Green Chem.*, **2018**, *20*, 3657.
- [165] Y. Nakagawa, K. Tomishige, *Catal. Commun.*, **2010**, *12*, 154.
- [166] J. Tuteja, H. Choudhary, S. Nishimura, K. Ebitani, *ChemSusChem*, **2014**, *7*, 96.
- [167] M. R. Nolan, G. Sun, B. H. Shanks, *Catal. Sci. Technol.*, **2014**, *4*, 2260.
- [168] T. Buntara, S. Noel, P. H. Phua, I. Melián-Cabrera, J. G. de Vries, H. J. Heeres, *Angew. Chem. Int. Ed. Engl.*, **2011**, *50*, 7083.
- [169] A. K. Vasishtha, R. K. Trivedi, G. Das, *J. Am. Oil Chem. Soc.*, **1990**, *67*, 333.
- [170] D. S. Ogunniyi, *Bioresour. Technol.*, **2006**, *97*, 1086.
- [171] R. A. Dytham, B. Weedon, *Tetrahedron*, **1960**, *8*, 246.
- [172] Q. Liu, D. Duan, Y. Wang, CN 103449971, **2013**.
- [173] M. R. Kamaruzaman, X. X. Jiang, X. de Hu, S. Y. Chin, *Chem. Eng. J.*, **2020**, *388*, 124186.
- [174] R. Williamson, J. Holladay, M. Jaffe, D. Brunelle, *Continuous Isosorbide Production From Sorbitol Using Solid Acid Catalysis*, **2006**.

-
- [175] R. J. Palmer in *Encyclopedia of polymer science and technology*, Wiley Interscience, Hoboken, NJ, **2004**.
- [176] P. Roose, K. Eller, E. Henkes, R. Rossbacher, H. Höke in *Ullmann's encyclopedia of industrial chemistry*, Wiley, Chichester, **2010**.
- [177] R. A. Smiley in *Ullmann's encyclopedia of industrial chemistry*, Wiley, Chichester, **2010**.
- [178] P. Pollak, G. Romeder, F. Hagedorn, H.-P. Gelbke in *Ullmann's encyclopedia of industrial chemistry*, Wiley, Chichester, **2010**.
- [179] W. J. Bartley, R. G. Cook, K. E. Curry, S. K. Mierau, WO2001066247, **2001**.
- [180] G. Hibert, O. Lamarzelle, L. Maisonneuve, E. Grau, H. Cramail, *Eur. Polym. J.*, **2016**, 82, 114.
- [181] K. Shimizu, K. Kon, W. Onodera, H. Yamazaki, J. N. Kondo, *ACS Catal.*, **2013**, 3, 112.
- [182] L. Xu, C. Shi, Z. He, H. Zhang, M. Chen, Z. Fang, Y. Zhang, *Energy Fuels*, **2020**, 34, 10441.
- [183] T. Wang, J. Ibañez, K. Wang, L. Fang, M. Sabbe, C. Michel, S. Paul, M. Peratitus, P. Sautet, *Nat. Catal.*, **2019**, 2, 773.
- [184] K. Kharas, WO2014065839A1, **2012**.
- [185] Y. Deng, L. Ma, Y. Mao, *Biochem. Eng. J.*, **2016**, 105, 16.
- [186] R. Santoro, C. Cameselle, S. Rodríguez-Couto, Á. Sanromán, *Bioprocess Eng.*, **1999**, 20, 1.
- [187] S. Picataggio, T. Rohrer, K. Deanda, D. Lanning, R. Reynolds, J. Mielenz, L. D. Eirich, *Nat. Biotechnol.*, **1992**, 10, 894.

-
- [188] R. Coeck, D. E. de Vos, *Green Chem.*, **2020**, *22*, 5105.
- [189] Y. Shi, P. C. J. Kamer, D. J. Cole-Hamilton, *Green Chem.*, **2017**, *19*, 5460.
- [190] J. H. Meessen, H. Petersen in *Ullmann's encyclopedia of industrial chemistry*, Wiley, Chichester, **2010**.
- [191] C. Nitschke, G. Scherr in *Ullmann's encyclopedia of industrial chemistry*, Wiley, Chichester, **2010**.
- [192] J. Meessen, *Chem. Ing Tech.*, **2014**, *86*, 2180.
- [193] L. Chen, Z. Qi, S. Zhang, J. Su, G. A. Somorjai, *Catalysts*, **2020**, *10*, 858.
- [194] J. Jia, L. C. Seitz, J. D. Benck, Y. Huo, Y. Chen, J. W. D. Ng, T. Bilir, J. S. Harris, T. F. Jaramillo, *Nat. Commun.*, **2016**, *7*, 13237.
- [195] Z. Yan, J. L. Hitt, J. A. Turner, T. E. Mallouk, *Proc. Natl. Acad. Sci. U.S.A.*, **2020**, *117*, 12558.
- [196] G. Stern, Muellner, Martin, Roessler, Markus, DE3928595A1, **1991**.
- [197] F. Arndt, E. D. Amstutz, R. Myers, *Org. Synth.*, **1935**, *15*, 48.
- [198] Buitink, Fredericus, Henricus, Maria, Dieltjens, Luc, Louis, Maria, WO2014104894A1.
- [199] D. R. Corbin, S. Schwarz, G. C. Sonnichsen, *Catal. Today*, **1997**, *37*, 71.
- [200] F. Brühne, E. Wright in *Ullmann's encyclopedia of industrial chemistry*, Wiley, Chichester, **2010**.
- [201] H. Zhang, M. Cao, X. Jiang, H. Zou, C. Wang, X. Xu, M. Xian, *BMC Biotechnol.*, **2014**, *14*, 30.
- [202] S. Pugh, R. McKenna, I. Halloum, D. R. Nielsen, *Metab. Eng. Commun.*, **2015**, *2*, 39.

-
- [203] M. Ghahremani, R. Ciriminna, V. Pandarus, A. Scurria, V. La Parola, F. Giordano, G. Avellone, F. Béland, B. Karimi, M. Pagliaro, *ACS Sustain. Chem. Eng.*, **2018**, *6*, 15441.
- [204] M. Zhang, Y. Zhai, S. Ru, D. Zang, S. Han, H. Yu, Y. Wei, *Chem. Commun.*, **2018**, *54*, 10164.
- [205] Z. Liu, J. Caner, A. Kudo, H. Naka, S. Saito, *Chemistry*, **2013**, *19*, 9452.
- [206] J. M. Snell, A. Weissberger, R. L. Shriner, N. S. Moon, *Org. Synth.*, **1940**, *20*, 92.
- [207] K. K. Miller, P. Zhang, Y. Nishizawa-Brennen, J. W. Frost, *ACS Sustain. Chem. Eng.*, **2014**, *2*, 2053.
- [208] A. R. Morais, S. Dworakowska, A. Reis, L. Gouveia, C. T. Matos, D. Bogdał, R. Bogel-Lukasik, *Catal. Today*, **2015**, *239*, 38.
- [209] M. B. Banella, C. Gioia, M. Vannini, M. Colonna, A. Celli, A. Gandini, *ChemSusChem*, **2016**, *9*, 942.
- [210] Z. Zhu, Z. Lu, S. Guo, J. Xie, Y. Song, CN101096333B, **2008**.
- [211] A. Anaby, M. Schelwies, J. Schwaben, F. Rominger, A. S. K. Hashmi, T. Schaub, *Organometallics*, **2018**, *37*, 2193.
- [212] X. Tan, Q. Wang, Y. Liu, F. Wang, H. Lv, X. Zhang, *Chem. Commun.*, **2015**, *51*, 12193.
- [213] S. Elangovan, B. Wendt, C. Topf, S. Bachmann, M. Scalone, A. Spannenberg, H. Jiao, W. Baumann, K. Junge, M. Beller, *Adv. Synth. Catal.*, **2016**, *358*, 820.
- [214] X. Zhao, Y. Zhou, A.-L. Jin, K. Huang, F. Liu, D.-J. Tao, *New J. Chem.*, **2018**, *42*, 15871.
- [215] C. Taeschler in *Encyclopedia of chemical technology* (Eds.: R. E. Kirk, D. F. Othmer), Wiley, New York, NY, **2003**.

-
- [216] Institut für Arbeitsschutz der Deutschen Gesetzlichen Unfallversicherung, “GESTIS-Stoffdatenbank. 4-Methylen-2-oxetanon, Diketene”, URL: <https://gestis.dguv.de/data?name=012680>, accessed 2021.02.04.
- [217] R. Miller, C. Abaecherli, A. Said, B. Jackson in *Ullmann’s encyclopedia of industrial chemistry*, Wiley, Chichester, **2010**.
- [218] J. W. WILLIAMS, C. D. HURD, *J. Org. Chem.*, **1940**, 05, 122.
- [219] T. T. Tidwell in *Science of synthesis. Houben-Weyl methods of molecular transformations* (Eds.: J. M. Aizpurua, R. L. Danheiser, D. Bellus, J. Houben, T. Weyl), Thieme, Stuttgart, **2006**.
- [220] L. Tenud, M. Weilenmann, E. Dallwigk, *Helv. Chim. Acta*, **1977**, 60, 975.
- [221] R. J. Clemens, *Chem. Rev.*, **1986**, 86, 241.
- [222] A. J. Kresge, Y. Chiang, P. H. Fitzgerald, R. S. McDonald, G. H. Schmid, *J. Am. Chem. Soc.*, **1971**, 93, 4907.
- [223] B. N. M. van Leeuwen, A. M. van der Wulp, I. Duijnste, A. J. A. van Maris, A. J. J. Straathof, *Appl. Microbiol. Biotechnol.*, **2012**, 93, 1377.
- [224] Global Bioenergies, “First production of isobutene from wheat straw at demo scale”, URL: <https://www.global-bioenergies.com/first-production-of-isobutene-from-wheat-straw-at-demo-scale/?lang=en>, accessed 2021.01.09.
- [225] M. F. Carroll, A. R. Bader, *J. Am. Chem. Soc.*, **1953**, 75, 5400.
- [226] J. Wang, M. Lin, M. Xu, S.-T. Yang, *Adv. Biochem. Eng./Biotechnol.*, **2016**, 156, 323.
- [227] E. Budsberg, R. Morales-Vera, J. T. Crawford, R. Bura, R. Gustafson, *Biotechnol. Biofuels*, **2020**, 13, 154.
- [228] N. Qureshi, H. P. Blaschek, *J. Ind. Microbiol. Biotechnol.*, **2001**, 27, 292.

-
- [229] W. Bauer in *Ullmann's encyclopedia of industrial chemistry*, Wiley, Chichester, **2010**.
- [230] P. B. V. Scholten, D. Moatsou, C. Detrembleur, M. A. R. Meier, *Macromol. Rapid Commun.*, **2020**, e2000266.
- [231] R. P. John, K. M. Nampoothiri, A. Pandey, *Appl. Microbiol. Biotechnol.*, **2007**, *74*, 524.
- [232] L. Matsakas, K. Hrůzová, U. Rova, P. Christakopoulos, *Fermentation*, **2018**, *4*, 13.
- [233] D. Decoster, S. Hoyt, S. Roach, WO2013192451A1, **2013**.
- [234] T. Blaschke, O. Lang, N. T. Wörz, C. Raith, M. Hartmann, M. Zajaczkowski-Fischer, US9630900B2, **2017**.
- [235] R. E. Holmen, US2859240A, **1958**.
- [236] T. Bonnotte, S. Paul, M. Araque, R. Wojcieszak, F. Dumeignil, B. Katryniok, *ChemBioEng Reviews*, **2018**, *5*, 34.
- [237] A. J. J. Straathof, S. Sie, T. T. Franco, L. A. M. van der Wielen, *Appl. Microbiol. Biotechnol.*, **2005**, *67*, 727.
- [238] T. Dishisha, S.-H. Pyo, R. Hatti-Kaul, *Microb. Cell Fact.*, **2015**, *14*, 200.
- [239] J. Lebeau, J. P. Efromson, M. D. Lynch, *Front. Bioeng. Biotechnol.*, **2020**, *8*, 207.
- [240] M. J. Darabi Mahboub, J.-L. Dubois, F. Cavani, M. Rostamizadeh, G. S. Patience, *Chem. Soc. Rev.*, **2018**, *47*, 7703.
- [241] K. Nagai, *Appl. Catal., A: General*, **2001**, *221*, 367.
- [242] Wacker Chemie AG, “2019 European Coatings Show. WACKER Presents New Product Line for Polymeric Binders Based on Renewable Raw Materials”, URL:

- https://www.wacker.com/cms/media/en/documents/pressrelease-pdf/10_wacker_vinneco_de.pdf, **2019**, accessed 2021.01.27.
- [243] B. Salisbury, M. E. Fitzpatrick, W. J. Brtko, N. C. Hallinan, US8399700B2, **2013**.
- [244] V. J. Johnston, L. Chen, J. H. Zink, J. T. Chapman, B. F. Kimmich, D. R. Repman, WO2010056299A1, **2010**.
- [245] J. Zhu, H. Bienaymè (Eds.) *Multicomponent reactions*, Wiley-VCH, Weinheim, **2005**.
- [246] I. Ugi, A. Dömling, W. Hörl, *Endeavour*, **1994**, *18*, 115.
- [247] Y. Gu, *Green Chem.*, **2012**, *14*, 2091.
- [248] R. C. Cioc, E. Ruijter, R. V. A. Orru, *Green Chem.*, **2014**, *16*, 2958.
- [249] I. Ugi, A. Dömling, B. Ebert in *Combinatorial Chemistry. Synthesis, Analysis, Screening* (Ed.: G. Jung), Wiley-VCH, Weinheim, Cambridge, **1999**.
- [250] A. Tuch, S. Wallé in *Handbook of Combinatorial Chemistry. Drugs, Catalysts, Materials* (Eds.: K. C. Nicolaou, R. Hanco, W. Hartwig), Wiley-VCH, Weinheim, **2002**.
- [251] A. Strecker, *Ann. Chem. Pharm.*, **1850**, *75*, 27.
- [252] A. Hantzsch, *Ann. Chem. Pharm.*, **1882**, *215*, 1.
- [253] N. Edraki, A. R. Mehdipour, M. Khoshneviszadeh, R. Miri, *Drug discovery today*, **2009**, *14*, 1058.
- [254] A. Hantzsch, *Ber. Dtsch. Chem. Ges.*, **1890**, *23*, 1474.
- [255] T. L. Poulos, *Chem. Rev.*, **2014**, *114*, 3919.
- [256] H. Scheer in *Chlorophylls and bacteriochlorophylls, Vol. 25* (Ed.: B. Grimm), Springer, Dordrecht, **2006**.

-
- [257] P. Biginelli, *Eur. J. Inorg. Chem.*, **1891**, 24, 1317.
- [258] C. Mannich, W. Krösche, *Arch. Pharm.*, **1912**, 250, 647.
- [259] R. Robinson, *J. Chem. Soc., Trans.*, **1917**, 111, 762.
- [260] B. Biersack, K. Ahmed, S. Padhye, R. Schobert, *Expert Opin. Drug Discovery*, **2018**, 13, 39.
- [261] M. Passerini, *Gazz. Chem. Ital.*, **1921**, 51, 121.
- [262] I. Ugi, R. meyr, U. Fetzer, C. Steinbrückner, *Angew. Chem.*, **1959**, 71, 373.
- [263] R. S. Bon, C. Hong, M. J. Bouma, R. F. Schmitz, F. J. J. de Kanter, M. Lutz, A. L. Spek, R. V. A. Orru, *Org. Lett.*, **2003**, 5, 3759.
- [264] S. Heck, A. Dömling, *Synlett*, **2000**, 2000, 424.
- [265] M. M. Heravi, V. Zadsirjan, *Curr. Org. Chem.*, **2020**, 24, 1331.
- [266] W. Zhang in *Green synthetic processes and procedures, Vol. 61* (Ed.: R. Ballini), Royal Society of Chemistry, Londres, **2019**.
- [267] B. Cornils, W. A. Herrmann, M. Rasch, *Angew. Chem. Int. Ed. Engl.*, **1994**, 33, 2144.
- [268] G. Dümbgen, D. Neubauer, *Chem. Ing Tech.*, **1969**, 41, 974.
- [269] W. Reppe, *Neue Entwicklungen auf dem Gebiete der Chemie des Acetylens und Kohlenoxyds*, Springer Berlin Heidelberg, Berlin, Heidelberg, s.l., **1949**.
- [270] I. Ugi, *J. Prakt. Chem.*, **1997**, 339, 499.
- [271] I. Ugi, *Pure Appl. Chem.*, **2001**, 73, 187.
- [272] A. Dömling, I. Ugi, *Angew. Chem. Int. Ed. Engl.*, **2000**, 39, 3168.

-
- [273] G. C. Tron, A. Minassi, G. Appendino, *Eur. J. Org. Chem.*, **2011**, 2011, 5541.
- [274] H. G. O. Alvim, E. N. da Silva Júnior, B. A. D. Neto, *RSC Adv.*, **2014**, 4, 54282.
- [275] K. Folkers, T. B. Johnson, *J. Am. Chem. Soc.*, **1933**, 55, 3784.
- [276] F. Sweet, J. D. Fissekis, *J. Am. Chem. Soc.*, **1973**, 95, 8741.
- [277] C. O. Kappe, *J. Org. Chem.*, **1997**, 62, 7201.
- [278] C. O. Kappe, P. Roschger, *J. Heterocycl. Chem.*, **1989**, 26, 55.
- [279] R. O. M. A. de Souza, E. T. da Penha, H. M. S. Milagre, S. J. Garden, P. M. Esteves, M. N. Eberlin, O. A. C. Antunes, *Chem. Eur. J.*, **2009**, 15, 9799.
- [280] L. M. Ramos, A. Y. Ponce de Leon y Tobio, M. R. dos Santos, H. C. B. de Oliveira, A. F. Gomes, F. C. Gozzo, A. L. de Oliveira, B. A. D. Neto, *J. Org. Chem.*, **2012**, 77, 10184.
- [281] L. M. Ramos, B. C. Guido, C. C. Nobrega, J. R. Corrêa, R. G. Silva, H. C. B. de Oliveira, A. F. Gomes, F. C. Gozzo, B. A. D. Neto, *Chem. Eur. J.*, **2013**, 19, 4156.
- [282] I. Capanec, M. Litvić, M. Filipan-Litvić, I. Grüngold, *Tetrahedron*, **2007**, 63, 11822.
- [283] M. Litvić, I. Večenaj, Z. M. Ladišić, M. Lovrić, V. Vinković, M. Filipan-Litvić, *Tetrahedron*, **2010**, 66, 3463.
- [284] H. G. O. Alvim, T. B. Lima, A. L. de Oliveira, H. C. B. de Oliveira, F. M. Silva, F. C. Gozzo, R. Y. Souza, W. A. da Silva, B. A. D. Neto, *J. Org. Chem.*, **2014**, 79, 3383.
- [285] N. Sahota, D. I. AbuSalim, M. L. Wang, C. J. Brown, Z. Zhang, T. J. El-Baba, S. P. Cook, D. E. Clemmer, *Chem. Sci.*, **2019**, 10, 4822.
- [286] Z.-L. Shen, X.-P. Xu, S.-J. Ji, *J. Org. Chem.*, **2010**, 75, 1162.

-
- [287] M. K. Raj, H. S. P. Rao, S. G. Manjunatha, R. Sridharan, S. Nambiar, J. Keshwan, J. Rappai, S. Bhagat, B. S. Shwetha, D. Hegde et al., *Tetrahedron Lett.*, **2011**, *52*, 4806.
- [288] C. Oliver Kappe, *Tetrahedron*, **1993**, *49*, 6937.
- [289] C. O. Kappe in *Multicomponent reactions* (Eds.: J. Zhu, H. Bienaymè), Wiley-VCH, Weinheim, **2005**.
- [290] S. Sandhu, J. S. Sandhu, *Arkivoc*, **2011**, *2012*, 66.
- [291] K. S. Atwal, B. C. O'Reilly, *Heterocycles*, **1987**, *26*, 1185.
- [292] K. S. Atwal, G. C. Rovnyak, B. C. O'Reilly, J. Schwartz, *J. Org. Chem.*, **1989**, *54*, 5898.
- [293] T. Jin, S. Zhang, S. Zhang, J. Guo, T. Li, *J. Chem. Res.*, **2002**, *2002*, 37.
- [294] A. Shaabani, A. Bazgir, F. Teimouri, *Tetrahedron Lett.*, **2003**, *44*, 857.
- [295] Q. Zhang, X. Wang, Z. Li, W. Wu, J. Liu, H. Wu, S. Cui, K. Guo, *RSC Adv.*, **2014**, *4*, 19710.
- [296] T. Jin, S. Zhang, T. Li, *Synth. Commun.*, **2002**, *32*, 1847.
- [297] P. P. Baruah, S. Gadhwal, D. Prajapati, J. S. Sandhu, *Chem. Lett.*, **2002**, *31*, 1038.
- [298] S. Khaleghi, M. M. Heravi, M. Khosroshahi, F. Kargar Behbahani, Z. Daroogheha, *Green Chem. Lett. Rev.*, **2008**, *1*, 133.
- [299] H. Salehi, Q.-X. Guo, *Synth. Commun.*, **2004**, *34*, 171.
- [300] S. Chitra, K. Pandiarajan, *Tetrahedron Lett.*, **2009**, *50*, 2222.
- [301] W. Su, J. Li, Z. Zheng, Y. Shen, *Tetrahedron Lett.*, **2005**, *46*, 6037.
- [302] A. S. Paraskar, G. K. Dewkar, A. Sudalai, *Tetrahedron Lett.*, **2003**, *44*, 3305.

-
- [303] J. Lu, Y. Bai, *Synthesis*, **2002**, 2002, 466.
- [304] J. Lu, Y.-J. Bai, Y.-H. Guo, Z.-J. Wang, H.-R. Ma, *Chin. J. Chem.*, **2002**, 20, 681.
- [305] C. Reddy, M. Mahesh, P. Raju, T. Babu, V. Reddy, *Tetrahedron Lett.*, **2002**, 43, 2657.
- [306] J. Lu, Y. Bai, Z. Wang, B. Yang, H. Ma, *Tetrahedron Lett.*, **2000**, 41, 9075.
- [307] D. S. Bose, L. Fatima, H. B. Mereyala, *J. Org. Chem.*, **2003**, 68, 587.
- [308] X. Fan, X. Zhang, Y. Zhang, *J. Chem. Res.*, **2002**, 2002, 436.
- [309] Y. Ma, C. Qian, L. Wang, M. Yang, *J. Org. Chem.*, **2000**, 65, 3864.
- [310] B. C. Ranu, A. Hajra, U. Jana, *J. Org. Chem.*, **2000**, 65, 6270.
- [311] K. Ramalinga, P. Vijayalakshmi, T. N. B. Kaimal, *Synlett*, **2001**, 2001, 863.
- [312] A. Arfan, L. Paquin, J. P. Bazureau, *Russ. J. Org. Chem.*, **2007**, 43, 1058.
- [313] X. Chen, Y. Peng, *Catal. Lett.*, **2008**, 122, 310.
- [314] Z.-T. Wang, S.-C. Wang, L.-W. Xu, *Helv. Chim. Acta*, **2005**, 88, 986.
- [315] R. V. Patil, J. U. Chavan, D. S. Dalal, V. S. Shinde, A. G. Beldar, *ACS Comb. Sci.*, **2019**, 21, 105.
- [316] M. Hechelski, A. Ghinet, B. Louvel, P. Dufrenoy, B. Rigo, A. Daïch, C. Waterlot, *ChemSusChem*, **2018**, 11, 1249.
- [317] F. Bigi, S. Carloni, B. Frullanti, R. Maggi, G. Sartori, *Tetrahedron Lett.*, **1999**, 40, 3465.
- [318] A. K. Mitra, K. Banerjee, *Synlett*, **2003**, 1509.

-
- [319] G. P. Romanelli, A. G. Sathicq, J. C. Autino, G. Baronetti, H. J. Thomas, *Synth. Commun.*, **2007**, *37*, 3907.
- [320] M. Kazemi, *Synth. Commun.*, **2020**, *50*, 1409.
- [321] P. Zhang, W. Li, G. Zhou, Y. Lai, S. Xu, *Heterocycles*, **2011**, *83*, 2067.
- [322] Y. Yu, W.-F. Lu, Z.-J. Yang, N. Wang, X.-Q. Yu, *Bioorg. Chem.*, **2020**, 104534.
- [323] L. V. Chopda, P. N. Dave, *ChemistrySelect*, **2020**, *5*, 5552.
- [324] A. M. A. Shumaila, A. A. N. Al-Thulaia, *Synth. Commun.*, **2019**, *49*, 1613.
- [325] B. A. Neto, T. de A. Fernandes, M. V. Correia, *Targets Heterocycl. Syst.*, **2019**, *22*, 356.
- [326] C. Kappe, *Eur. J. Med. Chem.*, **2000**, *35*, 1043.
- [327] J. Yu, F. Shi, L.-Z. Gong, *Acc. Chem. Res.*, **2011**, *44*, 1156.
- [328] C. de Graaff, E. Ruijter, R. V. A. Orru, *Chem. Soc. Rev.*, **2012**, *41*, 3969.
- [329] H. G. O. Alvim, D. L. J. Pinheiro, V. H. Carvalho-Silva, M. Fioramonte, F. C. Gozzo, W. A. da Silva, G. W. Amarante, B. A. D. Neto, *J. Org. Chem.*, **2018**, *83*, 12143.
- [330] R. Kaur, S. Chaudhary, K. Kumar, M. K. Gupta, R. K. Rawal, *Eur. J. Med. Chem.*, **2017**, *132*, 108.
- [331] Â. de Fátima, T. C. Braga, L. S. Da Neto, B. S. Terra, B. G. F. Oliveira, D. L. da Silva, L. V. Modolo, *J. Adv. Res.*, **2015**, *6*, 363.
- [332] L. H. S. Matos, F. T. Masson, L. A. Simeoni, M. Homem-de-Mello, *Eur. J. Med. Chem.*, **2018**, *143*, 1779.
- [333] L. Tao, C. Zhu, Y. Wei, Y. Zhao in *Multi-Component and Sequential Reactions in Polymer Synthesis* (Ed.: P. Theato), Springer International Publishing, Cham, **2015**.

-
- [334] Y. Zhao, H. Wu, Z. Wang, Y. Wei, Z. Wang, L. Tao, *Sci. China Chem.*, **2016**, *59*, 1541.
- [335] H. Nagarajaiah, A. Mukhopadhyay, J. N. Moorthy, *Tetrahedron Lett.*, **2016**, *57*, 5135.
- [336] R. Afshari, A. Shaabani, *ACS Comb. Sci.*, **2018**, *20*, 499.
- [337] T. Mao, G. Liu, H. Wu, Y. Wei, Y. Gou, J. Wang, L. Tao, *J. Am. Chem. Soc.*, **2018**, *140*, 6865.
- [338] T. Mao, X. He, G. Liu, Y. Wei, Y. Gou, X. Zhou, L. Tao, *Polym. Chem.*, **2021**.
- [339] L. Yang, Y. Zeng, H. Wu, C. Zhou, L. Tao, *J. Mater. Chem. B*, **2020**, *8*, 1383.
- [340] G. Springsteen, B. Wang, *Tetrahedron*, **2002**, *58*, 5291.
- [341] C. Zhu, B. Yang, Y. Zhao, C. Fu, L. Tao, Y. Wei, *Polym. Chem.*, **2013**, *4*, 5395.
- [342] Z. Huang, R. Wang, Y. Chen, X. Liu, L. Mao, J. Yuan, L. Tao, Y. Wei, X. Zhang, *J. Mater. Res.*, **2019**, *34*, 3011.
- [343] W. A. Cunningham, *J. Chem. Educ.*, **1935**, *12*, 120.
- [344] H. Wu, L. Yang, L. Tao, *Polym. Chem.*, **2017**, *8*, 5679.
- [345] J. Dong, M. Liu, R. Jiang, H. Huang, Q. Huang, Y. Wen, J. Tian, Y. Dai, X. Zhang, Y. Wei, *Dyes Pigm.*, **2019**, *165*, 90.
- [346] Z. Wang, Y. Yu, Y. Li, L. Yang, Y. Zhao, G. Liu, Y. Wei, X. Wang, L. Tao, *Polym. Chem.*, **2017**, *8*, 5490.
- [347] X. Ren, B. Yang, Y. Zhao, X. Zhang, X. Wang, Y. Wei, L. Tao, *Polymer*, **2015**, *64*, 210.
- [348] L. Rong, M. Zeng, H. Liu, B. Wang, Z. Mao, H. Xu, L. Zhang, Y. Zhong, J. Yuan, X. Sui, *Carbohydr. Polym.*, **2019**, *209*, 223.

-
- [349] E. Esen, M. A. R. Meier, *Macromol. Rapid Commun.*, **2020**, *41*, e1900375.
- [350] L. Xu, J. Dong, *Chin. J. Chem.*, **2020**, *38*, 414.
- [351] Y. Zhao, Y. Yu, Y. Zhang, X. Wang, B. Yang, Y. Zhang, Q. Zhang, C. Fu, Y. Wei, L. Tao, *Polym. Chem.*, **2015**, *6*, 4940.
- [352] H. Xue, Y. Zhao, H. Wu, Z. Wang, B. Yang, Y. Wei, Z. Wang, L. Tao, *J. Am. Chem. Soc.*, **2016**, *138*, 8690.
- [353] A. C. Boukis, A. Llevot, M. A. R. Meier, *Macromol. Rapid Commun.*, **2016**, *37*, 643.
- [354] H. Wu, C. Fu, Y. Zhao, B. Yang, Y. Wei, Z. Wang, L. Tao, *ACS Macro Lett.*, **2015**, *4*, 1189.
- [355] Y. Zhao, H. Wu, Y. Zhang, X. Wang, B. Yang, Q. Zhang, X. Ren, C. Fu, Y. Wei, Z. Wang et al., *ACS Macro Lett.*, **2015**, *4*, 843.
- [356] A. C. Boukis, B. Monney, M. A. R. Meier, *Beilstein J. Org. Chem.*, **2017**, *13*, 54.
- [357] B. Walekar, R. Mane, S. Nadaf, N. Valekar, P. Bhosale, S. Mane, *Macromol. Symp.*, **2016**, *361*, 106.
- [358] J. L. Bohlen, *Establishment of a potential Ligand-Library via the Biginelli Reaction. Bachelor Thesis*, Karlsruhe Institute of Technology, Karlsruhe, **2018**.
- [359] G. Morales, R. Martínez, T. Ziegler, *J. Phys. Chem. A*, **2008**, *112*, 3192.
- [360] R. J. Clemens, J. A. Hyatt, *J. Org. Chem.*, **1985**, *50*, 2431.
- [361] R. J. Clemens, *Kodak Lab. Chem. Bull.*, **1984**, *55*, 1.
- [362] J. S. Witzeman, W. D. Nottingham, *J. Org. Chem.*, **1991**, *56*, 1713.
- [363] A. E.-A. M. Gaber, H. McNab, *Synthesis*, **2001**, *2001*, 2059.

-
- [364] H. T. H. Nguyen, P. Qi, M. Rostagno, A. Feteha, S. A. Miller, *J. Mater. Chem. A*, **2018**, *6*, 9298.
- [365] S. R. Jaggavarapu, A. S. Kamalakaran, V. P. Jalli, S. K. Gangisetty, M. R. Ganesh, G. Gaddamanugu, *J. Chem. Sci.*, **2014**, *126*, 187.
- [366] M. J. García, F. Rebolledo, V. Gotor, *Tetrahedron Lett.*, **1993**, *34*, 6141.
- [367] M. J. García, F. Rebolledo, V. Gotor, *Tetrahedron*, **1994**, *50*, 6935.
- [368] V. Nagaraju, D. Purnachander, N. S. V. M. R. Mangina, S. Suresh, B. Sridhar, G. V. Karunakar, *Org. Biomol. Chem.*, **2015**, *13*, 3011.
- [369] D. Gravestock, M. C. Dovey, *Synthesis*, **2003**, *2003*, 523.
- [370] S. Koltzenburg, M. Maskos, O. Nuyken, *Polymere: Synthese, Eigenschaften und Anwendungen*, Springer Spektrum, Berlin, Heidelberg, **2014**.
- [371] P. J. Flory, *J. Am. Chem. Soc.*, **1936**, *58*, 1877.
- [372] L. N. Mizerovskii, V. A. Padokhin, *Fibre Chem.*, **2013**, *44*, 337.
- [373] S. Kuchanov, *Prog. Polym. Sci.*, **2004**, *29*, 563.
- [374] Y. Gnanou, M. Fontanille, *Organic and physical chemistry of polymers*, Wiley-Interscience, Hoboken, NJ, **2008**.
- [375] S. Tateyama, S. Masuo, P. Suvannasara, Y. Oka, A. Miyazato, K. Yasaki, T. Teerawatananond, N. Muangsin, S. Zhou, Y. Kawasaki et al., *Macromolecules*, **2016**, *49*, 3336.
- [376] L. Feng, W. Zhu, W. Zhou, C. Li, D. Zhang, Y. Xiao, L. Zheng, *Polym. Chem.*, **2015**, *6*, 7470.
- [377] A. Gandini, D. Coelho, M. Gomes, B. Reis, A. Silvestre, *J. Mater. Chem.*, **2009**, *19*, 8656.

-
- [378] M. Gomes, A. Gandini, A. J. D. Silvestre, B. Reis, *J. Polym. Sci. Part A: Polym. Chem.*, **2011**, *49*, 3759.
- [379] R. Storbeck, M. Ballauff, *Polymer*, **1993**, *34*, 5003.
- [380] S. Chatti, G. Schwarz, H. R. Kricheldorf, *Macromolecules*, **2006**, *39*, 9064.
- [381] S. Chatti, H. R. Kricheldorf, G. Schwarz, *J. Polym. Sci. Part A: Polym. Chem.*, **2006**, *44*, 3616.
- [382] A. Llevot, B. Monney, A. Sehlinger, S. Behrens, M. A. R. Meier, *Chem. Commun.*, **2017**, *53*, 5175.
- [383] P. S. Löser, *Sustainable Synthesis of Bio-based Recyclable Thermosets. PhD Thesis*, Karlsruhe Institute of Technology, Karlsruhe, **2020**.
- [384] C. E. Hoyle, T. Y. Lee, T. Roper, *J. Polym. Sci. Part A: Polym. Chem.*, **2004**, *42*, 5301.
- [385] B. J. Schmitt, *Makromolekulare Chemie. Ein Lehrbuch für Chemiker, Physiker, Materialwissenschaftler und Verfahrenstechniker*, Springer Spektrum, Berlin, Heidelberg, **2014**.
- [386] T. G. Fox, P. J. Flory, *J. Appl. Phys.*, **1950**, *21*, 581.
- [387] H. A. Schneider, *J. Therm. Anal. Calorim.*, **1999**, *56*, 983.
- [388] H. Daimon, H. Okitsu, J. Kumanotani, *Polym J*, **1975**, *7*, 460.
- [389] N. S. Vrandečić, M. Erceg, M. Jakić, I. Klarić, *Thermochim. Acta*, **2010**, *498*, 71.
- [390] J. G. Drobny, *Handbook of Thermoplastic Elastomers*, Elsevier, **2014**.
- [391] J. C. Brendel, G. Gody, S. Perrier, *Polym. Chem.*, **2016**, *7*, 5536.
- [392] F. L. Hatton, *Polym. Chem.*, **2020**, *11*, 220.

-
- [393] K. S. Khuong, W. H. Jones, W. A. Pryor, K. N. Houk, *J. Am. Chem. Soc.*, **2005**, *127*, 1265.
- [394] J. M. Briody, D. P. N. Satchell, *J. Chem. Soc.*, **1965**, 3778.
- [395] B. Vaisman, A. Shikanov, A. J. Domb, *J. Am. Oil Chem. Soc.*, **2008**, *85*, 169.
- [396] L. O. Kadidae, A. Usami, M. Honda, *Asian J. Chem.*, **2018**, *30*, 589.
- [397] J. E. McKeon, P. Fitton, *Tetrahedron*, **1972**, *28*, 233.
- [398] R. Jiang, Z. Chen, K. Zhan, L. Liu, J. Zhou, Y. Ai, S. Li, H. Bao, Z. Hu, L. Qi et al., *Tetrahedron Lett.*, **2018**, *59*, 3279.
- [399] J. Ziriakus, T. K. Zimmermann., A. Pöthig, M. Drees, S. Haslinger, D. Jantke, F. E. Kühn, *Adv. Synth. Catal.*, **2013**, *355*, 2845.
- [400] M. Jebrane, N. Terziev, I. Heinmaa, *Biomacromolecules*, **2017**, *18*, 498.
- [401] T. Shono, C. S. Marvel, *J. Polym. Sci. A Gen. Pap.*, **1963**, *1*, 2067.
- [402] C. Vilela, R. Rua, A. J. Silvestre, A. Gandini, *Ind. Crops Prod.*, **2010**, *32*, 97.
- [403] M. Destarac, D. Taton, S. Z. Zard, T. Saleh, Y. Six in *Green chemistry, Vol. 626* (Ed.: P. T. Anastas), American Chemical Society, Washington, DC, **1998**.
- [404] S. Harrison, X. Liu, J.-N. Ollagnier, O. Coutelier, J.-D. Marty, M. Destarac, *Polymers*, **2014**, *6*, 1437.
- [405] R.-P. Nzé, O. Colombani, E. Nicol, *J. Polym. Sci. Part A: Polym. Chem.*, **2012**, *50*, 4046.
- [406] S. A. Harrison, D. H. Wheeler, *J. Am. Chem. Soc.*, **1951**, *73*, 839.
- [407] C. S. Marvel, J. C. Hill, J. C. Cowan, J. P. Friedrich, J. L. O'Donnell, *J. Polym. Sci. A Gen. Pap.*, **1964**, *2*, 2523.
-

-
- [408] Z. Demchuk, O. Shevchuk, I. Tarnavchyk, V. Kirianchuk, A. Kohut, S. Voronov, A. Voronov, *ACS Sustain. Chem. Eng.*, **2016**, *4*, 6974.
- [409] Z. Demchuk, O. Shevchuk, I. Tarnavchyk, V. Kirianchuk, M. Lorensen, A. Kohut, S. Voronov, A. Voronov, *ACS omega*, **2016**, *1*, 1374.
- [410] G. Moad, E. Rizzardo, S. H. Thang, *Aust. J. Chem.*, **2009**, *62*, 1402.
- [411] D. J. Keddie, G. Moad, E. Rizzardo, S. H. Thang, *Macromolecules*, **2012**, *45*, 5321.
- [412] C. Barner-Kowollik, *Handbook of RAFT polymerization*, Wiley-VCH, Weinheim, **2008**.
- [413] S. Perrier, *Macromolecules*, **2017**, *50*, 7433.
- [414] B. Maiti, S. Kumar, P. De, *RSC Adv.*, **2014**, *4*, 56415.
- [415] B. Maiti, P. De, *RSC Adv.*, **2013**, *3*, 24983.
- [416] D. J. Keddie, *Chem. Soc. Rev.*, **2014**, *43*, 496.
- [417] C. Barner-Kowollik, M. Buback, B. Charleux, M. L. Coote, M. Drache, T. Fukuda, A. Goto, B. Klumperman, A. B. Lowe, J. B. Mcleary et al., *J. Polym. Sci. Part A: Polym. Chem.*, **2006**, *44*, 5809.
- [418] K. Skrabania, A. Miasnikova, A. M. Bivigou-Koumba, D. Zehm, A. Laschewsky, *Polym. Chem.*, **2011**, *2*, 2074.
- [419] A. Bowes, J. B. Mcleary, R. D. Sanderson, *J. Polym. Sci. Part A: Polym. Chem.*, **2007**, *45*, 588.
- [420] Reich Hans, "NMR Spectroscopy Database", URL:
<https://organicchemistrydata.org/hansreich/resources/nmr/?page=nmr-content%2F>,
accessed 2021.05.31.

- [421] Y. Matsushita in *Encyclopedia of polymeric nanomaterials* (Eds.: S. Kobayashi, K. Müllen), Springer, Berlin, **2015**.
- [422] W. C. Still, M. Kahn, A. Mitra, *J. Org. Chem.*, **1978**, *43*, 2923.

8 Appendix

8.1 List of Abbreviations

AIBN	2,2'-azobis(2-methylpropionitrile)
ATR	Attenuated total reflection
B-3CR	Biginelli-three-component reaction
BGR	<i>Bundesanstalt für Geowissenschaften und Rohstoffe</i>
bpy	2,2'-Bipyridine
cat.	Catalyst
CDI	Carbonyldiimidazole
COSY	Correlation spectroscopy
CTA	Chain transfer agent
DFT	Density functional theory
DHPM	3,4-dihydropyrimidin-2(1H)-ones
DMPA	2,2-Dimethoxy-2-phenylacetophenone
DMSO	Dimethyl sulfoxide
dRI	Differential refractive index
DSC	Differential scanning calorimetry
<i>e.g.</i>	<i>exempli gratia</i> Lat.: for example

8.1 List of Abbreviations

EI	Electron ionization
eq.	Equivalent
Eq.	Equation
ESI	Electrospray ionization
<i>et al.</i>	Lat.: <i>et alii, et aliae, et alia</i> : and others
<i>etc.</i>	Et cetera Lat.: and other similar things
FAB	Fast atom bombardment
FRP	Free radical polymerisation
GC-MS	Gas chromatography - mass spectrometry
GHS	Globally harmonised system of classification and Labelling of chemicals
HIV	Human immunodeficiency virus
HMBC	Heteronuclear multiple bond correlation
HMQC	Heteronuclear multiple quantum coherence
HRMS	High resolution mass spectrometry
HSQC	Heteronuclear single quantum coherence
<i>i.e.</i>	Id est Lat.: that is
<i>in situ</i>	Lat.: on site, locally without isolation
[IrCODCl] ₂	di- μ -chlorobis[(1,2,5,6- η^2)-1,5-cyclo- octadiene]diiridium

IR	Infrared spectroscopy
LCA	Life cycle assessment
MCR	Multicomponent reaction
MS	Mass spectrometry
NMP	<i>N</i> -methyl-2-pyrrolidone
NMR	Nuclear magnetic resonance
PEG	Poly(ethylene glycol)
Pd/C	Palladium on activated charcoal
polyDHPM	DHPM polymers
ppm	Parts per million
PPM	Post-polymerisation modification
<i>p</i> -TSA	<i>para</i> -Toluenesulfonic acid
r.t.	Room temperature (approximately 21 °C)
RAFT	Reversible addition–fragmentation chain transfer
RI	Refractive index
SEC	Size-exclusion chromatography
SLCA	Simplified life cycle assessment
t	Time factor
TBD	1,5,7-triazabicyclo[4.4.0]dec-5-en
TEMPO	2,2,6,6-Tetramethyl-1-piperidinyloxy

TGA	Thermo gravimetric analysis
TLC	Thin layer chromatography
UV	Ultra violet
UV/Vis	Ultraviolet–visible spectroscopy
<i>via</i>	Lat.: by way of, by means of, using
<i>vs.</i>	Versus Lat.: against
<i>v.s.</i>	Vide supra Lat.: see above

8.2 List of Symbols

ν	Wavenumber 1 cm^{-1}
$^{\circ}\text{C}$	Degree centigrade $0^{\circ}\text{C} = 273.15 \text{ K}$
Å	Ångström 10^{-10} m
a	year/s
<i>AE</i>	Atom economy
cm	Centimeter
d	Days
<i>D</i>	Dispersity $D = M_w \cdot M_n^{-1}$
<i>EE</i>	Energy efficiency
<i>E</i> -Factor	Environmental impact factor
<i>EMY</i>	Effective mass yield

<i>g</i>	Grams
<i>h</i>	Hours
<i>J</i>	Coupling constant 1 Hz
<i>M</i>	Molecular weight $1 \text{ g}\cdot\text{mol}^{-1}$
<i>m/z</i>	Mass-to-charge ratio
<i>mg</i>	Milligram
<i>min</i>	Minutes
<i>Mio.</i>	Million
<i>mL</i>	Milliliter
<i>mm</i>	Millimeter
<i>mmol</i>	Millimole 10^{-3} mol
<i>M_n</i>	Number averaged molecular weight $1 \text{ g}\cdot\text{mol}^{-1}$
<i>mol</i>	Mole $6.023\cdot 10^{23}$ particles
<i>mol%</i>	Mole percent
<i>M_w</i>	Mass averaged molecular weight $1 \text{ g}\cdot\text{mol}^{-1}$
<i>n</i>	Amount of substance 1 mol
<i>nm</i>	Nanometer
<i>P_i</i>	Penalty points for EcoScale
<i>PMI</i>	Process mass intensity

8.2 List of Symbols

R_f	Retention factor
RME_{global}	Global reaction mass efficiency
s	Second
sP	specific productivity
t	Tons
$T_{d5\%}$	Decomposition temperature
T_g	Glass transition temperature
T_m	Melting temperature
W	Watts
wt%	Weight percent
X	Conversion
δ	Chemical shift 1 ppm
α	Stoichiometric factor
β	Recovered material factor
ε	Yield
μL	Microliter
μm	Micrometer
μmol	Micromole
ρ	Density

8.3 List of Figures

- Figure 2.1** Visualization of the increase of publications related to the topic of “Sustainable Chemistry” from 1990 to 2019 relative to publications regarding the topic “chemistry” as a benchmark for the growing interest in sustainability (according to a search *via* SciFinder[®] and Scopus[®] on the research topic “Sustainable Chemistry”). 4
- Figure 2.2** The Four Challenges of Green Solvents.^[60] 18
- Figure 2.3** Popular cations (left) and anions (right) used in ionic liquid compositions: pyrrolidinium **4**, pyridinium **5**, imidazolium **6**, ammonium **7**, and tetraalkylphosphonium **8**, as well as hexafluorophosphate **9**, tetrachloroaluminate **10**, tetrafluoroborate **11**, chloride, and bromide.^[72,71] 21
- Figure 2.4** Popular hydrogen bond acceptors used for deep eutectic solvents are choline chloride (**12**) or trimethyl glycine (**13**), popular donors are lactic acid (**14**) or citric acid (**15**) 22
- Figure 2.5** Generic DHPM structures with anti-bacterial (**115**) and anti-inflammatory (**116**) effects.^[330] 62
- Figure 4.1** ¹H NMR spectra of **124d** (top) and **126d** (bottom) showing, as examples, the characteristic signals of diacetoacetates and diacetoacetamides. 75
- Figure 4.2** ¹H NMR spectrum of the crude product mixture of the reaction of ethyl acetoacetate (**90**) and butyl amine indicating the sole formation of an *E/Z*-mixture of the enamine (**130**) of 11:89 (signals 5 and 5' were assigned in accordance to the literature^[368,369]). 76
- Figure 4.3** SEC-determined evolution of the DP with *t* during the synthesis of **120e**, **131e**, **120f**, and **131f** showing a non-linear relation of DP with respect to the reaction time with a similar final chain length of approximately 10 repeat units for **120e**, **120f**, and **131f**. 83

-
- Figure 4.4** Evolution of the degree of polymerisation with the reaction time during the synthesis of **120e**, **131e**, **120f**, and **131f** determined *via* ^1H NMR analysis..... 84
- Figure 4.5** ^1H NMR spectra of **120d** (top) and **131d** (bottom) showing, as examples, the characteristic signals of polyDHPMs from diacetoacetates. 87
- Figure 4.6** SEC graphs of **120f** and **131f** showing a bimodal, broad shape. 89
- Figure 4.7** Dependence of the T_g of polyDHPMs on the spacer-length and the choice of either urea (**47**) or Me-urea (**49**). 91
- Figure 4.8** Evolution of the degree of polymerisation with reaction time during the synthesis of **132e** determined *via* ^1H NMR analysis. 93
- Figure 4.9** ^1H NMR spectra of **132d** (top) and **133d** (bottom) showing, as examples, the characteristic signals of polyDHPMs from diacetoacetamides. 94
- Figure 4.10** Optimisation of the synthesis of **141**, here shown by the results of the thiol-ene reaction in bulk: The crude ^1H NMR spectrum shows 92% conversion of the allyl double bond of **138** relative to the aldehyde signal; the product signals are visible besides minor impurities; the respective spectra of the reactions in CH_2Cl_2 or DMSO as solvent are comparable. 102
- Figure 4.11** Typical ^1H NMR spectrum of **144f** (top) and **144d** (bottom) with 5 mol% of **143**, the aldehyde end group signal is shown for **144d**. 109
- Figure 4.12** Estimation of end group conversion of **144d** in photoinitiated thiol-ene reaction with **145**: Integrals of the end group *CH* signal are given for reaction times of 15 h, 24 h, and 48 h relative to the starting material ($t = 0$ h), the signal of the *CH* proton of the polyDHPM backbone is used as reference. 113
- Figure 4.13** ^1H NMR spectrum of **144d** showing the typical signals of a polyDHPM-*b*-poly(ethylene glycol): besides the signal of the CH_2 groups of poly(ethylene glycol) at 3.5 ppm, the remaining signal of unreacted double bond end group at 5.8 ppm is visible. 116

-
- Figure 4.14** DSC graphs of **148a-e** showing two distinct thermal transitions, the T_m of the PEG block and the T_g of the respective polyDHPM block; the DSC graph of **148f** showed only one T_g 118
- Figure 4.15** Possible renewable starting materials for the synthesis of vinyl esters that carry an acetoacetate group. 124
- Figure 4.16** ^1H NMR spectrum of the crude reaction mixture of the synthesis of **153** from **149** using **64** after a reaction time of 4 h: the spectrum indicated approximately 30% conversion to the desired product..... 126
- Figure 4.17** ^1H NMR spectrum of the crude reaction mixture of the synthesis of **154** from **150** using **65** after a reaction time of 1 h: the spectrum indicated approximately 90% conversion to the desired product..... 128
- Figure 4.18** ^1H NMR spectra of **163** and **164** after purification..... 134
- Figure 4.19** ^1H NMR spectrum of **168**. 140
- Figure 4.20** SEC chromatograms of the RAFT polymerisation of **168** with CTA1 in a 7.5 M reaction mixture showing the development of a bimodal molecular weight distribution at reaction times longer than 2 – 3 h. 143
- Figure 4.21** Pseudo-first order kinetic plot showing the relation between $\ln([M_0]/[M])$ and the reaction time; a rate retarded induction period of 3 h was observed, the conversion was determined by ^1H NMR spectroscopy..... 145
- Figure 4.22** ^1H NMR spectrum of RAFT polymer **169** with a DP of 21. 147
- Figure 4.23** Example overlay of the normalised molecular weight distributions of the RI- and UV detector of **169** showing strong resemblance..... 148
- Figure 4.24** SEC chromatograms of the macro CTA and the chain extended polymer. . 149
- Figure 4.25** ^1H NMR spectrum of the block copolymer **170** in CDCl_3 150
-

Figure 4.26 ^1H NMR spectrum of the purified polymer 171a after PPM of 169 by B-3CR: both of the cis/trans-isomers of 171a are visible.....	152
Figure 4.27 SEC graphs of 169 and 171a	153
Figure 6.1 ^1H and ^{13}C NMR spectra of 124a in $\text{DMSO-}d_6$	167
Figure 6.2 ^1H and ^{13}C NMR spectra of 124b in $\text{DMSO-}d_6$	169
Figure 6.3 ^1H and ^{13}C NMR spectra of 124c in $\text{DMSO-}d_6$	171
Figure 6.4 ^1H and ^{13}C NMR spectra of 124d in $\text{DMSO-}d_6$	173
Figure 6.5 ^1H and ^{13}C NMR spectra of 124e in $\text{DMSO-}d_6$	175
Figure 6.6 ^1H and ^{13}C NMR spectra of 124f in $\text{DMSO-}d_6$	177
Figure 6.7 ^1H and ^{13}C NMR spectra of 126a in $\text{DMSO-}d_6$	179
Figure 6.8 ^1H and ^{13}C NMR spectra of 126d in $\text{DMSO-}d_6$	181
Figure 6.9 ^1H and ^{13}C NMR spectra of 126e in $\text{DMSO-}d_6$	183
Figure 6.10 Size exclusion chromatograms of the samples obtained from the polymerisation kinetics of 120e	185
Figure 6.11 Size exclusion chromatograms of the samples obtained from the polymerization kinetics of 131e	186
Figure 6.12 Size exclusion chromatograms of the samples obtained from the polymerisation kinetics of 120f	187
Figure 6.13 Size exclusion chromatograms of the samples obtained from the polymerisation kinetics of 131f	189
Figure 6.14 Size exclusion chromatograms of the samples obtained from the polymerisation kinetics of 132e	190

Figure 6.15 Size exclusion chromatograms of the samples obtained from the polymerisation kinetics of 133e	191
Figure 6.16 SEC chromatograms of polyDHMPs using acetoacetates and urea (120a-f , top) or Me-urea (131a-f , bottom).	193
Figure 6.17 DSC curves of polyDHMPs using acetoacetates and urea (120a-f , top) or Me-urea (131a-f , bottom) showing the respective T_g s.	194
Figure 6.18 ^1H NMR spectrum of 120a in $\text{DMSO-}d_6$	195
Figure 6.19 ^1H NMR spectrum of 120b in $\text{DMSO-}d_6$	196
Figure 6.20 ^1H NMR spectrum of 120c in $\text{DMSO-}d_6$	197
Figure 6.21 ^1H NMR spectrum of 120d in $\text{DMSO-}d_6$	198
Figure 6.22 ^1H NMR spectrum of 120e	199
Figure 6.23 ^1H NMR spectrum of 120f in $\text{DMSO-}d_6$	200
Figure 6.24 ^1H NMR spectrum of 131a in $\text{DMSO-}d_6$	201
Figure 6.25 ^1H NMR spectrum of 131b in $\text{DMSO-}d_6$	202
Figure 6.26 ^1H NMR spectrum of 131c in $\text{DMSO-}d_6$	203
Figure 6.27 ^1H NMR spectrum of 131d in $\text{DMSO-}d_6$	204
Figure 6.28 ^1H NMR spectrum of 131e in $\text{DMSO-}d_6$	205
Figure 6.29 ^1H NMR spectrum of 131f in $\text{DMSO-}d_6$	206
Figure 6.30 SEC chromatograms of the polyDHMPs using acetoacetamides and urea (132a,d,e , top) or Me-urea (133a,d,e , bottom).	208

Figure 6.31 DSC curves of the polyDHMPs 132a,d,e and 133a,d,e using acetoacetamides and urea (top) or Me-urea (bottom) showing the respective T_{gs} ; the baselines for the measurements of 132a , 133a , and 133d were not stable.....	209
Figure 6.32 ^1H NMR spectrum of 132a in $\text{DMSO-}d_6$	210
Figure 6.33 ^1H NMR spectrum of 132d in $\text{DMSO-}d_6$	211
Figure 6.34 ^1H NMR spectrum of 132e in $\text{DMSO-}d_6$	212
Figure 6.35 ^1H NMR spectrum of 133a in $\text{DMSO-}d_6$	213
Figure 6.36 ^1H NMR spectrum of 133d in $\text{DMSO-}d_6$	214
Figure 6.37 HSQC spectrum of 133d	215
Figure 6.38 ^1H NMR spectrum of 133e in $\text{DMSO-}d_6$	216
Figure 6.39 ^1H NMR spectrum of 137 in CDCl_3	219
Figure 6.40 ^1H NMR spectrum of 138 in $\text{DMSO-}d_6$	221
Figure 6.41 ^1H and ^{13}C NMR spectra of 140 in $\text{DMSO-}d_6$	224
Figure 6.42 ^1H and ^{13}C NMR spectra of 141 in $\text{DMSO-}d_6$	227
Figure 6.43 ^1H and ^{13}C NMR spectra of 143 in $\text{DMSO-}d_6$	230
Figure 6.44 SEC chromatograms of end group functionalised polyDHMPs 144a-e	232
Figure 6.45 DSC curves of end group functionalised polyDHMPs 144a-e showing the respective T_{gs}	233
Figure 6.46 ^1H NMR spectrum of 144a in $\text{DMSO-}d_6$	234
Figure 6.47 ^1H NMR spectrum of 144b in $\text{DMSO-}d_6$	235
Figure 6.48 ^1H NMR spectrum of 144c in $\text{DMSO-}d_6$	236

Figure 6.49 ^1H NMR spectrum of 144d in $\text{DMSO-}d_6$	237
Figure 6.50 ^1H NMR spectrum of 144e in $\text{DMSO-}d_6$	238
Figure 6.51 SEC chromatograms of polyDHPMs 144f with and without end-capping..	239
Figure 6.52 DSC curves showing the respective T_{gs} of the end group functionalised polyDHMPs 144f with and without end-capping.....	240
Figure 6.53 ^1H NMR spectrum of 144f in $\text{DMSO-}d_6$	242
Figure 6.54 ^1H NMR spectrum of 144f in $\text{DMSO-}d_6$	244
Figure 6.55 SEC chromatograms of the polyDHPM- <i>b</i> -poly(ethylene glycol)s 148a-f .	246
Figure 6.56 DSC curves showing the respective T_{gs}/T_{ms} of the polyDHPM- <i>b</i> -poly(ethylene glycol)s 148a-f .	247
Figure 6.57 ^1H NMR spectrum of 148a in $\text{DMSO-}d_6$	248
Figure 6.58 ^1H NMR spectrum of 148b in $\text{DMSO-}d_6$	249
Figure 6.59 ^1H NMR spectrum of 148c in $\text{DMSO-}d_6$	250
Figure 6.60 ^1H NMR spectrum of 148d in $\text{DMSO-}d_6$	251
Figure 6.61 ^1H NMR spectrum of 148e in $\text{DMSO-}d_6$	252
Figure 6.62 ^1H NMR spectrum of 148f in $\text{DMSO-}d_6$	253
Figure 6.63 SEC chromatograms and DSC curves of end group functionalised polyDHMPs 144a,b,c,eMe	255
Figure 6.64 ^1H NMR spectrum of 144aMe in $\text{DMSO-}d_6$	256
Figure 6.65 ^1H NMR spectrum of 144bMe in $\text{DMSO-}d_6$	257
Figure 6.66 ^1H NMR spectrum of 144cMe in $\text{DMSO-}d_6$	258

Figure 6.67 ^1H NMR spectrum of 144eMe in $\text{DMSO-}d_6$	259
Figure 6.68 SEC chromatograms and DSC curves of polyDHPM- <i>b</i> -poly(ethylene glycol)s (148a,b,c,eMe).	261
Figure 6.69 ^1H NMR spectrum of 148aMe in $\text{DMSO-}d_6$	262
Figure 6.70 ^1H NMR spectrum of 148bMe in $\text{DMSO-}d_6$	263
Figure 6.71 ^1H NMR spectrum of 148cMe in $\text{DMSO-}d_6$	264
Figure 6.72 ^1H NMR spectrum of 148eMe in $\text{DMSO-}d_6$	265
Figure 6.73 ^1H and ^{13}C NMR spectra of 157 in $\text{DMSO-}d_6$	268
Figure 6.74 ^1H and ^{13}C NMR spectra of 159 in $\text{DMSO-}d_6$	271
Figure 6.75 ^1H and ^{13}C NMR spectra of 160 in $\text{DMSO-}d_6$	274
Figure 6.76 ^1H and ^{13}C NMR spectra of 163 in $\text{DMSO-}d_6$	277
Figure 6.77 ^1H and ^{13}C NMR spectra of 164 in $\text{DMSO-}d_6$	280
Figure 6.78 ^1H and ^{13}C NMR spectra of 164 in $\text{DMSO-}d_6$	283
Figure 6.79 Example ^1H spectrum of 169 in CDCl_3	285
Figure 6.80 SEC graphs of the screening of the RAFT polymerisation of 168 at a 7.5 M concentration with CTA1 (top) and CTA2 (bottom).....	287
Figure 6.81 SEC graphs of the screening of the RAFT polymerisation of 168 at a 3.75 M concentration with CTA1.	288
Figure 6.82 SEC graphs of the screening of the RAFT polymerisation of 168 at a 1.8 M concentration with CTA1 (top) and CTA2 (bottom).....	290

Figure 6.83 SEC graphs of the RAFT polymerisations of 168 at a 1.8 M concentration with CTA1, stopped after certain reaction times to reach specific conversions.....	291
Figure 6.84 DSC graph of 169	292
Figure 6.85 Example ^1H spectrum of 169 in CDCl_3	294
Figure 6.86 SEC graphs of the applied macro CTA and the resulting polymer after chain extension <i>via</i> RAFT polymerisation.....	295
Figure 6.87 Example ^1H spectrum of 170 in CDCl_3	297
Figure 6.88 SEC graphs of the applied macro CTA and the resulting block copolymer 170	297
Figure 6.89 SEC and DSC graphs of 171a and 171b	299
Figure 6.90 ^1H NMR spectrum of 171a in $\text{DMSO-}d_6$	300
Figure 6.91 Phase edited HSQC spectrum of 171a : the picked signals indicate existence of an internal cis double bond and an internal trans double bond as the ^{13}C shift hardly differs between cis and trans while the ^1H shift does. ^[420]	301
Figure 6.92 ^1H NMR spectrum of 171b in $\text{DMSO-}d_6$	302

8.4 List of Schemes

Scheme 2.1 Generic reaction scheme of a linear stepwise reaction: x_i refer to stoichiometric coefficients of the intermediate C which is not part of the calculation of *AE*..... 7

Scheme 2.2 The four parts of a complete Life Cycle Assessment; data is continuously updated and interpreted allowing for an efficient adaptation of the sections.^[49] 14

-
- Scheme 2.3** Industrial oxirane production methods: traditional route over 2-chloroethanol and subsequent elimination of hydrogen chloride, improved route *via* direct oxidation of ethene.^[56,57] 16
- Scheme 2.4** Three types of switchable solvent systems using CO₂ as trigger: i. switchable polarity solvent, ii. switchable hydrophilicity solvent, iii. switchable water. 23
- Scheme 2.5** General concepts and comparison of traditional crude oil refinery and biorefinery: both share the same conceptual structure while biorefinery is designed as sustainable material cycle.^[101] 25
- Scheme 2.6** Considerable valorisation pathways for lignocellulose (gasification^[125,126], hydrolysis^[120] and pyrolysis^[127]): the possible product spectrum covers a variety of valuable product classes. 29
- Scheme 2.7** Syntheses pathways for the production of **18** from the renewable platform molecules **16** or **20** using biochemical and catalytic steps.^[57,128,134,135,137,149,150] Example reactions/conditions: **a)** microbial fermentation, *Saccharomyces cerevisiae*, water, 35 – 45°C, 3 – 5 d, no yield reported. **b)** dehydration, 95 wt% EtOH/H₂O, alumina based cat., 300 – 500°C, 1 – 2 bar, *SV* 0.1 – 1 h⁻¹, 94 – 99% yield. **c)** oxidation, 2 – 10 vol% **1**, alumina supported Ag, 220 – 277°C, 10 – 30 bar air, *SV* 2000 – 4000 h⁻¹, 16 – 52% yield. **d)** hydration, carboxylate salts as cat., 10 mol% H₂O/**3**, 100 – 120°C, 15 bar, 1 h, 98% yield. **e)** hydrogenation, Cu/Cr cat. on solid support, 50 wt% **16**/H₂O, 120 – 150°C, 70 bar H₂, 2 – 4 h, no yield reported. **f)** hydrogenolysis, Ru- or Ni-based catalyst, 200 – 275°C, 40 – 270 bar H₂, 20 min – 7 h, 8 – 25% yield. **g)** hydrogenolysis, Ru- or Ni-based catalyst, 120 – 230°C, 1 – 80 bar H₂ or N₂, 1 – 72 h, 6 – 30%. 32
- Scheme 2.8** Possible synthesis pathways for the production of **21** from the renewable platform molecules **16** and **20** *via* different biochemical processes or catalytic hydrogenolysis.^[142,144,146,147,152] Typical reactions/conditions: **a)** fermentation, *e.g.* genetically modified *Escherichia coli*, 0.2 wt% **16** in growth medium, 37°C, 1 d, 21% yield at 99% conversion. **b)** fermentation, genetically modified *Clostridium acetobutylicum*, 0.11 mol% **20** in growth medium, 35°C, volumetric productivity 3 g·L⁻¹·h⁻¹, 64% yield. **c)**

hydrogenolysis, 0.33 M **20** in H₂O, bohemite-supported Pt/W-oxide cat., 180°C, 50 bar H₂, 12 h, 69% yield at 99% conversion. 33

Scheme 2.9 Industrial production pathway of **24** from renewable **22** *via* drop-in strategy.^[153,156,157] Typical reactions/conditions: **a)** fermentation, *e.g.* genetically modified *Escherichia coli*, 40 – 100 g·L⁻¹ in growth medium, 30 – 40°C, volumetric productivity 1.1 – 3.8 g·L⁻¹·h⁻¹, 3 – 4 d, yield not given. **b)** hydrogenation, Ru/Sn catalyst on ZrO₂ support, 225°C, 140 bar H₂, 94% yield. 34

Scheme 2.10 Possible synthesis of **28** from the renewable **20** *via* subsequent catalytic reduction.^[158–162] Typical reactions/conditions: **a)** dehydration, 10 wt% **20** in H₂O, H₃PW₁₂O₄₀/Nb₂O₅ cat., *SV* 420 h⁻¹, 325°C, 92% yield. **b)** [4+2]-cycloaddition, 185 – 195°C, 45 – 75 min, up to 99% yield at 56% conversion. **c)** hydrogenation, 5 wt% **26** in MeOH, PtW/TiO₂ cat., 80°C, 6.6 bar H₂, 4 h, 60% yield (+27% **28**). **d)** hydrogenolysis, 2 wt% **27** in water, Rh/Re-oxide on carbon support, 100°C, 80 bar H₂, 24 h, 48% yield, at 50% conversion. 35

Scheme 2.11 Possible synthesis of **28** from the renewable **29** *via* subsequent catalytic reduction.^[164–168] Typical reactions/conditions: **a)** hydrogenation, 0.5 M **29** in H₂O, Ni–Pd/SiO₂ cat., 40°C, 80 bar H₂, 2 h, 96% yield. **b)** hydrogenolysis, 0.45 M **30** in water, Rh/Re-catalysts and NAFION™ SAC13, 120°C, 10 bar H₂, after 1 h 80 bar, 20 h, 86% yield. **c)** hydrogenolysis, 0.33 M in EtOH, Pd/ZrP, formic acid, 140°C, 21 h, 43% yield at 97% conversion. 36

Scheme 2.12 Possible synthesis of **34** from renewable castor oil *via* pyrolysis under alkaline conditions.^[169,170,172] Typical reactions/conditions: **a)** alkaline pyrolysis, mineral oil as solvent, NaOH, 280°C, 5 h, up to 70% yield. **b)** hydrogenation, Ru/Pd/Pt cat., 200°C, 150 bar H₂, ultrasonication, 98% yield. 37

Scheme 2.13 Synthesis of **35** *via* dehydration of **19**.^[173] Typical reactions/conditions: **a)** see **Scheme 2.7 e)**. **b)** dehydration, AMBERLYST 36™, 150°C, 4 h, 99.8% yield. 37

Scheme 2.14 Synthesis of renewable diamines **36**, **37**, and **38** by direct amination or two step synthesis over an intermediate dinitrile using diols as starting materials.^[179,180] Typical reactions/conditions: **a**) amination (*e.g.* of **18**), SiO₂/Al₂O₃-supported Ni/Re-cat., 130 – 225°C, 35 – 200 bar H₂/NH₃, 24% yield at 30% conversion. **b**) nitrile synthesis, 0.6 M **34** in MeCN, CuI/bipyridine/2,2,6,6-tetramethylpiperidiny-1-oxyl (TEMPO), NH₃, oxygen atmosphere, 30°C, 24 h, 93% yield. **c**) hydrogenation, 0.2 M in EtOH, Raney Ni, 70°C, 10 bar H₂. 16 h, 51% yield. 39

Scheme 2.15 Reported one-pot syntheses of aliphatic diamines from dicarboxylic acids over either an intermediate diol (shown for **43**) or diamide (shown for **39**).^[188,189] Typical reactions/conditions: **a**) hydrogenation, 0.1 M **40** in dioxane/water, Ru(acetylacetonate)₃/1,1,1-tris(diphenylphosphinomethyl)ethane/methanesulfonic acid, 220°C, 10 bar H₂. 20 h. **b**) amination, same as **a**) but 0.1 M in dioxane, aqueous NH₃, 83% yield. **c**) amidation, 0.1 M **33** in *c*-pentyl methyl ether, Ru/W-oxide cat. on solid support, 200°C, 6 bar NH₃, reaction time not given. **d**) hydrogenation, same as **c**) but 6 bar NH₃/50 bar H₂, 6.5 h, 30% yield. 40

Scheme 2.16 Synthesis of **47** and **49**.^[192,196–198] Typical reactions/conditions: **a**) addition/dehydration, 150 – 250°C, 120 – 400 bar. **b**) methylation, 380°C, 1 h, 60% yield. 41

Scheme 2.17 Synthesis of renewable **51** using carbohydrate feedstocks.^[203–205] Typical reactions/conditions: **a**) biosynthesis, 15 g·L⁻¹ **16** in growth medium, genetically modified *Escherichia coli*, 37°C, 96 h, 32% yield. **b**) oxidation, *hν* (>420 nm), 0.02 M **50** in toluene/H₃PO₄, Ru/SrTiO₃:Rh, 25°C, N₂, 18 h, >95% yield..... 42

Scheme 2.18 Synthesis route for **58** *via* **56** as intermediate using **52** and **53** as possible renewable precursors.^[204,207,210,214] Typical reactions/conditions: **a**) [4+2]-cycloaddition, TiCl₄-cat., 21°C, 24%, 94% yield. **b**) dehydroaromatisation, Pd/C, 240°C, 0.11 bar, 77% yield. **c**) oxidation, AcOH, Co(OAc)₂/Mn(OAc)₂ cat., O₂, 100°C, 94%. **d**) reduction, [RuCl₂(*p*-cumene)]₂, NaOEt, 80°C, 50 bar H₂, 16 h, 99% yield. **e**) oxidation, 0.2 M **57** in toluene, Co/N/C-cat., 100°C, O₂, 36 h, 99% yield. 43

-
- Scheme 2.19** Synthetic pathways for renewable **64** and **65**.^[215,217,218,220,221,225] Typical reactions/conditions: **a)** pyrolysis, 740 – 760°C, PO(OEt)₃ cat., no yield given. **b)** pyrolysis, 700 – 750°C, 10 h, 95% yield. **c)** [2+2]-cycloaddition, spontaneous below 200°C, up to 85% yield. **d)** ring-opening, 21-150°C, no further information given. **e)** addition, *p*-TsOH as cat., reflux, 3 h, 91 % yield. 44
- Scheme 2.20** The Strecker synthesis is the first MCR, reported in 1850; the *AE* was calculated using $R^1 = \text{CH}_3$.^[251] 47
- Scheme 2.21** Representative milestones of the development of MCRs with the names of the lead authors in the respective publication, year of publication, and an example *AE*; the *AE* was calculated using $R^x = \text{CH}_3$ and $X = \text{Cl}$.^[252,254,257,258] 48
- Scheme 2.22** Two examples for isocyanide-based MCRs are given with the names of the lead authors in the respective publication, year of publication, and an example *AE*; the *AE* was calculated using $R^x = \text{CH}_3$ and $X = \text{Cl}$.^[261,262] 49
- Scheme 2.23** Two examples industrially applied MCRs are given with the names of the lead authors in the respective publication, year of publication, and an example *AE*; the *AE* was calculated using $R^x = \text{CH}_3$.^[267,269] 50
- Scheme 2.24** Categorisation of multicomponent reactions into three types according to the reversibility of the mechanistic steps.^[270] 51
- Scheme 2.25** The first Biginelli-three-component reaction yielding the proposed open chain β -ureidocrotonate as originally reported by Biginelli in 1891.^[257] 52
- Scheme 2.26** The three possible primary reaction intermediates of a Biginelli-three-component reaction as proposed by Folkers and Johnson: a bisureide (red), an enamine (blue), or an enone (green).^[275] 53
- Scheme 2.27** Suggested enamine mechanism for the Biginelli-three-component reaction.^[275] 54
-

-
- Scheme 2.28** Suggested Knoevenagel-mechanism for the Biginelli-three-component reaction.^[276] 55
- Scheme 2.29** Results of the separate enamine formation and subsequent reaction towards a DHPM: only the enamine **100** was accessible which led to DHPM **101**. **101** differs in the position of the Me-N group from **103**, which is solely formed by direct B-3CR of **49**, **90**, and **51**;^[277] the position of the methyl group of interest is drawn in red. 56
- Scheme 2.30** Reaction of separately prepared **94** with **104** or **105** led to the formation of **106**, a regioisomer of the targeted DHPM.^[277] 57
- Scheme 2.31** Commonly accepted mechanism for the Brønsted acid-catalysed Biginelli-three-component reaction *via* the iminium intermediate **107** alongside common substituents of the components.^[277,288–290] 58
- Scheme 2.32** Atwal procedure for the synthesis of *N*3-substituted DHPMs through the efficient incorporation of aliphatic/sterically demanding aldehydes.^[292,291] 60
- Scheme 2.33** Synthesis of a DHPM-carrying methacrylate that is subsequently polymerised using FRP or RAFT polymerisation. 63
- Scheme 2.34** Two possible monomer systems for the synthesis of Biginelli-polycondensates: example of an AA/BB-monomer system as applied by Meier *et al.* and an AB-monomer system as applied by Tao *et al.*^[353,351] 67
- Scheme 4.1** Synthesis of acetoacetates (**129**) *via* the thermal *in situ* formation of acetylketene (**127**) using the precursors *tert*-butyl acetoacetate (**64**) or diketene acetone adduct (**65**) as an example. 73
- Scheme 4.2** Brønsted acid catalysed synthesis of polyDHPMs using six different diacetoacetates **124a-f** in combination with terephthalic aldehyde (**58**) and either urea (**47**) or *N*-methyl urea (**49**). 79

-
- Scheme 4.3** Synthesis scheme of polyDHPMs using three different diacetoacetamides **126a, d, e** in combination with terephthalic aldehyde (**58**) and either urea (**47**) or *N*-methyl urea (**49**). 92
- Scheme 4.4** Literature-known two-step synthesis of **138** from **134, 135, and 136**; reaction conditions: **a**) 7.50 eq **135**, 1.00 eq **136**, 0.01 eq TBD, 80°C, 1 h, 31% yield. **b**) 1.00 eq **134**, 2.50 eq **137**, 0.05 eq triphenyl phosphine, 0.001 eq Pd⁰/poly(vinylpyrrolidone), 0.370M in water, 90°C, 22 h, 80% yield.^[382,383] 99
- Scheme 4.5** Four step synthesis route to the renewable AB-monomer **141**; optimised reaction conditions: **a**) 1.00 eq **139**, 1.00 eq **64**, 150°C, 4.5 h, 63% yield. **b**) 1.00 eq **138**, 1.00 eq **140**, 0.01 eq DMPA, irradiation at 365 nm, over night, 85% yield..... 100
- Scheme 4.6** Reaction scheme for the synthesis of **143** by esterification of the respective alcohol **142** in bulk, 99% yield..... 103
- Scheme 4.7** Brønsted acid catalysed synthesis of end group functionalised polyDHPMs: top: using AA/BB-monomers, particularly the diacetoacetates **124a-e** in combination with terephthalic aldehyde (**58**) and urea (**47**), bottom: using the AB-monomer **141** together with **47**. 104
- Scheme 4.8** Idealised scheme of a generic polycondensation of a diol and a dicarboxylic acid: if both monomers are present in equal amounts, polymer chains with a statistical ratio of alcohol:dicarboxylic acid of 1:1 are formed; an excess of, *e.g.*, diol lowers the maximum DP and produces polymer diols at full conversion; addition of monofunctional alcohols equally lowers the DP and yields polymers with alcohol and “E” endgroups. 105
- Scheme 4.9** Reaction scheme of the photoinitiated thiol-ene reaction of **144a-f** with **147**. 114
- Scheme 4.10** Brønsted acid catalysed synthesis of end group functionalised polyDHPMs (**144a,b,c,eMe**) using AA/BB-monomers, particularly the diacetoacetates **124a,b,c,e** in combination with terephthalic aldehyde (**58**) and *N*-methyl urea (**49**)..... 119
-

Scheme 4.11 Attempts for the synthesis of 153 : a) 3.0 eq 64 , bulk, 140°C, 4.5 h, 30% yield, degradation upon isolation; b) 3.0 eq 65 , bulk, 95°C, 2 h, 0% yield.	125
Scheme 4.12 Reaction scheme for the synthesis of 157 using 64 or 65 : a) 3.00 eq 64 , 10 M in DMSO, 140°C, 3 h, 95% yield (not isolated); b) 3.00 eq 65 , bulk, 95°C, 3 h, 90% yield (not isolated); c) 1.10 eq 1M HCl _{aq} , room temperature, 30 min, 90 % yield (when 156 was prepared <i>via a</i>), extraction of the DMSO with EtOAc was necessary leading to a yield of 50%).	130
Scheme 4.13 Reaction scheme for the synthesis of 159 using 65 : a) 3.0 eq 65 , bulk, 95°C, 1 h, 68%.....	130
Scheme 4.14 Reaction scheme for the hydrogenation of 159 to 160 : a) 0.00125 eq Pd/C (10% Pd basis), 0.15M in EtOAc, room temperature, 15 bar H ₂ , 24 h, quantitative yield.	131
Scheme 4.15 Synthesis routes of the ricinoleic acid based vinyl esters 163 and 164 : a) 10 eq 161 , 0.01 eq [Ir(cod)Cl] ₂ , 0.03 eq NaOAc, degassed with Ar, 100°C, 16 h, 68% yield for 163 , 72% yield for 164	133
Scheme 4.16 Reaction scheme for the preparation of 166 from 159 using CDI and 2-hydroxyethyl methacrylate (165) and the subsequent esterification with 167 to 168 : a) 1.05 eq 165 , 0.43 M in anhydrous toluene, room temperature, 16 h, quantitative (¹ H NMR, no workup); b) 1.00 eq 167 , 0.43 M in toluene, 65°C, 8 h, 92%.....	139

8.5 List of Tables

Table 2.1 The 12 Principles of Green Chemistry published by Anastas and Warner in 1998 ^[17] as a guideline for the design of chemical processes and products.	6
--	---

Table 2.2 Annual production, accumulated waste and <i>E</i> -factors of four industrial sectors. ^[25,36]	10
Table 2.3 Comparison of prominent Green Chemistry metrics.....	13
Table 2.4 Categorisation of 18 common solvents according to their safety and impact on health and environment as recommended (green), problematic (yellow), and hazardous/highly hazardous (red). ^[67]	20
Table 2.5 Summary of biorefinery platforms, possible feedstocks, processing methodologies, and main products.	27
Table 4.1 Reaction Scheme for the synthesis of six different diacetoacetates (124a-f) with the respective yields and relative amounts of recovered excess of 64 and by-product 63 . 74	74
Table 4.2 Reaction Scheme for the synthesis of three different diacetoacetamides (126a, d, e) with the respective yields.....	77
Table 4.3 Results of the optimisation of the Biginelli polycondensation by varying the type of the catalyst and concentration of the reaction mixture.....	80
Table 4.4 SEC data of the kinetic investigation of 120e and 120f	82
Table 4.5 Molecular weight and DSC data for the polyDHPMs from diacetoacetates (120a-f and 131a-f).....	88
Table 4.6 Molecular weight data and DSC data for the polyDHPMs from diacetoacetamides (132a, d, e and 133a, d, e).....	95
Table 4.7 ¹ H NMR and SEC data of polyDHPMs using 124d or 141 with different amounts of 143	107
Table 4.8 ¹ H NMR and SEC data of polyDHPMs using 124a-e or 141 with 5 mol% of 143	111

Table 4.9 ^1H NMR, SEC, and DSC data and yields of polyDHPM- <i>b</i> -poly(ethylene glycol), 148a-f	115
Table 4.10 SEC and DSC data and yields of the end group functionalised polyDHPMs (144a,b,c,eMe) and the polyDHPM- <i>b</i> -poly(ethylene glycol)s (148a,b,c,eMe).	119
Table 4.11 Screening of conditions for the synthesis of 162 from 157 and 161 : a maximum of 34% of product was obtained within the crude mixture.	132
Table 4.12 Tested polymerisation conditions for 163 and 164 <i>via</i> RAFT polymerisation and FRP at 65°C.	137
Table 4.13 ^1H NMR and SEC results of the screening of the RAFT polymerisation of 168 at a 7.5 M concentration.	142
Table 4.14 ^1H NMR and SEC results from the screening of two different concentrations of the RAFT polymerisation of 168 with CTA1. ^a	144
Table 4.15 SEC and ^1H NMR data for the synthesis of RAFT polymers of specific molecular weights. ^a	146
Table 6.1 SEC data of the polymerisation kinetics of 120e	185
Table 6.2 SEC data of the polymerisation kinetics of 131e	186
Table 6.3 SEC data of the polymerization kinetics of 120f	188
Table 6.4 SEC data of the polymerization kinetics of 131f	189
Table 6.5 SEC data of the polymerization kinetics of 132e	190
Table 6.6 SEC data of the polymerization kinetics of 133e	191
Table 6.7 SEC and DSC data and yields of polyDHPMs 120a-f and 131a-f using diacetoacetates.	192

Table 6.8 SEC and DSC data and yields of polyDHPMs 132a-e using diacetoacetamides.	207
Table 6.9 Results of the TGA of the whole set of polyDHPMs.....	217
Table 6.10 SEC and DSC data and yields of end group functionalised polyDHPMs 144a-e from diacetoacetates 124a-e	232
Table 6.11 Analytical data (SEC, DSC, NMR, yield) of polyDHPMs 144f	239
Table 6.12 SEC and DSC data and yields of polyDHPM- <i>b</i> -poly(ethylene glycol)s 148a-f	246
Table 6.13 SEC and DSC data and yields of the end group functionalised polyDHPMs 144a,b,c,eMe from <i>N</i> -methyl urea.	254
Table 6.14 SEC and DSC data and yields of the the polyDHPM- <i>b</i> -poly(ethylene glycol)s (148a,b,c,eMe).	260
Table 6.15 ¹ H NMR and SEC results of the screening of the RAFT polymerisation of 168 at a 7.5 M and 3.75 M concentration using CTA1 or CTA2.	286
Table 6.16 ¹ H NMR and SEC results of the screening of the RAFT polymerisation of 168 at a 1.88 M concentration using CTA1 or CTA2.....	289
Table 6.17 SEC and ¹ H NMR data for the synthesis of RAFT polymers of specific molecular weights. ^a	291

8.6 Publications

J. T. Windbiel, M. A. R. Meier, *Polym Int*, **2020 // 2021**, *70*, 506. © 2020 Polymer International published by John Wiley & Sons Ltd on behalf of Society of Industrial Chemistry. DOI: 10.1002/pi.6106